University of Alberta

SCALED MODEL STUDIES OF THE IMMISCIBLE CARBON DIOXIDE WAG FLOODING PROCESS UNDER VARIOUS CONDITIONS

By
Tai Anh Nguyen ©

A thesis submitted to the Faculty of Graduate Studies and Research in Partial fulfillment of the requirements for the degree of Doctor of Philosophy
in
Petroleum Engineering

Department of Mining, Metallurgical and Petroleum Engineering

Edmonton, Alberta
Spring, 1997

National Library of Canada

Acquisitions and Bibliographic Services

395 Wellington Street
Ottawa ON K1A 0N4
Canada

Bibliothèque nationale du Canada

Acquisitions et services bibliographiques

395, rue Wellington
Ottawa ON K1A 0N4
Canada

Your file Votre référence

Our file Notre référence

The author has granted a non-exclusive licence allowing the National Library of Canada to reproduce, loan, distribute or sell copies of his/her thesis by any means and in any form or format, making this thesis available to interested persons.

L'auteur a accordé une licence non exclusive permettant à la Bibliothèque nationale du Canada de reproduire, prêter, distribuer ou vendre des copies de sa thèse de quelque manière et sous quelque forme que ce soit pour mettre des exemplaires de cette thèse à la disposition des personnes intéressées.

The author retains ownership of the copyright in his/her thesis. Neither the thesis nor substantial extracts from it may be printed or otherwise reproduced with the author's permission.

L'auteur conserve la propriété du droit d'auteur qui protège sa thèse. Ni la thèse ni des extraits substantiels de celle-ci ne doivent être imprimés ou autrement reproduits sans son autorisation.

0-612-21614-4

Canada

University of Alberta

Library Release Form

Name of Author: Tai Anh Nguyen

Title of Thesis: Scaled Model Studies of the Immiscible Carbon Dioxide WAG Flooding Process Under Various Conditions

Degree: Doctor of Philosophy

Year this Degree Granted: 1997

Permission is hereby granted to the University of Alberta to reproduce single copies of this thesis and to lend or sell such copies for private, scholarly, or scientific research purposes only.

The author reserves all other publication and other rights in association with the copyright in the thesis, and except as hereinbefore provided, neither the thesis nor any substantial portion thereof may be printed or otherwise reproduced in any material form whatever without the author's prior written permission.

Tai A Nguyen
#408 - 9023 - 105A Avenue
Edmonton, Alberta, Canada

DATED: Dec. 16/96

University of Alberta

Faculty of Graduate Studies and Research

The undersigned certify that they have read, and recommend to the Faculty of Graduate Studies and Research for acceptance, a thesis entitled SCALED MODEL STUDIES OF THE IMMISCIBLE CARBON DIOXIDE WAG FLOODING PROCESS UNDER VARIOUS CONDITIONS submitted by Tai Anh Nguyen in partial fulfillment of the requirements for the degree of DOCTOR OF PHILOSOPHY in PETROLEUM ENGINEERING.

Dr. S.M. Farouq Ali (Supervisor)

Carl Mendoza
Dr. C. Mendoza

Dr. J. Szymanski

Dr. Q.T. Doan

Ramon Bentsen
Dr. R.G. Bentsen

Teresa G. Monger-McClure
Dr. T.G. Monger-McClure (External Examiner)

DATE: Dec. 11, 96

Science is built up with facts, as a house is with stones.
But a collection of facts is no more a science than
a heap of stones is a house
Jules Henry Poincare´

1854-1912

ABSTRACT

This research was directed towards an experimental investigation of the performance of the immiscible carbon dioxide Water-Alternating-Gas (WAG) process, which holds considerable promise for the recovery of moderately viscous heavy oils from thin and/or deep formations, for which reservoir conditions do not favour the application of any of the thermal recovery techniques.

The experimental work was conducted to study the diffusion and gravity segregation phenomena occurring during the process. Work was also done to study the non-isothermal immiscible carbon dioxide WAG process.

A number of measurements were made to study the diffusivity of a gas phase into a liquid phase. In this study, two gases: carbon dioxide and methane were used as the diffusing gas phase. Oils of different physical properties were used to represent the liquid phase. The measurements were made at various pressure and temperature conditions. It was observed that, based on the results obtained, the diffusivity of gaseous carbon dioxide or methane increased with increasing pressure and temperature and decreased with increasing oil viscosity and oil molecular weight and that carbon dioxide diffused faster than methane. Using the data collected, an empirical correlation was also developed.

Several displacement experiments were performed to determine the possible application of a carbonated waterflood in place of an immiscible carbon dioxide WAG flood. A carbonated waterflood was found to be inferior to an immiscible carbon dioxide WAG flood, because the carbon dioxide requirement was too high.

Gravity segregation of carbon dioxide and water was investigated by conducting a number of vertical and horizontal displacement experiments. It was observed that gravity segregation affected the displacement efficiency of the immiscible WAG process. As well, it was noted that transverse diffusion of carbon dioxide in the horizontal direction normal to the vertical longitudinal direction helped delay the upward gravity channelling of carbon dioxide.

In addition to the studies mentioned above, a non-equilibrium mathematical model with phase change for the non-isothermal immiscible carbon dioxide WAG process was developed, using non-equilibrium thermodynamics theory. Two sets of scaling criteria for the non-isothermal carbon dioxide process were derived using the mathematical model. These were employed to design and perform non-isothermal experiments.

Moreover, the experimental results obtained in this investigation, as well as those obtained in previous investigations, were correlated using the scaling criteria derived, thus demonstrating the usefulness of the criteria.

ACKNOWLEDGMENTS

The author wishes to express his sincere gratitude and appreciation to Dr. S.M. Farouq Ali for his advice, encouragement, support, and guidance throughout the course of this study.

The author thanks Dr. R.G. Bentsen, Dr. Q.T. Doan, Dr. C. Mendoza, Dr. T.G. Monger-McClure and Dr. J. Szymanski for their valuable comments and suggestions.

Thanks are also expressed to Mr. Bob Smith and all the technical staff of the School of Mining and Petroleum Engineering in the Department of Civil and Environmental Engineering for their miscellaneous help and expertise in setting up the laboratory equipment.

Appreciation is given to Husky Oil Operations Ltd. and Sceptre Resources Ltd. for providing the oils used in this study.

Last, but not the least, the financial support for this research provided by the Alberta Oil Sands Technology and Research Authority (AOSTRA) is gratefully acknowledged.

TABLE OF CONTENTS

1 - Introduction 1

2 - Statement of the Problem 3

3 - Review of the Literature 4

3.1 - Diffusivity of Carbon Dioxide into Oil at Reservoir Conditions 4

3.1.1 - Measurement of Diffusion Coefficient 5

3.1.2 - Correlations of Diffusion Coefficients 7

3.2 - Carbonated Water Injection 7

3.3 - Gravity Segregation 8

3.3.1 - Effect of Gravity Segregation on Saturation Distribution 12

3.3.2 - Effect of Segregation on Sweep Efficiency 13

3.3.3 - Effect of Reservoir Heterogeneities 14

3.3.4 - Field Observation of Gravity Segregation 14

3.4 - Background to Non-Equilibrium Processes 15

3.4.1 - Background to Mathematical Modelling of Non-equilibrium 16

4 - Development of the Mathematical Model for the Non-Isothermal and Non-Equilibrium Immiscible CO_2 WAG Process 18

4.1 - Derivation of the Mathematical Model 18

4.2 - Derivation of Scaling Groups 37

4.2.1 - Inspectional Analysis 38

4.2.2 - Derivation of the Relaxed Scaling Groups 43

4.2.3 - Dimensional Analysis 46

5 - Experimental Apparatus and Procedure 47

5.1 - Experimental Apparatus 47

5.1.1 - Physical Models 47

5.1.2 - Fluids and Porous Medium 51

Oil 51

Carbon Dioxide Gas 51

Brine 51

Porous Medium 51
5.1.3 - Fluid Injection and Production System 53
Gas Injection 53
Oil Injection 53
Brine Injection 53
Fluid Production 53
5.1.4 - Data Acquisition System 53
5.2 - Experimental Procedures 54
5.2.1 - Packing 54
Linear Model 54
Two-Dimensional Model 54
5.2.2 - Pore Volume Determination 55
Linear Model 55
Two-Dimensional Model 55
5.2.3 - Permeability Determination 57
5.2.4 - Oil Saturation 57
5.2.5 - WAG Process, Post Waterflood, and Blowdown 58
5.2.6 - Data Processing 59
5.3 - Diffusivity Experiments 60
5.3.1 - Mathematical Analysis 60
5.3.2 - Experimental Measurement 62
6 - Discussion of Experimental Results 66
I - Diffusivity of Carbon Dioxide and Methane 66
6.1 - Effect of Pressure 66
6.2 - Effect of Increasing Temperature 72
6.3 - Effect of Oil Viscosity 72
6.4 - Effect of Oil Molecular Weight 75
6.5 - Diffusivity of Methane 75
6.6 - Correlations of the Diffusion Coefficients 77
II - Displacement Experiments 79

6.7 - Correlation of Displacement Results 89
6.7.1 - Single Slug and WAG Correlations 89
6.7.2 - WAG Ratio Correlations 91
6.7.3 - Total Carbon Dioxide Slug Size Correlations 93
II.1 - Isothermal Displacement Experiments 99
6.8 - Carbonated Waterflood 99
6.8.1 - Carbonated Waterflood vs. Immiscible WAG flood 99
6.8.2 - Effect of Carbon Dioxide Requirement 104
6.9 - Gravity Segregation 108
A - Linear Corefloods 108
6.9.1 - Vertical WAG Injection 108
6.9.2 - Continuous Carbon Dioxide Injection 113
6.9.3 - Effect of Pressure on Gravity Rise of Carbon Dioxide 116
6.9.4 - Effect of Gas Injection Rate 122
6.9.5 - Effect of Inverting the Core 124
B - Two-Dimensional Floods 126
6.9.6 - Effect of Rate 126
6.9.10 - Effect of Time 135
6.9.11 - Gravity vs. Transverse Diffusion 138
II.2 - Non-Isothermal Experiments 139
6.10 - Unscaled Experiments 139
6.10.1 - Effect of Temperature 139
6.10.2 - Effect of Oil Viscosity 141
6.10.3 - Effect of Carbon Dioxide Solubility 144
6.10.4 - Effect of Slug Size 147
6.11 - Scaled Experiments 150
6.11.1 - Experimental Design 150
6.11.2 - Discussion of The Results of The Scaled Experiments 155
6.12 - Reproducibility of the Experimental Results 158
7 - Summary and Conclusions 164

8 - Recommendations for Future Research 167
References 168
Appendix A - Initial and Boundary Conditions 179
Appendix B - Differential Equations in Dimensionless Form 181
Appendix C - Derivation of the Relaxed Scaling Groups 199
Appendix D - Tabulated Data of Diffusivity Experiments in Graphical Form 202
Appendix E - Tabulated Results of Displacement Experiments 222
Appendix F - Production Histories of All Experiments Conducted 330
Appendix G - Viscosity-Temperature Relationship for Different Oils 389

LIST OF TABLES

Table Caption Page

4.1 - Constitutive Relationships and Constraints 34
4.2 - Similarity Groups From Inspectional Analysis. 40
5.1 - Field Information 52
6.1 - Diffusivity of Carbon Dioxide 67
6.2 - Diffusivity of Methane. 69
6.3 - Summary of Previous Immiscible CO_2 Displacement Experiments. 80
6.4 - Summary of Carbonated Waterflood Experiments. 82
6.5 - Summary of Vertical Displacement Experiments in a Linear Model 83
6.6 - Summary of Horizontal WAG Displacement Experiments in a Quarter of a 5-Spot System 84
6.7 - Summary of Vertical Displacement Experiments in a Two-Dimensional Model 86
6.8 - Summary of Non-Isothermal Horizontal Displacement Experiments in a Scaled Model 87
E1 - Tabulated Results of Run CWF1 223
E2 - Tabulated Results of Run CWF2 224
E3 - Tabulated Results of Run CWF3 225
E4 - Tabulated Results of Run CWF4 226
E5 - Tabulated Results of Run VLC1 227
E6 - Tabulated Results of Run VLC2 229
E7 - Tabulated Results of Run VLC3 231
E8 - Tabulated Results of Run VLC4 232
E9 - Tabulated Results of Run VLC5 233
E10 - Tabulated Results of Run VLC6 234
E11 - Tabulated Results of Run VLC7 236
E12 - Tabulated Results of Run VLC8 237

E13 - Tabulated Results of Run VLC9 238
E14 - Tabulated Results of Run VLC10 239
E15 - Tabulated Results of Run VLC11 240
E16 - Tabulated Results of Run H2D1 241
E17 - Tabulated Results of Run H2D2 243
E18 - Tabulated Results of Run H2D3 245
E19 - Tabulated Results of Run H2D4 247
E20 - Tabulated Results of Run H2D5 249
E21 - Tabulated Results of Run H2D6 251
E22 - Tabulated Results of Run H2D7 253
E23 - Tabulated Results of Run H2D8 255
E24 - Tabulated Results of Run H2D9 257
E25 - Tabulated Results of Run H2D10 259
E26 - Tabulated Results of Run H2D11 261
E27 - Tabulated Results of Run H2D12 263
E28 - Tabulated Results of Run H2D13 265
E29 - Tabulated Results of Run H2D14 267
E30 - Tabulated Results of Run H2D15 269
E31 - Tabulated Results of Run H2D16 271
E32 - Tabulated Results of Run H2D17 273
E33 - Tabulated Results of Run H2D18 275
E34 - Tabulated Results of Run H2D19 277
E35 - Tabulated Results of Run H2D20 279
E36 - Tabulated Results of Run H2D21 281
E37 - Tabulated Results of Run H2D22 283
E38 - Tabulated Results of Run H2D23 285
E39 - Tabulated Results of Run H2D24 287
E40 - Tabulated Results of Run H2D25 289
E41 - Tabulated Results of Run H2D26 291
E42 - Tabulated Results of Run H2D27 293

E43 - Tabulated Results of Run H2D28 295
E44 - Tabulated Results of Run H2D29 297
E45 - Tabulated Results of Run H2D30 299
E46 - Tabulated Results of Run H2D31 301
E47 - Tabulated Results of Run H2D32 303
E48 - Tabulated Results of Run H2D33 305
E49 - Tabulated Results of Run H2D34 307
E50 - Tabulated Results of Run H2D35 308
E51 - Tabulated Results of Run H2D36 309
E52 - Tabulated Results of Run H2D37 310
E53 - Tabulated Results of Run V2D1 311
E54 - Tabulated Results of Run V2D2 312
E55 - Tabulated Results of Run H2D38 313
E56 - Tabulated Results of Run H2D39 315
E57 - Tabulated Results of Run H2D40 317
E58 - Tabulated Results of Run H2D41 319
E59 - Tabulated Results of Run H2D42a 321
E60 - Tabulated Results of Run H2D42b 322
E61 - Tabulated Results of Run H2D43a 324
E62 - Tabulated Results of Run H2D43b 325
E63 - Tabulated Results of Run H2D44a 327
E64 - Tabulated Results of Run H2D44b 328

LIST OF FIGURES

Figure Caption Page

5.1 - Schematic of the Experimental Apparatus 48
5.2 - Schematic of the Linear Model 49
5.3 - Cross sections of the Two-Dimensional Model. 50
5.4 - Two-Dimensional Model Fraction of Brine in Solution 56
5.5 - Two-Dimensional Model Pore Volume Determination 56
5.6 - Schematic of the Diffusion Cell 63
5.7 - Mass of CO_2 Injected into the Diffusion Cell vs. Square Root of Time. 65
6.1 - Diffusivities of Gaseous and Liquid CO_2 70
6.2 - Diffusivity of CO_2 in an 1842 mPa.s Oil as a Function of Pressure. 71
6.3 - Diffusivity of CO_2 in a 3607 mPa.s Oil as a Function of Pressure. 71
6.4 - Diffusivity of CO_2 in an 1842 mPa.s Oil as a Function of Temperature. 73
6.5 - Diffusivity of CO_2 in a 3607 mPa.s Oil as a Function of Temperature. 73
6.6 - Diffusivity of CO_2 as a Function of Oil Viscosity. 74
6.7 - Diffusivity of CO_2 as a Function of Oil Molecular Weight. 74
6.8 - Diffusivity of Methane in an 1842 mPa.s Oil. 76
6.9 - Comparison of Correlated and Measured Values for CO_2 Diffusivity in an 1842 mPa.s Oil. 78
6.10 - Comparison of Correlated and Measured Values for CO_2 Diffusivity in a 3607 mPa.s Oil. 78
6.11 - Map of Experiments Conducted in This Research 88
6.12 - Gas-Oil Ratio Correlations for Single CO_2 Slug Injection and WAG Injection. 90
6.13 - WAG Ratio Correlation 92
6.14 - Total CO_2 Slug Size Correlation 92

6.15 - Recovery-Slug Volume Correlation 94
6.16 - Total Slug Size Correlation for Low Pressure Operations 94
6.17 - Recovery-Slug Volume Correlation for Low Pressure Operations 96
6.18 - Total Slug Volume Correlation for Linear Coreflood 97
6.19 - Recovery-Slug Volume Correlation for Linear Coreflood 97
6.20 - Production History of Run CWF1 100
6.21 - Comparison of the GOR's of Runs CWF1 and LC31 102
6.22 - Comparison of Recoveries of Runs CWF1, LC31 and LC34 103
6.23 - Production History of Run CWF2 105
6.24 - Comparison of GOR's and WOR's of Runs CWF2 and GTD6 106
6.25 - Comparison of Recoveries of Runs CWF2, GTD6 and 21a 107
6.26 - Producing Gas-Oil Ratios of Runs VLC1, VLC2 and GTD6 109
6.27 - Producing Water-Oil Ratios of Runs VLC1, VLC2 and GTD6 111
6.28 - Comparison of Recoveries of Runs VLC1, VLC2 and GTD6 112
6.29 - Comparison of the Producing GOR's of Runs VLC3 and VLC5 114
6.30 - Comparison of the Oil Recoveries of Runs VLC3 and VLC5 115
6.31 - Comparison of the Producing WOR's of Runs VLC3 and VLC5 117
6.32 - Performance of Run VLC5 118
6.33 - Performance of Run VLC3 119
6.34 - Production History of Run VLC6 120
6.35 - Effect of Pressure on Gravity Rise of CO_2 Gas 121
6.36 - Effect of Gravity on Injection Rate 123
6.37 - Effect of Gravity on Volume of Oil Displaced 125
6.38 - Effect of Inverting the Model 127
6.39 - Oil Recovery vs. Ratio of Viscous-to-Gravitational Forces 129
6.40 - Oil Recovery vs. Ratio of Viscous-to-Gravitational Forces for Field Operations 130
6.41 - Oil Recovery vs. Ratio of Viscous-to-Gravitational Forces at 1.0 MPa 131
6.42 - Effect of Rate 133

6.43 - Oil Recovery vs. Ratio of Viscous-to-Gravitational Forces for Different CO_2 Injection Rates 134
6.44 - Effect of Time on Gravity Rise of CO_2 Gas 136
6.45 - Effect of Soak Time on Gas Breakthrough 137
6.46 - Production History of Run H2D38 140
6.47 - Comparison of GOR's of Runs H2D8 and H2D38 142
6.48 - Comparison of Oil Recoveries of Runs H2D8 and H2D38 143
6.49 - Comparison of GOR's of Runs H2D8 and H2D39 145
6.50 - Oil Recovery Comparison of Runs H2D8 and H2D39 146
6.51 - Effect of Similar CO_2 Solubility at Two Different Pressure and Temperature Conditions 148
6.52 - Comparison of Oil Recoveries of Runs H2D8 and H2D40 149
6.53 - Effect of Slug size on GOR's at Non-Isothermal Conditions 151
6.54 - Effect of Slug Size on Oil Recovery at Non-Isothermal Conditions 152
6.55 - GOR's of Run H2D42b vs. Those of Run H2D43b 156
6.56 - Recovery of Run H2D42b vs. That of Run H2D43b 157
6.57 - GOR Repeatability of Run CWF1. 159
6.58 - Recovery Repeatability of Run CWF1. 159
6.59 - GOR Repeatability of Run CWF2. 160
6.60 - Recovery Repeatability of Run CWF2. 160
6.61 - GOR Repeatability of Run VLC3. 161
6.62 - Recovery Repeatability of Run VLC3. 161
6.63 - GOR Repeatability of Run VLC7. 162
6.64 - Recovery Repeatability of Run VLC7. 162
6.65 - GOR Repeatability of Run H2D43b. 163
6.66 - Recovery Repeatability of Run H2D43b. 163
D1 - Mass of Gas Injected vs. Square Root of Time for Diffusion Experiments No. 1, 2, 3, and 4. 203
D2 - Mass of Gas Injected vs. Square Root of Time for Diffusion

Experiments No. 5, 6, 7, and 8. 204
D3 - Mass of Gas Injected vs. Square Root of Time for Diffusivity
Experiments No. 9, 10, 11, and 12. 205
D4 - Mass of Gas Injected vs. Square Root of Time for Diffusivity
Experiments No. 13, 14, 15, and 16. 206
D5 - Mass of Gas Injected vs. Square Root of Time for Diffusivity
Experiments No. 17, 18, 19, and 20. 207
D6 - Mass of Gas Injected vs. Square Root of Time for Diffusivity
Experiments No. 21, 22, 23, and 24. 208
D7 - Mass of Gas Injected vs. Square Root of Time for Diffusivity
Experiments No. 25, 26, 27, and 28. 209
D8 - Mass of Gas Injected vs. Square Root of Time for Diffusivity
Experiments No. 29, 30, 31, and 32. 210
D9 - Mass of Gas Injected vs. Square Root of Time for Diffusivity
Experiments No. 33, 34, 35, and 36. 211
D10 - Mass of Gas Injected vs. Square Root of Time for Diffusivity
Experiments No. 37, 38, 39, and 40. 212
D11 - Mass of Gas Injected vs. Square Root of Time for Diffusivity
Experiments No. 41, 42, 43, and 44. 213
D12 - Mass of Gas Injected vs. Square Root of Time for Diffusivity
Experiments No. 45, 46, 47, and 48. 214
D13 - Mass of Gas Injected vs. Square Root of Time for Diffusivity
Experiments No. 49, 50, 51, and 52. 215
D14 - Mass of Gas Injected vs. Square Root of Time for Diffusivity
Experiments No. 53, 54, 55, and 56. 216
D15 - Mass of Gas Injected vs. Square Root of Time for Diffusivity
Experiments No. 57, 58, 59, and 60. 217
D16 - Mass of Gas Injected vs. Square Root of Time for Diffusivity
Experiments No. 61, 62, 63, and 64. 218
D17 - Mass of Gas Injected vs. Square Root of Time for Diffusivity

Experiments No. 65, 66, 67, and 68. 219
D18 - Mass of Gas Injected vs. Square Root of Time for Diffusivity Experiments No. 69, 70, 71, and 72. 220
D19 - Mass of Gas Injected vs. Square Root of Time for Diffusivity Experiments No. 73, 74, 75, and 76. 221
F1 - Productin History of Run CWF3. 331
F2 - Productin History of Run CWF4. 332
F3 - Productin History of Run VLC1. 333
F4 - Productin History of Run VLC2. 334
F5 - Productin History of Run VLC3. 335
F6 - Productin History of Run VLC4. 336
F7 - Production History of Run VLC5. 337
F8 - Production History of Run VLC7. 338
F9 - Production History of Run VLC8. 339
F10 - Production History of Run VLC9. 340
F11 - Production History of Run VLC10. 341
F12 - Production History of Run VLC11. 342
F13 - Production History of Run H2D1. 343
F14 - Production History of Run H2D2. 344
F15 - Production History of Run H2D3. 345
F16 - Production History of Run H2D4. 346
F17 - Production History of Run H2D5. 347
F18 - Production History of Run H2D6. 348
F19 - Production History of Run H2D7. 349
F20 - Production History of Run H2D8. 350
F21 - Production History of Run H2D9. 351
F22 - Production History of Run H2D10. 352
F23 - Production History of Run H2D11. 353
F24 - Production History of Run H2D12. 354
F25 - Production History of Run H2D13. 355

F26 - Production History of Run H2D14. 356
F27 - Production History of Run H2D15. 357
F28 - Production History of Run H2D16. 358
F29 - Production History of Run H2D17. 359
F30 - Production History of Run H2D18. 360
F31 - Production History of Run H2D19. 361
F32 - Production History of Run H2D20. 362
F33 - Production History of Run H2D21. 363
F34 - Production History of Run H2D22. 364
F35 - Production History of Run H2D23. 365
F36 - Production History of Run H2D24. 366
F37 - Production History of Run H2D25. 367
F38 - Production History of Run H2D26. 368
F39 - Production History of Run H2D27. 369
F40 - Production History of Run H2D28. 370
F41 - Production History of Run H2D29. 371
F42 - Production History of Run H2D30. 372
F43 - Production History of Run H2D31. 373
F44 - Production History of Run H2D32. 374
F45 - Production History of Run H2D33. 375
F46 - Production History of Run H2D34. 376
F47 - Production History of Run H2D35. 377
F48 - Production History of Run H2D36. 378
F49 - Production History of Run H2D37. 379
F50 - Production History of Run H2D39. 380
F51 - Production History of Run H2D40. 381
F52 - Production History of Run H2D41. 382
F53a - Production History of Run H2D42a. 383
F53b - Production History of Run H2D42b. 384
F54a - Production History of Run H2D43a. 385

F54b - Production History of Run H2D43b. 386
F55a - Production History of Run H2D44a. 387
F55b - Production History of Run H2D44b. 388
G1 - Viscosity-Temperature Relationship for Battrum South Oil No.1. 390
G2 - Viscosity-Temperature Relationship for Battrum South Oil No.2. 391
G3 - Viscosity-Temperature Relationship for Kla-Da-Ing Oil. 392
G4 - Viscosity-Temperature Relationship for Della-Bell Oil. 393
G5 - Viscosity-Temperature Relationship for Epping Oil. 394
G6 - Viscosity-Temperature Relation ship for Senlac Oil. 395
G7 - Viscosity-Temperature Relationship for South Aberfeldy Oil No.1. 396
G8 - Viscosity-Temperature Relationship for South Aberfeldy Oil No.2. 397

NOMENCLATURE

A	area open for flow in an injection or production well, m^2
a	scaling factor
a_{jl}	interfacial area between phase j and l, m^2
$C_{i,j}$	concentration of the i component in the j phase, mass fraction
$\mathcal{D}^*$	molecular diffusion coefficient, m^2/s
$\mathcal{D}_L$	longitudinal hydrodynamic dispersion coefficient, m^2/s
$\mathcal{D}_T$	transverse hydrodynamic dispersion coefficient, m^2/s
$\overline{\overline{\mathcal{D}}}_j$	convective dispersion tensor of the j phase, m^2/s
$\overline{\overline{\mathcal{D}}}^*_{ij}$	molecular diffusion tensor of the i component in the j phase, m^2/s
$\overline{\overline{\mathcal{D}}}_{ij}$	hydrodynamic dispersion tensor of the i component in the j phase, m^2/s
$\mathcal{E}_j$	rate of total energy of the j phase injected at the injection well, kJ/s
F	formation electrical resistivity factor
F_{jB}	buoyancy force exerted on the j phase per unit volume, N/m^3
F_{jD}	drag force exerted on the j phase per unit volume, N/m^3
f_{ij}	fugacity of the i component in the j phase, kPa
g	gravitational acceleration, m/s^2
H	height or thickness of the reservoir or model, m
h_j	enthalpy of the j phase per unit mass, kJ/kg
k_i^{jl}	local mass transfer coefficient of the i component in the j phase related to the jl interface, $(m^2\text{-}s)^{-1}$
$\overline{\overline{k}}_j$	effective permeability tensor of the j phase, m^2
k_{rj}	relative permeability of the j phase, dimensionless
k_{hj}	thermal conductivity of the j phase, kW/m-K
k	absolute permeability, m^2
K	Boltzmann's constant (1.38E-23 J/K)
L	length of the reservoir or model, m
$\mathcal{M}_j$	rate of momentum of the j phase at the injection well, $kg\text{-}m/s^2$
$\dot{m}$	rate of water evaporation or condensation per unit volume, $kg/m^3\text{-}s$
$\mathcal{N}_{ijl}$	mass transfer rate of the i component in or out the j phase through jl interface per unit volume, $kg/m^3\text{-}s$
P_c	capillary pressure, kPa

p_j	pressure of the j phase, kPa
Q	volumetric injection rate, m^3/s
R	radius of molecule, cm
S_j	saturation of the j phase, fraction
$\mathfrak{s}_j$	entropy of the j phase per unit mass per absolute temperature, kJ/kg-K; or rate of entropy created at the injection well, kJ/s-K
T	temperature, °C or K
t	time, day or second
U_j	internal energy of the j phase per unit mass, kJ/kg
$\overline{\vartheta}_j$	superficial velocity vector of the j phase, m/s
ϑ_j	superficial velocity of the j phase, m/s
V	total volume of fluid injected, fraction
$V^*_{CO_2}$	slug volume of carbon dioxide, fraction
V^*_w	slug volume of water, fraction
W	width of the reservoir or model, m
$\mathcal{W}_i$	mass injection rate of the i component, kg/s
x,y,z	cartesian coordinates

Greek Symbols

ϕ	porosity, fraction
ρ_j	density of the j phase, kJ/kg
τ_j	shear stress of the j phase, N/m^2
η_{ij}	chemical potential of the i component in the j phase, kJ/kg
μ_j	dynamic viscosity of the j phase, mPa.s
σ_{jl}	interfacial tension between the j and l phases, kg/s^2

Subscripts

A	solute
B	solvent
D	dimensionless quantity
g	gas phase
CO_2,g	CO_2 component in the gas phase
CO_2,o	CO_2 component in the oil phase
CO_2,w	CO_2 component in the water phase

inj	located at the injection well
ℓ	liquid
M	model
o	oil phase
o,o	oil component in the oil phase
P	prototype
prod	located at the production well
R	reference quantity
r	rock matrix
v	vapour
w	water
w,w	water component in the water phase
x	x-direction
y	y-direction
z	z-direction

Superscripts

I	located at the interface
Ijl	located at the interface between the j and l phases

Abbreviations

Abs.	absolute
BD	blowdown
BT	breakthrough
d	darcy
GOR	gas-oil ratio
HCPV	hydrocarbon pore volume
Inj.	injected
LC	linear core
MW_o	oil molecular weight
Rec.	recovery
TD	two-dimensional
Vel.	velocity
Vis.	viscosity

WAG	water-alternating-gas
WF	waterflood
WOR	water-oil-ratio

INTRODUCTION

The immiscible carbon dioxide WAG (Water-Alternating-Gas) process holds promise for the recovery of moderately viscous heavy oils from thin (less than 10 m) and/or deep (greater than 1000 m) formations where thermal recovery methods are ineffective due to high heat loss and other limitations.

Many studies have been conducted to date to examine the effectiveness of the process, as well as its mechanism. Laboratory studies on the application of the process to the recovery of oil from thin and deep reservoirs showed that a substantial volume of oil, about 10 to 30% incremental oil compared to a waterflood, can be recovered by this process[1-8]. Field studies and projects conducted in the United States have produced good results[9,10]. In Alberta, the effectiveness of this process was demonstrated by the commercial immiscible carbon dioxide project in Retlaw, started in January 1991. Within six months after production began, the cumulative oil production exceeded 120,000 sm^3.[11]

The basic idea of this recovery process is to alternately inject small slugs of carbon dioxide and water. When carbon dioxide is injected into a reservoir, it will dissolve in the oil, causing swelling of the oil and lowering of the oil viscosity. Following this, water is injected to displace the carbon dioxide-swollen oil. The reason slugs of carbon dioxide and water are alternatively injected is to control the mobility of the gas phase. Carbon dioxide gas is preferred in this process because it has a very high solubility in oil, compared to other gases such as methane, propane, ethane, and nitrogen. In order to make the process more effective, carbon dioxide must be injected as gas rather than liquid because liquid carbon dioxide may only be sparingly soluble in oil.

Even though the process is quite successful in recovering moderately viscous heavy oils from thin and deep reservoirs, there are still a few problems associated with it. Two of the few problems existing in the process, which are also the focus of this current study, are non-equilibrium phenomena and gravity segregation of the injected carbon dioxide gas. The non-equilibrium phenomena arise because the concentration of carbon dioxide near or around the injection well is higher than that away from or near the production well. Consequently, mass transfer has to take place to even out the carbon dioxide concentration. One of the well known mass transfer processes is diffusion which occurs when a system is out of equilibrium. Diffusion is the mass transport process which involves the movement of molecules from one point to another and is known to play an important role in the immiscible carbon dioxide WAG process. Therefore, one of the objectives of this research is to measure the diffusivity of carbon dioxide in different heavy oils at various pressures and temperatures. A second objective is to develop a mathematical model which includes the non-equilibrium phenomena.

As mentioned above, because carbon dioxide is injected as gas rather than as liquid, its density is much lower than that of the reservoir oil. The density difference between the injected carbon dioxide and the reservoir oil results in segregation of the injected carbon dioxide, causing carbon dioxide to rise to the top of the reservoir and then to finger through the oil. Furthermore, the solution of carbon dioxide in oil increases the oil density, making the density difference worse.

Studies conducted to-date have been focussed on investigating gravity segregation in miscible gas displacements; none has been conducted to investigate the same phenomenon in immiscible gas displacements. Thus, there is a need to study gravity segregation in the immiscible carbon dioxide displacement process.

STATEMENT OF THE PROBLEM

Gravity segregation of the injected fluids and non-equilibrium phenomenon may have detrimental effects on the performance of the immiscible carbon dioxide WAG process. In this study, the effects of gravity segregation and non-equilibrium phenomena in the immiscible carbon dioxide WAG flooding process are to be investigated. The main objectives of this study can be summarized as follows:

1. To study the diffusivity of carbon dioxide into oil at various pressures and temperatures.

2. To design a mathematical model for the non-equilibrium and non-isothermal immiscible carbon dioxide WAG process, which is used to derive scaling groups.

3. To correlate the experimental results using the scaling groups derived in this study.

4. To investigate the effect of gravity segregation on the immiscible carbon dioxide WAG process and to determine whether gravity segregation increases or decreases the efficiency of the process, thus observing how it affects oil recovery from thin reservoirs.

REVIEW OF THE LITERATURE

The idea of using carbon dioxide as an enhanced oil recovery agent is not new. As early as in the 1950's, Martin[12-14] conducted the first study on the possibility of flooding an oil reservoir with carbonated water rather than with plain water. He found that carbon dioxide has a strong tendency to improve the mobility of the oil by lowering the viscosity of the oil after it dissolved in the oil. Following the pioneering work of Martin, other investigators[15-22] also recognized that viscosity reduction due to the solution of carbon dioxide in oil led to improved sweep efficiency, thus increasing oil recovery. Holm and Josendal[23] experimentally investigated the miscible displacement of a very light oil by carbon dioxide and discovered that using carbon dioxide to displace oil under miscible conditions could recover up to 95% of the in-place oil. However, at that time, due to relatively high primary oil production and the very high cost of carbon dioxide compared to the price of oil, the use of carbon dioxide in enhanced oil recovery was not attractive to most oil producers. Today, due to low primary oil production, high oil demands, and plentiful sources of carbon dioxide available at relatively low prices around the globe, there is an increasing emphasis on using carbon dioxide as an enhanced oil recovery agent.

The objective of this chapter is to provide a review of past work, to study the displacement of oil by carbon dioxide, and its relationship to the current study, which was directed towards an investigation of the immiscible displacement of moderately heavy oils by carbon dioxide and water.

3.1 - Diffusivity of Carbon Dioxide into Oil at Reservoir Conditions

In the immiscible carbon dioxide process, the four mechanisms contributing to oil recovery, according to Rojas and Farouq Ali's findings[24], are oil swelling, viscosity reduction, interfacial tension reduction leading to the formation of water-in-oil emulsions, and solution gas drive resulting from blowdown at the end of the displacement. The so-called oil swelling occurs when carbon dioxide dissolves in oil. There are two mass transfer processes which take place when carbon dioxide dissolves in oil: solution and diffusion. It is known that solution is a fast process whereas diffusion is a slow process.

In the current research, only the diffusion process is studied. Hence, the next section provides a review of the work done by other researchers on the diffusivity of a gas phase in a liquid phase.

3.1.1 - Measurement of Diffusion Coefficient

As mentioned in the above paragraph, diffusion is another means of mass transfer between carbon dioxide and oil, besides solution. It involves the movement of molecules from one point to another due to concentration, temperature, and pressure gradients; and it is independent of any convective forces in the system. It can also be defined as dispersion at the molecular level. Dispersion is the mixing of fluids which occurs when one fluid displaces another.

According to Grogan and Pinczewski[25], molecular diffusion plays an important role in the recovery of residual oil at the pore level since it is an important rate controlling mechanism in a carbon dioxide flood. Several authors[24-27] have pointed out the advantages of diffusion. It helps carbon dioxide to penetrate oil, inhibit viscous fingering, delay gas breakthrough and increase the oil rate.

Since 1933, efforts have been made by several investigators to measure experimentally molecular diffusion coefficients at elevated pressure and temperature conditions. Pomeroy, Lacey, Scudder, and Stapp[28] were the first to design an unsteady-state method which allowed the determination of diffusion constants at pressure up to 3 MPa. The method was based on Fick's second law of diffusion. They reported values in the range of 5×10^{-9} to 14×10^{-9} m^2/s for the diffusivity of methane in isopentane for pressures in the range of 0 to 2 MPa and at 30°C. Employing the same experimental apparatus, Hill and Lacey[29] measured the diffusivity of methane in different oils for temperatures in the range of 30°C to 60°C and at 2 MPa. The reported diffusion coefficients are in the range of 3.8×10^{-10} to 1.3×10^{-8} m^2/s. Diffusion was noted to increase with increasing temperature. Hill and Lacey[30] also presented a set of data for the diffusivity of propane in liquid hydrocarbons for pressures in the range of 0.2 to 1.4 MPa and temperatures from 30 to 60°C. They reported values in the range of 1.7×10^{-9} to 6.3×10^{-9} m^2/s. The diffusivity of propane was found to increase with increasing temperature and pressure. Other investigators[31-35] have also reported values for the diffusivity of methane and propane in various liquid hydrocarbons over various pressure and temperature ranges.

There have been many measurements of the diffusivity of methane in hydrocarbon solvents at elevated temperatures and pressures, but very few for the diffusivity of carbon dioxide. The only measurements reported are those of Schmidt, Leshchyshyn, and Puttagunta[36]; Denoyelle and Bardon[37]; de Boer, Wellington and Tschiedel[38]; Renner[39]; and Grogan, Pinczewski, Ruskauff, and Orr[40]. Schmidt et al.[36] performed the first work on determining the diffusivity in reservoir fluids at reservoir conditions. They measured the diffusivity of carbon dioxide in a 362,000 mPa.s bitumen at 5 MPa and temperatures ranging from 20 to 200°C. Their results demonstrated that the diffusivity of carbon dioxide in bitumen increased with increasing temperature. Denoyelle and Bardon[37] reported that the diffusivities of carbon dioxide in oil at reservoir conditions were about 5 to 10 times higher than those measured at atmospheric conditions. They concluded that the diffusivity coefficients at atmospheric conditions could not be used to estimate those at reservoir conditions. de Boer et al.[38] studied the diffusivity of carbon dioxide through an interface (water layer) into an oil droplet. Their observations are at variance with the work of Denoyelle and Bardon[37]. They observed that the diffusion rates of carbon dioxide in crude oil at elevated pressures were consistent with calculated rates based on diffusion coefficients measured at atmospheric conditions, provided that there was no precipitation of asphaltenes. They also observed that the precipitation of asphaltenes at the oil-water interface formed a highly resistive layer which retarded carbon dioxide mass transfer.

Employing the method of Reamer et al.[32], Renner[39] measured the diffusivity of carbon dioxide in decane and brine in consolidated porous media at pressures from 0.9 to 5.8 MPa and at 38°C. In this experimental study, he noted that the diffusivity of carbon dioxide increased with increasing pressure when the core was placed in the horizontal position and was independent of pressure when the core was in the vertical position. Grogan et al.[40] performed their measurements for carbon dioxide diffusion in pentane, decane and hexadecane. The reported data indicated that the diffusion coefficient decreased with increasing solvent molecular weight and increased with increasing carbon dioxide concentration. Furthermore, they also concluded that correlations for the diffusivity of carbon dioxide in hydrocarbon solvents in terms of solvent viscosity, developed from measurements at atmospheric pressure, provide realistic estimates for the diffusion coefficient at reservoir conditions. This is opposite to Denoyelle and Bardon's conclusion[37].

3.1.2 - Correlations of Diffusion Coefficients

In addition to experimentally determining the diffusion coefficient, efforts have been made to propose correlations for estimating the diffusivity of carbon dioxide. The first effort was made by McManamey and Wollen[41], who presented an empirical correlation for the diffusivity of carbon dioxide in organic liquids as a function of solvent viscosity only. This correlation was later shown by Denoyelle and Bardon[37] to give poor estimates of carbon dioxide diffusivity at pressures higher than atmospheric pressure. By fitting the data reported by Schmidt et al.[36] to the Nernst-Einstein equation (which is $\dot{\mathfrak{D}}_{AB} = \frac{KT}{6\pi R_A \mu_B}$), Schmidt[42] presented an empirical correlation for the diffusivity of carbon dioxide in bitumen as a function of viscosity and temperature. Renner[39] also correlated his data and others' to come up with a correlation for predicting the diffusivity of carbon dioxide, methane, ethane, and propane in liquid hydrocarbons. His correlation showed that increasing pressure decreased the diffusivity of a gas phase in oils. Mehrotra, Garg, and Svrcek[43] used Schmidt et al.'s data[36] to evaluate several correlations. They found that Umesi-Danner's correlation, together with the use of the corresponding states theory of Teja[44], could be used to predict the diffusivity of carbon dioxide in bitumen at reservoir conditions. The disadvantage of using this technique for field applications is that Teja's method is complicated; that is, it requires too many calculations and thermodynamics data.

3.2 - Carbonated Water Injection

The carbonated water injection process is quite different from the WAG injection process. Water is saturated with carbon dioxide at the surface before being injected into the reservoir. This process was first studied by

Martin[12-14] and Saxon, Breston, and Macfarlane[45] in the early 50's, and re-investigated by Holm[20] and de Nevers[21,46] in the 60's. Based on the results gathered, Saxon et al.[45] concluded that a carbonated waterflood would not reduce the oil saturation any further than a waterflood. Holm[23] reported higher carbon dioxide requirements and lower recoveries for a carbonated waterflood, as compared to a carbon dioxide slug flood.

In the 50's and 60's this oil recovery technology was tried in oilfields in New York and Oklahoma[46-48]. After more than a year of operation, no significant oil was recovered. It was tried again in Texas by Amoco in 1987. After only 7.5 months, injection was terminated because of extensive corrosion and plugging problems. There was no mention of any incremental recovery[49].

Perez, Poston, and Sharif[50] studied carbonated water imbibition in core plugs at various pressure and temperature conditions. They concluded that this method may hold promise for increasing oil production rates from fractured, low matrix permeability, and low gas-oil ratio oil reservoirs.

3.3 - Gravity Segregation

According to Morrow and Hornof[51], gravity segregation occurs when capillary and viscous forces are insufficient to overcome the effect of buoyancy forces. The first laboratory study of gravity segregation performed by Craig, Sanderlin, Moore, and Geffen[52] in 1957, showed that in linear gas or water injection operations in horizontal formations, segregation of the fluids due to the gravity effect could result in oil recoveries to breakthrough as low as 20% of those otherwise expected and that, in 5-spot injection operations in such formations, the oil recoveries at breakthrough could be as low as 40% of those predicted by methods which assume negligible gravity effects. Their results also indicated that the magnitude of segregation of the fluids due to gravity was influenced by the average injection rate rather than temporal variations.

Richardson and Perkins[53] studied experimentally the effect of rate on oil recovery by waterflooding. They concluded that decreasing the rate at which water is injected into a thick, homogeneous reservoir sand increases the tendency of the water to underrun the oil. Miller[54] also observed that water underran the oil in his study.

Blackwell, Terry, Rayne, Lindley, and Henderson[55] reported an investigation of the efficiency of water-solvent mixtures for oil recovery. They observed that, while flowing through sands the water and gas segregated into a gas layer on the top and a water layer at the bottom and that gas occupied a much smaller fraction of the vertical cross section than water. As a result, only the thin top layer was miscibly flooded by gas, whereas the bottom portion was waterflooded. This phenomenon was also observed by other investigators[54,56-57].

Stalkup[58] hypothesized that injection of solvent with low viscosity into a vertical cross section that contained oil more dense than the solvent led to the formation of a gravity tongue if the flow velocity was low enough so that vertical transport by gravity segregation dominated the viscous forces that induce instability. As the flow velocity increased, gravity forces played a diminishing role, and eventually viscous forces dominated.

Van der Poel[59], Miller[54], and Warner[56] studied miscible displacements in horizontal reservoirs. They all observed that when oil was displaced from a horizontal reservoir by a solvent of lower density, the latter tended to override the former in the shape of a tongue owing to gravity segregation. Fayers and Newley[57] noted that the tendency for solvent to rise became more pronounced when the flow rate was reduced. Miller[54] observed that the gravity override tongue pushed the reservoir oil down into the center of the reservoir which was then slowly displaced immiscibly by the water injected along with the gas. Based on this observation, he concluded that, in field operations, when the economic limit is reached, a substantial amount of the oil displaced by the miscible fluid early in the reservoir life is left unswept at abandonment.

According to Miller[54], there are two important mechanisms causing the formation of an overriding gravity tongue. They are the density difference between the two miscible fluids, which causes the injected lighter fluid to override the in-place fluid, and the vertical counterflow segregation resulting from a density difference between two immiscible fluids which results in the migration of the lighter hydrocarbon fluid to the top of the reservoir.

Miller[54] also investigated the effect of reservoir thickness on gravity-controlled displacements. He concluded that if a gravity finger was formed by density difference between two miscible fluids at the interface when a lighter fluid was injected, an increase in reservoir thickness would lead to more overriding because there was a greater gravity potential gradient at the top of the reservoir than at the bottom of the reservoir. However, if the gravity finger was caused by counterflow segregation, then a decrease in reservoir thickness would lead to poorer performance since the fluids would have a shorter distance to travel to segregate. He also suggested that capillary forces could prevent segregation, or at least retard the rate of segregation, in very thin sands.

Spivak[60] investigated gravity segregation in the two-phase displacement process, using a three-dimensional, three-phase and incompressible simulator, and found that gravity segregation increased with increasing permeability (either horizontal or vertical), density difference and viscosity ratio, but decreased with increasing rate and level of viscosity for a fixed viscosity ratio. In contrast to Miller's conclusion[54], Spivak found that gravity segregation in a 6 m thick reservoir could be as severe as in a 60 m thick reservoir. Based upon this finding, he concluded that formation thickness alone did not determine whether gravity segregation would be a problem.

Araktingi and Orr [61] used a simulator to study gravity segregation in miscible displacements in a vertical cross-section. Their study confirmed that, in homogeneous porous media, better displacement performance could be obtained at high viscous-to-gravity force ratios for any mobility ratio. As a result, high recoveries were reported at increasing viscous-to-gravity force ratios.

Thomas, Bergins, Monger and Bassiouni[62] conducted six horizontal cyclic carbon dioxide corefloods to investigate the influence of gravity segregation on oil recovery. They concluded that any effect of gravity segregation on the process was caused mainly during the huff (injection) stage and that gravity override benefited process performance. A few vertical cyclic carbon dioxide corefloods were carried out also. In these experiments, carbon dioxide was injected at the bottom. Gravity segregation was found to promote oil contact by facilitating the deeper penetration of carbon dioxide into the core resulting in improved oil recovery.

Using a compositional simulator to investigate the effect of solvent composition on displacement performance in two-dimensional (x-z) flow where both viscous and gravitational forces cause transverse transport or cross flow of fluids, Pande[63] concluded that the magnitude of the crossflow is affected by the oil-solvent density ratio and that the driving force for gravity crossflow is provided by the difference in fluid densities.

Gravity segregation has not only been studied in horizontal flood experiments, but also in vertical flood experiments. Hill[64], by conducting experiments on the displacement of sugar liquor by water from columns of granular bone of charcoal (sweetening off), came up with a critical velocity expression which predicts the rate above which instabilities can occur and viscous forces can dominate for vertically downward displacements. At rates less than this critical rate, gravity forces dominate and instabilities will not occur. The equation, defined in terms of the viscosities and densities of the two fluids, also accounts for the channelling which sometimes occurs when one fluid follows another along a uniformly packed column.

Using the same idea as did Hill[64], Dumore'[65] developed an analytical model for predicting a gravity stable rate for a miscible displacement which allows mixing between the solvent and oil.

Slobod and Howlett[66] used the critical velocity concept to determine the critical flow velocity for their vertically downward miscible displacement experiments. Their experiments were performed using fluids of various densities and viscosities. The results indicated that gravity segregation could act to shorten the mixing zone developed between the displaced and displacing phases when the displacing material was the less dense phase, and lengthen the mixing zone when the displacing phase was the more dense phase.

Experimental studies performed by Tiffin and Kremesec[67] showed that oil recovery at breakthrough was nearly doubled when carbon dioxide was injected at the top rather than at the bottom in vertical miscible displacement experiments. A comparison of vertical and horizontal displacement experiments was also made in their studies. Downward gravity-assisted displacements, even at velocities much greater than the critical rate, were shown to be more efficient than horizontal carbon dioxide displacements at comparable rates. Fong, Tang, Emanuel, and Sabat[68] recently conducted the same experimental studies as did Tiffin and Kremesec. Their results indicated that, at the same oil recovery, the producing gas-oil ratio of a vertical core flood experiment where gas was injected at the bottom, was twice that of a horizontal displacement.

3.3.1 - Effect of Gravity Segregation on Saturation Distribution

In 1951, Martin[69] performed a theoretical study on gravity segregation problems during two-phase flow in porous media. He concluded that only a short time would be required for an initially uniformly distributed gas saturation to reach a distribution in which most of the gas, which is free to flow, is segregated at the top of the reservoir.

During the course of their experiments, Richardson Perkin[53] observed that the volume of gas concentrated at the top of the sand due to gravity segregation was displaced by oil which in turn was displaced by water.

Walsh and Moon[70] theoretically analyzed the immiscible displacement of oil by water injection in a down dip reservoir. Their results showed that the final oil saturation increased as the gravity number increased. In their study, the water-oil gravity number was defined as $\frac{(\rho_o-\rho_w)kg\sin\alpha}{\mu_o u_T}$, where ρ_o and ρ_w are, respectively, the densities of oil and water; and k, g, μ_o, and u_T are, respectively, the absolute permeability, gravity, oil viscosity, and total velocity.

Hovanessian and Fayers[71] studied gravity effects in linear waterfloods and concluded that the gravitational forces had a pronounced effect on the saturation profiles.

Recently, Pande[63] and Belgrave and Win[72] used a three-phase, three-dimensional black oil simulator to study gas saturation distribution in homogeneous reservoirs at various viscous to gravity force ratios. They showed that, on moving upward from the bottom to the top of the reservoir, the gas saturation increased and decreased on moving outward to the production wells.

Cook[73], analyzing gravity segregation performance during natural depletion, concluded that gas liberated from solution can segregate to the top of sand developments in such a manner that a zone of high gas saturation forms along sand tops and is underlain by a zone of high oil saturation where flowing gas-oil ratios are maintained very low.

3.3.2 - Effect of Segregation on Sweep Efficiency

It is well established[52,60,74-75] that gravity tends to decrease vertical sweep efficiency in horizontal homogeneous reservoirs because of gravity tonguing. Belgrave and Win[72] observed that, for homogeneous reservoirs, vertical sweep efficiency increased with increasing gas injection rates. Recently, Ekrann[76] proposed an analytical model to predict the oil recovery at breakthrough with gravity effects for a waterflooding process, using vertical equilibrium theory. Using his model to generate results, he concluded that, in two-layer horizontal reservoirs, gravity may have a profound effect on the vertical sweep efficiency of a waterflooding process.

Stone[77] hypothesized that it takes some time for gravity segregation to occur; thus, there is a region near the injection well where vertical conformance is good, and the size of this region is determined principally by the injection rate, the vertical permeability, and the density difference between water and gas. Using this hypothesis, he proposed an analytical model to predict the size of this zone and, hence, the vertical sweep efficiency of a WAG flood. In deriving this analytical model, Stone assumed that a mobile gas zone was formed at the top of the reservoir and a mobile water zone at the bottom.

Craig et al.[52] measured vertical sweep at breakthrough in homogeneous and isotropic cross-sectional models. Their experiments showed a reduction in vertical sweep for increasing values of mobility ratio and decreasing viscous-to-gravity forces ratio.

3.3.3 - Effect of Reservoir Heterogeneities

Studies have shown that gravity segregation of the fluids is sensitive to reservoir heterogeneities[60,56-57,72]. A simulation study on gravity segregation on a two-layered reservoir conducted by Spivak[60] showed that gravity effects were diminished when the low-permeability layer was on the bottom and increased when the high-permeability layer was on the bottom. Warner[56] explained that if the high-permeability layer is located on the top of the reservoir, it provides a high-conductivity path to transport the carbon dioxide rapidly to the producer, once carbon dioxide has segregated into this layer .

Spivak[60] and Warner[56] also investigated gravity segregation in randomly heterogeneous reservoirs. Warner[56] reported a nearly doubled oil recovery for the carbon dioxide slug process when random heterogeneity was used in place of homogeneity in his simulation study. They both agreed that the random heterogeneity tended to reduce gravity segregation.

Araktingi and Orr[61] also showed that for injection of a light solvent into a layered reservoir with high permeability low in the reservoir, better displacement efficiency was observed at intermediate values of viscous-to-gravity forces ratio than at high or low values. If the high permeability was at the top, a high value of viscous-to-gravity force ratios was preferred.

3.3.4 - Field Observation of Gravity Segregation

Wilcox, Polzin, Kuo, Saidikowski, and Humphrey[78] noted the overriding of the injected gas in the Prudhoe Bay Miscible Gas Project in Alaska due to high vertical permeability and the large difference in density between the gas and reservoir fluids. The injected gas rose to the top of the reservoir or underneath shales, forming cone-shaped swept intervals around WAG Injectors.

Pritchard and Nieman[79] reported segregation of the injected gas after examining the dynamics of a hydrocarbon miscible flood in the Judy Creek field through the inspection of saturation cross-section between the injector-producer pair. Early in the solvent injection life, the solvent displaced an oil bank from the swept zone out into the reservoir. With further miscible injection, the solvent tended to override the water flowing interval and traveled along the top of the reservoir to the producers. This solvent then displaced oil that resided in the upper portion of the reservoir. As long as injection of the miscible fluid was continued, oil continued to be produced from either within or below the gas flowing zone. When water was injected, the oil bank also migrated upward in the reservoir due primarily to density differences between oil and water. The oil would then move into the previously oil swept gas flowing zone and re-saturate this region back to the residual oil saturation to waterflooding. This oil would become immobile and could not be recovered.

3.4 - Background to Non-Equilibrium Processes

Non-equilibrium thermodynamics, also known as irreversible thermodynamics, considers systems which are not in thermodynamic equilibrium, or which are approaching equilibrium. Historically, its roots are found in the phenomenological laws of viscous flow (Newton), heat conduction (Fourier), diffusion (Fick), and electrical conduction (Ohm). Its theory restricts itself to large systems that can be treated as continuous media and can be assumed to be in local equilibrium. That is to say, a non-equilibrium system in local equilibrium can be divided into cells small enough so that any thermodynamic properties – such as mass, density, pressure, and temperature – which in non-equilibrium situations can be functions of space and time, vary slightly over one cell. On the other hand, these cells must be large on a microscopic scale – large enough so that they can still be treated as thermodynamic subsystems in contact with their surroundings. It should as well be kept in mind that local equilibrium cells must be open for energy and/or mass transport in order to account for the overall macroscopic time evolution of the system[80].

Non-equilibrium thermodynamics has many applications in petroleum engineering. The idea of petroleum reservoir engineering simulation is analogous to the theory of non-equilibrium thermodynamics. The reservoir under study is divided into many blocks. In each block, the fluid properties and saturations, pressure, and temperature are everywhere uniform, but vary from block to block. In the immiscible carbon dioxide injection process which is the subject of this research, when carbon dioxide is injected into a heavy oil reservoir, initially, because the concentrations of carbon dioxide in the injected gas stream and those in the reservoir fluids are not equal to the thermodynamic equilibrium values, mass transfer occurs, tending to even out the concentrations. Furthermore, as was already mentioned in Chapter 1, the concentration of carbon dioxide near or around the injection well is higher than that away from or near the production well. Thus, mass transfer has to take place to even out the carbon dioxide concentration. Consequently, it is important to know the conditions and the time required for thermodynamic equilibrium to be reached. The time at which equilibrium is reached is known as the equilibrium time. Goss and Exall[81] performed an experimental study on the equilibrium time of a carbon dioxide-bitumen mixture. An 18,000 mPa.s sample of bitumen was left exposed to carbon dioxide at 6.8 MPa and 50°C. After 12.5 days, they observed that concentrations of carbon dioxide in the gas phase equaled those in the bitumen phase.

Martin, Combarnous, and Charpentier[82] conducted an experimental study on mass transfer and phase distribution in two-phase flow through porous media under conditions similar to hydrodynamic reservoir conditions. The gas phase was carbon dioxide and the liquid phase iso-octane. Based upon the experimental results and observations, they concluded that the mass transfer process was not instantaneous while the phases are flowing co-currently inside a porous medium, that the equilibrium lag varied as a function of the ratio of gas to liquid velocity, and that mass transfer variations were mainly due to specific interfacial area variations.

3.4.1 - Background to Mathematical Modelling of Non-equilibrium

In order to model the mass transport phenomena under non-equilibrium conditions, a mass balance for each phase has to be written. A set of macroscopic mass balances with interfacial mass transfer phenomena were presented by Bird, Stewart, and Lightfoot[83]. By considering each phase separately in a two-phase flow system, interfacial balance equations, and interfacial boundary, and using a time averaging procedure, Ishii[84] developed a mathematical model which consists of two sets of equations which govern the mass, momentum, and energy balances for each phase. This so-called two-fluid model was later shown by Kataoka and Ishii[85] to predict accurately mechanical and thermal non-equilibrium between phases, if interfacial transfer terms are modelled accurately.

Farouq Ali, Chakma and Islam[86] proposed a non-equilibrium mathematical model for the simulation of alkaline/polymer injections. The model consists of mass balances for water, oil, gas, and chemical transport in the porous medium. A numerical simulation study was performed to investigate the time effects of absorption, dispersion, and interfacial tension. Bree[87] developed a non-equilibrium thermodynamic theory of continuous media for simple mixtures. Global and local entropy inequalities were derived for the mixture and for each of its constituents. He found that the set of entropy inequalities for the constituents was not equivalent to the single entropy inequality for the mixture. Mathieu and Lebon[88] presented a non-equilibrium thermodynamic model for describing the flow of a two-phase fluid with phase transition. A non-zero slip velocity, as well as a temperature jump between the two phases, was taken into account. They also devised a method for calculating the velocity of condensation which is based on the Knudsen number, which is the ratio of the molecular mean free path to the mean diameter of the particle. Lozada and Farouq Ali[89] proposed a set of mass balance equations which governed non-equilibrium transport phenomena in an immiscible carbon dioxide flood. Interfacial mass transfer effects were taken into account. The two-film theory was employed to model the interfacial mass transfer effect. They obtained six sets of scaling criteria, which were used to design the experiment for a non-equilibrium immiscible carbon dioxide drive[90]. Their equations were not complete because momentum, total energy , and entropy balances were not included.

4 - DEVELOPMENT OF THE MATHEMATICAL MODEL FOR THE NON-ISOTHERMAL AND NON-EQUILIBRIUM IMMISCIBLE CARBON DIOXIDE WAG PROCESS

To-date there has been no mathematical model for an immiscible carbon dioxide flood which includes non-equilibrium and phase change phenomena for non-isothermal cases, where the reservoir temperature is different from the surface temperature. The mathematical model previously presented by Lozada and Farouq Ali[89], which consists of mass balances for each component i in each phase j, includes the non-equilibrium phenomena amongst the oil, gas, and water phases only. Their model is valid for isothermal cases, where the reservoir temperature is the same as the surface temperature. A phase change was not considered in their model either, for the gas phase was assumed to consist of pure carbon dioxide only. Consequently, there is a need to develop a non-isothermal and non-equilibrium mathematical model including phase changes and interfacial mass transfer, which was one of the objectives of this research.

4.1 - Derivation of the Mathematical Model

The following assumptions were made when developing the model. The process was treated as three-phase flow (oleic, aqueous, and vapour). The gas phase was assumed to consist of carbon dioxide and water vapour, while the oil phase consisted of carbon dioxide and heavy oil, and the water phase consisted of carbon dioxide and water. Mass transfer was assumed to occur from the gas phase to the oil phase and from the oil phase to the water phase. Mass transfer was assumed to result from diffusion, convection, and dispersion. Interfacial mass transfer between the oleic phase and the vapour phase and/or the water phase for any component i was modelled using an interfacial film model. Darcy's, Fourier's, and Fick's laws were assumed to be valid. The system was assumed to be in local thermodynamic equilibrium. Chemical reactions were neglected. Negligible potential energy was assumed. Gas bubbles were assumed to be of a single and constant size. The velocity of the i component in the j phase was assumed to be that of the j phase. Instantaneous phase equilibrium was assumed to exist at the interfaces between the oil and gas phases and the oil and water phases. No accumulation at the interfaces was involved. Oil, gas, and water were considered to be Newtonian fluids. The viscosity of the gas phase was that of carbon dioxide. The above assumptions lead to the following mathematical model for a non-isothermal and non-equilibrium immiscible carbon dioxide flood. The diagram below presents a schematic of the system under consideration.

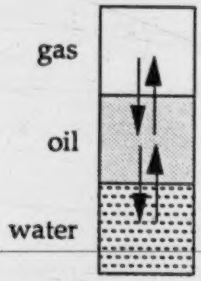

In the mass balance for each component, the following terms are considered: convective mass flux, diffusive mass flux, and interfacial mass transfer.

Mass Balance for Carbon Dioxide in the Oil Phase[89]

$$\frac{\partial}{\partial x}\left[C_{CO_2,o}\rho_o\vartheta_{ox}+\phi S_o\left(\overline{\overline{\mathfrak{D}}}_o+\overline{\overline{\mathfrak{D}}}^{*}_{CO_2,o}\right)\frac{\partial}{\partial x}\left(C_{CO_2,o}\rho_o\right)\right]+$$
$$\frac{\partial}{\partial y}\left[C_{CO_2,o}\rho_o\vartheta_{oy}+\phi S_o\left(\overline{\overline{\mathfrak{D}}}_o+\overline{\overline{\mathfrak{D}}}^{*}_{CO_2,o}\right)\frac{\partial}{\partial y}\left(C_{CO_2,o}\rho_o\right)\right]+$$
$$\frac{\partial}{\partial z}\left[C_{CO_2,o}\rho_o\vartheta_{oz}+\phi S_o\left(\overline{\overline{\mathfrak{D}}}_o+\overline{\overline{\mathfrak{D}}}^{*}_{CO_2,o}\right)\frac{\partial}{\partial z}\left(C_{CO_2,o}\rho_o\right)\right]+\mathcal{N}_{CO_2,ogx}+\mathcal{N}_{CO_2,ogy}+$$
$$\mathcal{N}_{CO_2,ogz}+\mathcal{N}_{CO_2,owx}+\mathcal{N}_{CO_2,owy}+\mathcal{N}_{CO_2,owz}=\frac{\partial}{\partial t}\left(\phi S_o\rho_o C_{CO_2,o}\right). \qquad (4.1)$$

Mass Balance for Carbon Dioxide in the Gas Phase[89]

$$\frac{\partial}{\partial x}\left[C_{CO_2,g}\rho_g\vartheta_{gx}+\phi S_g\left(\overline{\overline{\mathfrak{D}}}_g+\overline{\overline{\mathfrak{D}}}^{*}_{CO_2,g}\right)\frac{\partial}{\partial x}\left(C_{CO_2,g}\rho_g\right)\right]+$$
$$\frac{\partial}{\partial y}\left[C_{CO_2,g,g}\rho_g\vartheta_{gy}+\phi S_g\left(\overline{\overline{\mathfrak{D}}}_g+\overline{\overline{\mathfrak{D}}}^{*}_{CO_2,g}\right)\frac{\partial}{\partial y}\left(C_{CO_2,g}\rho_g\right)\right]+$$
$$\frac{\partial}{\partial z}\left[C_{CO_2,g}\rho_g\vartheta_{gz}+\phi S_g\left(\overline{\overline{\mathfrak{D}}}_g+\overline{\overline{\mathfrak{D}}}^{*}_{CO_2,g}\right)\frac{\partial}{\partial z}\left(C_{CO_2,g}\rho_g\right)\right]+\mathcal{N}_{CO_2,gox}+\mathcal{N}_{CO_2,goy}$$
$$+\mathcal{N}_{CO_2,goz}=\frac{\partial}{\partial t}\left(\phi S_g\rho_g C_{CO_2,g}\right). \qquad (4.2)$$

Mass Balance for Carbon Dioxide in the Water Phase[89]

$$\frac{\partial}{\partial x}\left[C_{CO_2,w}\rho_w\vartheta_{wx}+\phi S_w\left(\overline{\overline{\mathfrak{D}}}_w+\overline{\overline{\mathfrak{D}}}^{*}_{CO_2,w}\right)\frac{\partial}{\partial x}\left(C_{CO_2,w}\rho_w\right)\right]+$$
$$\frac{\partial}{\partial y}\left[C_{CO_2,w}\rho_w\vartheta_{wy}+\phi S_w\left(\overline{\overline{\mathfrak{D}}}_w+\overline{\overline{\mathfrak{D}}}^{*}_{CO_2,w}\right)\frac{\partial}{\partial y}\left(C_{CO_2,w}\rho_w\right)\right]+$$
$$\frac{\partial}{\partial z}\left[C_{CO_2,w}\rho_w\vartheta_{wz}+\phi S_w\left(\overline{\overline{\mathfrak{D}}}_w+\overline{\overline{\mathfrak{D}}}^{*}_{CO_2,w}\right)\frac{\partial}{\partial z}\left(C_{CO_2,w}\rho_w\right)\right]+\mathcal{N}_{CO_2,wox}+\mathcal{N}_{CO_2,woy}$$
$$+\mathcal{N}_{CO_2,woz}=\frac{\partial}{\partial t}\left(\phi S_w\rho_w C_{CO_2,w}\right). \tag{4.3}$$

Mass Balance for Oil in the Oil Phase[89]

$$\frac{\partial}{\partial x}\left[C_{o,o}\rho_o\vartheta_{ox}+\phi S_o\left(\overline{\overline{\mathfrak{D}}}_o+\overline{\overline{\mathfrak{D}}}^{*}_{o,o}\right)\frac{\partial}{\partial x}\left(C_{o,o}\rho_o\right)\right]+$$
$$\frac{\partial}{\partial y}\left[C_{o,o}\rho_o\vartheta_{oy}+\phi S_o\left(\overline{\overline{\mathfrak{D}}}_o+\overline{\overline{\mathfrak{D}}}^{*}_{o,o}\right)\frac{\partial}{\partial y}\left(C_{o,o}\rho_o\right)\right]+$$
$$\frac{\partial}{\partial z}\left[C_{o,o}\rho_o\vartheta_{oz}+\phi S_o\left(\overline{\overline{\mathfrak{D}}}_o+\overline{\overline{\mathfrak{D}}}^{*}_{o,o}\right)\frac{\partial}{\partial z}\left(C_{o,o}\rho_o\right)\right]=\frac{\partial}{\partial t}\left(\phi S_o\rho_o C_{o,o}\right). \tag{4.4}$$

Mass Balance for Water in the Water Phase

$$\frac{\partial}{\partial x}\left[C_{w,w}\rho_w\vartheta_{wx}+\phi S_w\left(\overline{\overline{\mathfrak{D}}}_w+\overline{\overline{\mathfrak{D}}}^{*}_{w,w}\right)\frac{\partial}{\partial x}\left(C_{w,w}\rho_w\right)\right]+$$
$$\frac{\partial}{\partial y}\left[C_{w,w}\rho_w\vartheta_{wy}+\phi S_w\left(\overline{\overline{\mathfrak{D}}}_w+\overline{\overline{\mathfrak{D}}}^{*}_{w,w}\right)\frac{\partial}{\partial y}\left(C_{w,w}\rho_w\right)\right]+$$
$$\frac{\partial}{\partial z}\left[C_{w,w}\rho_w\vartheta_{wz}+\phi S_w\left(\overline{\overline{\mathfrak{D}}}_w+\overline{\overline{\mathfrak{D}}}^{*}_{w,w}\right)\frac{\partial}{\partial z}\left(C_{w,w}\rho_w\right)\right]+\mathcal{N}_{wx,v\to\ell}+\mathcal{N}_{wy,v\to\ell}$$
$$+\mathcal{N}_{wz,v\to\ell}=\frac{\partial}{\partial t}\left(\phi S_w\rho_w C_{w,w}\right). \tag{4.5}$$

Mass Balance for Water in the Gas Phase

$$\frac{\partial}{\partial x}\left[C_{w,g}\rho_g\vartheta_{gx}+\phi S_g\left(\overline{\overline{\mathfrak{D}}}_g+\overline{\overline{\mathfrak{D}}}^{*}_{w,g}\right)\frac{\partial}{\partial x}\left(C_{w,g}\rho_g\right)\right]+$$
$$\frac{\partial}{\partial y}\left[C_{w,g}\rho_g\vartheta_{gy}+\phi S_g\left(\overline{\overline{\mathfrak{D}}}_g+\overline{\overline{\mathfrak{D}}}^{*}_{w,g}\right)\frac{\partial}{\partial y}\left(C_{w,g}\rho_g\right)\right]+$$
$$\frac{\partial}{\partial z}\left[C_{w,g}\rho_g\vartheta_{gz}+\phi S_g\left(\overline{\overline{\mathfrak{D}}}_g+\overline{\overline{\mathfrak{D}}}^{*}_{w,g}\right)\frac{\partial}{\partial z}\left(C_{w,g}\rho_g\right)\right]+\mathcal{N}_{wx,\ell\to v}+\mathcal{N}_{wy,\ell\to v}$$

$$+\mathcal{N}_{wz,\ell\to v} = \frac{\partial}{\partial t}\left(\phi S_g \rho_g C_{w,g}\right). \tag{4.6}$$

where,

$\mathcal{N}_{w,v\to\ell}$ = rate of mass flux of water from vapour phase to liquid phase,

$\mathcal{N}_{w,\ell\to v}$ = rate of mass flux of water from liquid phase to vapour phase.

It is assumed that when water vapour condenses it has to give up a certain amount of latent heat which is enough to vaporize the same amount of water to the vapour phase. Therefore, $\mathcal{N}_{w,v\to\ell}$ can be equated to $\mathcal{N}_{w,\ell\to v}$. Adding these two mass balances for water will eliminate these two terms and result in one single mass balance for water, which is as follows:

$$\begin{aligned}
&\frac{\partial}{\partial x}\left[C_{w,w}\rho_w \vartheta_{wx} + \phi S_w\left(\overline{\overline{\mathcal{D}}}_w + \overline{\overline{\mathcal{D}}}^{*}_{w,w}\right)\frac{\partial}{\partial x}\left(C_{w,w}\rho_w\right)\right] + \\
&\frac{\partial}{\partial y}\left[C_{w,w}\rho_w \vartheta_{wy} + \phi S_w\left(\overline{\overline{\mathcal{D}}}_w + \overline{\overline{\mathcal{D}}}^{*}_{w,w}\right)\frac{\partial}{\partial y}\left(C_{w,w}\rho_w\right)\right] + \\
&\frac{\partial}{\partial z}\left[C_{w,w}\rho_w \vartheta_{wz} + \phi S_w\left(\overline{\overline{\mathcal{D}}}_w + \overline{\overline{\mathcal{D}}}^{*}_{w,w}\right)\frac{\partial}{\partial z}\left(C_{w,w}\rho_w\right)\right] + \\
&\frac{\partial}{\partial x}\left[C_{w,g}\rho_g \vartheta_{gx} + \phi S_g\left(\overline{\overline{\mathcal{D}}}_g + \overline{\overline{\mathcal{D}}}^{*}_{w,g}\right)\frac{\partial}{\partial x}\left(C_{w,g}\rho_g\right)\right] + \\
&\frac{\partial}{\partial y}\left[C_{w,g}\rho_g \vartheta_{gy} + \phi S_g\left(\overline{\overline{\mathcal{D}}}_g + \overline{\overline{\mathcal{D}}}^{*}_{w,g}\right)\frac{\partial}{\partial y}\left(C_{w,g}\rho_g\right)\right] + \\
&\frac{\partial}{\partial z}\left[C_{w,g}\rho_g \vartheta_{gz} + \phi S_g\left(\overline{\overline{\mathcal{D}}}_g + \overline{\overline{\mathcal{D}}}^{*}_{w,g}\right)\frac{\partial}{\partial z}\left(C_{w,g}\rho_g\right)\right] \\
&= \frac{\partial}{\partial t}\left(\phi S_w \rho_w C_{w,w} + \phi S_g \rho_g C_{w,g}\right).
\end{aligned} \tag{4.7}$$

Note that in the case where the condensing gas phase is carbon dioxide and the vaporizing liquid phase water, the assumption as stated above is not valid because the latent heats of carbon dioxide and water are not the same. In such a case, in order to determine the amount of water that vaporizes for each mole or mass of carbon dioxide that condenses and/or diffuses, one needs to perform a heat balance at the interface using the latent heat as shown below.

$$\lambda_{CO_2}\mathcal{N}_{CO_2,wo(v\to\ell)} = -\lambda_w \mathcal{N}_{w,wo(\ell\to v)}.$$

Knowing the latent heats, the relationship between the two fluxes can be determined from the above heat balance.

In the momentum balance for each component, the following terms are considered: momentum gain by convection, diffusive momentum flux, gravitational force, pressure force, drag force, buoyancy force, momentum gain by viscous transfer, and momentum gain by interfacial mass flux.

Momentum Balance for Carbon Dioxide in the Oil Phase

$$
\begin{aligned}
&-\frac{\partial}{\partial x}\left[C_{CO_2,o}\rho_o\left(\vartheta_{ox}\vartheta_{ox}+\vartheta_{ox}\vartheta_{oy}+\vartheta_{ox}\vartheta_{oz}\right)+\phi S_o\left(\overline{\overline{\mathfrak{D}}}_o+\overline{\overline{\mathfrak{D}}}^{*}_{CO_2,o}\right)\frac{\partial}{\partial x}\left(C_{CO_2,o}\rho_o\vartheta_{ox}\right)\right]\\
&-\frac{\partial}{\partial y}\left[C_{CO_2,o}\rho_o\left(\vartheta_{oy}\vartheta_{ox}+\vartheta_{oy}\vartheta_{oy}+\vartheta_{oy}\vartheta_{oz}\right)+\phi S_o\left(\overline{\overline{\mathfrak{D}}}_o+\overline{\overline{\mathfrak{D}}}^{*}_{CO_2,o}\right)\frac{\partial}{\partial y}\left(C_{CO_2,o}\rho_o\vartheta_{oy}\right)\right]\\
&-\frac{\partial}{\partial z}\left[C_{CO_2,o}\rho_o\left(\vartheta_{oz}\vartheta_{ox}+\vartheta_{oz}\vartheta_{oy}+\vartheta_{oz}\vartheta_{oz}\right)+\phi S_o\left(\overline{\overline{\mathfrak{D}}}_o+\overline{\overline{\mathfrak{D}}}^{*}_{CO_2,o}\right)\frac{\partial}{\partial z}\left(C_{CO_2,o}\rho_o\vartheta_{oz}\right)\right]\\
&+C_{CO_2,o}\rho_o\left(g_x+g_y+g_z\right)-\frac{\partial}{\partial x}\left(p_{CO_2,o}\right)-\frac{\partial}{\partial y}\left(p_{CO_2,o}\right)-\frac{\partial}{\partial z}\left(p_{CO_2,o}\right)+\mathcal{N}_{CO_2,ogx}\vartheta_{ox}\\
&+\mathcal{N}_{CO_2,ogy}\vartheta_{oy}+\mathcal{N}_{CO_2,ogz}\vartheta_{oz}+\mathcal{N}_{CO_2,owx}\vartheta_{ox}+\mathcal{N}_{CO_2,owy}\vartheta_{oy}+\mathcal{N}_{CO_2,owz}\vartheta_{oz}\\
&=\frac{\partial}{\partial t}\left[\phi C_{CO_2,o}\rho_o S_o\left(\vartheta_{ox}+\vartheta_{oy}+\vartheta_{oz}\right)\right]. \qquad (4.8)
\end{aligned}
$$

Momentum Balance for Carbon Dioxide in the Gas Phase

$$
\begin{aligned}
&-\frac{\partial}{\partial x}\left[C_{CO_2,g}\rho_g\left(\vartheta_{gx}\vartheta_{gx}+\vartheta_{gx}\vartheta_{gy}+\vartheta_{gx}\vartheta_{gz}\right)+\phi S_g\left(\overline{\overline{\mathfrak{D}}}_g+\overline{\overline{\mathfrak{D}}}^{*}_{CO_2,g}\right)\frac{\partial}{\partial x}\left(C_{CO_2,g}\rho_g\vartheta_{gx}\right)\right]\\
&-\frac{\partial}{\partial y}\left[C_{CO_2,g}\rho_g\left(\vartheta_{gy}\vartheta_{gx}+\vartheta_{gy}\vartheta_{gy}+\vartheta_{gy}\vartheta_{gz}\right)+\phi S_g\left(\overline{\overline{\mathfrak{D}}}_g+\overline{\overline{\mathfrak{D}}}^{*}_{CO_2,g}\right)\frac{\partial}{\partial y}\left(C_{CO_2,g}\rho_g\vartheta_{gy}\right)\right]\\
&-\frac{\partial}{\partial z}\left[C_{CO_2,g}\rho_g\left(\vartheta_{gz}\vartheta_{gx}+\vartheta_{gz}\vartheta_{gy}+\vartheta_{gz}\vartheta_{gz}\right)+\phi S_g\left(\overline{\overline{\mathfrak{D}}}_g+\overline{\overline{\mathfrak{D}}}^{*}_{CO_2,g}\right)\frac{\partial}{\partial z}\left(C_{CO_2,g}\rho_g\vartheta_{gz}\right)\right]\\
&-\frac{\partial}{\partial x}\left(\tau_{gxx}+\tau_{gxy}+\tau_{gxz}\right)-\frac{\partial}{\partial y}\left(\tau_{gyx}+\tau_{gyy}+\tau_{gyz}\right)-\frac{\partial}{\partial z}\left(\tau_{gzx}+\tau_{gzy}+\tau_{gzz}\right)\\
&+C_{CO_2,g}\rho_g\left(g_x+g_y+g_z\right)-\frac{\partial}{\partial x}\left(p_{CO_2,g}\right)-\frac{\partial}{\partial y}\left(p_{CO_2,g}\right)-\frac{\partial}{\partial z}\left(p_{CO_2,g}\right)-F_{CO_2,gBx}-F_{CO_2,gBy}\\
&-F_{CO_2,gBz}-F_{CO_2,gDx}-F_{CO_2,gDy}-F_{CO_2,gDz}+\mathcal{N}_{CO_2,gox}\left(\vartheta_{gx}-\vartheta_{ox}\right)+\mathcal{N}_{CO_2,goy}\left(\vartheta_{gy}-\vartheta_{oy}\right)\\
&+\mathcal{N}_{CO_2,goz}\left(\vartheta_{gz}-\vartheta_{oz}\right)=\frac{\partial}{\partial t}\left[\phi C_{CO_2,g}\rho_g S_g\left(\vartheta_{gx}+\vartheta_{gy}+\vartheta_{gz}\right)\right]. \qquad (4.9)
\end{aligned}
$$

Momentum Balance for Carbon Dioxide in the Water Phase

$$\begin{aligned}
&-\frac{\partial}{\partial x}\left[C_{CO_2,w}\rho_w\left(\vartheta_{wx}\vartheta_{wx}+\vartheta_{wx}\vartheta_{wy}+\vartheta_{wx}\vartheta_{wz}\right)+\phi S_w\left(\overline{\overline{\mathfrak{D}}}_w+\overline{\overline{\mathfrak{D}}}^{*}_{CO_2,w}\right)\frac{\partial}{\partial x}\left(C_{CO_2,w}\rho_w\vartheta_{wx}\right)\right]\\
&-\frac{\partial}{\partial y}\left[C_{CO_2,w}\rho_w\left(\vartheta_{wy}\vartheta_{wx}+\vartheta_{wy}\vartheta_{wy}+\vartheta_{wy}\vartheta_{wz}\right)+\phi S_w\left(\overline{\overline{\mathfrak{D}}}_w+\overline{\overline{\mathfrak{D}}}^{*}_{CO_2,w}\right)\frac{\partial}{\partial y}\left(C_{CO_2,w}\rho_w\vartheta_{wy}\right)\right]\\
&-\frac{\partial}{\partial z}\left[C_{CO_2,w}\rho_w\left(\vartheta_{wz}\vartheta_{wx}+\vartheta_{wz}\vartheta_{wy}+\vartheta_{wz}\vartheta_{wz}\right)+\phi S_w\left(\overline{\overline{\mathfrak{D}}}_w+\overline{\overline{\mathfrak{D}}}^{*}_{CO_2,w}\right)\frac{\partial}{\partial z}\left(C_{CO_2,w}\rho_w\vartheta_{wz}\right)\right]\\
&+C_{CO_2,w}\rho_w\left(g_x+g_y+g_z\right)-\frac{\partial}{\partial x}\left(p_{CO_2,w}\right)-\frac{\partial}{\partial y}\left(p_{CO_2,w}\right)-\frac{\partial}{\partial z}\left(p_{CO_2,w}\right)\\
&+\mathcal{N}_{CO_2,wox}\left(\vartheta_{wx}-\vartheta_{ox}\right)+\mathcal{N}_{CO_2,woy}\left(\vartheta_{wy}-\vartheta_{oy}\right)+\mathcal{N}_{CO_2,woz}\left(\vartheta_{wz}-\vartheta_{oz}\right)\\
&=\frac{\partial}{\partial t}\left[\phi C_{CO_2,w}\rho_w S_w\left(\vartheta_{wx}+\vartheta_{wy}+\vartheta_{wz}\right)\right]. \qquad (4.10)
\end{aligned}$$

Momentum Balance for Oil in the Oil Phase

$$\begin{aligned}
&-\frac{\partial}{\partial x}\left[C_{o,o}\rho_o\left(\vartheta_{ox}\vartheta_{ox}+\vartheta_{ox}\vartheta_{oy}+\vartheta_{ox}\vartheta_{oz}\right)+\phi S_o\left(\overline{\overline{\mathfrak{D}}}_o+\overline{\overline{\mathfrak{D}}}^{*}_{o,o}\right)\frac{\partial}{\partial x}\left(C_{o,o}\rho_o\vartheta_{ox}\right)\right]\\
&-\frac{\partial}{\partial y}\left[C_{o,o}\rho_o\left(\vartheta_{oy}\vartheta_{ox}+\vartheta_{oy}\vartheta_{oy}+\vartheta_{oy}\vartheta_{oz}\right)+\phi S_o\left(\overline{\overline{\mathfrak{D}}}_o+\overline{\overline{\mathfrak{D}}}^{*}_{o,o}\right)\frac{\partial}{\partial y}\left(C_{o,o}\rho_o\vartheta_{oy}\right)\right]\\
&-\frac{\partial}{\partial z}\left[C_{o,o}\rho_o\left(\vartheta_{oz}\vartheta_{ox}+\vartheta_{oz}\vartheta_{oy}+\vartheta_{oz}\vartheta_{oz}\right)+\phi S_o\left(\overline{\overline{\mathfrak{D}}}_o+\overline{\overline{\mathfrak{D}}}^{*}_{o,o}\right)\frac{\partial}{\partial z}\left(C_{o,o}\rho_o\vartheta_{oz}\right)\right]\\
&-\frac{\partial}{\partial x}\left(\tau_{oxx}+\tau_{oxy}+\tau_{oxz}\right)-\frac{\partial}{\partial y}\left(\tau_{oyx}+\tau_{oyy}+\tau_{oyz}\right)-\frac{\partial}{\partial z}\left(\tau_{ozx}+\tau_{ozy}+\tau_{ozz}\right)\\
&+C_{o,o}\rho_o\left(g_x+g_y+g_z\right)-\frac{\partial}{\partial x}\left(p_o\right)-\frac{\partial}{\partial y}\left(p_o\right)-\frac{\partial}{\partial z}\left(p_o\right)+F_{CO_2,gDx}+F_{CO_2,gDy}+F_{CO_2,gDz}\\
&=\frac{\partial}{\partial t}\left[\phi C_{o,o}\rho_o S_o\left(\vartheta_{ox}+\vartheta_{oy}+\vartheta_{oz}\right)\right]. \qquad (4.11)
\end{aligned}$$

Momentum Balance for Water

$$\begin{aligned}
&-\frac{\partial}{\partial x}\left[C_{w,w}\rho_w\left(\vartheta_{wx}\vartheta_{wx}+\vartheta_{wx}\vartheta_{wy}+\vartheta_{wx}\vartheta_{wz}\right)+\phi S_w\left(\overline{\overline{\mathfrak{D}}}_w+\overline{\overline{\mathfrak{D}}}^{*}_{w,w}\right)\frac{\partial}{\partial x}\left(C_{w,w}\rho_w\vartheta_{wx}\right)\right]\\
&-\frac{\partial}{\partial y}\left[C_{w,w}\rho_w\left(\vartheta_{wy}\vartheta_{wx}+\vartheta_{wy}\vartheta_{wy}+\vartheta_{wy}\vartheta_{wz}\right)+\phi S_w\left(\overline{\overline{\mathfrak{D}}}_w+\overline{\overline{\mathfrak{D}}}^{*}_{w,w}\right)\frac{\partial}{\partial y}\left(C_{w,w}\rho_w\vartheta_{wy}\right)\right]\\
&-\frac{\partial}{\partial z}\left[C_{w,w}\rho_w\left(\vartheta_{wz}\vartheta_{wx}+\vartheta_{wz}\vartheta_{wy}+\vartheta_{wz}\vartheta_{wz}\right)+\phi S_w\left(\overline{\overline{\mathfrak{D}}}_w+\overline{\overline{\mathfrak{D}}}^{*}_{w,w}\right)\frac{\partial}{\partial z}\left(C_{w,w}\rho_w\vartheta_{wz}\right)\right]\\
&-\frac{\partial}{\partial x}\left[C_{w,g}\rho_w\left(\vartheta_{gx}\vartheta_{gx}+\vartheta_{gx}\vartheta_{gy}+\vartheta_{gx}\vartheta_{gz}\right)+\phi S_g\left(\overline{\overline{\mathfrak{D}}}_g+\overline{\overline{\mathfrak{D}}}^{*}_{w,g}\right)\frac{\partial}{\partial x}\left(C_{w,g}\rho_g\vartheta_{gx}\right)\right]
\end{aligned}$$

$$
\begin{aligned}
&-\frac{\partial}{\partial y}\left[C_{w,g}\rho_w\left(\vartheta_{gy}\vartheta_{gx}+\vartheta_{gy}\vartheta_{gy}+\vartheta_{gy}\vartheta_{gz}\right)+\phi S_g\left(\overline{\overline{\mathfrak{D}}}_g+\overline{\overline{\mathfrak{D}}}^{*}_{w,g}\right)\frac{\partial}{\partial y}\left(C_{w,g}\rho_g\vartheta_{gy}\right)\right]\\
&-\frac{\partial}{\partial z}\left[C_{w,g}\rho_w\left(\vartheta_{gz}\vartheta_{gx}+\vartheta_{gz}\vartheta_{gy}+\vartheta_{gz}\vartheta_{gz}\right)+\phi S_g\left(\overline{\overline{\mathfrak{D}}}_g+\overline{\overline{\mathfrak{D}}}^{*}_{w,g}\right)\frac{\partial}{\partial z}\left(C_{w,g}\rho_g\vartheta_{gz}\right)\right]\\
&-\frac{\partial}{\partial x}\left(\tau_{wxx}+\tau_{wxy}+\tau_{wxz}\right)-\frac{\partial}{\partial y}\left(\tau_{wyx}+\tau_{wyy}+\tau_{wyz}\right)-\frac{\partial}{\partial z}\left(\tau_{wzx}+\tau_{wzy}+\tau_{wzz}\right)\\
&+C_{w,w}\rho_w\left(g_x+g_y+g_z\right)-\frac{\partial}{\partial x}\left(p_w\right)-\frac{\partial}{\partial y}\left(p_w\right)-\frac{\partial}{\partial z}\left(p_w\right)+C_{w,g}\rho_g\left(g_x+g_y+g_z\right)\\
&-\frac{\partial}{\partial x}\left(p_{w,g}\right)-\frac{\partial}{\partial y}\left(p_{w,g}\right)-\frac{\partial}{\partial z}\left(p_{w,g}\right)+\dot{m}\left[\left(\vartheta_{gx}-\vartheta_{wx}\right)+\left(\vartheta_{gy}-\vartheta_{wy}\right)+\left(\vartheta_{gz}-\vartheta_{wz}\right)\right]\\
&=\frac{\partial}{\partial t}\left[\phi C_{w,w}\rho_w S_w\left(\vartheta_{wx}+\vartheta_{wy}+\vartheta_{wz}\right)+\phi C_{w,g}\rho_g S_g\left(\vartheta_{gx}+\vartheta_{gy}+\vartheta_{gz}\right)\right].
\end{aligned}
\tag{4.12}
$$

In the total energy balance for each phase, the following terms are considered: convective transport of kinetic energy along with the fluid across the system boundary, kinetic energy of diffusion, work done by pressure forces, work done by viscous forces, work done by mass forces, reversible conversion of kinetic energy to internal energy due to viscosity, irreversible conversion of kinetic energy to internal energy due to viscosity (i.e., the energy that is dissipated), work done by drag forces, work done by buoyancy forces, convective heat and kinetic energy transport due to interfacial mass transfer, and convective/conductive heat flux.

Total Energy Balance for Carbon Dioxide in the Oil Phase

$$
\begin{aligned}
&-\frac{\partial}{\partial x}\left[C_{CO_2,o}\frac{1}{2}\vartheta_{ox}^2\vartheta_{ox}\rho_o\right]-\frac{\partial}{\partial x}\left[\phi S_o\left(\overline{\overline{\mathfrak{D}}}_o+\overline{\overline{\mathfrak{D}}}^{*}_{CO_2,o}\right)\frac{\partial}{\partial x}\left(C_{CO_2,o}\frac{1}{2}\rho_o\vartheta_{ox}^2\right)\right]\\
&-\frac{\partial}{\partial y}\left[C_{CO_2,o}\frac{1}{2}\vartheta_{oy}^2\vartheta_{oy}\rho_o\right]-\frac{\partial}{\partial y}\left[\phi S_o\left(\overline{\overline{\mathfrak{D}}}_o+\overline{\overline{\mathfrak{D}}}^{*}_{CO_2,o}\right)\frac{\partial}{\partial y}\left(C_{CO_2,o}\frac{1}{2}\rho_o\vartheta_{oy}^2\right)\right]\\
&-\frac{\partial}{\partial z}\left[C_{CO_2,o}\frac{1}{2}\vartheta_{oz}^2\vartheta_{oz}\rho_o\right]-\frac{\partial}{\partial z}\left[\phi S_o\left(\overline{\overline{\mathfrak{D}}}_o+\overline{\overline{\mathfrak{D}}}^{*}_{CO_2,o}\right)\frac{\partial}{\partial z}\left(C_{CO_2,o}\frac{1}{2}\rho_o\vartheta_{oz}^2\right)\right]\\
&-\frac{\partial}{\partial x}\left(p_{CO_2,o}\vartheta_{ox}\right)-\frac{\partial}{\partial y}\left(p_{CO_2,o}\vartheta_{oy}\right)-\frac{\partial}{\partial z}\left(p_{CO_2,o}\vartheta_{oz}\right)-p_{CO_2,o}\frac{\partial}{\partial x}\left(\vartheta_{ox}\right)-p_{CO_2,o}\frac{\partial}{\partial y}\left(\vartheta_{oy}\right)\\
&-p_{CO_2,o}\frac{\partial}{\partial z}\left(\vartheta_{oz}\right)+C_{CO_2,o}\rho_o\left(g_x\vartheta_{ox}+g_y\vartheta_{oy}+g_z\vartheta_{oz}\right)+\mathcal{N}_{CO_2,ogx}\left\{h_{CO_2}+\frac{1}{2}\left(\vartheta_{gx}^2-\vartheta_{ox}^2\right)\right\}\\
&+\mathcal{N}_{CO_2,ogy}\left\{h_{CO_2}+\frac{1}{2}\left(\vartheta_{gy}^2-\vartheta_{oy}^2\right)\right\}+\mathcal{N}_{CO_2,ogz}\left\{h_{CO_2}+\frac{1}{2}\left(\vartheta_{gz}^2-\vartheta_{oz}^2\right)\right\}\\
&+\mathcal{N}_{CO_2,owx}\left\{h_{CO_2}+\frac{1}{2}\left(\vartheta_{wx}^2-\vartheta_{ox}^2\right)\right\}+\mathcal{N}_{CO_2,owy}\left\{h_{CO_2}+\frac{1}{2}\left(\vartheta_{wy}^2-\vartheta_{oy}^2\right)\right\}
\end{aligned}
$$

$$
\begin{aligned}
&+\mathcal{N}_{CO_2,owz}\left\{h_{CO_2}+\frac{1}{2}\left(\vartheta_{wz}^2-\vartheta_{oz}^2\right)\right\}+\frac{\partial}{\partial x}\left[C_{CO_2,o}\rho_o h_{CO_2}\vartheta_{ox}\right]+\frac{\partial}{\partial y}\left[C_{CO_2,o}\rho_o h_{CO_2}\vartheta_{oy}\right]\\
&+\frac{\partial}{\partial z}\left[C_{CO_2,o}\rho_o h_{CO_2}\vartheta_{oz}\right]\\
&=\frac{\partial}{\partial t}\left[\phi C_{CO_2,o}\rho_o S_o U_{CO_2}+\frac{1}{2}\phi C_{CO_2,o}\rho_o S_o\left(\vartheta_{ox}^2+\vartheta_{oy}^2+\vartheta_{oz}^2\right)\right]. \qquad (4.13)
\end{aligned}
$$

Total Energy Balance for Carbon Dioxide in the Gas Phase

$$
\begin{aligned}
&-\frac{\partial}{\partial x}\left[C_{CO_2,g}\frac{1}{2}\vartheta_{gx}^2\vartheta_{gx}\rho_g\right]-\frac{\partial}{\partial x}\left[\phi S_g\left(\overline{\overline{\mathfrak{D}}}_g+\overline{\overline{\mathfrak{D}}}^{*}_{CO_2,g}\right)\frac{\partial}{\partial x}\left(C_{CO_2,g}\frac{1}{2}\rho_g\vartheta_{gx}^2\right)\right]\\
&-\frac{\partial}{\partial y}\left[C_{CO_2,g}\frac{1}{2}\vartheta_{gy}^2\vartheta_{gy}\rho_g\right]-\frac{\partial}{\partial y}\left[\phi S_g\left(\overline{\overline{\mathfrak{D}}}_g+\overline{\overline{\mathfrak{D}}}^{*}_{CO_2,g}\right)\frac{\partial}{\partial y}\left(C_{CO_2,g}\frac{1}{2}\rho_g\vartheta_{gy}^2\right)\right]\\
&-\frac{\partial}{\partial z}\left[C_{CO_2,g}\frac{1}{2}\vartheta_{gz}^2\vartheta_{gz}\rho_g\right]-\frac{\partial}{\partial z}\left[\phi S_g\left(\overline{\overline{\mathfrak{D}}}_g+\overline{\overline{\mathfrak{D}}}^{*}_{CO_2,g}\right)\frac{\partial}{\partial z}\left(C_{CO_2,g}\frac{1}{2}\rho_g\vartheta_{gz}^2\right)\right]\\
&-\frac{\partial}{\partial x}\left(p_{CO_2,g}\vartheta_{gx}\right)-\frac{\partial}{\partial y}\left(p_{CO_2,g}\vartheta_{gy}\right)-\frac{\partial}{\partial z}\left(p_{CO_2,g}\vartheta_{gz}\right)-\frac{\partial}{\partial x}\left(\tau_{gxx}\vartheta_{gx}+\tau_{gxy}\vartheta_{gy}+\tau_{gxz}\vartheta_{gz}\right)\\
&-\frac{\partial}{\partial y}\left(\tau_{gyx}\vartheta_{gx}+\tau_{gyy}\vartheta_{gy}+\tau_{gyz}\vartheta_{gz}\right)-\frac{\partial}{\partial z}\left(\tau_{gzx}\vartheta_{gx}+\tau_{gzy}\vartheta_{gy}+\tau_{gzz}\vartheta_{gz}\right)-p_{CO_2,g}\frac{\partial}{\partial x}\left(\vartheta_{gx}\right)\\
&-p_{CO_2,g}\frac{\partial}{\partial y}\left(\vartheta_{gy}\right)-p_{CO_2,g}\frac{\partial}{\partial z}\left(\vartheta_{gz}\right)-\tau_{gxx}\left(\frac{\partial\vartheta_{gx}}{\partial x}\right)-\tau_{gyy}\left(\frac{\partial\vartheta_{gy}}{\partial y}\right)-\tau_{gzz}\left(\frac{\partial\vartheta_{gz}}{\partial z}\right)\\
&-\tau_{gxy}\left(\frac{\partial\vartheta_{gx}}{\partial y}+\frac{\partial\vartheta_{gy}}{\partial x}\right)-\tau_{gyz}\left(\frac{\partial\vartheta_{gy}}{\partial z}+\frac{\partial\vartheta_{gz}}{\partial y}\right)-\tau_{gzx}\left(\frac{\partial\vartheta_{gz}}{\partial x}+\frac{\partial\vartheta_{gx}}{\partial z}\right)\\
&+C_{CO_2,g}\rho_g\left(g_x\vartheta_{gx}+g_y\vartheta_{gy}+g_z\vartheta_{gz}\right)-F_{CO_2,gBx}\vartheta_{gx}-F_{CO_2,gBy}\vartheta_{gy}-F_{CO_2,gBz}\vartheta_{gz}\\
&-F_{CO_2,gDx}\vartheta_{gx}-F_{CO_2,gDy}\vartheta_{gy}-F_{CO_2,gDz}\vartheta_{gz}+\mathcal{N}_{CO_2,gox}\left\{h_{CO_2}+\frac{1}{2}\left(\vartheta_{gx}^2-\vartheta_{ox}^2\right)\right\}\\
&+\mathcal{N}_{CO_2,goy}\left\{h_{CO_2}+\frac{1}{2}\left(\vartheta_{gy}^2-\vartheta_{oy}^2\right)\right\}+\mathcal{N}_{CO_2,goz}\left\{h_{CO_2}+\frac{1}{2}\left(\vartheta_{gz}^2-\vartheta_{oz}^2\right)\right\}\\
&+\frac{\partial}{\partial x}\left[C_{CO_2,g}\rho_g h_{CO_2}\vartheta_{gx}\right]+\frac{\partial}{\partial y}\left[C_{CO_2,g}\rho_g h_{CO_2}\vartheta_{gy}\right]+\frac{\partial}{\partial z}\left[C_{CO_2,g}\rho_g h_{CO_2}\vartheta_{gz}\right]\\
&=\frac{\partial}{\partial t}\left[\phi C_{CO_2,g}\rho_g S_g U_{CO_2}+\frac{1}{2}\phi C_{CO_2,g}\rho_g S_g\left(\vartheta_{gx}^2+\vartheta_{gy}^2+\vartheta_{gz}^2\right)\right]. \qquad (4.14)
\end{aligned}
$$

The Total Energy Balance for Carbon Dioxide in the Water Phase

$$
\begin{aligned}
&-\frac{\partial}{\partial x}\left[C_{CO_2,w}\frac{1}{2}\vartheta_{wx}^2\vartheta_{wx}\rho_w\right]-\frac{\partial}{\partial x}\left[\phi S_w\left(\overline{\overline{\mathfrak{D}}}_w+\overline{\overline{\mathfrak{D}}}^{*}_{CO_2,w}\right)\frac{\partial}{\partial x}\left(C_{CO_2,w}\frac{1}{2}\rho_w\vartheta_{wx}^2\right)\right]\\
&-\frac{\partial}{\partial y}\left[C_{CO_2,w}\frac{1}{2}\vartheta_{wy}^2\vartheta_{wy}\rho_w\right]-\frac{\partial}{\partial y}\left[\phi S_w\left(\overline{\overline{\mathfrak{D}}}_w+\overline{\overline{\mathfrak{D}}}^{*}_{CO_2,w}\right)\frac{\partial}{\partial y}\left(C_{CO_2,w}\frac{1}{2}\rho_w\vartheta_{wy}^2\right)\right]
\end{aligned}
$$

$$
\begin{aligned}
&-\frac{\partial}{\partial z}\left[C_{CO_2,w}\frac{1}{2}\vartheta_{wz}^2\vartheta_{wz}\rho_w\right]-\frac{\partial}{\partial z}\left[\phi S_w\left(\overline{\overline{\mathfrak{D}}}_w+\overline{\overline{\mathfrak{D}}}^*_{CO_2,w}\right)\frac{\partial}{\partial z}\left(C_{CO_2,w}\frac{1}{2}\rho_w\vartheta_{wz}^2\right)\right]\\
&-\frac{\partial}{\partial x}\left(p_{CO_2,w}\vartheta_{wx}\right)-\frac{\partial}{\partial y}\left(p_{CO_2,w}\vartheta_{wy}\right)-\frac{\partial}{\partial z}\left(p_{CO_2,w}\vartheta_{wz}\right)-p_{CO_2,w}\frac{\partial}{\partial x}\left(\vartheta_{wx}\right)\\
&-p_{CO_2,w}\frac{\partial}{\partial y}\left(\vartheta_{wy}\right)-p_{CO_2,w}\frac{\partial}{\partial z}\left(\vartheta_{wz}\right)+C_{CO_2,w}\rho_w\left(g_x\vartheta_{wx}+g_y\vartheta_{wy}+g_z\vartheta_{wz}\right)\\
&+\mathcal{N}_{CO_2,wox}\left\{h_{CO_2}+\frac{1}{2}\left(\vartheta_{wx}^2-\vartheta_{ox}^2\right)\right\}+\mathcal{N}_{CO_2,woy}\left\{h_{CO_2}+\frac{1}{2}\left(\vartheta_{wy}^2-\vartheta_{oy}^2\right)\right\}\\
&+\mathcal{N}_{CO_2,woz}\left\{h_{CO_2}+\frac{1}{2}\left(\vartheta_{wz}^2-\vartheta_{oz}^2\right)\right\}+\frac{\partial}{\partial x}\left[C_{CO_2,w}\rho_w h_{CO_2}\vartheta_{wx}\right]\\
&+\frac{\partial}{\partial y}\left[C_{CO_2,w}\rho_w h_{CO_2}\vartheta_{wy}\right]+\frac{\partial}{\partial z}\left[C_{CO_2,w}\rho_w h_{CO_2}\vartheta_{wz}\right]\\
&=\frac{\partial}{\partial t}\left[\phi C_{CO_2,w}\rho_w S_w U_{CO_2}+\frac{1}{2}\phi C_{CO_2,w}\rho_w S_w\left(\vartheta_{wx}^2+\vartheta_{wy}^2+\vartheta_{wz}^2\right)\right].
\end{aligned}
\tag{4.15}
$$

Total Energy Balance for Oil in the Oil Phase

$$
\begin{aligned}
&-\frac{\partial}{\partial x}\left[C_{o,o}\frac{1}{2}\vartheta_{ox}^2\vartheta_{ox}\rho_o\right]-\frac{\partial}{\partial x}\left[\phi S_o\left(\overline{\overline{\mathfrak{D}}}_o+\overline{\overline{\mathfrak{D}}}^*_{o,o}\right)\frac{\partial}{\partial x}\left(C_{o,o}\frac{1}{2}\rho_o\vartheta_{ox}^2\right)\right]\\
&-\frac{\partial}{\partial y}\left[C_{o,o}\frac{1}{2}\vartheta_{oy}^2\vartheta_{oy}\rho_o\right]-\frac{\partial}{\partial y}\left[\phi S_o\left(\overline{\overline{\mathfrak{D}}}_o+\overline{\overline{\mathfrak{D}}}^*_{o,o}\right)\frac{\partial}{\partial y}\left(C_{o,o}\frac{1}{2}\rho_o\vartheta_{oy}^2\right)\right]\\
&-\frac{\partial}{\partial z}\left[C_{o,o}\frac{1}{2}\vartheta_{oz}^2\vartheta_{oz}\rho_o\right]-\frac{\partial}{\partial z}\left[\phi S_o\left(\overline{\overline{\mathfrak{D}}}_o+\overline{\overline{\mathfrak{D}}}^*_{o,o}\right)\frac{\partial}{\partial z}\left(C_{o,o}\frac{1}{2}\rho_o\vartheta_{oz}^2\right)\right]-\frac{\partial}{\partial x}\left(p_o\vartheta_{ox}\right)\\
&-\frac{\partial}{\partial y}\left(p_o\vartheta_{oy}\right)-\frac{\partial}{\partial z}\left(p_o\vartheta_{oz}\right)-\frac{\partial}{\partial x}\left(\tau_{oxx}\vartheta_{ox}+\tau_{oxy}\vartheta_{oy}+\tau_{oxz}\vartheta_{oz}\right)\\
&-\frac{\partial}{\partial y}\left(\tau_{oyx}\vartheta_{ox}+\tau_{oyy}\vartheta_{oy}+\tau_{oyz}\vartheta_{oz}\right)-\frac{\partial}{\partial z}\left(\tau_{ozx}\vartheta_{ox}+\tau_{ozy}\vartheta_{oy}+\tau_{ozz}\vartheta_{oz}\right)-p_o\frac{\partial}{\partial x}\left(\vartheta_{ox}\right)\\
&-p_o\frac{\partial}{\partial y}\left(\vartheta_{oy}\right)-p_o\frac{\partial}{\partial z}\left(\vartheta_{oz}\right)-\tau_{oxx}\left(\frac{\partial\vartheta_{ox}}{\partial x}\right)-\tau_{oyy}\left(\frac{\partial\vartheta_{oy}}{\partial y}\right)-\tau_{ozz}\left(\frac{\partial\vartheta_{oz}}{\partial z}\right)\\
&-\tau_{oxy}\left(\frac{\partial\vartheta_{ox}}{\partial y}+\frac{\partial\vartheta_{oy}}{\partial x}\right)-\tau_{oyz}\left(\frac{\partial\vartheta_{oy}}{\partial z}+\frac{\partial\vartheta_{oz}}{\partial y}\right)-\tau_{ozx}\left(\frac{\partial\vartheta_{oz}}{\partial x}+\frac{\partial\vartheta_{ox}}{\partial z}\right)+F_{CO_2,gDx}\vartheta_{gx}\\
&+F_{CO_2,gDy}\vartheta_{gy}+F_{CO_2,gDz}\vartheta_{gz}+C_{o,o}\rho_o\left(g_x\vartheta_{ox}+g_y\vartheta_{oy}+g_z\vartheta_{oz}\right)+\frac{\partial}{\partial x}\left[C_{o,o}\rho_o h_o\vartheta_{ox}\right]\\
&+\frac{\partial}{\partial y}\left[C_{o,o}\rho_o h_o\vartheta_{oy}\right]+\frac{\partial}{\partial z}\left[C_{o,o}\rho_o h_o\vartheta_{oz}\right]\\
&=\frac{\partial}{\partial t}\left[\phi C_{o,o}\rho_o S_o U_o+\frac{1}{2}\phi C_{o,o}\rho_o S_o\left(\vartheta_{ox}^2+\vartheta_{oy}^2+\vartheta_{oz}^2\right)\right].
\end{aligned}
\tag{4.16}
$$

Total Energy Balance for Water

$$\begin{aligned}
&-\frac{\partial}{\partial x}\left[C_{w,w}\frac{1}{2}\vartheta_{wx}^2\vartheta_{wx}\rho_w\right]-\frac{\partial}{\partial x}\left[\phi S_w\left(\overline{\overline{\mathfrak{D}}}_w+\overline{\overline{\mathfrak{D}}}^{*}_{w,w}\right)\frac{\partial}{\partial x}\left(C_{w,w}\frac{1}{2}\rho_w\vartheta_{wx}^2\right)\right]\\
&-\frac{\partial}{\partial y}\left[C_{w,w}\frac{1}{2}\vartheta_{wy}^2\vartheta_{wy}\rho_w\right]-\frac{\partial}{\partial y}\left[\phi S_w\left(\overline{\overline{\mathfrak{D}}}_w+\overline{\overline{\mathfrak{D}}}^{*}_{w,w}\right)\frac{\partial}{\partial y}\left(C_{w,w}\frac{1}{2}\rho_w\vartheta_{wy}^2\right)\right]\\
&-\frac{\partial}{\partial z}\left[C_{w,w}\frac{1}{2}\vartheta_{wz}^2\vartheta_{wz}\rho_w\right]-\frac{\partial}{\partial z}\left[\phi S_w\left(\overline{\overline{\mathfrak{D}}}_w+\overline{\overline{\mathfrak{D}}}^{*}_{w,w}\right)\frac{\partial}{\partial z}\left(C_{w,w}\frac{1}{2}\rho_w\vartheta_{wz}^2\right)\right]-\frac{\partial}{\partial x}\left(p_w\vartheta_{wx}\right)\\
&-\frac{\partial}{\partial y}\left(p_w\vartheta_{wy}\right)-\frac{\partial}{\partial z}\left(p_w\vartheta_{wz}\right)-\frac{\partial}{\partial x}\left(\tau_{wxx}\vartheta_{wx}+\tau_{wxy}\vartheta_{wy}+\tau_{wxz}\vartheta_{wz}\right)\\
&-\frac{\partial}{\partial y}\left(\tau_{wyx}\vartheta_{wx}+\tau_{wyy}\vartheta_{wy}+\tau_{wyz}\vartheta_{wz}\right)-\frac{\partial}{\partial z}\left(\tau_{wzx}\vartheta_{wx}+\tau_{wzy}\vartheta_{wy}+\tau_{wzz}\vartheta_{wz}\right)\\
&-p_w\frac{\partial}{\partial x}\left(\vartheta_{wx}\right)-p_w\frac{\partial}{\partial y}\left(\vartheta_{wy}\right)-p_w\frac{\partial}{\partial z}\left(\vartheta_{wz}\right)-\tau_{wxx}\left(\frac{\partial\vartheta_{wx}}{\partial x}\right)-\tau_{wyy}\left(\frac{\partial\vartheta_{wy}}{\partial y}\right)-\tau_{wzz}\left(\frac{\partial\vartheta_{wz}}{\partial z}\right)\\
&-\tau_{wxy}\left(\frac{\partial\vartheta_{wx}}{\partial y}+\frac{\partial\vartheta_{wy}}{\partial x}\right)-\tau_{wyz}\left(\frac{\partial\vartheta_{wy}}{\partial z}+\frac{\partial\vartheta_{wz}}{\partial y}\right)-\tau_{wzx}\left(\frac{\partial\vartheta_{wz}}{\partial x}+\frac{\partial\vartheta_{wx}}{\partial z}\right)\\
&+C_{w,w}\rho_w\left(g_x\vartheta_{wx}+g_y\vartheta_{wy}+g_z\vartheta_{wz}\right)+\frac{\partial}{\partial x}\left[C_{w,w}\rho_w h_w\vartheta_{wx}\right]+\frac{\partial}{\partial y}\left[C_{w,w}\rho_w h_w\vartheta_{wy}\right]\\
&+\frac{\partial}{\partial z}\left[C_{w,w}\rho_w h_w\vartheta_{wz}\right]\\
&-\frac{\partial}{\partial x}\left[C_{w,g}\frac{1}{2}\vartheta_{gx}^2\vartheta_{gx}\rho_g\right]-\frac{\partial}{\partial x}\left[\phi S_g\left(\overline{\overline{\mathfrak{D}}}_g+\overline{\overline{\mathfrak{D}}}^{*}_{w,g}\right)\frac{\partial}{\partial x}\left(C_{w,g}\frac{1}{2}\rho_g\vartheta_{gx}^2\right)\right]\\
&-\frac{\partial}{\partial y}\left[C_{w,g}\frac{1}{2}\vartheta_{gy}^2\vartheta_{gy}\rho_g\right]-\frac{\partial}{\partial y}\left[\phi S_g\left(\overline{\overline{\mathfrak{D}}}_g+\overline{\overline{\mathfrak{D}}}^{*}_{w,g}\right)\frac{\partial}{\partial y}\left(C_{w,g}\frac{1}{2}\rho_g\vartheta_{gy}^2\right)\right]\\
&-\frac{\partial}{\partial z}\left[C_{w,g}\frac{1}{2}\vartheta_{gz}^2\vartheta_{gz}\rho_g\right]-\frac{\partial}{\partial z}\left[\phi S_g\left(\overline{\overline{\mathfrak{D}}}_g+\overline{\overline{\mathfrak{D}}}^{*}_{w,g}\right)\frac{\partial}{\partial z}\left(C_{w,g}\frac{1}{2}\rho_g\vartheta_{gz}^2\right)\right]-\frac{\partial}{\partial x}\left(p_{w,g}\vartheta_{gx}\right)\\
&-\frac{\partial}{\partial y}\left(p_{w,g}\vartheta_{gy}\right)-\frac{\partial}{\partial z}\left(p_{w,g}\vartheta_{gz}\right)-p_{w,g}\frac{\partial}{\partial x}\left(\vartheta_{gx}\right)-p_{w,g}\frac{\partial}{\partial y}\left(\vartheta_{gy}\right)-p_{w,g}\frac{\partial}{\partial z}\left(\vartheta_{gz}\right)\\
&+C_{w,g}\rho_g\left(g_x\vartheta_{gx}+g_y\vartheta_{gy}+g_z\vartheta_{gz}\right)+\frac{\partial}{\partial x}\left[C_{w,g}\rho_g h_{w*}\vartheta_{gx}\right]+\frac{\partial}{\partial y}\left[C_{w,g}\rho_g h_{w*}\vartheta_{gy}\right]\\
&+\frac{\partial}{\partial z}\left[C_{w,g}\rho_g h_{w*}\vartheta_{gz}\right]+\dot{m}\left\{\left(h_{w*}-h_w\right)+\frac{1}{2}\left[\left(\vartheta_{gx}^2-\vartheta_{wx}^2\right)+\left(\vartheta_{gy}^2-\vartheta_{wy}^2\right)+\left(\vartheta_{gz}^2-\vartheta_{wz}^2\right)\right]\right\}\\
&=\frac{\partial}{\partial t}\left[\phi C_{w,w}\rho_w S_w U_w+\frac{1}{2}\phi C_{w,w}\rho_w S_w\left(\vartheta_{wx}^2+\vartheta_{wy}^2+\vartheta_{wz}^2\right)+\phi C_{w,g}\rho_g S_g U_{w*}+\right.\\
&\qquad\qquad\left.\frac{1}{2}\phi C_{w,g}\rho_g S_g\left(\vartheta_{gx}^2+\vartheta_{gy}^2+\vartheta_{gz}^2\right)\right]. \qquad (4.17)
\end{aligned}$$

Total Energy Balance for the Rock Matrix

$$(1-\phi)\rho_r \frac{\partial U_r}{\partial t} = \frac{\partial}{\partial x}\left(k_{hr}\frac{\partial T}{\partial x}\right) + \frac{\partial}{\partial y}\left(k_{hr}\frac{\partial T}{\partial y}\right) + \frac{\partial}{\partial z}\left(k_{hr}\frac{\partial T}{\partial z}\right). \tag{4.18}$$

The following balance equations express the changes of the entropy of each component with time, which are due to the flows of entropy into the volume element and the presence of an entropy source due to irreversible phenomena inside the volume element. The following terms are considered in the entropy balance for each component: convective entropy flux, diffusive entropy flux, entropy created due to convective heat flux, entropy transport due to temperature gradient, entropy transport due to chemical potential gradient, entropy created by work done by buoyancy forces, entropy created by work done by drag forces, entropy created by work done by mass forces, entropy flux due to velocity gradient, and entropy flux due to interfacial mass transfer.

Entropy Balance for Carbon Dioxide in the Oil Phase

$$\begin{aligned}
&\frac{\partial}{\partial x}\left(C_{CO_2,o}\rho_o\vartheta_{ox}\mathfrak{s}_{CO_2}\right) + \frac{\partial}{\partial x}\left[\frac{\phi S_o\left(\overline{\overline{\mathfrak{D}}}_o + \overline{\overline{\mathfrak{D}}}^*_{CO_2,o}\right)}{T}\eta_{CO_2,o}\frac{\partial}{\partial x}\left(C_{CO_2,o}\rho_o\right)\right] \\
&+\frac{\partial}{\partial y}\left(C_{CO_2,o}\rho_o\vartheta_{oy}\mathfrak{s}_{CO_2}\right) + \frac{\partial}{\partial y}\left[\frac{\phi S_o\left(\overline{\overline{\mathfrak{D}}}_o + \overline{\overline{\mathfrak{D}}}^*_{CO_2,o}\right)}{T}\eta_{CO_2,o}\frac{\partial}{\partial y}\left(C_{CO_2,o}\rho_o\right)\right] \\
&+\frac{\partial}{\partial z}\left(C_{CO_2,o}\rho_o\vartheta_{oz}\mathfrak{s}_{CO_2}\right) + \frac{\partial}{\partial z}\left[\frac{\phi S_o\left(\overline{\overline{\mathfrak{D}}}_o + \overline{\overline{\mathfrak{D}}}^*_{CO_2,o}\right)}{T}\eta_{CO_2,o}\frac{\partial}{\partial z}\left(C_{CO_2,o}\rho_o\right)\right] \\
&+\frac{\partial}{\partial x}\left(C_{CO_2,o}\rho_o\frac{h_{CO_2}}{T}\vartheta_{ox}\right) + \frac{\partial}{\partial y}\left(C_{CO_2,o}\rho_o\frac{h_{CO_2}}{T}\vartheta_{oy}\right) + \frac{\partial}{\partial z}\left(C_{CO_2,o}\rho_o\frac{h_{CO_2}}{T}\vartheta_{oz}\right) \\
&+C_{CO_2,o}\rho_o h_{CO_2}\vartheta_{ox}\frac{\partial}{\partial x}\left(\frac{1}{T}\right) + C_{CO_2,o}\rho_o h_{CO_2}\vartheta_{oy}\frac{\partial}{\partial y}\left(\frac{1}{T}\right) + C_{CO_2,o}\rho_o h_{CO_2}\vartheta_{oz}\frac{\partial}{\partial z}\left(\frac{1}{T}\right)
\end{aligned}$$

$$+\phi S_o\left(\overline{\overline{\mathfrak{D}}}_o+\overline{\overline{\mathfrak{D}}}^*_{CO_2,o}\right)\frac{\partial}{\partial x}\left(C_{CO_2,o}\rho_o\right)\frac{\partial}{\partial x}\left(\frac{\eta_{CO_2,o}}{T}\right)$$

$$+\phi S_o\left(\overline{\overline{\mathfrak{D}}}_o+\overline{\overline{\mathfrak{D}}}^*_{CO_2,o}\right)\frac{\partial}{\partial x}\left(C_{CO_2,o}\rho_o\right)\frac{\partial}{\partial y}\left(\frac{\eta_{CO_2,o}}{T}\right)$$

$$+\phi S_o\left(\overline{\overline{\mathfrak{D}}}_o+\overline{\overline{\mathfrak{D}}}^*_{CO_2,o}\right)\frac{\partial}{\partial x}\left(C_{CO_2,o}\rho_o\right)\frac{\partial}{\partial z}\left(\frac{\eta_{CO_2,o}}{T}\right)+\frac{C_{CO_2,o}\rho_o}{T}\left(\vartheta_{ox}g_x+\vartheta_{oy}g_y+\vartheta_{oz}g_z\right)$$

$$+\mathcal{N}_{CO_2,ogx}\mathfrak{s}_{CO_2}+\mathcal{N}_{CO_2,ogx}\frac{1}{2T}\left(\vartheta^2_{gx}-\vartheta^2_{ox}\right)+\mathcal{N}_{CO_2,ogy}\mathfrak{s}_{CO_2}+\mathcal{N}_{CO_2,ogy}\frac{1}{2T}\left(\vartheta^2_{gy}-\vartheta^2_{oy}\right)$$

$$+\mathcal{N}_{CO_2,ogz}\mathfrak{s}_{CO_2}+\mathcal{N}_{CO_2,ogz}\frac{1}{2T}\left(\vartheta^2_{gz}-\vartheta^2_{oz}\right)+\mathcal{N}_{CO_2,owx}\mathfrak{s}_{CO_2}+\mathcal{N}_{CO_2,owx}\frac{1}{2T}\left(\vartheta^2_{wx}-\vartheta^2_{ox}\right)$$

$$+\mathcal{N}_{CO_2,owy}\mathfrak{s}_{CO_2}+\mathcal{N}_{CO_2,owy}\frac{1}{2T}\left(\vartheta^2_{wy}-\vartheta^2_{oy}\right)+\mathcal{N}_{CO_2,owz}\mathfrak{s}_{CO_2}$$

$$+\mathcal{N}_{CO_2,owz}\frac{1}{2T}\left(\vartheta^2_{wz}-\vartheta^2_{oz}\right)=\frac{\partial}{\partial t}\left(\phi S_o\rho_o C_{CO_2,o}\mathfrak{s}_{CO_2}\right). \tag{4.19}$$

Entropy Balance for Carbon Dioxide in the Gas Phase

$$\frac{\partial}{\partial x}\left(C_{CO_2,g}\rho_g\vartheta_{gx}\mathfrak{s}_{CO_2}\right)+\frac{\partial}{\partial x}\left[\frac{\phi S_g\left(\overline{\overline{\mathfrak{D}}}_g+\overline{\overline{\mathfrak{D}}}^*_{CO_2,g}\right)}{T}\eta_{CO_2,g}\frac{\partial}{\partial x}\left(C_{CO_2,g}\rho_g\right)\right]$$

$$+\frac{\partial}{\partial y}\left(C_{CO_2,g}\rho_g\vartheta_{gy}\mathfrak{s}_{CO_2}\right)+\frac{\partial}{\partial y}\left[\frac{\phi S_g\left(\overline{\overline{\mathfrak{D}}}_g+\overline{\overline{\mathfrak{D}}}^*_{CO_2,g}\right)}{T}\eta_{CO_2,g}\frac{\partial}{\partial y}\left(C_{CO_2,g}\rho_g\right)\right]$$

$$+\frac{\partial}{\partial z}\left(C_{CO_2,g}\rho_g\vartheta_{gz}\mathfrak{s}_{CO_2}\right)+\frac{\partial}{\partial z}\left[\frac{\phi S_g\left(\overline{\overline{\mathfrak{D}}}_g+\overline{\overline{\mathfrak{D}}}^*_{CO_2,g}\right)}{T}\eta_{CO_2,g}\frac{\partial}{\partial z}\left(C_{CO_2,g}\rho_g\right)\right]$$

$$+\frac{\partial}{\partial x}\left(C_{CO_2,g}\rho_g\frac{h_{CO_2,g}}{T}\vartheta_{gx}\right)+\frac{\partial}{\partial y}\left(C_{CO_2,g}\rho_g\frac{h_{CO_2,g}}{T}\vartheta_{gy}\right)+\frac{\partial}{\partial z}\left(C_{CO_2,g}\rho_g\frac{h_{CO_2,g}}{T}\vartheta_{gz}\right)$$

$$+C_{CO_2,g}\rho_g h_{CO_2}\vartheta_{gx}\frac{\partial}{\partial x}\left(\frac{1}{T}\right)+C_{CO_2,g}\rho_g h_{CO_2}\vartheta_{gy}\frac{\partial}{\partial y}\left(\frac{1}{T}\right)+C_{CO_2,g}\rho_g h_{CO_2}\vartheta_{gz}\frac{\partial}{\partial z}\left(\frac{1}{T}\right)$$

$$+\phi S_g\left(\overline{\overline{\mathfrak{D}}}_g+\overline{\overline{\mathfrak{D}}}^*_{CO_2,g}\right)\frac{\partial}{\partial x}\left(C_{CO_2,g}\rho_g\right)\frac{\partial}{\partial x}\left(\frac{\eta_{CO_2,g}}{T}\right)$$

$$+\phi S_g\left(\overline{\overline{\mathfrak{D}}}_g+\overline{\overline{\mathfrak{D}}}^*_{CO_2,g}\right)\frac{\partial}{\partial y}\left(C_{CO_2,g}\rho_g\right)\frac{\partial}{\partial y}\left(\frac{\eta_{CO_2,g}}{T}\right)$$

$$+\phi S_g\left(\overline{\overline{\mathfrak{D}}}_g+\overline{\overline{\mathfrak{D}}}^*_{CO_2,g}\right)\frac{\partial}{\partial z}\left(C_{CO_2,g}\rho_g\right)\frac{\partial}{\partial z}\left(\frac{\eta_{CO_2,g}}{T}\right)+\frac{C_{CO_2,g}\rho_g}{T}\left(\vartheta_{gx}g_x+\vartheta_g g_y+\vartheta_{gz}g_z\right)$$

$$+\frac{F_{CO_2,gBx}\vartheta_{gx}}{T}+\frac{F_{CO_2,gBy}\vartheta_{gy}}{T}+\frac{F_{CO_2,gBz}\vartheta_{gz}}{T}+\frac{F_{CO_2,gDx}\vartheta_{gx}}{T}+\frac{F_{CO_2,gDy}\vartheta_{gy}}{T}$$

$$+\frac{F_{CO_2,gDz}\vartheta_{gz}}{T}+\frac{1}{T}\tau_{gxx}\left(\frac{\partial\vartheta_{gx}}{\partial x}\right)+\frac{1}{T}\tau_{gyy}\left(\frac{\partial\vartheta_{gy}}{\partial y}\right)+\frac{1}{T}\tau_{gzz}\left(\frac{\partial\vartheta_{gz}}{\partial z}\right)$$
$$+\frac{1}{T}\tau_{gxy}\left(\frac{\partial\vartheta_{gx}}{\partial y}+\frac{\partial\vartheta_{gy}}{\partial x}\right)+\frac{1}{T}\tau_{gyz}\left(\frac{\partial\vartheta_{gy}}{\partial z}+\frac{\partial\vartheta_{gz}}{\partial y}\right)+\frac{1}{T}\tau_{gzx}\left(\frac{\partial\vartheta_{gz}}{\partial x}+\frac{\partial\vartheta_{gx}}{\partial z}\right)$$
$$+\mathcal{N}_{CO_2,gox}\mathscr{s}_{CO_2}+\mathcal{N}_{CO_2,goy}\mathscr{s}_{CO_2}+\mathcal{N}_{CO_2,goz}\mathscr{s}_{CO_2}+\mathcal{N}_{CO_2,gox}\frac{1}{2T}\left(\vartheta_{gx}^2-\vartheta_{ox}^2\right)$$
$$+\mathcal{N}_{CO_2,goy}\frac{1}{2T}\left(\vartheta_{gy}^2-\vartheta_{oy}^2\right)+\mathcal{N}_{CO_2,goz}\frac{1}{2T}\left(\vartheta_{gz}^2-\vartheta_{oz}^2\right)=\frac{\partial}{\partial t}\left(\phi\rho_g S_g C_{CO_2,g}\mathscr{s}_{CO_2}\right). \qquad (4.20)$$

Entropy Balance for Carbon Dioxide in the Water Phase

$$\frac{\partial}{\partial x}\left(C_{CO_2,w}\rho_w\vartheta_{wx}\mathscr{s}_{CO_2}\right)+\frac{\partial}{\partial x}\left[\frac{\phi S_w\left(\overline{\overline{\mathfrak{D}}}_w+\overline{\overline{\mathfrak{D}}}^*_{CO_2,w}\right)}{T}\eta_{CO_2,w}\frac{\partial}{\partial x}\left(C_{CO_2,w}\rho_w\right)\right]$$
$$+\frac{\partial}{\partial y}\left(C_{CO_2,w}\rho_w\vartheta_{wy}\mathscr{s}_{CO_2}\right)+\frac{\partial}{\partial y}\left[\frac{\phi S_w\left(\overline{\overline{\mathfrak{D}}}_w+\overline{\overline{\mathfrak{D}}}^*_{CO_2,w}\right)}{T}\eta_{CO_2,w}\frac{\partial}{\partial y}\left(C_{CO_2,w}\rho_w\right)\right]$$
$$+\frac{\partial}{\partial z}\left(C_{CO_2,w}\rho_w\vartheta_{wz}\mathscr{s}_{CO_2}\right)+\frac{\partial}{\partial z}\left[\frac{\phi S_w\left(\overline{\overline{\mathfrak{D}}}_w+\overline{\overline{\mathfrak{D}}}^*_{CO_2,w}\right)}{T}\eta_{CO_2,w}\frac{\partial}{\partial z}\left(C_{CO_2,w}\rho_w\right)\right]$$
$$+\frac{\partial}{\partial x}\left(C_{CO_2,w}\rho_w\frac{h_{CO_2}}{T}\vartheta_{wx}\right)+\frac{\partial}{\partial y}\left(C_{CO_2,w}\rho_w\frac{h_{CO_2}}{T}\vartheta_{wy}\right)+\frac{\partial}{\partial z}\left(C_{CO_2,w}\rho_w\frac{h_{CO_2}}{T}\vartheta_{wz}\right)$$
$$+C_{CO_2,w}\rho_w h_{CO_2}\vartheta_{wx}\frac{\partial}{\partial x}\left(\frac{1}{T}\right)+C_{CO_2,w}\rho_w h_{CO_2}\vartheta_{wy}\frac{\partial}{\partial y}\left(\frac{1}{T}\right)+C_{CO_2,w}\rho_w h_{CO_2}\vartheta_{wz}\frac{\partial}{\partial z}\left(\frac{1}{T}\right)$$
$$+\phi S_w\left(\overline{\overline{\mathfrak{D}}}_w+\overline{\overline{\mathfrak{D}}}^*_{CO_2,w}\right)\frac{\partial}{\partial x}\left(C_{CO_2,w}\rho_w\right)\frac{\partial}{\partial x}\left(\frac{\eta_{CO_2,w}}{T}\right)$$
$$+\phi S_w\left(\overline{\overline{\mathfrak{D}}}_w+\overline{\overline{\mathfrak{D}}}^*_{CO_2,w}\right)\frac{\partial}{\partial y}\left(C_{CO_2,w}\rho_w\right)\frac{\partial}{\partial y}\left(\frac{\eta_{CO_2,w}}{T}\right)$$
$$+\phi S_w\left(\overline{\overline{\mathfrak{D}}}_w+\overline{\overline{\mathfrak{D}}}^*_{CO_2,w}\right)\frac{\partial}{\partial z}\left(C_{CO_2,w}\rho_w\right)\frac{\partial}{\partial z}\left(\frac{\eta_{CO_2,w}}{T}\right)$$
$$+\frac{C_{CO_2,w}\rho_w}{T}\left(\vartheta_{wx}g_x+\vartheta_w g_y+\vartheta_{wz}g_z\right)+\mathcal{N}_{CO_2,wox}\mathscr{s}_{CO_2}+\mathcal{N}_{CO_2,wox}\frac{1}{2T}\left(\vartheta_{wx}^2-\vartheta_{ox}^2\right)$$
$$+\mathcal{N}_{CO_2,woy}\mathscr{s}_{CO_2}+\mathcal{N}_{CO_2,woy}\frac{1}{2T}\left(\vartheta_{wy}^2-\vartheta_{oy}^2\right)+\mathcal{N}_{CO_2,woz}\mathscr{s}_{CO_2}$$
$$+\mathcal{N}_{CO_2,woz}\frac{1}{2T}\left(\vartheta_{wz}^2-\vartheta_{oz}^2\right)=\frac{\partial}{\partial t}\left(\phi S_w\rho_w C_{CO_2,w}\mathscr{s}_{CO_2}\right). \qquad (4.21)$$

Entropy Balance for Oil in the Oil Phase

$$
\begin{aligned}
&\frac{\partial}{\partial x}\left(C_{o,o}\rho_o\vartheta_{ox}\mathscr{s}_o\right)+\frac{\partial}{\partial x}\left[\frac{\phi S_o\left(\overline{\overline{\mathfrak{D}}}_o+\overline{\overline{\mathfrak{D}}}^{*}_{o,o}\right)}{T}\eta_o\frac{\partial}{\partial x}\left(C_{o,o}\rho_o\right)\right]\\
&+\frac{\partial}{\partial y}\left(C_{o,o}\rho_o\vartheta_{oy}\mathscr{s}_o\right)+\frac{\partial}{\partial y}\left[\frac{\phi S_o\left(\overline{\overline{\mathfrak{D}}}_o+\overline{\overline{\mathfrak{D}}}^{*}_{o,o}\right)}{T}\eta_o\frac{\partial}{\partial y}\left(C_{o,o}\rho_o\right)\right]\\
&+\frac{\partial}{\partial z}\left(C_{o,o}\rho_o\vartheta_{oz}s_o\right)+\frac{\partial}{\partial z}\left[\frac{\phi S_o\left(\overline{\overline{\mathfrak{D}}}_o+\overline{\overline{\mathfrak{D}}}^{*}_{o,o}\right)}{T}\eta_o\frac{\partial}{\partial z}\left(C_{o,o}\rho_o\right)\right]\\
&+\frac{\partial}{\partial x}\left(C_{o,o}\rho_o\frac{h_o}{T}\vartheta_{ox}\right)+\frac{\partial}{\partial y}\left(C_{o,o}\rho_o\frac{h_o}{T}\vartheta_{oy}\right)+\frac{\partial}{\partial z}\left(C_{o,o}\rho_o\frac{h_o}{T}\vartheta_{oz}\right)\\
&+C_{o,o}\rho_o h_o\vartheta_{ox}\frac{\partial}{\partial x}\left(\frac{1}{T}\right)+C_{o,o}\rho_o h_o\vartheta_{oy}\frac{\partial}{\partial y}\left(\frac{1}{T}\right)+C_{o,o}\rho_o h_o\vartheta_{oz}\frac{\partial}{\partial z}\left(\frac{1}{T}\right)\\
&+\phi S_o\left(\overline{\overline{\mathfrak{D}}}_o+\overline{\overline{\mathfrak{D}}}^{*}_{o,o}\right)\frac{\partial}{\partial x}\left(C_{o,o}\rho_o\right)\frac{\partial}{\partial x}\left(\frac{\eta_o}{T}\right)+\phi S_o\left(\overline{\overline{\mathfrak{D}}}_o+\overline{\overline{\mathfrak{D}}}^{*}_{o,o}\right)\frac{\partial}{\partial y}\left(C_{o,o}\rho_o\right)\frac{\partial}{\partial y}\left(\frac{\eta_o}{T}\right)\\
&+\phi S_o\left(\overline{\overline{\mathfrak{D}}}_o+\overline{\overline{\mathfrak{D}}}^{*}_{o,o}\right)\frac{\partial}{\partial z}\left(C_{o,o}\rho_o\right)\frac{\partial}{\partial z}\left(\frac{\eta_o}{T}\right)+\frac{C_{o,o}\rho_o}{T}\left(\vartheta_{ox}g_x+\vartheta_o g_y+\vartheta_{oz}g_z\right)\\
&+\frac{1}{T}\tau_{oxx}\left(\frac{\partial\vartheta_{ox}}{\partial x}\right)+\frac{1}{T}\tau_{oyy}\left(\frac{\partial\vartheta_{oy}}{\partial y}\right)+\frac{1}{T}\tau_{ozz}\left(\frac{\partial\vartheta_{oz}}{\partial z}\right)+\frac{1}{T}\tau_{oxy}\left(\frac{\partial\vartheta_{ox}}{\partial y}+\frac{\partial\vartheta_{oy}}{\partial x}\right)\\
&+\frac{1}{T}\tau_{oyz}\left(\frac{\partial\vartheta_{oy}}{\partial z}+\frac{\partial\vartheta_{oz}}{\partial y}\right)+\frac{1}{T}\tau_{ozx}\left(\frac{\partial\vartheta_{oz}}{\partial x}+\frac{\partial\vartheta_{ox}}{\partial z}\right)=\frac{\partial}{\partial t}\left(\phi S_o\rho_o C_{o,o}\mathscr{s}_o\right).
\end{aligned}
\tag{4.22}
$$

Entropy Balance for Water

$$
\begin{aligned}
&\frac{\partial}{\partial x}\left(C_{w,w}\rho_w\vartheta_{wx}\mathscr{s}_w\right)+\frac{\partial}{\partial x}\left[\frac{\phi S_w\left(\overline{\overline{\mathfrak{D}}}_w+\overline{\overline{\mathfrak{D}}}^{*}_{w,w}\right)}{T}\eta_w\frac{\partial}{\partial x}\left(C_{w,w}\rho_w\right)\right]\\
&+\frac{\partial}{\partial y}\left(C_{w,w}\rho_w\vartheta_{wy}\mathscr{s}_w\right)+\frac{\partial}{\partial y}\left[\frac{\phi S_w\left(\overline{\overline{\mathfrak{D}}}_w+\overline{\overline{\mathfrak{D}}}^{*}_{w,w}\right)}{T}\eta_w\frac{\partial}{\partial y}\left(C_{w,w}\rho_w\right)\right]\\
&+\frac{\partial}{\partial z}\left(C_{w,w}\rho_w\vartheta_{wz}\mathscr{s}_w\right)+\frac{\partial}{\partial z}\left[\frac{\phi S_w\left(\overline{\overline{\mathfrak{D}}}_w+\overline{\overline{\mathfrak{D}}}^{*}_{w,w}\right)}{T}\eta_w\frac{\partial}{\partial z}\left(C_{w,w}\rho_w\right)\right]\\
&+\frac{\partial}{\partial x}\left(C_{w,w}\rho_w\frac{h_w}{T}\vartheta_{wx}\right)+\frac{\partial}{\partial y}\left(C_{w,w}\rho_w\frac{h_w}{T}\vartheta_{wy}\right)+\frac{\partial}{\partial z}\left(C_{w,w}\rho_w\frac{h_w}{T}\vartheta_{wz}\right)
\end{aligned}
$$

$$
\begin{aligned}
&+C_{w,w}\rho_w h_w \vartheta_{wx}\frac{\partial}{\partial x}\left(\frac{1}{T}\right)+C_{w,w}\rho_w h_w \vartheta_{wy}\frac{\partial}{\partial y}\left(\frac{1}{T}\right)+C_{w,w}\rho_w h_w \vartheta_{wz}\frac{\partial}{\partial z}\left(\frac{1}{T}\right)\\
&+\phi S_w\left(\overline{\overline{\mathfrak{D}}}_w+\overline{\overline{\mathfrak{D}}}^{*}_{w,w}\right)\frac{\partial}{\partial x}\left(C_{w,w}\rho_w\right)\frac{\partial}{\partial x}\left(\frac{\eta_w}{T}\right)+\phi S_w\left(\overline{\overline{\mathfrak{D}}}_w+\overline{\overline{\mathfrak{D}}}^{*}_{w,w}\right)\frac{\partial}{\partial y}\left(C_{w,w}\rho_w\right)\frac{\partial}{\partial y}\left(\frac{\eta_w}{T}\right)\\
&+\phi S_w\left(\overline{\overline{\mathfrak{D}}}_w+\overline{\overline{\mathfrak{D}}}^{*}_{w,w}\right)\frac{\partial}{\partial z}\left(C_{w,w}\rho_w\right)\frac{\partial}{\partial z}\left(\frac{\eta_w}{T}\right)+\frac{C_{w,w}\rho_w}{T}\left(\vartheta_{wx}g_x+\vartheta_w g_y+\vartheta_{wz}g_z\right)\\
&+\frac{1}{T}\tau_{wxx}\left(\frac{\partial\vartheta_{wx}}{\partial x}\right)+\frac{1}{T}\tau_{wyy}\left(\frac{\partial\vartheta_{wy}}{\partial y}\right)+\frac{1}{T}\tau_{wzz}\left(\frac{\partial\vartheta_{wz}}{\partial z}\right)+\frac{1}{T}\tau_{wxy}\left(\frac{\partial\vartheta_{wx}}{\partial y}+\frac{\partial\vartheta_{wy}}{\partial x}\right)\\
&+\frac{1}{T}\tau_{wyz}\left(\frac{\partial\vartheta_{wy}}{\partial z}+\frac{\partial\vartheta_{wz}}{\partial y}\right)+\frac{1}{T}\tau_{wzx}\left(\frac{\partial\vartheta_{wz}}{\partial x}+\frac{\partial\vartheta_{wx}}{\partial z}\right)+\frac{\partial}{\partial x}\left(C_{w,g}\rho_g\vartheta_{gx}s_{w\circledast}\right)\\
&+\frac{\partial}{\partial x}\left[\frac{\phi S_g\left(\overline{\overline{\mathfrak{D}}}_g+\overline{\overline{\mathfrak{D}}}^{*}_{w,g}\right)}{T}\eta_{w\circledast}\frac{\partial}{\partial x}\left(C_{w,g}\rho_g\right)\right]+\frac{\partial}{\partial y}\left(C_{w,g}\rho_g\vartheta_{gy}s_{w\circledast}\right)\\
&+\frac{\partial}{\partial y}\left[\frac{\phi S_g\left(\overline{\overline{\mathfrak{D}}}_g+\overline{\overline{\mathfrak{D}}}^{*}_{w,g}\right)}{T}\eta_{w\circledast}\frac{\partial}{\partial y}\left(C_{w,g}\rho_g\right)\right]+\frac{\partial}{\partial z}\left(C_{w,g}\rho_g\vartheta_{gz}s_{w\circledast}\right)\\
&+\frac{\partial}{\partial z}\left[\frac{\phi S_g\left(\overline{\overline{\mathfrak{D}}}_g+\overline{\overline{\mathfrak{D}}}^{*}_{w,g}\right)}{T}\eta_{w\circledast}\frac{\partial}{\partial z}\left(C_{w,g}\rho_g\right)\right]+\frac{\partial}{\partial x}\left(C_{w,g}\rho_g\frac{h_{w\circledast}}{T}\vartheta_{gx}\right)\\
&+\frac{\partial}{\partial y}\left(C_{w,g}\rho_g\frac{h_{w\circledast}}{T}\vartheta_{gy}\right)+\frac{\partial}{\partial z}\left(C_{w,g}\rho_g\frac{h_{w\circledast}}{T}\vartheta_{gz}\right)+C_{w,g}\rho_g h_{w\circledast}\vartheta_{gx}\frac{\partial}{\partial x}\left(\frac{1}{T}\right)\\
&+C_{w,g}\rho_g h_{w\circledast}\vartheta_{gy}\frac{\partial}{\partial y}\left(\frac{1}{T}\right)+C_{w,g}\rho_g h_{w\circledast}\vartheta_{gz}\frac{\partial}{\partial z}\left(\frac{1}{T}\right)\\
&+\phi S_g\left(\overline{\overline{\mathfrak{D}}}_g+\overline{\overline{\mathfrak{D}}}^{*}_{w,g}\right)\frac{\partial}{\partial x}\left(C_{w,g}\rho_g\right)\frac{\partial}{\partial x}\left(\frac{\eta_{w\circledast}}{T}\right)+\phi S_g\left(\overline{\overline{\mathfrak{D}}}_g+\overline{\overline{\mathfrak{D}}}^{*}_{w,g}\right)\frac{\partial}{\partial y}\left(C_{w,g}\rho_g\right)\frac{\partial}{\partial y}\left(\frac{\eta_{w\circledast}}{T}\right)\\
&+\phi S_g\left(\overline{\overline{\mathfrak{D}}}_g+\overline{\overline{\mathfrak{D}}}^{*}_{w,g}\right)\frac{\partial}{\partial z}\left(C_{w,g}\rho_g\right)\frac{\partial}{\partial z}\left(\frac{\eta_{w\circledast}}{T}\right)+\frac{C_{w,g}\rho_g}{T}\left(\vartheta_{gx}g_x+\vartheta_g g_y+\vartheta_{gz}g_z\right)\\
&+\left(s_{w\circledast}-s_w\right)\dot{m}+\dot{m}\frac{1}{2T}\left\{\left(\vartheta_{gx}^2-\vartheta_{wx}^2\right)+\left(\vartheta_{gy}^2-\vartheta_{wy}^2\right)+\left(\vartheta_{gz}^2-\vartheta_{wz}^2\right)\right\}\\
&=\frac{\partial}{\partial t}\left(\phi S_w\rho_w C_{w,w}s_w+\phi S_g\rho_g C_{w,g}s_{w\circledast}\right)
\end{aligned}
\tag{4.23}
$$

Entropy Balance for the Rock Matrix

$$
\begin{aligned}
&\frac{\partial}{\partial x}\left(\frac{k_{hr}}{T}\frac{\partial T}{\partial x}\right)+\frac{\partial}{\partial y}\left(\frac{k_{hr}}{T}\frac{\partial T}{\partial y}\right)+\frac{\partial}{\partial z}\left(\frac{k_{hr}}{T}\frac{\partial T}{\partial z}\right)+\left(k_{hr}\frac{\partial T}{\partial x}\right)\frac{\partial}{\partial x}\left(\frac{1}{T}\right)+\left(k_{hr}\frac{\partial T}{\partial y}\right)\frac{\partial}{\partial y}\left(\frac{1}{T}\right)\\
&+\left(k_{hr}\frac{\partial T}{\partial z}\right)\frac{\partial}{\partial z}\left(\frac{1}{T}\right)=(1-\phi)\rho_r\frac{\partial s_r}{\partial t}.
\end{aligned}
\tag{4.24}
$$

These partial differential equations represent the conservation of mass, momentum, total energy, and entropy for the non-isothermal and non-equilibrium immiscible displacement of oil by carbon dioxide and brine. They require additional constitutive relationships, constraint equations, and initial and boundary conditions. Table 4.1 (on the next page) lists the constitutive relationships and constraints. Appendix A contains a possible set of boundary conditions.

Table 4.1 - Constitutive Relationships and Constraints

1. $S_o + S_w + S_g = 1$
2. $C_{CO_2,o} = C_{CO_2,o}(x, y, z, t, p, T)$
3. $C_{CO_2,w} = C_{CO_2,w}(x, y, z, t, p, T)$
4. $C_{CO_2,g} = C_{CO_2,g}(x, y, z, t, p, T)$
5. $C_{CO_2,o} + C_{o,o} = 1$
6. $C_{CO_2,g} + C_{w,g} = 1$
7. $C_{CO_2,w} + C_{w,w} = 1$
8. $p_o = p_o(x, y, z, t)$
9. $p_w = p_w(x, y, z, t)$
10. $p_g = p_g(x, y, z, t)$
11. $P_{cow} = p_o - p_w$
12. $P_{cgo} = p_g - p_o$
13. $\mathcal{X}_{CO_2,og} = -\mathcal{X}_{CO_2,go}$
14. $\mathcal{X}_{CO_2,ow} = -\mathcal{X}_{CO_2,wo}$
15. $f_{io}^{I} = f_{io}^{I}(x, y, z, t, p, T)$
16. $f_{ig}^{I} = f_{ig}^{I}(x, y, z, t, p, T)$
17. $f_{iw}^{I} = f_{iw}^{I}(x, y, z, t, p, T)$
18. $f_{io}^{I} = f_{ig}^{I}$ i=CO$_2$, o, w I=interface o/g
19. $f_{io}^{I} = f_{iw}^{I}$ i=CO$_2$, o, w I=interface o/w
20. $\rho_o = \rho_o\left(p_o, T, C_{CO_2,o}, x, y, z, t\right)$
21. $\rho_g = \rho_g\left(p_g, T, C_{CO_2,g}, x, y, z, t\right)$
22. $\rho_w = \rho_w\left(p_w, T, C_{CO_2,w}, x, y, z, t\right)$
23. $\mu_o = \mu_o\left(p_o, T, C_{CO_2,o}, x, y, z, t\right)$
24. $\mu_g = \mu_g\left(p_g, T, C_{CO_2,g}, x, y, z, t\right)$
25. $\mu_w = \mu_w\left(p_w, T, C_{CO_2,w}, x, y, z, t\right)$
26. ϕ=constant
27. g=constant
28. $k_o = k_o\left(S_o, S_g, S_w, k\right)$
29. $k_g = k_g\left(S_o, S_g, S_w, k\right)$
30. $k_w = k_w\left(S_o, S_g, S_w, k\right)$
31. $\overline{\overline{\mathcal{D}}}_{CO_2,o} = \overline{\overline{\mathcal{D}}}_o + \overline{\overline{\mathcal{D}}}_{CO_2,o} = \overline{\overline{\mathcal{D}}}_{CO_2,o}\left(\mathcal{D}_{LCO_2,o}, \mathcal{D}_{TCO_2,o}\right)$

32. $\overline{\overline{\mathcal{D}}}_{CO_2,g} = \overline{\overline{\mathcal{D}}}_g + \overline{\overline{\mathcal{D}}}^*_{CO_2,g} = \overline{\overline{\mathcal{D}}}_{CO_2,g}\left(\mathcal{D}_{LCO_2,g}, \mathcal{D}_{TCO_2,g}\right)$

33. $\overline{\overline{\mathcal{D}}}_{CO_2,w} = \overline{\overline{\mathcal{D}}}_w + \overline{\overline{\mathcal{D}}}^*_{CO_2,w} = \overline{\overline{\mathcal{D}}}_{CO_2,w}\left(\mathcal{D}_{LCO_2,w}, \mathcal{D}_{TCO_2,w}\right)$

34. $\overline{\overline{\mathcal{D}}}_{w,w} = \overline{\overline{\mathcal{D}}}_w + \overline{\overline{\mathcal{D}}}^*_{w,w} = \overline{\overline{\mathcal{D}}}_{w,w}\left(\mathcal{D}_{Lw,w}, \mathcal{D}_{Tw,w}\right)$

35. $\overline{\overline{\mathcal{D}}}_{w,g} = \overline{\overline{\mathcal{D}}}_g + \overline{\overline{\mathcal{D}}}^*_{w,g} = \overline{\overline{\mathcal{D}}}_{w,g}\left(\mathcal{D}_{Lw,g}, \mathcal{D}_{Tw,g}\right)$

36. $\overline{\overline{\mathcal{D}}}_{o,o} = \overline{\overline{\mathcal{D}}}_o + \overline{\overline{\mathcal{D}}}^*_{o,o} = \overline{\overline{\mathcal{D}}}_{o,o}\left(\mathcal{D}_{Lo,o}, \mathcal{D}_{To,o}\right)$

37. $\mathcal{N}_{CO_2,og} = \mathcal{N}_{CO_2,og}\left(k^{og}_{CO_2}, a_{og}, \phi, \rho_o, S_o, C_{CO_2,o}, C^I_{CO_2,o}, x, y, z, t\right)$

38. $\mathcal{N}_{CO_2,go} = \mathcal{N}_{CO_2,go}\left(k^{go}_{CO_2}, a_{og}, \phi, \rho_g, S_g, C_{CO_2,g}, C^I_{CO_2,g}, x, y, z, t\right)$

39. $\mathcal{N}_{CO_2,ow} = \mathcal{N}_{CO_2,ow}\left(k^{ow}_{CO_2}, a_{ow}, \phi, \rho_o, S_o, C_{CO_2,o}, C^I_{CO_2,o}, x, y, z, t\right)$

40. $\mathcal{N}_{CO_2,wo} = \mathcal{N}_{CO_2,wo}\left(k^{wo}_{CO_2}, a_{ow}, \phi, \rho_w, S_w, C_{CO_2,w}, C^I_{CO_2,w}, x, y, z, t\right)$

41. $\dot{m} = \dot{m}(p, T, x, y, z, t)$

42. $h_g = h_g\left(p, T, C_{CO_2,g}, x, y, z, t\right)$

43. $h_w = h_w\left(p, T, C_{CO_2,w}, x, y, z, t\right)$

44. $h_{wv} = h_{wv}\left(p, T, C_{CO_2,g}, x, y, z, t\right)$

45. $h_o = h_o\left(p, T, C_{CO_2,o}, x, y, z, t\right)$

46. $U_g = h_g - \dfrac{p_g}{\rho_g} = U_g\left(p, T, C_{CO_2,g}, x, y, z, t\right)$

47. $U_w = h_w - \dfrac{p_w}{\rho_w} = U_w\left(p, T, C_{CO_2,w}, x, y, z, t\right)$

48. $U_o = h_o - \dfrac{p_o}{\rho_o} = U_o\left(p, T, C_{CO_2,o}, x, y, z, t\right)$

49. $U_{wv} = h_{wv} - \dfrac{p_g}{\rho_g} = U_{wv}\left(p, T, C_{CO_2,g}, x, y, z, t\right)$

50. $U_r = U_r(T, x, y, z, t)$

51. $s_g = s_g\left(U_g, \rho_g^{-1}, C_{CO_2,g}, x, y, z, t\right)$

52. $s_w = s_w\left(U_w, \rho_w^{-1}, C_{CO_2,w}, x, y, z, t\right)$

53. $s_{wv} = s_{wv}\left(U_{wv}, \rho_g^{-1}, C_{CO_2,g}, x, y, z, t\right)$

54. $s_o = s_o\left(U_o, \rho_o^{-1}, C_{CO_2,o}, x, y, z, t\right)$

55. $\eta_g = U_g + \dfrac{p_g}{\rho_g} - T_g s_g = \eta_g\left(p, T, C_{CO_2,g}, x, y, z, t\right)$

56. $\eta_w = U_w + \dfrac{p_w}{\rho_w} - T_w s_w = \eta_w\left(p, T, C_{CO_2,w}, x, y, z, t\right)$

57. $\eta_{w*} = U_{w*} + \frac{p_g}{\rho_g} - T_g s_{w*} = \eta_{w*}(p, T, C_{CO_2,g}, x, y, z, t)$

58. $\eta_o = U_o + \frac{p_o}{\rho_o} - T_o s_o = \eta_o(p, T, C_{CO_2,o}, x, y, z, t)$

59. $Z = Z(x,y,z)$ fixed coordinates

According to Perkins and Johnston[26], the dispersion tensor consists of molecular diffusion and convective terms. Bear and Buchlin[91] conducted a thorough study on transport processes of materials in porous media and showed that for porous media that are isotropic with respect to dispersion and where an orthonormal coordinate system parallel to the directional flow is chosen, the dispersion tensor becomes

$$\overline{\overline{\mathcal{D}}} = \begin{bmatrix} \mathcal{D}_L & 0 & 0 \\ 0 & \mathcal{D}_T & 0 \\ 0 & 0 & \mathcal{D}_T \end{bmatrix}. \tag{4.25}$$

Also, Newtonian fluids were assumed. Therefore, the following relationships for the shear-stress components are true.

$$\tau_{xx} = -2\mu \frac{\partial \vartheta_x}{\partial x} + \frac{2}{3}\mu\left(\frac{\partial \vartheta_x}{\partial x} + \frac{\partial \vartheta_y}{\partial y} + \frac{\partial \vartheta_z}{\partial z}\right), \tag{4.26}$$

$$\tau_{yy} = -2\mu \frac{\partial \vartheta_y}{\partial y} + \frac{2}{3}\mu\left(\frac{\partial \vartheta_x}{\partial x} + \frac{\partial \vartheta_y}{\partial y} + \frac{\partial \vartheta_z}{\partial z}\right), \tag{4.27}$$

$$\tau_{zz} = -2\mu \frac{\partial \vartheta_z}{\partial z} + \frac{2}{3}\mu\left(\frac{\partial \vartheta_x}{\partial x} + \frac{\partial \vartheta_y}{\partial y} + \frac{\partial \vartheta_z}{\partial z}\right), \tag{4.28}$$

$$\tau_{xy} = \tau_{yx} = -\mu\left(\frac{\partial \vartheta_x}{\partial y} + \frac{\partial \vartheta_y}{\partial x}\right), \tag{4.29}$$

$$\tau_{yz} = \tau_{zy} = -\mu\left(\frac{\partial \vartheta_y}{\partial z} + \frac{\partial \vartheta_z}{\partial y}\right), \tag{4.30}$$

$$\tau_{zx} = \tau_{xz} = -\mu\left(\frac{\partial \vartheta_z}{\partial x} + \frac{\partial \vartheta_x}{\partial z}\right). \tag{4.31}$$

For mass transfer across the inteface, the two film theory was assumed to be valid. The theory assumes that the phases are in equilibrium at the actual points of contact at the interface, and the bulk of each phase being well mixed; thus, the flux equations can be written as[89]

$$\mathcal{N}_{ijl} = k_i^{jl} a_{jl} \phi S_j \left(\rho_j C_{ij} - \rho_j C_{ij}^{Ijl} \right) \tag{4.32}$$

where,

$\mathcal{N}_{ijl}$ = mass transfer rate of component i in or out the j phase through the jl interface,

k_i^{jl} = local mass transfer coefficient of component i in j phase related to the jl interface,

a_{jl} = interfacial area between phase j and l,

C_{ij} = average mass fraction of component i in the bulk of j phase,

C_{ij}^{Ijl} = mass fraction of component i in j phase at the jl interface.

Furthermore, Darcy's law for flow in porous media was assumed to be valid. Thus, Darcy's equation, which can be expressed as follows, applies.

$$\bar{\vartheta}_j = -\frac{\bar{\bar{k}}_j}{\mu_j} \left(\nabla p_j + \rho_j g \nabla Z \right). \tag{4.33}$$

4.2 - Derivation of Scaling Groups

This section deals with the derivation of similarity groups which are used to design experiments for a non-isothermal and non-equilibrium carbon dioxide WAG process. There are two approaches for deriving the similarity groups: Inspectional Analysis and Dimensional Analysis. Inspectional Analysis requires the variables in a set of equations which fully describe the whole process. In almost all instances, the equations describing a flow process are partial differential equations, and the relevant boundary and initial conditions need to be specified for the process to be completely described. Dimensional Analysis requires knowledge of all of the relevant variables influencing the process. This method is employed to derive the similarity groups when the partial differential equations describing the flow process of interest are not known. Geertsma, Croes, and Schwarz[92] showed that Dimensional Analysis often yields a larger set of similarity groups than inspectional analysis, but the physical meaning of the similarity groups themselves is more apparent from Inspectional Analysis. For this reason, Inspectional Analysis is often preferred. Dimensional Analysis is always used in conjunction with Inspectional Analysis to ensure that important groups are not omitted. Both of these methods have been used extensively by many other researchers to design their physical models[3,92-97].

4.2.1 - Inspectional Analysis

The procedure to derive the similarity groups by this method is to first express the governing partial differential equations, initial and boundary conditions, constitutive relationships, and constraints in terms of the dimensionless variables and their reference quantities. In other words, it is necessary to divide each variable and or property by some characteristic reference quantity. The following example can clearly illustrate this step. The general property M can be written as $M = M_D M_R$, where M_D is the dimensionless form of the property M, and M_R some constant characteristic reference quantity. Replacing M with $M_D M_R$ in the governing partial differential equations, as well as in the constraints, constitutive relationships, initial and boundary conditions, results in an equation with the form as shown below for the mass balance of carbon dioxide in the oil phase. Appendix B lists the dimensionless form of the momentum, energy and entropy balances for carbon dioxide in the oil phase.

Mass Balance for CO_2 in the Oil Phase in Dimensionless Form

$$\left\{C_{CO_2,oR}\rho_{oR}\frac{k_{oR}}{\mu_{oR}}\frac{p_{oR}}{x_R^2}\right\}\frac{\partial}{\partial x_D}\left[C_{CO_2,oD}\rho_{oD}\frac{k_{oD}}{\mu_{oD}}\frac{\partial p_{oD}}{\partial x_D}\right]+$$

$$\left\{C_{CO_2,oR}\rho_{oR}^2 g_{xR}\frac{k_{oR}}{\mu_{oR}}\frac{Z_R}{x_R^2}\right\}\frac{\partial}{\partial x_D}\left[C_{CO_2,oD}\rho_{oD}^2 g_{xD}\frac{k_{oD}}{\mu_{oD}}\frac{\partial Z_D}{\partial x_D}\right]+$$

$$\left\{\frac{\phi_R S_{oR}\mathcal{D}_{LoR}C_{CO_2,oR}\rho_{oR}}{x_R^2}\right\}\frac{\partial}{\partial x_D}\left[\phi_D S_{oD}\mathcal{D}_{LoD}\frac{\partial}{\partial x_D}\left(C_{CO_2,oD}\rho_{oD}\right)\right]+$$

$$\left\{\frac{\phi_R S_{oR}\mathcal{D}^*_{LCO_2,oR}C_{CO_2,oR}\rho_{oR}}{x_R^2}\right\}\frac{\partial}{\partial x_D}\left[\phi_D S_{oD}\mathcal{D}^*_{LCO_2,oD}\frac{\partial}{\partial x_D}\left(C_{CO_2,oD}\rho_{oD}\right)\right]+$$

$$\left\{C_{CO_2,oR}\rho_{oR}\frac{k_{oR}}{\mu_{oR}}\frac{p_{oR}}{y_R^2}\right\}\frac{\partial}{\partial y_D}\left[C_{CO_2,oD}\rho_{oD}\frac{k_{oD}}{\mu_{oD}}\frac{\partial p_{oD}}{\partial y_D}\right]+$$

$$\left\{C_{CO_2,oR}\rho_{oR}^2 g_{yR}\frac{k_{oR}}{\mu_{oR}}\frac{Z_R}{y_R^2}\right\}\frac{\partial}{\partial y_D}\left[C_{CO_2,oD}\rho_{oD}^2 g_{yD}\frac{k_{oD}}{\mu_{oD}}\frac{\partial Z_D}{\partial y_D}\right]+$$

$$\left\{\frac{\phi_R S_{oR}\mathcal{D}_{ToR}C_{CO_2,oR}\rho_{oR}}{y_R^2}\right\}\frac{\partial}{\partial y_D}\left[\phi_D S_{oD}\mathcal{D}_{ToD}\frac{\partial}{\partial y_D}\left(C_{CO_2,oD}\rho_{oD}\right)\right]+$$

$$\begin{aligned}
&\left\{\frac{\phi_R S_{oR} \mathcal{D}^{*}_{TCO_2,oR} C_{CO_2,oR} \rho_{oR}}{y_R^2}\right\} \frac{\partial}{\partial y_D}\left[\phi_D S_{oD} \mathcal{D}^{*}_{TCO_2,oD} \frac{\partial}{\partial y_D}\left(C_{CO_2,oD} \rho_{oD}\right)\right] + \\
&\left\{C_{CO_2,oR} \rho_{oR} \frac{k_{oR}}{\mu_{oR}} \frac{p_{oR}}{z_R^2}\right\} \frac{\partial}{\partial z_D}\left[C_{CO_2,oD} \rho_{oD} \frac{k_{oD}}{\mu_{oD}} \frac{\partial p_{oD}}{\partial z_D}\right] + \\
&\left\{C_{CO_2,oR} \rho_{oR}^2 g_{zR} \frac{k_{oR}}{\mu_{oR}} \frac{Z_R}{z_R^2}\right\} \frac{\partial}{\partial z_D}\left[C_{CO_2,oD} \rho_{oD}^2 g_{zD} \frac{k_{oD}}{\mu_{oD}} \frac{\partial Z_D}{\partial z_D}\right] + \\
&\left\{\frac{\phi_R S_{oR} \mathcal{D}_{ToR} C_{CO_2,oR} \rho_{oR}}{z_R^2}\right\} \frac{\partial}{\partial z_D}\left[\phi_D S_{oD} \mathcal{D}_{ToD} \frac{\partial}{\partial z_D}\left(C_{CO_2,oD} \rho_{oD}\right)\right] + \\
&\left\{\frac{\phi_R S_{oR} \mathcal{D}^{*}_{TCO_2,oR} C_{CO_2,oR} \rho_{oR}}{z_R^2}\right\} \frac{\partial}{\partial z_D}\left[\phi_D S_{oD} \mathcal{D}^{*}_{TCO_2,oD} \frac{\partial}{\partial z_D}\left(C_{CO_2,oD} \rho_{oD}\right)\right] + \\
&\mathcal{N}_{CO_2,ogR} \mathcal{N}_{CO_2,ogD} + \mathcal{N}_{CO_2,owR} \mathcal{N}_{CO_2,owD} \\
&= \left\{\frac{\phi_R S_{oR} \rho_{oR} C_{CO_2,oR}}{t_R}\right\} \frac{\partial}{\partial t_D}\left(\phi_D S_{oD} \rho_{oD} C_{CO_2,oD}\right) \qquad (4.34)
\end{aligned}$$

For other components, their dimensionless balances can be written in a similar manner. The reference quantities in the braces represent the coefficient for that term in the equation. All coefficients have the same units. To obtain similarity groups, the entire equation is divided by any one of these coefficients. This gives the dimensionless forms of the equations and their similarity groups. Similarly, the dimensionless forms of other governing equations are obtained in the same manner. They are included in Appendix B. Table 4.2 lists the similarity groups and their physical meanings.

Table 4.2 - Similarity Groups From Inspectional Analysis.

Now, let $x_R=L$, $y_R=W$, and $z_R=H$

Group	Physical Meaning
1. ϕ_R	porosity
2. $\frac{L}{W}$	geometric scaling factor
3. $\frac{H}{W}$	geometric scaling factor
4. $\frac{\phi_R S_{oR} \mu_{oR} L^2}{k_{oR} p_{oR} t_R}$	time scaling factor
5. $\frac{\rho_{oR} g_R H}{p_{oR}}$	ratio of gravitational to viscous forces
6. $\frac{\rho_{gR}}{\rho_{oR}}$	ratio of gas to oil density
7. $\frac{\rho_{wR}}{\rho_{oR}}$	ratio of water to oil density
8. $\frac{\mu_{oR} k_{gR}}{\mu_{gR} k_{oR}}$	gas-oil mobility ratio
9. $\frac{\mu_{oR} k_{wR}}{\mu_{wR} k_{oR}}$	water-oil mobility ratio
10. $\frac{S_{gR}}{S_{oR}}$	ratio of gas to oil saturation
11. $\frac{S_{wR}}{S_{oR}}$	ratio of water to oil saturation
12. $\frac{S_{wiR}}{S_{oiR}}$	ratio of initial water to initial oil saturation
13. $\frac{p_{prodR}}{p_{oR}}$	ratio of production to oil pressure
14. $\frac{P_{cowR}}{p_{cgoR}}$	ratio of oil-water capillary to gas-oil capillary pressure
16. $\frac{p_{wR}}{p_{oR}}$	ratio of water to oil pressure
17. $\frac{p_{CO_2,gR}}{p_{w\text{[illegible]},gR}}$	ratio of CO_2 partial pressure to water vapour partial pressure in the gas phase
18. $\frac{S_{oR} \mu_{oR} \phi_R \mathcal{D}_{LCO_2,oR}}{k_{oR} p_{oR}}$	ratio of dispersive forces to viscous forces

Table 4.2 - (Continued)

Group	Physical Meaning
19. $\frac{\mathcal{D}_{TCO_2,oR}}{\mathcal{D}_{LCO_2,oR}}$	ratio of transverse dispersion to longitudinal dispersion of CO_2 in the oil phase
20. $\frac{\mathcal{D}_{LCO_2,gR}}{\mathcal{D}_{TCO_2,gR}}$	ratio of longitudinal dispersion to transverse dispersion of CO_2 in the gas phase
21. $\frac{\mathcal{D}_{LCO_2,wR}}{\mathcal{D}_{TCO_2,wR}}$	ratio of longitudinal dispersion to transverse dispersion of CO_2 in the water phase
22. $\frac{\mathcal{D}_{Lo,oR}}{\mathcal{D}_{To,oR}}$	ratio of longitudinal dispersion to transverse dispersion of oil in the oil phase
23. $\frac{\mathcal{D}_{Lw,wR}}{\mathcal{D}_{Tw,wR}}$	ratio of longitudinal dispersion to transverse dispersion of water in the water phase
24. $\frac{\mathcal{D}_{Lwv,gR}}{\mathcal{D}_{Twv,gR}}$	ratio of longitudinal dispersion to transverse dispersion of water vapour in the gas phase
25. $\frac{\mathcal{D}_{Lg,gR}}{\mathcal{D}_{Tg,gR}}$	ratio of longitudinal dispersion to transverse dispersion of gas in the gas phase
26. $\frac{\mathcal{N}_{CO_2,ogR}\mu_{oR}L^2}{C_{CO_2,oR}\rho_{oR}k_{oR}p_{oR}}$	ratio of mass transfer rate of CO_2 in or out of the oil phase through the oil/gas interface to viscous forces
27. $\frac{\mathcal{N}_{CO_2,goR}}{\mathcal{N}_{CO_2,ogR}}$	ratio of mass transfer rate of CO_2 in or out of the oil and gas phases
28. $\frac{\mathcal{N}_{CO_2,owR}}{\mathcal{N}_{CO_2,woR}}$	ratio of mass transfer rate of CO_2 in or out of the water and oil phases
29. $\frac{C_{CO_2,wR}}{C_{CO_2,oR}}$	ratio of CO_2 concentration in the water and oil phases
30. $\frac{C_{CO_2,gR}}{C_{o,oR}}$	ratio of CO_2 concentration in the gas and oil phases
31. $\frac{C_{wv,gR}}{C_{w,wR}}$	ratio of water vapour concentration in the gas and water phases
32. $\frac{F_{CO_2,gBR}}{C_{CO_2,gR}\rho_{gR}g_R}$	ratio of buoyancy force to mass force
33. $\frac{F_{CO_2,gBR}}{F_{CO_2,gDR}}$	ratio of buoyancy force to dragforce
34. $\frac{\dot{m}_R\mu_{wR}L^2}{C_{w,wR}\rho_{wR}k_{wR}p_{wR}}$	ratio of the rate of water condenses or evaporates to viscous forces

Table 4.2 - (Continued)

Group	Physical Meaning
35. $\frac{h_{CO_2R}}{h_{oR}}$	ratio of CO_2 enthalpy to oil enthalpy
36. $\frac{h_{w\ast R}}{h_{wR}}$	ratio of water vapour enthalpy to water enthalpy
37. $\frac{U_{CO_2R}}{U_{oR}}$	ratio of CO_2 internal energy to oil internal energy
38. $\frac{U_{w\ast R}}{U_{wR}}$	ratio of water vapour internal energy to water internal energy
39. $\frac{\rho_r U_{rR}}{\rho_{oR} h_{oR}}$	ratio of the energy stored in the rock to that in the oil
40. $\frac{(h_{w\ast R} - h_{wR})\dot{m}_R t_R}{C_{w,wR}\rho_{wR} h_{wR}\phi_R S_{wR}}$	ratio of amount of latent heat released/absorbed when water condenses/evaporates to water enthalpy
41. $\frac{A_{injR}\dot{m}_R L}{\mathcal{W}_{wR} C_{w,wR}}$	ratio of the rate of water condenses or evaporates to water injection rate
42. $\frac{h_{oR}\rho_{oR} k_{oR} p_{oR}}{k_{hrR} T_R \mu_{oR}}$	ratio of convective to conductive heat transfer
43. $\frac{\phi_R S_{gR} \mathcal{D}_{LCO_2,gR} \eta_{CO_2,g} \mu_{gR}}{T_R s_{CO_2R} p_{gR} k_{gR}}$	ratio of the longitudinal dispersive entropy flux of CO_2 in the gas phase to CO_2 entropy
44. $\frac{h_{CO_2R}}{T_R s_{CO_2R}}$	ratio of entropy gained or lost by CO_2 due to convective heat transfer to CO_2 entropy
45. $\frac{s_{wR}}{s_{oR}}$	ratio of water entropy to oil entropy
46. $\frac{s_{CO_2R}}{s_{w\ast R}}$	ratio of CO_2 entropy to water vapour entropy
47. $\frac{s_{rR}}{s_{wR}}$	ratio of the entropy of the rock matrix to water entropy
48. $\frac{g_R H}{T_R s_{oR}}$	ratio of the conversion of gravitational forces to entropy to oil entropy
49. $\frac{\mathcal{W}_{CO_2R} \mu_{gR}}{\rho_{gR} k_{gR} p_{gR} L}$	ratio of CO_2 injection rate to viscous forces
50. $\frac{\mathcal{W}_{wR}}{\mathcal{W}_{CO_2R}}$	ratio of water injection rate to gas injection rate
51. $\frac{\mathcal{M}_{CO_2R} \mu_{gR}}{\rho_{gR} k_{gR} p_{gR} \phi_R S_{oR} \mathcal{D}_{LCO_2,oR}}$	ratio of the momentum of the injected CO_2 to the longitudinal dispersive momentum of CO_2 in the oil phase at the injection well

Table 4.2 - (Continued)

Group	Physical Meaning
52. $\frac{\mathcal{M}_{CO_2R}}{\mathcal{M}_{wR}}$	ratio of CO_2 momentum to water momentum
53. $\frac{\mathcal{E}_{CO_2R}L}{k_{hrR}T_RA_{injR}}$	ratio of the kinematic energy of CO_2 to conduction heat transfer at the injection well
54. $\frac{\mathcal{E}_{wR}L}{k_{hrR}T_RA_{injR}}$	ratio of the kinematic energy of water to conduction heat transfer at the injection well
55. $\frac{(\mathscr{s}_{weR}-\mathscr{s}_{wR})\dot{m}_Rt_R}{C_{w,wR}\rho_{wR}s_{wR}\phi_RS_{wR}}$	ratio of the entropy released/absorbed when water condenses/evaporates to water entropy
56. $\frac{\mathscr{s}_{CO_2R}\mathcal{W}_{CO_2R}L}{k_{hrR}A_{injR}}$	ratio of the CO_2 entropy to the entropy created due to conduction heat transfer at the injection well
57. $\frac{U_{rR}}{T_R\mathscr{s}_{rR}}$	ratio of entropy gained or lost by the rock due to conductive heat transfer to the rock entropy
58. $\frac{T_{oiR}}{T_R}$	ratio of initial oil and reservoir temperatures

4.2.2 - Derivation of the Relaxed Scaling Groups

The aim is to obtain sets of similarity groups which can be used with the scaled physical model, which was previously designed and built by Rojas[1]. The derivation of these groups is found in Appendix C.

Approach No. 1

In this approach, it is assumed that both the reservoir and the model have the same porous medium, fluids, pressure drops, temperature, and geometric similarity is satisfied. The advantage of approach is that it leads to the satisfaction of the scaling requirements for viscosity, density, solubility, diffusivity, equilibrium constants, mass transfer rate, condensation and/or evaporation of water, and other properties which depend on pressure and temperature. Using the same porous medium (same porosity, same permeability, same grain size, and same wettability) allows the residual saturations to be the same in the model and in the prototype. Therefore, viscous forces, capillary forces, and diffusive forces are properly scaled. This leads to the following set of relaxed scaling groups.

$$\phi_R, \frac{H}{W}, \frac{L}{W}, \frac{\mu_{oR} S_{oR} \mathcal{D}^*_{CO_2,oR}}{p_{oR} k_{oR} F_R}, \frac{\phi_R S_{oR} \mu_{oR} L^2}{k_{oR} p_{oR} t_R}, \frac{\mathcal{N}_{CO_2,ogR} \mu_{oR} L^2}{C_{CO_2,oR} \rho_{oR} k_{oR} p_{oR}}, \frac{\mathcal{N}_{CO_2,owR}}{\mathcal{N}_{CO_2,ogR}}, \frac{\mathcal{N}_{CO_2,goR}}{\mathcal{N}_{CO_2,woR}},$$

$$\frac{\mathcal{D}^*_{CO_2,gR}}{\mathcal{D}^*_{CO_2,oR}}, \frac{\mathcal{D}^*_{CO_2,wR}}{\mathcal{D}^*_{w,wR}}, \frac{\mathcal{D}^*_{o,oR}}{\mathcal{D}^*_{w\bullet,gR}}, \frac{\mu_{oR} k_{gR}}{\mu_{gR} k_{oR}}, \frac{\mu_{oR} k_{wR}}{\mu_{wR} k_{oR}}, \frac{S_{gR}}{S_{oR}}, \frac{S_{wR}}{S_{oR}}, \frac{S_{oiR}}{S_{wiR}}, \frac{p_{CO_2,gR}}{p_{w\bullet,gR}}, \frac{p_{wR}}{p_{oR}},$$

$$\frac{p_{prodR}}{p_{oR}}, \frac{P_{cgoR}}{P_{cowR}}, \frac{p_{oiR}}{p_{wiR}}, \frac{\mathcal{W}_{CO_2R} \mu_{gR}}{\rho_{gR} k_{gR} p_{gR} L}, \frac{\mathcal{W}_{wR}}{\mathcal{W}_{CO_2R}}, \frac{A_{injR}}{L^2}, \frac{\rho_{gR}}{\rho_{oR}}, \frac{\rho_{wR}}{\rho_{oR}}, \frac{C_{CO_2,gR}}{C_{CO_2,oR}}, \frac{C_{CO_2,wR}}{C_{o,oR}},$$

$$\frac{C_{w,wR}}{C_{w\bullet,gR}}, \frac{F_{CO_2,gBR} H}{p_{gR}}, \frac{F_{CO_2,gBR}}{F_{CO_2,gDR}}, \frac{\dot{m}_R \mu_{wR} L^2}{C_{w,wR} \rho_{wR} k_{wR} p_{wR}}, \frac{h_{CO_2R}}{h_{oR}}, \frac{h_{w\bullet R}}{h_{wR}}, \frac{U_{CO_2R}}{U_{oR}}, \frac{U_{w\bullet R}}{U_{wR}},$$

$$\frac{\rho_r U_{rR}}{\rho_{oR} h_{oR}}, \frac{F_{CO_2,gBR} H}{C_{CO_2,gR} \rho_{gR} h_{CO_2R}}, \frac{(h_{wvR} - h_{wR}) \dot{m}_R t_R}{C_{w,wR} \rho_{wR} h_{wR} \phi_R S_{wR}}, \frac{A_{injR} \dot{m}_R L}{\mathcal{W}_{wR} C_{w,wR}}, \frac{h_{oR} \rho_{oR} k_{oR} p_{oR}}{k_{hrR} T_R \mu_{oR}},$$

$$\frac{S_{gR} \mathcal{D}^*_{CO_2,gR} \eta_{CO_2,g} \mu_{gR}}{T_R \mathfrak{s}_{CO_2R} p_{gR} k_{gR} F_R}, \frac{h_{CO_2R}}{T_R \mathfrak{s}_{CO_2R}}, \frac{U_{rR}}{T_R \mathfrak{s}_{rR}}, \frac{\mathfrak{s}_{CO_2R}}{\mathfrak{s}_{oR}}, \frac{\mathfrak{s}_{w\bullet R}}{\mathfrak{s}_{wR}}, \frac{\mathfrak{s}_{rR}}{\mathfrak{s}_{oR}}, \frac{\mathfrak{s}_{CO_2R} \mathcal{W}_{CO_2R} L}{k_{hrR} A_{injR}}, \frac{T_{oiR}}{T_R}$$

$$\frac{(\mathfrak{s}_{w\bullet R} - \mathfrak{s}_{wR}) \dot{m}_R t_R}{C_{w,wR} \rho_{wR} \mathfrak{s}_{wR} \phi_R S_{wR}}, \frac{\mathcal{M}_{CO_2R} \mu_{gR}}{\rho_{gR} k_{gR} p_{gR} \phi_R S_{oR} \mathcal{D}^*_{CO_2R}}, \frac{\mathcal{M}_{CO_2R}}{\mathcal{M}_{wR}}, \frac{\mathcal{E}_{CO_2R} L}{k_{hrR} T_R A_{injR}}, \frac{\mathcal{E}_{wR} L}{k_{hrR} T_R A_{injR}}.$$

In addition, it should be noted that all the dimensionless properties must be the same function of their dimensionless variables for the model and the prototype. For a model reduced in length by a scaling factor "a" and employing the same fluids as the prototype, Δp_{max}, p_{oi}, p_{prod}, T, k, ϕ, S_{oi}, S_{wi}, and F must be the same in the model and the prototype. The parameters H, W, $\mathcal{W}_{CO_2}$, $\mathcal{W}_w$, must be reduced by "a" and t by "a^2".

Approach No. 2

In this approach, the reservoir and the model are assumed to have different fluids and pressure drops, the same porous medium, and geometric similarity. This approach is rather similar to Approach No. 1. The only differences are the model oil and the experimental pressure and temperature conditions. The model oil is selected so that its viscosity at room temperature equals that of the prototype oil at reservoir temperature. The experimental model pressure and temperature are different from the reservoir pressure and temperature.

In this approach, the determination of the experimental pressure at atmospheric temperature is crucial, because it is hypothesized that the solubilities of carbon dioxide in oil at two different pressure and temperature conditions can be the same. In other words, the experimental pressure at 21°C is determined such that the solubility of carbon dioxide in the model oil at this pressure is equal to that in the reservoir oil at the field pressure and temperature.

In addition, in order to balance viscous forces (viscous x/viscous y) and viscous divided by gravitational forces while maintaining geometric similarity, the pressure drop is relaxed. It is proposed to use the same porous medium in the model as in the field. In other words, the model will have the same permeability, porosity, and saturation distributions as the prototype. The main weakness of this approach is that all properties (except solubility) which depend on pressure and temperature, and composition are not scaled because of the different pressure and temperature in the model and the prototype. The resulting groups are as follows:

$$\phi_R, \frac{L}{W}, \frac{H}{W}, \frac{\phi_R S_{oR} \mu_{oR} L^2}{k_{oR} p_{oR} t_R}, \frac{\mu_{oR} S_{oR} \overset{*}{\mathcal{D}}_{CO_2,oR}}{p_{oR} k_{oR} F_R}, \frac{\rho_{oR} g_R H}{p_{oR}}, \frac{\rho_{gR}}{\rho_{oR}}, \frac{\rho_{wR}}{\rho_{oR}}, \frac{\mu_{oR} k_{gR}}{\mu_{gR} k_{oR}}, \frac{\mu_{oR} k_{wR}}{\mu_{wR} k_{oR}},$$

$$\frac{\mathcal{N}_{CO_2,ogR} \mu_{oR} L^2}{C_{CO_2,oR} \rho_{oR} k_{oR} p_{oR}}, \frac{\mathcal{N}_{CO_2,goR}}{\mathcal{N}_{CO_2,ogR}}, \frac{\mathcal{N}_{CO_2,owR}}{\mathcal{N}_{CO_2,woR}}, \frac{\overset{*}{\mathcal{D}}_{CO_2,gR}}{\overset{*}{\mathcal{D}}_{CO_2,oR}}, \frac{\overset{*}{\mathcal{D}}_{CO_2,wR}}{\overset{*}{\mathcal{D}}_{o,oR}}, \frac{\overset{*}{\mathcal{D}}_{w\bullet,gR}}{\overset{*}{\mathcal{D}}_{w,wR}}, \frac{C_{CO_2,gR}}{C_{CO_2,oR}},$$

$$\frac{C_{CO_2,wR}}{C_{o,oR}}, \frac{C_{w\bullet,gR}}{C_{w,wR}}, \frac{S_{gR}}{S_{oR}}, \frac{S_{wR}}{S_{oR}}, \frac{S_{oiR}}{S_{wiR}}, \frac{p_{CO_2,gR}}{p_{w\bullet,gR}}, \frac{p_{wR}}{p_{oR}}, \frac{p_{prodR}}{p_{oR}}, \frac{p_{oiR}}{p_{wiR}}, \frac{F_{CO_2,gBR}}{C_{CO_2R} \rho_{gR} g_R},$$

$$\frac{F_{CO_2,gBR}}{F_{CO_2,gDR}}, \frac{\mathcal{N}_{CO_2,ogR} h_{CO_2R} L F_R}{C_{CO_2R} \rho_{gR} g_R \overset{*}{\mathcal{D}}_{CO_2,oR} S_{oR}}, \frac{h_{CO_2R}}{h_{oR}}, \frac{h_{w\bullet R}}{h_{wR}}, \frac{U_{CO_2R}}{U_{oR}}, \frac{U_{w\bullet R}}{U_{wR}}, \frac{\rho_r U_{rR}}{\rho_{oR} h_{oR}},$$

$$\frac{(h_{w\bullet R} - h_{wR}) \dot{m}_R t_R}{C_{w,wR} \rho_{wR} h_{wR} \phi_R S_{wR}}, \frac{S_{gR} \overset{*}{\mathcal{D}}_{CO_2,gR} \eta_{CO_2,g} \mu_{gR}}{T_R s_{CO_2R} p_{gR} k_{gR} F_R}, \frac{h_{CO_2R}}{T_R s_{CO_2R}}, \frac{g_R H}{s_{CO_2R} T_R}, \frac{s_{CO_2R}}{s_{oR}}, \frac{s_{w\bullet R}}{s_{wR}}, \frac{s_{rR}}{s_{oR}},$$

$$\frac{(s_{w\bullet R} - s_{wR}) \dot{m}_R t_R}{C_{w,wR} \rho_{wR} s_{wR} \phi_R S_{wR}}.$$

In addition to these requirements, the dimensionless properties as functions of dimensionless variables should be the same in the model and the prototype. For a model reduced in length by "a", and considering the same fluids, ϕ, S_{oi}, S_{wi} and K must be the same in the model and the prototype. The parameters W, H, and t must be reduced by "a". The parameters W_{CO_2} and W_W must be reduced by "a^2".

4.2.3 - Dimensional Analysis

The dimensional analysis approach to derive the similarity groups for a process is based on the Buckingham π-Theorem, which uses the Principle of Similarity. The procedure is to first select the relevant variables for the process. The similarity groups can be determined using the Buckingham π-Theorem. The general rule for this approach is that if there are n separate variables and m primary quantities, then the set will be complete when there are (n-m) dimensionless groups. More details on this approach can be found in Ref. 98. The similarity groups derived by this method are given below.

$$\phi, \frac{H}{L}, \frac{W}{L}, \frac{\rho_o g H}{p_o}, \frac{\rho_g}{\rho_o}, \frac{\rho_w}{\rho_o}, \frac{\mu_o k_w}{\mu_w k_o}, \frac{\mu_o k_g}{\mu_g k_o}, \frac{p_{CO_2,g}}{p_o}, \frac{p_{w*,g}}{p_w}, \frac{p_{prod}}{p_o}, \frac{P_{cow}}{P_{cgo}}, \frac{\sigma_{go}}{P_{cgo} k^{1/2}}, \frac{\sigma_{go}}{\sigma_{ow}},$$

$$\frac{\rho_g \vartheta_g k_g^{1/2}}{\mu_g}, \frac{\mathcal{W}_{CO_2} \mu_g}{L \rho_g k_g p_g}, \frac{\mathcal{W}_w}{\mathcal{W}_{CO_2}}, \frac{\phi S_o \mathcal{D}_{LCO_2,o} \mu_o}{k_o p_o}, \frac{\mathcal{D}_{TCO_2,o}}{\mathcal{D}_{LCO_2,o}}, \frac{\mathcal{D}_{LCO_2,w}}{\mathcal{D}_{TCO_2,w}}, \frac{\mathcal{D}_{Lo,o}}{\mathcal{D}_{To,o}}, \frac{\mathcal{D}_{Lw,w}}{\mathcal{D}_{Tw,w}},$$

$$\frac{\mathcal{D}_{LCO_2,g}}{\mathcal{D}_{TCO_2,g}}, \frac{\mathcal{D}_{Lw*,g}}{\mathcal{D}_{Tw*,g}}, \frac{\mathcal{D}_{Lg,g}}{\mathcal{D}_{Tg,g}}, \frac{\mathcal{N}_{CO_2,og} \mu_o L^2}{C_{CO_2,o} \rho_o k_o p_o}, \frac{\mathcal{N}_{CO_2,go}}{\mathcal{N}_{CO_2,og}}, \frac{\mathcal{N}_{CO_2,ow}}{\mathcal{N}_{CO_2,wo}}, \frac{\dot{m} \mu_w L^2}{C_{w,w} \rho_w k_w p_w},$$

$$\frac{\dot{m} A_{inj} L}{\mathcal{W}_w C_{w,w}}, \frac{F_{CO_2,gB}}{C_{CO_2,g} \rho_g g}, \frac{F_{CO_2,gB}}{F_{CO_2,gD}}, \frac{h_{CO_2}}{h_o}, \frac{h_{w*}}{h_w}, \frac{U_{CO_2}}{U_o}, \frac{U_{w*}}{U_w}, \frac{\rho_r \mathcal{U}_r}{\rho_o U_o}, \frac{h_{CO_2}}{T \mathfrak{s}_{CO_2}}, \frac{U_r}{T \mathfrak{s}_r}, \frac{\mathfrak{s}_{CO_2}}{\mathfrak{s}_o},$$

$$\frac{\mathfrak{s}_{w*}}{\mathfrak{s}_w}, \frac{\mathfrak{s}_r}{\mathfrak{s}_o}, \frac{gH}{T \mathfrak{s}_o}, \frac{F_{CO_2,gB} H}{C_{CO_2,g} \rho_g h_{CO_2}}, \frac{h_o \rho_o k_o p_o}{k_{hr} T \mu_o}, \frac{\sigma_{go}}{L \rho_o h_o}, \frac{\phi S_g \mathcal{D}_{LCO_2,g} \eta_{CO_2,g} \mu_g}{T \mathfrak{s}_{CO_2,g} p_g k_g},$$

$$\frac{\mathcal{M}_{CO_2} \mu_g \vartheta_g}{L \mathcal{D}_{LCO_2,o} p_g k_g \rho_g \phi S_o}, \frac{\mathcal{M}_{CO_2}}{\mathcal{M}_w}, \frac{\mathfrak{E}_{CO_2} L}{k_{hr} T A_{inj}}, \frac{\mathfrak{E}_w L}{k_{hr} T A_{inj}}, \frac{k_{hr} A_{inj}}{\mathfrak{s}_{CO_2}}, \frac{C_{CO_2,w}}{C_{o,o}}, \frac{C_{CO_2,g}}{C_{CO_2,o}}, \frac{C_{w*,g}}{C_{w,w}},$$

$$\frac{T_{oi}}{T}, \frac{S_g}{S_o}, \frac{S_w}{S_o}, \frac{S_{oi}}{S_{wi}}, \frac{k}{L^2}, \frac{\mathfrak{s}_{CO_2} \mathcal{W}_{CO_2} L}{k_{hr} A_{inj}}, \frac{V_w^*}{V_{CO_2}^*}, \frac{\mu_o \vartheta_g}{g k \Delta\rho_{go}}, \frac{\mu_o \vartheta_w}{g \Delta\rho_{ow}}.$$

The group $\frac{\mu_o \vartheta_g}{g k \Delta\rho_{go}}$ appears in the above set derived using the dimensional analysis approach because $g\Delta\rho_{go}$ was taken as a variable.

5 - EXPERIMENTAL APPARATUS and PROCEDURE

This chapter presents a description of the apparatus, materials, and procedures used in the present research. The first part describes the procedure for packing and saturating the model prior to conducting an experiment, and the second part gives details of how the diffusivity and solubility of carbon dioxide in oil, in the presence of nitrogen, were measured. A discussion of the procedure for conducting an immiscible WAG experiment is also provided.

5.1 - Experimental Apparatus

Figure 5.1 shows a schematic of the apparatus used for the displacement experiments. As shown, the apparatus used in this study consists of the physical model, fluids and porous medium, fluid injection and production systems, and the data acquisition system.

5.1.1 - Physical Models

Two models: linear and two-dimensional, were used in the present research. The linear model was partially scaled while the two-dimensional model was fully scaled to the Aberfeldy reservoir in Saskatchewan. The similarity groups which were used to design the model can be found in Ref. 1. The linear model was built to act as a screening model for the two-dimensional model. It was 415 mm in length and 98 mm in diameter. Chevron-type fittings were used to seal the ends of the pipe, as well as to form the injection and production ports. Figure 5.2 presents a schematic of the linear model.

In contrast to the linear model, the two-dimensional model was more complex. Cross sections of the two-dimensional model are shown in Figure 5.3. Much effort was expended in designing and fabricating it[1]. A brief description of this model is given below.

- Rectangular shape: 45.7 cm x 45.7 cm x 2.2 cm.
- Three reinforcing members.

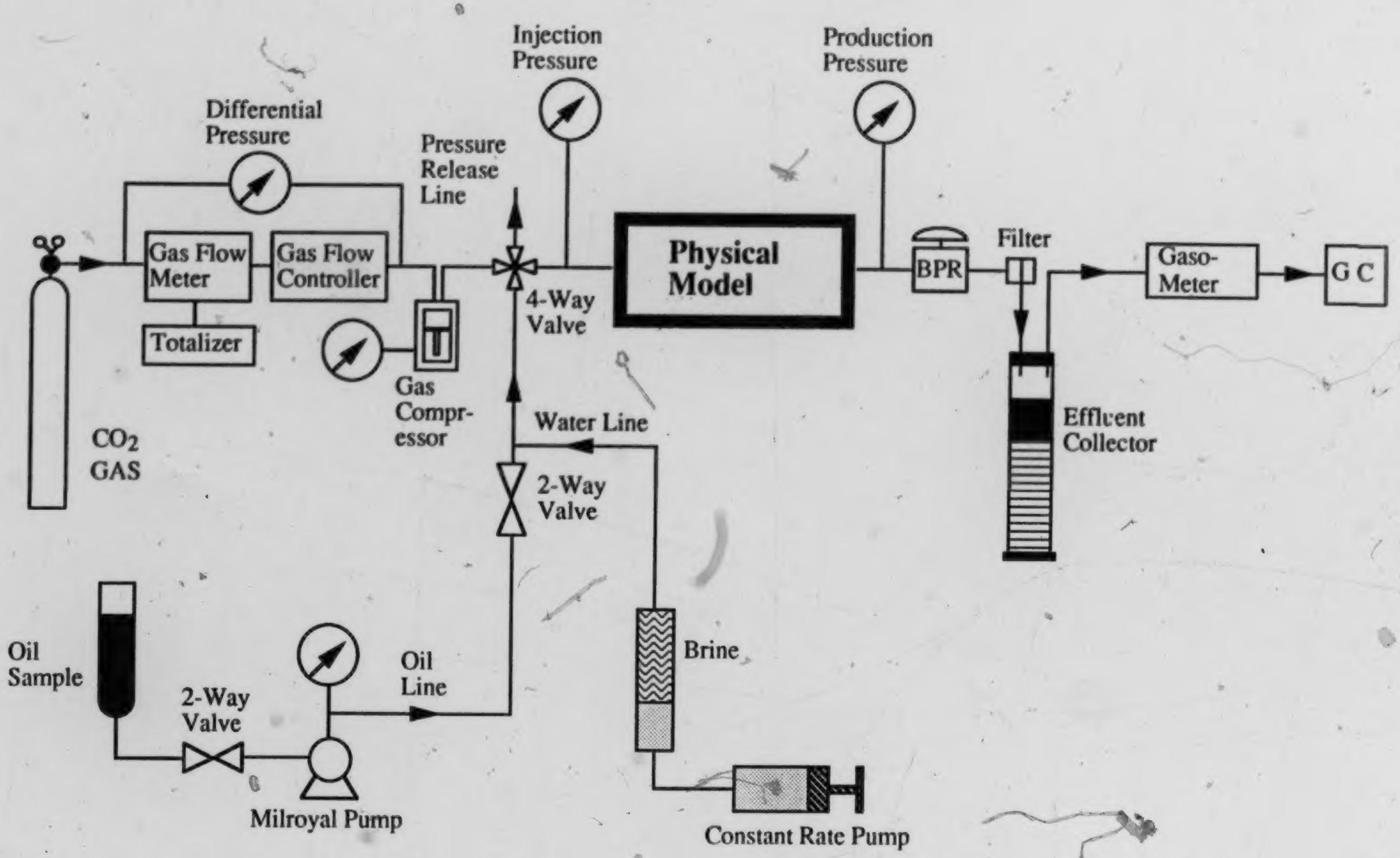
Differential Pressure
Injection Pressure
Production Pressure
Pressure Release Line
Gas Flow Meter
Gas Flow Controller
Totalizer
Physical Model
BPR
Filter
Gaso-Meter
G C
4-Way Valve
Gas Compr-essor
Water Line
Effluent Collector
CO_2 GAS
2-Way Valve
Oil Sample
2-Way Valve
Oil Line
Brine
Milroyal Pump
Constant Rate Pump

Figure 5.1 - Schematic of the Experimental Apparatus.

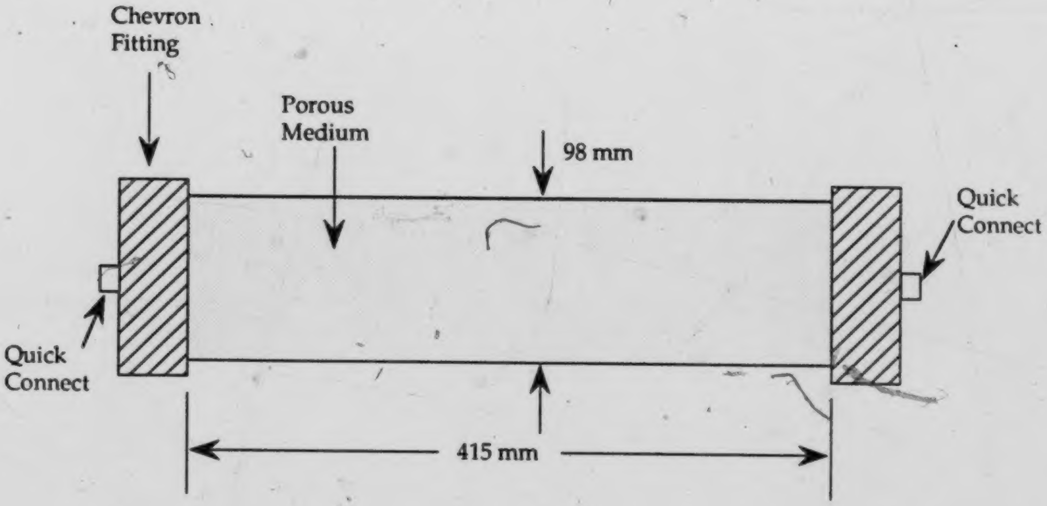
Chevron Fitting
Porous Medium
98 mm
Quick Connect
Quick Connect
415 mm

Figure 5.2 - Schematic of the Linear Model.

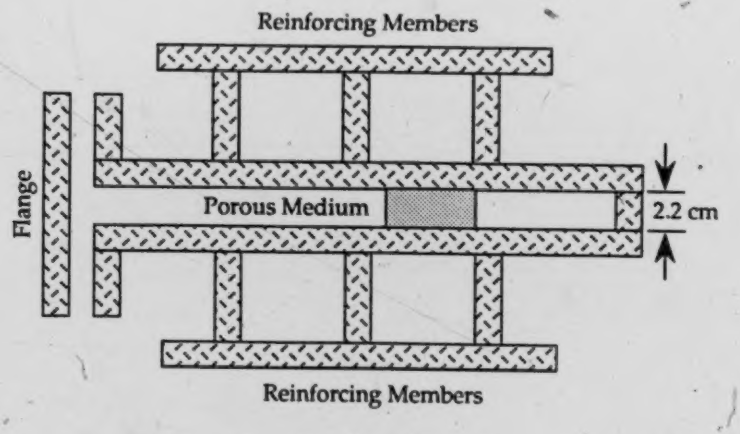
Reinforcing Members
Flange
Porous Medium
2.2 cm
Reinforcing Members

a) Horizontal Cross-Section

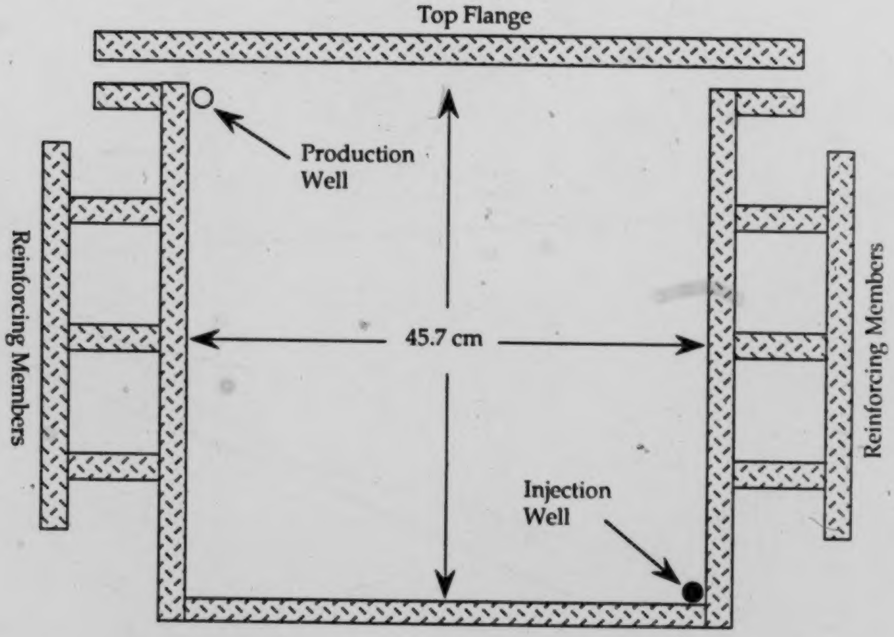
Top Flange
Production Well
Reinforcing Members
45.7 cm
Reinforcing Members
Injection Well

b) Vertical Cross-Section

Figure 5.3 - Cross-Sections of the Two-Dimensional Model.

- Maximum internal pressure: 10.0 MPa at 51°C.
- Maximum deflections of walls at 10.0 MPa: < 0.01 mm.
- Weight of model: 1.0 tonne.
- Number of wells: 9.
- Possible patterns to simulate: 5-spot, 9-spot, line drive.
- The model can be rotated for horizontal, inclined, or vertical floods.

In this research, in addition to conducting experiments at iso-thermal conditions, it was intended to perform experiments at non-isothermal conditions. The field data that were used to design the scaled non-isothermal experiments are given in Table 5.1, on the next page.

5.1.2 - Fluids and Porous Medium

Oil

The oils used in all experiments were from the Aberfeldy and Battrum South fields in Lloydminster, Saskatchewan and from a heavy oil field in Oklahoma.

Carbon Dioxide Gas

Commercial carbon dioxide gas with a purity of up to 99.9%, purchased from Medigas, was used in all runs.

Brine

Field-simulated brines were used in all runs.

Porous Medium

For most of the runs, Ottawa Silica Sand from Ottawa, Michigan, was used to represent the field porous medium since it has a grain size similar to that of the reservoir sands (70-140 mesh).

Table 5.1 - Field Information

Field name	X
Date discovered	November, 1987
Producing depth	912 m
Net sand thickness	5.1 m
Original reservoir pressure	8560 kPa
Current reservoir pressure	4799 kPa
Production pressure	2600 kPa
Reservoir temperature	37°C
Oil gravity	17.3° API
Oil density (@ surface temperature)	950 kg
Formation volume factor	1.024 rm^3/sm^3
Initial oil saturation	60.7%
Current oil saturation	44.0%
Oil viscosity at bottom hole temperature	160 mPa.s
Porosity	25.1%
Permeability	0.1 to 2.5 darcies
Geometry	inverted 9-spot
Well spacing	161,875 m^2

5.1.3 - Fluid Injection and Production System

Gas Injection

Carbon dioxide was injected using a Matheson gas metering system. This system controlled and measured the gas entering the model. The Matheson Dyna-Blender helped to control the flow rate of gas. A gas compressor was also used to maintain a constant gas injection pressure. A Matheson totalizer provided the cumulative volume of gas injected into the model.

Oil Injection

A positive displacement Milroyal pump was employed to inject heavy oil into the model.

Brine Injection

Brine was injected by a constant rate screw-type piston pump. The pump flow rate was controlled by varying the pump speed.

Fluid Production

The effluent was collected in a glass cylinder at atmospheric conditions (101.325 kPa and 23°C). Oil and water, because their densities were greater than that of gas, were collected at the bottom of the cylinder while gas displaced a volume of water in the upright glass burette equal to the total volume of gas produced. Since oil and water mixed with each other at the time of collection, they had to be heat-separated to determine the produced volumes of each.

5.1.4 - Data Acquisition System

The production pressure was controlled by a back-pressure regulator which was connected to the production end of the model. Two Heise pressure gauges were used to measure the injection and production pressures.

5.2 - Experimental Procedures

In this research, as mentioned previously, two models: linear and two-dimensional, were used to conduct experiments. The terms 'Linear' and 'Two-Dimensional' are used for convenience only; in fact, flow in any physical model is three-dimensional. Much effort was made to minimize the effect of gravity, which acts in the third dimension.

For both models, the experimental procedures used were identical, except that dry packing was used for the linear model and wet packing for the two-dimensional model. The procedures are as discussed below.

5.2.1 - Packing

Linear Model

Dry packing was used for the linear model. The packing procedure is relatively simple. After the bottom Chevron end cap was installed on the production end of the model, the model was inverted so that the open (injection) end was up and so that it was perfectly vertical. A level gauge was used to check if it was in the vertical position. An air vibrator was then strapped on the side of the model. Next, Ottawa sand was slowly poured into the model while it was being vibrated. In this way, a tight sand pack was achieved. Afterwards, the model was left vibrating for eight-to-ten hours. After vibration, the top Chevron end cap was mounted, and a vacuum pump was connected to the top end to evacuate air from the model while it was again being vibrated for another eight-to-ten hours. A vacuum was drawn at the top to achieve the best vacuum possible. At this point, the model was ready for pore volume determination.

Two-Dimensional Model

While the linear model was dry-packed, the two-dimensional model was wet-packed for convenience. Similar to the linear model, the two-dimensional model was first inverted so that the open cavity was facing up. Next, an aluminium extension was temporarily mounted on the top of the model, and distilled water was added to the model. The purpose of the extension was to maintain a 10-cm head of water above the sand level. An air vibrator was clamped on the top of the model and activated, and Ottawa sand was slowly poured in until the sand level was about 2 cm above the head of the model. The model was then vibrated for at least eight-to-ten hours. Afterwards, the 10-cm head of water, air vibrator, and aluminium extension were removed, and the top flange was put on and bolted. Finally, the model was pressure-tested at about 6.0 MPa or higher to check for leaks. If no leak was detected, the model was now ready for pore volume determination.

5.2.2 - Pore Volume Determination

Linear Model

After a vacuum was drawn on the model, a plastic tube from a calibrated cylinder containing an initially known volume of brine was connected to the bottom end of the model and brine was drawn up into the model due to the pressure difference between the model and the atmosphere. By injecting water from the bottom of the model, a more accurate pore volume and a more uniform water saturation could be achieved. The difference between the initial and final volumes of brine yielded the pore volume of the model. The porosity was calculated by dividing the pore volume by the bulk volume of the model.

Two-Dimensional Model

For the two-dimensional model, the determination of the pore volume was more time-consuming than that for the linear model. First, the model was rotated so that the flange side faced down. Next, brine with a refractive index of 1.3446 was injected at the bottom of the model using the constant rate screw-type piston pump, while distilled water was being produced and collected at the top of the model. Brine injection was continued until the refractive index of the produced water reached 1.3446. At this time, the model was believed to be 100% brine saturated, and the injection was stopped. For each sample of water collected, its refractive index was measured using a refractometer to estimate a gradual change from water to brine solution. The refractive indices of the first and last water samples were plotted versus the percent of brine in solution, since it was believed that the first sample contained 0.0% brine and the last 100.0% brine (Figure 5.4). From this plot,

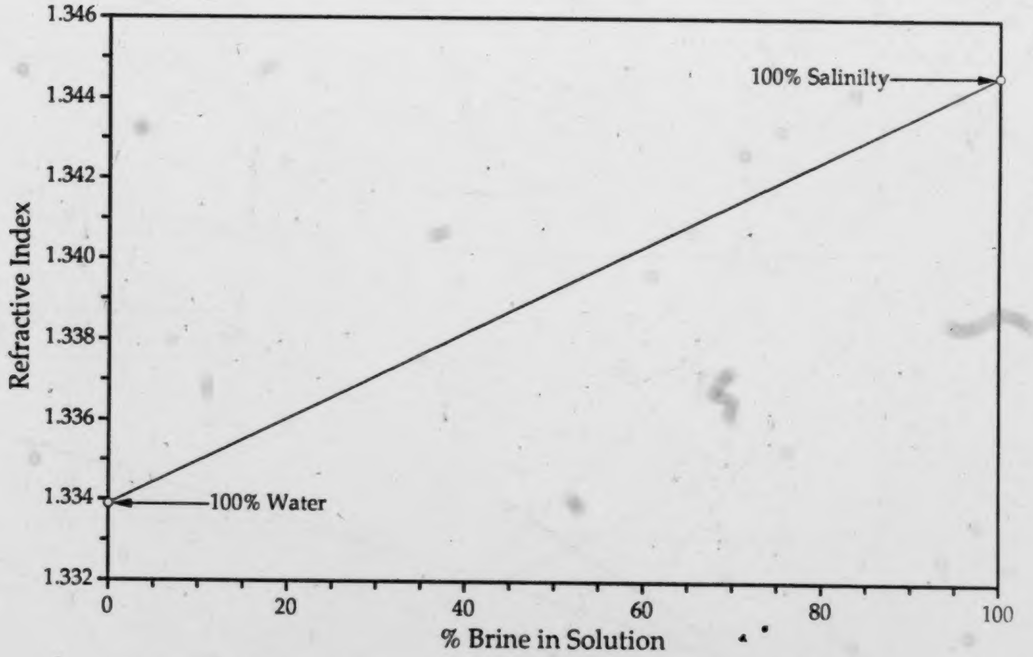

Figure 5.4 - Two-Dimensional Model Fraction of Brine in Solution.

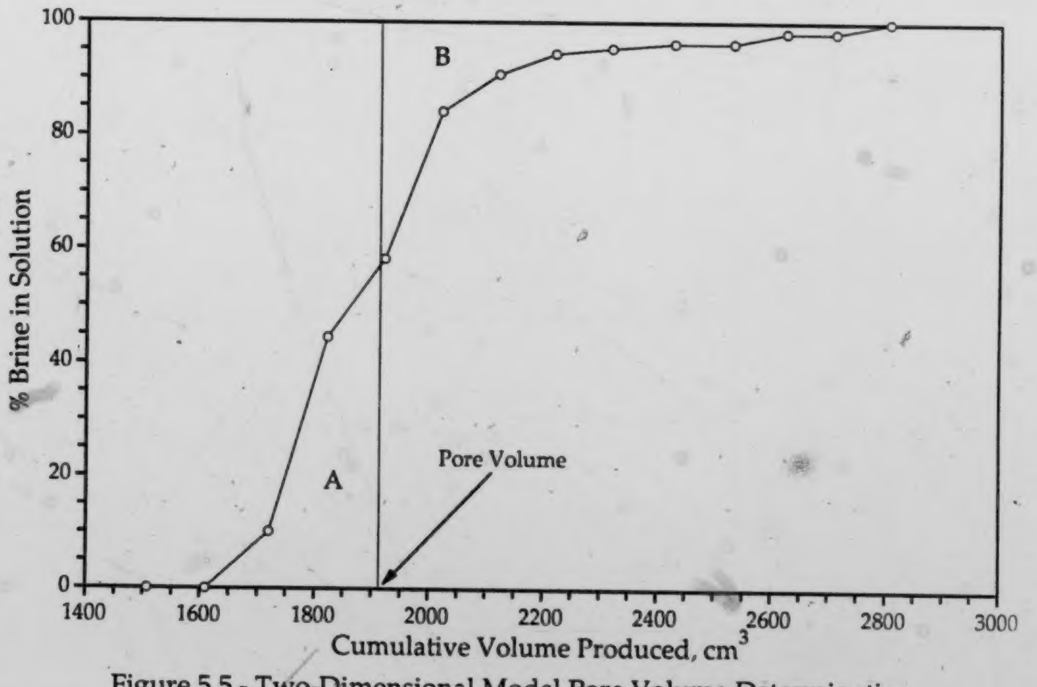

Figure 5.5 - Two-Dimensional Model Pore Volume Determination.

knowing the refractive index of each water sample, the percent of brine in solution could be found. To determine the pore volume of the model, the percent of brine in solution was plotted versus the cumulative volume of water produced, and the area under the curve was divided into two equal portions (Figure 5.5 on the previous page). The pore volume was the cumulative volume at which area A equalled area B.

5.2.3 - Permeability Determination

For both the linear and the two-dimensional models, the permeability was measured using the same approach. Note that after the pore volume determination, the model was brine saturated; thus, brine was used as the fluid to measure the permeability of the sand pack. The horizontal permeability of the model was measured by flowing brine through the model in a horizontal position, at a specific flow rate and pressure differential. A known volume of water was collected at a given time and pressure differential, and the permeability was determined using Darcy's linear flow equation for the linear model and Muskat's equation[99] for the two-dimensional model.

5.2.4 - Oil Saturation

For both physical models, the procedures to saturate the model sand pack with oil were similar. First, the model was inverted so that the injection port was facing up and the production port facing down, and the model pressure was brought to the experimental pressure by injecting brine into the model with the production back-pressure regulator (BPR) closed. Also, oil had to be pressurized to the experimental pressure by activating the constant rate Milroyal pump, with the inlet valve closed, until the oil pressure was at least a little higher than or equal to the model pressure. Then it was injected into the model at a very slow rate by fully opening the inlet valve. Right after oil breakthrough occurred, injection was stopped and the volume of brine produced was recorded. This volume of brine was used to predict the initial oil saturation, as follows.

$$S_{oi} = \frac{\text{HCPV}}{\text{Pore Volume}}$$

For the linear model:

$$S_{oi} = \frac{\text{Brine Volume Produced - Oil Volume in Chevron - Type Caps}}{\text{Pore Volume}} \times 100\%$$

For the two-dimensional model:

$$S_{oi} = \frac{\text{Brine Volume Produced}}{\text{Pore Volume}} \times 100\%$$

At this time, the model was believed to be oil-saturated and ready for an experiment.

5.2.5 - WAG Process, Post Waterflood, and Blowdown

The same procedure was used to conduct an experiment in both physical models. To start an experiment, the volumes of gas and brine to be injected had to be calculated first. The calculation procedure is shown below.

Since it was found by previous researchers[1,5] that a total gas slug size of 20% HCPV and a water volume four times the gas volume, both of which were divided into ten equal slugs, were optimal, they were used in all experiments in this study.

$$\text{Total Gas Volume @ Experimental Conditions} = 0.20 \times \text{HCPV} \quad [\text{cm}^3]$$

It had to be converted to its equivalent volume at the meter (standard) conditions.

Total Gas Volume @ Meter Conditions

$$= 0.20 \times \text{HCPV} \times \frac{\text{MD @ Experimental Conditions } \left(\text{mol/cm}^3\right)}{\text{MD @ Meter Conditions } \left(\text{mol/cm}^3\right)} \quad [\text{cm}^3]$$

where,

MD = molar density calculated using the Starling Equation of State[100].

$$\text{Total Brine Volume} = 4 \times \text{Total Gas Volume @ Experimental Conditions} \quad [\text{cm}^3].$$

Finally, the total gas and brine volumes were divided into ten slugs each.

After the preliminary calculations had been completed, the model was prepared to start an experiment. With the model in the horizontal position, a gas slug was first injected then followed by a water slug until ten slug pairs of gas and water had been injected, and the WAG process ended.

The WAG process was followed by the "post-WAG waterflood". This waterflood was carried out only when, after the WAG process, the producing WOR was still below 20:1. The model was flooded with brine until the WOR reached 20:1, or higher, when the waterflood was terminated. The "blowdown" was commenced by first closing the injection valve and then slowly lowering the pressure to atmospheric pressure by releasing the production BPR. Subsequently, the model was left for at least eight hours to make sure all gas was produced. At this time, the experiment was terminated.

After the termination of the experiment, the model was opened and the sand pack was removed and discarded. The model, as well as the injection and production ports, were cleaned first with Varsol, then toluene, and readied for the next experiment. The data collected were analyzed to determine various parameters indicative of the overall performance of the experiment. A typical run took a total of two weeks.

5.2.6 - Data Processing

The experimental data were processed using a previously developed computer program[5]. The program was based on the material balance of oil, water, and carbon dioxide mixture. The volume of fluids injected was calculated by this program. It also computed the water-oil ratios (WOR), gas-oil ratios (GOR), oil recovery, the total volume of oil produced, oil produced-fluid injected ratio (OPFIR), carbon dioxide retention and carbon dioxide required to produce a unit volume of oil.

The carbon dioxide material balance used the Starling equation of state[100]. The equation of state is as follows:

$$p = \rho RT + \left(B_o RT - A_o - \frac{C_o}{T^2} + \frac{D_o}{T^3} - \frac{E_o}{T^4}\right)\rho^2 + \left(bRT - a - \frac{d}{T}\right)\rho^3 + \alpha\left(a + \frac{d}{T}\right)\rho^6$$

$$+\frac{c\rho^3}{T^2}\left(1+\gamma\rho^2\right)\exp\left(-\gamma\rho^2\right) \qquad (5.1)$$

where,

p = pressure (MPa)
T = Temperature (K)
ρ = molar density (kmol/m^3)

The constants for carbon dioxide in SI units are:

$A_o = 0.176976$ $\quad B_o = 0.024588$ $\quad C_o = 2.451876E04$
$D_o = 1.883482E06$ $\quad E_o = 2.631556E04$ $\quad R = 0.008314$
$a = 0.009434$ $\quad b = 0.003784$ $\quad c = 1.4197888E03$
$d = 0.055761$ $\quad \alpha = 0.0000961229$ $\quad \gamma = 0.006421$

Newton-Raphson's method was applied to the above equation to determine the molar densities of nitrogen-carbon dioxide mixtures of various compositions. According to Starling[100], the above equation predicts experimental density data with an average error of less than 1.0%.

5.3 - Diffusivity Experiments

This section is divided into two sub-sections. The first presents the mathematical analysis leading to the determination of the diffusivity coefficient, and the second discusses the experimental technique.

5.3.1 - Mathematical Analysis

The one-dimensional unsteady-state diffusivity equation is

$$\frac{\partial C_i}{\partial t} = \mathcal{D}^{*}_{ij}\frac{\partial^2 C_i}{\partial x^2} \qquad (5.2)$$

subject to the following initial condition:

$$C_i(x, t=0) = 0 \text{ for } 0 \le x \le \infty \qquad (5.3)$$

and the following two boundary conditions (assuming an infinite length):

$$C_i(x=0, t>0) = C_{ie} \tag{5.4}$$

$$C_i(x=\infty, t>0) = 0 \tag{5.5}$$

where,

C_{ie} = equilibrium concentration at the interface.

The solution to equation (5.2) subject to the above conditions is[101]

$$C_i(x,t) = C_{ie}\,\mathrm{erfc}\left[\frac{x}{2\sqrt{\mathcal{D}^{*}_{ij}t}}\right] \tag{5.6}$$

The total mass of the gas component i, m_t, absorbed after time t can be defined as

$$m_t = A\int_0^{\infty} C_i(x,t)\,dx \tag{5.7}$$

where,

A = diffusional cross-sectional area.

Inserting equation (5.6) into equation (5.7) gives

$$m_t = AC_{ie}\int_0^{\infty}\mathrm{erfc}\left[\frac{x}{2\sqrt{\mathcal{D}^{*}_{ij}t}}\right]dx \tag{5.8}$$

The solution to equation (5.8) given by other investigators[28, 32, 37,39] is

$$m_t = 2AC_{ie}\sqrt{\frac{\mathcal{D}^{*}_{ij}t}{\pi}} \tag{5.9}$$

The parameter, m_t, is mass of gas component i injected into the diffusion cell after time t to maintain a constant pressure during the duration of a diffusion experiment, which can be determined directly from the observed volume of gas injected into the cell, which can be converted to mass by using an appropriate equation of state. For carbon dioxide, the Starling equation of state is the most accurate. The interfacial equilibrium concentration, C_{ie}, in kg/m^3 of solution, which can be measured experimentally by taking a sample at the top of the oil column. The diffusional cross-sectional area, A, can be measured directly. By plotting m_t vs. $\sqrt{t}$, a straight line with a slope equal to $2AC_{s}\sqrt{\frac{\mathcal{D}_{ij}^{*}}{\pi}}$ can be obtained. The diffusivity coefficient, $\mathcal{D}_{ij}^{*}$, can be determined from the slope of the straight line.

5.3.2 - Experimental Measurement

The method of measuring the carbon dioxide diffusivity in oils presented here is quite similar to the one designed by Pomeroy et al.[28], except for the completion of the experiment. In Pomeroy et al.[28]'s method, at the end of the diffusion period, the diffusion cell was shaken or continuously rotated to obtain equilibrium and complete mixing of the gas and oil. Then, a sample was taken, and the equilibrium concentration was determined. In this method, at the end of the time allowed for the diffusion to occur, a sample at the top of the oil column was taken, and the volume of gas released from the oil was used to determine the equilibrium concentration.

The diffusion cell used in this study is shown in Figure 5.6. It consisted of a stainless steel cylinder fitted with two flanges. The internal cross-sectional area of the cell was 32.17 cm^2 and the length was 122.0 cm. The cell was always placed in the vertical position during packing and cleaning, as well as during the actual experiments. The top flange was connected to a high pressure carbon dioxide cylinder. A Heise pressure gauge was also connected to the top flange to measure the pressure inside the cell during the experiment. The bottom flange was equipped with a two-way high pressure valve which permitted collection of oil samples for determining the concentration of diffused carbon dioxide in the oil at the end of the experiment.

The procedure for conducting a diffusion experiment was as follows. First, the diffusion cell was evacuated for six hours using a vacuum pump connected to the top flange of the cell. Next, while the cell was still being evacuated, a plastic tube from a calibrated cylinder containing an initially known volume of oil was connected to the bottom valve, and oil was drawn up into the cell to obtain an oil column of at least 20 cm, and the bottom valve was closed. Carbon dioxide at the desired experimental pressure was

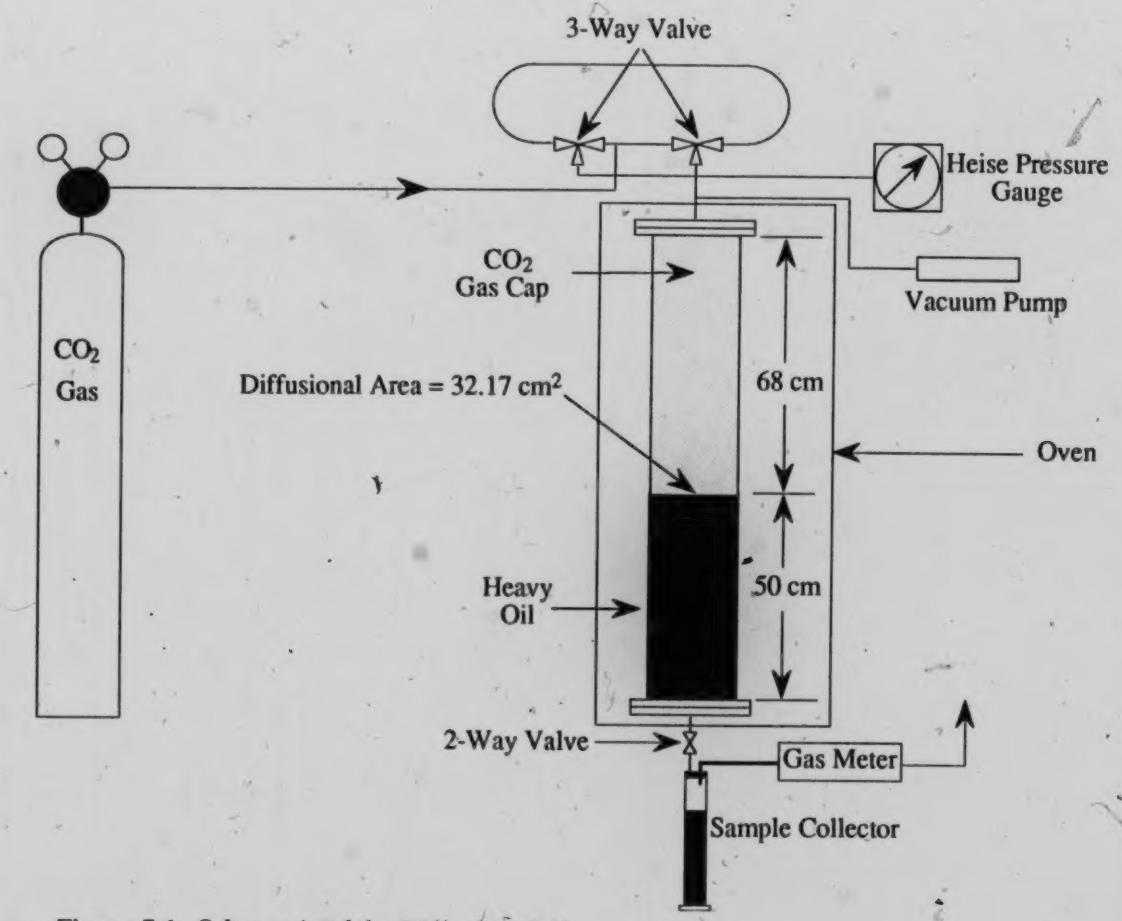
3-Way Valve
Heise Pressure Gauge
CO_2 Gas Cap
Vacuum Pump
CO_2 Gas
Diffusional Area = 32.17 cm^2
68 cm
Oven
Heavy Oil
50 cm
2-Way Valve
Gas Meter
Sample Collector

Figure 5.6 - Schematic of the Diffusion Cell.

injected into the cell at the top flange, and the pressure was kept constant during the course of the experiment by injecting carbon dioxide. The volume of car bon dioxide injected and the time it was injected were recorded. As the injection of carbon dioxide continued, a straight line was obtained on the plot of m_t vs. $\sqrt{t}$. At this time, a sample at the top of the oil column was taken. The volume of gas released was trapped and measured. The experiment was then terminated. The cell was opened and cleaned to prepare for the next experiment.

A sample plot of m_t vs. $\sqrt{t}$ for one of the diffusivity experiments is provided in Figure 5.7, on the next page. The lower part of the curve near the origin where the data points are scattered indicates the period during which the interfacial equilibrium concentration is becoming established. The upper part of the curve where the curve rises rapidly indicates the diffusing gas has reached the bottom of the diffusion cell. When this has occurred, it means that the infinite boundary condition assumption is no longer tenable. The middle section (between A and B), where a straight line is established indicates the diffusion period which may be used to determine the diffusivity coefficient.

It should be noted that when carbon dioxide diffuses in oil, it causes the oil to swell. In this study, the effect of swelling was included in the calculation of the equilibrium concentration at the interface by using Welker and Dunlop's correlation[17].

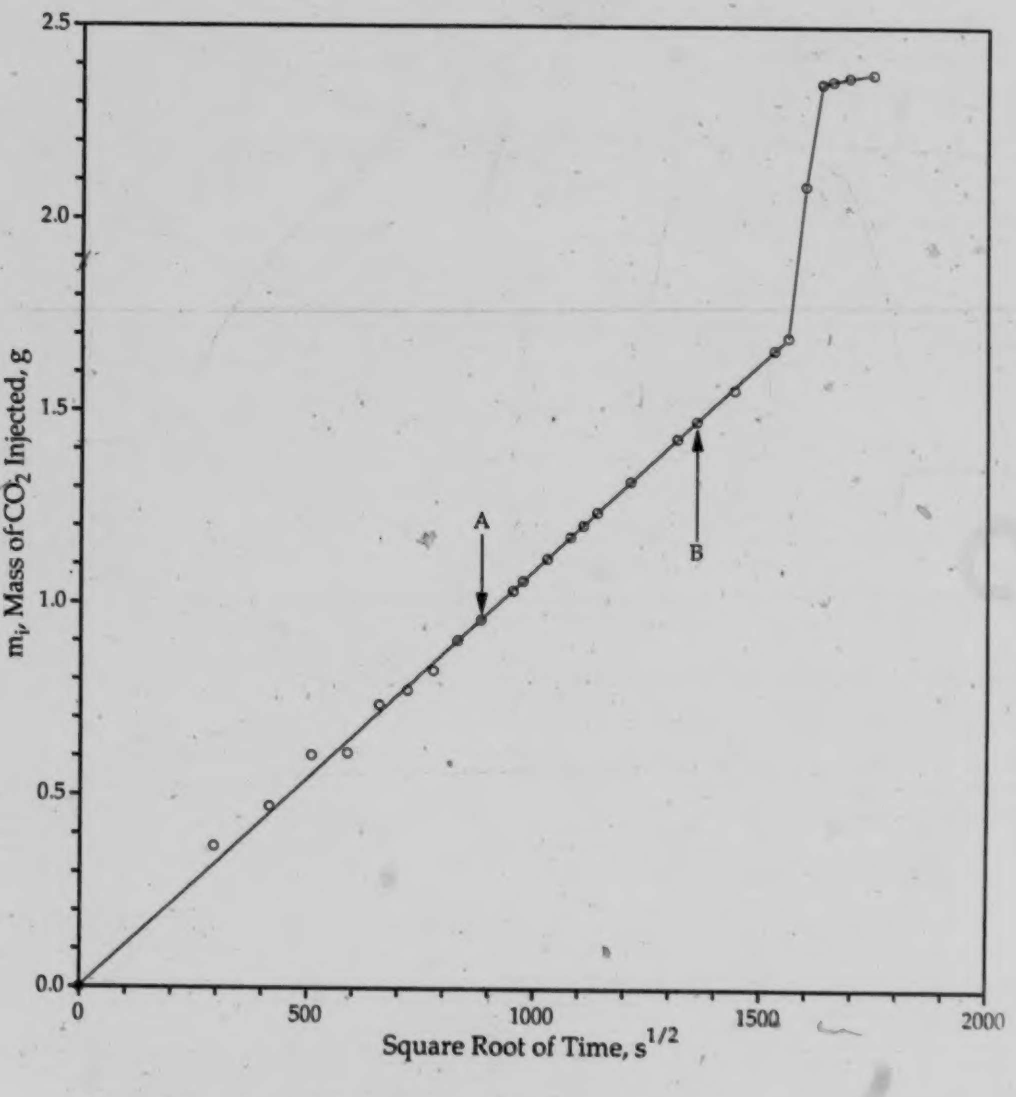

Figure 5.7 - Mass of Carbon Dioxide Injected into Diffusion Cell vs. Square Root of Time.

6 - DISCUSSION OF EXPERIMENTAL RESULTS

This chapter consists of two parts. The first part deals with the presentation and discussion of the work done to investigate the diffusivity of a gas phase into a liquid phase. The second part contains the discussion of the displacement experiments – isothermal and non-isothermal.

I - Diffusivity of Carbon Dioxide and Methane

Tables 6.1 and 6.2, respectively, present the 76 measurements made to investigate the diffusivities of carbon dioxide and methane into different oils. The raw data were plotted and are included in Appendix D. The conditions at which the measurements were made are given in Tables 6.1 and 6.2.

6.1 - Effect of Pressure

Figure 6.1 shows a log-log plot of the diffusivities of carbon dioxide versus pressure for an 1842 mPa.s oil at 294.15 K. Figures 6.2 and 6.3, respectively, present the logarithm of the diffusivity of carbon dioxide in 1842 and 3607 mPa.s oils vs. the logarithm of pressure at the temperature conditions at which carbon dioxide is gaseous. It is apparent in these two figures that as long as carbon dioxide is in a gas phase, its diffusivity increases linearly with increasing pressure. In Figure 6.1, there are two distinct regions: gaseous and liquid carbon dioxide diffusion. First consider gaseous carbon dioxide diffusion consisting of Experiments 3 to 7 conducted at 0.69 to 5.17 MPa. As is shown by the gaseous carbon dioxide diffusion line, the diffusivity of carbon dioxide into oil increased with increasing pressure, under the experimental conditions. Now, consider the liquid carbon dioxide diffusion region, consisting of Experiments 8 to 11 performed at pressures from 6.89 to 10.34 MPa. Clearly, liquid carbon dioxide diffusion remained unchanged and was much lower than gaseous carbon dioxide diffusion. The reasons can be as follows. When carbon dioxide is in a gas phase, molecular forces are weak, thus allowing carbon dioxide molecules to move quickly and freely into the oil. Hence, high carbon dioxide diffusion can result. On the other hand, at 6.89 to 10.34 MPa and 294.15°K, carbon dioxide is in a liquid phase, which means that the molecular speed of the carbon dioxide molecules is low due to the strong

Table 6.1 - Diffusivity of Carbon Dioxide.

Experiment No.	Oil Viscosity at 21°C and 0.101 MPa (mPa.s)	Temperature (°C)	Pressure (MPa)	Diffusivity (m^2/s)
1	603	57.1	6.89	2.5452E-08
2	1058	57.1	6.89	7.2971E-09
3	1842	21.0	0.69	1.2677E-09
4	1842	21.0	1.38	1.6529E-09
5	1842	21.0	2.07	2.0635E-09
6	1842	21.0	3.45	2.4311E-09
7	1842	21.0	5.17	2.7448E-09
8	1842	21.0	6.89	1.0025E-09
9	1842	21.0	6.89	1.0693E-09
10	1842	21.0	8.62	1.1857E-09
11	1842	21.0	10.34	1.0811E-09
12	1842	57.1	0.69	2.3648E-09
13	1842	57.1	2.07	3.8234E-09
14	1842	57.1	3.45	4.6159E-09
15	1842	57.1	6.89	6.1387E-09
16	1842	57.1	10.34	7.2715E-09
17	1842	57.1	13.79	8.4097E-09
18	1842	57.1	17.24	9.0767E-09
19	1842	65.4	0.69	2.8093E-09
20	1842	65.4	2.07	4.4365E-09
21	1842	65.4	3.45	5.5934E-09
22	1842	65.4	6.89	7.5272E-09
23	1842	65.4	10.34	8.3963E-09
24	1842	65.4	13.79	9.5944E-09
25	1842	65.4	17.24	1.1040E-08
26	1842	79.3	0.69	3.5671E-09
27	1842	79.3	2.07	5.4081E-09
28	1842	79.3	3.45	6.7305E-09

Table 6.1 - Cont'd.

Experiment No.	Oil Viscosity at 21°C and 0.101 MPa (mPa.s)	Temperature (°C)	Pressure (MPa)	Diffusivity (m^2/s)
29	1842	79.3	6.89	9.1780E-09
30	1842	79.3	10.34	1.1575E-08
31	1842	79.3	13.79	1.2812E-08
32	1842	79.3	17.24	1.3679E-08
33	1842	93.2	0.69	4.6817E-09
34	1842	93.2	2.07	6.7744E-09
35	1842	93.2	3.45	8.1905E-09
36	1842	93.2	6.89	1.0645E-08
37	1842	93.2	10.34	1.3065E-08
38	1842	93.2	13.79	1.5105E-08
39	1842	93.2	17.24	1.6902E-08
40	3607	21.0	0.69	4.1527E-10
41	3607	21.0	2.07	6.4930E-10
42	3607	21.0	3.45	7.8370E-10
43	3607	57.1	0.69	7.8582E-10
44	3607	57.1	2.07	1.2149E-09
45	3607	57.1	3.45	1.5023E-09
46	3607	57.1	6.89	2.1191E-09
47	3607	57.1	10.34	2.4231E-09
48	3607	57.1	13.79	2.7780E-09
49	3607	57.1	17.24	2.9223E-09
50	3607	65.4	0.69	9.6930E-10
51	3607	65.4	2.07	1.3922E-09
52	3607	65.4	3.45	1.6866E-09
53	3607	65.4	6.89	2.3515E-09
54	3607	65.4	10.34	2.9077E-09
55	3607	65.4	13.79	3.3766E-09
56	3607	65.4	17.24	3.5797E-09

Table 6.1 - Cont'd.

Experiment No.	Oil Viscosity at 21°C and 0.101 MPa (mPa.s)	Temperature (°C)	Pressure (MPa)	Diffusivity (m^2/s)
57	3607	79.3	0.69	1.1724E-09
58	3607	79.3	2.07	1.7455E-09
59	3607	79.3	3.45	2.1320E-09
60	3607	79.3	6.89	2.8408E-09
61	3607	79.3	10.34	3.3845E-09
62	3607	79.3	13.79	3.9272E-09
63	3607	79.3	17.24	4.4053E-09
64	3607	93.2	0.69	1.4052E-09
65	3607	93.2	2.07	2.4581E-09
66	3607	93.2	3.45	2.8765E-09
67	3607	93.2	6.89	3.6291E-09
68	3607	93.2	10.34	4.2601E-09
69	3607	93.2	13.79	4.8763E-09
70	3607	93.2	17.24	5.0193E-09
71	15402	57.1	6.89	4.9337E-10

Table 6.2 - Diffusivity of Methane.

Experiment No.	Oil Viscosity at 21°C and 0.101 MPa (mPa.s)	Temperature (°C)	Pressure (MPa)	Diffusivity (m^2/s)
72	1842	57.1	0.69	3.1151E-11
73	1842	57.1	3.45	6.9301E-11
74	1842	57.1	6.89	8.4217E-11
75	1842	57.1	13.79	4.1067E-10
76	1842	57.1	17.24	4.5441E-10

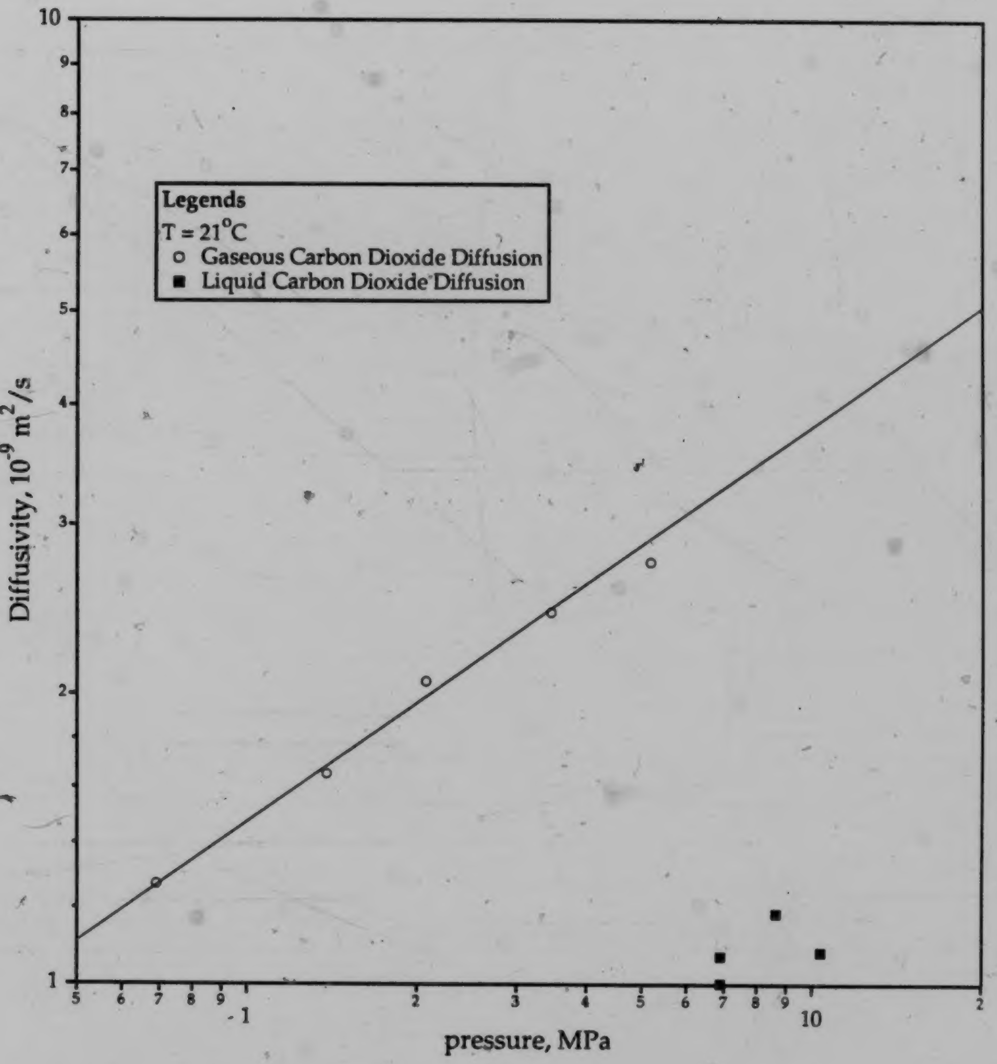

Figure 6.1 - Diffusivities of Gaseous and Liquid Carbon Dioxide.

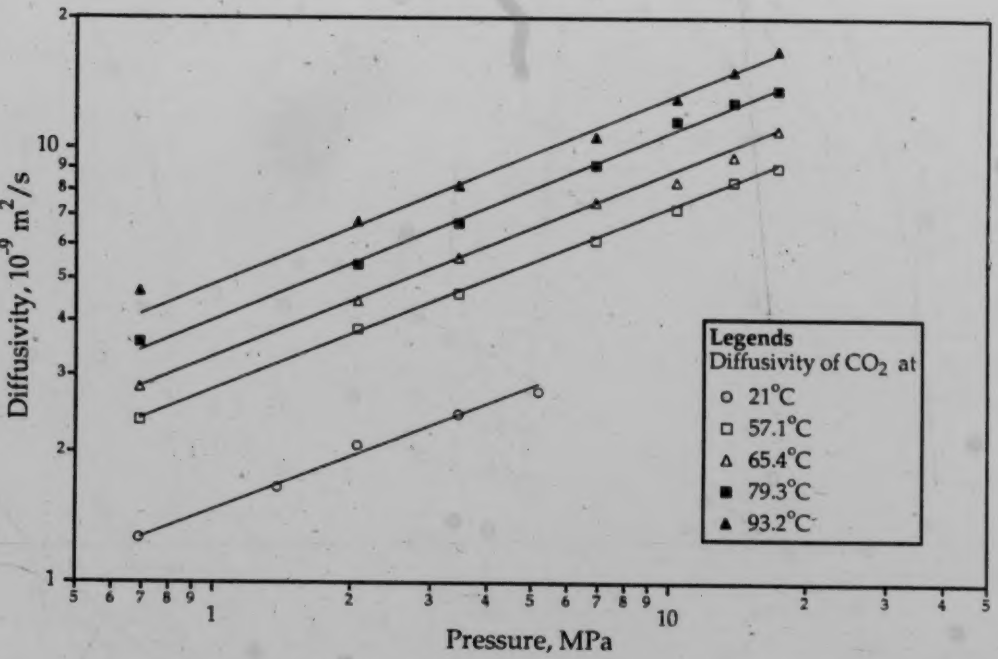

Figure 6.2 - Diffusivity of CO_2 in an 1842 mPa.s Oil as a Function of Pressure.

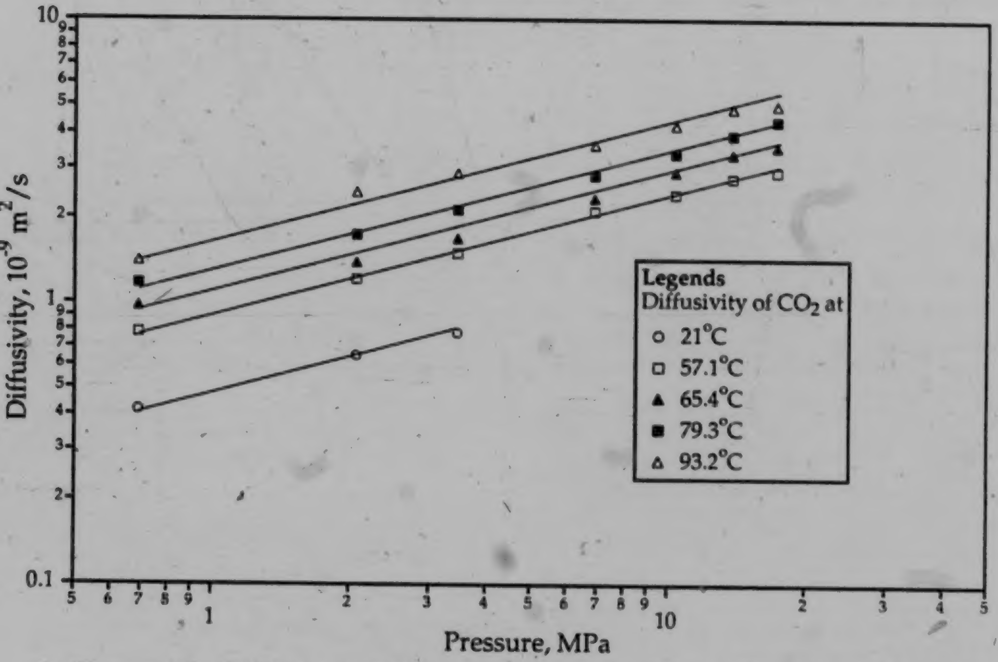

Figure 6.3 - Diffusivity of CO_2 in a 3607 mPa.s Oil as a Function of Pressure.

molecular forces. As a result, the diffusivity of carbon dioxide is reduced. This is why low diffusion coefficients were obtained at 6.89 to 1034 MPa and 294.15 K, at which carbon dioxide was liquid.

This finding of low liquid carbon dioxide diffusion helps explain the low oil recoveries reported by Rojas[1], who injected liquid carbon dioxide rather than gaseous carbon dioxide in some of his immiscible carbon dioxide WAG displacement experiments.

6.2 - Effect of Increasing Temperature

One of the objectives of this research was to investigate the effect of increasing temperature on the diffusivity of carbon dioxide. Figures 6.4 and 6.5 depict the effect of temperature on the diffusivity of carbon dioxide into 1842 and 3607 mPa.s oils at different temperatures. In these figures, the log-log plot of the diffusion coefficient in m^2/s versus temperature in K is presented. A straight line was obtained, indicating that the diffusivity of carbon dioxide increases exponentially with increasing temperature. The reason for an increase in carbon dioxide diffusion with temperature increase is that increasing temperature causes an increase in the kinetic energy which accelerates the movement of the carbon dioxide molecules, consequently leading to an increase in carbon dioxide diffusion. Also, at an elevated temperature, oil molecules are more spread out, the "holes" among the oil molecules are bigger, the intermolecular forces between the oil molecules are weaker, and the viscosity of the oil is less, thus allowing the carbon dioxide molecules to diffuse through more easily.

6.3 - Effect of Oil Viscosity

Five experiments were performed using oils having different viscosities to study the influence of oil viscosity on the diffusivity of carbon dioxide. They were Experiments 1, 2, 15, 46, and 71. The viscosities of the oils used in these five experiments were 603, 1058, 1848, 3607 and 15402 mPa.s, respectively. The pressure and temperature at which these five experiments were conducted were 6.89 MPa and 330.26°K, respectively. The results are shown in Figure 6.6 as the logarithm of the diffusivity versus the logarithm of the oil

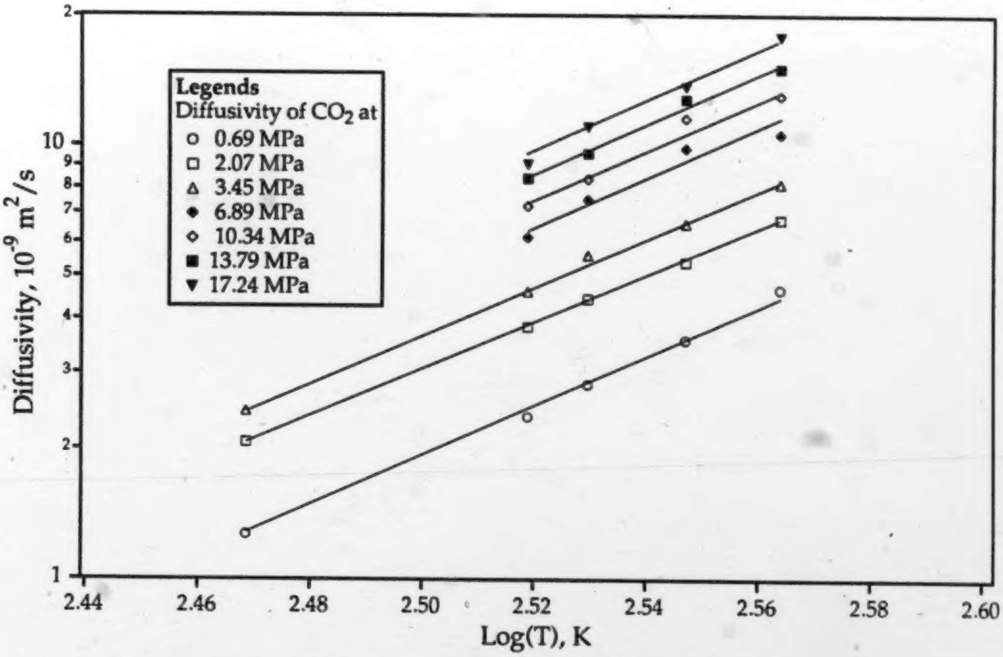

Figure 6.4 - Diffusivity of CO_2 in an 1842 mPa.s Oil as a Function of Temperature.

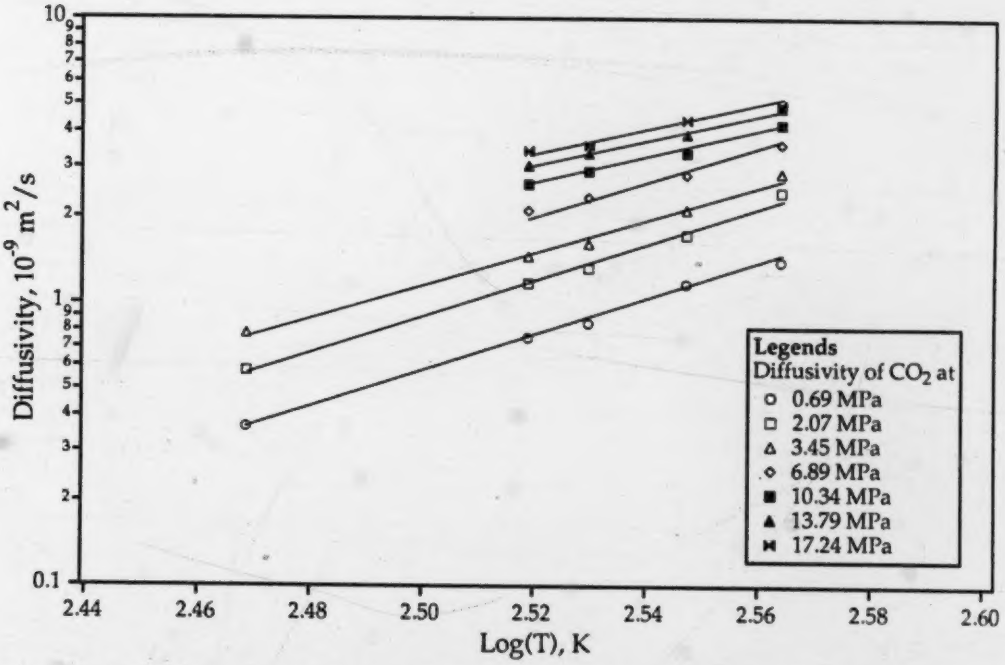

Figure 6.5 - Diffusivity of CO_2 in a 3607 mPa.s Oil as a Function of Temperature.

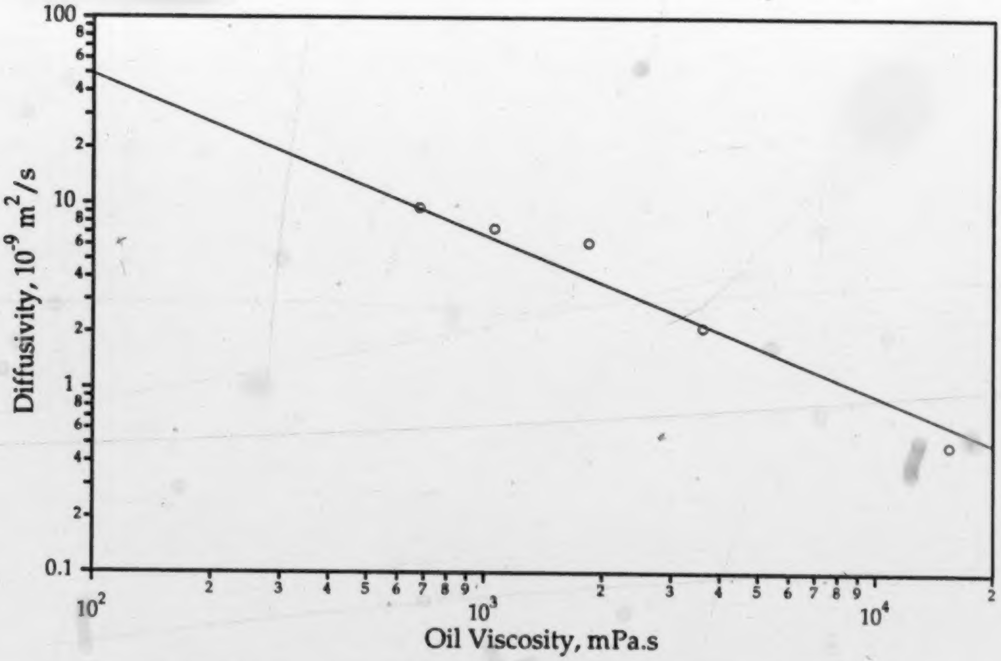

Figure 6.6 - Diffusivity of Carbon Dioxide as a Function of Oil Viscosity.

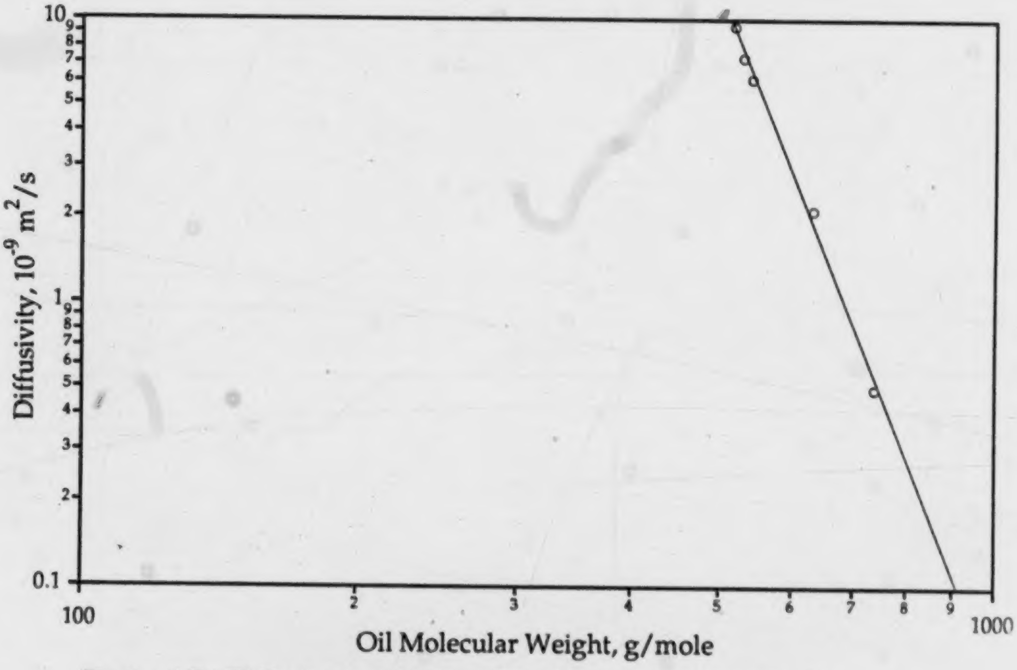

Figure 6.7 - Diffusivity of Carbon Dioxide as a Function of Oil Molecular Weight.

viscosity. It is noted that the diffusivity-oil viscosity relationship is exponential and that the diffusivity decreases with increasing oil viscosity. This is because lower viscosity oils have weaker molecular bonds.

6.4 - Effect of Oil Molecular Weight

Besides oil viscosity, oil molecular weight was also found to have an effect on the diffusivity of carbon dioxide. Figure 6.7 (on the previous page) shows the logarithm of the carbon dioxide diffusivity vs. the logarithm of the oil molecular weight. The diffusivity coefficients plotted in this figure are those of Experiments 1, 2, 15, 46, and 71, which were discussed in Section 6.3. As shown, the diffusivity of carbon dioxide exponentially decreases with increasing oil molecular weight.

6.5 - Diffusivity of Methane

Besides studying the diffusivity of carbon dioxide, the diffusivity of methane into oil was also studied. Five experiments (Experiments 72 to 76) were performed using methane as the diffusing gas at 330.26 K and 0.69 to 17.24 MPa. The results are given in Table 6.2 and plotted in Figure 6.8. Like carbon dioxide diffusivity, the diffusivity of methane into oil increased with increasing pressure. In Figure 6.8, the diffusivities of carbon dioxide into an oil of identical viscosity (i.e., 1846 mPa.s) are also shown. Comparing the two straight lines in the figure reveals that more carbon dioxide than methane could diffuse into the oil under the experimental conditions. The reason is as follows. According to the Stokes-Einstein equation, for diffusing molecules large with respect to solvent molecules, the rate of diffusion depends inversely on the radius of the diffusing molecule (i.e., $\mathcal{D}_{ij}^{*} \alpha 1/V^{1/3}$)[102]. Ross and Hildebrand[103], Nakanishi, Voigt and Hildebrand[104] showed that with dissolved gas molecules the diffusivity mainly depends on the cross-sectional area ($V^{2/3}$) of the diffusing molecules. Based on these two theories, it can be said that diffusivity varies inversely with the molecular volume to the third power ($\mathcal{D}_{ij}^{*} \alpha 1/V^{2/3}$). Under experimental conditions, the molecular volumes of methane (eg., 763.75 cm^3/mol at 3.45 MPa and 57.1°C) were much higher than those of carbon dioxide (eg., 686.20 cm^3/mol at 3.45 MPa and

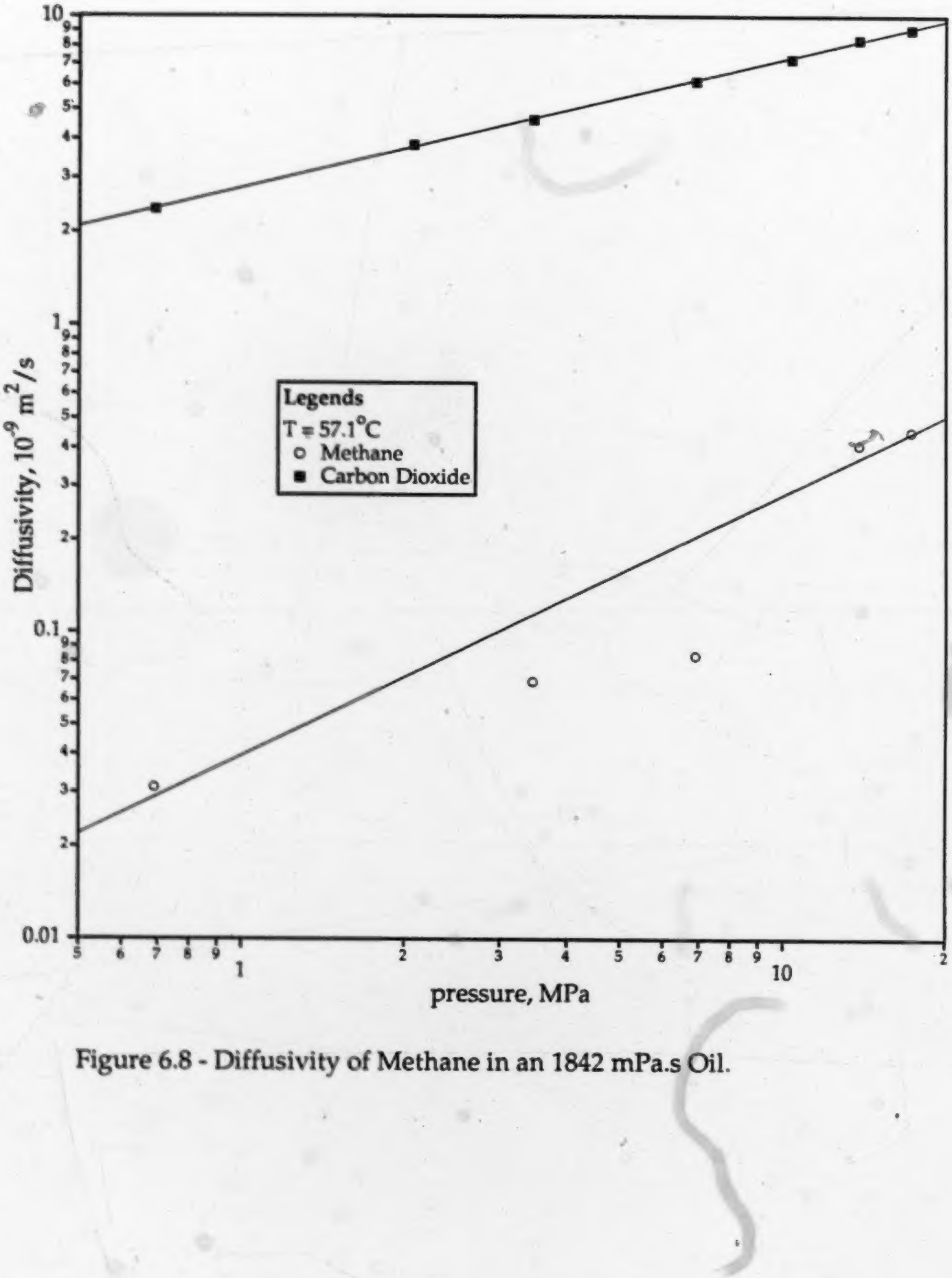

Figure 6.8 - Diffusivity of Methane in an 1842 mPa.s Oil.

57.1°C). Therefore, the diffusivity of methane was found to be lower than that of carbon dioxide.

6.6 - Correlations of the Diffusion Coefficients

The technique of correlating the experimental data employed in this work is the one first proposed by Wilke and Chang[105], which is widely used. The main idea of this technique is to collapse all data points on one single straight line. More details on this technique can be found in Reference 105. From the discussions presented in Sections 6.1 to 6.4, it is obvious that the diffusivity of carbon dioxide in oils depends on pressure, temperature, oil viscosity, and oil molecular weight. As a result, an empirical equation which is similar to the one proposed by McManamey and Wollen.[41], that has a form as shown below, is adopted.

$$\mathcal{D}^{*}_{CO_2-oil} = \omega p^{\alpha} T^{\beta} \mu_o^{\gamma} MW_o^{\varepsilon}. \tag{6.1}$$

where ω, α, β, γ, and ε are the correlation parameters which are to be determined.

By linear regression analysis, the numerical values of ω, α, β, γ, and ε were respectively found to be 5.7582×10^{-9}, 0.3734, 5.6110, -0.6606, and -4.4851. Thus the final form of the correlation is

$$\mathcal{D}^{*}_{CO_2-oil} = 5.7582 \times 10^{-9} \frac{p^{0.3734} T^{5.6110}}{\mu_o^{0.6606} MW_o^{4.4851}}. \tag{6.2}$$

where, p = MPa,
T = K,
μ_o = mPa.s,
MW_o = g/mole.

Figures 6.9 to 6.10 compare the experimental and calculated values. This correlation was found to predict the diffusivity of carbon dioxide in heavy oils with an average error of less than 6%.

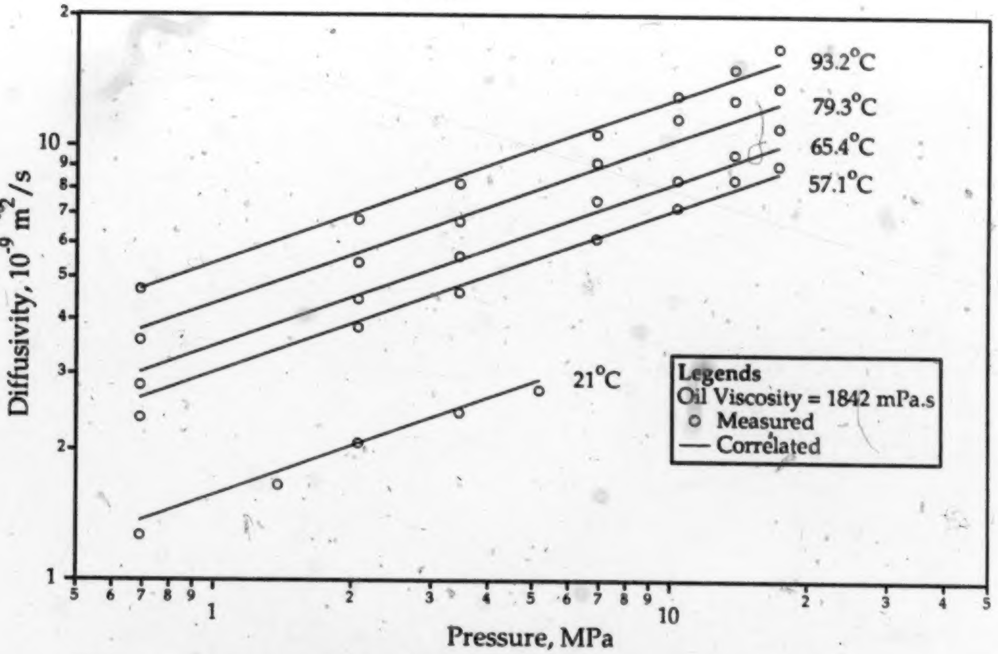

Figure 6.9 - Comparison of Correlated and Measured Values for Kla-Da-Ing Oil.

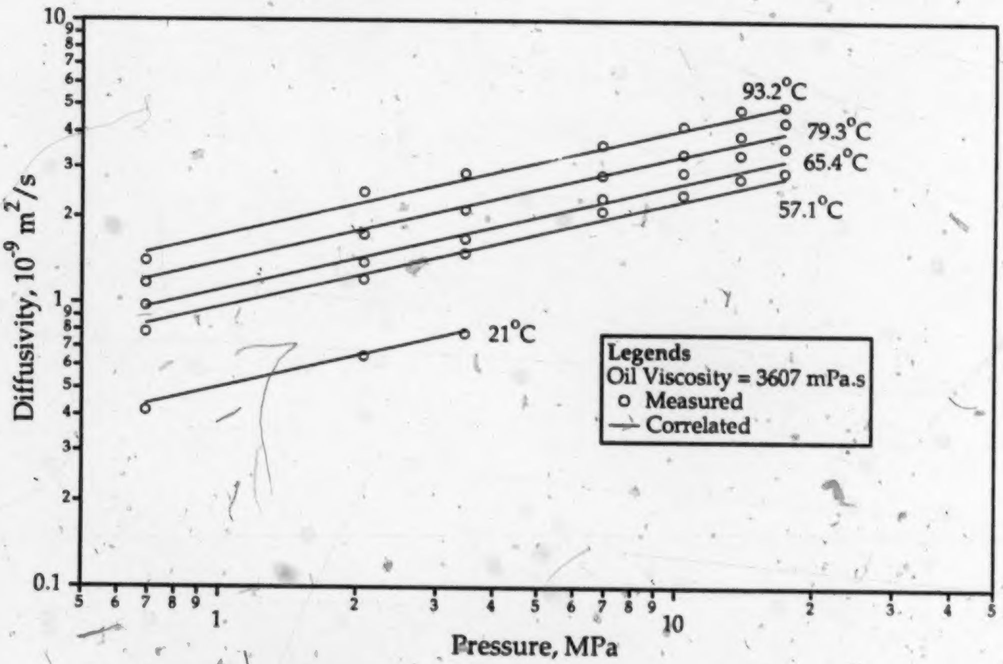

Figure 6.10 - Comparison of Correlated and Measured Values for Della-Bell Oil.

II - Displacement Experiments

The second part of this chapter presents a discussion of the displacement experiments conducted in previous and present studies. The first section presents correlations of the experimental data (included in Table 6.3 on page 80) reported by the former investigators at the University of Alberta[1,4,5,7] with the dimensionless groups. The second section presents a discussion of the experiments made in this study. Most of the experiments conducted in this study and previous studies[1,4,5,7] were completed S_{oi} (initial oil saturation) instead of S_{or} (residual oil saturation) because the process is apt to be employed in reservoirs where primary recoveries are very low and waterflooding is inefficient. Four experiments were performed to investigate the possibility of using a carbonated waterflood in place of an immiscible carbon dioxide WAG flood. Table 6.4 contains the results of these four carbonated waterflood experiments. Fifty experiments were made to study the gravity segregation of the injected fluids. Seven experiments were conducted to observe the performance of the immiscible carbon dioxide WAG process under non-isothermal conditions. Two physical models, one linear and one two-dimensional, were used to conduct the experiments. The results reported in this study are summarized in Tables 6.5 and 6.6. The prefixes "V" and "H" in the run No. refer to vertical and horizontal, respectively. A typical run took a total of two weeks or longer, depending on the type of run. For non-isothermal runs the results of which are summarized in Table 6.8, the model had to be heated to the experimental temperature and pressure conditions for at least 5 to 7 days or even longer to make sure the temperature in the model was uniform, as shown by a constant temperature on the temperature controller.

Figure 6.11 provides a pictorial view of the different experiments conducted in the linear and two-dimensional models. The tabulated results of the experiments can be found in Appendix E. Appendix F contains the production histories of all experiments conducted.

Table 6.3 - Summary of Previous Immiscible Carbon Dioxide Displacement Experiments.

Run No.	Model Type	Process Description	ϕ (%)	Abs. k (d)	Oil Vis. (μ_o) (mPa.s)	S_{oi} (%)	p (MPa)	Flow Vel. (m/d)	CO_2 Vol. Inj. (HCPV)	CO_2 Moles Inj. (mol)	CO_2 Required (sm^3/sm^3)	CO_2 Retained (%Inj)	Total Recovery (%HCPV)
6R[1]	TD	1 CO_2 Slug =>2.32 HCPV WF	43.14	24.3	1032	88.6	5.5	0.18	0.20	1.42	47.33	54.19	39.2
7R[1]	TD	1 CO_2 Slug =>0.66 HCPV WF	43.70	15.4	1032	90.1	5.5	0.20	0.21	1.47	70.31	84.03	26.4
8R[1]	TD	1 CO_2 Slug =>1.90 HCPV WF	45.50	15.4	1032	91.0	5.5	2.90	0.20	1.53	48.37	25.22	38.3
9R[1]	TD	1 CO_2 Slug =>2.06HCPV WF & 1.66 m/d CO_2 Slug	45.67	16.8	1032	91.1	5.5	1.05	0.20	1.54	55.31	64.76	33.5
10R[1]	TD	1 CO_2 Slug =>2.13HCPV WF & 0.72 m/d CO_2 Slug	47.00	17.9	1032	87.7	5.5	2.32	0.20	1.52	40.35	19.95	45.9
14R[1]	TD	1:1 WAG (10 CO_2 Slugs)	41.19	10.9	1032	88.3	5.5	1.16	0.20	1.35	47.28	48.99	39.4
15R[1]	TD	3:1 WAG (10 CO_2 Slugs)	43.22	11.7	1032	88.9	5.5	1.16	0.20	1.42	43.72	74.39	42.3
16R[1]	TD	4:1 WAG (10 CO_2 Slugs)	44.40	14.9	1032	88.7	5.5	1.44	0.20	1.46	39.04	67.54	47.5
17R[1]	TD	5:1 WAG (10 CO_2 Slugs)	42.78	12.4	1032	87.6	5.5	1.16	0.20	1.4	40.46	53.53	46.4
18R[1]	TD	6:1 WAG (10 CO_2 Slugs)	43.71	14.1	1032	87.8	5.5	1.47	0.20	1.43	43.29	61.34	43.3
21aR[1]	TD	1.66 HCPV Waterflood	43.15	9.26	1032	88.1	5.5	0.88	0.0	0.0	0.0	0.0	33.8
23R[1]	TD	4:1 WAG (10 CO_2 Slugs)	42.14	9.3	4681	89.1	5.5	0.87	0.20	1.39	83.58	75.21	22.2
12Z[4]	TD	1 CO_2 Slug =>2.48 HCPV WF	40.48	12.4	1116	92.4	5.5	2.07	0.20	1.43	60.3	23.76	33.0
13Z[4]	TD	4:1 WAG (10 CO_2 Slugs)	38.71	5.3	1116	90.3	5.5	2.59	0.20	1.33	54.9	37.05	35.9
16Z[4]	TD	4:1 WAG (10 CO_2 Slugs)	39.26	14.3	1116	90.5	5.5	1.55	0.20	1.34	45.1	45.82	43.0
24Z[4]	TD	4:1 WAG (10 CO_2 Slugs)	41.39	15.4	1233	91.1	5.5	1.55	0.20	1.42	68.5	98.17	28.2
25Z[4]	TD	4:1 WAG (10 CO_2 Slugs)	40.81	8.2	1092	89.9	5.5	0.78	0.20	1.38	72.1	84.93	26.8
TD1[5]	TD	4:1 WAG (10 CO_2 Slugs) Senlac Oil	43.10	7.6	3295	86.8	2.5	0.78	0.61	1.41	45.38	48.91	40.9

Table 6.3 - Summary of Previous Immiscible Carbon Dioxide Displacements Experiments (Cont'd).

Run No.	Model Type	Process Description	ø (%)	Abs. k (d)	Oil Vis. (μ_o) (mPa.s)	S_{oi} (%)	p (MPa)	Flow Vel. (m/d)	CO_2 Vol. Inj. (HCPV)	CO_2 Moles Inj. (mol)	CO_2 Required (sm^3/sm^3)	CO_2 Retained (%Inj)	Total Recovery (%HCPV)
GTD1[7]	TD	4:1 WAG (10 CO_2 Slugs)	41.6	13.6	1230	85.9	2.5	1.29	0.02	0.42	19.7	95.4	32.8
GTD3[7]	TD	4:1 WAG (10 CO_2 Slugs)	41.1	18.7	1115	91.3	2.5	2.6	0.10	0.45	7.3	99.1	42.5
GTD4[7]	TD	4:1 WAG (10 CO_2 Slugs)	41.6	13.6	1130	93.2	2.5	2.6	0.30	0.68	22.5	75.3	40.6
GTD5[7]	TD	4:1 WAG (10 CO_2 Slugs)	43.2	11.5	1135	85.6	1.0	2.6	0.10	0.078	4.5	99.9	35.8
GTD7[7]	TD	4:1 WAG (10 CO_2 Slugs)	38.0	11.9	1279	91.1	1.0	2.6	0.30	0.22	7.2	4.0	43.6
GTD8[7]	TD	4:1 WAG (10 CO_2 Slugs)	38.0	12.2	1046	88.9	1.0	1.29	0.10	0.071	3.0	15.0	36.8
GTD10[7]	TD	4:1 WAG (10 CO_2 Slugs)	39.5	12.1	1046	91.7	1.0	1.29	0.30	0.23	6.1	12.3	44.1
LC16[5]	LC	4:1 WAG (10 CO_2 Slugs)	34.8	9.0	1059	79.1	2.5	0.98	0.64	0.75	29.71	93.91	52.73
LC17[5]	LC	4:1 WAG (10 CO_2 Slugs)	37.7	12.3	1055	89.2	2.5	0.98	0.20	0.26	12.64	20.46	48.02
LC30[7]	LC	4:1 WAG (10 CO_2 Slugs)	37.6	11.4	1055	90.2	2.5	0.98	0.89	1.13	47.6	16.8	50.2
LC31[7]	LC	4:1 WAG (10 CO_2 Slugs)	36.4	11.0	1055	79.4	2.5	0.98	0.20	0.22	9.5	14.3	57.0
LC32[7]	LC	4:1 WAG (10 CO_2 Slugs)	37.6	14.1	1055	93.7	2.5	0.98	0.40	0.53	27.7	25.0	41.1
LC33[7]	LC	4:1 WAG (10 CO_2 Slugs)	37.4	13.1	1230	94.9	2.5	0.98	0.20	0.22	11.1	12.4	51.1
LC34[7]	LC	Waterflood	36.5	9.9	1134	92.5	2.5	0.98	0.0	0.0	0.0	0.0	40.5
LC36[7]	LC	4:1 WAG (10 CO_2 Slugs)	37.1	11.2	1130	91.8	2.5	0.98	0.05	0.064	3.3	99.4	46.4

Table 6.4 - Summary of Carbonated Waterflood Experiments.

Run No.	ø (%)	Abs. k (d)	Oil Vis. (μ_o) (mPa.s)	S_{oi} (%)	p (MPa)	Ave. Flow Velocity (m/d)	CO_2 Required (sm^3/sm^3)	CO_2 Retained (sm^3/sm^3)	Total Recovery (%HCPV OOIP)
CWF1	35.8	14.4	1058.0	92.2	2.5	0.98	63.4	29.8	56.5
CWF2	37.8	11.6	1058.0	89.9	1.0	2.60	5.3	36.6	39.2
CWF3	36.0	11.3	1058.0	96.2	2.5	0.98	62.7	31.1	57.1
CWF4	37.5	10.9	1058.0	90.1	1.0	2.60	4.9	23.6	42.2

Note: Runs CWF1 and CWF3 were conducted in the linear core model. Run CWF3 was conducted to check the result of Run CWF1.
Run CWF2 was made in the 2-D model. In this run, 20% HCPV carbon dioxide was mixed with water at 4:1 ratio.
Run CWF4 was conducted to check the result of Run CWF2.

Table 6.5 - Summary of Vertical Displacement Experiments in a Linear Model.

Run No.	Process Description	Injection At	WAG Ratio	CO_2 Injected (%HC-PV)	No. of Slugs	ø (%)	Abs. k (d)	Oil Vis. (μ_o) (mPa.s)	S_{oi} (%)	p (MPa)	Injection Velocity (cc/h)	CO_2 Required (sm³/sm³)	CO_2 Retained (sm³/sm³)	CO_2 WAG Rec. (%)	Post-wf Rec. (%)	BD Rec. (%)	Total Recovery (%HCPV OOIP)
VLC1	WAG	bottom	4	20	10	35.9	11.3	1053	95.4	1.0	0.98	3.8	37.2	41.6	11.0	1.9	54.5
VLC2	WAG	top	4	20	10	35.5	11.1	1053	90.7	1.0	0.98	4.3	54.1	38.2	7.2	2.5	47.9
VLC3	Continuous	bottom		20		34.7	9.2	1053	94.4	1.0	0.98	5.3	59.6	0.2	38.6	1.1	39.9
VLC4	Continuous	bottom		20		35.5	10.2	1053	92.0	1.0	0.98	6.5	99.9	0.7	36.0	1.7	38.4
VLC5	Continuous	top		20		35.4	11.3	1053	91.8	1.0	0.98	7.2	99.2	1.7	28.0	0.3	30.0
VLC6	WAG	bottom	4	20	10	35.3	9.9	1053	92.0	2.5	0.98	12.1	75.3	37.5	9.8	0.7	48.0
VLC7	Continuous	top		till BT		35.4	10.0	1053	90.7	1.0	0.98	20.7	87.4	4.8	51.6	1.2	57.6
VLC8	Continuous	top		till BT		35.5	9.4	1053	91.9	1.0	0.98	15.5	67.9	5.6	54.8	0.4	60.8
VLC9	Continuous	top		till BT		35.4	10.6	1053	92.6	1.0	0.49	15.8	79.5	9.6	58.7	0.9	69.2
VLC10	Continuous	top		till BT		35.4	11.0	1053	91.5	1.0	0.49	17.5	87.9	10.8	63.9	2.0	76.7
VLC11	Continuous	top		till BT		35.6	10.8	1053	92.3	1.0	0.98	16.9	71.4	7.0	51.1	2.0	60.1

Table 6.6 - Summary of Horizontal WAG Displacement Experiments in a Quarter of a 5-Spot System.

Run No.	Process Description	WAG Ratio	CO_2 Injected (%HC-PV)	No. of Slugs	ø (%)	Abs. k (d)	Oil Vis. (μ_o) (mPa.s)	S_{oi} (%)	p (MPa)	CO_2 Injection Velocity (m/d)	Water Injection Velocity (m/d)	CO_2 Required (sm^3/sm^3)	CO_2 Retained (sm^3/sm^3)	CO_2 WAG Rec. (%)	Post-wf Rec. (%)	BD Rec. (%)	Total Recovery (%HCPV OOIP)
H2D1	WAG	4	20	10	40.1	12.0	603	93.3	2.5	0.83	0.83	5.0	50.2	28.6	12.2	0.8	41.6
H2D2	WAG	4	20	10	39.7	14.5	603	90.7	2.5	1.55	1.55	4.7	47.0	30.7	13.0	0.8	44.5
H2D3	WAG	4	20	10	39.8	13.2	603	86.9	2.5	2.54	2.54	4.4	42.2	32.9	13.2	1.4	47.5
H2D4	WAG	4	20	10	38.7	15.7	603	89.9	2.5	3.17	3.17	4.5	45.1	31.8	13.5	0.9	46.2
H2D5	WAG	4	20	10	42.8	12.3	603	81.2	2.5	3.81	3.81	5.0	33.6	31.0	10.5	0.4	41.9
H2D6	WAG	4	20	10	37.4	12.2	1058	88.1	2.5	0.83	0.83	6.3	75.4	29.7	2.4	0.8	32.9
H2D7	WAG	4	20	10	41.6	13.9	1058	91.3	2.5	1.55	1.55	6.1	44.2	29.1	4.5	0.3	33.9
H2D8	WAG	4	20	10	40.5	12.5	1058	90.7	2.5	2.60	2.60	4.6	65.3	30.9	8.1	6.1	45.1
H2D9	WAG	4	20	10	38.5	14.5	1058	89.9	2.5	3.17	3.17	4.8	43.3	31.8	9.6	1.7	43.1
H2D10	WAG	4	20	10	38.1	12.3	1058	89.1	2.5	3.81	3.81	5.1	29.7	29.9	7.9	3.0	40.8
H2D11	WAG	4	20	10	41.3	12.7	1842	93.2	2.5	0.83	0.83	7.7	55.9	21.3	4.1	1.8	27.2
H2D12	WAG	4	20	10	43.7	14.1	1842	91.4	2.5	1.55	1.55	6.8	56.8	24.2	4.8	1.8	30.8
H2D13	WAG	4	20	10	41.1	13.5	1842	87.8	2.5	2.54	2.54	16.2	52.6	28.3	5.4	2	35.7
H2D14	WAG	4	20	10	39.5	13.4	1842	90.1	2.5	3.17	3.17	16.5	52.3	27.6	5.4	2.0	35.0
H2D15	WAG	4	20	10	39.8	13.1	1842	90.3	2.5	3.81	3.81	17.8	45.9	24.6	4.2	3.6	32.4
H2D16	WAG	4	20	10	39.9	12.7	3295	90.0	2.5	0.83	0.83	25.9	60.7	20.7	0.6	1.1	22.4
H2D17	WAG	4	20	10	42.4	14.0	3295	87.8	2.5	1.55	1.55	23.0	65.0	23.0	1.4	0.8	25.2
H2D18	WAG	4	20	10	39.1	12.9	3295	89.5	2.5	2.54	2.54	17.3	56.4	29.8	1.5	2.2	33.5

Table 6.6 - Summary of Horizontal WAG Displacement Experiments in a Quarter of a 5-Spot System (Cont'd).

Run No.	Process Description	WAG Ratio	CO_2 Injected (%HC-PV)	No. of Slugs	ø (%)	Abs. k (d)	Oil Vis. (μ_o) (mPa.s)	S_{oi} (%)	p (MPa)	CO_2 Injection Velocity (m/d)	Water Injection Velocity (m/d)	CO_2 Required (sm^3/sm^3)	CO_2 Retained (sm^3/sm^3)	CO_2 WAG Rec. (%)	Post-wf Rec. (%)	BD Rec. (%)	Total Recovery (%HCPV OOIP)
H2D19	WAG	4	20	10	38.5	13.6	3295	93.1	2.5	3.17	3.17	20.4	25.5	24.1	1.4	2.8	28.3
H2D20	WAG	4	20	10	38.1	13.6	3295	94.0	2.5	3.81	3.81	24.5	36.8	18.9	2.2	2.5	23.6
H2D21	WAG	4	20	10	44.3	12.6	3607	92.1	2.5	0.83	0.83	30.9	66.9	17.0	0.6	1.1	18.7
H2D22	WAG	4	20	10	39.5	12.4	3607	91.5	2.5	1.55	1.55	9.4	62.9	20.4	0.4	1.4	22.2
H2D23	WAG	4	20	10	39.7	12.4	3607	89.0	2.5	2.54	2.54	6.9	39.9	23.8	4.4	2.0	30.2
H2D24	WAG	4	20	10	40.2	12.8	3607	90.3	2.5	3.17	3.17	8.3	59.5	21.3	1.7	2.0	25.0
H2D25	WAG	4	20	10	41.0	12.9	3607	90.6	2.5	3.81	3.81	9.4	51.3	18.0	2.5	1.6	22.1
H2D26	WAG	4	20	10	36.1	22.0	1058	92.3	1.0	0.26	2.60	4.7	96.3	30.7	12.3	1.2	44.2
H2D27	WAG	4	20	10	40.0	14.1	1058	91.1	1.0	0.52	2.60	4.9	96.9	31.1	10.7	0.9	42.7
H2D28	WAG	4	20	10	42.1	14.5	1058	84.9	1.0	2.6	2.6	4.1	54.1	35.7	13.2	2.4	51.3
H2D29	WAG	4	20	10	39.5	16.6	1058	90.3	1.0	5.20	2.60	4.5	90.7	35.5	9.9	0.7	46.1
H2D30	WAG	4	20	10	40.6	13.3	1058	90.6	1.0	4.15	0.83	4.5	81.9	37.0	8.8	0.9	46.7
H2D31	WAG	4	20	10	41.4	13.3	1058	86.4	1.0	1.29	1.29	4.5	44.0	33.6	9.5	3.3	46.4
H2D32	WAG	4	20	10	40.6	13.3	1058	91.3	1.0	0.83	0.83	4.8	65.7	31.5	10.1	1.7	43.3
H2D33	WAG	4	20	10	38.5	12.5	1058	89.2	1.0	2.08	2.08	6.3	75.4	29.7	2.4	0.8	32.9

Table 6.6 - Summary of Horizontal WAG Displacement Experiments in a Quarter of a 5-Spot System (Cont'd).

Run No.	Process Description	CO_2 Injected (%HC-PV)	ø (%)	Abs. k (d)	Oil Vis. (μ_o) (mPa.s)	S_{oi} (%)	p (MPa)	CO_2 Injection Velocity (m/d)	Water Injection Velocity (m/d)	Soak Time (days)	CO_2 Required (sm^3/sm^3)	CO_2 Retained (sm^3/sm^3)	CO_2 WAG Rec. (%)	Post-wf Rec. (%)	BD Rec. (%)	Total Recovery (%HCPV OOIP)
H2D34	Continuous	5	39.2	14.1	1058	90.6	2.5	1.27	2.54	0	5.5	98.9	1.7	34.6	1.3	37.6
H2D35	Continuous	5	38.5	14.0	1058	91.6	2.5	1.59	3.17	3.0	5.5	99.3	1.5	35.0	1.6	38.1
H2D36	Continuous	5	38.6	10.7	1058	91.7	2.5	1.27	2.54	4.83	5.8	97.4	1.3	32.3	2.6	36.2
H2D37	Continuous	5	39.4	11.3	1058	89.1	2.5	1.27	2.54	10	5.4	99.0	1.7	36.1	0.7	38.5

Table 6.7 - Summary of Vertical Displacement Experiments in a Two-Dimensional Model.

Run No.	Process Description	Injection At	WAG Ratio	CO_2 Injected (%HC-PV)	No. of Slugs	ø (%)	Abs. k (d)	Oil Vis. (μ_o) (mPa.s)	S_{oi} (%)	p (MPa)	Injection Velocity (m/d)	CO_2 Required (sm^3/sm^3)	CO_2 Retained (sm^3/sm^3)	CO_2 WAG Rec. (%)	Post-wf Rec. (%)	BD Rec. (%)	Total Recovery (%HCPV OOIP)
V2D1	Continuous	bottom		5		39.4	11.3	1058	88.7	2.5	2.60	2.4	55.0				47.7
V2D2	Continuous	bottom		5		40.4	12.0	1058	90.0	2.5	2.60	3.42	20.8				41.8

V2D2 - Nitrogen was used in place of carbon dioxide.

Table 6.8 - Summary of Non-Isothermal Horizontal Displacement Experiments in a Scaled Model.

Run No.	CO_2 Injected (%HC-PV)	WAG Ratio	Flood Pattern A Quarter of a	ø (%)	Abs. k (d)	Oil Vis. (μ_o) (mPa.s)	S_{oi} (%)	p (MPa)	T (°C)	CO_2 Injection Velocity (m/d)	Water Injection Velocity (m/d)	CO_2 Required (sm^3/sm^3)	CO_2 Retained (sm^3/sm^3)	CO_2 WAG Rec. (%)	Post-wf Rec. (%)	BD Rec. (%)	Total Recovery (%HCPV OOIP)
H2D38	20	4	5-Spot	38.9	12.2	1058	88.6	2.5	37.0	2.54	2.54	9.7	44.2	40.0	11.4	3.5	54.9
H2D39	20	4	5-Spot	37.7	4.4	5200	87.1	2.5	37.0	2.54	2.54	12.9	55.0	27.8	11.2	2.1	41.1
H2D40	20	4	5-Spot	37.6	3.2	5200	86.9	3.14	37.0	2.54	2.54	13.5	35.4	30.8	9.9	3.0	43.7
H2D41	10	4	5-Spot	37.6	3.9	5200	86.9	2.5	37.0	2.54	2.54	8.8	59.2	19.6	10.5	1.1	31.2
H2D42a			9-Spot	37.3	6.2	603	82.1	4.8	37.0		2.54						50.7
H2D42b	20	2	9-Spot	37.3	6.2	603	40.5	4.8	37.0	2.54	2.54	96.4	33.3	2.4	9.0	1.2	12.6
H2D43a			9-Spot	37.0	11.9	282	82.8	3.58	21.0		2.54						50.7
H2D43b	20	2	9-Spot	37.0	11.9	282	40.8	3.58	21.0	2.54	2.54	77.2	16.3	2.8	9.3	2.7	14.8
H2D44a			9-Spot	37.3	8.1	282	81.0	3.58	21.0		2.54						48.3
H2D44b	20	2	9-Spot	37.3	8.1	282	41.9	3.58	21.0	2.54	2.54	82.1	28.8	2.9	9.2	3.0	15.1

All non-isothermal displacement experiments were performed in the WAG mode, utilizing 10 slugs.

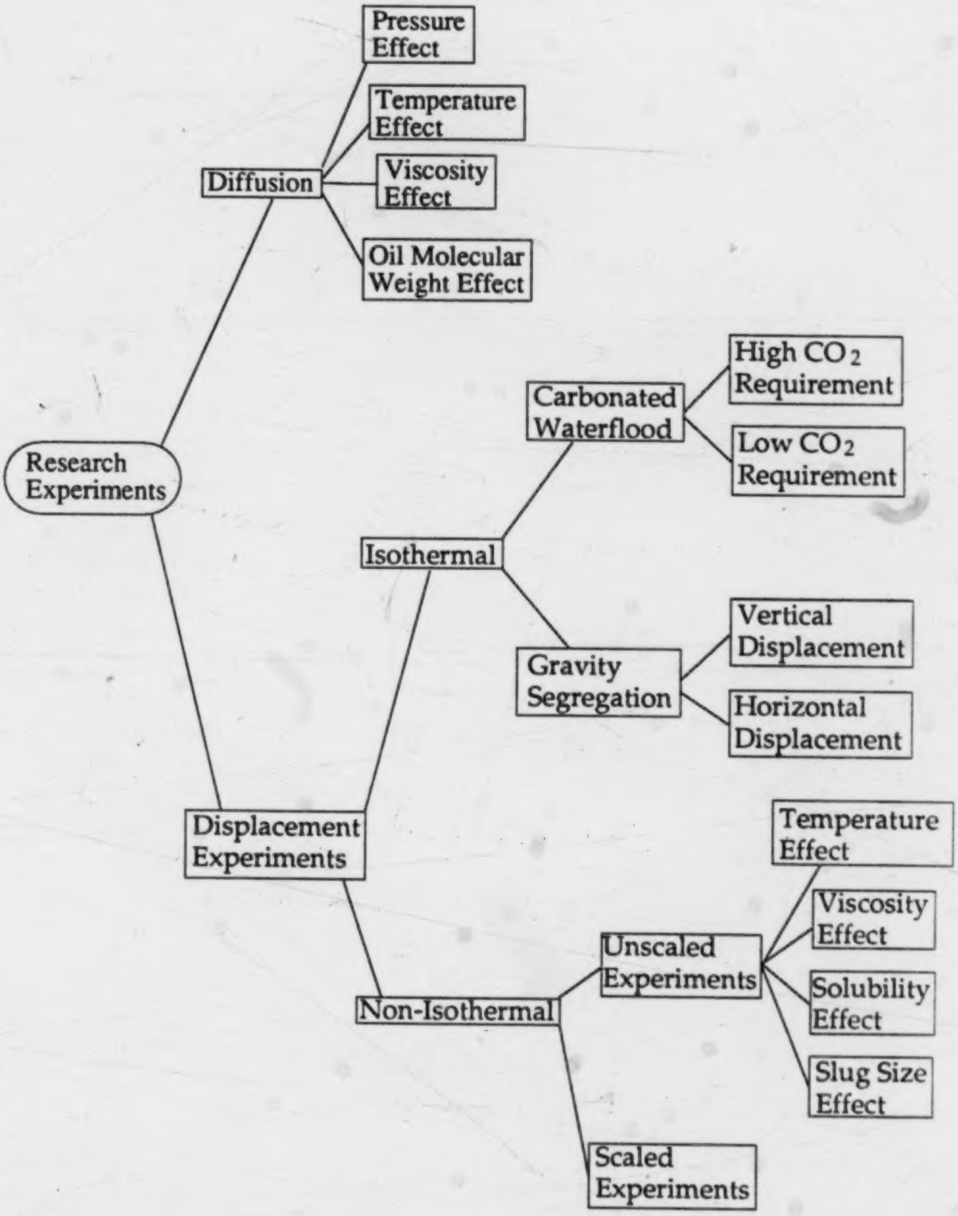
Research Experiments
Diffusion
Pressure Effect
Temperature Effect
Viscosity Effect
Oil Molecular Weight Effect
Displacement Experiments
Isothermal
Carbonated Waterflood
High CO_2 Requirement
Low CO_2 Requirement
Gravity Segregation
Vertical Displacement
Horizontal Displacement
Non-Isothermal
Unscaled Experiments
Temperature Effect
Viscosity Effect
Solubility Effect
Slug Size Effect
Scaled Experiments

Figure 6.11 - Map of experiments conducted in this research.

6.7 - Correlation of Displacement Results

This section presents the correlations of the experimental displacement results reported by Rojas[1], Zhu[4], Dyer[5], Prosper[7], and in this study. The dimensionless groups used in the correlations are those previously derived by Rojas[1]. Note that the groups derived by Rojas[1] are a sub-set of the two sets derived in this study.

6.7.1 - Single Slug and WAG Correlations

Figure 6.12 presents the correlations of the overall average gas-oil ratios[1,4] with the dimensionless group $\frac{\vartheta_g \mu_o}{g k \Delta\rho_{go}}$ (which is the ratio of viscous forces to gravitational forces) for single slug immiscible carbon dioxide displacements and immiscible carbon dioxide WAG displacements in a quarter of a 5-spot flood pattern. Let us first consider the upper line representing the overall average gas-oil ratios for single slug carbon dioxide injection experiments (Runs 6R-10R[1] and 12Z[4]) conducted using injection velocities ranging from 0.18 to 2.9 m/d, and a total carbon dioxide slug size of 20% HCPV. In these runs, carbon dioxide was continuously injected until 20% HCPV had been injected; then, water was injected to displace the carbon-dioxide swollen oil until the water-oil ratio reached about 20 to 1, which is the cut-off water-oil ratio. As is shown in the figure, the overall average gas-oil ratio linearly increases from 22 to 508 sm^3/sm^3 as $\frac{\vartheta_g \mu_o}{g k \Delta\rho_{go}}$ increases from 0.0096 to 0.23, or the injection velocity increases from 0.18 to 2.9 m/d. In other words, there is an exponential relationship between the overall average gas-oil ratio and the ratio of viscous forces to gravitational forces for single slug immiscible carbon dioxide injection. It is clearly shown by the straight line that a higher gas injection rate results in a higher overall average gas-oil ratio. This is basically due to a higher mobility ratio at a higher injection rate. It should also be noted that when carbon dioxide is injected at a high rate, it does not have enough time to dissolve as much as it can to develop a complete phase equilibrium with the oil phase. Therefore, at a higher rate, a larger volume of carbon dioxide is produced during the flood. In contrast to this, a lower injection rate will give carbon dioxide more time to dissolve and to develop a better phase equilibrium with the oil. As is indicated in the figure, at a viscous-

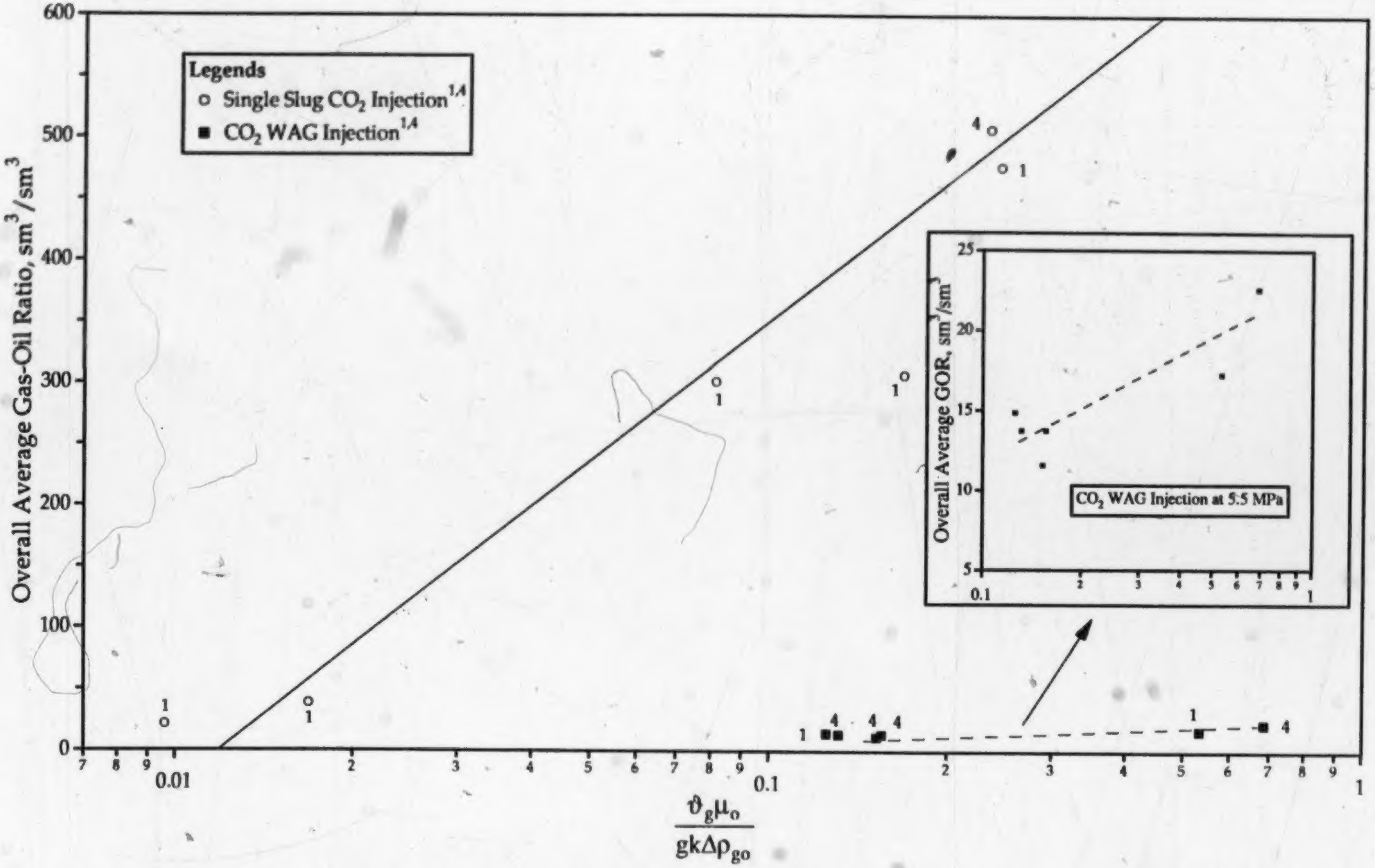

Figure 6.12 - Gas-Oil Ratio Correlations for Single Carbon Dioxide Slug Injection and WAG Injection (Data from Refs. 1 and 4).

gravitational force ratio equal to 0.0096, the overall average gas-oil ratio is 22 sm^3/sm^3, which is about one-twenty fifth of that at 0.23, for single slug immiscible carbon dioxide injection.

On the bottom of the same figure, there is a dashed line which represents the overall average gas-oil ratios for experiments (Runs 16R[1], 23R[1], 13Z[4], 16Z[4], 24Z[4] and 25Z[4]) carried out utilizing the immiscible carbon dioxide WAG injection method. Similar to the single slug carbon dioxide injection, the overall average gas-oil ratio for the carbon dioxide WAG process rises to a higher value at a higher viscous-to-gravitational forces ratio. The inserted picture shows this more clearly. Observing the two gas-oil ratio curves, one sees that much less gas, even at a higher viscous to gravitational force ratio, is produced during the carbon dioxide WAG injection than during the single slug carbon dioxide injection. This means that injecting carbon dioxide in the WAG mode reduces the mobility of the gas phase, which consequently leads to an increased amount of carbon dioxide going into solution in the oil.

6.7.2 - WAG Ratio Correlations

It has been shown that injecting carbon dioxide in the WAG fashion yields better mobility control on the gas phase than injecting it in the single slug mode[1]. One can ask at what WAG ratio the carbon dioxide WAG injection will give its best performance. Referring to Figure 6.13, where the overall average gas-oil ratios of Runs 14R-18R[1] conducted using the same carbon dioxide slug volume but different WAG ratios[1] are plotted versus the products of the viscous-gravitational forces ratio and WAG ratio, the dashed concave downward curve represents the overall average gas-oil ratio curve while the solid concave upward curve represents the oil recovery. The WAG ratios employed in the experiments were varied from 1:1 to 6:1. In order to make a fair comparison, the same injection velocity and oil were used in these runs. It is shown by the overall average gas-oil ratio curve that the volume of produced gas decreases as the WAG ratio increases until the WAG ratio reaches 4:1, where the gas-oil ratio is minimum. Then it rises back up when the WAG ratio increases to 5:1 then to 6:1. The reasons may be most likely as follows. When a WAG ratio lower than 4:1 is utilized, the slug volume of water is not enough to reduce the mobility of the carbon dioxide gas phase. When a

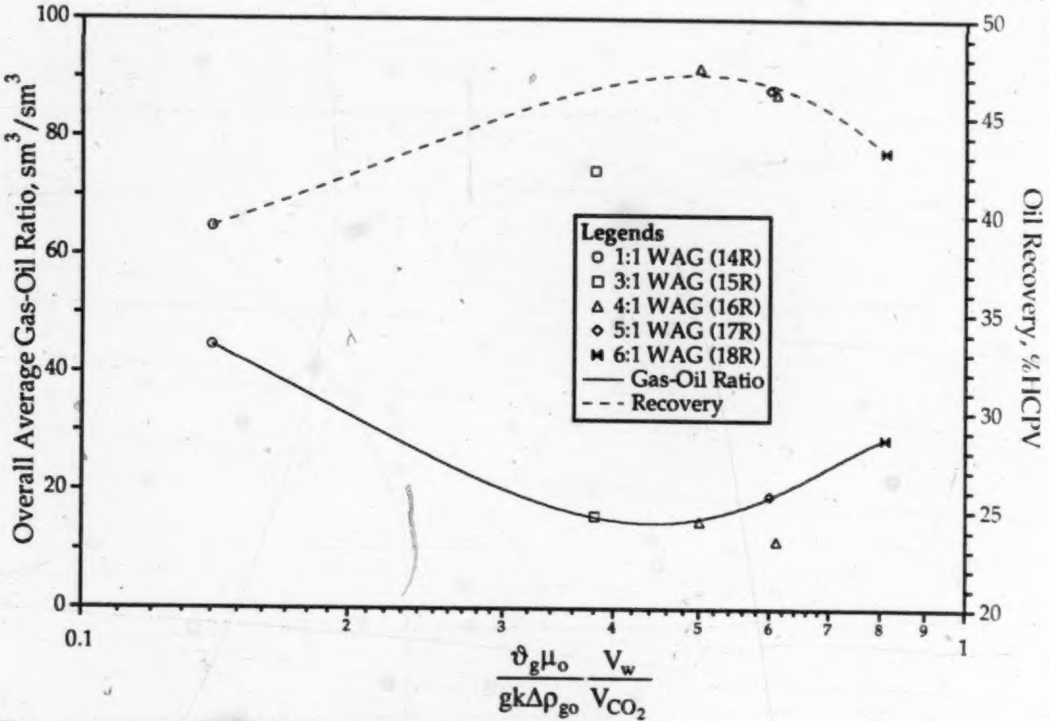

Figure 6.13 - WAG Ratio Correlation (Data from Ref. 1).

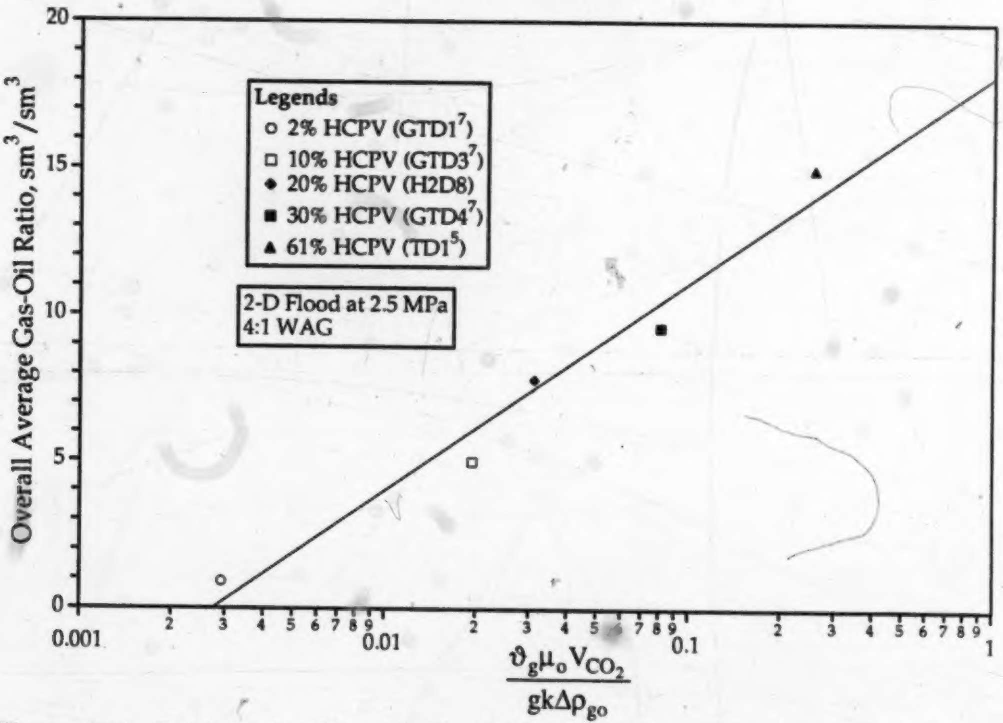

Figure 6.14 - Total Carbon Dioxide Slug Size Correlation (Data from Refs. 5 & 7).

WAG ratio higher than 4:1 is used, the water saturation in the flushed zone is higher while the corresponding oil saturation is lower, compared to when a 4:1 WAG ratio is used. This seems to affect the mass transfer rate of carbon dioxide to oil. It is known that the mass transfer rate of carbon dioxide to oil in porous media depends on the oil saturation, i.e., the lower the oil saturation, the lower the rate of mass transfer of carbon dioxide to oil. Experimental work done by Denoyelle and Bardon[37] verifies this. Thus, the lower is the oil saturation, the lower is the interfacial area available for mass transfer between carbon dioxide and oil. This plays a very important role in mass transfer. It is because a lower/higher interfacial area will lead to a lower/higher mass transfer rate. As a result of this, when the next carbon dioxide slug is injected following the preceding water slug, more carbon dioxide will go into the water phase, or remain in the gas phase, than goes into the oil phase, thus resulting in the production of large gas volumes.

In terms of displacement efficiency, the 4:1 WAG ratio is the most effective. As is shown by the oil recovery curve, the highest recovery was obtained with the 4:1 WAG ratio.

Summarizing, the use of a 4:1 WAG ratio in the immiscible carbon dioxide displacement process yields the most effective mobility control of the gas phase and the highest displacement efficiency.

6.7.3 - Total Carbon Dioxide Slug Size Correlations

Five experiments (Runs GTD1[7], GTD3[7], GTD4[7], TD1[5], and H2D3) were performed using slug sizes of 2, 10, 20, 30, and 61% HCPV at 2.5 MPa and 21°C. These runs were conducted using a 4:1 WAG ratio. Also, the same injection rate and oil were utilized in these runs. The results of these runs were correlated with the product of the ratio of viscous-to-gravitational forces and slug size[1,5,7] and are shown in Figures 6.14 and 6.15. Figure 6.14 provides a correlation of the overall average gas-oil ratios with the product of the ratio of viscous-to-gravitational forces and slug size. As indicated, there is an exponential relationship between the gas-oil ratio and the dimensionless group $\frac{\vartheta_g \mu_o V_{CO_2}}{g k \Delta\rho_{go}}$, and the gas-oil ratio increases when the slug size increases. This is

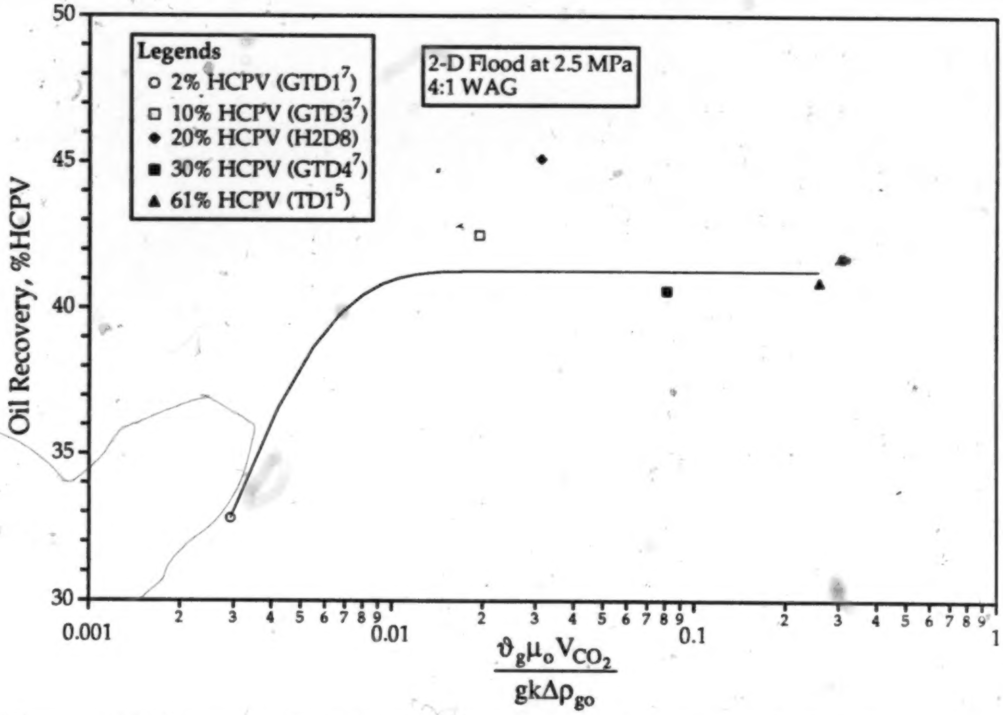

Figure 6.15 - Recovery-Slug Volume Correlation (Data from Refs. 5 & 7).

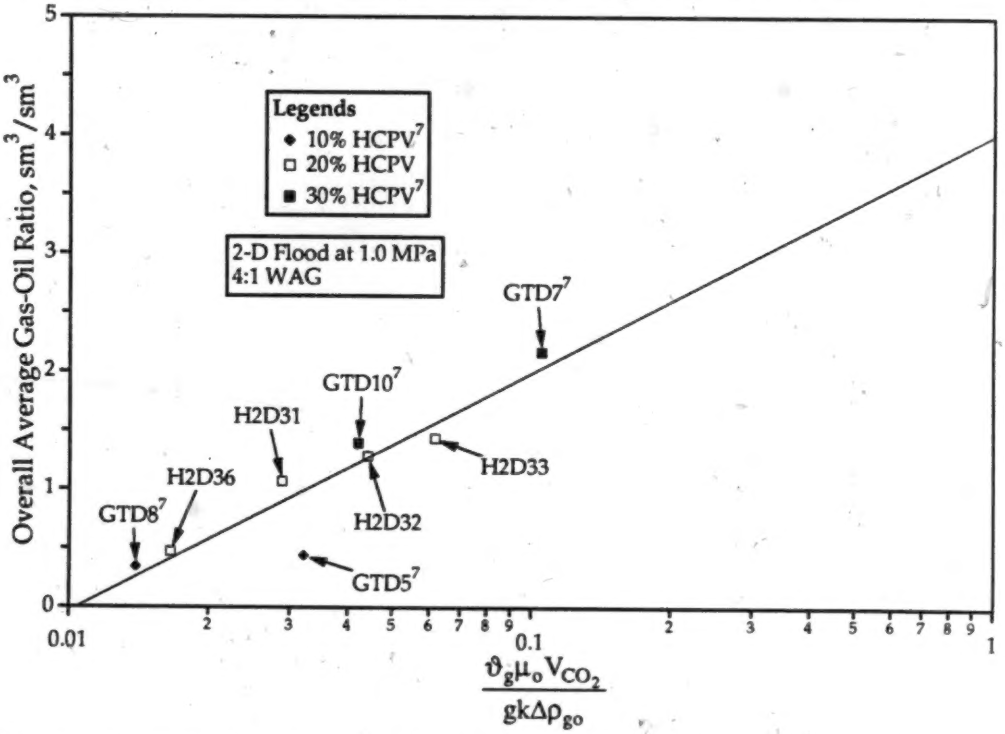

Figure 6.16 - Total Slug Size Correlation for Low Pressure Operations (Data from Ref. 7).

because, under a given pressure and temperature condition only a certain volume of carbon dioxide can dissolve in the oil and the excess remains in the gas phase, which will then bypass the oil. The higher is the slug size, the higher are therefore the gas volume and the producing gas-oil ratio.

The correlation of recovery with the same dimensionless group as mentioned above was also made and is shown in Figure 6.15. The recovery increases with a larger slug size and reaches its maximum at a slug size equal to 20% HCPV, then flattens out when the slug size is greater than 20% HCPV. The same correlations were performed as well for Runs GTD5[7], GTD7[7], GTD8[7], GTD10[7], H2D26 and H2D31-33 conducted at 1.0 MPa. Figure 6.16 presents a correlation of the overall average gas-oil ratios with the product of the ratio of viscous-to-gravitational forces and slug size for these runs. The total carbon dioxide slug sizes used in these runs were varied from 10 to 30% HCPV, in an increment of 10% HCPV. The same feature observed in Figure 6.14 can also be observed in Figure 6.16. As is shown in Figure 6.16, at 1.0 MPa, increasing the volume of carbon dioxide used in the immiscible carbon dioxide WAG process increases the producing GOR. The explanation mentioned the preceding paragraph applies here also.

Figure 6.17 provides the correlation of recovery with the same dimensionless group for Runs GTD5[7], GTD7[7], GTD8[7], GTD10[7], H2D26 and H2D31-33 conducted at 1.0 MPa. The figure shows three different straight lines for the oil recoveries of runs utilizing total carbon dioxide slug sizes of 10, 20, and 30% HCPV. It is indicated in Figure 6.17 that the recovery at 1.0 MPa is optimal when the volume of carbon dioxide utilized in the immiscible WAG process is 20% HCPV.

In addition to correlating the results of the experiments conducted utilizing a quarter of a 5-spot flood pattern, correlations were also done for those conducted utilizing linear core floods. Figure 6.18 presents a correlation of the overall average gas-oil ratios with the product of the ratio of viscous-to-gravitational forces and slug size for Runs LC16[5], LC17[5], LC30-33[7] and LC36[7] conducted at 2.5 MPa, in the linear model. The total carbon dioxide used in these runs were 5, 20, 40, 64, and 89% HCPV. In these experiments, an oil with a viscosity of 1055 mPa.s was used; except in a few runs, oils with viscosi-

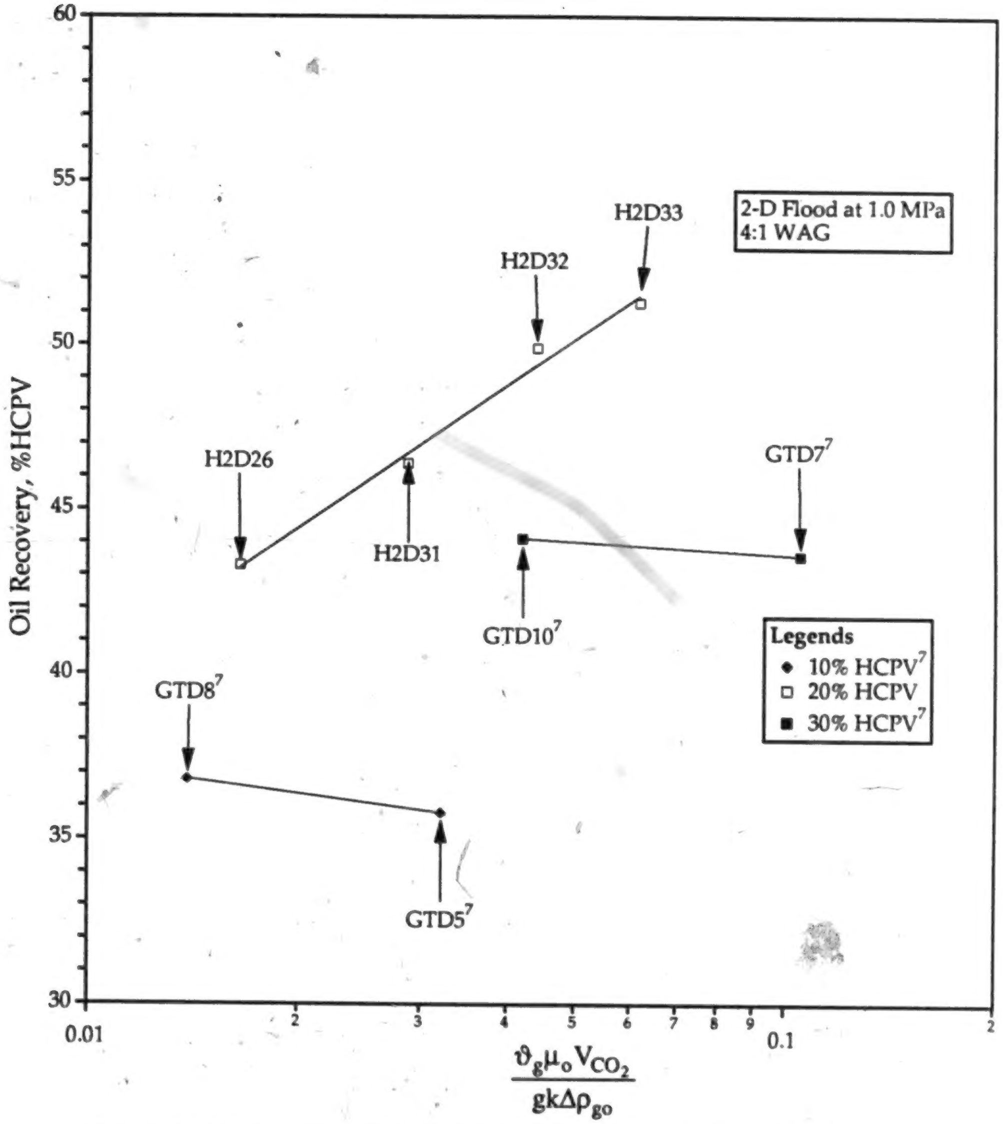

Figure 6.17 - Recovery-Slug Volume Correlation for Low Pressure Operations (Data from Ref. 7).

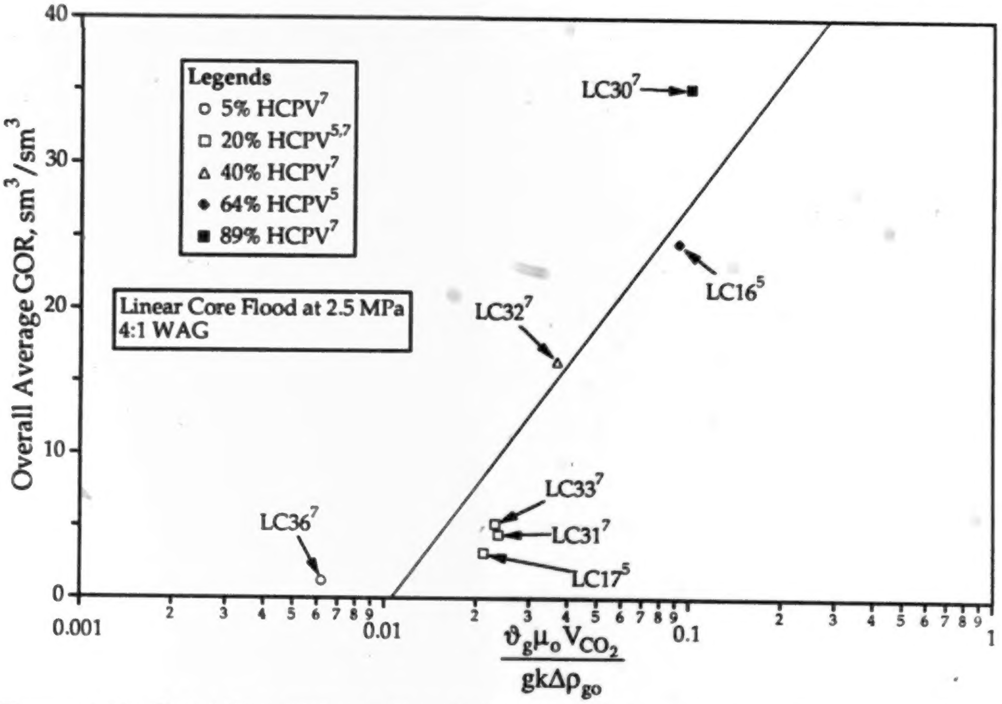

Figure 6.18 - Total Slug Volume Correlation for a Linear Coreflood (Data from Refs. 5 & 7).

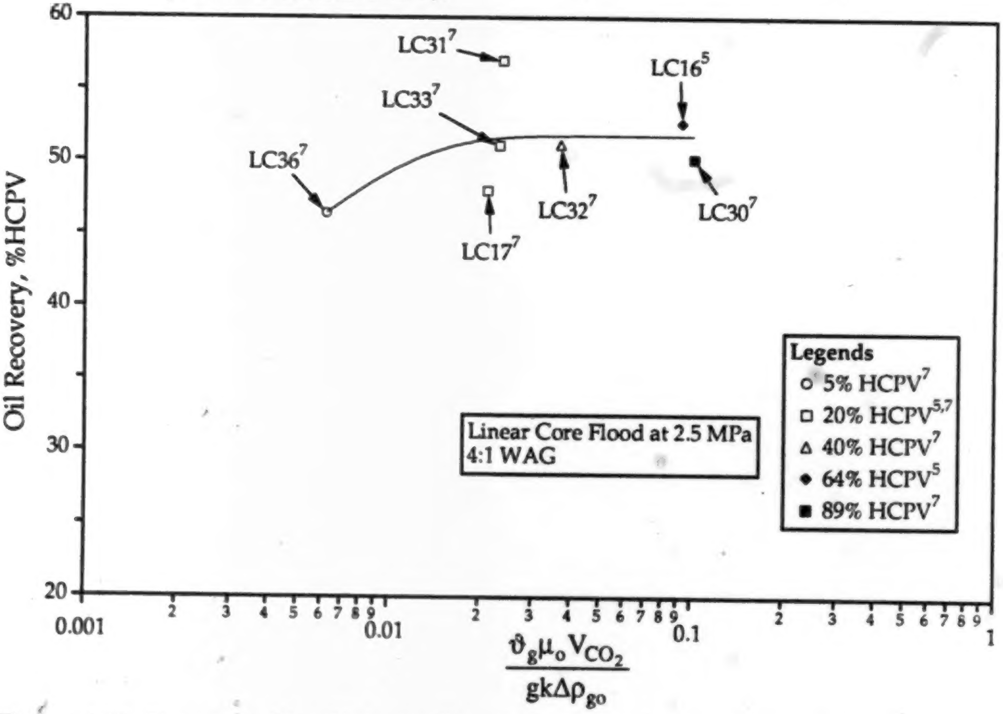

Figure 6.19 -Recovery-Slug Volume Correlation for a Linear Coreflood (Data from Refs. 5 & 7).

ties of 1230 mPa.s and 1130 mPa.s were used. Similar to what already observed, the producing GOR increases with increasing the total carbon dioxide slug size for the experiments conducted in the linear model. The correlation of recovery with the same dimensionless group for linear coreflood experiments performed at 2.5 MPa is shown in Figure 6.19. The curve in the figure reveals that there is no increase in oil recovery when the slug size greater than 20% HCPV is used. This is similar to the observation made on Figure 6.15.

In conclusion, the immiscible carbon dioxide process has its best performance when it is employed in the WAG mode, with a WAG ratio of 4 to 1 and a total slug size equal to 20% HCPV.

II.1 - Isothermal Displacement Experiments

6.8 - Carbonated Waterflood

As has already been mentioned in Chapter 3, the idea of flooding an oil reservoir with carbonated water is not new. The method was first tested in the laboratory and tried in the field in the 50's and 60's. In this study, several experiments were made by injecting carbonated water, instead of injecting carbon dioxide alternately with water. The experimental results for these runs are summarized in Table 6.4 on page 82.

6.8.1 - Carbonated Waterflood vs. Immiscible WAG flood

Run CWF1 was conducted by injecting carbonated water at 2.5 MPa and 21°C, in a linear model. The carbonated water was prepared by mixing brine with carbon dioxide at experimental pressure and temperature conditions until equilibrium was reached, which could be ascertained by observing the constant pressure on the pressure gauge. Before the carbonated water was injected, the solubility of carbon dioxide in brine was measured to be 16.25 sm^3/sm^3 at 2.5 MPa and 21°C. The pH of the carbonic acid formed due to the chemical reaction taking place between carbon dioxide and brine was also measured using a pH meter. It was measured to be 5.1.

The experiment was conducted by continuously injecting carbonated brine until the producing water-oil ratio reached 20:1; then injection was stopped to start blowdown. Figures 6.20 depicts the production history of this run.

The oil recoveries of this run at each phase of production were 51.71% of oil recovered in the carbonated brine flood phase and 4.82% in the blowdown phase, thus giving a total recovery of 56.53%. The GOR curve shows that during the early part of the flood no carbon dioxide gas was produced, which is very good in terms of controlling the mobility of the gas phase. After gas breakthrough occurred at 0.72 PV, the production of gas climbed and reached its maximum value at 228 sm^3/sm^3 at the end of the flood, which is at 1.73 PV as indicated in the figure. This very high producing GOR is undesirable in any enhanced oil recovery method where the injected

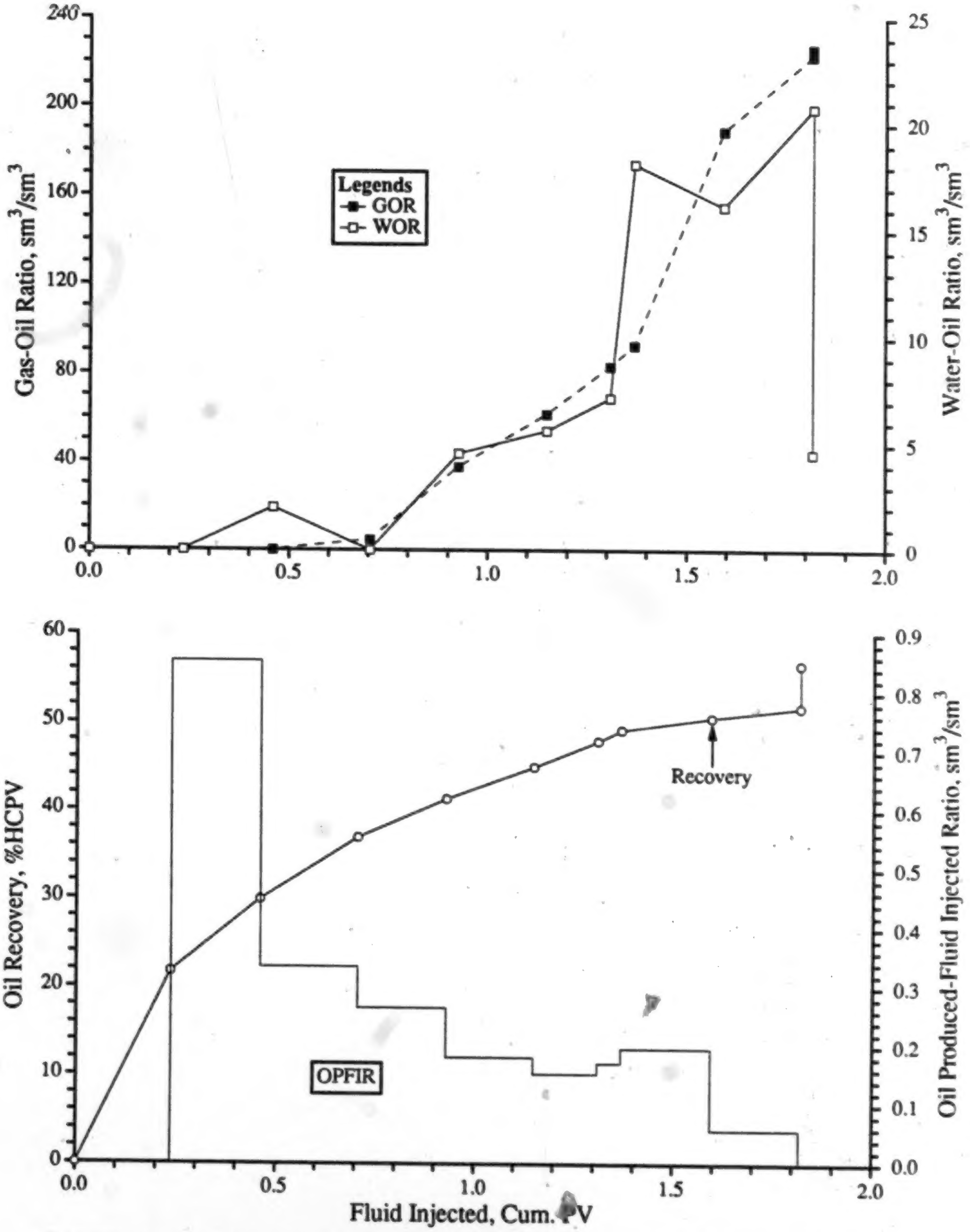

NOTE: Average Run Conditions: Carbonated Waterflood at 2.5 MPa and 21°C
Model Parameters: Average Injection Rate = 308 cc/hr, μ_o = 1058.0 mPa.s,
$\emptyset$ = 35.80 %, k = 11.44 darcies, S_o = 92.18 %, S_{wc} = 7.82 %
Flood Pattern: Linear Core

Figure 6.20 - Production History of Run CWF1.

gas plays a dominant role.

In order to compare the performance of this recovery method, the GOR of this run (i.e., Run CWF1) was plotted on the same graph as that of Run LC31[7], which was done using an immiscible carbon dioxide WAG flood utilizing a 4:1 WAG ratio and a total slug size of 20% HCPV at 2.5 MPa. Figure 6.21 shows the comparison. Examining the two GOR curves reveals some interesting features. At early time, the same volumes of gas were produced in both runs; but after gas breakthrough, much more gas was produced in Run CWF1 than in Run LC31[7]. Gas breakthrough occurred earlier in Run CWF1 than in Run LC31[7], at 0.72 PV in Run CWF1 and at 1.02 PV in Run LC31[7]. As indicated in the figure, at 1.0 PV both runs seemed to have nearly the same GOR; but after 1.0 PV, the GOR in Run CWF1 steeply and continuously rose while it gradually decreased in Run LC31[7]. On average, after gas breakthrough the GOR of Run CWF1 was about 10 times higher than that of Run LC31[7]. It can also be seen easily that Run CWF1 had a shorter flood life than Run LC31[7].

Figure 6.22 depicts the oil recoveries of Runs CWF1, LC31[7], and LC34[7], which was conducted by injecting brine only. It is clearly shown in the figure that the recovery curve for Run CWF1 nearly lies on that for Run LC31[7] and that both runs have nearly an identical recovery. The recoveries for Runs CWF1 and LC31[7] were, respectively, 56.53 and 57.1%. In terms of oil recovery, the two runs are comparable; but, in terms of carbon dioxide requirement, which is the volume of carbon dioxide required to produce one cubic meter of oil at standard conditions, the two runs are not comparable. In Run CWF1, it required 63.6 sm^3 to produce one standard cubic meter of oil while it required only 10.29 sm^3 to produce the same volume of oil in Run LC31[7]. This indicates that in order to recover as much oil as the immiscible WAG process, the amount of carbon dioxide required for the carbonated brine flood should be 6 times higher. The very high GOR and carbon dioxide requirement in Run CWF1 is due to the slow mass transfer process from carbon dioxide to oil. In Run CWF1, carbon dioxide had to diffuse out of the non-diffusing liquid water phase before contacting the oil, whereas in Run LC31[7] carbon dioxide was in direct contact with the oil.

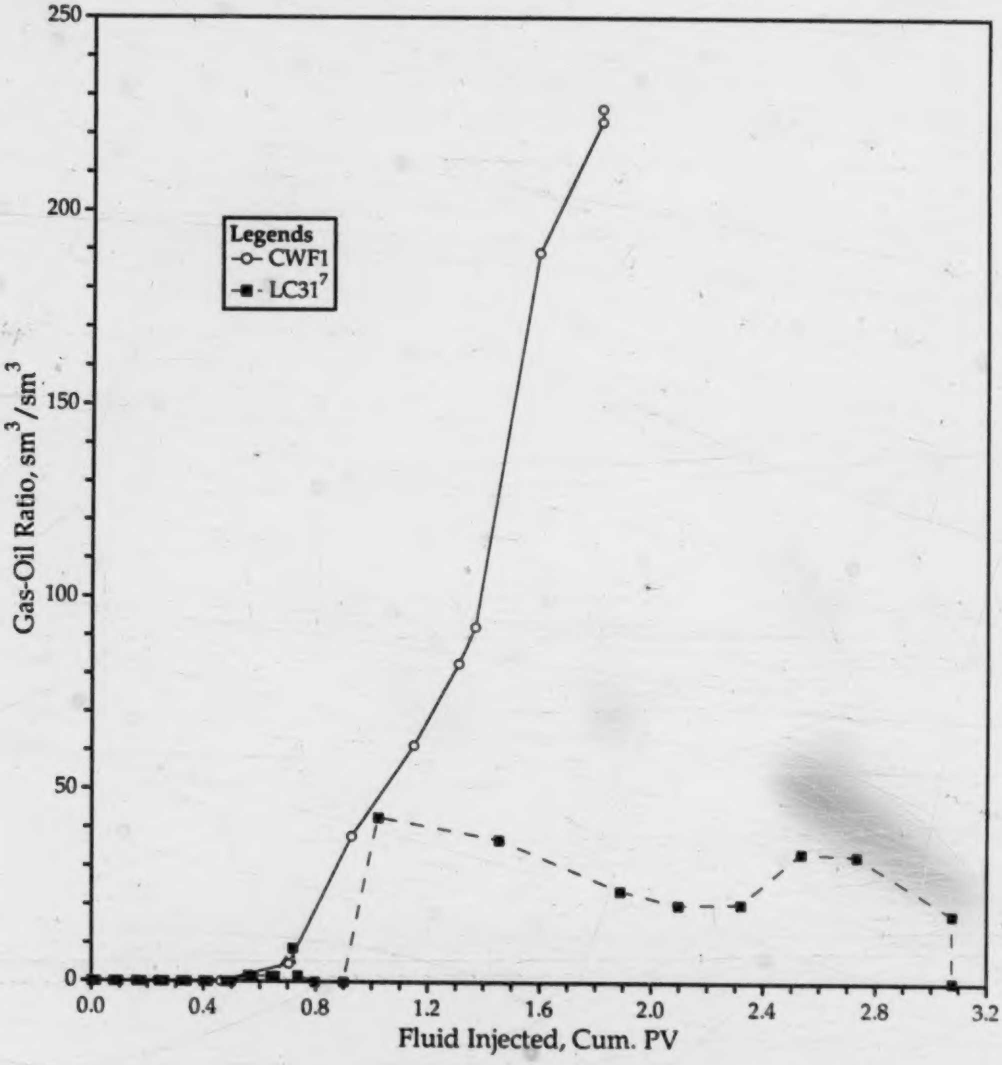

Figure 6.21 - Comparison of the GOR's of Runs CWF1 and LC31[7].

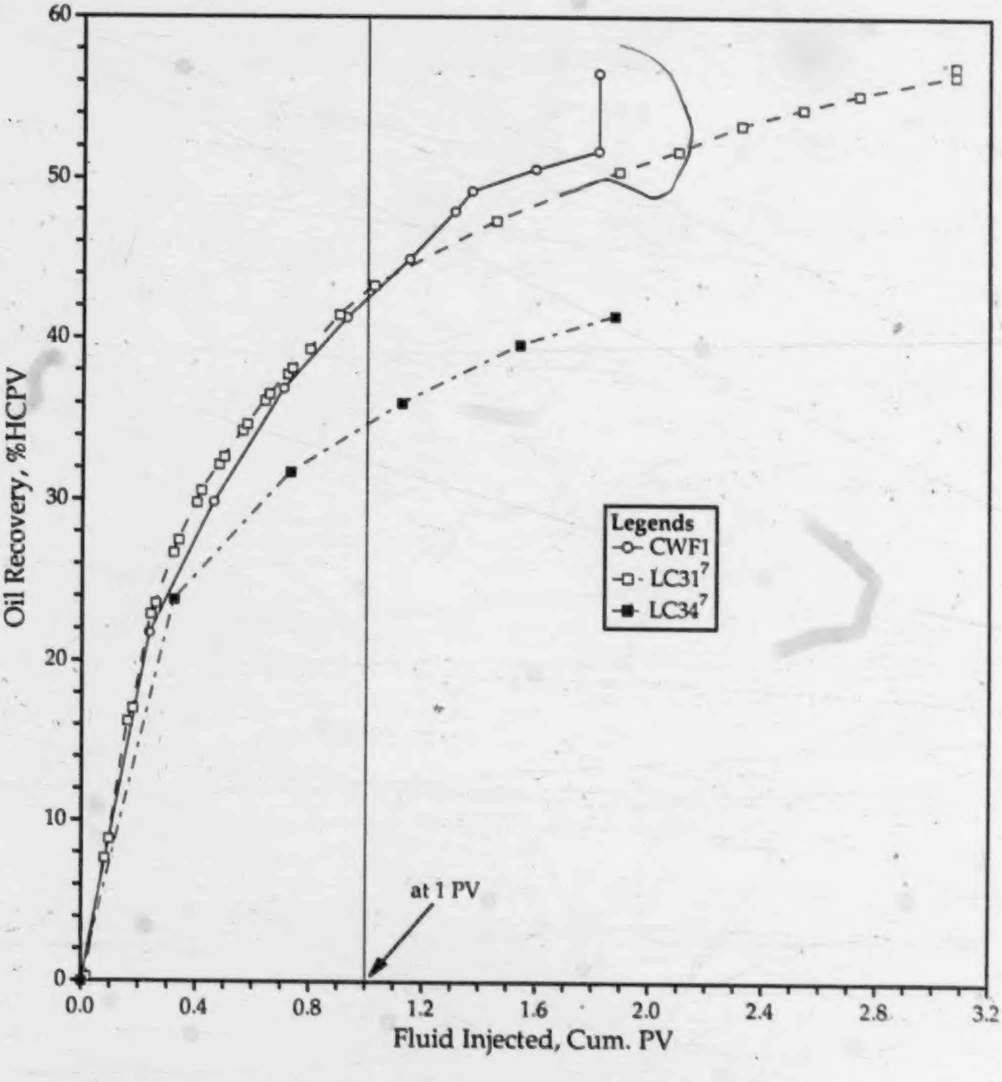

Figure 6.22 - Comparison of Recoveries of Runs CWF1, LC31[7], and LC34[7].

Figure 6.22 also shows a comparison of Run CWF1 with Run LC34[7] (a waterflood run). Examining the two recovery curves reveals that both runs had nearly the same flood life, but Run CWF1 had a higher recovery than Run LC34[7], which had a recovery of 41.45%. Comparing the two recoveries, approximately 36% more oil was produced in Run CWF1 than in Run LC34[7].

Summarizing, the carbonated brine flood method is as effective as the immiscible WAG method when the volume of carbon dioxide used in the former is 6 times higher than that in the latter.

6.8.2 - Effect of Carbon Dioxide Requirement

To study the effect of the carbon dioxide requirement on flooding an oil reservoir with carbonated brine, Run CWF2 was performed in a scaled model, utilizing a quarter of a five-spot pattern. In this run, the carbonated brine was prepared by mixing 20% HCPV of carbon dioxide with brine at a 4 to 1 ratio and at 1.0 MPa and 21°C. After the carbonated brine was injected, water was injected to bring the WOR to the limiting WOR. The production history of this run is depicted in Figure 6.23.

Figure 6.24 depicts a comparison of Run CWF2 with Run GTD6[7], which was conducted employing the immiscible carbon dioxide WAG process with a total carbon dioxide slug size equal to 20% HCPV and a 4:1 WAG ratio. It is shown in Figure 6.24 that from 0 to 1.04 PV, the GOR of Run CWF2 is higher than that of Run GTD6[7], that after 1.04 PV the reverse is true, and that gas breakthrough in Run CWF2 occurred at 0.28 PV, which is earlier than that in Run GTD6[7]. Moreover, Run CWF2 had a shorter flood life than Run GTD6[7] because the limiting WOR was reached earlier in Run CWF2, as shown in the figure.

Figure 6.25 presents the recoveries of the three runs CWF2, GTD6[7] and 21a[1,3]. Run 21a[1,3] was done by injecting brine only. The figure clearly demonstrates that at 1.0 PV 37% of the oil was recovered by the carbon dioxide WAG flood, 32% by carbonated brine flood, and 30% by waterflood. This shows that up to 1.0 PV, a carbonated brine flood is no better than a waterflood. It is also shown in the figure that, up to nearly 0.6 PV, the recovery curve of Run

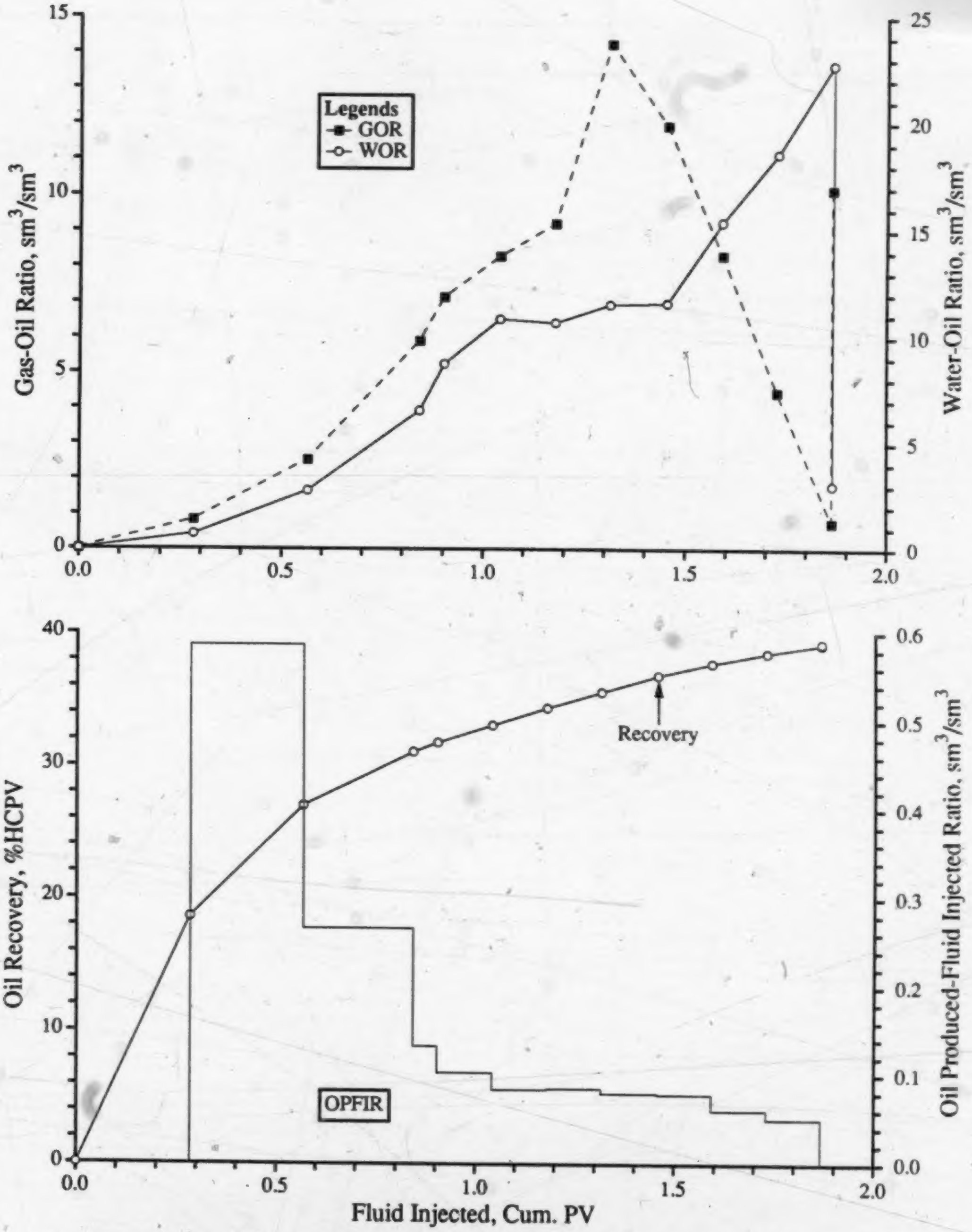

NOTE: Average Run Conditions: Carbonated Waterflood at 1.0 MPa and 21°C
Model Parameters: Average Injection Rate = 308 cc/hr, μ_o = 1058.0 mPa.s,
ϕ = 37.84%, k = 11.56 darcies, S_o = 89.94%, S_{wc} = 10.06%
Flood Pattern: Quarter of a 5-Spot
[20% HCPV of CO_2 Mixed with Brine at 4:1 Ratio]

Figure 6.23 - Production History of Run CWF2.

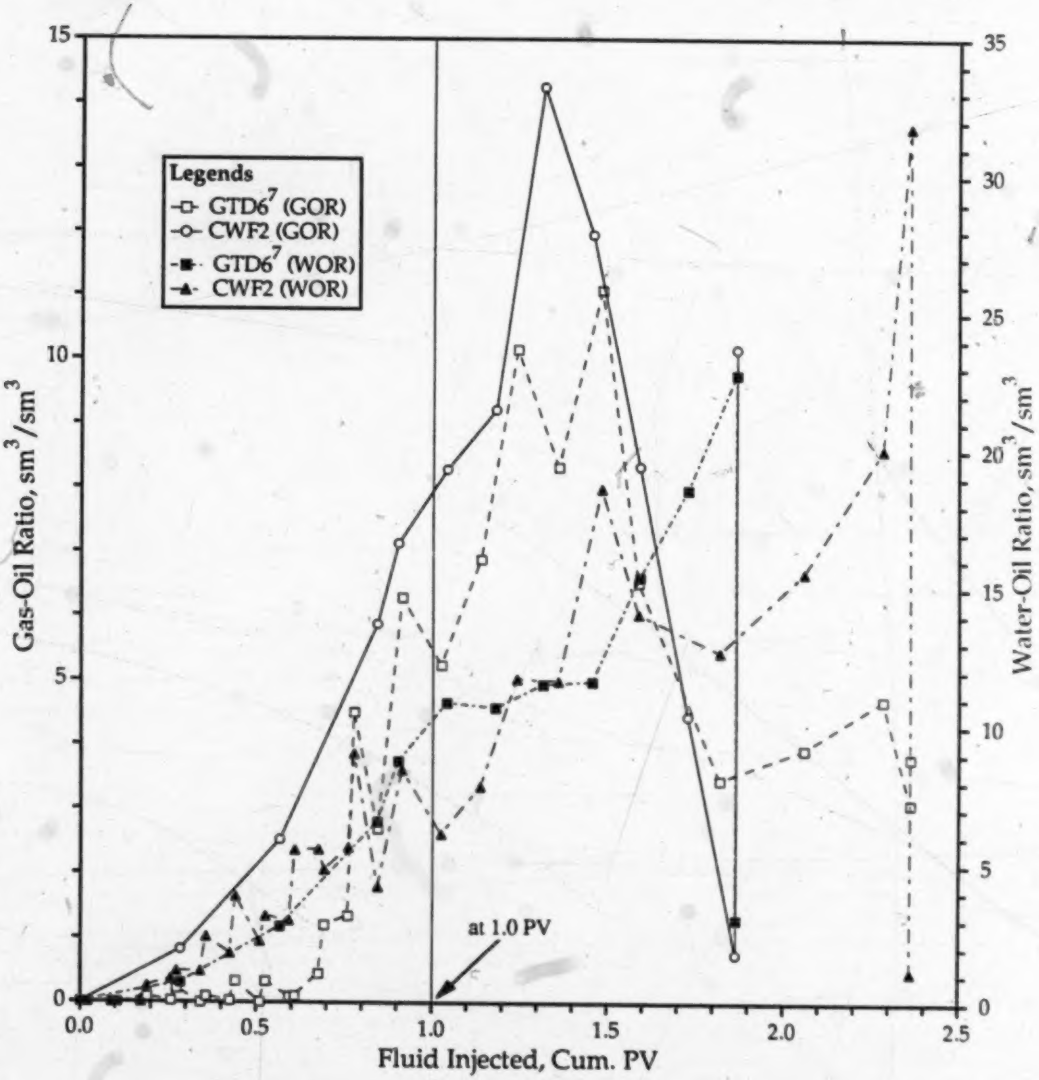

Figure 6.24 - Comparison of GOR's and WOR's of Runs CWF2 and GTD6[7]

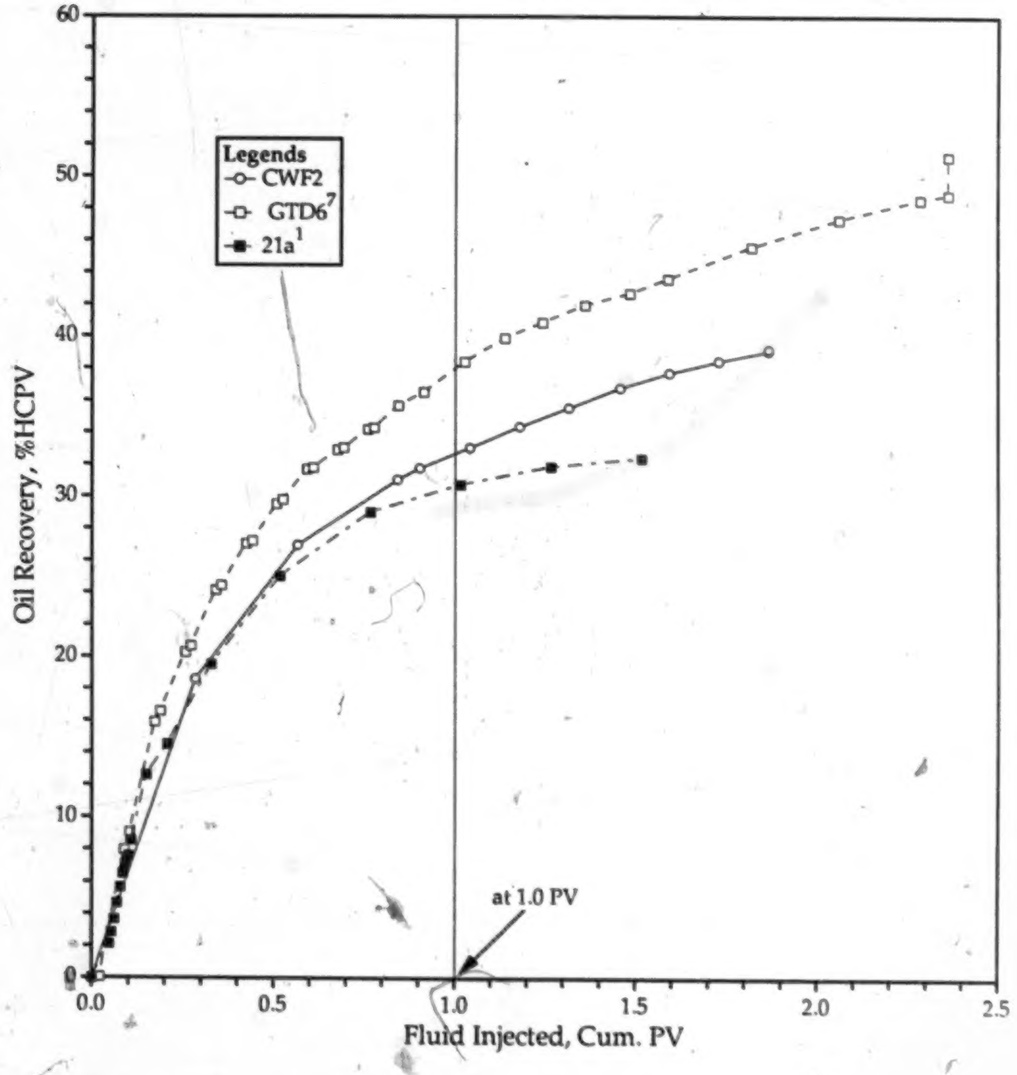

Figure 6.25 - Comparison of Recoveries of Runs CWF2, GTD6[7], and 21a[1].

CWF2 almost overlaps that of Run 21a[1,3]. Examining the three curves reveals that during the duration of the flood more oil was recovered in Run GTD6[7] than in Runs CWF2 and 21a[1,3]. The total recoveries for the three Runs CWF2, GTD6[7] and 21a[1,3] were respectively 51.3, 39.2 and 32.4%, which indicates that the WAG flood recovered 12.1% more oil than the carbonated brine flood and that the oil recovered by the carbonated brine flood followed by a waterflood up to 1.0 PV is almost the same as that by a waterflood alone.

In short, a carbonated waterflood followed by a waterflood is not comparable to an immiscible WAG flood when the same amount of carbon dioxide is used. The former is no more effective than a waterflood.

6.9 - Gravity Segregation

In this section, the results of the experiments conducted to investigate the effect of gravity segregation on the performance of an immiscible carbon dioxide WAG process are discussed.

A - Linear Corefloods

6.9.1 - Vertical WAG Injection

Two vertical runs, VLC1 and VLC2, were performed by, respectively, injecting the carbon dioxide WAG at the bottom and top of the model to study the effect of gravity segregation of the injected fluids. The results of the two runs are given in Table 6.5 (page 83), along with those for the others. Figure 6.26 shows the producing GOR's of the two runs, along with that for the horizontal WAG injection run[7] (GTD6) conducted at identical conditions and utilizing identical experimental parameters.

The figure shows that a smaller volume of carbon dioxide was produced when carbon dioxide was injected at the top than at the bottom of the model. This is because when carbon dioxide is injected at the bottom, the buoyancy forces (acting in the same direction as the viscous forces) cause the carbon dioxide to rise to the top, resulting in early carbon dioxide breakthrough and the production of high carbon dioxide volume. The comparison of the GOR's reveals that at the same carbon dioxide injection rate (i.e. 308.0 cc/h) more gas was produced in the horizontal WAG injection run[7] (GTD6)

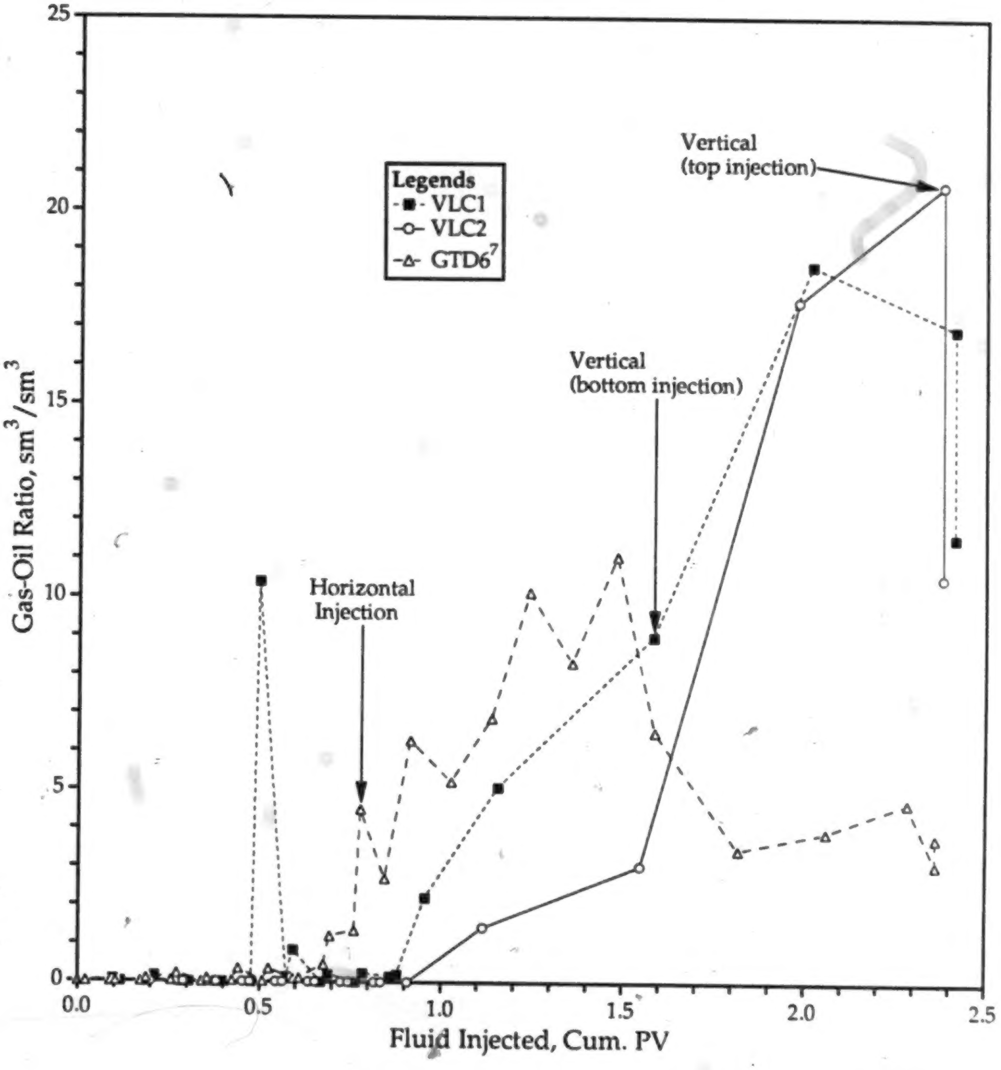

Figure 6.26 - Producing Gas-Oil Ratios of Runs VLC1, VLC2, and GTD6[7].

than in Runs VLC1 and VLC2 and that, in the horizontal WAG injection run, carbon dioxide production started after about 0.25 PV of fluids injected, showing that at the same injection rate the viscous forces acting in the horizontal direction (Run GTD6[7]) were greater than the sum of the buoyancy forces and viscous forces both acting the vertical direction (Runs VLC1 and VLC2).

To examine the gravity segregation effect on water slugs, it is necessary to refer to Figure 6.27, where the producing WOR's of the three runs are shown. In contrast to what was observed with the carbon dioxide slugs, injecting water slugs at the top of the model led to early water breakthrough and high WOR's, as indicated in the figure. This was basically due to a higher water density compared to oil. Furthermore, when carbon dioxide dissolved in oil, in addition to reducing the oil viscosity it reduced the oil density, which induced a greater oil-water density difference, which consequently encouraged early water breakthrough.

The immiscible carbon dioxide WAG process for different model positions: top (Run VLC2), bottom (Run VLC1), and horizontal (Run GTD6[7]) has an effect on the oil recovery as well. As is shown in Figure 6.28, the highest oil recovery was obtained when the WAG injection was conducted at the bottom of the model. The reason is that when carbon dioxide was injected at the bottom, gravity helped to induce the mass transfer rate of carbon dioxide by solution and diffusion into the oil, causing a significant reduction in the viscosity and density of the oil. When water slugs were injected following the injection of carbon dioxide slugs, due to its greater density compared to that of carbon dioxide-oil mixture, water resided at the bottom and pushed the carbon dioxide-oil mixture upwards. Gravity also helped to stabilize the water front, resulting in a high displacement efficiency. As a result of these two advantages, a high recovery was achieved in Run VLC1.

In Run VLC2, where the immiscible carbon dioxide WAG was injected at the top rather than at the bottom, gravity kept the injected carbon dioxide at the top due to its lower density compared to that of oil, causing an adverse effect on the mass transfer rate of carbon dioxide by solution and diffusion into oil. When water was injected, due to its higher density, it quickly found a

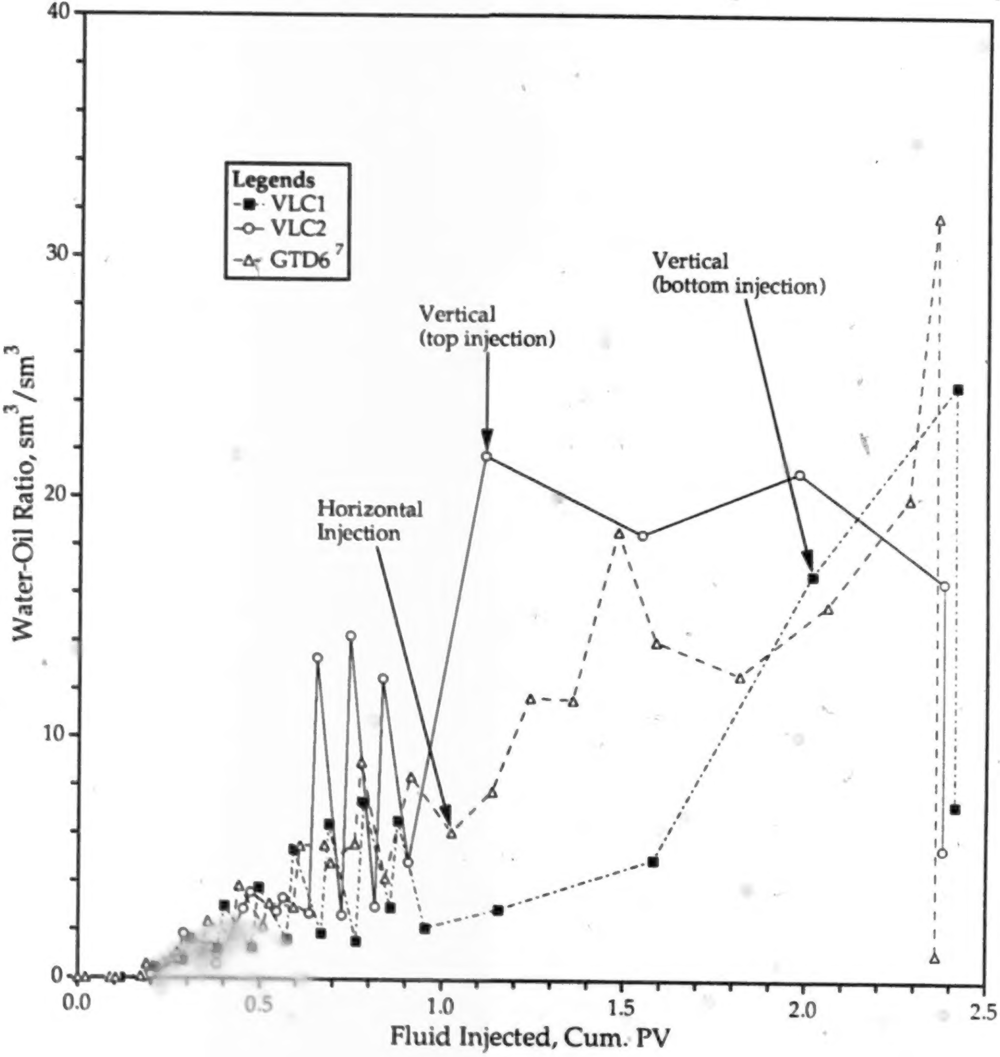

Figure 6.27 - Producing Water-Oil Ratios of Runs VLC1, VLC2, and GTD6[7].

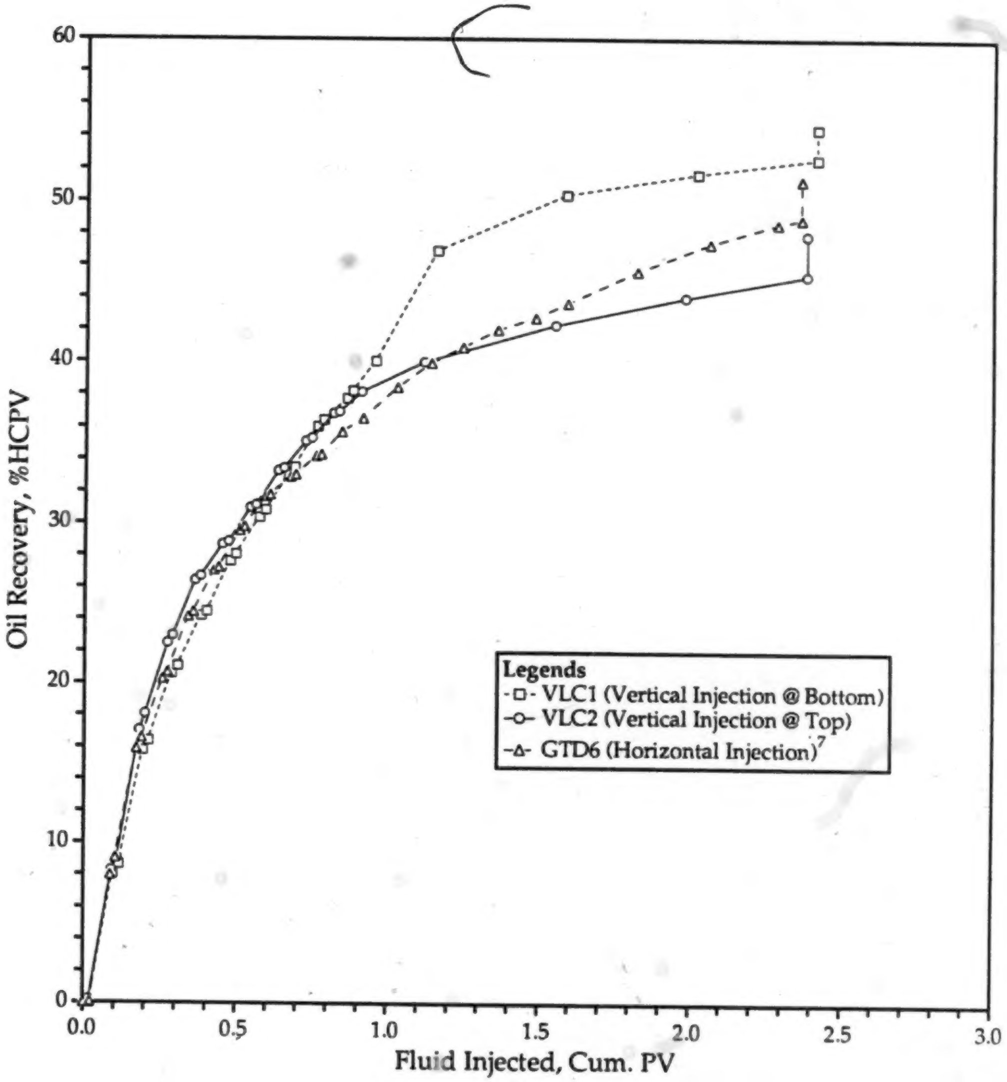

Figure 6.28 - Comparison of Oil Recoveries of Runs VLC1, VLC2, and GTD6[7].

way to finger through and pushed the oil upwards, resulting in the production of oil at high WOR's.

6.9.2 - Continuous Carbon Dioxide Injection

Runs VLC3 and VLC5 were conducted to demonstrate more clearly segregation of the injected fluids. Continuous injection of carbon dioxide was carried out until 20% HCPV of carbon dioxide was injected, which was then followed by the injection of water to displace oil.

Figure 6.29 shows the GOR curves of the two runs. Examining the GOR curve of Run VLC5, where carbon dioxide injection was conducted at the top of the model, reveals that gravity kept carbon dioxide at the top, inducing the formation of a gas cap which pushed the oil downwards. This can be observed by looking at the volume of oil produced after injecting 20% HCPV carbon dioxide. As indicated by the recovery curve of Run VLC5 in Figure 6.30, after 20% HCPV carbon dioxide was injected, approximately 2.0% of the oil was recovered, while none was produced when injecting the identical volume of carbon dioxide at the bottom (Run VLC3). This volume of oil produced was relatively small compared to the volume of carbon dioxide injected. However, it clearly demonstrates that in the immiscible carbon dioxide WAG process, as time goes on, carbon dioxide will segregate and rise to the top to form a gas zone which pushes the reservoir oil downwards. The GOR curve of Run VLC3 shows a totally different trend. As shown in Figure 6.29, after the injection of 20% HCPV carbon dioxide and 0.95 total fluid PV, a very small amount of carbon dioxide was produced, showing that gravity segregation of the injected carbon dioxide does not occur right away. As more water was injected, the water pushed the carbon dioxide upward. Since carbon dioxide occurred as free gas, it could travel upward at a much higher rate than oil, resulting in the increased production of carbon dioxide. This clearly shows that water slugs injected following the carbon dioxide slugs in the WAG process induce the gravity rise of carbon dioxide to the top of the reservoir.

The continuous water injection following carbon dioxide injection in Run VLC5 helps to illustrate the gravity segregation of the water slugs in the

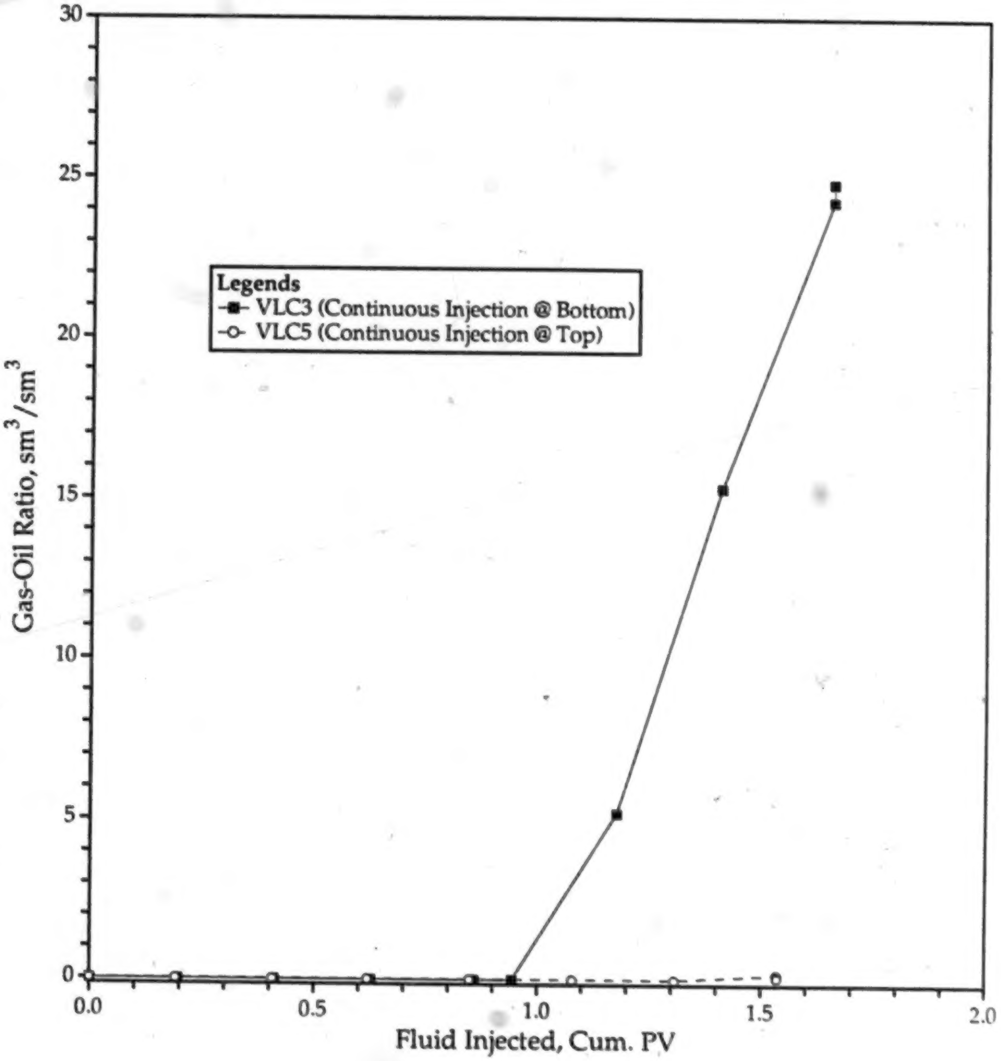

Figure 6.29 - Comparison of the Producing GOR's of Runs VLC3 and VLC5.

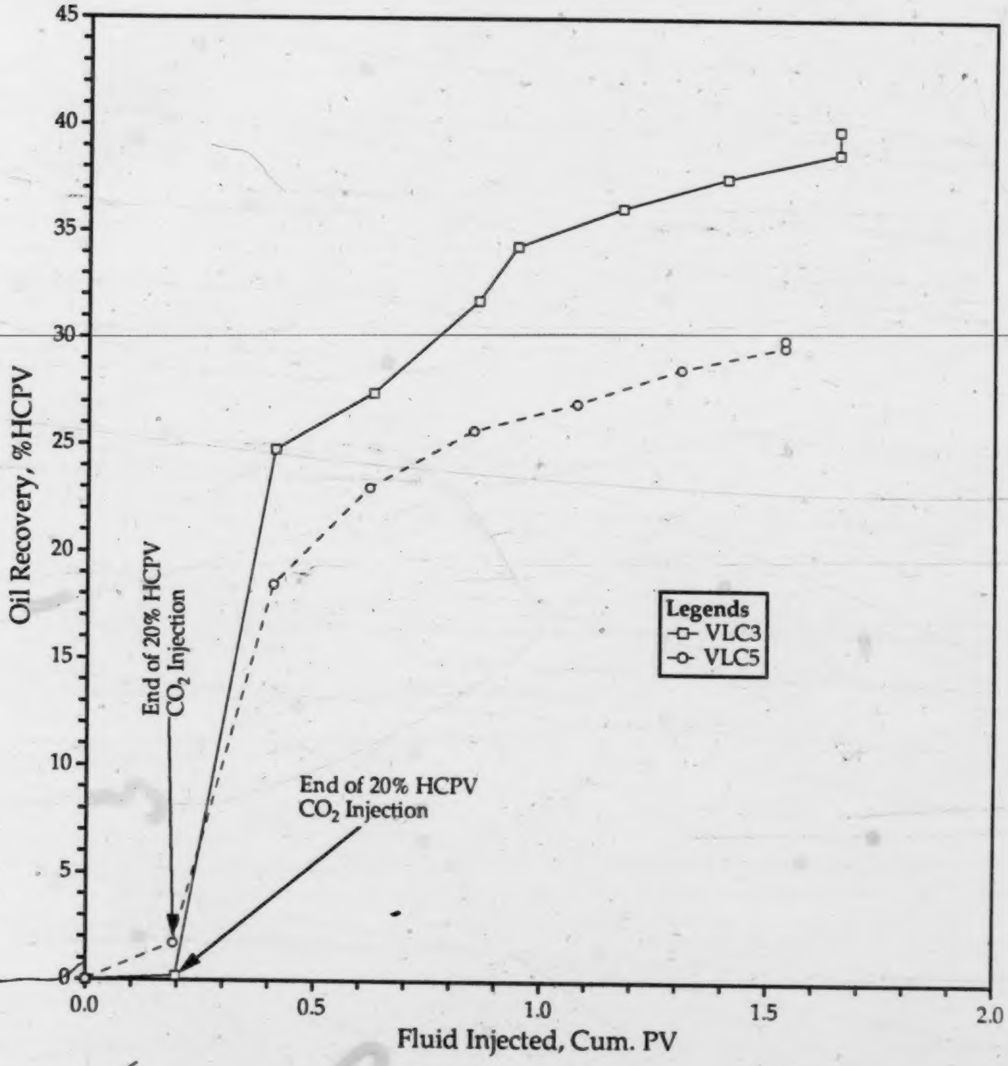

Figure 6.30 - Comparison of the Oil Recoveries of Runs VLC3 and VLC5.

WAG process. It is indicated by the WOR curve of Run VLC5 (where water was injected at the top) in Figure 6.31 that high volumes of water were collected during the course of the experiment, which is thought to have a detrimental effect on the immiscible WAG displacement process. To clarify this, the GOR's, WOR's, and recovery of Run VLC5 are plotted on the same graph, as shown in Figure 6.32. It is demonstrated by this figure that at the same pore volume of fluids injected much more water was produced than carbon dioxide and oil, which shows that in the immiscible WAG process the slugs of water push carbon dioxide and oil to the top of the reservoir, which causes the oil to re-saturate the zone already swept by the carbon dioxide gas. The same phenomenon can also be observed by considering Figure 6.33, where the GOR's, WOR's and recovery of Run VLC3 are plotted.

Based on the phenomena observed in these two runs and those described in Section 6.9.1, it can be said that the immiscible carbon dioxide WAG displacement process performs the best when carbon dioxide and water are injected at the bottom.

6.9.3 - Effect of Pressure on Gravity Rise of Carbon Dioxide

The effect of pressure on the gravity rise of carbon dioxide was observed by Conducting Run VLC6 at 2.5 MPa. The experimental parameters used in this run, as included in Table 6.5 (page 83), were similar to those used in Run VLC1 in order to make a fair comparison. The tabulated experimental data of this run are provided in Appendix E. Figure 6.34 depicts the production history of this run.

Figure 6.35 details the GOR's of Runs VLC1 and VLC6 at each time fluids were injected. As already mentioned, Run VLC1 was carried out at 1.0 MPa. An observation of the GOR curves of both runs reveals that pressure has the effect of retarding the gravity rise of the injected carbon dioxide gas. Gas breakthrough occurred at 0.48 PV in Run VLC1 (conducted at 1.0 MPa), whereas it occurred at 0.88 PV in Run VLC6 (conducted at 2.5 MPa). This is basically due to higher carbon dioxide solubility in Run VLC6. Other factors contributing to the earlier gas breakthrough in Run VLC1 can be as follows. When carbon dioxide dissolves in oil, it swells the oil and forms dispersed

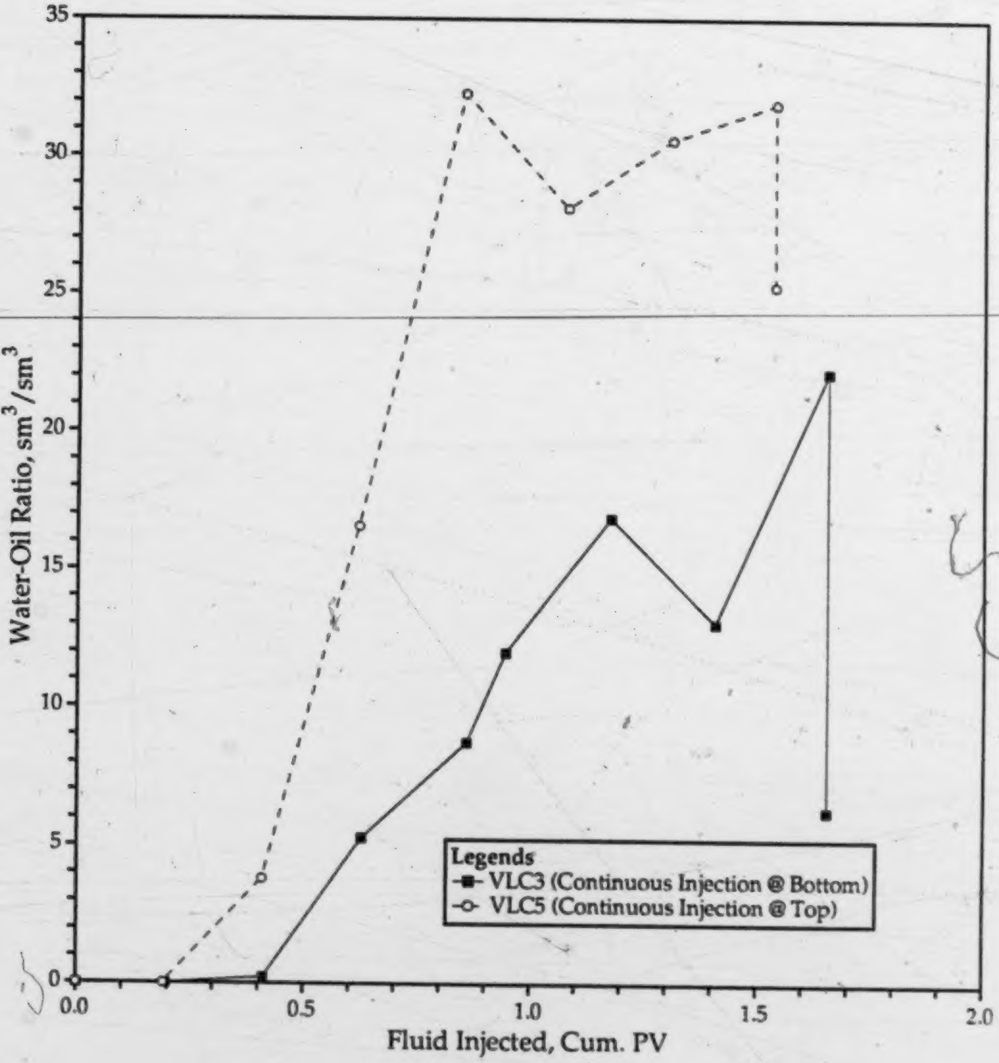

Figure 6.31 - Comparison of the Producing WOR's of Runs VLC3 and VLC5.

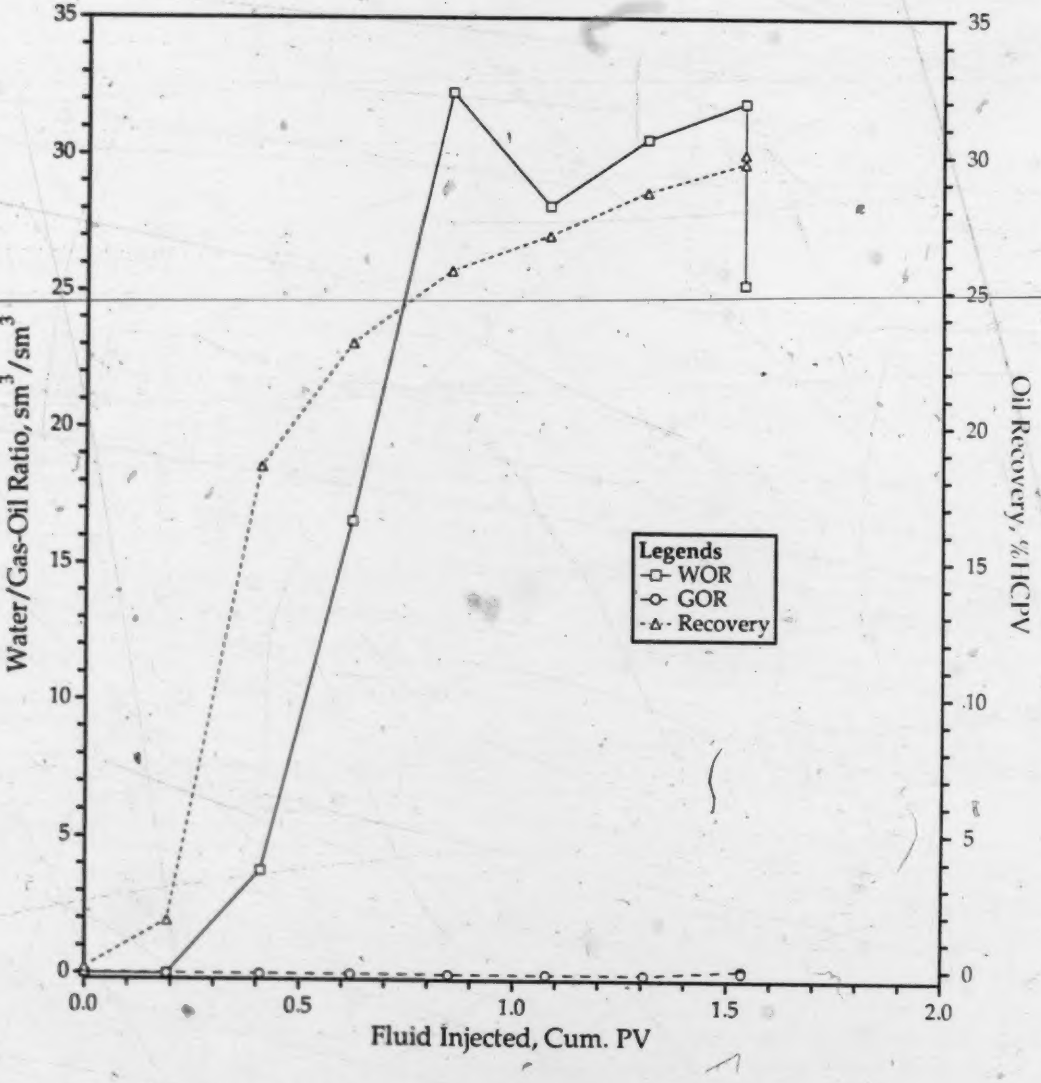

Figure 6.32 - Performance of Run VLC5 (Continuous Injection @ Top).

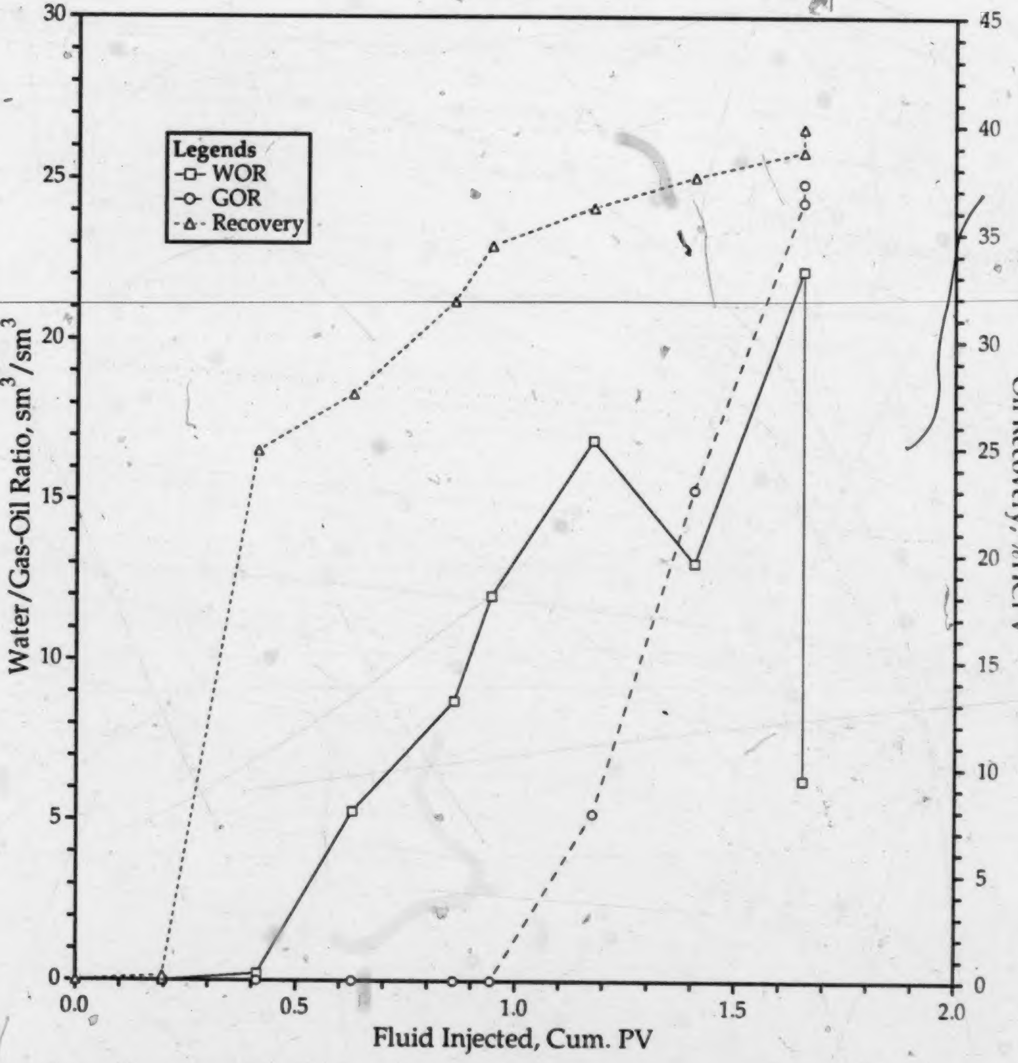

Figure 6.33 - Performance of Run VLC3 (Continuous Injection at Bottom).

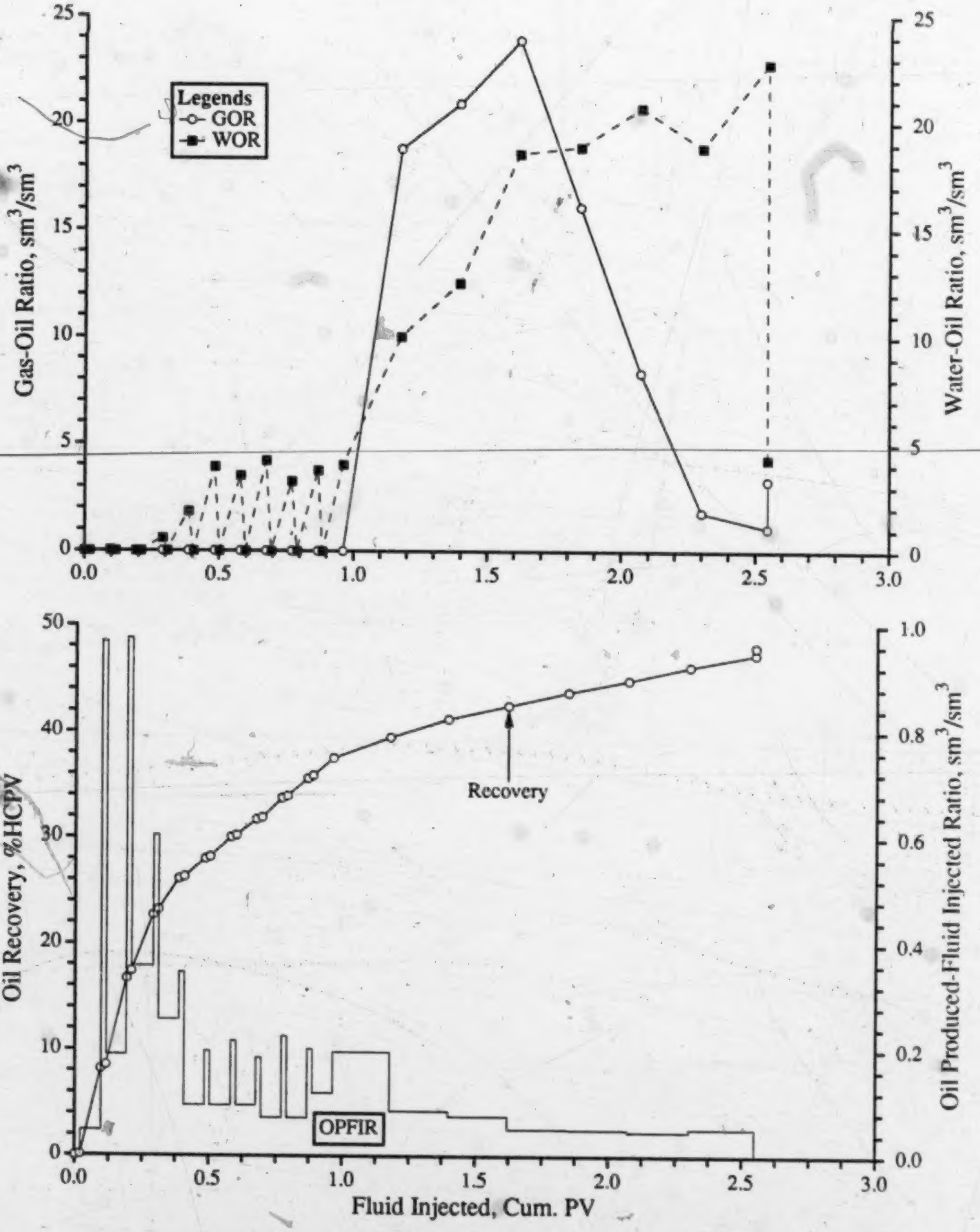

NOTE: Average Run Conditions: Vertical WAG Flood at Bottom, 2.5 MPa, 21°C
Model Parameters: Average Injection Rate = 308 cc/hr, μ_o = 1058.0 mPa.s, ϕ = 35.3 %, k = 9.87 darcies, S_o = 92.0 %, S_{wc} = 8.0 %
Model Type: Linear
[0.20 HCPV CO_2 @ 2.5 MPa (0.087 mol), 4:1 WAG, 10 Slugs]

Figure 6.34 - Production History of Run VLC06.

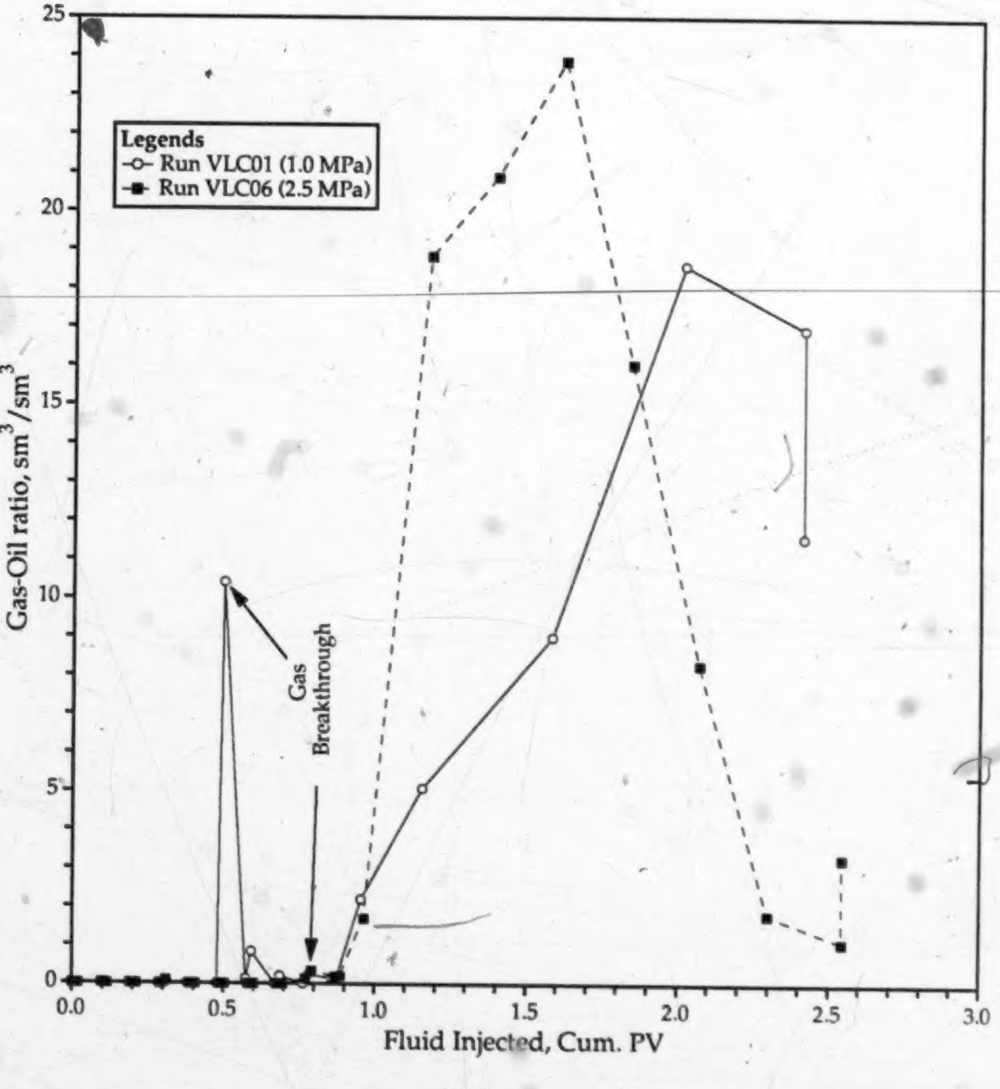

Figure 6.35 - Effect of Pressure on Gravity Rise of Carbon Dioxide Gas.

bubbles of carbon dioxide gas, which travel faster than the oil, at a velocity equal to the velocity of the oil plus the rise velocity due to the buoyancy of the bubbles. It is known that the size of the bubbles formed depends on the pressure, assuming that spherical gas bubbles of a single and constant size are formed. The lower is the pressure, the bigger are the bubbles. The larger bubbles will rise faster because the buoyancy forces grow faster than the drag forces. The buoyancy forces depend on the bubble volume (or $V \alpha r^3$), while the drag forces depend on the bubble surface area ($A \alpha r^2$). That is why gas breakthrough occurred earlier in Run VLC1 than in Run VLC6. Moreover, having been conducted at 1.0 MPa, the density of carbon dioxide injected in Run VLC1 was lower, which also contributed to a faster rate of gas rising.

After 1.0 PV of fluids had been injected, more gas was produced in Run VLC6 than in Run VLC1 as is shown in Figure 6.35. This is because a higher volume of carbon dioxide gas at standard conditions was injected in Run VLC6.

In short, the gravity rise of the carbon dioxide gas injected in the immiscible WAG process is affected by the operating pressure. Gravity rise occurs faster at a lower operating pressure. Therefore, it can be speculated that in the miscible carbon dioxide displacement process conducted at a pressure at which there is only one fluid phase present, the gravity rise of carbon dioxide is less severe than in the immiscible one.

6.9.4 - Effect of Gas Injection Rate

Two runs, VLC7 and VLC9, were conducted in the linear model by continuously injecting carbon dioxide gas at the top of the model until gas breakthrough at the bottom. The injection rates used in the two runs were 0.984 and 0.492 m/d, respectively. The pressure and temperature at which they were conducted were, respectively, 1.0 MPa and 21°C. After gas breakthrough, the total volume of carbon dioxide injected was recorded and water was then injected at the bottom, while the model was still in the vertical position.

Figure 6.36 shows the GOR histories of the two runs. An interesting feature of this plot becomes evident by considering the volume of carbon dioxide injected until gas breakthrough. In Run VLC7, utilizing a 0.894 m/d

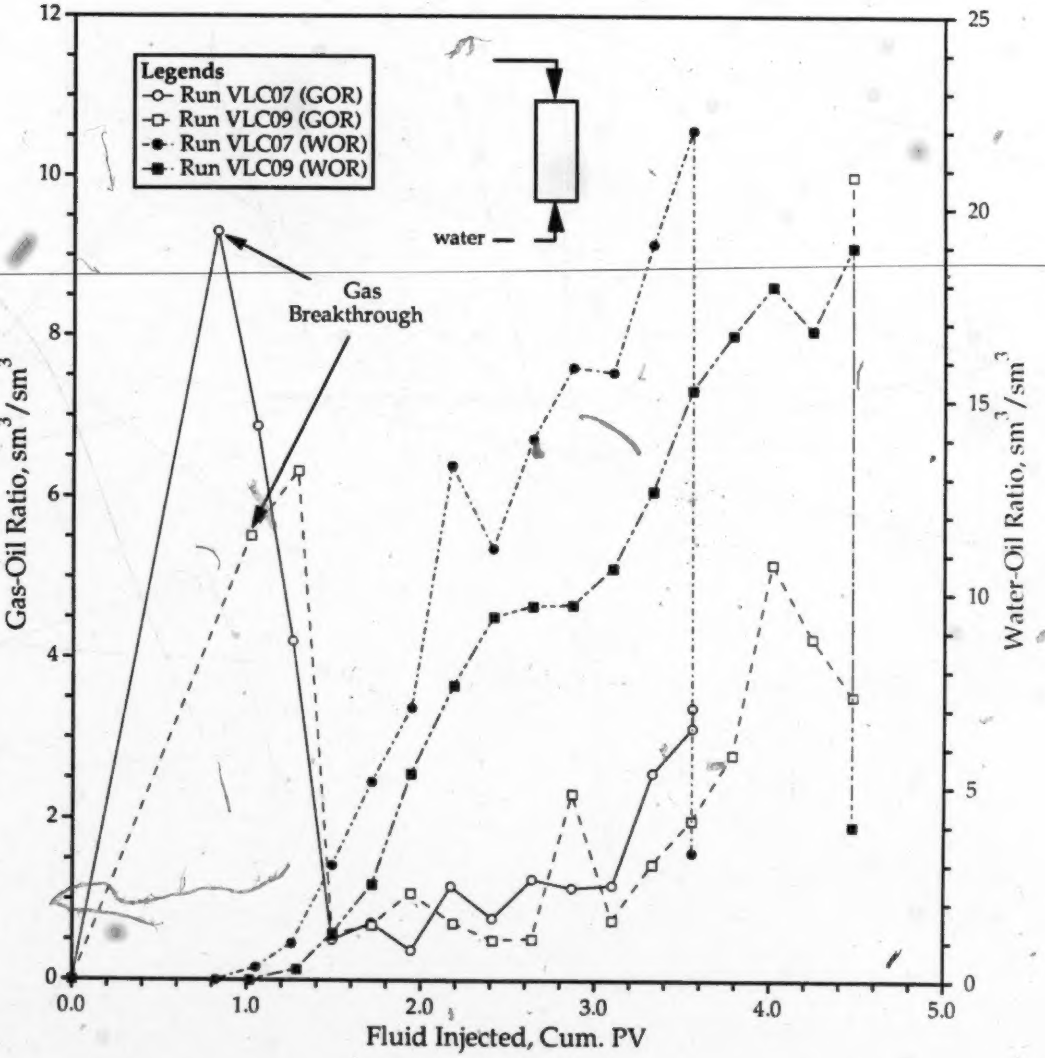

Figure 6.36 - Effect of Gravity on Injection Rate.

injection rate, gas breakthrough was noted when 0.8 PV of carbon dioxide was injected while it was noted when 1.0 PV of carbon dioxide was injected in Run VLC9 utilizing a 0.492 m/d injection rate. This indicates that at a lower rate, the residence time is longer, permitting more gravity segregation to occur. The figure also shows that the GOR of Run VLC7 is approximately twice that of Run VLC9, at breakthrough. This indicates that in a downdip displacement, when carbon dioxide is injected at the top, a higher injection rate will result in a longer mixing zone between carbon dioxide and oil.

Also presented in Figure 6.36 are the GOR's of both runs when water was injected at the bottom. As shown, both GOR curves have nearly the same trend and there is little difference between the two even though the water injection rate employed in Run VLC7 was twice that used in Run VLC9. This shows that over the range of the water injection rate employed to displace the carbon dioxide-swollen oil in the immiscible process the gravitational forces dominate the segregation of the gas.

The effect of gravity on the rise of the injected water can be viewed in Figure 6.36. As indicated in the figure, the WOR's of Run VLC7 were higher than those of Run VLC9, showing that gravity had less effect at a water injection rate of 0.984 m/d than at 0.492 m/d. In other words, had gravity the same effect at a water rate of 0.984 m/d as it had at 0.492 m/d, then the two WOR curves would overlap. Furthermore, it also showed that at 0.984 m/d the viscous forces played a more dominant role than the gravitational forces.

The volume of oil displaced in each run is shown in Figure 6.37. At gas breakthrough, 5.1% of the oil was displaced by carbon dioxide in Run VLC7, whereas 9.5% of the oil was displaced in Run VLC9. Overall, as shown, more oil was displaced in Run VLC9 than in Run VLC7, because more carbon dioxide was injected until breakthrough in the former run.

6.9.5 - Effect of Inverting the Core

Run VLC10 was done a little differently from those already mentioned. In this experiment, carbon dioxide was injected at the top until breakthrough, then the core was inverted to injected water at the bottom. It was performed at 1.0 MPa and 21°C, utilizing an injection rate of 0.492 m/d. In other words,

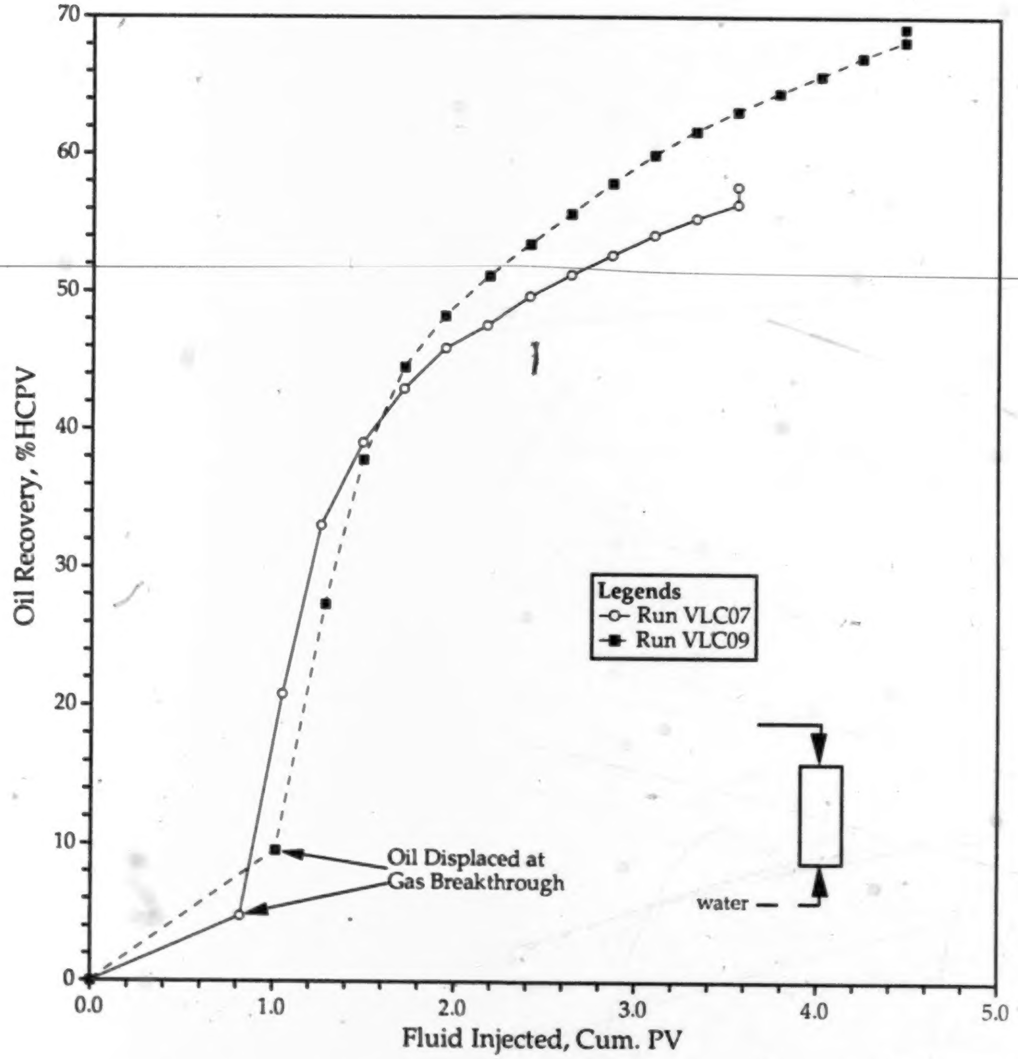

Figure 6.37 - Effect of Gravity on the Volume of Oil Displaced.

the experimental conditions and parameters utilized in this experiment were identical to those utilized in Run VLC9, except that the model was inverted to inject water at the bottom.

The GOR for this run is plotted in Figure 6.38. As shown, by inverting the model, the GOR at the first volume of water injected was 2.75 sm^3/sm^3, which is 2.5 times less than that of Run VLC9 which was done without inverting the model. The reason for the lower GOR at the first volume of water injected is as follows. After carbon dioxide was injected until breakthrough, the carbon dioxide saturation at the top was higher than that at the bottom. When water was injected following inversion of the model, the gas (which was at the bottom) now at the top was produced. This indicates that it still took time for a larger volume of carbon dioxide at the bottom (which had been initially at the top) to rise to the top even though with the help of the driving forces provided by the water injected at the bottom. It also shows that the solubility of carbon dioxide in oil plays a role in retarding the rise of carbon dioxide by virtue of gravity segregation. This is to say that had there been no carbon dioxide solubility in oil, all carbon dioxide would have risen to the top immediately once the model was inverted and water injected.

B - Two-Dimensional Floods

6.9.6 - Effect of Rate

The immiscible carbon dioxide WAG process was proved to be successful in recovering oils from thin, deep and moderately heavy oil reservoirs underlain by a bottom water layer[1-8]. A number of experiments conducted in a quarter of a five-spot system utilizing oils of different viscosities were made in this study to investigate the effect of injection rate. They were Runs H2D1 to H2D25. All these experiments were conducted at 2.5 MPa, 21°C and utilizing a carbon dioxide slug volume of 20% HCPV, a 4:1 WAG ratio and injection rates varying from 0.78 to 3.81 m/d. The oils used in these experiments had viscosities from 603 to 3607 mPa.s. This viscosity range is normally encountered in thin, deep, and moderately heavy oil reservoirs in Alberta and Saskatchewan. Table 6.6 (pages 84 to 86) contains a summary of these experiments.

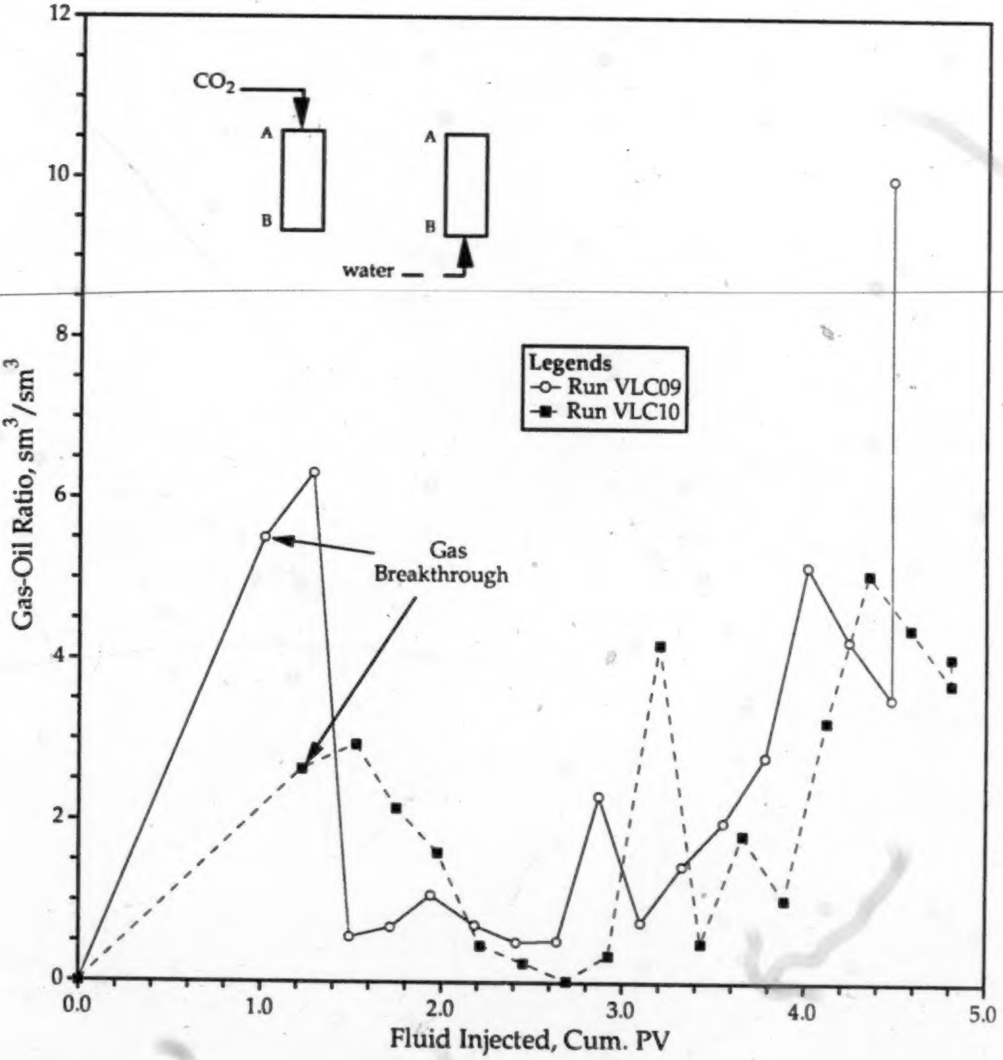

Figure 6.38 - Effect of Inverting the Model.

Figure 6.39 presents the results of the experiments expressed as the oil recovery vs. the dimensionless group $\frac{\vartheta_g \mu_o}{g k \Delta\rho_{go}}$. It is shown in Table 6.6 (pages 85 and 87) that for all oils tested the recovery climbs to its maximum as the injection rate increases to 2.54 m/d and falls off when the injection rate exceeds 2.54 m/d, indicating that 2.54 m/d is the optimal injection rate. The reasons could be as follows. When carbon dioxide is injected at a lower rate, it has a longer time to diffuse into the oil phase. The reverse is true when carbon dioxide is injected at a higher rate. Therefore, the higher is the volume of carbon dioxide that goes into solution in the oil, the greater is the oil viscosity reduction. The greater oil viscosity reduction always leads to a higher oil recovery. In the immiscible carbon dioxide WAG process, carbon dioxide and water are generally injected at the same rate. This means that when the injection rate of carbon dioxide is low, the injection rate of water is as well low. When water is injected at a low rate, the gravity effect is large. The viscous-to-gravitational force ratio is small. As a result, the water injected, instead of displacing oil, segregates at the bottom of the model or flows downward vertically to the bottom, which causes the displacing front to be nearly flat or horizontal. Therefore, only portions of oil near and at the bottom of the model are removed, resulting in a poor volumetric sweep and hence low oil recovery. On the other hand, when water is injected at a high rate, it will, instead of displacing the oil, bypass the oil, leading to a poor volumetric sweep and hence low oil recovery. This is why a lower oil recovery was obtained when an injection rate lower or higher than 2.54 m/d was employed.

Figure 6.40 shows a similar plot for field conditions, assuming the laboratory recovery equals the field recovery; but the results were expressed as the oil recovery vs. the dimensionless group $\frac{Q_g \mu_o}{4 k g \Delta\rho_{go} H^2}$. A similar correlation was done for runs conducted at 1.0 MPa. Figure 6.41 contains such a correlation. Similar to the observation made on Figure 6.39, the volume of oil produced increases as the injection rate increases as shown in Figure 6.41. The volume of oil produced is maximum at the injection rate of 2.54 m/d. Combining this observation and the one made on Figure 6.39 reveals that the optimal injection rate for the two experimental pressures: 2.5 and 1.0 MPa is 2.54 m/d.

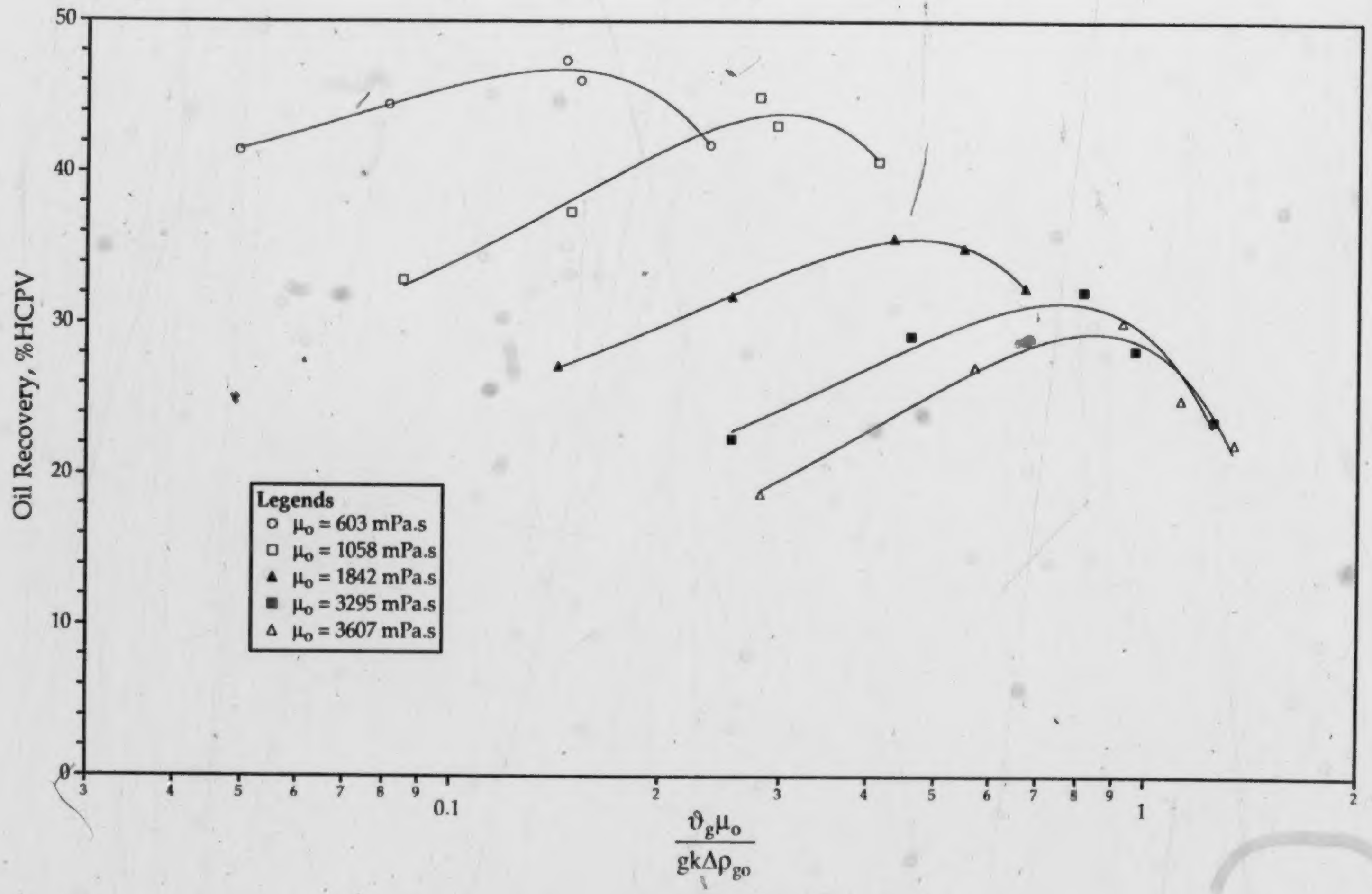

Figure 6.39 - Oil Recovery vs. Ratio of Viscous-to-Gravitational Forces.

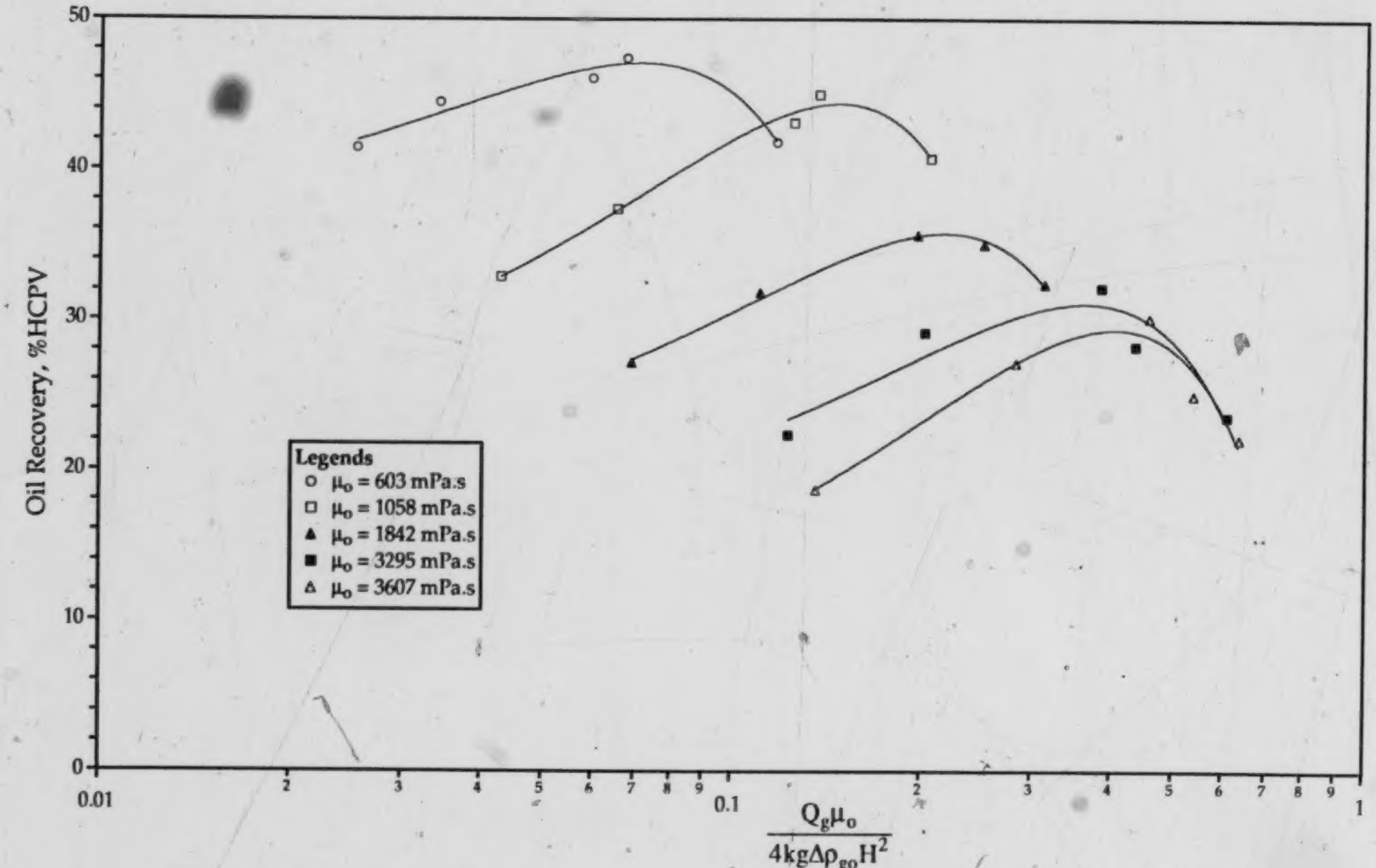

Figure 6.40 - Oil Recovery vs. Ratio of Viscous-to-Gravitational Forces for Field Operations.

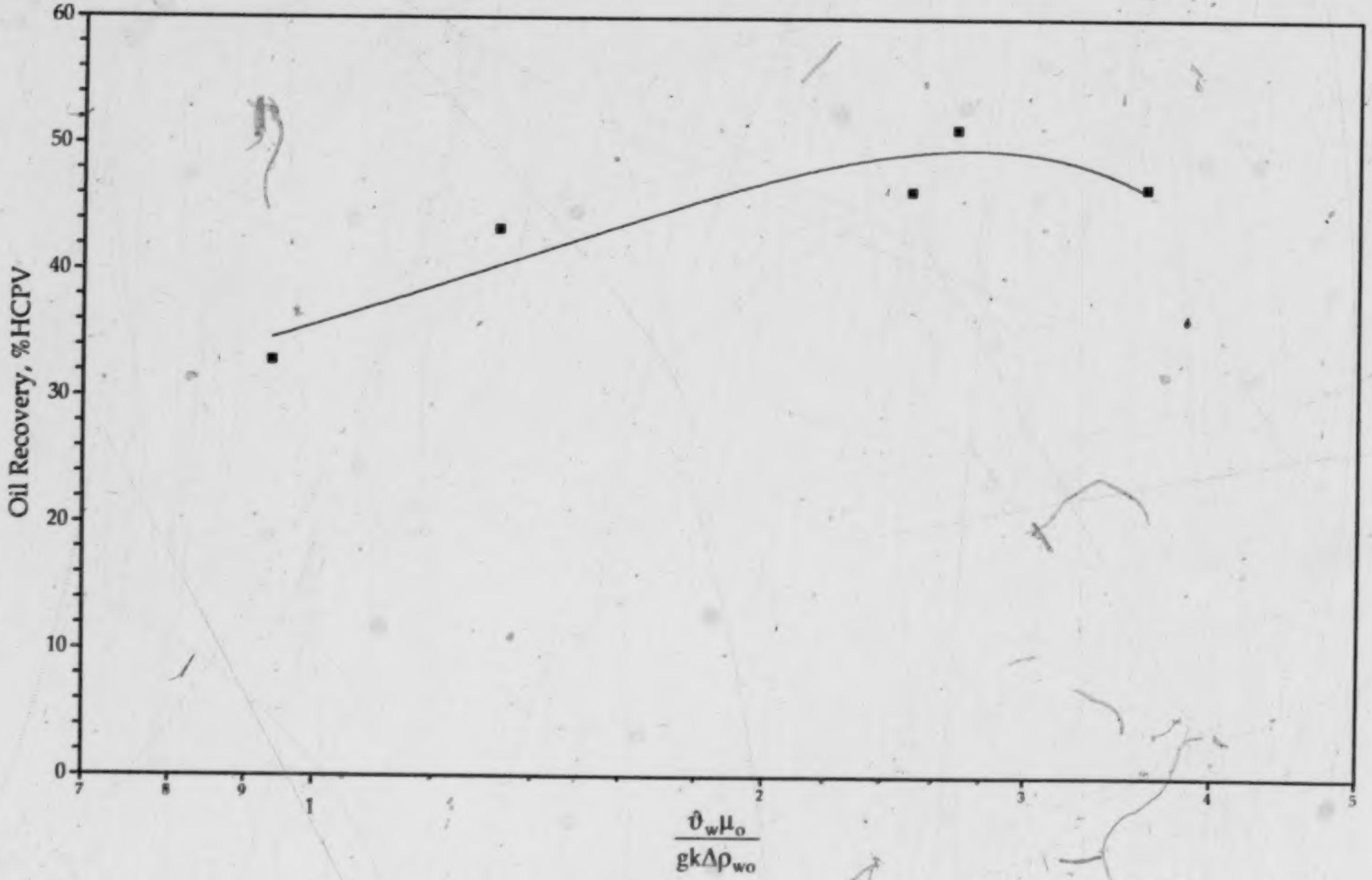

Figure 6.41 - Oil Recovery vs. Ratio of Viscous-to-Gravitational Forces at 1.0 MPa.

To investigate further the effect of carbon dioxide injection rate and to determine the optimal carbon dioxide injection rate at low pressures, a number of experiments were performed by injecting carbon dioxide gas at different injection rates. They were Runs H2D26 to H2D29. The gas injection rates employed in the four runs were, respectively, 0.26, 0.52, 2.6, and 5.2 m/d, while the water injection rate was maintained at 2.6 m/d. The volume of carbon dioxide injected in these runs was 20% HCPV, and the WAG ratio was 4:1. The instantaneous GOR's of the four runs are plotted in Figure 6.42. The effect of gas injection rate becomes evident by observing the GOR curves in the figure. Gas breakthrough occurred earliest at the highest injection rate, i.e., at 5.2 m/d, and more gas was produced in Run H2D29 than in Runs H2D26, H2D27 and H2D28. Observing the GOR curves of Runs H2D26 and H2D27 raises a very interesting feature about the effect of gas injection rate on the solubility of carbon dioxide in the oil. There was very little or almost no production of gas in these two runs until 0.9 PV of fluids were injected, indicating that the low injection rates (0.26 and 0.52 m/d) used in these two runs helped retard gas breakthrough and gave the carbon dioxide enough time to dissolve as much as it could at the pressure and temperature conditions in the oil and thus to establish a close (but not complete) phase equilibrium with the oil. It should be noted that, based on experience, in order for carbon dioxide to reach complete phase equilibrium with the oil, mechanical mixing of carbon dioxide and oil is needed for at least 3 weeks or longer; whereas, in Runs H2D26 and H2D27, the flood time was about 3 days. After the occurrence of gas breakthrough, the GOR's of both runs were almost similar, showing that injecting carbon dioxide at 0.26 or 0.52 m/d produced the same effect.

Figure 6.43 compares the oil recoveries of the four runs. There is very little distinction in the oil recovery when carbon dioxide was injected at 0.26 (Run H2D26), 0.52 (Run H2D27), or 2.6 m/d (Run H2D28). A lower recovery was noted when carbon dioxide was injected at 5.2 m/d (Run H2D29).

To sum up, the injection rate of carbon dioxide has an important effect on the performance of the immiscible carbon dioxide WAG process. That is, when it is very low, it helps to delay gas breakthrough and reach more complete phase equilibrium between carbon dioxide and oil than when it is high. The experimental results show little or no effect of gravity on the gas

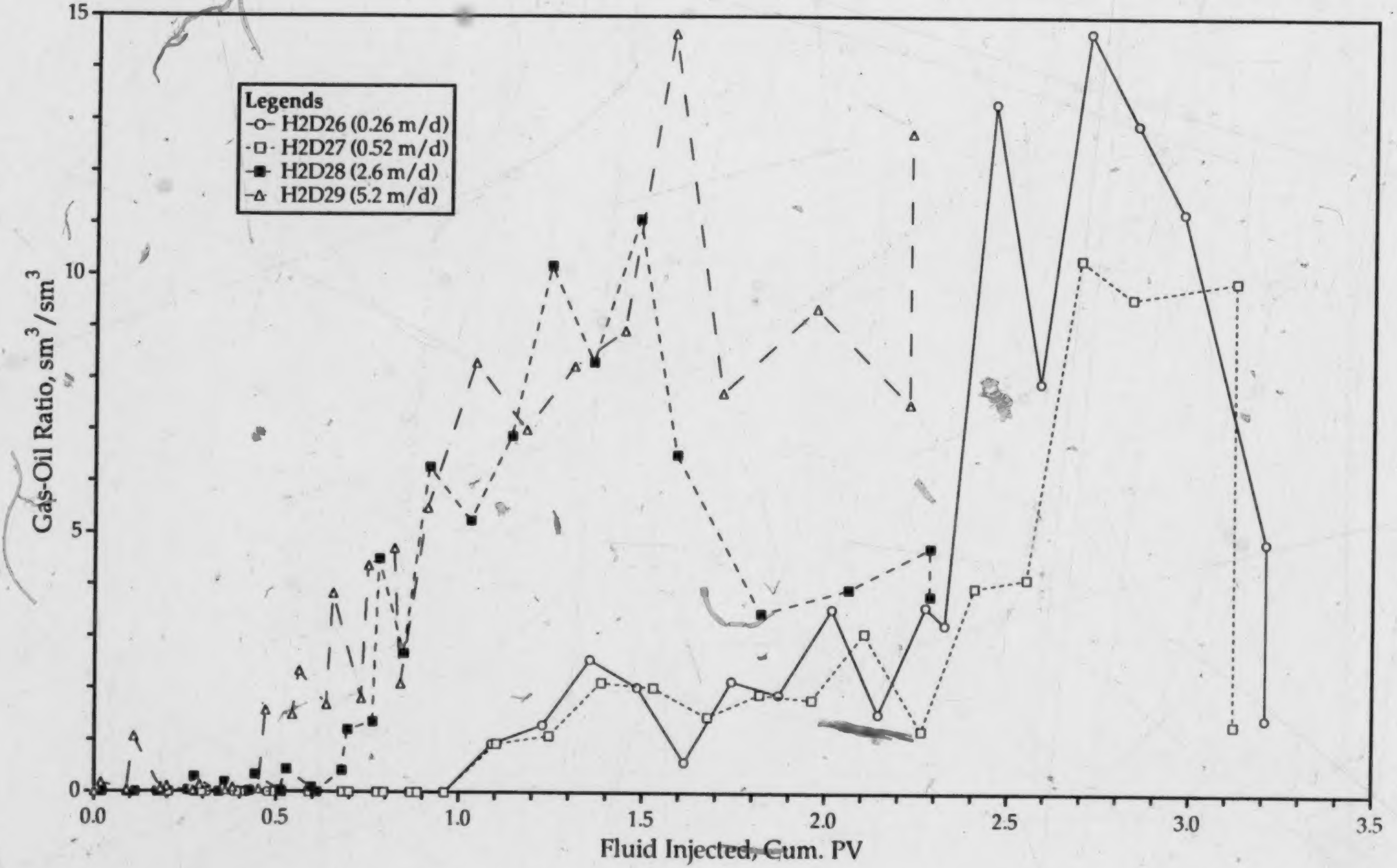

Figure 6.42 - Effect of Rate.

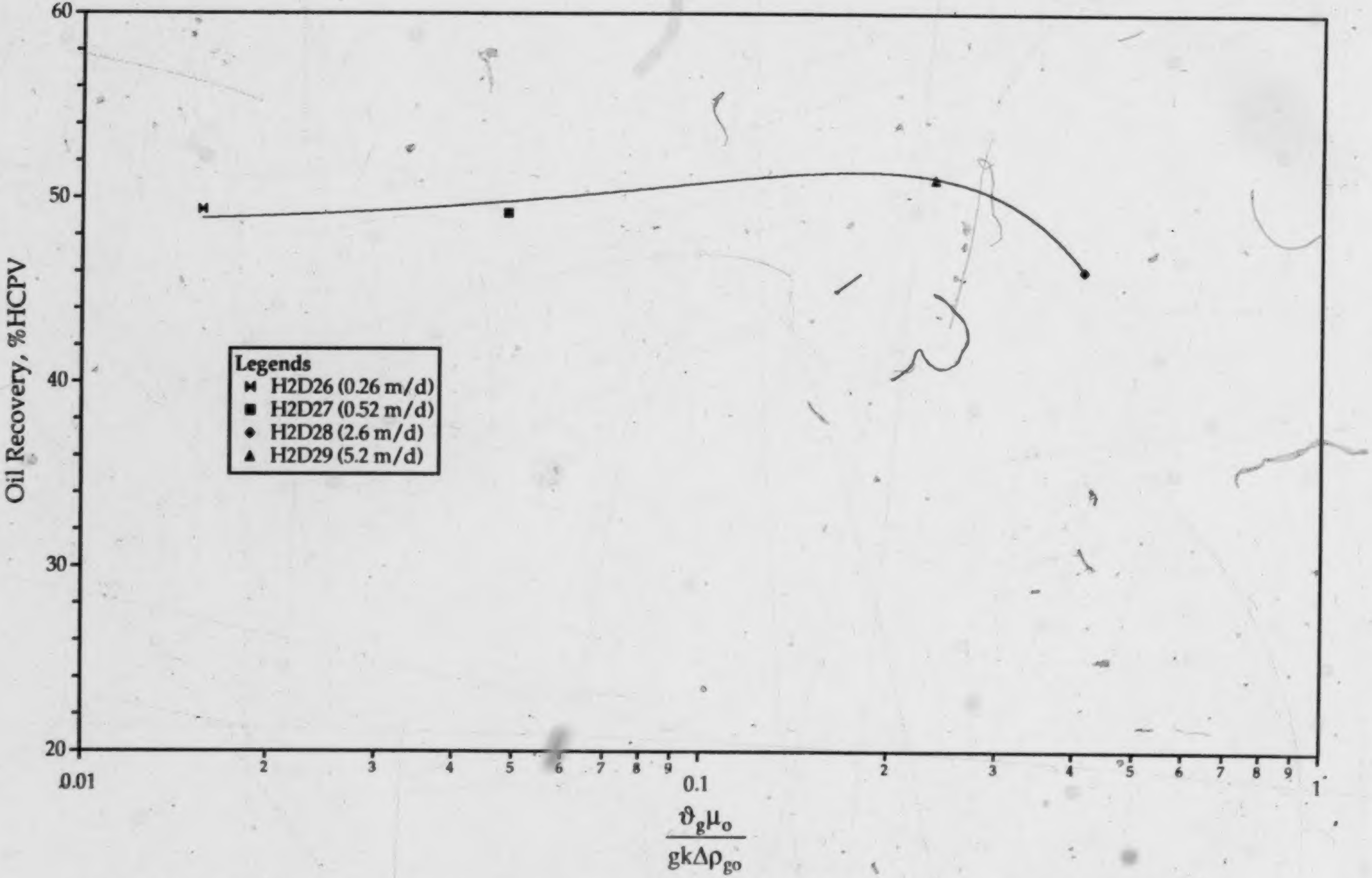

Figure 6.43 - Oil Recovery vs. Ratio of Viscous-to-Gravitational Forces for Different CO_2 Injection Rates.

injection rate, particularly at low rates, because the experiments were conducted in short time spans. It is also obvious from the experimental results that, based on the oil recovery, the immiscible carbon dioxide WAG process performs best when carbon dioxide is injected at a rate less than or equal to the optimal water injection rate. This is true in the laboratory. In the field, because the reservoir thickness and well spacing are much larger than those in the model and the flood can take many years, injecting carbon dioxide at a rate lower than the optimal water injection rate will result in gravity segregation of the carbon dioxide, which will cause gas tonguing, consequently causing an adverse effect on the performance of the process. As such, for field applications, it is recommended that carbon dioxide be injected at a rate equal to the optimal water injection rate.

6.9.10 - Effect of Time

The effect of time on the gravity segregation of carbon dioxide was investigated by conducting Runs H2D34 to 37, which were performed in a two-dimensional model utilizing a carbon dioxide gas slug volume of 5% HCPV at 2.5 MPa and 21°C. Other parameters used in these runs are provided in Table 6.6 (page 86). These experiments were done differently from those already discussed. After 5% HCPV of carbon dioxide was injected, a certain amount of time was allowed to let carbon dioxide "soak" into the oil, then water was injected to displace the oil. The soak times for the runs were, respectively, 0, 3, 4.83 and 10 days. Note that the same injection rate was employed in all runs.

Figure 6.44 shows the GOR's of all four runs as a function of the volume of fluids injected. A close observation of the GOR at breakthrough reveals an interesting aspect of the effect of soak time on gravity segregation of the injected carbon dioxide gas: increasing the soak time increased the breakthrough GOR. The breakthrough GOR's for soak times of 0, 3, 4.83, and 10 days were respectively 0.06, 0.16, 0.27, and 0.33 sm^3/sm^3. A more obvious demonstration of the effect of soak time on gravity segregation of the injected carbon dioxide gas is shown by Figure 6.45, where the breakthrough GOR's are plotted versus soak time. As noted, the breakthrough GOR increased by 3, 4.5, and 5 fold when the soak time increased to 3, 4.83, and 10 days, respectively.

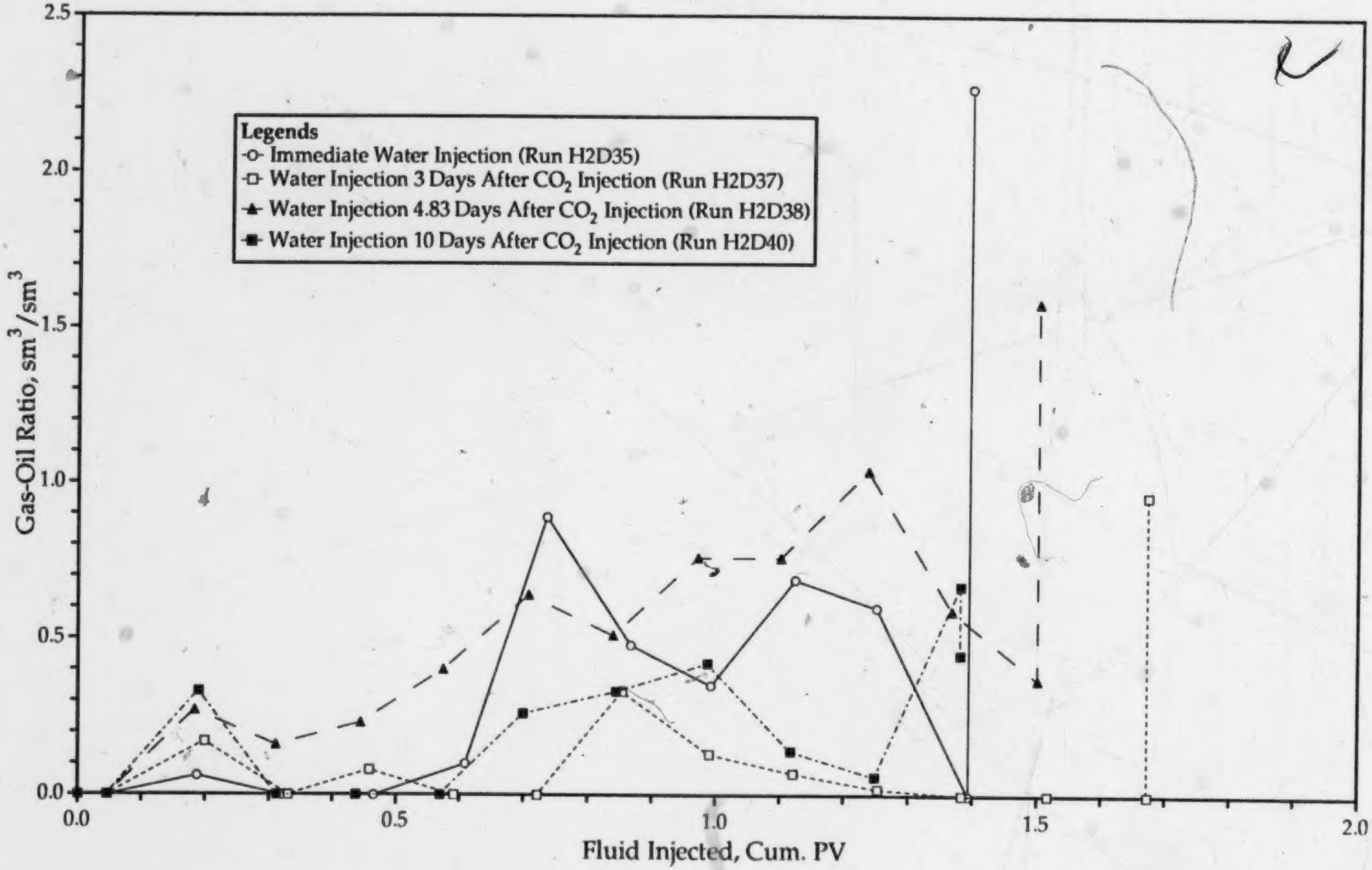

Figure 6.44 - Effect of Time on Gravity Rise of Carbon Dioxide Gas.

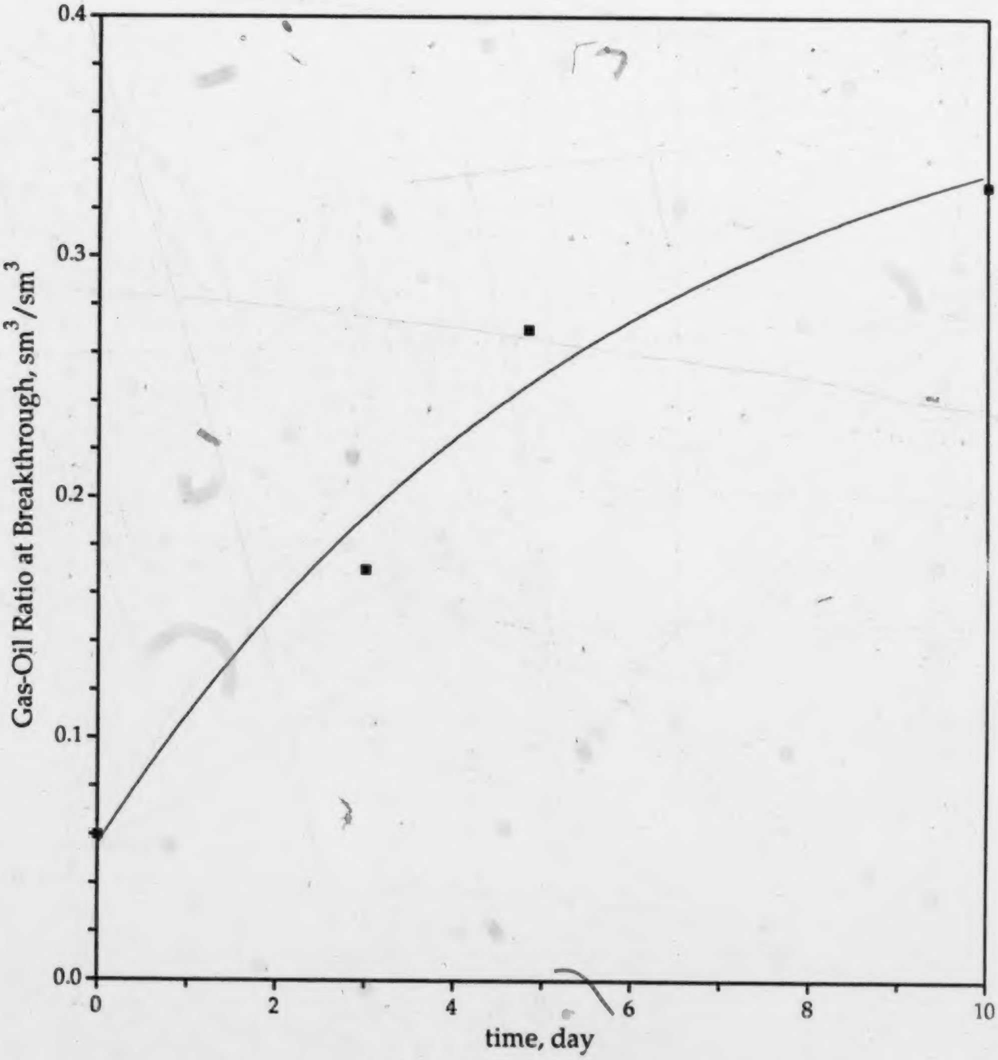

Figure 6.45 - Effect of Soak Time on Gas Breakthrough.

The breakthrough GOR increases with soak time because as more time is allowed more carbon dioxide gas segregates and rises to the top by virtue of the density difference between carbon dioxide and oil, thus leading to a higher GOR at breakthrough. Based on this observation, it is speculated that gravity segregation of carbon dioxide will continue until no more segregation is possible, assuming enough time is allowed. At that time, because the concentration of carbon dioxide on the top is higher than that on the bottom, carbon dioxide will diffuse downward. Then, the GOR at breakthrough will be constant with soak time.

The problem of gravity segregation becomes more pronounced with time. Based on this laboratory observation, it can be said that for field applications where the flood can be as long as many years, the gravity segregation of the carbon dioxide gas will reduce the contact between carbon dioxide and oil, thus leading to a drastic reduction in the amount of carbon dioxide going into solution in the oil as the carbon dioxide moves farther away from the injection well.

6.9.11 - Gravity vs. Transverse Diffusion

Two experiments, V2D1 and V2D2, were performed to investigate the role of transverse diffusion, normal to the vertical direction, on delaying the gravity rise of carbon dioxide. The gases used in Runs V2D1 and V2D2 were, respectively, carbon dioxide and nitrogen. The reason for the choice of nitrogen in the second experiment was because it was to investigate only the gravity rise of the injected gas without any mass transfer involved. Nitrogen has a very low solubility and diffusivity in oil, compared to other gases.

The two experiments were done as follows. With the two-dimensional model in the vertical position, 5% HCPV of carbon dioxide or nitrogen was injected at the bottom. Then, the model was left undisturbed until gas was detected at the top. The time when the gas was detected was recorded. Finally, water was injected at the bottom to complete the experiment. Table 6.7 (page 87) summarizes the results of the two runs.

In Run V2D1, carbon dioxide was noted at the top after 65.4 days, while nitrogen was noted after 37.6 days in Run V2D2. The longer time in Run V2D1 indicates that the transverse diffusivity of carbon dioxide in the direction normal to the longitudinal direction helped delay the gravity rise of the carbon dioxide gas travelling at a velocity equal to the sum of the diffusive velocity due to diffusion and the convective velocity due to gravitational forces.

II.2 - Non-Isothermal Experiments

In addition to conducting experiments under isothermal conditions, it was also intended to conduct experiments under non-isothermal conditions. As has already been defined, non-isothermal in this study means fluids at the atmospheric temperature are injected into a reservoir at a higher temperature. Hence, phase changes and heat transfer from the reservoir fluids to the injected fluids will take place.

6.10 - Unscaled Experiments

6.10.1 - Effect of Temperature

To investigate the effect of temperature, Run H2D38 was performed at 37°C and 2.5 MPa in the two-dimensional model. Note that this experiment was not a scaled experiment. The 37°C temperature was arbitrarily selected. A carbon dioxide volume of 20% HCPV divided into ten equal slugs and a 4:1 WAG ratio were utilized in this run. The oil used had a viscosity of 1058 mPa.s at 21°C and atmospheric pressure. Both carbon dioxide and water were injected at 2.54 m/d. In short, the experimental parameters utilized in this run were identical to those used in Run H2D8 conducted at 21°C. The only difference between the two was the experimental temperature. The tabulated experimental data for this run can be found in Appendix E.

Figure 6.46 details the producing GOR's and production history of Run H2D38. The compositions by mole percent of the gas produced in this run were measured to be on average 0.39 propane, 6.96 water, 1.41 methane, and 91.24 carbon dioxide, while the produced gas in Run H2D8 was found to be mostly carbon dioxide and negligible amounts of water and methane. This

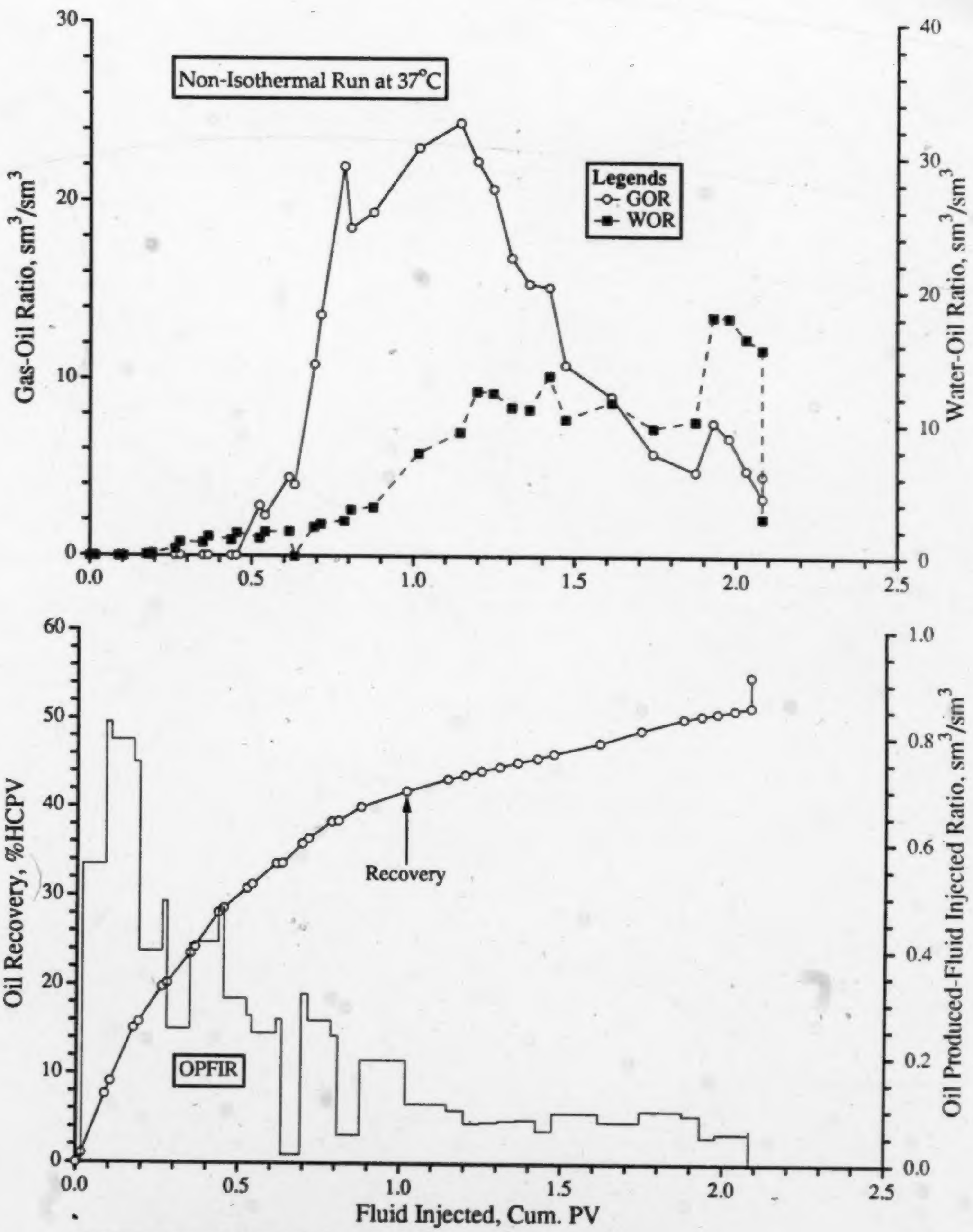

NOTE: Quarter of A 5-Spot

Model Parameters: Average Injection Rate =308.0 cc/hr, μ_o = 1058 mPa.s, ϕ = 38.9 %, k = 12.2 darcies, S_{oi} = 88.6 %, S_{wc} = 11.4 %

[0.20 HCPV CO_2 @ 2.5 MPa & 37°C (0.372 mol), 4:1 WAG, 10 Slugs]

Figure 6.46 - Production History of Run H2D38.

shows that the temperature affected the composition of the gas produced in Run H2D38. It caused some of the injected and reservoir water to vaporize and made the light components of the oil more volatile.

Figure 6.47 presents a comparison of the GOR's of Run H2D38 with those of Run H2D8. As shown, gas breakthrough occurred earlier in Run H2D8 (21°C) than in Run H2D38 (37°C). This is due to the lower gas-oil mobility ratio encountered in the latter run. The viscosity of the oil in Run H2D8 was higher than that in Run H2D38 because the latter was conducted at 37°C while the former was conducted at 21°C. At 37°C and atmospheric pressure, an oil with a viscosity of 1058 mPa.s at 21°C and atmospheric pressure was measured to be 327 mPa.s. Appendix G contains the experimentally measured viscosities of different oils as functions of temperature. Empirical correlations based on Walther's equation were also made and are included. Even though gas breakthrough occurred earlier in Run H2D8, the GOR curve for Run H2D38 is higher than that for Run H2D8, as shown in the figure. There were two factors which caused the higher gas production in Run H2D38. The first was the higher temperature which reduced the solubility of carbon dioxide in oil. The second might be as follows. Due to the presence of water vapour, propane, and methane in Run H2D38 (conducted at 37°C), when carbon dioxide was injected, it mixed faster with the water vapour, methane, and propane than with the oil because mass transfer occurs much faster from gas to gas than from gas to liquid. Once carbon dioxide mixed with these gases, its solubility in oil decreased. However, the diffusivity of carbon dioxide was higher at 37°C, but this did not contribute much because diffusion is a very slow mass transfer process compared to solution.

Figure 6.48 compares the oil recovery of Run H2D08 with that of Run H2D38. As shown, the recoveries were 54% and 45% for Runs H2D38 and H2D8, respectively. This clearly indicates that temperature affects the displacement efficiency of the immiscible WAG process.

6.10.2 - Effect of Oil Viscosity

It was noted in the preceding section that more oil was recovered at a higher temperature because the viscosity of a 1058 mPa.s oil at 21°C reduced to

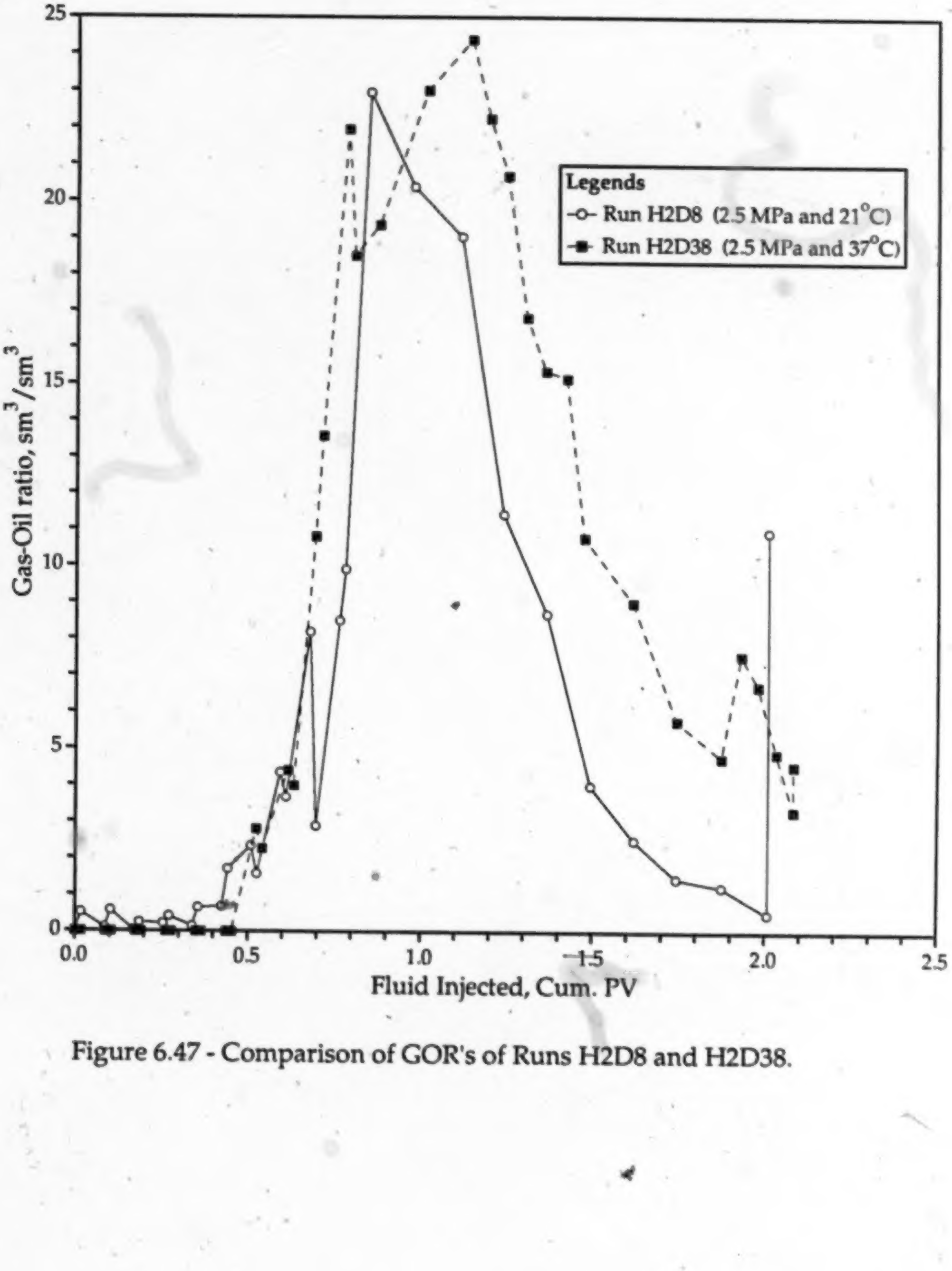

Figure 6.47 - Comparison of GOR's of Runs H2D8 and H2D38.

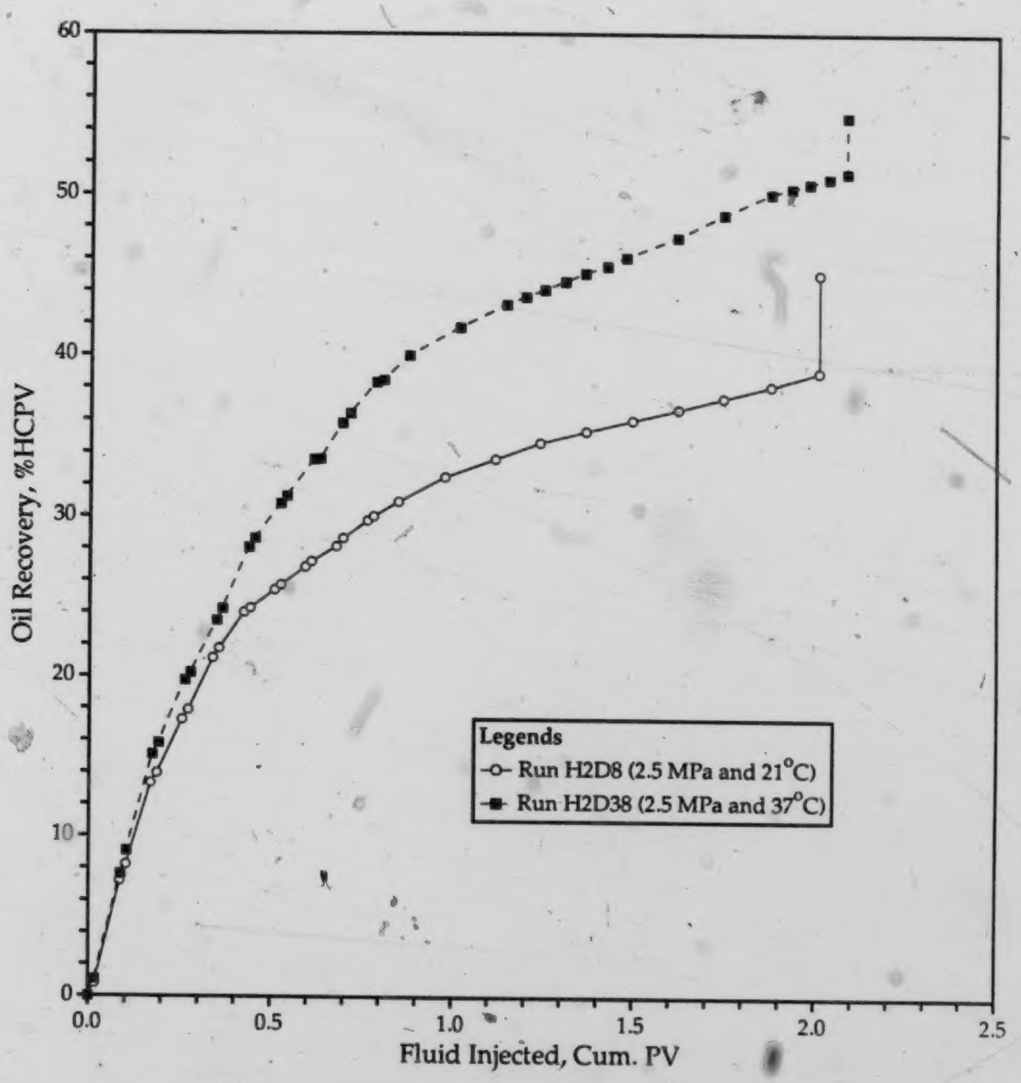

Figure 6.48 - Comparison of Oil Recoveries of Runs H2D8 and H2D38.

327 mPa.s at 37°C. Consequently, it was intended to conduct an experiment using an oil with a viscosity equal to 1058 mPa.s at 37°C. Therefore, an oil with a viscosity of 5200 mPa.s at 21°C was chosen because it viscosity became 1058 mPa.s at 37°C. Run H2D39 was conducted using this oil. The experimental parameters employed in this run were exactly the same as those used in Runs H2D8 and H2D38. Note that it was done at 37°C. Appendix E contains the tabulated experimental data for this run.

The instantaneous GOR's of Run H2D39, together with those of Run H2D8, are shown in Figure 6.49. It is shown in the figure that gas breakthrough occurred earlier in Run H2D39 and that the GOR curve for Run H2D39 is higher than that for Run H2D8, even though the two runs were conducted using oils with the same viscosity at two different temperatures. The earlier gas breakthrough and higher instantaneous GOR's occurring in Run H2D39 were due to the lower gas viscosity and solubility of carbon dioxide in oil at a higher temperature, which did not cause the same viscosity reduction as it did in Run H2D8.

The recoveries of the two runs are shown in Figure 6.50. The curve with a lower trend represents the recovery history of Run H2D39. It is clearly shown in the figure that the total recovery of Runs H2D39 is 4% lower than that of H2D8, which was basically, as has been recently mentioned, due to the lower carbon dioxide solubility at a higher temperature.

The observation made above reveals that in order to correlate a non-isothermal experiment to an isothermal one or vice-versa, not only the oil viscosity must be considered but also the solubility of carbon dioxide in the oil.

6.10.3 - Effect of Carbon Dioxide Solubility

Based on the observation made in the preceding section, it was intended to conduct an experiment at 37°C and at a predetermined pressure such that the solubility of carbon dioxide in oil at this pressure and temperature condition was identical to that at 21°C and 2.5 MPa, ignoring the effects of water vapour and hydrocarbon gases at the higher temperature. To determine this experimental pressure, Chung, Jones, and Nguyen's correlation[106]

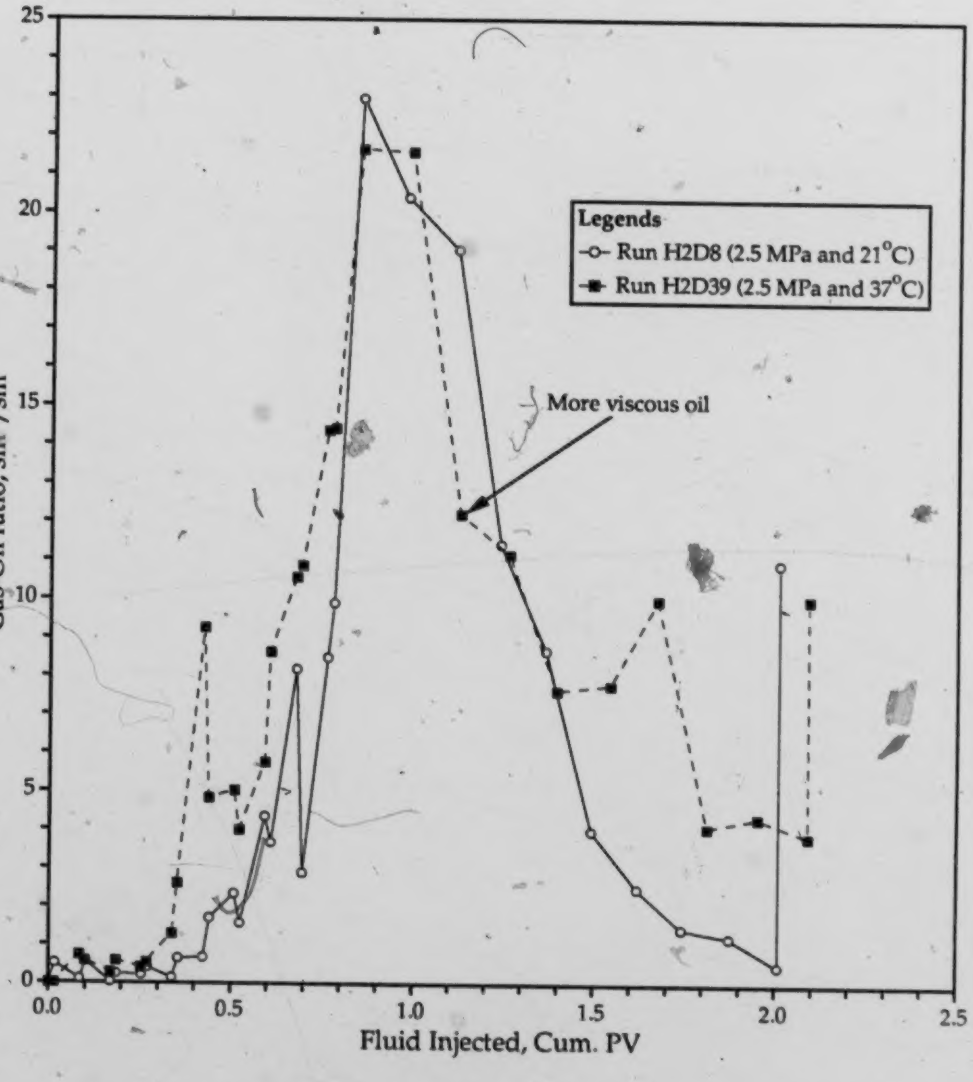

Figure 6.49 - Comparison of GOR's of Runs H2D8 and H2D39.

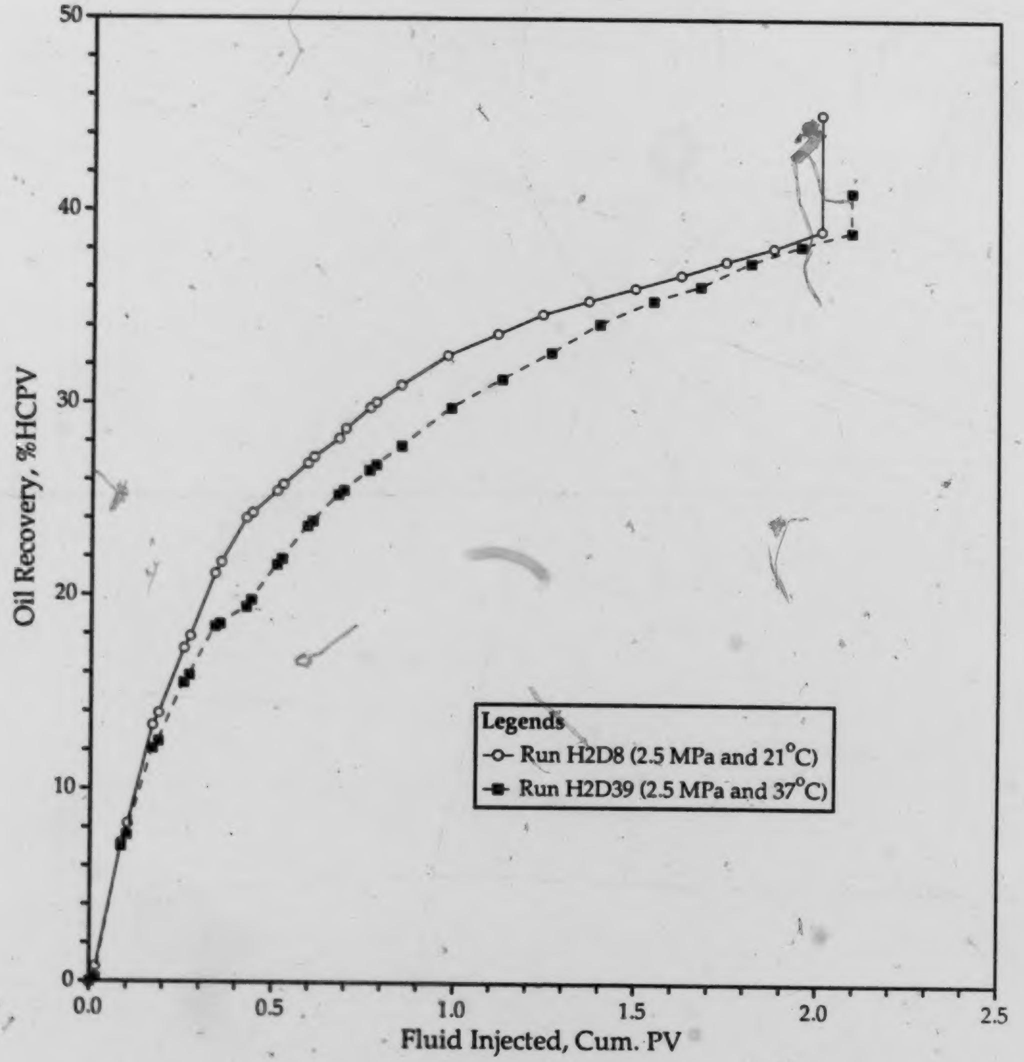

Figure 6.50 - Oil Recovery Comparison of Runs H2D8 and H2D39.

for carbon dioxide solubility in oils was used. At 3.14 MPa and 37°C the solubility of carbon dioxide was identical to that at 2.5 MPa and 21°C. Hence, Run H2D40 was performed at 3.14 MPa and 37°C utilizing the same experimental parameters as used in Run H2D8. The same oil used in Run H2D39 was used in this run. Appendix E contains the tabulated results of this run.

The instantaneous GOR's of Run H2D40 are plotted in Figure 6.51, along with those of Run H2D8. Observing the GOR's of both runs raises an interesting point. As indicated, gas breakthrough occurred at the same time in both runs. Also shown in the figure is that the GOR curve for Run H2D40 has a higher trend than that for Run H2D8. This is because a higher carbon dioxide volume at standard conditions was utilized in Run H2D40. Another reason which is believed to cause the higher GOR's in Run H2D40 is the lower solubility of carbon dioxide due to the higher concentration of water vapour at 37°C.

Figure 6.52 compares the volume of oil displaced in the two runs. The two recovery curves nearly overlay, demonstrating that almost the same oil recoveries were obtained in the WAG, post-waterflood, and blowdown phases in both runs, and consequently the total recoveries of the two differ by less than 2% (45.4% for Run H2D8 vs. 43.7% for Run H2D40). This recovery difference is small and can be neglected. The almost similar oil recoveries reported in the two runs indicate that the same viscosity reduction was approximately achieved in both runs.

In short, combining the observations made in the preceding section and this, it can be concluded that in order to correlate an isothermal experiment to non-isothermal conditions, or vice-versa, the oil viscosities and carbon dioxide solubilities in the two runs be equal.

6.10.4 - Effect of Slug Size

Based on the observation made in Section 6.10.1, it is hypothesized that because the solubility of carbon dioxide is lower at a higher temperature, a smaller volume of carbon dioxide should be used instead. Run H2D41 was conducted using a total carbon dioxide slug size of 10% HCPV. In order to make a fair comparison with Run H2D39, the same oil with identical physical

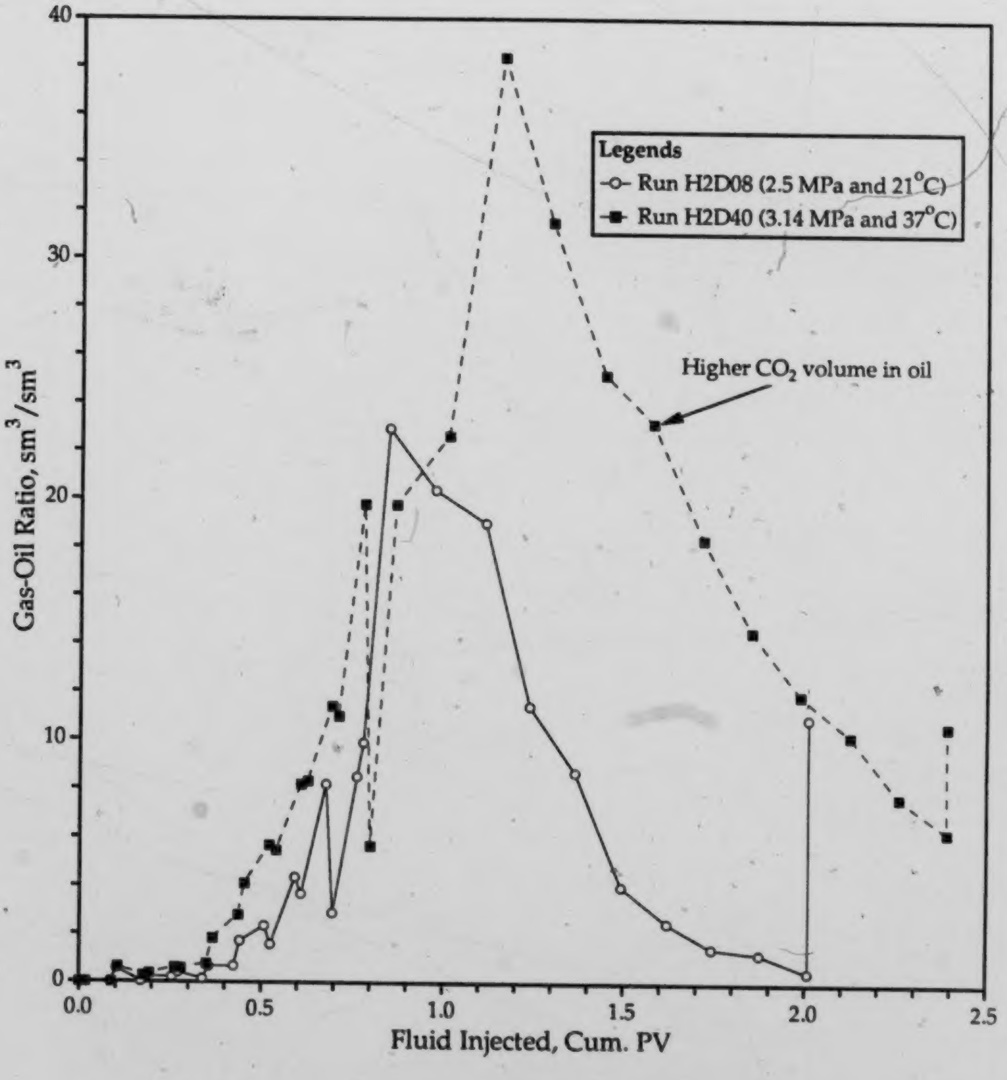

Figure 6.51 - Effect of Similar Carbon Dioxide Solubility at Two Different Pressure and Temperature Conditions.

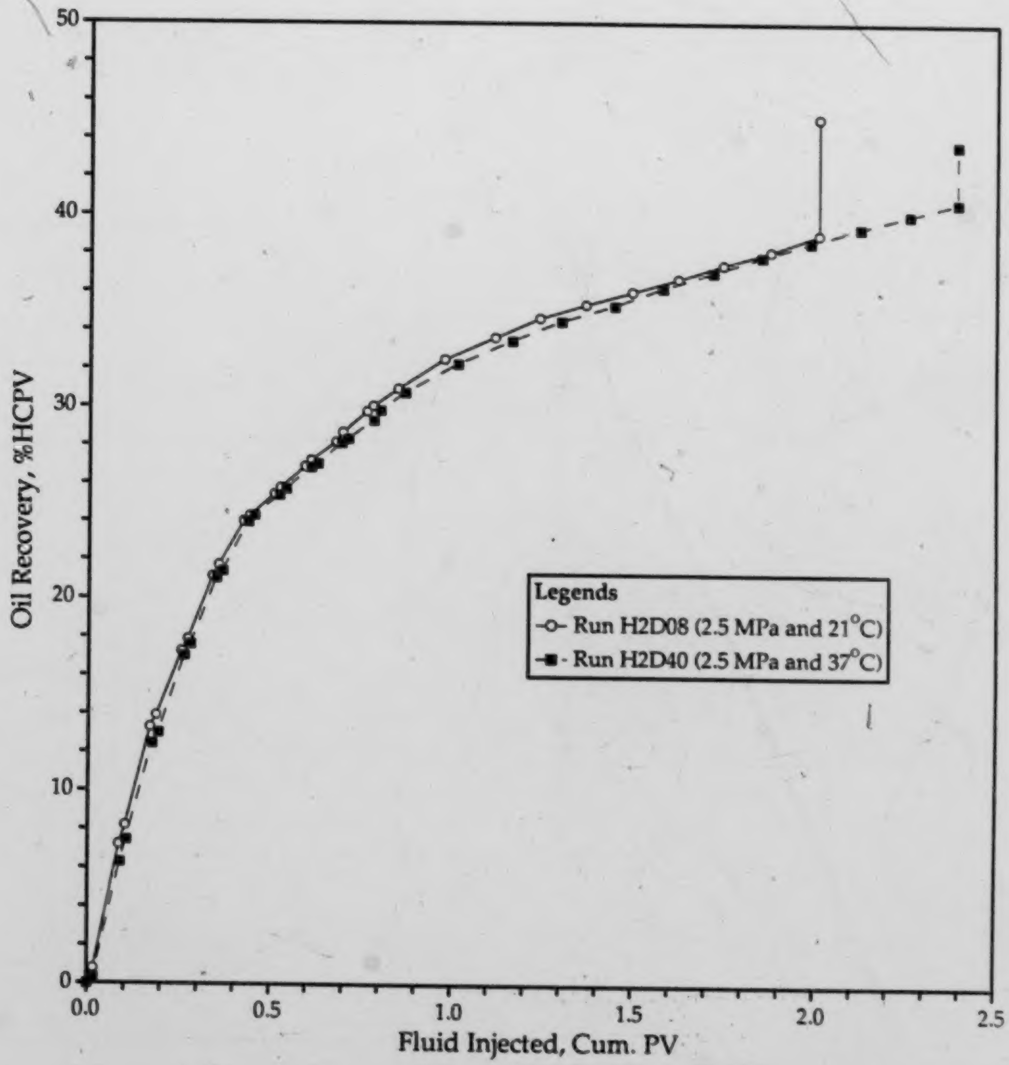

Figure 6.52 - Comparison of Oil Recoveries of Runs H2D8 and H2D40.

properties and the same injection rate and experimental parameters used in Run H2D39 were used in Run H2D41. The tabulated experimental results of this experiment can be seen in Appendix E.

Figures 6.53 and 6.54 show the comparisons of Runs H2D41 and H2D39. As shown in Figure 6.53, similar to what was observed in Section 6.7.3, a higher producing GOR curve corresponds to a higher volume of carbon dioxide injected. In Figure 6.54, a comparison of the recoveries of the two runs reveals that a higher oil recovery was obtained with a higher volume of carbon dioxide injected. The total volume of oil recovered in Run H2D41 (10% HCPV CO_2) was 31.2% while it was 41.1% in Run H2D39 (20% HCPV CO_2). As explained previously, a lower recovery was obtained when a 10% HCPV of carbon dioxide was injected because the volume of carbon dioxide utilized was insufficient to cause the maximum oil viscosity reduction.

6.11 - Scaled Experiments

6.11.1 - Experimental Design

The purpose of this section is to use the scaling criteria derived in Chapter 4 (page 18) to design the scaled experiments according to the field data presented in Table 5.1 (page 52). The first parameter to be determined is the scaling factor, a, which is the ratio of the length in the prototype to that in the model. It is usually determined by the maximum physical size available for the experiment. In this study, it is desired to design the scaled experiments in such a way that they can be conducted in the existing scaled physical model. The length of the existing model, as mentioned in Chapter 5 (page 47), is 0.457 m; the scaling factor, a, is therefore

$$a = \frac{\text{field well spacing}}{\text{model well spacing}} = \frac{201.17\ \text{m}}{0.457\ \text{m}} = 440.2.$$

Model Thickness: it is calculated by the group $\left(\frac{H}{L}\right)$ as follows:

$$\left(\frac{H}{L}\right)_M = \left(\frac{H}{L}\right)_P$$

$$H_M = \frac{H_P \times L_M}{L_P} = \frac{5.1\ \text{m}}{440.2} = 0.012\ \text{m}$$

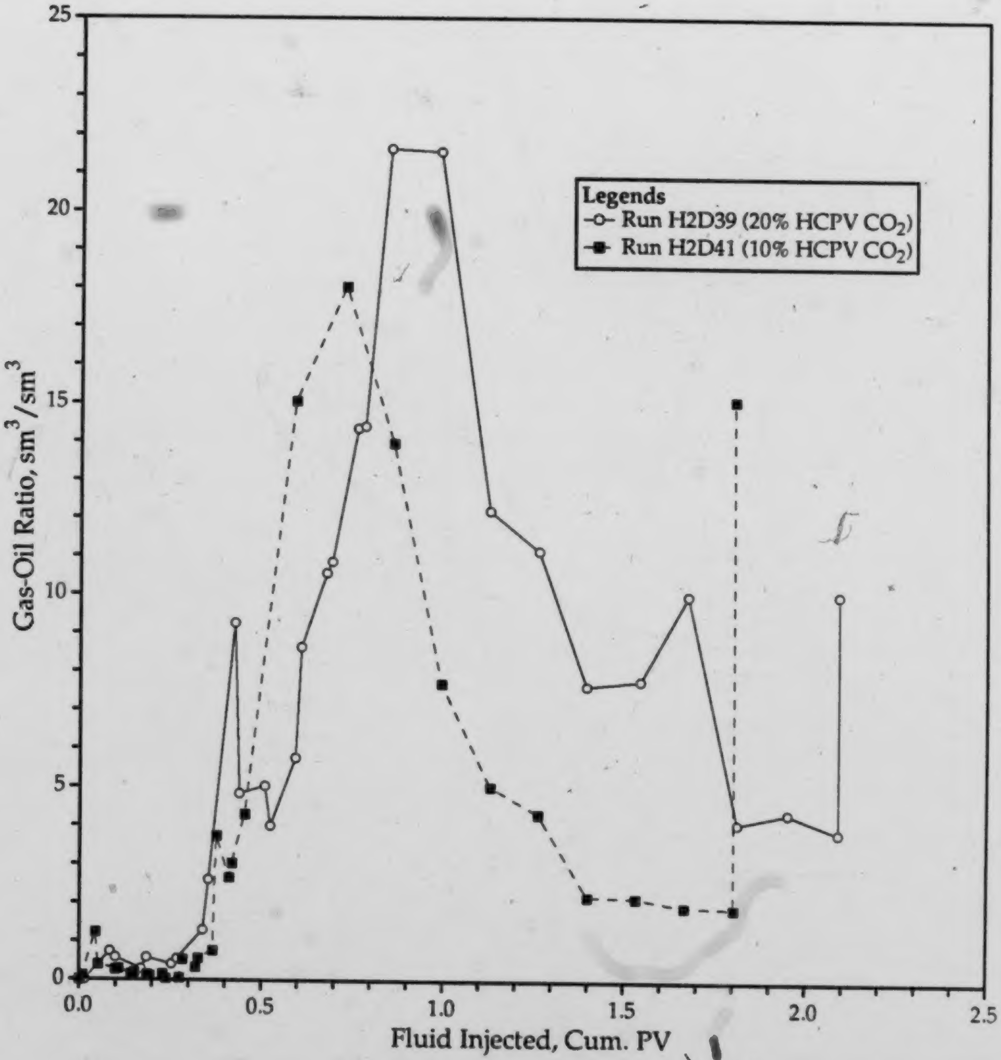

Figure 6.53 - Effect of Slug Size on GOR's at Non-Isothermal Conditions.

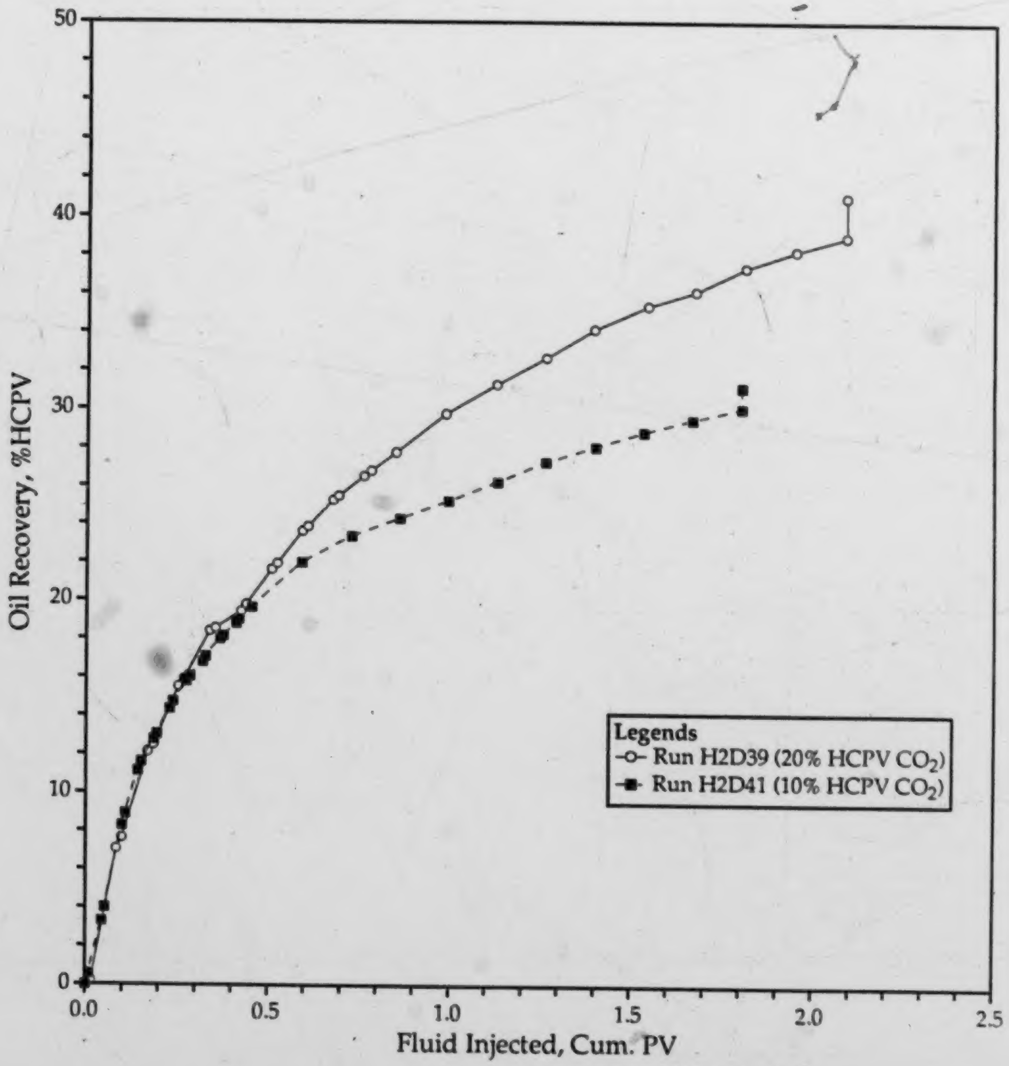

Figure 6.54 - Effect of Slug Size on Oil Recovery at Non-Isothermal Conditions.

Thus, the desired model representing the reservoir will have dimensions of $0.457\ \mathrm{m} \times 0.457\ \mathrm{m} \times 0.012\ \mathrm{m}$. As it is very costly to fabricate a model with these dimensions, the existing scaled physical model with dimensions of $0.457\ \mathrm{m} \times 0.457\ \mathrm{m} \times 0.022\ \mathrm{m}$ is used instead. The existing model is 0.010 m thicker that the desired model.

Fluid Properties: each dimensionless fluid property should be the same function of dimensionless pressure and temperature for the model as it is for the field. To satisfy this requirement, it is best to use the reservoir fluids in the model; thus, fluid properties such as density, viscosity, solubility, and diffusivity are automatically scaled. This is true if the model pressure and temperature are identical to the reservoir pressure and temperature.

For Approach 1, the fluid properties are scaled because the reservoir fluids are used in the model; moreover, the pressure and temperature are the same in the model and the prototype. As for Approach 2, only two fluid properties are scaled: viscosity and diffusivity, because the viscosity of the model oil and the solubility of carbon dioxide in the model oil at the laboratory temperature and experimental pressure are chosen to be respectively the same as those in the reservoir oil at the reservoir temperature and pressure. The viscosity of the reservoir oil at 37°C is 160 mPa.s; therefore, the viscosity of the model oil must be 160 mPa.s at 21°C.

Model Pressure: for Approach 1, there is no need to determine the model pressure because it is chosen to be equal to the field pressure. As for Approach 2, it is necessary to determine a model pressure such that the solubility of carbon dioxide at 21°C and the model pressure equals that at field temperature and pressure, i.e., at 37°C and 4.8 MPa, respectively. By using Chung et al.'s correlation[106], the model pressure is 3.58 MPa.

In addition , it is necessary to select the pressure drop in the model such that the gravitational-to-viscous forces ratio is scaled. This can be done as follows:

$$\frac{(p - p_{\mathrm{prod}})_{\mathrm{Model}}}{(p - p_{\mathrm{prod}})_{\mathrm{Field}}} = \frac{(\Delta\rho_{og} g H)_{\mathrm{Model}}}{(\Delta\rho_{og} g H)_{\mathrm{Field}}}$$

Re-arranging gives

$$\left(p-p_{prod}\right)_{Model}=\left(p-p_{prod}\right)_{Field}\times\frac{\left(\Delta\rho_{og}H\right)_{Model}}{\left(\Delta\rho_{og}H\right)_{Field}}$$

Therefore, the model pressure drop, by virtue of this expression, is reduced by a factor "a". Given the densities of oils and carbon dioxide at the two pressure and temperature conditions, the true model pressure can be determined as shown below.

$\rho_{CO_2} = 83.5$ kg/m^3 at 3.58 MPa and 21°C
$\rho_{CO_2} = 111.0$ kg/m^3 at 4.8 MPa and 37°C
$\rho_{oil} = 950.0$ kg/m^3 at 3.58 MPa and 21°C
$\rho_{oil} = 943.8$ kg/m^3 at 4.8 MPa and 37°C

and the field production pressure is 2.6 MPa. The expression for the model pressure can be written as

$$p_{Model}=\left(p_{prod}\right)_{Model}+0.00987$$

If the model production pressure is chosen to be 3.58 MPa, then the actual average pressure of the model will be 3.59 MPa, which is not very different from the pressure determined using Chung et al's correlation[106] for predicting solubility of carbon dioxide in viscous crudes.

Permeability Determination: for both approaches, the permeability is the same in the model and the prototype because the reservoir sand is used to represent the field porous medium.

Injection Rate: to calculate the injection rate of carbon dioxide and water, the group $\frac{\alpha w_{CO_2R}\mu_{gR}}{\rho_{gR}k_{gR}p_{gR}H}$ is used. The field current injection rate, being unavailable, the optimal injection rate determined in Section 6.9.6 (page 122) is used in the scaled experiments.

6.11.2 - Discussion of The Results of The Scaled Experiments

Two scaled experiments were performed according to the design discussed in the preceding section to investigate the possible application of the immiscible carbon dioxide WAG recovery technique in the pre-waterflooded reservoir under consideration (moderately heavy oil reservoir in Saskatchewan) for which reservoir description is provided in Table 6.8 (page 147). They were tertiary Runs H2D42b and H2D43b. Run H2D42b was conducted using the design for Approach 1 and Run H2D43b was conducted using Approach 2. The total volume of carbon dioxide injected in both runs was 20% HCPV in a 2:1 WAG mode. The 2:1 WAG ratio was selected because a previous study on this reservoir showed that utilizing a 2:1 WAG ratio is as effective as utilizing a 4:1 WAG ratio, for the reservoir under study. The temperature and pressure conditions at which Runs H2D42b and H2D43b were conducted were respectively 37°C at 4.8 MPa and 21°C at 3.58 MPa. Even though they were conducted at two different temperatures, the viscosities of the oils used in the two runs were similar, and the solubilities of carbon dioxide in the oils were supposed to be the same as well. Hence, a fair comparison could be made, assuming there was no oil density difference.

Figure 6.55 presents a comparison of the instantaneous GOR's of the two runs. It is shown in the figure that the GOR curve of Run H2D42b (37°C) is higher for the most part than that of Run H2D43b (21°C). This is because a higher volume of water vapour was present in Run H2D42b. The water vapour from the analysis of the produced gas in Run H2D42b was 3.88 mole%, while it was 0.81 mole% in Run H2D43b. This higher concentration of water vapour prevented carbon dioxide from going into the oil. That is, it reduced the carbon dioxide solubility, causing carbon dioxide to remain in a free gas phase which would then bypass the oil. Another interesting feature can be spotted when comparing the late time GOR's of the two runs. The late time GOR of Run H2D42b (non-isothermal at 37°C), as shown in the figure, is 3 times higher than that of Run H2D43b, which indicates that in the blowdown stage when the pressure is depleted, the higher temperature enhances the release of the carbon dioxide gas dissolved in the oil.

The comparison of the recoveries of the two runs, according to the two recovery curves in Figure 6.56, reveals that the same volume of oil was

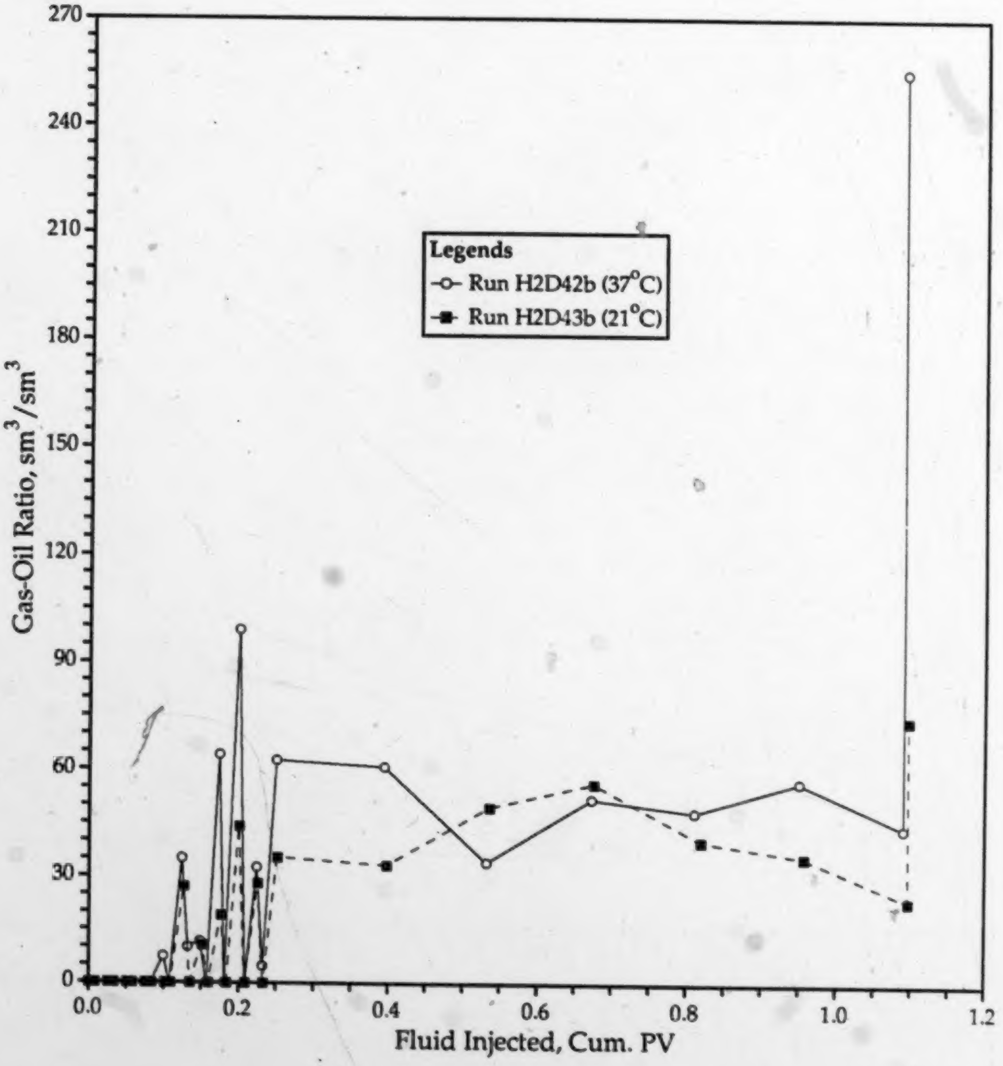

Figure 6.55 - GOR's of Run H2D42b vs. Those of Run H2D43b.

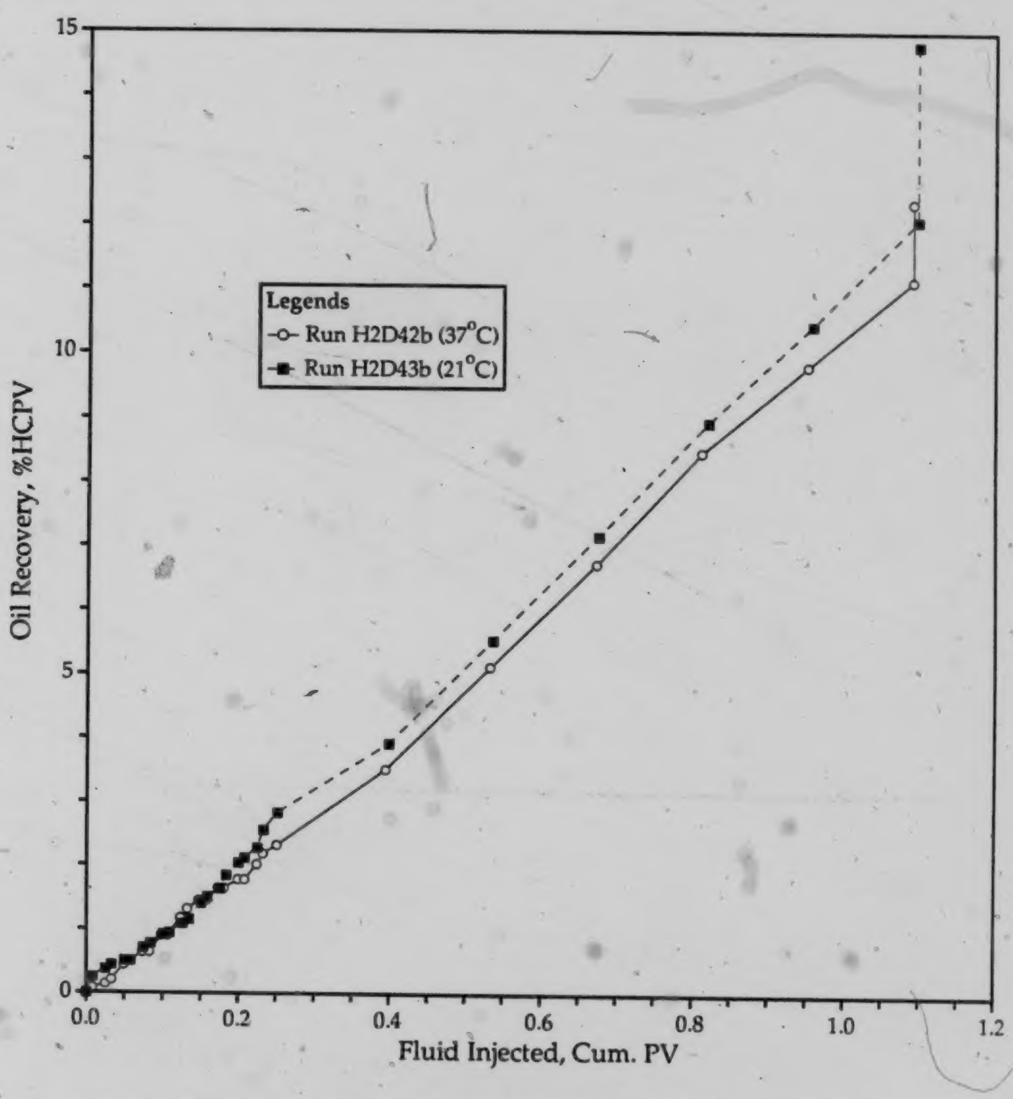

Figure 6.56 - Recovery of Run H2D42b vs. That of Run H2D43b.

recovered in the WAG stage (from 0 to 0.3 PV) and the post-water recoveries of the two runs differed by less than 0.5% HCPV. Overall, the total recoveries differed by less than 1.5% HCPV. This total recovery difference is very small, indicating that both approaches can be used to predict the performance of the immiscible carbon dioxide process under non-isothermal conditions.

6.12 - Reproducibility of the Experimental Results

An important aspect of this study concerns the reproducibility of the experimental results.

Repeatability of the experiments was examined further by conducting Runs CWF3, CWF4, VLC4, VLC8 and H2D44b to check respectively the results of Runs CWF1, CWF2, VLC3, VLC7 and H2D43b. Run VLC11 was performed to check also Run VLC7. The results of these experiments were also tabulated and are contained in Appendix E.

Figures 6.57, 6.59, 6.61, 6.63, and 6.65 present the reproducibilities of the GOR's of Runs CWF1, CWF2, VLC3, VLC7, and H2D43b, respectively. They show that the reproducibilities of the GOR's of these experiments were fairly good, because the overall errors involved were small–in the range of 15 to 30 %. This range of error is normally encountered in any experiment involving the flow of a gas phase, because gases do not flow at a constant rate. Consequently, it is very difficult to have a constant gas flow rate.

Figures 6.58, 6.60, 6.62, 6.64 and 6.66 present the reproducibilities of the recoveries of Runs CWF1, CW2, VLC3, VLC7 and H2D43b, respectively. Unlike those of the GOR's, the reproducibilities of the oil recoveries were good, the errors being in the range of 5 to 10%.

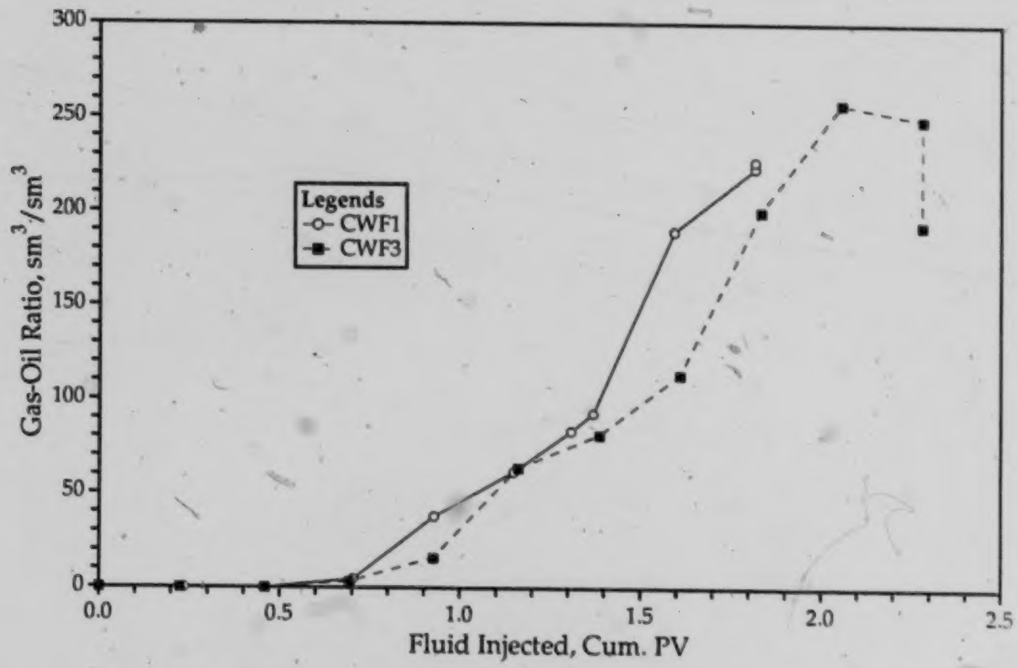

Figure 6.57 - GOR Repeatability of Run CWF1.

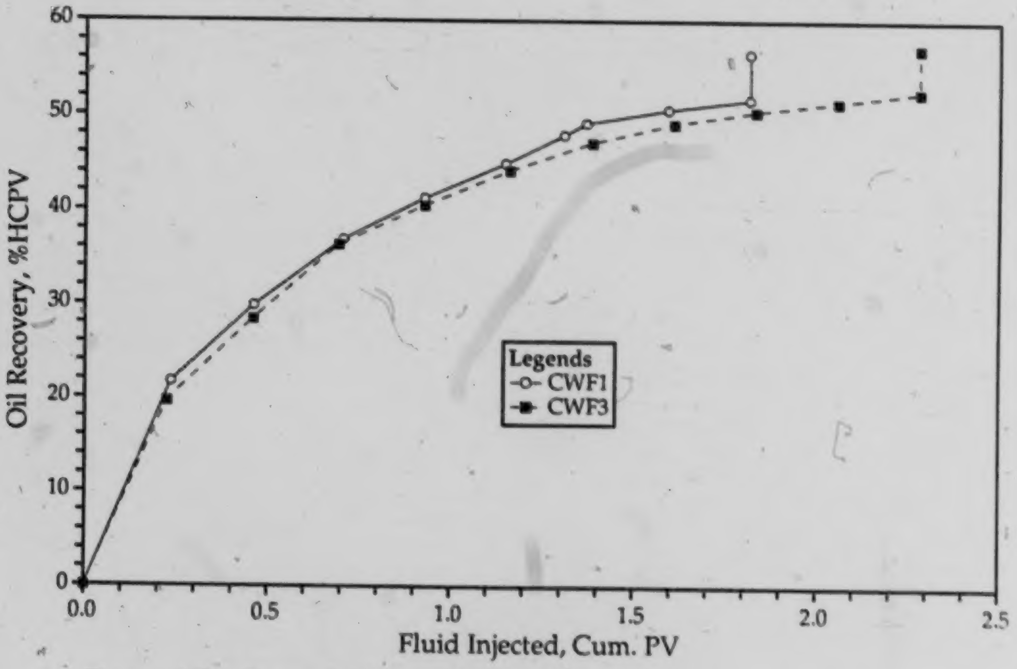

Figure 6.58 - Recovery Repeatability of Run CWF1.

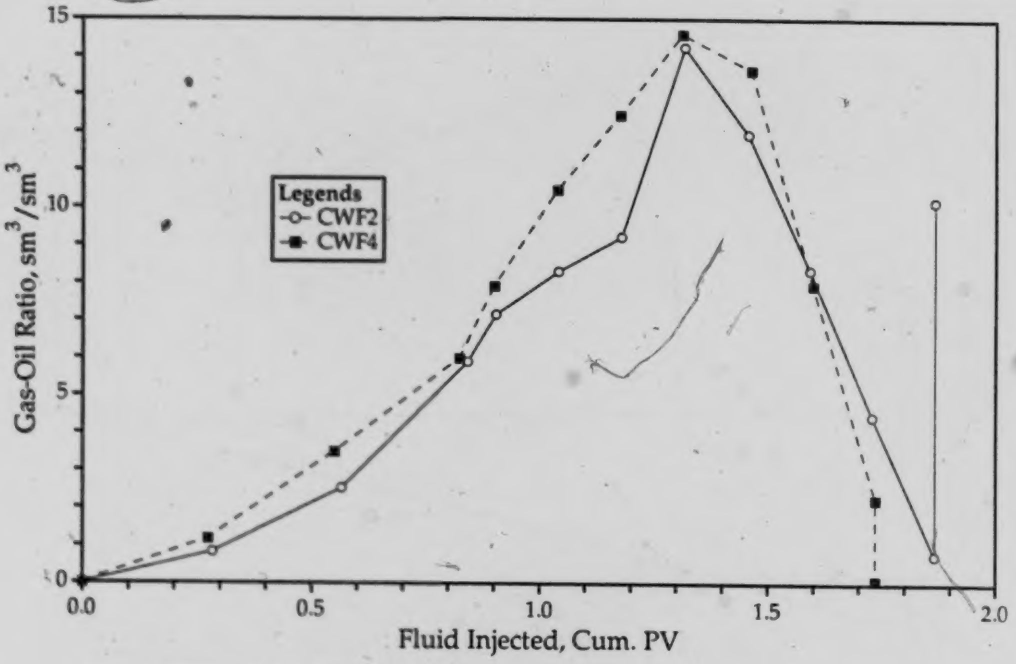

Figure 6.59 - GOR Repeatability of Run CWF2.

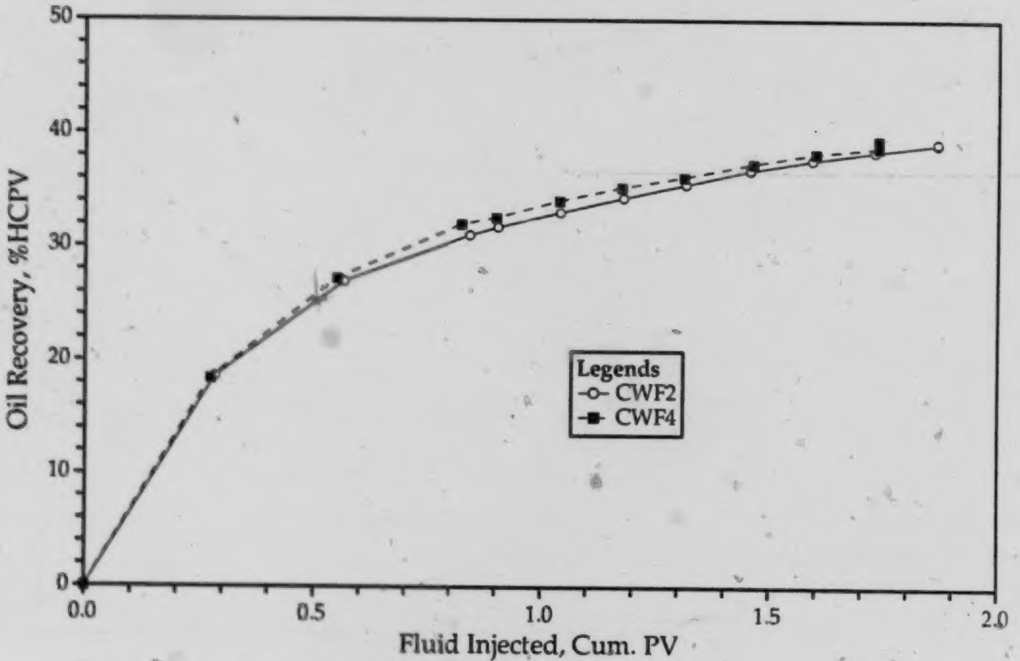

Figure 6.60 - Recovery Repeatability of Run CWF2.

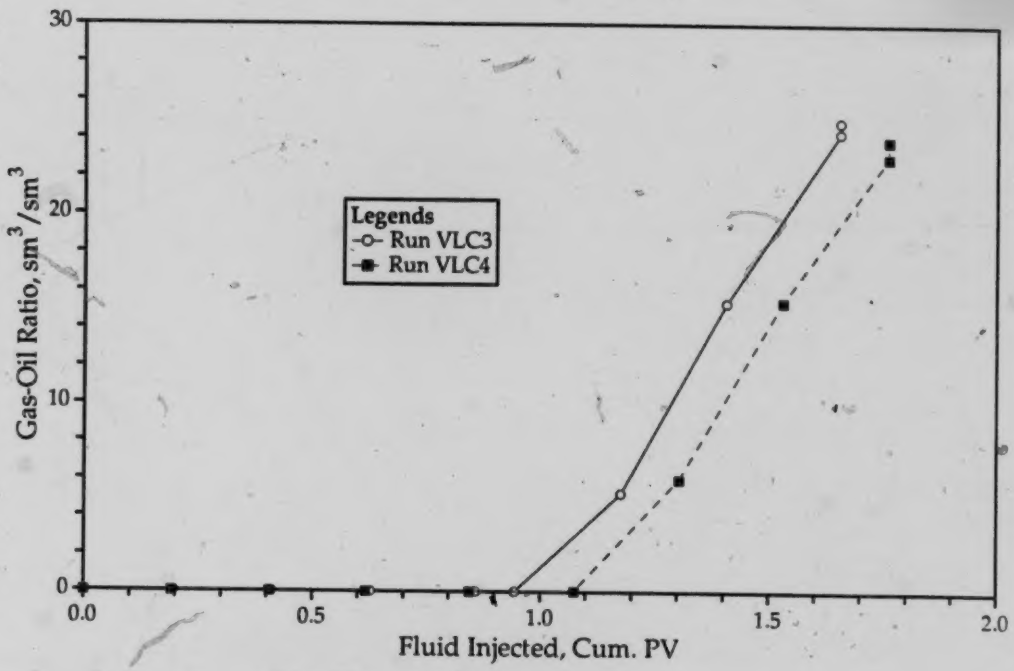

Figure 6.61 - GOR Repeatability of Run VLC3.

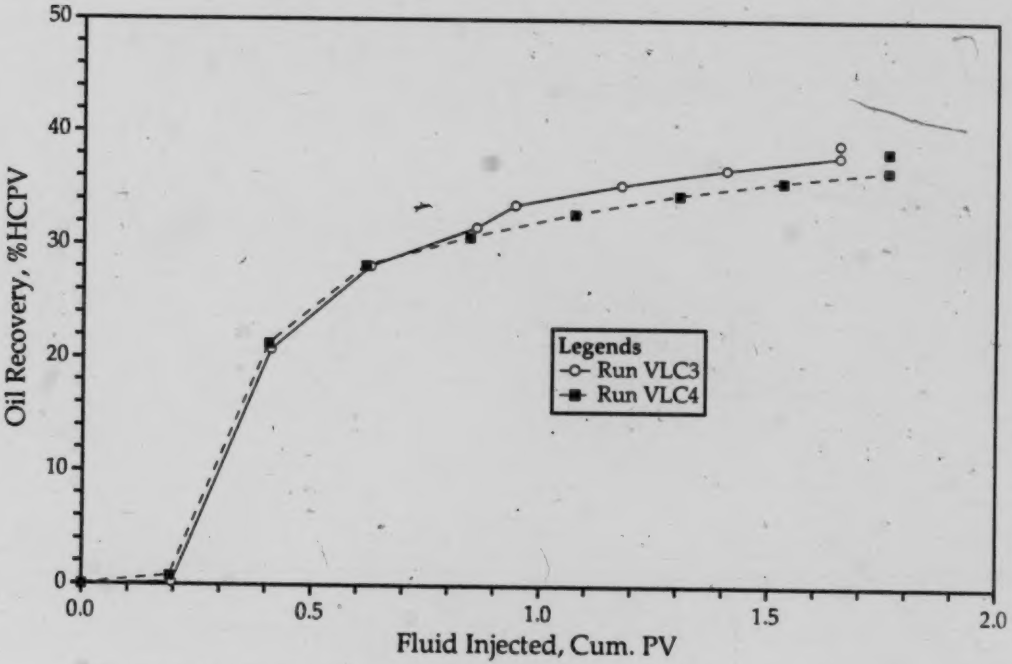

Figure 6.62 - Recovery Repeatability of Run VLC3.

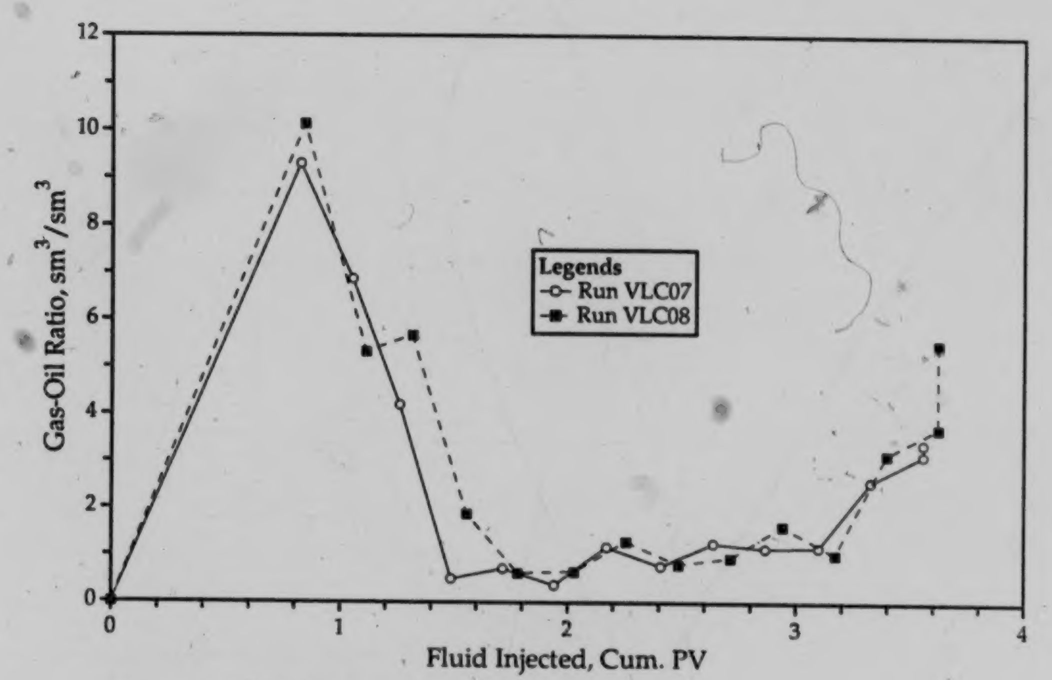

Figure 6.63 - GOR Repeatability of Run VLC7.

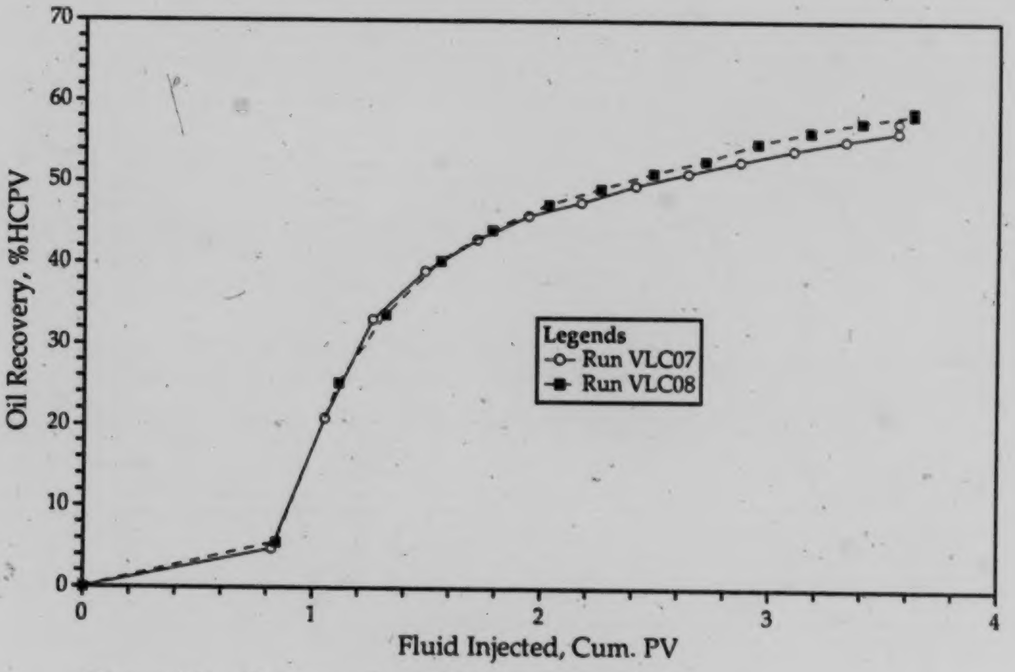

Figure 6.64 - Recovery Repeatability of Run VLC7.

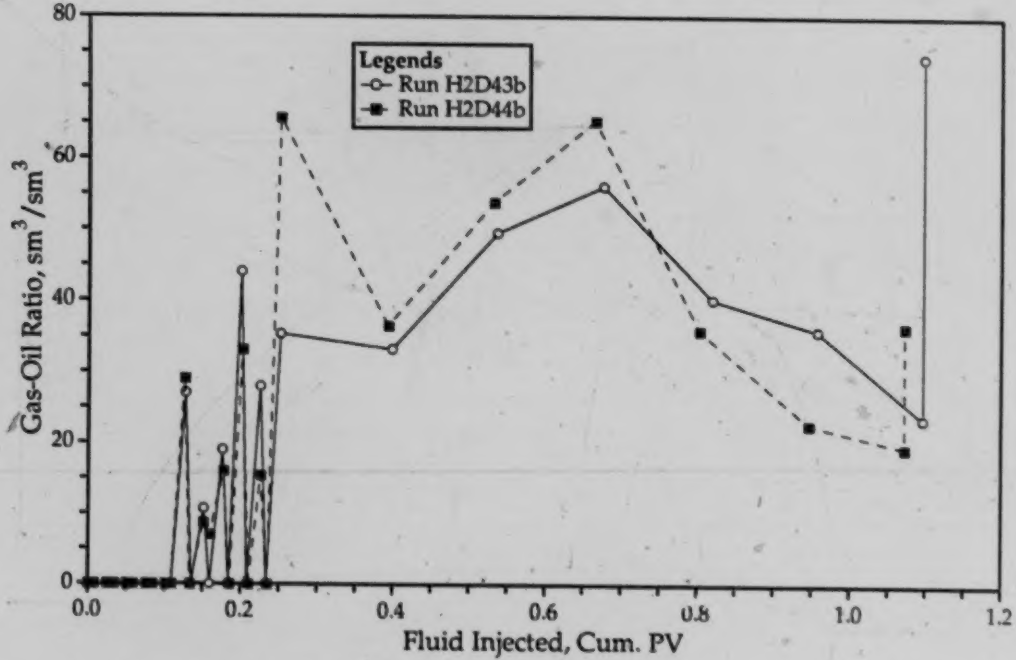

Figure 6.65 - GOR Repeatability of Run H2D43b.

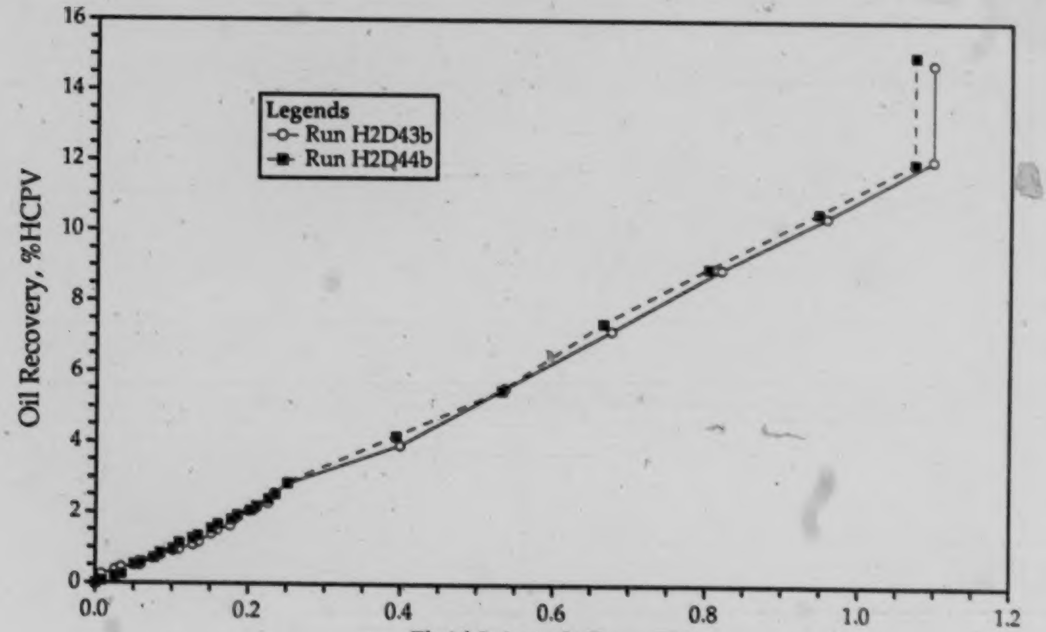

Figure 6.66 - Recovery Repeatability of Run H2D43b.

7 - SUMMARY and CONCLUSIONS

This investigation was devoted to several aspects of the immiscible (subcritical) carbon dioxide WAG process for the recovery of moderately viscous oils. In this study, experimental data reported by Rojas[1], Zhu[4], Dyer[5], Wilson[7], and in this work were correlated with the dimensionless similarity groups derived in this work. A method supported by a mathematical model was developed to measure experimentally the diffusivity of a gas into a liquid. Seventy-six experiments were conducted to measure the diffusivities of carbon dioxide and methane in various oils. An empirical correlation for predicting the diffusivity of carbon dioxide in oil was developed using the data obtained. Vertical and horizontal displacement experiments were conducted in two scaled models to examine gravity segregation of the injected fluids. Horizontal displacement data were correlated with the dimensionless group describing the ratio of viscous-to-gravitational forces. In addition, a non-isothermal and non-equilibrium mathematical model including phase change and interfacial mass transfer was developed. Two sets of similarity groups for the non-isothermal immiscible carbon dioxide WAG displacement process were derived. Non-isothermal displacement experiments were also designed and performed.

Based upon the experimental observations, the following conclusions can be reached.

Carbon Dioxide Diffusion into Oils

1. Diffusivities of carbon dioxide and methane increase with increasing pressure, as long as both gases are in the gas phase (2.3648E-09 at 0.69 MPa vs. 6.1387E-09 at 6.89 MPa).

2. Increasing temperature and/or decreasing the oil viscosity increases the diffusivity of carbon dioxide into oil (6.1387E-09 at 57.1°C vs. 7.5272E-09 at 65.4°C).

3. The diffusivity of carbon dioxide is affected by the molecular weight of the oil. It decreases as the oil molecular weight increases (2.5452E-08 in a 516.73 g/mol oil vs. 4.9337E-10 in a 737.59 g/mol oil).

4. Carbon dioxide, having a smaller molecular size than methane, can diffuse faster in oils than methane (6.1387E-09 for carbon dioxide vs. 8.4217E-11 for methane).

Correlation of Experimental Data

1. Dimensionless groups were derived for a comprehensive mathematical model of the immiscible carbon dioxide flooding process.

2. The groups can be used to correlate the previous and present experimental data.

Gravity Segregation of Carbon Dioxide

1. Based on the results of the vertical displacement experiments conducted, it can be concluded that gravity plays an important role in the immiscible carbon dioxide WAG displacement process. It causes the injected carbon dioxide to rise to the top, which results in the formation of a gas zone which is believed to both finger through and push the oil down towards the bottom, which would then be displaced by the injected water. Gravity segregation of the injected water slugs encourages the rise of carbon dioxide to the top and pushes the oil upwards, which will then re-saturate the zone already swept by carbon dioxide. This volume of oil will never be recovered, consequently causing the loss of oil recovery.

2. In horizontal floods, transverse diffusion of carbon dioxide in the horizontal direction normal to the horizontal longitudinal direction can help delay the gravity rise of the gas.

Non-Isothermal Experiments

1. Experiments at an elevated temperature showed distinct effects on the mechanism of the process, mainly due to evaporation of water and mixing of water vapour with carbon dioxide, thereby reducing its solubility in oil.

2. Experimental results show that if two oils have the same viscosity and gas solubility at two different temperatures, the overall performance of the immiscible carbon dioxide WAG process will be very similar in the two

cases, thereby indicating that the experimental results can be extended to other temperatures.

8 - RECOMMENDATIONS for FUTURE RESEARCH

The following studies are recommended to extend the scope of this research.

1. The effect of a bottom water layer on the performance of the immiscible carbon dioxide process should be examined. This can be done by creating a water layer underneath the oil zone. This study should be carried out because the field reservoir is underlain by a water layer and the experimental results will more accurately predict the true field performance of the process.

2. The improvement in the relative permeability to oil afforded by carbon dioxide at immiscible conditions should be studied.

3. A study should also be conducted to investigate the effect of gas trapping which occurs due to gravity segregation.

REFERENCES

1. Rojas, G.: "Scaled Model Studies of Immiscible Carbon Dioxide Displacement of Heavy Oil," Ph.D. Thesis, University of Alberta, Edmonton, Alberta (1985).

2. Rojas, G. and Farouq Ali, S.M.: "Scaled Model Studies of Carbon Dioxide/Brine Injection Strategies for Heavy Oil Recovery from Thin Formations," JCPT (Jan. - Feb. 1986) 85-94.

3. Rojas, G.A., Zhu, T., Dyer, S.B., Thomas, S., and Farouq Ali, S.M.: "Scaled Model Studies of CO_2 Floods," SPE Res. Eng. (May 1991) 169-178.

4. Zhu, T.: "Displacement of a Heavy Oil By Carbon Dioxide and Nitrogen in a Scaled Model," M.Sc. Thesis, University of Alberta, Edmonton, Alberta (1986).

5. Dyer, S.: "Performance of the Immiscible Carbon Dioxide WAG Process at Low Pressure," M.Sc. Thesis, University of Alberta, Edmonton, Alberta (1989).

6. Dyer, S.B. and Farouq Ali, S.M.: "Linear Model Studies of the Immiscible Carbon Dioxide WAG Process for the Recovery of Heavy Oils," Paper SPE 21162 presented at the SPE Latin America Petroleum Engineering Conference, Rio de Janeiro (Oct. 14-19, 1990).

7. Prosper, G.W.: "Study of the Immiscible Carbon Dioxide Process at Low Pressures," M.Sc. Thesis, University of Alberta, Edmonton, Alberta (1992).

8. Prosper, G.W. and Farouq Ali, S.M.: "Scaled Model Studies of the Immiscible Carbon Dioxide Flooding Process at Low Pressures," Paper CIM/AOSTRA 91-2 presented at the CIM/AOSTRA 1991 Technical Conference, Banff, Alberta (April 21-24, 1991).

9. Brock, W.R., and Bryan, L.A.: "Summary Results of CO_2 EOR Field Test, 1972-1987," Paper SPE 18977 presented at the SPE Joint Rocky Mountain Regional/Low Permeability Reservoirs Symposium and Exhibition, Denver (March 6-8, 1989), 499-507.

10. Moritis, G.: "CO_2 and HC Injection Lead EOR Production Increase," Oil and Gas Journal (April 23, 1990) 49-82.

11. Anonymous: "Immiscible Carbon Dioxide Flood Proving Effective: Ulster Retlaw Project Goes Commercial," The TAR Paper, published by AOSTRA (June 1991) **14**, No. 2.

12. Martin, J.W.: "The Use of Carbon Dioxide Increasing the Recovery of Oil," Producers Monthly (May, 1951) 13-15.

13. Martin, J.W.: "Additional Oil Production Through Flooding With Carbonated Water," Producers Monthly (July, 1951) 18-22.

14. Martin, J.W.: "Additional Oil Production Through Flooding With Carbonated Water," Oil and Gas Journal (August 30, 1951) 70-71, 86-87.

15. Beeson, D.M. and Ortloff, G.D.: "Laboratory Investigation of the Water-Driven Carbon Dioxide Process for Oil Recovery," JPT (April 1959) 63-66.

16. Dickerson, L.R. and Crawford, G.W.: "Laboratory Tests Show That CO_2 Scores Highest in Reducing Oil Viscosity," Oil and Gas Journal (Feb. 1960) 96-98.

17. Welker, J.R. and Dunlop, D.D.: "Physical Properties of Carbonated Oils," JPT (August 1963) 873-876.

18. Holm, L.W.: "A Comparison of Propane and CO_2 Solvent Flooding Processes," AIChE Journal (August 30, 1951) 70-71, 86-87.

19. Holm, L.W.: "Carbon Dioxide Solvent Flooding for Increased Oil Recovery," Trans., AIME (1959) **216**, 225-231.

20. Holm, L.W.: "CO_2 Requirements in CO_2 Slug and Carbonated Water Oil Recovery Processes," Producers Monthly (Sept. 1963) 6-8, 26-28.

21. de Nevers, N.H.: "A Calculation Method for Carbonated Water Flooding," SPEJ (Mar. 1964) 9-20.

22. Simon, R. and Graue, D.J.: "Generalized Correlations for Predicting Solubility, Swelling and Viscosity Behaviour of CO_2-Crude Oil System," JPT (Jan. 1965) 102-106.

23. Holm, L.W. and Josendal, V.A.: "Mechanisms of Oil Displacement by Carbon Dioxide," JPT (Dec. 1974) 1427-1438.

24. Rojas, G. and Farouq Ali, S.M.: "Dynamics of Subcritical CO_2/Brine Floods for Heavy Oil Recovery," SPERE (Feb. 1988) 35-44.

25. Grogan, A.T. and Pinczewski, V.W.: "The Role of Molecular Diffusion Processes in Tertiary CO_2 Flooding," JPT (May 1987) 591-601.

26. Perkins, T.K. and Johnston, O.C.: "A Review of Diffusion and Dispersion in Porous Media," SPEJ (March 1963) 70-84.

27. Spivak, A., Karaoguz, D. and Issever, K.: "Simulation of Immiscible CO_2 Injection in a Fractured Carbonate Reservoir, Bati Raman Field, Turkey," Paper SPE 18765 presented at the SPE California Regional Meeting, Bakersfield, CA (April 5-7, 1989) 179-192.

28. Pomeroy, R.D., Lacey, W.N., Scudder, N.F. and Stapp, F.P.: "Rate of Solution of Methane in Quiescent Liquid Hydrocarbons," Ind. Eng. Chem (Sept. 1933) **25**, No. 9, 1014-1019.

29. Hill, E.S. and Lacey, W.N.: "Rate of Solution of Methane in Quiescent Liquid Hydrocarbons. II," Ind. Eng. Chem (Dec. 1934) **26**, No. 12, 1324-1327.

30. Hill, E.S. and Lacey, W.N.: "Rate of Solution of Propane in Quiescent Liquid Hydrocarbons," Ind. Eng. Chem (Dec. 1934) **26**, No. 12, 1327-1331.

31. Bertram, E.A. and Lacey, W.N.: "Rate of Solution of Methane in Oils Filling Spaces between Sand Grains," Ind. Eng. Chem (Dec. 1934) **28**, No. 3, 316-318.

32. Reamer, H.H., Opfell, J.B. and Sage, B.H.: "Diffusion Coefficients in Hydrocarbon Systems: Methane-White Oil-Methane in Liquid Phase," Ind. Eng. Chem (Feb. 1956) **48**, No. 2, 275-284.

33. Reamer, H.H., Duffy, C.H. and Sage, B.H.: "Diffusion Coefficients in Hydrocarbon Systems: Methane-Decane-Methane in Liquid Phase," Ind. Eng. Chem (Feb. 1956) **48**, No. 2, 285-288.

34. Hayduk, W. and Buckley, W.D.: "Effect of Molecular Size and Shape on Diffusivity in Dilute Liquid Solutions," Chem. Eng. Sci. (1972) **27**, 1997-2003.

35. Sigmund, P.M.: "Prediction of Molecular Diffusion at Reservoir Conditions: Part II – Estimating the Effects of Molecular Diffusion and Convective Mixing in Multicomponent Systems," JCPT (July-Sept. 1976) 53-62.

36. Schmidt, T., Leshchyshyn, T. and Puttagunta, V.R.: "Diffusivity of Carbon Dioxide in Athabasca Bitumen," Paper CIM 82-33-100 presented at the 33rd Annual Meeting of the Petroleum Section of CIM, Calgary, Alberta (June 6-9, 1982).

37. Denoyelle, L. and Bardon, C.: "Diffusivity of Carbon Dioxide into Reservoir Fluids," Paper No. 115 presented at the 86th Annual Meeting of the Canadian Institute of Mining and Metallurgy, Ottawa (April 1984).

38. de Boer, R.B., Wellington, S.L. and Tschiedel, K.L.: "Measurements on CO_2-Diffusion Through Unusually Resistive Layers on Oil-Water Interfaces," Colloids and Surfaces (1984) **9**, 79-83.

39. Renner, T.A.: "Measurement and Correlation of Diffusion Coefficients for CO_2 and Rich Gas Applications," SPERE (May 1988) **3**, No. 2, 517-523.

40. Grogan, A.T., Pinczewski, V.W., Ruskauff, G.J. and Orr Jr., F.M.: "Diffusion of CO_2 at Reservoir Conditions: Models and Measurements," SPERE (Feb. 1988) 93-102.

41. McManamey, W.J. and Wollen, J.M.: "The Diffusivity of Carbon Dioxide in Some Organic Liquids at 25°C and 50°C," AIChE Journal (May 1973) 667-669.

42. Schmidt, T.: "Viscosity Dependence of Diffusion Coefficient of Carbon Dioxide in Bitumen," Paper No. 19 presented at the Fourth UNITAR/UNDP International Conference on Heavy Crude and Tar Sands, Edmonton, Alberta (Aug. 7-12, 1988) 721-726.

43. Mehrotra, A.K., Garg, A. and Svrcek, W.Y.: "Prediction of Mass Diffusivity of CO_2 into Bitumen," Canadian Journal of Chemical Engineering (Oct. 1987) **65**, 826-832.

44. Teja, A.S.: "Correlation and Prediction of Diffusion Coefficients by Use of a Generalized Corresponding States Principle," Ind. Eng. Chem. Fundam. (1985) **24**, No.1, 39-44.

45. Saxon Jr., J., Breston, J.N. and Macfarlane, R.M.: "Laboratory Tests with Carbon Dioxide and Carbonated Water as Flooding Medium," Producers Monthly (Nov. 1951) 8-14.

46. de Nevers, N.H.: "Carbonated Waterflooding," World Oil (Sept. 1966) 93-96.

47. Anonymous: "How Carbonated Waterfloods Stack up with Conventional type Waterfloods," Oil and Gas Journal (July 1962) 106-107.

48. Scott, J.O.: "Performance of Domes Unit Carbonated Waterflood – First Stage," AIChE Journal (May 1973) 667-669.

49. Blackford, T.A.: "Carbonated Waterflood Implementation and Its Impact on Material Performance in a Pilot Project," Paper SPE 16831 presented at the 62nd Annual Technical Conference and Exhibition, Dallas, TX (Sept. 27-30, 1987) 55-60.

50. Perez, J.M., Poston, S.W. and Sharif, Q.J.: "Carbonated Water Imbition Flooding: An Enhanced Oil Recovery Process for Fractured Reservoirs," Paper SPE/DOE 24164 presented at the SPE/DOE Eighth Symposium on Enhanced Oil Recovery, Tulsa, OK (April 22-24, 1992) 79-90.

51. Morrow, N.R. and Hornof, V.: "Gravity Effects in the Displacement of Oil by Surfactant Solutions," Paper SPE 13573 presented at the International Symposium on Oilfield and Geothermal Chemistry, Phoenix, Arizona (April 9-11, 1985) 255-264.

52. Craig, F.F., Sanderlin, J.L., Moore, D.W. and Geffen, T.M.: "A Laboratory Study of Gravity Segregation in Frontal Drives," Trans., AIME (1957) **210**, 275-282.

53. Richardson, J.G. and Perkins Jr., F.M.: "A Laboratory Investigation of the effect of Rate on Recovery of Oil by Waterflooding," Trans., AIME (1957) **210**, 114-121.

54. Miller, M.C.: "Gravity Effects in Miscible Displacement," Paper SPE 1531 presented at the 41st Annual Fall Meeting, Dallas, TX (Oct. 2-5, 1966) 12p.

55. Blackwell, R.J., Terry, W.M., Rayne, J.R., Lindley, D.C. and Henderson, J.R.: "Recovery of Oil by Displacement With Water-Solvent Mixtures," Trans., AIME (1960) **219**, 293-300.

56. Warner, H.R.: "An Evaluation of Miscible CO_2 Flooding in Waterflooded Sandstone Reservoirs," JPT (Oct. 1977) 1339-1347.

57. Fayers, F.J. and Newley, T.M.J.: "Detailed Validation of an Empirical Model for Viscous Fingering With Gravity Effects," Paper SPE 15993 presented at the 9th SPE Symposium on Reservoir Simulation, San Antonio, TX (Feb. 1-4, 1987) 7-19.

58. Stalkup, F.I., Jr.: Miscible Displacement, Monograph 8, SPE of AIME, New York (1983).

59. Van Der Poel, C.: "Effect of Lateral Diffusivity on Miscible Displacement in Horizontal Reservoirs," SPEJ (Dec. 1962) 317-326.

60. Spivak, A.: "Gravity Segregation in Two-Phase Displacement Process," SPEJ (Dec. 1974) 619-632.

61. Araktingi, U.G. and Orr, F.M., Jr.: "Viscous Fingering, Gravity Segregation, and Reservoir Heterogeneity in Miscible Displacements in Vertical Cross Sections," Paper SPE/DOE 20176 presented at the SPE/DOE 7th Symposium on Enhanced Oil Recovery, Tulsa, OK (April 22-25, 1990) 39-46.

62. Thomas, J., Berzins, T.V., Monger, T.G. and Bassiouni, Z.: "Light Oil Recovery from Cyclic CO_2 Injection: Influence of Gravity Segregation and Remaining Oil," Paper SPE 20531 presented at the 65th Annual Technical Conference and Exhibition, New Orleans, LA (Sept. 23-26, 1990) 609-616.

63. Pande, K.K.: "Effects of Gravity and Viscous Crossflow on Hydrocarbon Miscible Flood Performance in Heterogeneous Reservoirs," Paper SPE 24935 presented at the 67th Annual Technical Conference and Exhibition, Washington, DC, (Oct. 4-7, 1992) 839-849.

64. Hill, S.: "Chanelling in Packed Columns," Chem. Eng. Sci. (1952) **1**, No. 6, 247-253.

65. Dumore, J.M.: "Stability Considerations in Downward Miscible Displacement," SPEJ (Dec. 1964) 356-362.

66. Slobod, R.L. and Howlett, W.E.: "The effects of Gravity Segregation in Laboratory Studies of Miscible Displacement in Vertical Unconsolidated Porous Media," SPEJ (March 1964) 1-8.

67. Tiffin, D.L. and Kremesec, V.J.: "A Mechanistic Study of Gravity-Assisted CO_2 Flooding," Paper SPE/DOE 14895 presented at the SPE/DOE 5th Symposium on Enhanced Oil Recovery, Tulsa, OK (April 20-23, 1986) 205-222.

68. Fong, W.S., Tang, R.W, Emanuel, A.S. and Sabat, P.J.: "EOR for California Diatomites: Flue Gas and Water Corefloods, and Computer Simulations," Paper SPE 24039 presented at the Western Regional Meeting, Bakersfield, CA (March 30-April 1, 1992) 159-170.

69. Martin, J.C.: "Some Mathematical Aspects of Two-Phase Flow With Applications to Flooding and Gravity Segregation Problems," Producers Monthly (April 1958), 22-35.

70. Walsh, M.P. and Moon, G.M.: "An Analysis of Gravity-Dominated, Immiscible Flows in Dipping Reservoirs," Paper SPE 21651 presented at the Production Symposium, Oklahoma City, OK (April 7-9, 1991) 197-207.

71. Hovanessian, S.A. and Fayers, F.J.: "Linear Waterflood With Gravity and Capillary Effects," SPEJ (March 1961) 32-36.

72. Belgrade, J.D.M. and Win, T.: "Vertical Sweep Efficiency and Oil Recovery From Gas Injection in Heterogeneous Horizontal Reservoirs," Paper SPE 26085 presented at the Western Regional Meeting, Anchorage, Alaska (May 26-28, 1993) 569-579.

73. Cook, R.E.: "Analysis of Gravity Segregation Performance During Natural Depletion," SPEJ (Sept. 1962) 261-274.

74. Craig, F.F.: The Reservoir Engineering Aspects of Waterflooding, Monograph 3, SPE of AIME, Dallas, TX (1963).

75. Willhite, G.P.: Waterflooding, Textbook Series, SPE of AIME, Richardson, TX (1986).

76. Erkrann, S.: "Gravity and Vertical Sweep Efficiency," In Situ (1993) **17**, No. 2, 183-199.

77. Stone, H.L.: "Vertical Conformance in an Alternating Water-Miscible Gas Flood," Paper SPE 11130 presented at the 57th Annual Fall Technical and Exhibition, New Orleans, LA (Sept. 26-29, 1992) 15p.

78. Wilcox, T.C., Polzin, M.W., Kuo, S.S., Saidikowski, R.M. and Humphrey, K.J.,: "Infill Drilling in Gravity-Dominated WAG Floods, Prudhoe Bay Field, Alaska," Paper SPE 26130 presented at the Western Regional Meeting, Anchorage, Alaska (May 26-28, 1993) 751-752.

79. Pritchard, D.W.L. and Nieman, R.E.: "Improving Oil Recovery Through WAG Cycle Optimization in a Gravity-Override-Dominated Miscible Flood," Paper SPE/DOE 24181 presented at the SPE/DOE Eighth Symposium on Enhanced Oil Recovery, Tulsa, OK (April 22-24, 1992) 263-278.

80. Kreuzer, H.J.: Non-equilibrium Thermodynamics and its Statistical Foundations, Clarendon Press, Oxford, 1981.

81. Goss, M.J. and Exall, D.I.: "Experimental Investigations of the Transport Mechanisms Controlling In Situ Recovery from Heavy Oil Sands," The Oil Sands of Canada-Venezuela, CIM Special Volume 17 (1977) 327-333.

82. Martin, J.M., Combarnous, M. and Charpentier, J.C.: "Mass transfer and Phase Distribution for Two-Phase Flow Through Porous Media," Chem. Eng. Commun. (1981) **10**, 269-281.

83. Bird, R.B., Stewart, W.E. and Lightfoot, E.N.: Transport Phenomena, Wiley & Sons, New York, 1960.

84. Ishii, M.: Thermo-Fluid Dynamic Theory of Two-Phase Flow, Eyrolles, Paris, 1975.

85. Kataoka, I. and Ishii, M.: "Local Formulation and Measurements of Interfacial Area Concentration in Two-Phase Flow," Int. J. Multiphase Floe (1986) **12**, No. 4, 505-529.

86. Farouq Ali, S.M., Chakma, A. and Islam, M.R.: "Mathematical Modelling of Non-Equilibrium Phenomena in Chemical Injections," Paper presented at the Fifth European Symposium on Improved Oil Recovery, Budapest, Hungary, (April 25-27, 1989) 419-428.

87. Bree, J.: "Non-Equilibrium Thermodynamics of Simple Mixtures," J. Non-Equilib. Thermodyn. (1980) **5**, 73-90.

88. Mathieu, P. and Lebon, G.: "A Non-Equilibrium Thermodynamic Model of Two-Phase Fluids with Mass Transfer," J. Non-Equilib. Thermodyn. (1982), **7**, 129-144.

89. Lozada, D. and Farouq Ali, S.M.: "New Sets of Scaling Criteria for Partial Equilibrium Immiscible Carbon Dioxide Drive," Paper CIM 87-38-23 presented at the 38th Annual Technical Meeting of the Petroleum Society of CIM, Calgary, Alberta, (June 7-10, 1987) 393-411.

90. Lozada, D. and Farouq Ali, S.M.: "Experimental Design for Non-Equilibrium Immiscible Carbon Dioxide Flood," Paper No. 159 presented at the

Fourth UNITAR/UNDP International Conference on Heavy Crude and Tar Sands, Edmonton, Alberta, (Aug. 7-12, 1988) 275-296.

91. Bear, J. and Buchlin, J.M.: Modelling and Applications of Transport Phenomena in Porous Media, Kluwer Academic Publishers, Boston, 1991.

92. Geertsma, J., Croes, G. and Schwarz, N.:"Theory of Dimensionally Scaled Models of Petroleum Reservoirs," Trans., AIME (1956) **207**, 118-127.

93. Leverett, M.C., Lewis, W.B. and True, M.E.:"Dimensional-Model Studies of Oil-Field Behavior,"Trans., AIME (1942) **146**, 175-193.

94. Rapoport, L.A. and Leas, W.J.:"Properties of Linear Water Floods,"Trans., AIME (1953) **198**, 139-148.

95. Croes, G.A. and Schwarz, N.:"Dimensionally Scaled Experiments and the Theories on the Water-Drive Process,"Trans., AIME (1955) **204**, 35-42.

96. Offeringa, J. and van der Poel, C.:"Displacement of Oil from Porous Media by Miscible Liquids," Trans., AIME (1954) **201**, 310-316.

97. Loomis, A.G. and Crowell, D.C.:"Theory and Applications of Dimensional and Inspectional Analysis to Model Study of Fluid Displacements in Petroleum Reservoirs," Bureau of Mines Report RI6546, 1964.

98. Langhaar, H.L.: Dimensional Analysis and Theory of Models, John Wiley & Sons, New York (1951).

99. Muskat, M.: Physical Principles of Oil Production, McGraw-Hill Book Company Inc., New York (1949).

100. Starling, K.E.: Fluid Thermodynamic Properties for Light Petroleum System, Gulf Publishing Company, Houston, TX (1973).

101. Crank, J.: The Mathematics of Diffusion, 2nd Edition, Clarendon Press, Oxford (1975).

102. Reid, R.C., Prausnitz, J.M. and Polling, B.E., The Properties of Gases and Liquids, 4th Edition, McGraw-Hill Book Co. Inc. (1987).

103. Ross, M. and Hildebrand, J.H.:"Diffusion of Hydrogen, Deuterium, Nitrogen, Argon, Methane, and Carbon Tetraflouride in Carbon Tetrachloride," Journal of Chemical Physics (1964) 40, 2397.

104. Nakanishi, K., Voigt, E.M. and Hildebrand, J.H.:"Quantum Effect in the Diffusion of Gases in Liquids at 25°C," Journal of Chemical Physics (1965) 42, 1860.

105. Wilke, C.R. and Chang, P.:"Correlation of Diffusion Coefficients in Dilute Solutions," AIChE Journal (June 1955) 264-270.

106. Chung, T.H. Frank, Jones, A. Ray and Nguyen, T. Hai.:"Measurements and Correlations of the Physical Properties of CO_2/Heavy-Crude-Oil Mixtures," SPERE (August 1988) 822-828.

APPENDIX A

INITIAL AND BOUNDARY CONDITIONS

A.1 - Initial and Boundary Conditions

No fluid flow across top and bottom of reservoir

$$\rho_o \overline{\vartheta}_{on} = -\frac{\rho_o}{\mu_o}\bar{\bar{k}}_o\left(\nabla_n p_o + \rho_o g \nabla_n Z\right) = 0$$

$$\rho_g \overline{\vartheta}_{gn} = -\frac{\rho_g}{\mu_g}\bar{\bar{k}}_g\left(\nabla_n p_g + \rho_g g \nabla_n Z\right) = 0$$

$$\rho_w \overline{\vartheta}_{wn} = -\frac{\rho_w}{\mu_w}\bar{\bar{k}}_w\left(\nabla_n p_w + \rho_w g \nabla_n Z\right) = 0$$

A.2 - Injection Well

$$\int_{A_{inj}} \rho_g \frac{\bar{\bar{k}}_g}{\mu_g}\left(\nabla p_g + \rho_g g \nabla Z\right) dA = \mathcal{W}_{CO_2}$$

$$\int_{A_{inj}} \rho_g \left[\frac{\bar{\bar{k}}_g}{\mu_g}\left(\nabla p_g + \rho_g g \nabla Z\right)\right]^2 dA = \mathcal{M}_{CO_2}$$

$$\int_{A_{inj}} \rho_w \frac{\bar{\bar{k}}_w}{\mu_w}\left(\nabla p_w + \rho_w g \nabla Z\right) dA = \mathcal{W}_w$$

$$\int_{A_{inj}} \rho_w \left[\frac{\bar{\bar{k}}_w}{\mu_w}\left(\nabla p_w + \rho_w g \nabla Z\right)\right]^2 dA = \mathcal{M}_w$$

$$\int_{A_{inj}} \rho_g \left\{\frac{1}{2}\left[\frac{\bar{\bar{k}}_g}{\mu_g}\left(\nabla p_g + \rho_g\right)\right]^2 \left[\frac{\bar{\bar{k}}_g}{\mu_g}\left(\nabla p_g + \rho_g\right)\right] + h_g \frac{\bar{\bar{k}}_g}{\mu_g}\left(\nabla p_g + \rho_g\right)\right\} dA$$

$$+ \int_{A_{inj}} \rho_o h_o \frac{\bar{\bar{k}}_o}{\mu_o}\left(\nabla p_o + \rho_o\right) dA + \int_{A_{inj}} \left(k_{hr} \nabla_n T\right) dA = \mathcal{E}_{CO_2}$$

$$\int_{A_{inj}} \rho_w \left\{\frac{1}{2}\left[\frac{\bar{\bar{k}}_w}{\mu_w}\left(\nabla p_w + \rho_w\right)\right]^2 \left[\frac{\bar{\bar{k}}_w}{\mu_w}\left(\nabla p_w + \rho_w\right)\right] + h_w \frac{\bar{\bar{k}}_w}{\mu_w}\left(\nabla p_w + \rho_w\right)\right\} dA$$

$$+ \int_{A_{inj}} \rho_o h_o \frac{\bar{\bar{k}}_o}{\mu_o}\left(\nabla p_o + \rho_o\right) dA + \int_{A_{inj}} \left(k_{hr} \nabla_n T\right) dA = \mathcal{E}_w$$

$$\int_{A_{inj}} \rho_g \left\{ \left[\frac{\bar{\bar{k}}_g}{\mu_g} \left(\nabla p_g + \rho_g g \nabla Z \right) \right] s_g + \frac{h_g}{T} \frac{\bar{\bar{k}}_g}{\mu_g} \left(\nabla p_g + \rho_g g \nabla Z \right) \right\} dA$$

$$+ \int_{A_{inj}} \rho_o \frac{h_o}{T} \frac{\bar{\bar{k}}_o}{\mu_o} (\nabla p_o + \rho_o g \nabla Z) dA + \int_{A_{inj}} \frac{k_{hr} \nabla_n T}{T} dA = 8_{CO_2}$$

$$\int_{A_{inj}} \rho_w \left\{ \left[\frac{\bar{\bar{k}}_w}{\mu_w} (\nabla p_w + \rho_w g \nabla Z) \right] s_w + \frac{h_w}{T} \frac{\bar{\bar{k}}_w}{\mu_w} (\nabla p_w + \rho_w g \nabla Z) \right\} dA$$

$$+ \int_{A_{inj}} \rho_o \frac{h_o}{T} \frac{\bar{\bar{k}}_o}{\mu_o} (\nabla p_o + \rho_o g \nabla Z) dA + \int_{A_{inj}} \frac{k_{hr} \nabla_n T}{T} dA = 8_w$$

A3 - Production Well

$p_o = p_{prod}$
$p_g = p_{prod} + P_{cgo}$
$p_w = p_{prod} + P_{cow}$

Initial Conditions

$p_o(0,x,y,z) = p_{oi}(0,x,y,z)$
$S_o(0,x,y,z) = S_{oi}(0,x,y,z)$
$S_w(0,x,y,z) = S_{wi}(0,x,y,z)$
$T(0,x,y,z) = T_i(0,x,y,z)$

APPENDIX B

DIFFERENTIAL EQUATIONS IN DIMENSIONLESS FORM

B.1 - Momentum Balance for CO_2 in the Oil Phase in Dimensionless Form

$$
\begin{aligned}
&-\left\{C_{CO_2,oR}\rho_{oR}\frac{k_{oR}^2}{\mu_{oR}^2}\frac{p_{oR}^2}{x_R^3}\right\}\frac{\partial}{\partial x_D}\left[C_{CO_2,oD}\rho_{oD}\frac{k_{oD}^2}{\mu_{oD}^2}\left(\frac{\partial p_{oD}}{\partial x_D}\right)^2\right]\\
&-\left\{2C_{CO_2,oR}\rho_{oR}^2 g_{xR}\frac{k_{oR}^2}{\mu_{oR}^2}\frac{p_{oR}}{x_R^3}Z_R\right\}\frac{\partial}{\partial x_D}\left[C_{CO_2,oD}\rho_{oD}^2 g_{xD}\frac{k_{oD}^2}{\mu_{oD}^2}\frac{\partial p_{oD}}{\partial x_D}\frac{\partial Z_D}{\partial x_D}\right]\\
&-\left\{C_{CO_2,oR}\rho_{oR}^3 g_{xR}^2\frac{k_{oR}^2}{\mu_{oR}^2}\frac{Z_R^2}{x_R^3}\right\}\frac{\partial}{\partial x_D}\left[C_{CO_2,oD}\rho_{oD}^3 g_{xD}^2\frac{k_{oD}^2}{\mu_{oD}^2}\left(\frac{\partial Z_D}{\partial x_D}\right)^2\right]\\
&-\left\{C_{CO_2,oR}\rho_{oR}\frac{k_{oR}^2}{\mu_{oR}^2}\frac{p_{oR}^2}{x_R^2 y_R}\right\}\frac{\partial}{\partial x_D}\left[C_{CO_2,oD}\rho_{oD}\frac{k_{oD}^2}{\mu_{oD}^2}\frac{\partial p_{oD}}{\partial x_D}\frac{\partial p_{oD}}{\partial y_D}\right]\\
&-\left\{C_{CO_2,oR}\rho_{oR}^2 g_{yR}\frac{k_{oR}^2}{\mu_{oR}^2}\frac{p_{oR}Z_R}{x_R^2 y_R}\right\}\frac{\partial}{\partial x_D}\left[C_{CO_2,oD}\rho_{oD}^2 g_{yD}\frac{k_{oD}^2}{\mu_{oD}^2}\frac{\partial p_{oD}}{\partial x_D}\frac{\partial Z_D}{\partial y_D}\right]\\
&-\left\{C_{CO_2,oR}\rho_{oR}^2 g_{xR}\frac{k_{oR}^2}{\mu_{oR}^2}\frac{p_{oR}Z_R}{x_R^2 y_R}\right\}\frac{\partial}{\partial x_D}\left[C_{CO_2,oD}\rho_{oD}^2 g_{xD}\frac{k_{oD}^2}{\mu_{oD}^2}\frac{\partial p_{oD}}{\partial y_D}\frac{\partial Z_D}{\partial x_D}\right]\\
&-\left\{C_{CO_2,oR}\rho_{oR}^3 g_{xR}g_{yR}\frac{k_{oR}^2}{\mu_{oR}^2}\frac{Z_R}{x_R^2 y_R}\right\}\frac{\partial}{\partial x_D}\left[C_{CO_2,oD}\rho_{oD}^3 g_{xD}g_{yD}\frac{k_{oD}^2}{\mu_{oD}^2}\frac{\partial Z_D}{\partial y_D}\frac{\partial Z_D}{\partial x_D}\right]\\
&-\left\{C_{CO_2,oR}\rho_{oR}\frac{k_{oR}^2}{\mu_{oR}^2}\frac{p_{oR}^2}{x_R^2 z_R}\right\}\frac{\partial}{\partial x_D}\left[C_{CO_2,oD}\rho_{oD}\frac{k_{oD}^2}{\mu_{oD}^2}\frac{\partial p_{oD}}{\partial x_D}\frac{\partial p_{oD}}{\partial z_D}\right]\\
&-\left\{C_{CO_2,oR}\rho_{oR}^2 g_{zR}\frac{k_{oR}^2}{\mu_{oR}^2}\frac{p_{oR}Z_R}{x_R^2 z_R}\right\}\frac{\partial}{\partial x_D}\left[C_{CO_2,oD}\rho_{oD}^2 g_{zD}\frac{k_{oD}^2}{\mu_{oD}^2}\frac{\partial p_{oD}}{\partial x_D}\frac{\partial Z_D}{\partial z_D}\right]\\
&-\left\{C_{CO_2,oR}\rho_{oR}^2 g_{xR}\frac{k_{oR}^2}{\mu_{oR}^2}\frac{p_{oR}Z_R}{x_R^2 z_R}\right\}\frac{\partial}{\partial x_D}\left[C_{CO_2,oD}\rho_{oD}^2 g_{xD}\frac{k_{oD}^2}{\mu_{oD}^2}\frac{\partial p_{oD}}{\partial z_D}\frac{\partial Z_D}{\partial x_D}\right]\\
&-\left\{C_{CO_2,oR}\rho_{oR}^3 g_{xR}g_{zR}\frac{k_{oR}^2}{\mu_{oR}^2}\frac{Z_R^2}{z_R x_R^2}\right\}\frac{\partial}{\partial x_D}\left[C_{CO_2,oD}\rho_{oD}^3 g_{xD}g_{zD}\frac{k_{oD}^2}{\mu_{oD}^2}\frac{\partial Z_D}{\partial x_D}\frac{\partial Z_D}{\partial z_D}\right]\\
&+\left\{\phi_R S_{oR}\mathcal{D}_{LoR}C_{CO_2,oR}\rho_{oR}\frac{k_{oR}}{\mu_{oR}}\frac{p_{oR}}{x_R^3}\right\}\frac{\partial}{\partial x_D}\left[\phi_D S_{oD}\mathcal{D}_{LoD}\frac{\partial}{\partial x_D}\left(C_{CO_2,oD}\rho_{oD}\frac{k_{oD}}{\mu_{oD}}\frac{\partial p_{oD}}{\partial x_D}\right)\right]\\
&+\left\{\phi_R S_{oR}\dot{\mathcal{D}}_{LCO_2,oR}C_{CO_2,oR}\rho_{oR}\frac{k_{oR}}{\mu_{oR}}\frac{p_{oR}}{x_R^3}\right\}\bullet\\
&\qquad\frac{\partial}{\partial x_D}\left[\phi_D S_{oD}\dot{\mathcal{D}}_{LCO_2,oD}\frac{\partial}{\partial x_D}\left(C_{CO_2,oD}\rho_{oD}\frac{k_{oD}}{\mu_{oD}}\frac{\partial p_{oD}}{\partial x_D}\right)\right]
\end{aligned}
$$

$$
\begin{aligned}
&+\left\{\phi_R S_{oR}\mathcal{D}_{LoR}C_{CO_2,oR}\rho_{oR}^2 g_{xR}\frac{k_{oR}}{\mu_{oR}}\frac{Z_D}{x_R^3}\right\}\bullet \\
&\qquad\frac{\partial}{\partial x_D}\left[\phi_D S_{oD}\mathcal{D}_{LoD}\frac{\partial}{\partial x_D}\left(C_{CO_2,oD}\rho_{oD}^2 g_{xD}\frac{k_{oD}}{\mu_{oD}}\frac{\partial Z_D}{\partial x_D}\right)\right] \\
&+\left\{\phi_R S_{oR}\mathcal{D}^*_{LCO_2,oR}C_{CO_2,oR}\rho_{oR}^2 g_{xR}\frac{k_{oR}}{\mu_{oR}}\frac{Z_D}{x_R^3}\right\}\bullet \\
&\qquad\frac{\partial}{\partial x_D}\left[\phi_D S_{oD}\mathcal{D}^*_{LCO_2,oD}\frac{\partial}{\partial x_D}\left(C_{CO_2,oD}\rho_{oD}^2 g_{xD}\frac{k_{oD}}{\mu_{oD}}\frac{\partial Z_D}{\partial x_D}\right)\right] \\
&-\left\{C_{CO_2,oR}\rho_{oR}\frac{k_{oR}^2}{\mu_{oR}^2}\frac{p_{oR}^2}{y_R^2 x_R}\right\}\frac{\partial}{\partial y_D}\left[C_{CO_2,oD}\rho_{oD}\frac{k_{oD}^2}{\mu_{oD}^2}\frac{\partial p_{oD}}{\partial y_D}\frac{\partial p_{oD}}{\partial x_D}\right] \\
&-\left\{C_{CO_2,oR}\rho_{oR}^2 g_{xR}\frac{k_{oR}^2}{\mu_{oR}^2}\frac{p_{oR}Z_R}{y_R^2 x_R}\right\}\frac{\partial}{\partial y_D}\left[C_{CO_2,oD}\rho_{oD}^2 g_{xD}\frac{k_{oD}^2}{\mu_{oD}^2}\frac{\partial p_{oD}}{\partial y_D}\frac{\partial Z_D}{\partial x_D}\right] \\
&-\left\{C_{CO_2,oR}\rho_{oR}^2 g_{yR}\frac{k_{oR}^2}{\mu_{oR}^2}\frac{p_{oR}Z_R}{y_R^2 x_R}\right\}\frac{\partial}{\partial y_D}\left[C_{CO_2,oD}\rho_{oD}^2 g_{yD}\frac{k_{oD}^2}{\mu_{oD}^2}\frac{\partial p_{oD}}{\partial x_D}\frac{\partial Z_D}{\partial y_D}\right] \\
&-\left\{C_{CO_2,oR}\rho_{oR}^3 g_{xR}g_{yR}\frac{k_{oR}^2}{\mu_{oR}^2}\frac{Z_R}{y_R^2 x_R}\right\}\frac{\partial}{\partial y_D}\left[C_{CO_2,oD}\rho_{oD}^3 g_{xD}g_{yD}\frac{k_{oD}^2}{\mu_{oD}^2}\frac{\partial Z_D}{\partial y_D}\frac{\partial Z_D}{\partial x_D}\right] \\
&-\left\{C_{CO_2,oR}\rho_{oR}\frac{k_{oR}^2}{\mu_{oR}^2}\frac{p_{oR}^2}{y_R^3}\right\}\frac{\partial}{\partial y_D}\left[C_{CO_2,oD}\rho_{oD}\frac{k_{oD}^2}{\mu_{oD}^2}\left(\frac{\partial p_{oD}}{\partial y_D}\right)^2\right] \\
&-\left\{2C_{CO_2,oR}\rho_{oR}^2 g_{yR}\frac{k_{oR}^2}{\mu_{oR}^2}\frac{p_{oR}}{y_R^3}Z_R\right\}\frac{\partial}{\partial y_D}\left[C_{CO_2,oD}\rho_{oD}^2 g_{yD}\frac{k_{oD}^2}{\mu_{oD}^2}\frac{\partial p_{oD}}{\partial y_D}\frac{\partial Z_D}{\partial y_D}\right] \\
&-\left\{C_{CO_2,oR}\rho_{oR}^3 g_{yR}^2\frac{k_{oR}^2}{\mu_{oR}^2}\frac{Z_R^2}{y_R^3}\right\}\frac{\partial}{\partial y_D}\left[C_{CO_2,oD}\rho_{oD}^3 g_{yD}^2\frac{k_{oD}^2}{\mu_{oD}^2}\left(\frac{\partial Z_D}{\partial y_D}\right)^2\right] \\
&-\left\{C_{CO_2,oR}\rho_{oR}\frac{k_{oR}^2}{\mu_{oR}^2}\frac{p_{oR}^2}{y_R^2 z_R}\right\}\frac{\partial}{\partial y_D}\left[C_{CO_2,oD}\rho_{oD}\frac{k_{oD}^2}{\mu_{oD}^2}\frac{\partial p_{oD}}{\partial y_D}\frac{\partial p_{oD}}{\partial z_D}\right] \\
&-\left\{C_{CO_2,oR}\rho_{oR}^2 g_{zR}\frac{k_{oR}^2}{\mu_{oR}^2}\frac{p_{oR}Z_R}{y_R^2 z_R}\right\}\frac{\partial}{\partial y_D}\left[C_{CO_2,oD}\rho_{oD}^2 g_{zD}\frac{k_{oD}^2}{\mu_{oD}^2}\frac{\partial p_{oD}}{\partial y_D}\frac{\partial Z_D}{\partial z_D}\right] \\
&-\left\{C_{CO_2,oR}\rho_{oR}^2 g_{yR}\frac{k_{oR}^2}{\mu_{oR}^2}\frac{p_{oR}Z_R}{y_R^2 z_R}\right\}\frac{\partial}{\partial y_D}\left[C_{CO_2,oD}\rho_{oD}^2 g_{yD}\frac{k_{oD}^2}{\mu_{oD}^2}\frac{\partial p_{oD}}{\partial z_D}\frac{\partial Z_D}{\partial y_D}\right] \\
&-\left\{C_{CO_2,oR}\rho_{oR}^3 g_{yR}g_{zR}\frac{k_{oR}^2}{\mu_{oR}^2}\frac{Z_R^2}{z_R y_R^2}\right\}\frac{\partial}{\partial y_D}\left[C_{CO_2,oD}\rho_{oD}^3 g_{yD}g_{zD}\frac{k_{oD}^2}{\mu_{oD}^2}\frac{\partial Z_D}{\partial y_D}\frac{\partial Z_D}{\partial z_D}\right] \\
&+\left\{\phi_R S_{oR}\mathcal{D}_{ToR}C_{CO_2,oR}\rho_{oR}\frac{k_{oR}}{\mu_{oR}}\frac{p_{oR}}{y_R^3}\right\}\frac{\partial}{\partial y_D}\left[\phi_D S_{oD}\mathcal{D}_{ToD}\frac{\partial}{\partial y_D}\left(C_{CO_2,oD}\rho_{oD}\frac{k_{oD}}{\mu_{oD}}\frac{\partial p_{oD}}{\partial y_D}\right)\right]
\end{aligned}
$$

$$
\begin{aligned}
&+\left\{\phi_R S_{oR}\mathcal{D}^{*}_{TCO_2,oR}C_{CO_2,oR}\rho_{oR}\frac{k_{oR}}{\mu_{oR}}\frac{p_{oR}}{y_R^3}\right\}\bullet\\
&\qquad\frac{\partial}{\partial y_D}\left[\phi_D S_{oD}\mathcal{D}^{*}_{TCO_2,oD}\frac{\partial}{\partial y_D}\left(C_{CO_2,oD}\rho_{oD}\frac{k_{oD}}{\mu_{oD}}\frac{\partial p_{oD}}{\partial y_D}\right)\right]\\
&+\left\{\phi_R S_{oR}\mathcal{D}_{ToR}C_{CO_2,oR}\rho_{oR}^2 g_{yR}\frac{k_{oR}}{\mu_{oR}}\frac{Z_D}{y_R^3}\right\}\bullet\\
&\qquad\frac{\partial}{\partial y_D}\left[\phi_D S_{oD}\mathcal{D}_{ToD}\frac{\partial}{\partial y_D}\left(C_{CO_2,oD}\rho_{oD}^2 g_{yD}\frac{k_{oD}}{\mu_{oD}}\frac{\partial Z_D}{\partial y_D}\right)\right]\\
&+\left\{\phi_R S_{oR}\mathcal{D}^{*}_{TCO_2,oR}C_{CO_2,oR}\rho_{oR}^2 g_{yR}\frac{k_{oR}}{\mu_{oR}}\frac{Z_R}{y_R^3}\right\}\bullet\\
&\qquad\frac{\partial}{\partial y_D}\left[\phi_D S_{oD}\mathcal{D}^{*}_{TCO_2,oD}\frac{\partial}{\partial y_D}\left(C_{CO_2,oD}\rho_{oD}^2 g_{yD}\frac{k_{oD}}{\mu_{oD}}\frac{\partial Z_D}{\partial y_D}\right)\right]\\
&-\left\{C_{CO_2,oR}\rho_{oR}\frac{k_{oR}^2}{\mu_{oR}^2}\frac{p_{oR}^2}{z_R^2 x_R}\right\}\frac{\partial}{\partial z_D}\left[C_{CO_2,oD}\rho_{oD}\frac{k_{oD}^2}{\mu_{oD}^2}\frac{\partial p_{oD}}{\partial z_D}\frac{\partial p_{oD}}{\partial x_D}\right]\\
&-\left\{C_{CO_2,oR}\rho_{oR}^2 g_{xR}\frac{k_{oR}^2}{\mu_{oR}^2}\frac{p_{oR}Z_R}{z_R^2 x_R}\right\}\frac{\partial}{\partial z_D}\left[C_{CO_2,oD}\rho_{oD}^2 g_{xD}\frac{k_{oD}^2}{\mu_{oD}^2}\frac{\partial p_{oD}}{\partial z_D}\frac{\partial Z_D}{\partial x_D}\right]\\
&-\left\{C_{CO_2,oR}\rho_{oR}^2 g_{zR}\frac{k_{oR}^2}{\mu_{oR}^2}\frac{p_{oR}Z_R}{z_R^2 x_R}\right\}\frac{\partial}{\partial z_D}\left[C_{CO_2,oD}\rho_{oD}^2 g_{zD}\frac{k_{oD}^2}{\mu_{oD}^2}\frac{\partial p_{oD}}{\partial x_D}\frac{\partial Z_D}{\partial z_D}\right]\\
&-\left\{C_{CO_2,oR}\rho_{oR}^3 g_{zR}^2\frac{k_{oR}^2}{\mu_{oR}^2}\frac{Z_R^2}{x_R z_R^2}\right\}\frac{\partial}{\partial z_D}\left[C_{CO_2,oD}\rho_{oD}^3 g_{zD}^2\frac{k_{oD}^2}{\mu_{oD}^2}\frac{\partial Z_D}{\partial x_D}\frac{\partial Z_D}{\partial z_D}\right]\\
&-\left\{C_{CO_2,oR}\rho_{oR}\frac{k_{oR}^2}{\mu_{oR}^2}\frac{p_{oR}^2}{z_R^2 y_R}\right\}\frac{\partial}{\partial z_D}\left[C_{CO_2,oD}\rho_{oD}\frac{k_{oD}^2}{\mu_{oD}^2}\frac{\partial p_{oD}}{\partial z_D}\frac{\partial p_{oD}}{\partial y_D}\right]\\
&-\left\{C_{CO_2,oR}\rho_{oR}^2 g_{yR}\frac{k_{oR}^2}{\mu_{oR}^2}\frac{p_{oR}Z_R}{z_R^2 y_R}\right\}\frac{\partial}{\partial z_D}\left[C_{CO_2,oD}\rho_{oD}^2 g_{yD}\frac{k_{oD}^2}{\mu_{oD}^2}\frac{\partial p_{oD}}{\partial z_D}\frac{\partial Z_D}{\partial y_D}\right]\\
&-\left\{C_{CO_2,oR}\rho_{oR}^2 g_{zR}\frac{k_{oR}^2}{\mu_{oR}^2}\frac{p_{oR}Z_R}{z_R^2 y_R}\right\}\frac{\partial}{\partial z_D}\left[C_{CO_2,oD}\rho_{oD}^2 g_{zD}\frac{k_{oD}^2}{\mu_{oD}^2}\frac{\partial p_{oD}}{\partial y_D}\frac{\partial Z_D}{\partial z_D}\right]\\
&-\left\{C_{CO_2,oR}\rho_{oR}^3 g_{yR}g_{zR}\frac{k_{oR}^2}{\mu_{oR}^2}\frac{Z_R}{z_R^2 y_R}\right\}\frac{\partial}{\partial z_D}\left[C_{CO_2,oD}\rho_{oD}^3 g_{yD}g_{zD}\frac{k_{oD}^2}{\mu_{oD}^2}\frac{\partial Z_D}{\partial z_D}\frac{\partial Z_D}{\partial y_D}\right]\\
&-\left\{C_{CO_2,oR}\rho_{oR}\frac{k_{oR}^2}{\mu_{oR}^2}\frac{p_{oR}^2}{z_R^3}\right\}\frac{\partial}{\partial z_D}\left[C_{CO_2,oD}\rho_{oD}\frac{k_{oD}^2}{\mu_{oD}^2}\left(\frac{\partial p_{oD}}{\partial z_D}\right)^2\right]\\
&-\left\{2C_{CO_2,oR}\rho_{oR}^2 g_{zR}\frac{k_{oR}^2}{\mu_{oR}^2}\frac{p_{oR}}{z_R^3}Z_R\right\}\frac{\partial}{\partial z_D}\left[C_{CO_2,oD}\rho_{oD}^2 g_{zD}\frac{k_{oD}^2}{\mu_{oD}^2}\frac{\partial p_{oD}}{\partial z_D}\frac{\partial Z_D}{\partial z_D}\right]\\
&-\left\{C_{CO_2,oR}\rho_{oR}^3 g_{zR}^2\frac{k_{oR}^2}{\mu_{oR}^2}\frac{Z_R^2}{z_R^3}\right\}\frac{\partial}{\partial z_D}\left[C_{CO_2,oD}\rho_{oD}^3 g_{zD}^2\frac{k_{oD}^2}{\mu_{oD}^2}\left(\frac{\partial Z_D}{\partial z_D}\right)^2\right]
\end{aligned}
$$

$$+\left\{\phi_R S_{oR} \mathcal{D}_{ToR} C_{CO_2,oR} \rho_{oR} \frac{k_{oR}}{\mu_{oR}} \frac{p_{oR}}{z_R^3}\right\} \frac{\partial}{\partial z_D}\left[\phi_D S_{oD} \mathcal{D}_{ToD} \frac{\partial}{\partial z_D}\left(C_{CO_2,oD} \rho_{oD} \frac{k_{oD}}{\mu_{oD}} \frac{\partial p_{oD}}{\partial z_D}\right)\right]$$

$$+\left\{\phi_R S_{oR} \overset{*}{\mathcal{D}}_{TCO_2,oR} C_{CO_2,oR} \rho_{oR} \frac{k_{oR}}{\mu_{oR}} \frac{p_{oR}}{z_R^3}\right\} \bullet$$

$$\frac{\partial}{\partial z_D}\left[\phi_D S_{oD} \overset{*}{\mathcal{D}}_{TCO_2,oD} \frac{\partial}{\partial z_D}\left(C_{CO_2,oD} \rho_{oD} \frac{k_{oD}}{\mu_{oD}} \frac{\partial p_{oD}}{\partial z_D}\right)\right]$$

$$+\left\{\phi_R S_{oR} \mathcal{D}_{ToR} C_{CO_2,oR} \rho_{oR}^2 g_{zR} \frac{k_{oR}}{\mu_{oR}} \frac{Z_D}{z_R^3}\right\} \bullet$$

$$\frac{\partial}{\partial z_D}\left[\phi_D S_{oD} \mathcal{D}_{ToD} \frac{\partial}{\partial z_D}\left(C_{CO_2,oD} \rho_{oD}^2 g_{zD} \frac{k_{oD}}{\mu_{oD}} \frac{\partial Z_D}{\partial z_D}\right)\right]$$

$$+\left\{\phi_R S_{oR} \overset{*}{\mathcal{D}}_{TCO_2,oR} C_{CO_2,oR} \rho_{oR}^2 g_{zR} \frac{k_{oR}}{\mu_{oR}} \frac{Z_R}{z_R^3}\right\} \bullet$$

$$\frac{\partial}{\partial z_D}\left[\phi_D S_{oD} \overset{*}{\mathcal{D}}_{TCO_2,oD} \frac{\partial}{\partial z_D}\left(C_{CO_2,oD} \rho_{oD}^2 g_{zD} \frac{k_{oD}}{\mu_{oD}} \frac{\partial Z_D}{\partial z_D}\right)\right]$$

$$+\left\{C_{CO_2,oR} \rho_{oR} g_{xR}\right\} C_{CO_2,oD} \rho_{oD} g_{xD} + \left\{C_{CO_2,oR} \rho_{oR} g_{yR}\right\} C_{CO_2,oD} \rho_{oD} g_{yD}$$

$$+\left\{C_{CO_2,oR} \rho_{oR} g_{zR}\right\} C_{CO_2,oD} \rho_{oD} g_{zD} - \left\{\frac{p_{CO_2,oR}}{x_R}\right\} \frac{\partial}{\partial x_D}\left(p_{CO_2,oD}\right)$$

$$-\left\{\frac{p_{CO_2,oR}}{y_R}\right\} \frac{\partial}{\partial y_D}\left(p_{CO_2,oD}\right) - \left\{\frac{p_{CO_2,oR}}{z_R}\right\} \frac{\partial}{\partial z_D}\left(p_{CO_2,oD}\right)$$

$$-\left\{\mathcal{N}_{CO_2,ogxR} \frac{k_{oR}}{\mu_{oR}} \frac{p_{oR}}{x_R}\right\} \mathcal{N}_{CO_2,ogxD} \frac{k_{oD}}{\mu_{oD}} \frac{\partial p_{oD}}{\partial x_D}$$

$$-\left\{\mathcal{N}_{CO_2,ogxR} \frac{k_{oR}}{\mu_{oR}} \rho_{oR} g_R \frac{Z_R}{x_R}\right\} \mathcal{N}_{CO_2,ogxD} \frac{k_{oD}}{\mu_{oD}} \rho_{oD} g_D \frac{\partial Z_D}{\partial x_D}$$

$$-\left\{\mathcal{N}_{CO_2,ogyR} \frac{k_{oR}}{\mu_{oR}} \frac{p_{oR}}{y_R}\right\} \mathcal{N}_{CO_2,ogyD} \frac{k_{oD}}{\mu_{oD}} \frac{\partial p_{oD}}{\partial y_D}$$

$$-\left\{\mathcal{N}_{CO_2,ogyR} \frac{k_{oR}}{\mu_{oR}} \rho_{oR} g_R \frac{Z_R}{y_R}\right\} \mathcal{N}_{CO_2,ogyD} \frac{k_{oD}}{\mu_{oD}} \rho_{oD} g_D \frac{\partial Z_D}{\partial y_D}$$

$$-\left\{\mathcal{N}_{CO_2,ogzR} \frac{k_{oR}}{\mu_{oR}} \frac{p_{oR}}{z_R}\right\} \mathcal{N}_{CO_2,ogzD} \frac{k_{oD}}{\mu_{oD}} \frac{\partial p_{oD}}{\partial z_D}$$

$$-\left\{\mathcal{N}_{CO_2,ogzR} \frac{k_{oR}}{\mu_{oR}} \rho_{oR} g_R \frac{Z_R}{z_R}\right\} \mathcal{N}_{CO_2,ogzD} \frac{k_{oD}}{\mu_{oD}} \rho_{oD} g_D \frac{\partial Z_D}{\partial z_D}$$

$$-\left\{\mathcal{N}_{CO_2,owxR} \frac{k_{oR}}{\mu_{oR}} \frac{p_{oR}}{x_R}\right\} \mathcal{N}_{CO_2,owxD} \frac{k_{oD}}{\mu_{oD}} \frac{\partial p_{oD}}{\partial x_D}$$

$$-\left\{\mathcal{N}_{CO_2,owxR}\frac{k_{oR}}{\mu_{oR}}\rho_{oR}g_{xR}\frac{Z_R}{x_R}\right\}\mathcal{N}_{CO_2,owxD}\frac{k_{oD}}{\mu_{oD}}\rho_{oD}g_{xD}\frac{\partial Z_D}{\partial x_D}$$

$$-\left\{\mathcal{N}_{CO_2,owyR}\frac{k_{oR}}{\mu_{oR}}\frac{p_{oR}}{y_R}\right\}\mathcal{N}_{CO_2,owyD}\frac{k_{oD}}{\mu_{oD}}\frac{\partial p_{oD}}{\partial y_D}$$

$$-\left\{\mathcal{N}_{CO_2,owyR}\frac{k_{oR}}{\mu_{oR}}\rho_{oR}g_{yR}\frac{Z_R}{y_R}\right\}\mathcal{N}_{CO_2,owyD}\frac{k_{oD}}{\mu_{oD}}\rho_{oD}g_{yD}\frac{\partial Z_D}{\partial y_D}$$

$$-\left\{\mathcal{N}_{CO_2,owzR}\frac{k_{oR}}{\mu_{oR}}\frac{p_{oR}}{z_R}\right\}\mathcal{N}_{CO_2,owzD}\frac{k_{oD}}{\mu_{oD}}\frac{\partial p_{oD}}{\partial z_D}$$

$$-\left\{\mathcal{N}_{CO_2,owzR}\frac{k_{oR}}{\mu_{oR}}\rho_{oR}g_{zR}\frac{Z_R}{z_R}\right\}\mathcal{N}_{CO_2,owzD}\frac{k_{oD}}{\mu_{oD}}\rho_{oD}g_{zD}\frac{\partial Z_D}{\partial z_D}$$

$$=-\left\{\phi_R C_{CO_2,oR}\rho_{oR}S_{oR}\frac{k_{oR}}{\mu_{oR}}\frac{p_{oR}}{x_R t_R}\right\}\frac{\partial}{\partial t_D}\left[\phi_D C_{CO_2,oD}\rho_{oD}S_{oD}\frac{k_{oD}}{\mu_{oD}}\frac{\partial p_{oD}}{\partial x_D}\right]$$

$$-\left\{\phi_R C_{CO_2,oR}\rho_{oR}^2 S_{oR}g_{xR}\frac{k_{oR}}{\mu_{oR}}\frac{Z_D}{x_R t_R}\right\}\frac{\partial}{\partial t_D}\left[\phi_D C_{CO_2,oD}\rho_{oD}^2 S_{oD}g_{xD}\frac{k_{oD}}{\mu_{oD}}\frac{\partial Z_D}{\partial x_D}\right]$$

$$-\left\{\phi_R C_{CO_2,oR}\rho_{oR}S_{oR}\frac{k_{oR}}{\mu_{oR}}\frac{p_{oR}}{y_R t_R}\right\}\frac{\partial}{\partial t_D}\left[\phi_D C_{CO_2,oD}\rho_{oD}S_{oD}\frac{k_{oD}}{\mu_{oD}}\frac{\partial p_{oD}}{\partial y_D}\right]$$

$$-\left\{\phi_R C_{CO_2,oR}\rho_{oR}^2 S_{oR}g_{yR}\frac{k_{oR}}{\mu_{oR}}\frac{Z_R}{y_R t_R}\right\}\frac{\partial}{\partial t_D}\left[\phi_D C_{CO_2,oD}\rho_{oD}^2 S_{oD}g_{yD}\frac{k_{oD}}{\mu_{oD}}\frac{\partial Z_D}{\partial y_D}\right]$$

$$-\left\{\phi_R C_{CO_2,oR}\rho_{oR}S_{oR}\frac{k_{oR}}{\mu_{oR}}\frac{p_{oR}}{z_R t_R}\right\}\frac{\partial}{\partial t_D}\left[\phi_D C_{CO_2,oD}\rho_{oD}S_{oD}\frac{k_{oD}}{\mu_{oD}}\frac{\partial p_{oD}}{\partial z_D}\right]$$

$$-\left\{\phi_R C_{CO_2,oR}\rho_{oR}^2 S_{oR}g_{zR}\frac{k_{oR}}{\mu_{oR}}\frac{Z_R}{z_R t_R}\right\}\frac{\partial}{\partial t_D}\left[\phi_D C_{CO_2,oD}\rho_{oD}^2 S_{oD}g_{zD}\frac{k_{oD}}{\mu_{oD}}\frac{\partial Z_D}{\partial z_D}\right]$$

B.2 - Total Energy Balance for Carbon Dioxide in the Oil Phase in Dimensionless Form

$$\left\{C_{CO_2,oR}\frac{1}{2}\rho_{oR}\frac{k_{oR}^3}{\mu_{oR}^3}\frac{p_{oR}^3}{x_R^4}\right\}\frac{\partial}{\partial x_D}\left[C_{CO_2,oD}\rho_{oD}\frac{k_{oD}^3}{\mu_{oD}^3}\left(\frac{\partial p_{oD}}{\partial x_D}\right)^3\right]$$

$$+\left\{C_{CO_2,oR}\frac{3}{2}\rho_{oR}^2 g_{xR}\frac{k_{oR}^3}{\mu_{oR}^3}\frac{p_{oR}^2}{x_R^4}Z_R\right\}\frac{\partial}{\partial x_D}\left[C_{CO_2,oD}\rho_{oD}^2 g_{xD}\frac{k_{oD}^3}{\mu_{oD}^3}\left(\frac{\partial p_{oD}}{\partial x_D}\right)^2\frac{\partial Z_D}{\partial x_D}\right]$$

$$+\left\{C_{CO_2,oR}\frac{3}{2}\rho_{oR}^3 g_{xR}^2\frac{k_{oR}^3}{\mu_{oR}^3}p_{oR}\frac{Z_R^2}{x_R^4}\right\}\frac{\partial}{\partial x_D}\left[C_{CO_2,oD}\rho_{oD}^3 g_{xD}^2\frac{k_{oD}^3}{\mu_{oD}^3}\frac{\partial p_{oD}}{\partial x_D}\left(\frac{\partial Z_D}{\partial x_D}\right)^2\right]$$

$$+\left\{C_{CO_2,oR}\frac{1}{2}\rho_{oR}^4 g_{xR}^3\frac{k_{oR}^3}{\mu_{oR}^3}\frac{Z_R^3}{x_R^4}\right\}\frac{\partial}{\partial x_D}\left[C_{CO_2,oD}\rho_{oD}^4 g_{xD}^3\frac{k_{oD}^3}{\mu_{oD}^3}\left(\frac{\partial Z_D}{\partial x_D}\right)^3\right]$$

$$-\left\{\phi_R S_{oR} \mathfrak{D}_{LoR} C_{CO_2,oR} \frac{1}{2} \rho_{oR} \frac{k_{oR}^2}{\mu_{oR}^2} \frac{p_{oR}^2}{x_R^4}\right\} \bullet$$

$$\frac{\partial}{\partial x_D}\left[\phi_D S_{oD} \mathfrak{D}_{LoD} \frac{\partial}{\partial x_D}\left\{C_{CO_2,oD}\rho_{oD}\frac{k_{oD}^2}{\mu_{oD}^2}\left(\frac{\partial p_{oD}}{\partial x_D}\right)^2\right\}\right]$$

$$-\left\{\phi_R S_{oR} \mathfrak{D}_{LoR} C_{CO_2,oR} \rho_{oR}^2 g_{xR} \frac{k_{oR}^2}{\mu_{oR}^2} \frac{p_{oR}}{x_R^4} Z_R\right\} \bullet$$

$$\frac{\partial}{\partial x_D}\left[\phi_D S_{oD} \mathfrak{D}_{LoD} \frac{\partial}{\partial x_D}\left(C_{CO_2,oD}\rho_{oD}^2 g_{xD}\frac{k_{oD}^2}{\mu_{oD}^2}\frac{\partial p_{oD}}{\partial x_D}\frac{\partial Z_D}{\partial x_D}\right)\right]$$

$$-\left\{\phi_R S_{oR} \mathfrak{D}_{LoR} C_{CO_2,oR} \frac{1}{2} \rho_{oR}^3 g_{xR}^2 \frac{k_{oR}^2}{\mu_{oR}^2} \frac{Z_R^2}{x_R^4}\right\} \bullet$$

$$\frac{\partial}{\partial x_D}\left[\phi_D S_{oD} \mathfrak{D}_{LoD} \frac{\partial}{\partial x_D}\left\{C_{CO_2,oD}\rho_{oD}^3 g_{xD}^2\frac{k_{oD}^2}{\mu_{oD}^2}\left(\frac{\partial Z_D}{\partial x_D}\right)^2\right\}\right]$$

$$-\left\{\phi_R S_{oR} \mathfrak{D}^*_{LCO_2,oR} C_{CO_2,oR} \frac{1}{2} \rho_{oR} \frac{k_{oR}^2}{\mu_{oR}^2} \frac{p_{oR}^2}{x_R^4}\right\} \bullet$$

$$\frac{\partial}{\partial x_D}\left[\phi_D S_{oD} \mathfrak{D}^*_{LCO_2,oD} \frac{\partial}{\partial x_D}\left\{C_{CO_2,oD}\rho_{oD}\frac{k_{oD}^2}{\mu_{oD}^2}\left(\frac{\partial p_{oD}}{\partial x_D}\right)^2\right\}\right]$$

$$-\left\{\phi_R S_{oR} \mathfrak{D}^*_{LCO_2,oR} C_{CO_2,oR} \rho_{oR}^2 g_{xR} \frac{k_{oR}^2}{\mu_{oR}^2} \frac{p_{oR}}{x_R^4} Z_R\right\} \bullet$$

$$\frac{\partial}{\partial x_D}\left[\phi_D S_{oD} \mathfrak{D}^*_{LCO_2,oD} \frac{\partial}{\partial x_D}\left(C_{CO_2,oD}\rho_{oD}^2 g_{xD}\frac{k_{oD}^2}{\mu_{oD}^2}\frac{\partial p_{oD}}{\partial x_D}\frac{\partial Z_D}{\partial x_D}\right)\right]$$

$$-\left\{\phi_R S_{oR} \mathfrak{D}^*_{LCO_2,oR} C_{CO_2,oR} \frac{1}{2} \rho_{oR}^3 g_{xR}^2 \frac{k_{oR}^2}{\mu_{oR}^2} \frac{Z_R^2}{x_R^4}\right\} \bullet$$

$$\frac{\partial}{\partial x_D}\left[\phi_D S_{oD} \mathfrak{D}^*_{LCO_2,oD} \frac{\partial}{\partial x_D}\left\{C_{CO_2,oD}\rho_{oD}^3 g_{xD}^2\frac{k_{oD}^2}{\mu_{oD}^2}\left(\frac{\partial Z_D}{\partial x_D}\right)^2\right\}\right]$$

$$+\left\{C_{CO_2,oR} \frac{1}{2} \rho_{oR} \frac{k_{oR}^3}{\mu_{oR}^3} \frac{p_{oR}^3}{y_R^4}\right\} \frac{\partial}{\partial y_D}\left[C_{CO_2,oD}\rho_{oD}\frac{k_{oD}^3}{\mu_{oD}^3}\left(\frac{\partial p_{oD}}{\partial y_D}\right)^3\right]$$

$$+\left\{C_{CO_2,oR} \frac{3}{2} \rho_{oR}^2 g_{yR} \frac{k_{oR}^3}{\mu_{oR}^3} \frac{p_{oR}^2}{y_R^4} Z_R\right\} \frac{\partial}{\partial y_D}\left[C_{CO_2,oD}\rho_{oD}^2 g_{yD}\frac{k_{oD}^3}{\mu_{oD}^3}\left(\frac{\partial p_{oD}}{\partial y_D}\right)^2\frac{\partial Z_D}{\partial y_D}\right]$$

$$+\left\{C_{CO_2,oR} \frac{3}{2} \rho_{oR}^3 g_{yR}^2 \frac{k_{oR}^3}{\mu_{oR}^3} p_{oR} \frac{Z_R^2}{y_R^4}\right\} \frac{\partial}{\partial y_D}\left[C_{CO_2,oD}\rho_{oD}^3 g_{yD}^2\frac{k_{oD}^3}{\mu_{oD}^3}\frac{\partial p_{oD}}{\partial y_D}\left(\frac{\partial Z_D}{\partial y_D}\right)^2\right]$$

$$
\begin{aligned}
&+\left\{C_{CO_2,oR}\frac{1}{2}\rho_{oR}^{4}g_{yR}^{3}\frac{k_{oR}^{3}}{\mu_{oR}^{3}}\frac{Z_R^{3}}{y_R^{4}}\right\}\frac{\partial}{\partial y_D}\left[C_{CO_2,oD}\rho_{oD}^{4}g_{yD}^{3}\frac{k_{oD}^{3}}{\mu_{oD}^{3}}\left(\frac{\partial Z_D}{\partial y_D}\right)^{3}\right]\\
&-\left\{\phi_R S_{oR}\mathcal{D}_{ToR}C_{CO_2,oR}\frac{1}{2}\rho_{oR}\frac{k_{oR}^{2}}{\mu_{oR}^{2}}\frac{p_{oR}^{2}}{y_R^{4}}\right\}\bullet\\
&\qquad\frac{\partial}{\partial y_D}\left[\phi_D S_{oD}\mathcal{D}_{ToD}\frac{\partial}{\partial y_D}\left\{C_{CO_2,oD}\rho_{oD}\frac{k_{oD}^{2}}{\mu_{oD}^{2}}\left(\frac{\partial p_{oD}}{\partial y_D}\right)^{2}\right\}\right]\\
&-\left\{\phi_R S_{oR}\mathcal{D}_{ToR}C_{CO_2,oR}\rho_{oR}^{2}g_{yR}\frac{k_{oR}^{2}}{\mu_{oR}^{2}}\frac{p_{oR}}{y_R^{4}}Z_R\right\}\bullet\\
&\qquad\frac{\partial}{\partial y_D}\left[\phi_D S_{oD}\mathcal{D}_{ToD}\frac{\partial}{\partial y_D}\left(C_{CO_2,oD}\rho_{oD}^{2}g_{yD}\frac{k_{oD}^{2}}{\mu_{oD}^{2}}\frac{\partial p_{oD}}{\partial y_D}\frac{\partial Z_D}{\partial y_D}\right)\right]\\
&-\left\{\phi_R S_{oR}\mathcal{D}_{ToR}C_{o,oR}\frac{1}{2}\rho_{oR}^{3}g_{yR}^{2}\frac{k_{oR}^{2}}{\mu_{oR}^{2}}\frac{Z_R^{2}}{y_R^{4}}\right\}\bullet\\
&\qquad\frac{\partial}{\partial y_D}\left[\phi_D S_{oD}\mathcal{D}_{ToD}\frac{\partial}{\partial y_D}\left\{C_{CO_2,oD}\rho_{oD}^{3}g_{yD}^{2}\frac{k_{oD}^{2}}{\mu_{oD}^{2}}\left(\frac{\partial Z_D}{\partial y_D}\right)^{2}\right\}\right]\\
&-\left\{\phi_R S_{oR}\mathcal{D}^{*}_{TCO_2,oR}C_{CO_2,oR}\frac{1}{2}\rho_{oR}\frac{k_{oR}^{2}}{\mu_{oR}^{2}}\frac{p_{oR}^{2}}{y_R^{4}}\right\}\bullet\\
&\qquad\frac{\partial}{\partial y_D}\left[\phi_D S_{oD}\mathcal{D}^{*}_{TCO_2,oD}\frac{\partial}{\partial y_D}\left\{C_{CO_2,oD}\rho_{oD}\frac{k_{oD}^{2}}{\mu_{oD}^{2}}\left(\frac{\partial p_{oD}}{\partial y_D}\right)^{2}\right\}\right]\\
&-\left\{\phi_R S_{oR}\mathcal{D}^{*}_{TCO_2,oR}C_{CO_2,oR}\rho_{oR}^{2}g_{yR}\frac{k_{oR}^{2}}{\mu_{oR}^{2}}\frac{p_{oR}}{y_R^{4}}Z_R\right\}\bullet\\
&\qquad\frac{\partial}{\partial y_D}\left[\phi_D S_{oD}\mathcal{D}^{*}_{TCO_2,oD}\frac{\partial}{\partial y_D}\left(C_{CO_2,oD}\rho_{oD}^{2}g_{yD}\frac{k_{oD}^{2}}{\mu_{oD}^{2}}\frac{\partial p_{oD}}{\partial y_D}\frac{\partial Z_D}{\partial y_D}\right)\right]\\
&-\left\{\phi_R S_{oR}\mathcal{D}^{*}_{TCO_2,oR}C_{o,oR}\frac{1}{2}\rho_{oR}^{3}g_{yR}^{2}\frac{k_{oR}^{2}}{\mu_{oR}^{2}}\frac{Z_R^{2}}{y_R^{4}}\right\}\bullet\\
&\qquad\frac{\partial}{\partial y_D}\left[\phi_D S_{oD}\mathcal{D}^{*}_{TCO_2,oD}\frac{\partial}{\partial y_D}\left\{C_{CO_2,oD}\rho_{oD}^{3}g_{yD}^{2}\frac{k_{oD}^{2}}{\mu_{oD}^{2}}\left(\frac{\partial Z_D}{\partial y_D}\right)^{2}\right\}\right]\\
&+\left\{C_{CO_2,oR}\frac{1}{2}\rho_{oR}\frac{k_{oR}^{3}}{\mu_{oR}^{3}}\frac{p_{oR}^{3}}{z_R^{4}}\right\}\frac{\partial}{\partial z_D}\left[C_{CO_2,oD}\rho_{oD}\frac{k_{oD}^{3}}{\mu_{oD}^{3}}\left(\frac{\partial p_{oD}}{\partial z_D}\right)^{3}\right]\\
&+\left\{C_{CO_2,oR}\frac{3}{2}\rho_{oR}^{2}g_{zR}\frac{k_{oR}^{3}}{\mu_{oR}^{3}}\frac{p_{oR}^{2}}{z_R^{4}}Z_R\right\}\frac{\partial}{\partial z_D}\left[C_{CO_2,oD}\rho_{oD}^{2}g_{zD}\frac{k_{oD}^{3}}{\mu_{oD}^{3}}\left(\frac{\partial p_{oD}}{\partial z_D}\right)^{2}\frac{\partial Z_D}{\partial z_D}\right]
\end{aligned}
$$

$$+\left\{C_{CO_2,oR}\frac{3}{2}\rho_{oR}^3 g_{zR}^2\frac{k_{oR}^3}{\mu_{oR}^3}p_{oR}\frac{Z_R^2}{z_R^4}\right\}\frac{\partial}{\partial z_D}\left[C_{CO_2,oD}\rho_{oD}^3 g_{zD}^2\frac{k_{oD}^3}{\mu_{oD}^3}\frac{\partial p_{oD}}{\partial z_D}\left(\frac{\partial Z_D}{\partial z_D}\right)^2\right]$$

$$+\left\{C_{CO_2,oR}\frac{1}{2}\rho_{oR}^4 g_{zR}^3\frac{k_{oR}^3}{\mu_{oR}^3}\frac{Z_R^3}{z_R^4}\right\}\frac{\partial}{\partial z_D}\left[C_{CO_2,oD}\rho_{oD}^4 g_{zD}^3\frac{k_{oD}^3}{\mu_{oD}^3}\left(\frac{\partial Z_D}{\partial z_D}\right)^3\right]$$

$$-\left\{\phi_R S_{oR}\mathcal{D}_{ToR}C_{CO_2,oR}\frac{1}{2}\rho_{oR}\frac{k_{oR}^2}{\mu_{oR}^2}\frac{p_{oR}^2}{z_R^4}\right\}\bullet$$

$$\frac{\partial}{\partial z_D}\left[\phi_D S_{oD}\mathcal{D}_{ToD}\frac{\partial}{\partial z_D}\left\{C_{CO_2,oD}\rho_{oD}\frac{k_{oD}^2}{\mu_{oD}^2}\left(\frac{\partial p_{oD}}{\partial z_D}\right)^2\right\}\right]$$

$$-\left\{\phi_R S_{oR}\mathcal{D}_{ToR}C_{CO_2,oR}\rho_{oR}^2 g_{zR}\frac{k_{oR}^2}{\mu_{oR}^2}\frac{p_{oR}}{z_R^4}Z_R\right\}\bullet$$

$$\frac{\partial}{\partial z_D}\left[\phi_D S_{oD}\mathcal{D}_{ToD}\frac{\partial}{\partial z_D}\left(C_{CO_2,oD}\rho_{oD}^2 g_{zD}\frac{k_{oD}^2}{\mu_{oD}^2}\frac{\partial p_{oD}}{\partial z_D}\frac{\partial Z_D}{\partial z_D}\right)\right]$$

$$-\left\{\phi_R S_{oR}\mathcal{D}_{ToR}C_{CO_2,oR}\frac{1}{2}\rho_{oR}^3 g_{zR}^2\frac{k_{oR}^2}{\mu_{oR}^2}\frac{Z_R^2}{z_R^4}\right\}\bullet$$

$$\frac{\partial}{\partial z_D}\left[\phi_D S_{oD}\mathcal{D}_{ToD}\frac{\partial}{\partial z_D}\left\{C_{CO_2,oD}\rho_{oD}^3 g_{zD}^2\frac{k_{oD}^2}{\mu_{oD}^2}\left(\frac{\partial Z_D}{\partial z_D}\right)^2\right\}\right]$$

$$-\left\{\phi_R S_{oR}\mathcal{D}_{TCO_2,oR}C_{CO_2,oR}\frac{1}{2}\rho_{oR}\frac{k_{oR}^2}{\mu_{oR}^2}\frac{p_{oR}^2}{z_R^4}\right\}\bullet$$

$$\frac{\partial}{\partial z_D}\left[\phi_D S_{oD}\mathcal{D}_{TCO_2,oD}\frac{\partial}{\partial z_D}\left\{C_{CO_2,oD}\rho_{oD}\frac{k_{oD}^2}{\mu_{oD}^2}\left(\frac{\partial p_{oD}}{\partial z_D}\right)^2\right\}\right]$$

$$-\left\{\phi_R S_{oR}\dot{\mathcal{D}}_{TCO_2,oR}C_{CO_2,oR}\rho_{oR}^2 g_{zR}\frac{k_{oR}^2}{\mu_{oR}^2}\frac{p_{oR}}{z_R^4}Z_R\right\}$$

$$\bullet\frac{\partial}{\partial z_D}\left[\phi_D S_{oD}\dot{\mathcal{D}}_{TCO_2,oD}\frac{\partial}{\partial z_D}\left\{C_{CO_2,oD}\rho_{oD}^2 g_{zD}\frac{k_{oD}^2}{\mu_{oD}^2}\frac{\partial p_{oD}}{\partial z_D}\frac{\partial Z_D}{\partial z_D}\right\}\right]$$

$$-\left\{\phi_R S_{oR}\dot{\mathcal{D}}_{TCO_2,oR}C_{CO_2,oR}\frac{1}{2}\rho_{oR}^3 g_{zR}^2\frac{k_{oR}^2}{\mu_{oR}^2}\frac{Z_R^2}{z_R^4}\right\}$$

$$\bullet\frac{\partial}{\partial z_D}\left[\phi_D S_{oD}\mathcal{D}_{TCO_2,oD}\frac{\partial}{\partial z_D}\left\{C_{CO_2,oD}\rho_{oD}^3 g_{zD}^2\frac{k_{oD}^2}{\mu_{oD}^2}\left(\frac{\partial Z_D}{\partial z_D}\right)^2\right\}\right]$$

$$+\left\{p_{CO_2,oR}\frac{k_{oR}}{\mu_{oR}}\frac{p_{oR}}{x_R^2}\right\}\frac{\partial}{\partial x_D}\left[p_{CO_2,oD}\frac{k_{oD}}{\mu_{oD}}\frac{\partial p_{oD}}{\partial x_D}\right]$$

$$+\left\{p_{CO_2,oR}\frac{k_{oR}}{\mu_{oR}}\rho_{oR}g_{xR}\frac{Z_R}{x_R^2}\right\}\frac{\partial}{\partial x_D}\left[p_{CO_2,oD}\frac{k_{oD}}{\mu_{oD}}\rho_{oD}g_{xD}\frac{\partial Z_D}{\partial x_D}\right]$$

$$+\left\{p_{CO_2,oR}\frac{k_{oR}}{\mu_{oR}}\frac{p_{oR}}{y_R^2}\right\}\frac{\partial}{\partial y_D}\left[p_{CO_2,oD}\frac{k_{oD}}{\mu_{oD}}\frac{\partial p_{oD}}{\partial y_D}\right]$$

$$+\left\{p_{CO_2,oR}\frac{k_{oR}}{\mu_{oR}}\rho_{oR}g_{yR}\frac{Z_R}{y_R^2}\right\}\frac{\partial}{\partial y_D}\left[p_{CO_2,oD}\frac{k_{oD}}{\mu_{oD}}\rho_{oD}g_{D}\frac{\partial Z_D}{\partial y_D}\right]$$

$$+\left\{p_{CO_2,oR}\frac{k_{oR}}{\mu_{oR}}\frac{p_{oR}}{z_R^2}\right\}\frac{\partial}{\partial z_D}\left[p_{CO_2,oD}\frac{k_{oD}}{\mu_{oD}}\frac{\partial p_{oD}}{\partial z_D}\right]$$

$$+\left\{p_{CO_2,oR}\frac{k_{oR}}{\mu_{oR}}\rho_{oR}g_{zR}\frac{Z_R}{z_R^2}\right\}\frac{\partial}{\partial z_D}\left[p_{CO_2,oD}\frac{k_{oD}}{\mu_{oD}}\rho_{oD}g_{zD}\frac{\partial Z_D}{\partial z_D}\right]$$

$$+\left\{p_{CO_2,oR}\frac{k_{oR}}{\mu_{oR}}\frac{p_{oR}}{x_R^2}\right\}p_{CO_2,oD}\frac{\partial}{\partial x_D}\left[\frac{k_{oD}}{\mu_{oD}}\frac{\partial p_{oD}}{\partial x_D}\right]$$

$$+\left\{p_{CO_2,oR}\frac{k_{oR}}{\mu_{oR}}\rho_{oR}g_{xR}\frac{Z_R}{x_R^2}\right\}p_{CO_2,oD}\frac{\partial}{\partial x_D}\left[\frac{k_{oD}}{\mu_{oD}}\rho_{oD}g_{xD}\frac{\partial Z_D}{\partial x_D}\right]$$

$$+\left\{p_{CO_2,oR}\frac{k_{oR}}{\mu_{oR}}\frac{p_{oR}}{y_R^2}\right\}p_{CO_2,oD}\frac{\partial}{\partial y_D}\left[\frac{k_{oD}}{\mu_{oD}}\frac{\partial p_{oD}}{\partial y_D}\right]$$

$$+\left\{p_{CO_2,oR}\frac{k_{oR}}{\mu_{oR}}\rho_{oR}g_{yR}\frac{Z_R}{y_R^2}\right\}p_{CO_2,oD}\frac{\partial}{\partial y_D}\left[\frac{k_{oD}}{\mu_{oD}}\rho_{oD}g_{yD}\frac{\partial Z_D}{\partial y_D}\right]$$

$$+\left\{p_{CO_2,oR}\frac{k_{oR}}{\mu_{oR}}\frac{p_{oR}}{z_R^2}\right\}p_{CO_2,oD}\frac{\partial}{\partial z_D}\left[\frac{k_{oD}}{\mu_{oD}}\frac{\partial p_{oD}}{\partial z_D}\right]$$

$$+\left\{p_{CO_2,oR}\frac{k_{oR}}{\mu_{oR}}\rho_{oR}g_{zR}\frac{Z_R}{z_R^2}\right\}p_{CO_2,oD}\frac{\partial}{\partial z_D}\left[\frac{k_{oD}}{\mu_{oD}}\rho_{oD}g_{zD}\frac{\partial Z_D}{\partial z_D}\right]$$

$$-\left\{C_{CO_2,oR}\rho_{oR}g_{xR}\frac{k_{oR}}{\mu_{oR}}\frac{p_{oR}}{x_R}\right\}C_{CO_2,oD}\rho_{oD}g_{xD}\frac{k_{oD}}{\mu_{oD}}\frac{\partial p_{oD}}{\partial x_D}$$

$$-\left\{C_{CO_2,oR}\rho_{oR}^2g_{xR}^2\frac{k_{oR}}{\mu_{oR}}\frac{Z_R}{x_R}\right\}C_{CO_2,oD}\rho_{oD}^2g_{xD}^2\frac{k_{oD}}{\mu_{oD}}\frac{\partial Z_D}{\partial x_D}$$

$$-\left\{C_{CO_2,oR}\rho_{oR}g_{yR}\frac{k_{oR}}{\mu_{oR}}\frac{p_{oR}}{y_R}\right\}C_{CO_2,oD}\rho_{oD}g_{yD}\frac{k_{oD}}{\mu_{oD}}\frac{\partial p_{oD}}{\partial y_D}$$

$$-\left\{C_{CO_2,oR}\rho_{oR}^2g_{yR}^2\frac{k_{oR}}{\mu_{oR}}\frac{Z_R}{y_R}\right\}C_{CO_2,oD}\rho_{oD}^2g_{yD}^2\frac{k_{oD}}{\mu_{oD}}\frac{\partial Z_D}{\partial y_D}$$

$$-\left\{C_{CO_2,oR}\rho_{oR}g_{zR}\frac{k_{oR}}{\mu_{oR}}\frac{p_{oR}}{z_R}\right\}C_{CO_2,oD}\rho_{oD}g_{zD}\frac{k_{oD}}{\mu_{oD}}\frac{\partial p_{oD}}{\partial z_D}$$

$$-\left\{C_{CO_2,oR}\rho_{oR}^2g_{zR}^2\frac{k_{oR}}{\mu_{oR}}\frac{Z_R}{z_R}\right\}C_{CO_2,oD}\rho_{oD}^2g_{zD}^2\frac{k_{oD}}{\mu_{oD}}\frac{\partial Z_D}{\partial z_D}$$

$$+\left\{\mathcal{N}_{CO_2,ogxR}h_{CO_2R}\right\}\mathcal{N}_{CO_2,ogxD}h_{CO_2D}$$

$$+\left\{\mathcal{N}_{CO_2,ogxR}\frac{1}{2}\frac{k_{gR}^2}{\mu_{gR}^2}\frac{p_{gR}^2}{x_R^2}\right\}\mathcal{N}_{CO_2,ogxD}\frac{1}{2}\left(\frac{k_{gD}}{\mu_{gD}}\frac{\partial p_{gD}}{\partial x_D}\right)^2$$

$$-\left\{\mathcal{N}_{CO_2,ogxR}\frac{1}{2}\frac{k_{oR}^2}{\mu_{oR}^2}\frac{p_{oR}^2}{x_R^2}\right\}\mathcal{N}_{CO_2,ogxD}\frac{1}{2}\left(\frac{k_{oD}}{\mu_{oD}}\frac{\partial p_{oD}}{\partial x_D}\right)^2$$

$$+\left\{\mathcal{N}_{CO_2,ogxR}\frac{k_{gR}^2}{\mu_{gR}^2}\rho_{gR}g_{xR}\frac{p_{gR}Z_R}{x_R^2}\right\}\mathcal{N}_{CO_2,ogxD}\frac{k_{gD}^2}{\mu_{gD}^2}\frac{\partial p_{gD}}{\partial x_D}\rho_{gD}g_{xD}\frac{\partial Z_D}{\partial x_D}$$

$$-\left\{\mathcal{N}_{CO_2,ogxR}\frac{k_{oR}^2}{\mu_{oR}^2}\rho_{oR}g_{xR}\frac{p_{oR}Z_R}{x_R^2}\right\}\mathcal{N}_{CO_2,ogxD}\frac{k_{oD}^2}{\mu_{oD}^2}\frac{\partial p_{oD}}{\partial x_D}\rho_{oD}g_{xD}\frac{\partial Z_D}{\partial x_D}$$

$$+\left\{\mathcal{N}_{CO_2,ogxR}\frac{1}{2}\frac{k_{gR}^2}{\mu_{gR}^2}\rho_{gR}^2g_{xR}^2\frac{Z_R^2}{x_R^2}\right\}\mathcal{N}_{CO_2,ogxD}\frac{1}{2}\left(\frac{k_{gD}}{\mu_{gD}}\rho_{gD}g_{xD}\frac{\partial Z_D}{\partial x_D}\right)^2$$

$$-\left\{\mathcal{N}_{CO_2,ogxR}\frac{1}{2}\frac{k_{oR}^2}{\mu_{oR}^2}\rho_{oR}^2g_{xR}^2\frac{Z_R^2}{x_R^2}\right\}\mathcal{N}_{CO_2,ogxD}\frac{1}{2}\left(\frac{k_{oD}}{\mu_{oD}}\rho_{oD}g_{xD}\frac{\partial Z_D}{\partial x_D}\right)^2$$

$$+\left\{\mathcal{N}_{CO_2,ogyR}h_{CO_2R}\right\}\mathcal{N}_{CO_2,ogyD}h_{CO_2D}$$

$$+\left\{\mathcal{N}_{CO_2,ogyR}\frac{1}{2}\frac{k_{gR}^2}{\mu_{gR}^2}\frac{p_{gR}^2}{y_R^2}\right\}\mathcal{N}_{CO_2,ogyD}\frac{1}{2}\left(\frac{k_{gD}}{\mu_{gD}}\frac{\partial p_{gD}}{\partial y_D}\right)^2$$

$$-\left\{\mathcal{N}_{CO_2,ogyR}\frac{1}{2}\frac{k_{oR}^2}{\mu_{oR}^2}\frac{p_{oR}^2}{y_R^2}\right\}\mathcal{N}_{CO_2,ogyD}\frac{1}{2}\left(\frac{k_{oD}}{\mu_{oD}}\frac{\partial p_{oD}}{\partial y_D}\right)^2$$

$$+\left\{\mathcal{N}_{CO_2,ogyR}\frac{k_{gR}^2}{\mu_{gR}^2}\rho_{gR}g_{yR}\frac{p_{gR}Z_R}{y_R^2}\right\}\mathcal{N}_{CO_2,ogyD}\frac{k_{gD}^2}{\mu_{gD}^2}\frac{\partial p_{gD}}{\partial y_D}\rho_{gD}g_{yD}\frac{\partial Z_D}{\partial y_D}$$

$$-\left\{\mathcal{N}_{CO_2,ogyR}\frac{k_{oR}^2}{\mu_{oR}^2}\rho_{oR}g_{yR}\frac{p_{oR}Z_R}{y_R^2}\right\}\mathcal{N}_{CO_2,ogyD}\frac{k_{oD}^2}{\mu_{oD}^2}\frac{\partial p_{oD}}{\partial y_D}\rho_{oD}g_{yD}\frac{\partial Z_D}{\partial y_D}$$

$$+\left\{\mathcal{N}_{CO_2,ogyR}\frac{1}{2}\frac{k_{gR}^2}{\mu_{gR}^2}\rho_{gR}^2g_{yR}^2\frac{Z_R^2}{y_R^2}\right\}\mathcal{N}_{CO_2,ogyD}\frac{1}{2}\left(\frac{k_{gD}}{\mu_{gD}}\rho_{gD}g_{yD}\frac{\partial Z_D}{\partial y_D}\right)^2$$

$$-\left\{\mathcal{N}_{CO_2,ogyR}\frac{1}{2}\frac{k_{oR}^2}{\mu_{oR}^2}\rho_{oR}^2g_{yR}^2\frac{Z_R^2}{y_R^2}\right\}\mathcal{N}_{CO_2,ogyD}\frac{1}{2}\left(\frac{k_{oD}}{\mu_{oD}}\rho_{oD}g_{yD}\frac{\partial Z_D}{\partial y_D}\right)^2$$

$$+\left\{\mathcal{N}_{CO_2,ogzR}h_{CO_2R}\right\}\mathcal{N}_{CO_2,ogzD}h_{CO_2D}$$

$$+\left\{\mathcal{N}_{CO_2,ogzR}\frac{1}{2}\frac{k_{gR}^2}{\mu_{gR}^2}\frac{p_{gR}^2}{z_R^2}\right\}\mathcal{N}_{CO_2,ogzD}\frac{1}{2}\left(\frac{k_{gD}}{\mu_{gD}}\frac{\partial p_{gD}}{\partial z_D}\right)^2$$

$$-\left\{\mathcal{N}_{CO_2,ogzR}\frac{1}{2}\frac{k_{oR}^2}{\mu_{oR}^2}\frac{p_{oR}^2}{z_R^2}\right\}\mathcal{N}_{CO_2,ogzD}\frac{1}{2}\left(\frac{k_{oD}}{\mu_{oD}}\frac{\partial p_{oD}}{\partial z_D}\right)^2$$

$$+\left\{\mathcal{N}_{CO_2,ogzR}\frac{k_{gR}^2}{\mu_{gR}^2}\rho_{gR}g_{zR}\frac{p_{gR}Z_R}{z_R^2}\right\}\mathcal{N}_{CO_2,ogzD}\frac{k_{gD}^2}{\mu_{gD}^2}\frac{\partial p_{gD}}{\partial z_D}\rho_{gD}g_{zD}\frac{\partial Z_D}{\partial z_D}$$

$$-\left\{\mathcal{N}_{CO_2,ogzR}\frac{k_{oR}^2}{\mu_{oR}^2}\rho_{oR}g_{zR}\frac{p_{oR}Z_R}{z_R^2}\right\}\mathcal{N}_{CO_2,ogzD}\frac{k_{oD}^2}{\mu_{oD}^2}\frac{\partial p_{oD}}{\partial z_D}\rho_{oD}g_{zD}\frac{\partial Z_D}{\partial z_D}$$

$$+\left\{\mathcal{N}_{CO_2,ogzR}\frac{1}{2}\frac{k_{gR}^2}{\mu_{gR}^2}\rho_{gR}^2g_{zR}^2\frac{Z_R^2}{z_R^2}\right\}\mathcal{N}_{CO_2,ogzD}\frac{1}{2}\left(\frac{k_{gD}}{\mu_{gD}}\rho_{gD}g_{zD}\frac{\partial Z_D}{\partial z_D}\right)^2$$

$$-\left\{\mathcal{N}_{CO_2,ogzR}\frac{1}{2}\frac{k_{oR}^2}{\mu_{oR}^2}\rho_{oR}^2g_{zR}^2\frac{Z_R^2}{z_R^2}\right\}\mathcal{N}_{CO_2,ogzD}\frac{1}{2}\left(\frac{k_{oD}}{\mu_{oD}}\rho_{oD}g_{zD}\frac{\partial Z_D}{\partial z_D}\right)^2$$

$$+\left\{\mathcal{N}_{CO_2,owxR}h_{CO_2R}\right\}\mathcal{N}_{CO_2,owxD}h_{CO_2D}$$

$$+\left\{\mathcal{N}_{CO_2,owxR}\frac{1}{2}\frac{k_{wR}^2}{\mu_{wR}^2}\frac{p_{wR}^2}{x_R^2}\right\}\mathcal{N}_{CO_2,owxD}\frac{1}{2}\left(\frac{k_{wD}}{\mu_{wD}}\frac{\partial p_{wD}}{\partial x_D}\right)^2$$

$$-\left\{\mathcal{N}_{CO_2,owxR}\frac{1}{2}\frac{k_{oR}^2}{\mu_{oR}^2}\frac{p_{oR}^2}{x_R^2}\right\}\mathcal{N}_{CO_2,owxD}\frac{1}{2}\left(\frac{k_{oD}}{\mu_{oD}}\frac{\partial p_{oD}}{\partial x_D}\right)^2$$

$$+\left\{\mathcal{N}_{CO_2,owxR}\frac{k_{wR}}{\mu_{wR}}\rho_{wR}g_{xR}\frac{p_{oR}Z_R}{x_R^2}\right\}\mathcal{N}_{CO_2,owxD}\frac{k_{wD}}{\mu_{wD}}\frac{\partial p_{wD}}{\partial x_D}\rho_{wD}g_{yD}\frac{\partial Z_D}{\partial x_D}$$

$$-\left\{\mathcal{N}_{CO_2,owxR}\frac{k_{oR}}{\mu_{oR}}\rho_{oR}g_{xR}\frac{p_{oR}Z_R}{x_R^2}\right\}\mathcal{N}_{CO_2,owxD}\frac{k_{oD}}{\mu_{oD}}\frac{\partial p_{oD}}{\partial x_D}\rho_{oD}g_{yD}\frac{\partial Z_D}{\partial x_D}$$

$$+\left\{\mathcal{N}_{CO_2,owxR}\frac{1}{2}\frac{k_{wR}^2}{\mu_{wR}^2}\rho_{wR}^2g_{xR}^2\frac{Z_R^2}{x_R^2}\right\}\mathcal{N}_{CO_2,owxD}\frac{1}{2}\left(\frac{k_{wD}}{\mu_{wD}}\rho_{wD}g_{xD}\frac{\partial Z_D}{\partial x_D}\right)^2$$

$$-\left\{\mathcal{N}_{CO_2,owxR}\frac{1}{2}\frac{k_{oR}^2}{\mu_{oR}^2}\rho_{oR}^2g_{xR}^2\frac{Z_R^2}{x_R^2}\right\}\mathcal{N}_{CO_2,owxD}\frac{1}{2}\left(\frac{k_{oD}}{\mu_{oD}}\rho_{oD}g_{xD}\frac{\partial Z_D}{\partial x_D}\right)^2$$

$$+\left\{\mathcal{N}_{CO_2,owyR}h_{CO_2R}\right\}\mathcal{N}_{CO_2,owyD}h_{CO_2D}$$

$$+\left\{\mathcal{N}_{CO_2,owyR}\frac{1}{2}\frac{k_{wR}^2}{\mu_{wR}^2}\frac{p_{wR}^2}{y_R^2}\right\}\mathcal{N}_{CO_2,owyD}\frac{1}{2}\left(\frac{k_{wD}}{\mu_{wD}}\frac{\partial p_{wD}}{\partial y_D}\right)^2$$

$$-\left\{\mathcal{N}_{CO_2,owyR}\frac{1}{2}\frac{k_{oR}^2}{\mu_{oR}^2}\frac{p_{oR}^2}{y_R^2}\right\}\mathcal{N}_{CO_2,owyD}\frac{1}{2}\left(\frac{k_{oD}}{\mu_{oD}}\frac{\partial p_{oD}}{\partial y_D}\right)^2$$

$$+\left\{\mathcal{N}_{CO_2,owyR}\frac{k_{wR}}{\mu_{wR}}\rho_{wR}g_{yR}\frac{p_{wR}Z_R}{y_R^2}\right\}\mathcal{N}_{CO_2,owyD}\frac{k_{wD}}{\mu_{wD}}\frac{\partial p_{wD}}{\partial y_D}\rho_{wD}g_{yD}\frac{\partial Z_D}{\partial y_D}$$

$$
\begin{aligned}
&-\left\{\mathcal{N}_{CO_2,owyR}\frac{k_{oR}}{\mu_{oR}}\rho_{oR}g_{yR}\frac{p_{oR}Z_R}{y_R^2}\right\}\mathcal{N}_{CO_2,owyD}\frac{k_{oD}}{\mu_{oD}}\frac{\partial p_{oD}}{\partial y_D}\rho_{oD}g_{yD}\frac{\partial Z_D}{\partial y_D}\\
&+\left\{\mathcal{N}_{CO_2,owyR}\frac{1}{2}\frac{k_{wR}^2}{\mu_{wR}^2}\rho_{wR}^2g_{yR}^2\frac{Z_R^2}{y_R^2}\right\}\mathcal{N}_{CO_2,owyD}\frac{1}{2}\left(\frac{k_{wD}}{\mu_{wD}}\rho_{wD}g_{yD}\frac{\partial Z_D}{\partial y_D}\right)^2\\
&-\left\{\mathcal{N}_{CO_2,owyR}\frac{1}{2}\frac{k_{oR}^2}{\mu_{oR}^2}\rho_{oR}^2g_{yR}^2\frac{Z_R^2}{y_R^2}\right\}\mathcal{N}_{CO_2,owyD}\frac{1}{2}\left(\frac{k_{oD}}{\mu_{oD}}\rho_{oD}g_{yD}\frac{\partial Z_D}{\partial y_D}\right)^2\\
&+\left\{\mathcal{N}_{CO_2,owzR}h_{CO_2R}\right\}\mathcal{N}_{CO_2,owzD}h_{CO_2D}\\
&+\left\{\mathcal{N}_{CO_2,owzR}\frac{1}{2}\frac{k_{wR}^2}{\mu_{wR}^2}\frac{p_{wR}^2}{z_R^2}\right\}\mathcal{N}_{CO_2,owzD}\frac{1}{2}\left(\frac{k_{wD}}{\mu_{wD}}\frac{\partial p_{wD}}{\partial z_D}\right)^2\\
&-\left\{\mathcal{N}_{CO_2,owzR}\frac{1}{2}\frac{k_{oR}^2}{\mu_{oR}^2}\frac{p_{oR}^2}{z_R^2}\right\}\mathcal{N}_{CO_2,owzD}\frac{1}{2}\left(\frac{k_{oD}}{\mu_{oD}}\frac{\partial p_{oD}}{\partial z_D}\right)^2\\
&+\left\{\mathcal{N}_{CO_2,owzR}\frac{k_{wR}}{\mu_{wR}}\rho_{wR}g_{zR}\frac{p_{wR}Z_R}{z_R^2}\right\}\mathcal{N}_{CO_2,owzD}\frac{k_{wD}}{\mu_{wD}}\frac{\partial p_{wD}}{\partial z_D}\rho_{wD}g_{zD}\frac{\partial Z_D}{\partial z_D}\\
&-\left\{\mathcal{N}_{CO_2,owzR}\frac{k_{oR}}{\mu_{oR}}\rho_{oR}g_{zR}\frac{p_{oR}Z_R}{z_R^2}\right\}\mathcal{N}_{CO_2,owzD}\frac{k_{oD}}{\mu_{oD}}\frac{\partial p_{oD}}{\partial z_D}\rho_{oD}g_{zD}\frac{\partial Z_D}{\partial z_D}\\
&+\left\{\mathcal{N}_{CO_2,owzR}\frac{1}{2}\frac{k_{wR}^2}{\mu_{wR}^2}\rho_{wR}^2g_{zR}^2\frac{Z_R^2}{z_R^2}\right\}\mathcal{N}_{CO_2,owzD}\frac{1}{2}\left(\frac{k_{wD}}{\mu_{wD}}\rho_{wD}g_{zD}\frac{\partial Z_D}{\partial z_D}\right)^2\\
&-\left\{\mathcal{N}_{CO_2,owzR}\frac{1}{2}\frac{k_{oR}^2}{\mu_{oR}^2}\rho_{oR}^2g_{zR}^2\frac{Z_R^2}{z_R^2}\right\}\mathcal{N}_{CO_2,owzD}\frac{1}{2}\left(\frac{k_{oD}}{\mu_{oD}}\rho_{oD}g_{zD}\frac{\partial Z_D}{\partial z_D}\right)^2\\
&-\left\{C_{CO_2,oR}\rho_{oR}h_{CO_2R}\frac{k_{oR}}{\mu_{oR}}\frac{p_{oR}}{x_R^2}\right\}\frac{\partial}{\partial x_D}\left[C_{CO_2,oD}\rho_{oD}h_{CO_2D}\frac{k_{oD}}{\mu_{oD}}\frac{\partial p_{oD}}{\partial x_D}\right]\\
&-\left\{C_{CO_2,oR}\rho_{oR}^2h_{CO_2R}g_{xR}\frac{k_{oR}}{\mu_{oR}}\frac{Z_R}{x_R^2}\right\}\frac{\partial}{\partial x_D}\left[C_{CO_2,oD}\rho_{oD}^2h_{CO_2D}g_{xD}\frac{k_{oD}}{\mu_{oD}}\frac{\partial Z_D}{\partial x_D}\right]\\
&-\left\{C_{CO_2,oR}\rho_{oR}h_{CO_2R}\frac{k_{oR}}{\mu_{oR}}\frac{p_{oR}}{y_R^2}\right\}\frac{\partial}{\partial y_D}\left[C_{CO_2,oD}\rho_{oD}h_{CO_2D}\frac{k_{oD}}{\mu_{oD}}\frac{\partial p_{oD}}{\partial y_D}\right]\\
&-\left\{C_{CO_2,oR}\rho_{oR}^2h_{CO_2R}g_{y_R}\frac{k_{oD}}{\mu_{oD}}\frac{Z_R}{y_R^2}\right\}\frac{\partial}{\partial y_D}\left[C_{CO_2,oD}\rho_{oD}^2h_{CO_2D}g_{y_D}\frac{k_{oD}}{\mu_{oD}}\frac{\partial Z_D}{\partial y_D}\right]\\
&-\left\{C_{CO_2,oR}\rho_{oR}h_{CO_2R}\frac{k_{oR}}{\mu_{oR}}\frac{p_{oR}}{z_R^2}\right\}\frac{\partial}{\partial z_D}\left[C_{CO_2,oD}\rho_{oD}h_{CO_2D}\frac{k_{oD}}{\mu_{oD}}\frac{\partial p_{oD}}{\partial z_D}\right]\\
&-\left\{C_{CO_2,oR}\rho_{oR}^2h_{CO_2R}g_{zD}\frac{k_{oD}}{\mu_{oD}}\frac{Z_R}{z_R^2}\right\}\frac{\partial}{\partial z_D}\left[C_{CO_2,oD}\rho_{oD}^2h_{CO_2D}g_{zD}\frac{k_{oD}}{\mu_{oD}}\frac{\partial Z_D}{\partial z_D}\right]\\
&=\left\{\frac{\phi_R C_{CO_2,oR}\rho_{oR}S_{oR}U_{CO_2R}}{t_R}\right\}\frac{\partial}{\partial t_D}\left[\phi_D C_{CO_2,oD}\rho_{oD}S_{oD}U_{CO_2D}\right]
\end{aligned}
$$

$$+\left\{\frac{1}{2}\frac{\phi_R C_{CO_2,oR}\rho_{oR}S_{oR}}{t_R}\frac{k_{oR}^2}{\mu_{oR}^2}\frac{p_{oR}^2}{x_R^2}\right\}\frac{\partial}{\partial t_D}\left[\phi_D C_{CO_2,oD}\rho_{oD}S_{oD}\frac{k_{oD}^2}{\mu_{oD}^2}\left(\frac{\partial p_{oD}}{\partial x_D}\right)^2\right]$$

$$+\left\{\frac{\phi_R C_{CO_2,oR}\rho_{oR}^2 S_{oR}g_{xR}}{t_R}\frac{k_{oR}^2}{\mu_{oR}^2}\frac{p_{oR}Z_R}{x_R^2}\right\}\frac{\partial}{\partial t_D}\left[\phi_D C_{CO_2,oD}\rho_{oD}^2 S_{oD}g_{xD}\frac{k_{oD}^2}{\mu_{oD}^2}\frac{\partial p_{oD}}{\partial x_D}\frac{\partial Z_D}{\partial x_D}\right]$$

$$+\left\{\frac{1}{2}\frac{\phi_R C_{CO_2,oR}\rho_{oR}^3 S_{oR}g_{xR}^2}{t_R}\frac{k_{oR}^2}{\mu_{oR}^2}\frac{Z_R^2}{x_R^2}\right\}\frac{\partial}{\partial t_D}\left[\phi_D C_{CO_2,oD}\rho_{oD}^3 S_{oD}g_{xD}^2\frac{k_{oD}^2}{\mu_{oD}^2}\left(\frac{\partial Z_D}{\partial x_D}\right)^2\right]$$

$$+\left\{\frac{1}{2}\frac{\phi_R C_{CO_2,oR}\rho_{oR}S_{oR}}{t_R}\frac{k_{oR}^2}{\mu_{oR}^2}\frac{p_{oR}^2}{y_R^2}\right\}\frac{\partial}{\partial t_D}\left[\phi_D C_{CO_2,oD}\rho_{oD}S_{oD}\frac{k_{oD}^2}{\mu_{oD}^2}\left(\frac{\partial p_{oD}}{\partial y_D}\right)^2\right]$$

$$+\left\{\frac{\phi_R C_{CO_2,oR}\rho_{oR}^2 S_{oR}g_{yR}}{t_R}\frac{k_{oR}^2}{\mu_{oR}^2}\frac{p_{oR}Z_R}{y_R^2}\right\}\frac{\partial}{\partial t_D}\left[\phi_D C_{CO_2,oD}\rho_{oD}^2 S_{oD}g_{yD}\frac{k_{oD}^2}{\mu_{oD}^2}\frac{\partial p_{oD}}{\partial y_D}\frac{\partial Z_D}{\partial y_D}\right]$$

$$+\left\{\frac{1}{2}\frac{\phi_R C_{CO_2,oR}\rho_{oR}^3 S_{oR}g_{yR}^2}{t_R}\frac{k_{oR}^2}{\mu_{oR}^2}\frac{Z_R^2}{y_R^2}\right\}\frac{\partial}{\partial t_D}\left[\phi_D C_{CO_2,oD}\rho_{oD}^3 S_{oD}g_{yD}^2\frac{k_{oD}^2}{\mu_{oD}^2}\left(\frac{\partial Z_D}{\partial y_D}\right)^2\right]$$

$$+\left\{\frac{1}{2}\frac{\phi_R C_{CO_2,oR}\rho_{oR}S_{oR}}{t_R}\frac{k_{oR}^2}{\mu_{oR}^2}\frac{p_{oR}^2}{z_R^2}\right\}\frac{\partial}{\partial t_D}\left[\phi_D C_{CO_2,oD}\rho_{oD}S_{oD}\frac{k_{oD}^2}{\mu_{oD}^2}\left(\frac{\partial p_{oD}}{\partial z_D}\right)^2\right]$$

$$+\left\{\frac{\phi_R C_{CO_2,oR}\rho_{oR}^2 S_{oR}g_{zR}}{t_R}\frac{k_{oR}^2}{\mu_{oR}^2}\frac{p_{oR}Z_R}{z_R^2}\right\}\frac{\partial}{\partial t_D}\left[\phi_D C_{CO_2,oD}\rho_{oD}^2 S_{oD}g_{zD}\frac{k_{oD}^2}{\mu_{oD}^2}\frac{\partial p_{oD}}{\partial z_D}\frac{\partial Z_D}{\partial z_D}\right]$$

$$+\left\{\frac{1}{2}\frac{\phi_R C_{CO_2,oR}\rho_{oR}^3 S_{oR}g_{zR}^2}{t_R}\frac{k_{oR}^2}{\mu_{oR}^2}\frac{Z_R^2}{z_R^2}\right\}\frac{\partial}{\partial t_D}\left[\phi_D C_{CO_2,oD}\rho_{oD}^3 S_{oD}g_{zD}^2\frac{k_{oD}^2}{\mu_{oD}^2}\left(\frac{\partial Z_D}{\partial z_D}\right)^2\right]$$

B.3 - Entropy Balance for CO_2 in the Oil Phase in Dimensionless Form

$$-\left\{C_{CO_2,oR}\rho_{oR}s_{CO_2R}\frac{k_{oR}}{\mu_{oR}}\frac{p_{oR}}{x_R^2}\right\}\frac{\partial}{\partial x_D}\left[C_{CO_2,oD}\rho_{oD}s_{CO_2D}\frac{k_{oD}}{\mu_{oD}}\frac{\partial p_{oD}}{\partial x_D}\right]$$

$$-\left\{C_{CO_2,oR}\rho_{oR}^2 s_{CO_2R}g_{xR}\frac{k_{oR}}{\mu_{oR}}\frac{Z_R}{x_R^2}\right\}\frac{\partial}{\partial x_D}\left[C_{CO_2,oD}\rho_{oD}^2 s_{CO_2D}g_{xD}\frac{k_{oD}}{\mu_{oD}}\frac{\partial Z_D}{\partial x_D}\right]$$

$$-\left\{C_{CO_2,oR}\rho_{oR}s_{CO_2R}\frac{k_{oR}}{\mu_{oR}}\frac{p_{oR}}{y_R^2}\right\}\frac{\partial}{\partial y_D}\left[C_{CO_2,oD}\rho_{oD}s_{CO_2D}\frac{k_{oD}}{\mu_{oD}}\frac{\partial p_{oD}}{\partial y_D}\right]$$

$$-\left\{C_{CO_2,oR}\rho_{oR}^2 s_{CO_2R}g_{yR}\frac{k_{oR}}{\mu_{oR}}\frac{Z_R}{y_R^2}\right\}\frac{\partial}{\partial y_D}\left[C_{CO_2,oD}\rho_{oD}^2 s_{CO_2D}g_{yD}\frac{k_{oD}}{\mu_{oD}}\frac{\partial Z_D}{\partial y_D}\right]$$

$$-\left\{C_{CO_2,oR}\rho_{oR}\mathfrak{s}_{CO_2R}\frac{k_{oR}}{\mu_{oR}}\frac{p_{oR}}{z_R^2}\right\}\frac{\partial}{\partial z_D}\left[C_{CO_2,oD}\rho_{oD}\mathfrak{s}_{CO_2D}\frac{k_{oD}}{\mu_{oD}}\frac{\partial p_{oD}}{\partial z_D}\right]$$

$$-\left\{C_{CO_2,oR}\rho_{oR}^2\mathfrak{s}_{CO_2R}g_{zR}\frac{k_{oR}}{\mu_{oR}}\frac{Z_R}{z_R^2}\right\}\frac{\partial}{\partial z_D}\left[C_{CO_2,oD}\rho_{oD}^2\mathfrak{s}_{CO_2D}g_{zD}\frac{k_{oD}}{\mu_{oD}}\frac{\partial Z_D}{\partial z_D}\right]$$

$$+\left\{\frac{\phi_R S_{oR}\mathfrak{D}_{LoR}}{T_R}\eta_{CO_2,oR}\frac{C_{CO_2,oR}\rho_{oR}}{x_R^2}\right\}\frac{\partial}{\partial x_D}\left[\frac{\phi_D S_{oD}\mathfrak{D}_{LoD}}{T_D}\eta_{CO_2,oD}\frac{\partial}{\partial x_D}\left(C_{CO_2,oD}\rho_{oD}\right)\right]$$

$$+\left\{\frac{\phi_R S_{oR}\mathfrak{D}^*_{LCO_2,oR}}{T_R}\eta_{CO_2,oR}\frac{C_{CO_2,oR}\rho_{oR}}{x_R^2}\right\}\bullet$$

$$\frac{\partial}{\partial x_D}\left[\frac{\phi_D S_{oD}\mathfrak{D}^*_{LCO_2,oD}}{T_D}\eta_{CO_2,oD}\frac{\partial}{\partial x_D}\left(C_{CO_2,oD}\rho_{oD}\right)\right]$$

$$+\left\{\frac{\phi_R S_{oR}\mathfrak{D}_{ToR}}{T_R}\eta_{CO_2,oR}\frac{C_{CO_2,oR}\rho_{oR}}{y_R^2}\right\}\frac{\partial}{\partial y_D}\left[\frac{\phi_D S_{oD}\mathfrak{D}_{ToD}}{T_D}\eta_{CO_2,oD}\frac{\partial}{\partial y_D}\left(C_{CO_2,oD}\rho_{oD}\right)\right]$$

$$+\left\{\frac{\phi_R S_{oR}\mathfrak{D}^*_{TCO_2,oR}}{T_R}\eta_{CO_2,oR}\frac{C_{CO_2,oR}\rho_{oR}}{y_R^2}\right\}\bullet$$

$$\frac{\partial}{\partial y_D}\left[\frac{\phi_D S_{oD}\mathfrak{D}^*_{TCO_2,oD}}{T_D}\eta_{CO_2,oD}\frac{\partial}{\partial y_D}\left(C_{CO_2,oD}\rho_{oD}\right)\right]$$

$$+\left\{\frac{\phi_R S_{oR}\mathfrak{D}_{ToR}}{T_R}\eta_{CO_2,oR}\frac{C_{CO_2,oR}\rho_{oR}}{z_R^2}\right\}\frac{\partial}{\partial z_D}\left[\frac{\phi_D S_{oD}\mathfrak{D}_{ToD}}{T_D}\eta_{CO_2,oD}\frac{\partial}{\partial z_D}\left(C_{CO_2,oD}\rho_{oD}\right)\right]$$

$$+\left\{\frac{\phi_R S_{oR}\mathfrak{D}^*_{TCO_2,oR}}{T_R}\eta_{CO_2,oR}\frac{C_{CO_2,oR}\rho_{oR}}{z_R^2}\right\}\bullet$$

$$\frac{\partial}{\partial z_D}\left[\frac{\phi_D S_{oD}\mathfrak{D}^*_{TCO_2,oD}}{T_D}\eta_{CO_2,oD}\frac{\partial}{\partial z_D}\left(C_{CO_2,oD}\rho_{oD}\right)\right]$$

$$-\left\{C_{CO_2,oR}\rho_{oR}\frac{h_{CO_2R}}{T_R}\frac{k_{oR}}{\mu_{oR}}\frac{p_{oR}}{x_R^2}\right\}\frac{\partial}{\partial x_D}\left[C_{CO_2,oD}\rho_{oD}\frac{h_{CO_2D}}{T_D}\frac{k_{oD}}{\mu_{oD}}\frac{\partial p_{oD}}{\partial x_D}\right]$$

$$-\left\{C_{CO_2,oR}\rho_{oR}^2 g_{xR}\frac{h_{CO_2R}}{T_R}\frac{k_{oR}}{\mu_{oR}}\frac{Z_R}{x_R^2}\right\}\frac{\partial}{\partial x_D}\left[C_{CO_2,oD}\rho_{oD}^2 g_{xD}\frac{h_{CO_2D}}{T_D}\frac{k_{oD}}{\mu_{oD}}\frac{\partial Z_D}{\partial x_D}\right]$$

$$-\left\{C_{CO_2,oR}\rho_{oR}\frac{h_{CO_2R}}{T_R}\frac{k_{oR}}{\mu_{oR}}\frac{p_{oR}}{y_R^2}\right\}\frac{\partial}{\partial y_D}\left[C_{CO_2,oD}\rho_{oD}\frac{h_{CO_2D}}{T_D}\frac{k_{oD}}{\mu_{oD}}\frac{\partial p_{oD}}{\partial y_D}\right]$$

$$-\left\{C_{CO_2,oR}\rho_{oR}^2 g_{yR}\frac{h_{CO_2R}}{T_R}\frac{k_{oR}}{\mu_{oR}}\frac{Z_R}{y_R^2}\right\}\frac{\partial}{\partial y_D}\left[C_{CO_2,oD}\rho_{oD}^2 g_{yD}\frac{h_{CO_2D}}{T_D}\frac{k_{oD}}{\mu_{oD}}\frac{\partial Z_D}{\partial y_D}\right]$$

$$-\left\{C_{CO_2,oR}\rho_{oR}\frac{h_{CO_2R}}{T_R}\frac{k_{oR}}{\mu_{oR}}\frac{p_{oR}}{z_R^2}\right\}\frac{\partial}{\partial z_D}\left[C_{CO_2,oD}\rho_{oD}\frac{h_{CO_2D}}{T_D}\frac{k_{oD}}{\mu_{oD}}\frac{\partial p_{oD}}{\partial z_D}\right]$$

$$-\left\{C_{CO_2,oR}\rho_{oR}^2 g_{zR}\frac{h_{CO_2R}}{T_R}\frac{k_{oR}}{\mu_{oR}}\frac{Z_R}{z_R^2}\right\}\frac{\partial}{\partial z_D}\left[C_{CO_2,oD}\rho_{oD}^2 g_{zD}\frac{h_{CO_2D}}{T_D}\frac{k_{oD}}{\mu_{oD}}\frac{\partial Z_D}{\partial z_D}\right]$$

$$-\left\{C_{CO_2,oR}\rho_{oR}h_{CO_2R}\frac{k_{oR}}{\mu_{oR}}\frac{p_{oR}}{x_R^2}\frac{1}{T_R}\right\}C_{CO_2,oD}\rho_{oD}h_{CO_2D}\frac{k_{oD}}{\mu_{oD}}\frac{\partial p_{oD}}{\partial x_D}\frac{\partial}{\partial x_D}\left(\frac{1}{T_D}\right)$$

$$-\left\{C_{CO_2,oR}\rho_{oR}^2 h_{CO_2R}g_{xR}\frac{k_{oR}}{\mu_{oR}}\frac{Z_R}{x_R^2}\frac{1}{T_R}\right\}\frac{1}{T_R}C_{CO_2,oD}\rho_{oD}^2 h_{CO_2D}g_{xD}\frac{k_{oD}}{\mu_{oD}}\frac{\partial Z_D}{\partial x_D}\frac{\partial}{\partial x_D}\left(\frac{1}{T_D}\right)$$

$$-\left\{C_{CO_2,oR}\rho_{oR}h_{CO_2R}\frac{k_{oR}}{\mu_{oR}}\frac{p_{oR}}{y_R^2}\frac{1}{T_R}\right\}C_{CO_2,oD}\rho_{oD}h_{CO_2D}\frac{k_{oD}}{\mu_{oD}}\frac{\partial p_{oD}}{\partial y_D}\frac{\partial}{\partial y_D}\left(\frac{1}{T_D}\right)$$

$$-\left\{C_{CO_2,oR}\rho_{oR}^2 h_{CO_2R}g_{yR}\frac{k_{oR}}{\mu_{oR}}\frac{Z_R}{y_R^2}\frac{1}{T_R}\right\}C_{CO_2,oD}\rho_{oD}^2 h_{CO_2D}g_{yD}\frac{k_{oD}}{\mu_{oD}}\frac{\partial Z_D}{\partial y_D}\frac{\partial}{\partial y_D}\left(\frac{1}{T_D}\right)$$

$$-\left\{C_{CO_2,oR}\rho_{oR}h_{CO_2R}\frac{k_{oR}}{\mu_{oR}}\frac{p_{oR}}{z_R^2}\frac{1}{T_R}\right\}C_{CO_2,oD}\rho_{oD}h_{CO_2D}\frac{k_{oD}}{\mu_{oD}}\frac{\partial p_{oD}}{\partial z_D}\frac{\partial}{\partial z_D}\left(\frac{1}{T_D}\right)$$

$$-\left\{C_{CO_2,oR}\rho_{oR}^2 h_{CO_2R}g_{zR}\frac{k_{oR}}{\mu_{oR}}\frac{Z_R}{z_R^2}\frac{1}{T_R}\right\}C_{CO_2,oD}\rho_{oD}^2 h_{CO_2D}g_{zD}\frac{k_{oD}}{\mu_{oD}}\frac{\partial Z_D}{\partial z_D}\frac{\partial}{\partial z_D}\left(\frac{1}{T_D}\right)$$

$$-\left\{\frac{C_{CO_2,oR}\rho_{oR}k_{oR}}{T_R\mu_{oR}}g_{xR}\frac{p_{oR}}{x_R}\right\}\frac{C_{CO_2,oD}\rho_{oD}k_{wD}}{T_D\mu_{oD}}g_{xD}\frac{\partial p_{oD}}{\partial x_D}$$

$$-\left\{\frac{C_{CO_2,oR}\rho_{oR}^2 k_{oR}}{T_R\mu_{oR}}g_{xR}^2\frac{Z_R}{x_R}\right\}\frac{C_{CO_2,oD}\rho_{oD}^2 k_{oD}}{T_D\mu_{oD}}g_{xD}^2\frac{\partial Z_D}{\partial x_D}$$

$$-\left\{\frac{C_{CO_2,oR}\rho_{oR}k_{oR}}{T_R\mu_{oR}}g_{yR}\frac{p_{oR}}{y_R}\right\}\frac{C_{CO_2,oD}\rho_{oD}k_{wD}}{T_D\mu_{oD}}g_{yD}\frac{\partial p_{oD}}{\partial y_D}$$

$$-\left\{\frac{C_{CO_2,oR}\rho_{oR}^2 k_{oR}}{T_R\mu_{oR}}g_{yR}^2\frac{Z_R}{y_R}\right\}\frac{C_{CO_2,oD}\rho_{oD}^2 k_{oD}}{T_D\mu_{oD}}g_{yD}^2\frac{\partial Z_D}{\partial y_D}$$

$$-\left\{\frac{C_{CO_2,oR}\rho_{oR}k_{oR}}{T_R\mu_{oR}}g_{zR}\frac{p_{oR}}{z_R}\right\}\frac{C_{CO_2,oD}\rho_{oD}k_{wD}}{T_D\mu_{oD}}g_{zD}\frac{\partial p_{oD}}{\partial z_D}$$

$$-\left\{\frac{C_{CO_2,oR}\rho_{oR}^2 k_{oR}}{T_R\mu_{oR}}g_{zR}^2\frac{Z_R}{z_R}\right\}\frac{C_{CO_2,oD}\rho_{oD}^2 k_{oD}}{T_D\mu_{oD}}g_{zD}^2\frac{\partial Z_D}{\partial z_D}$$

$$-\left\{C_{CO_2,oR}\rho_{oR}\frac{k_{oR}}{\mu_{oR}}\frac{p_{oR}}{x_R^2}\frac{\eta_{CO_2,oR}}{T_R}\right\}C_{CO_2,oD}\rho_{oD}\frac{k_{oD}}{\mu_{oD}}\frac{\partial p_{oD}}{\partial x_D}\frac{\partial}{\partial x_D}\left(\frac{\eta_{CO_2,oD}}{T_D}\right)$$

$$-\left\{C_{CO_2,oR}\rho_{oR}^2 g_{xR}\frac{k_{oR}}{\mu_{oR}}\frac{Z_R}{x_R^2}\frac{\eta_{CO_2,oR}}{T_R}\right\}C_{CO_2,oD}\rho_{oD}^2 g_{xD}\frac{k_{oD}}{\mu_{oD}}\frac{\partial Z_D}{\partial x_D}\frac{\partial}{\partial x_D}\left(\frac{\eta_{CO_2,oD}}{T_D}\right)$$

$$-\left\{C_{CO_2,oR}\rho_{oR}\frac{k_{oR}}{\mu_{oR}}\frac{p_{oR}}{y_R^2}\frac{\eta_{CO_2,oR}}{T_R}\right\}C_{CO_2,oD}\rho_{oD}\frac{k_{oD}}{\mu_{oD}}\frac{\partial p_{oD}}{\partial y_D}\frac{\partial}{\partial y_D}\left(\frac{\eta_{CO_2,oD}}{T_D}\right)$$

$$-\left\{C_{CO_2,oR}\rho_{oR}^2 g_{yR}\frac{k_{oR}}{\mu_{oR}}\frac{Z_R}{y_R^2}\frac{\eta_{CO_2,oR}}{T_R}\right\}C_{CO_2,oD}\rho_{oD}^2 g_{yD}\frac{k_{oD}}{\mu_{oD}}\frac{\partial Z_D}{\partial y_D}\frac{\partial}{\partial y_D}\left(\frac{\eta_{CO_2,oD}}{T_D}\right)$$

$$-\left\{C_{CO_2,oR}\rho_{oR}\frac{k_{oR}}{\mu_{oR}}\frac{p_{oR}}{z_R^2}\frac{\eta_{CO_2,oR}}{T_R}\right\}C_{CO_2,oD}\rho_{oD}\frac{k_{oD}}{\mu_{oD}}\frac{\partial p_{oD}}{\partial z_D}\frac{\partial}{\partial z_D}\left(\frac{\eta_{CO_2,oD}}{T_D}\right)$$
$$-\left\{C_{CO_2,oR}\rho_{oR}^2 g_{zR}\frac{k_{oR}}{\mu_{oR}}\frac{Z_R}{z_R^2}\frac{\eta_{CO_2,oR}}{T_R}\right\}C_{CO_2,oD}\rho_{oD}^2 g_{zD}\frac{k_{oD}}{\mu_{oD}}\frac{\partial Z_D}{\partial z_D}\frac{\partial}{\partial z_D}\left(\frac{\eta_{CO_2,oD}}{T_D}\right)$$
$$+\left\{\mathcal{N}_{CO_2,ogxR}g_{CO_2R}\right\}\mathcal{N}_{CO_2,ogxD}g_{CO_2D}+\left\{\mathcal{N}_{CO_2,ogyR}g_{CO_2R}\right\}\mathcal{N}_{CO_2,ogyD}g_{CO_2D}$$
$$+\left\{\mathcal{N}_{CO_2,ogzR}g_{CO_2R}\right\}\mathcal{N}_{CO_2,ogzD}g_{CO_2D}+\left\{\mathcal{N}_{CO_2,owxR}g_{CO_2R}\right\}\mathcal{N}_{CO_2,owxD}g_{CO_2D}$$
$$+\left\{\mathcal{N}_{CO_2,owyR}g_{CO_2R}\right\}\mathcal{N}_{CO_2,owyD}g_{CO_2D}+\left\{\mathcal{N}_{CO_2,owzR}g_{CO_2R}\right\}\mathcal{N}_{CO_2,owzD}g_{CO_2D}$$
$$+\left\{\mathcal{N}_{CO_2,ogxR}\frac{1}{2T_R}\frac{k_{gR}^2}{\mu_{gR}^2}\frac{p_{gR}^2}{x_R^2}\right\}\mathcal{N}_{CO_2,ogxD}\frac{1}{2T_D}\frac{k_{gD}^2}{\mu_{gD}^2}\left(\frac{\partial p_{gD}}{\partial x_D}\right)^2$$
$$-\left\{\mathcal{N}_{CO_2,ogxR}\frac{1}{2T_R}\frac{k_{oR}^2}{\mu_{oR}^2}\frac{p_{oR}^2}{x_R^2}\right\}\mathcal{N}_{CO_2,ogxD}\frac{1}{2T_D}\frac{k_{oD}^2}{\mu_{oD}^2}\left(\frac{\partial p_{oD}}{\partial x_D}\right)^2$$
$$+\left\{\mathcal{N}_{CO_2,ogyR}\frac{1}{2T_R}\frac{k_{gR}^2}{\mu_{gR}^2}\frac{p_{gR}^2}{y_R^2}\right\}\mathcal{N}_{CO_2,ogyD}\frac{1}{2T_D}\frac{k_{gD}^2}{\mu_{gD}^2}\left(\frac{\partial p_{gD}}{\partial y_D}\right)^2$$
$$-\left\{\mathcal{N}_{CO_2,ogyR}\frac{1}{2T_R}\frac{k_{oR}^2}{\mu_{oR}^2}\frac{p_{oR}^2}{y_R^2}\right\}\mathcal{N}_{CO_2,ogyD}\frac{1}{2T_D}\frac{k_{oD}^2}{\mu_{oD}^2}\left(\frac{\partial p_{oD}}{\partial y_D}\right)^2$$
$$+\left\{\mathcal{N}_{CO_2,ogzR}\frac{1}{2T_R}\frac{k_{gR}^2}{\mu_{gR}^2}\frac{p_{gR}^2}{z_R^2}\right\}\mathcal{N}_{CO_2,ogzD}\frac{1}{2T_D}\frac{k_{gD}^2}{\mu_{gD}^2}\left(\frac{\partial p_{gD}}{\partial z_D}\right)^2$$
$$-\left\{\mathcal{N}_{CO_2,ogzR}\frac{1}{2T_R}\frac{k_{oR}^2}{\mu_{oR}^2}\frac{p_{oR}^2}{z_R^2}\right\}\mathcal{N}_{CO_2,ogzD}\frac{1}{2T_D}\frac{k_{oD}^2}{\mu_{oD}^2}\left(\frac{\partial p_{oD}}{\partial z_D}\right)^2$$
$$+\left\{\mathcal{N}_{CO_2,ogxR}\frac{1}{T_R}\frac{k_{gR}^2}{\mu_{gR}^2}\rho_{gR}g_{xR}\frac{p_{gR}Z_R}{x_R^2}\right\}\mathcal{N}_{CO_2,ogxD}\frac{1}{T_D}\frac{k_{gD}^2}{\mu_{gD}^2}\rho_{gD}g_{xD}\frac{\partial p_{gD}}{\partial x_D}\frac{\partial Z_D}{\partial x_D}$$
$$-\left\{\mathcal{N}_{CO_2,ogxR}\frac{1}{T_R}\frac{k_{oR}^2}{\mu_{oR}^2}\rho_{oR}g_{xR}\frac{p_{oR}Z_R}{x_R^2}\right\}\mathcal{N}_{CO_2,ogxD}\frac{1}{T_D}\frac{k_{oD}^2}{\mu_{oD}^2}\rho_{oD}g_{xD}\frac{\partial p_{oD}}{\partial x_D}\frac{\partial Z_D}{\partial x_D}$$
$$+\left\{\mathcal{N}_{CO_2,ogyR}\frac{1}{T_R}\frac{k_{gR}^2}{\mu_{gR}^2}\rho_{gR}g_{yR}\frac{p_{gR}Z_R}{y_R^2}\right\}\mathcal{N}_{CO_2,ogyD}\frac{1}{T_D}\frac{k_{gD}^2}{\mu_{gD}^2}\rho_{gD}g_{yD}\frac{\partial p_{gD}}{\partial y_D}\frac{\partial Z_D}{\partial y_D}$$
$$-\left\{\mathcal{N}_{CO_2,ogyR}\frac{1}{T_R}\frac{k_{oR}^2}{\mu_{oR}^2}\rho_{oR}g_{yR}\frac{p_{oR}Z_R}{y_R^2}\right\}\mathcal{N}_{CO_2,ogyD}\frac{1}{T_D}\frac{k_{oD}^2}{\mu_{oD}^2}\rho_{oD}g_{yD}\frac{\partial p_{oD}}{\partial y_D}\frac{\partial Z_D}{\partial y_D}$$
$$+\left\{\mathcal{N}_{CO_2,ogzR}\frac{1}{T_R}\frac{k_{gR}^2}{\mu_{gR}^2}\rho_{gR}g_{zR}\frac{p_{gR}Z_R}{z_R^2}\right\}\mathcal{N}_{CO_2,ogzD}\frac{1}{T_D}\frac{k_{gD}^2}{\mu_{gD}^2}\rho_{gD}g_{zD}\frac{\partial p_{gD}}{\partial z_D}\frac{\partial Z_D}{\partial z_D}$$
$$-\left\{\mathcal{N}_{CO_2,ogzR}\frac{1}{T_R}\frac{k_{oR}^2}{\mu_{oR}^2}\rho_{oR}g_{zR}\frac{p_{oR}Z_R}{z_R^2}\right\}\mathcal{N}_{CO_2,ogzD}\frac{1}{T_D}\frac{k_{oD}^2}{\mu_{oD}^2}\rho_{oD}g_{zD}\frac{\partial p_{oD}}{\partial z_D}\frac{\partial Z_D}{\partial z_D}$$

$$+\left\{\mathcal{N}_{CO_2,ogxR}\frac{1}{2T_R}\frac{k_{gR}^2}{\mu_{gR}^2}\rho_{gR}^2 g_{xR}^2\frac{Z_R^2}{x_R^2}\right\}\mathcal{N}_{CO_2,ogxD}\frac{1}{2T_D}\frac{k_{gD}^2}{\mu_{gD}^2}\rho_{gD}^2 g_{xD}^2\left(\frac{\partial Z_D}{\partial x_D}\right)^2$$

$$-\left\{\mathcal{N}_{CO_2,ogxR}\frac{1}{2T_R}\frac{k_{oR}^2}{\mu_{oR}^2}\rho_{oR}^2 g_{xR}^2\frac{Z_R^2}{x_R^2}\right\}\mathcal{N}_{CO_2,ogxD}\frac{1}{2T_D}\frac{k_{oD}^2}{\mu_{oD}^2}\rho_{oD}^2 g_{xD}^2\left(\frac{\partial Z_D}{\partial x_D}\right)^2$$

$$+\left\{\mathcal{N}_{CO_2,ogyR}\frac{1}{2T_R}\frac{k_{gR}^2}{\mu_{gR}^2}\rho_{gR}^2 g_{yR}^2\frac{Z_R^2}{y_R^2}\right\}\mathcal{N}_{CO_2,ogyD}\frac{1}{2T_D}\frac{k_{gD}^2}{\mu_{gD}^2}\rho_{gD}^2 g_{yD}^2\left(\frac{\partial Z_D}{\partial y_D}\right)^2$$

$$-\left\{\mathcal{N}_{CO_2,ogyR}\frac{1}{2T_R}\frac{k_{oR}^2}{\mu_{oR}^2}\rho_{oR}^2 g_{yR}^2\frac{Z_R^2}{y_R^2}\right\}\mathcal{N}_{CO_2,ogyD}\frac{1}{2T_D}\frac{k_{oD}^2}{\mu_{oD}^2}\rho_{oD}^2 g_{yD}^2\left(\frac{\partial Z_D}{\partial y_D}\right)^2$$

$$+\left\{\mathcal{N}_{CO_2,ogzR}\frac{1}{2T_R}\frac{k_{gR}^2}{\mu_{gR}^2}\rho_{gR}^2 g_{zR}^2\frac{Z_R^2}{z_R^2}\right\}\mathcal{N}_{CO_2,ogzD}\frac{1}{2T_D}\frac{k_{gD}^2}{\mu_{gD}^2}\rho_{gD}^2 g_{zD}^2\left(\frac{\partial Z_D}{\partial z_D}\right)^2$$

$$-\left\{\mathcal{N}_{CO_2,ogzR}\frac{1}{2T_R}\frac{k_{oR}^2}{\mu_{oR}^2}\rho_{oR}^2 g_{zR}^2\frac{Z_R^2}{z_R^2}\right\}\mathcal{N}_{CO_2,ogzD}\frac{1}{2T_D}\frac{k_{oD}^2}{\mu_{oD}^2}\rho_{oD}^2 g_{zD}^2\left(\frac{\partial Z_D}{\partial z_D}\right)^2$$

$$+\left\{\mathcal{N}_{CO_2,owxR}\frac{1}{2T_R}\frac{k_{wR}^2}{\mu_{wR}^2}\frac{p_{wR}^2}{x_R^2}\right\}\mathcal{N}_{CO_2,owxD}\frac{1}{2T_D}\frac{k_{wD}^2}{\mu_{wD}^2}\left(\frac{\partial p_{wD}}{\partial x_D}\right)^2$$

$$-\left\{\mathcal{N}_{CO_2,owxR}\frac{1}{2T_R}\frac{k_{oR}^2}{\mu_{oR}^2}\frac{p_{oR}^2}{x_R^2}\right\}\mathcal{N}_{CO_2,owxD}\frac{1}{2T_D}\frac{k_{oD}^2}{\mu_{oD}^2}\left(\frac{\partial p_{oD}}{\partial x_D}\right)^2$$

$$+\left\{\mathcal{N}_{CO_2,owyR}\frac{1}{2T_R}\frac{k_{wR}^2}{\mu_{wR}^2}\frac{p_{wR}^2}{y_R^2}\right\}\mathcal{N}_{CO_2,owyD}\frac{1}{2T_D}\frac{k_{wD}^2}{\mu_{wD}^2}\left(\frac{\partial p_{wD}}{\partial y_D}\right)^2$$

$$-\left\{\mathcal{N}_{CO_2,owyR}\frac{1}{2T_R}\frac{k_{oR}^2}{\mu_{oR}^2}\frac{p_{oR}^2}{y_R^2}\right\}\mathcal{N}_{CO_2,owyD}\frac{1}{2T_D}\frac{k_{oD}^2}{\mu_{oD}^2}\left(\frac{\partial p_{oD}}{\partial y_D}\right)^2$$

$$+\left\{\mathcal{N}_{CO_2,owzR}\frac{1}{2T_R}\frac{k_{wR}^2}{\mu_{wR}^2}\frac{p_{wR}^2}{z_R^2}\right\}\mathcal{N}_{CO_2,owzD}\frac{1}{2T_D}\frac{k_{wD}^2}{\mu_{wD}^2}\left(\frac{\partial p_{wD}}{\partial z_D}\right)^2$$

$$-\left\{\mathcal{N}_{CO_2,owzR}\frac{1}{2T_R}\frac{k_{oR}^2}{\mu_{oR}^2}\frac{p_{oR}^2}{z_R^2}\right\}\mathcal{N}_{CO_2,owzD}\frac{1}{2T_D}\frac{k_{oD}^2}{\mu_{oD}^2}\left(\frac{\partial p_{oD}}{\partial z_D}\right)^2$$

$$+\left\{\mathcal{N}_{CO_2,owxR}\frac{1}{T_R}\frac{k_{wR}^2}{\mu_{wR}^2}\rho_{wR}g_{xR}\frac{p_{wR}Z_R}{x_R^2}\right\}\mathcal{N}_{CO_2,owxD}\frac{1}{T_D}\frac{k_{wD}^2}{\mu_{wD}^2}\rho_{wD}g_{xD}\frac{\partial p_{wD}}{\partial x_D}\frac{\partial Z_D}{\partial x_D}$$

$$-\left\{\mathcal{N}_{CO_2,owxR}\frac{1}{T_R}\frac{k_{oR}^2}{\mu_{oR}^2}\rho_{oR}g_{xR}\frac{p_{oR}Z_R}{x_R^2}\right\}\mathcal{N}_{CO_2,owxD}\frac{1}{T_D}\frac{k_{oD}^2}{\mu_{oD}^2}\rho_{oD}g_{xD}\frac{\partial p_{oD}}{\partial x_D}\frac{\partial Z_D}{\partial x_D}$$

$$+\left\{\mathcal{N}_{CO_2,owyR}\frac{1}{T_R}\frac{k_{wR}^2}{\mu_{wR}^2}\rho_{wR}g_{yR}\frac{p_{wR}Z_R}{y_R^2}\right\}\mathcal{N}_{CO_2,owyD}\frac{1}{T_D}\frac{k_{wD}^2}{\mu_{wD}^2}\rho_{wD}g_{yD}\frac{\partial p_{wD}}{\partial y_D}\frac{\partial Z_D}{\partial y_D}$$

$$-\left\{\mathcal{N}_{CO_2,owyR}\frac{1}{T_R}\frac{k_{oR}^2}{\mu_{oR}^2}\rho_{oR}g_{yR}\frac{p_{oR}Z_R}{y_R^2}\right\}\mathcal{N}_{CO_2,owyD}\frac{1}{T_D}\frac{k_{oD}^2}{\mu_{oD}^2}\rho_{oD}g_{yD}\frac{\partial p_{oD}}{\partial y_D}\frac{\partial Z_D}{\partial y_D}$$

$$
\begin{aligned}
&+\left\{\mathcal{N}_{CO_2,owzR}\frac{1}{T_R}\frac{k_{wR}^2}{\mu_{wR}^2}\rho_{wR}g_{zR}\frac{p_{wR}Z_R}{z_R^2}\right\}\mathcal{N}_{CO_2,owzD}\frac{1}{T_D}\frac{k_{wD}^2}{\mu_{wD}^2}\rho_{wD}g_{zD}\frac{\partial p_{wD}}{\partial z_D}\frac{\partial Z_D}{\partial z_D}\\
&-\left\{\mathcal{N}_{CO_2,owzR}\frac{1}{T_R}\frac{k_{oR}^2}{\mu_{oR}^2}\rho_{oR}g_{zR}\frac{p_{oR}Z_R}{z_R^2}\right\}\mathcal{N}_{CO_2,owzD}\frac{1}{T_D}\frac{k_{oD}^2}{\mu_{oD}^2}\rho_{oD}g_{zD}\frac{\partial p_{oD}}{\partial z_D}\frac{\partial Z_D}{\partial z_D}\\
&+\left\{\mathcal{N}_{CO_2,owxR}\frac{1}{2T_R}\frac{k_{wR}^2}{\mu_{wR}^2}\rho_{wR}^2g_{xR}^2\frac{Z_R^2}{x_R^2}\right\}\mathcal{N}_{CO_2,owxD}\frac{1}{2T_D}\frac{k_{wD}^2}{\mu_{wD}^2}\rho_{wD}^2g_{xD}^2\left(\frac{\partial Z_D}{\partial x_D}\right)^2\\
&-\left\{\mathcal{N}_{CO_2,owxR}\frac{1}{2T_R}\frac{k_{oR}^2}{\mu_{oR}^2}\rho_{oR}^2g_{xR}^2\frac{Z_R^2}{x_R^2}\right\}\mathcal{N}_{CO_2,owxD}\frac{1}{2T_D}\frac{k_{oD}^2}{\mu_{oD}^2}\rho_{oD}^2g_{xD}^2\left(\frac{\partial Z_D}{\partial x_D}\right)^2\\
&+\left\{\mathcal{N}_{CO_2,owyR}\frac{1}{2T_R}\frac{k_{wR}^2}{\mu_{wR}^2}\rho_{wR}^2g_{yR}^2\frac{Z_R^2}{y_R^2}\right\}\mathcal{N}_{CO_2,owyD}\frac{1}{2T_D}\frac{k_{wD}^2}{\mu_{wD}^2}\rho_{wD}^2g_{yD}^2\left(\frac{\partial Z_D}{\partial y_D}\right)^2\\
&-\left\{\mathcal{N}_{CO_2,owyR}\frac{1}{2T_R}\frac{k_{oR}^2}{\mu_{oR}^2}\rho_{oR}^2g_{yR}^2\frac{Z_R^2}{y_R^2}\right\}\mathcal{N}_{CO_2,owyD}\frac{1}{2T_D}\frac{k_{oD}^2}{\mu_{oD}^2}\rho_{oD}^2g_{yD}^2\left(\frac{\partial Z_D}{\partial y_D}\right)^2\\
&+\left\{\mathcal{N}_{CO_2,owzR}\frac{1}{2T_R}\frac{k_{wR}^2}{\mu_{wR}^2}\rho_{wR}^2g_{zR}^2\frac{Z_R^2}{z_R^2}\right\}\mathcal{N}_{CO_2,owzD}\frac{1}{2T_D}\frac{k_{wD}^2}{\mu_{wD}^2}\rho_{wD}^2g_{zD}^2\left(\frac{\partial Z_D}{\partial z_D}\right)^2\\
&-\left\{\mathcal{N}_{CO_2,owzR}\frac{1}{2T_R}\frac{k_{oR}^2}{\mu_{oR}^2}\rho_{oR}^2g_{zR}^2\frac{Z_R^2}{z_R^2}\right\}\mathcal{N}_{CO_2,owzD}\frac{1}{2T_D}\frac{k_{oD}^2}{\mu_{oD}^2}\rho_{oD}^2g_{zD}^2\left(\frac{\partial Z_D}{\partial z_D}\right)^2\\
&=\left\{\frac{\phi_R S_{oR}\rho_{oR}C_{CO_2,oR}g_{CO_2R}}{t_R}\right\}\frac{\partial}{\partial t_D}\left(\phi_D S_{oD}\rho_{oD}C_{CO_2,oD}g_{CO_2D}\right)
\end{aligned}
$$

APPENDIX C

DERIVATION OF THE RELAXED SCALING GROUPS

For the two approaches, the method of deriving a relaxed set of similarity groups is similar. Based on the assumption made in each approach, the terms corresponding to these assumptions are deleted from the governing partial differential equations. Each equation is then divided by one of its own remaining coefficients to yield the dimensionless form of the equation. The coefficients represent the relaxed set of similarity groups which can subsequently be reduced to their simplest form. The constitutive relationships, constraints, and initial and boundary conditions are treated in a similar manner.

C.1 - Approach No. 1

For approach no. 1, the effects of gravity and transverse and longitudinal dispersion are assumed to be neglible. For the sake of simplicity the following model for diffusion in porous media was adopted[29].

$$\mathcal{D}^*_{\text{eff}} = \frac{\mathcal{D}^*}{F\phi}. \qquad \text{(C.1)}$$

Mass Balance for CO_2 in the Oil Phase

$$\begin{aligned}
&\frac{C_{CO_2,oR}\rho_{oR}k_{oR}p_{oR}}{\mu_{oR}x_R^2}\frac{\partial}{\partial x_D}\left[C_{CO_2,oD}\frac{\rho_{oD}}{\mu_{oD}}k_{oD}\frac{\partial p_{oD}}{\partial x_D}\right] \\
&+\frac{S_{oR}C_{CO_2,oR}\rho_{oR}\mathcal{D}^*_{CO_2,oR}}{F_R x_R^2}\frac{\partial}{\partial x_D}\left[S_{oD}\frac{\mathcal{D}^*_{CO_2,oD}}{F_D}\frac{\partial}{\partial x_D}\left(C_{CO_2,oD}\rho_{oD}\right)\right] \\
&+\frac{C_{CO_2,oR}\rho_{oR}k_{oR}p_{oR}}{\mu_{oR}y_R^2}\frac{\partial}{\partial y_D}\left[C_{CO_2,oD}\frac{\rho_{oD}}{\mu_{oD}}k_{oD}\frac{\partial p_{oD}}{\partial y_D}\right] \\
&+\frac{S_{oR}C_{CO_2,oR}\rho_{oR}\mathcal{D}^*_{CO_2,oR}}{F_R y_R^2}\frac{\partial}{\partial y_D}\left[S_{oD}\frac{\mathcal{D}^*_{CO_2,oD}}{F_D}\frac{\partial}{\partial y_D}\left(C_{CO_2,oD}\rho_{oD}\right)\right] \\
&+\frac{C_{CO_2,oR}\rho_{oR}k_{oR}p_{oR}}{\mu_{oR}z_R^2}\frac{\partial}{\partial z_D}\left[C_{CO_2,oD}\frac{\rho_{oD}}{\mu_{oD}}k_{oD}\frac{\partial p_{oD}}{\partial z_D}\right]
\end{aligned}$$

$$
\begin{aligned}
&+\frac{S_{oR}C_{CO_2,oR}\rho_{oR}\mathcal{D}^{*}_{CO_2,oR}}{F_R z_R^2}\frac{\partial}{\partial z_D}\left[S_{oD}\frac{\mathcal{D}^{*}_{CO_2,oD}}{F_D}\frac{\partial}{\partial z_D}\left(C_{CO_2,oD}\rho_{oD}\right)\right]+\mathcal{N}_{CO_2,ogR}\mathcal{N}_{CO_2,ogD}\\
&+\mathcal{N}_{CO_2,owR}\mathcal{N}_{CO_2,owD}=\frac{\phi_R C_{CO_2,oR}\rho_{oR}S_{oR}}{t_R}\frac{\partial}{\partial t_D}\left(\phi_D S_{oD}\rho_{oD}C_{CO_2,oD}\right) \qquad \text{(C.2)}
\end{aligned}
$$

Dividing by $\frac{C_{CO_2,oR}\rho_{oR}k_{oR}p_{oR}}{\mu_{oR}x_R^2}$ and collecting dimensionless groups give

$$
\frac{S_{oR}\mu_{oR}\mathcal{D}^{*}_{CO_2,oR}}{k_{oR}p_{oR}F_R},\ \frac{x_R^2}{y_R^2},\ \frac{S_{oR}\mu_{oR}\mathcal{D}^{*}_{CO_2,oR}x_R^2}{k_{oR}p_{oR}F_R y_R^2},\ \frac{x_R^2}{z_R^2},\ \frac{S_{oR}\mu_{oR}\mathcal{D}^{*}_{CO_2,oR}x_R^2}{k_{oR}p_{oR}F_R z_R^2},
$$

$$
\frac{\mathcal{N}_{CO_2,ogR}\mu_{oR}x_R^2}{C_{CO_2,oR}\rho_{oR}k_{oR}p_{oR}},\ \frac{\mathcal{N}_{CO_2,owR}\mu_{oR}x_R^2}{C_{CO_2,oR}\rho_{oR}k_{oR}p_{oR}},\ \frac{\phi_R S_{oR}\mu_{oR}x_R^2}{k_{oR}p_{oR}t_R}
$$

C.2 - Approach No.2

For approach no. 2, with the exclusion of the pressure drop term from the governing equation the mass balance for carbon dioxide in the oil phase becomes

$$
\begin{aligned}
&\frac{C_{CO_2,oR}\rho_{oR}^2k_{oR}g_R Z_R}{\mu_{oR}x_R^2}\frac{\partial}{\partial x_D}\left[C_{CO_2,oD}\frac{\rho_{oD}^2}{\mu_{oD}}k_{oD}g_D\frac{\partial Z_D}{\partial x_D}\right]\\
&+\frac{\phi_R S_{oR}C_{CO_2,oR}\rho_{oR}\mathcal{D}^{*}_{CO_2,oR}}{x_R^2}\frac{\partial}{\partial x_D}\left[\phi_D S_{oD}\mathcal{D}^{*}_{CO_2,oD}\frac{\partial}{\partial x_D}\left(C_{CO_2,oD}\rho_{oD}\right)\right]\\
&+\frac{C_{CO_2,oR}\rho_{oR}^2k_{oR}g_R Z_R}{\mu_{oR}y_R^2}\frac{\partial}{\partial y_D}\left[C_{CO_2,oD}\frac{\rho_{oD}^2}{\mu_{oD}}k_{oD}g_D\frac{\partial Z_D}{\partial y_D}\right]\\
&+\frac{\phi_R S_{oR}C_{CO_2,oR}\rho_{oR}\mathcal{D}^{*}_{CO_2,oR}}{y_R^2}\frac{\partial}{\partial y_D}\left[\phi_D S_{oD}\mathcal{D}^{*}_{CO_2,oD}\frac{\partial}{\partial y_D}\left(C_{CO_2,oD}\rho_{oD}\right)\right]\\
&+\frac{C_{CO_2,oR}\rho_{oR}^2k_{oR}g_R Z_R}{\mu_{oR}z_R^2}\frac{\partial}{\partial z_D}\left[C_{CO_2,oD}\frac{\rho_{oD}^2}{\mu_{oD}}k_{oD}g_D\frac{\partial Z_D}{\partial z_D}\right]\\
&+\frac{\phi_R S_{oR}C_{CO_2,oR}\rho_{oR}\mathcal{D}^{*}_{CO_2,oR}}{z_R^2}\frac{\partial}{\partial z_D}\left[\phi_D S_{oD}\mathcal{D}^{*}_{CO_2,oD}\frac{\partial}{\partial z_D}\left(C_{CO_2,oD}\rho_{oD}\right)\right]\\
&+\mathcal{N}_{CO_2,ogR}\mathcal{N}_{CO_2,ogD}+\mathcal{N}_{CO_2,owR}\mathcal{N}_{CO_2,owD}\\
&=\frac{\phi_R S_{oR}\rho_{oR}C_{CO_2,oR}}{t_R}\frac{\partial}{\partial t_D}\left(\phi_D S_{oD}\rho_{oD}C_{CO_2,oD}\right) \qquad \text{(C.3)}
\end{aligned}
$$

Dividing by $\frac{C_{CO_2,oR}\rho_{oR}^2 k_{oR} g_R Z_R}{\mu_{oR} x_R^2}$ and collecting the dimensionless groups lead to

$$\frac{\phi_R S_{oR} \mathcal{D}^{*}_{CO_2,oR}\mu_{oR}}{\rho_{oR} k_{oR} g_R Z_R}, \frac{x_R^2}{y_R^2}, \frac{\phi_R S_{oR} \mathcal{D}^{*}_{CO_2,oR}\mu_{oR} x_R^2}{\rho_{oR} k_{oR} g_R Z_R y_R^2}, \frac{x_R^2}{z_R^2}, \frac{\phi_R S_{oR} \mathcal{D}^{*}_{CO_2,oR}\mu_{oR} x_R^2}{\rho_{oR} k_{oR} g_R Z_R z_R^2},$$

$$\frac{\mathcal{N}_{CO_2,ogR}\mu_{oR} x_R^2}{C_{CO_2,oR}\rho_{oR} k_{oR} p_{oR}}, \frac{\mathcal{N}_{CO_2,ogR}\mu_{oR} x_R^2}{C_{CO_2,oR}\rho_{oR}^2 k_{oR} g_R Z_R}, \frac{\phi_R S_{oR}\mu_{oR} x_R^2}{\rho_{oR} k_{oR} g_R Z_R t_R}$$

APPENDIX D

Tabulated Data of Diffusivity Experiments in Graphical Form

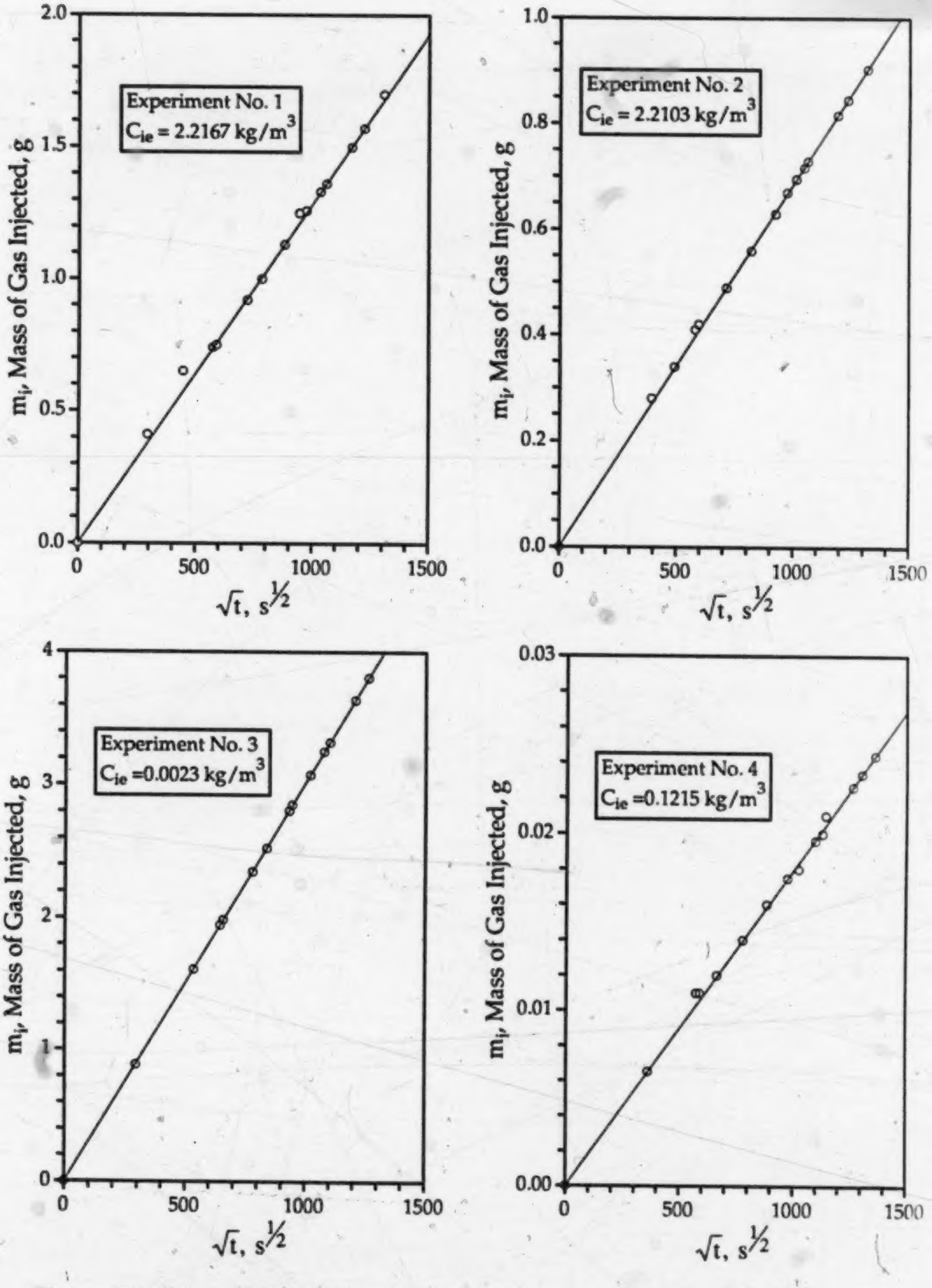

Figure D1 - Mass of CO_2 Injected vs. Square Root of Time for Diffusivity Experiments No. 1, 2, 3, and 4.

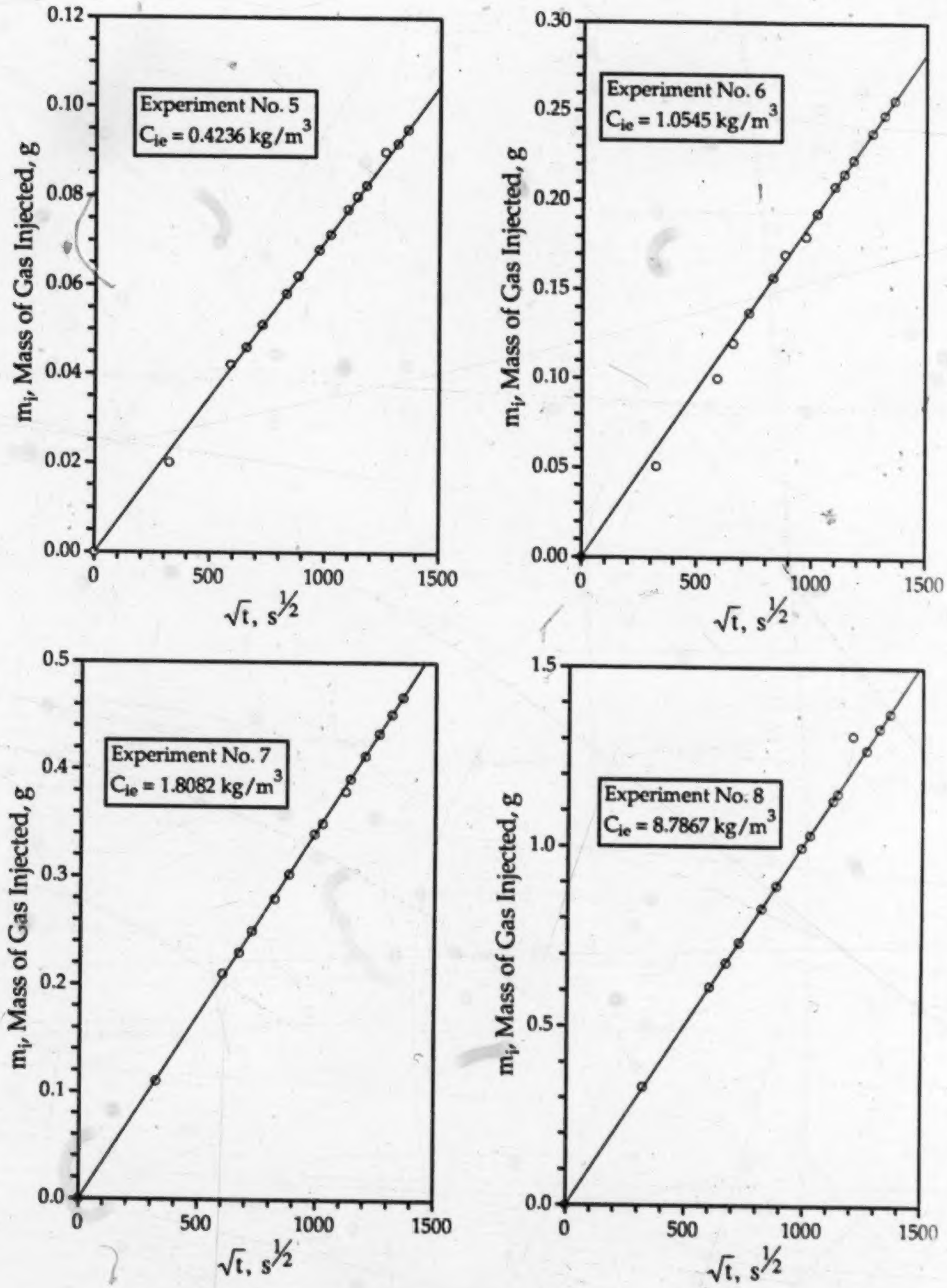

Figure D2 - Mass of CO_2 Injected vs. Square Root of Time for Diffusivity Experiments No. 5, 6, 7, and 8.

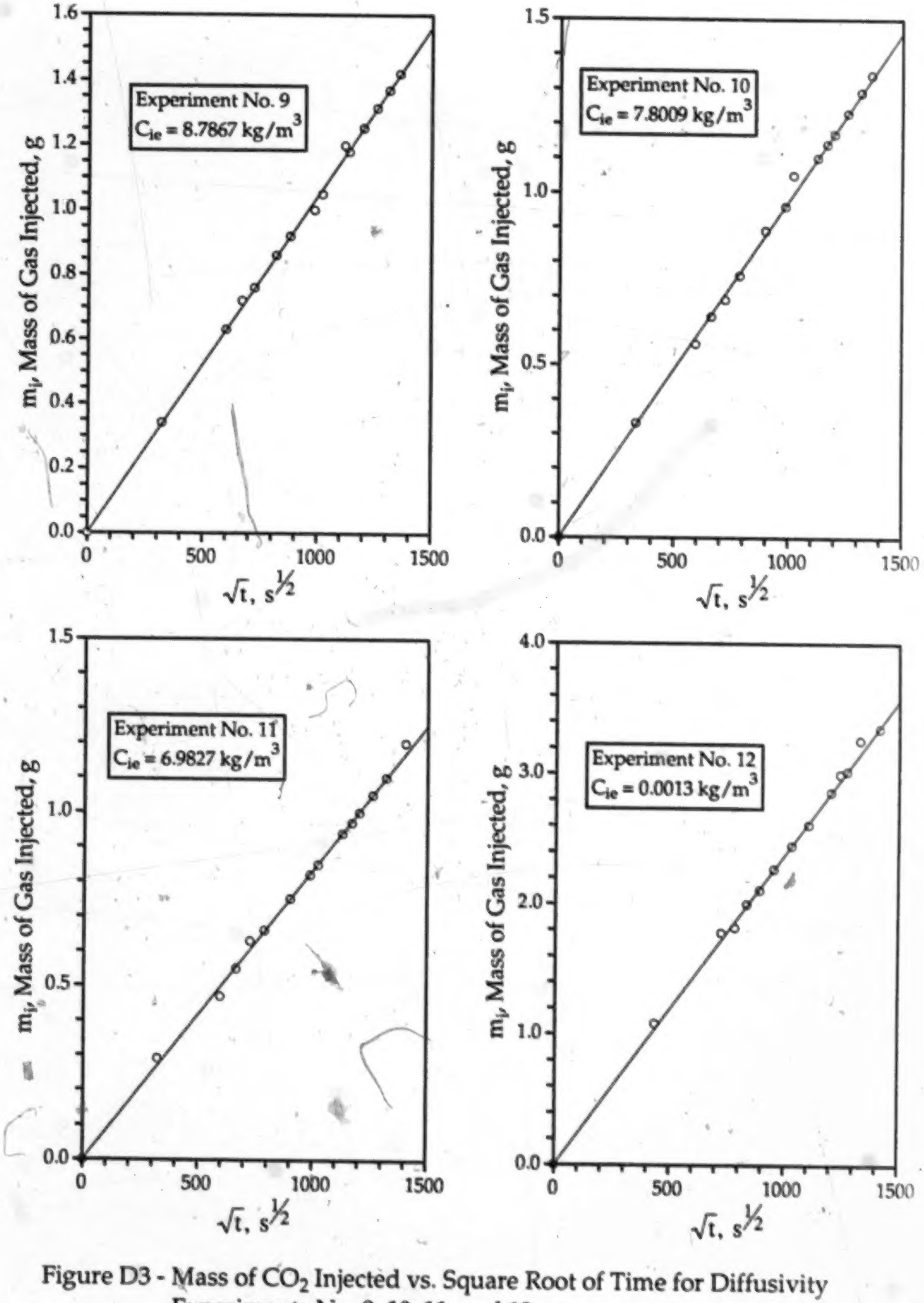

Figure D3 - Mass of CO_2 Injected vs. Square Root of Time for Diffusivity Experiments No. 9, 10, 11, and 12.

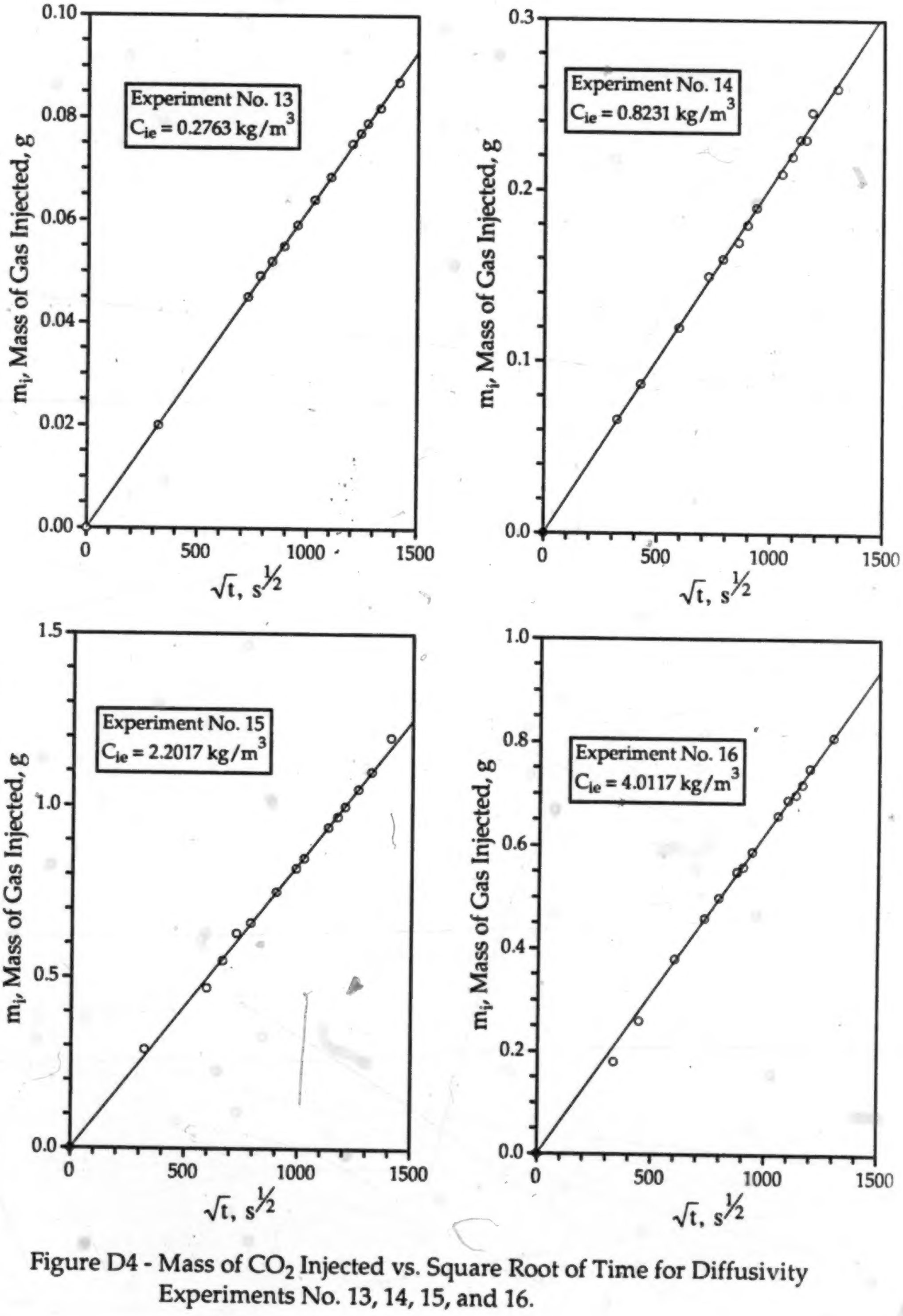

Figure D4 - Mass of CO_2 Injected vs. Square Root of Time for Diffusivity Experiments No. 13, 14, 15, and 16.

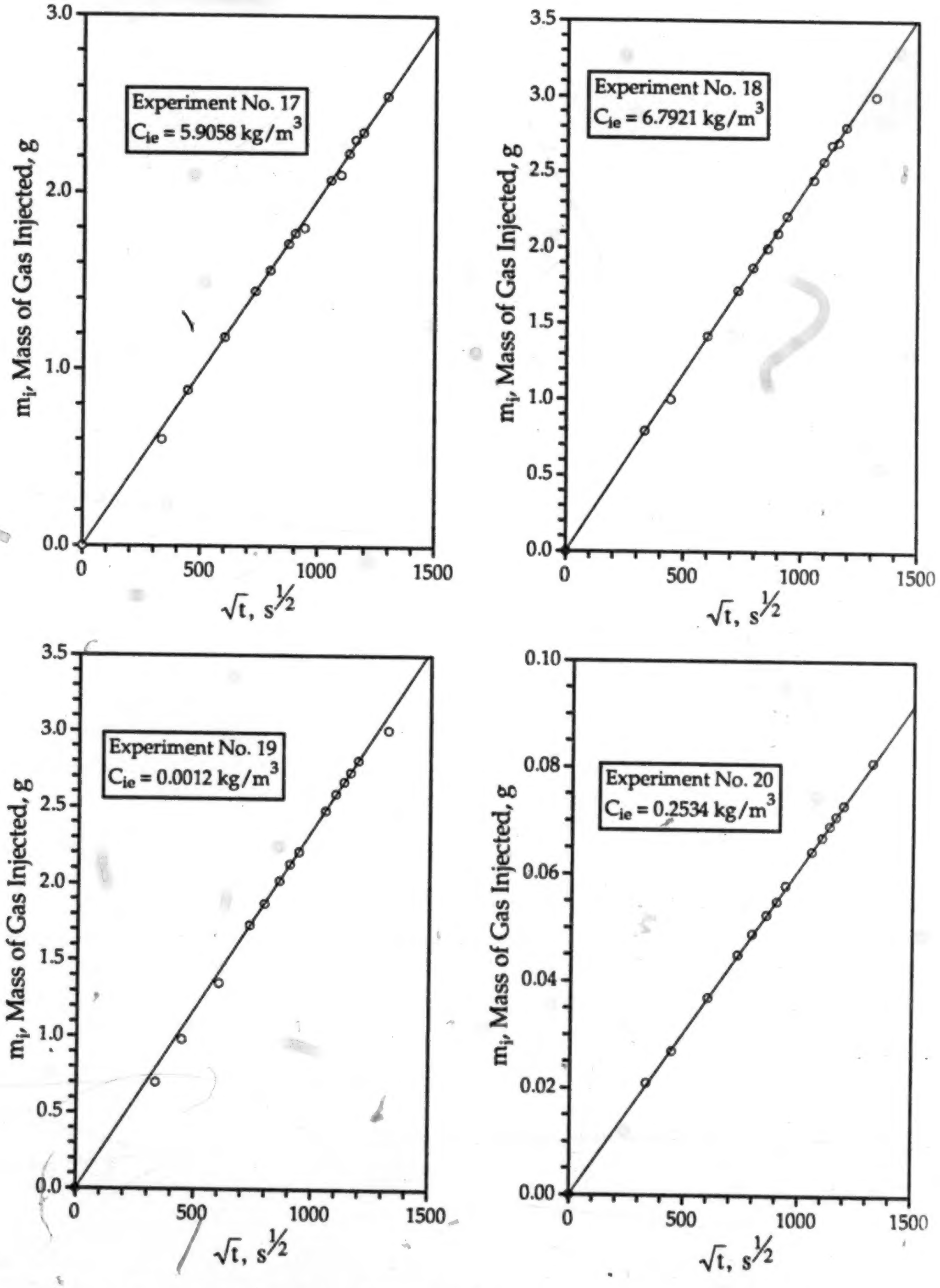

Figure D5 - Mass of CO_2 Injected vs. Square Root of Time for Diffusivity Experiments No. 17, 18, 19 and 20.

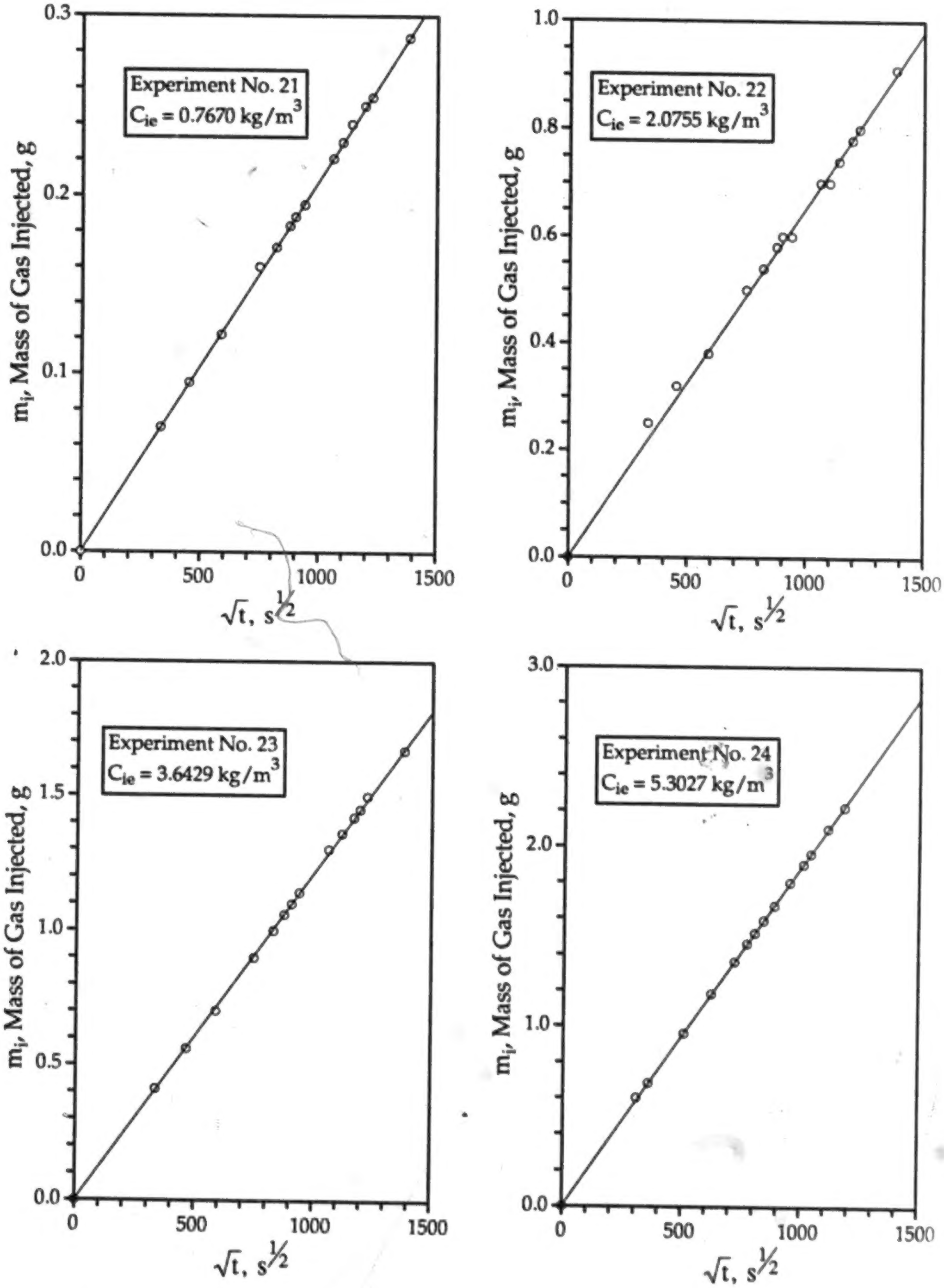

Figure D6 - Mass of CO_2 Injected vs. Square Root of Time for Diffusivity Experiments No. 21, 22, 23, and 24.

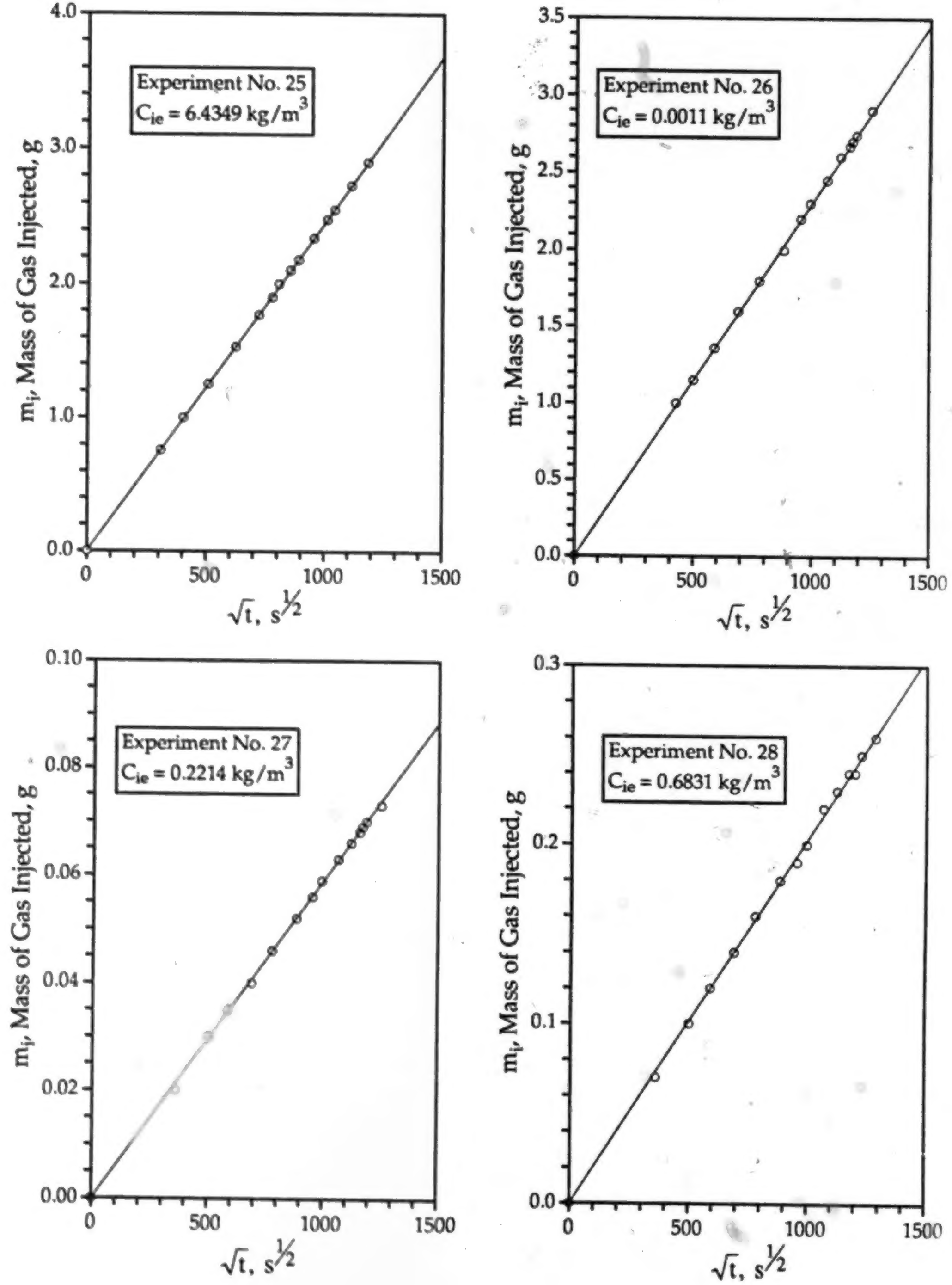

Figure D7 - Mass of CO_2 Injected vs. Square Root of Time for Diffusivity Experiments No. 25, 26, 27, and 28.

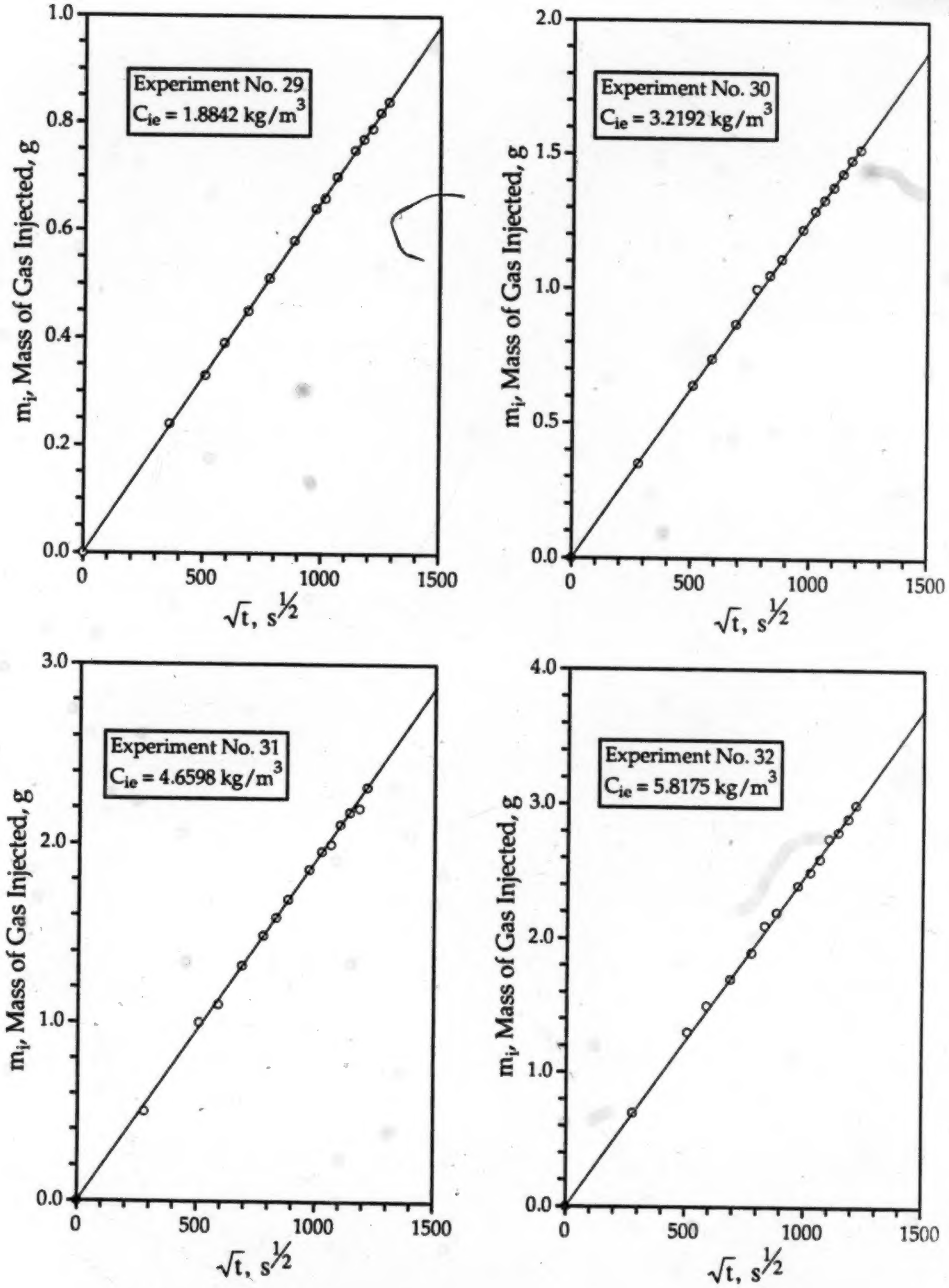

Figure D8 - Mass of CO_2 Injected vs. Square Root of Time for Diffusivity Experiments No. 29, 30, 31, and 32.

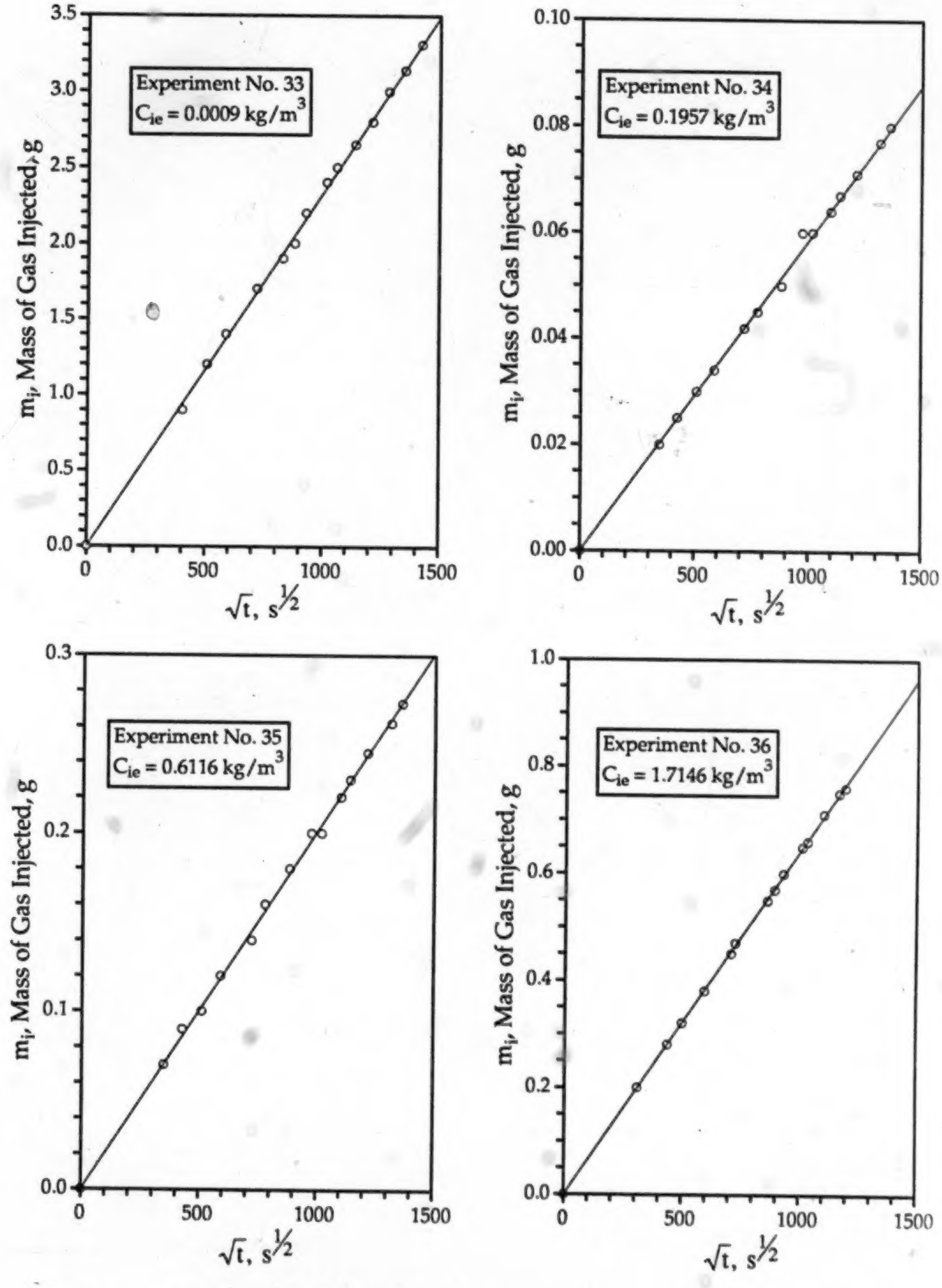

Figure D9 - Mass of CO_2 Injected vs. Square Root of Time for Diffusivity Experiments No. 33, 34, 35, and 36.

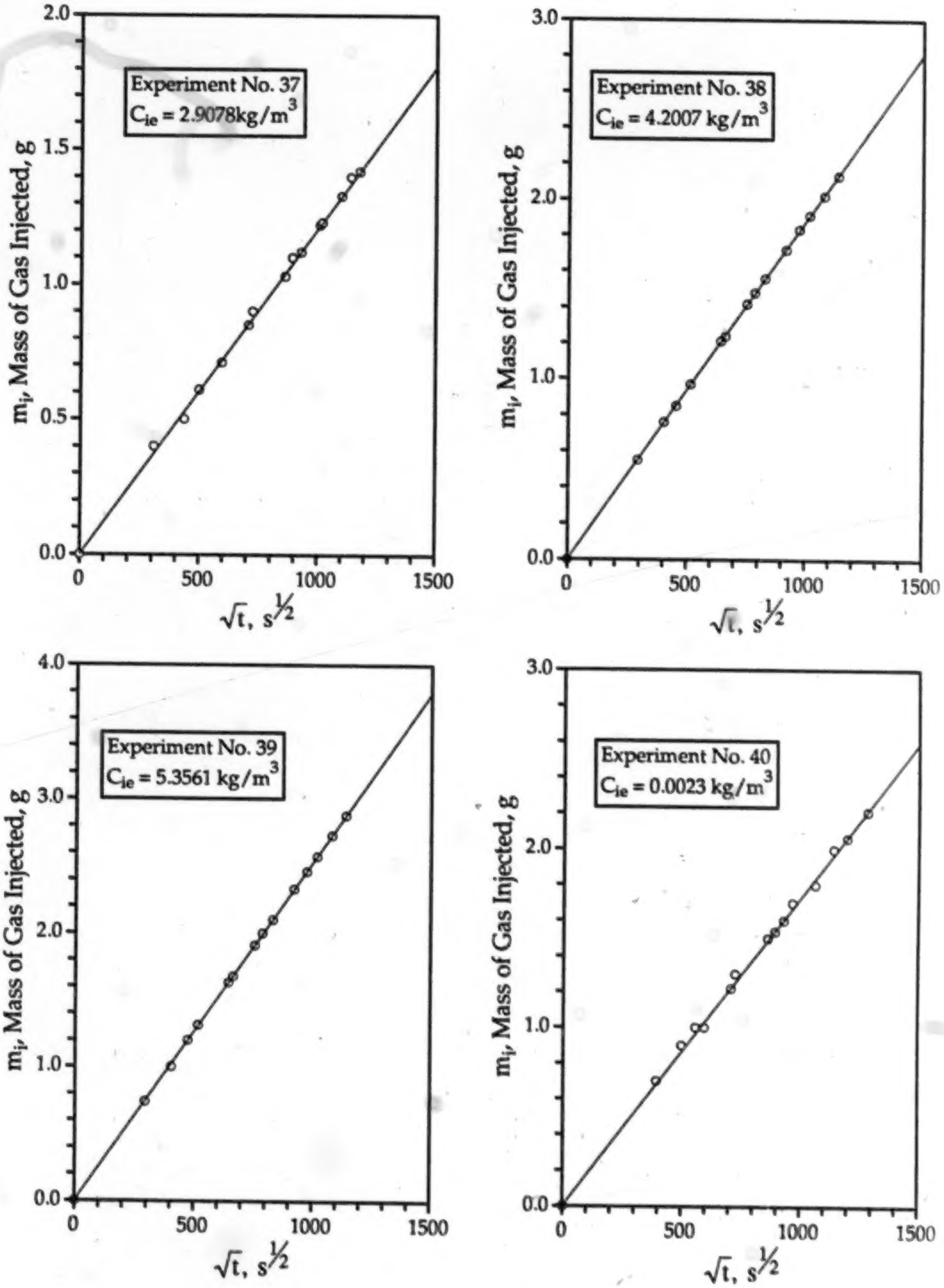

Figure D10 - Mass of CO_2 Injected vs. Square Root of Time for Diffusivity Experiments No. 37, 38, 39, and 40.

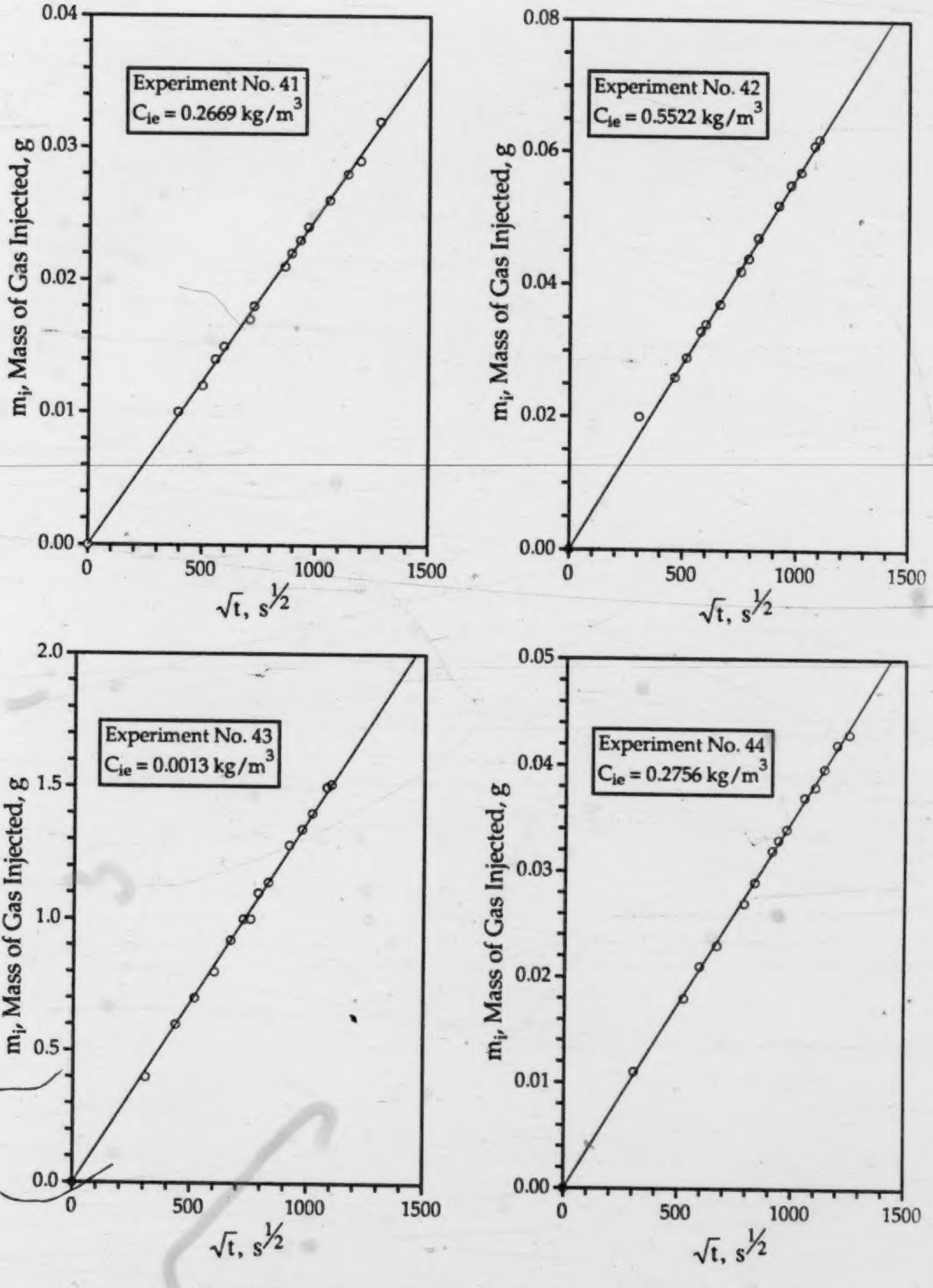

Figure D11 - Mass of CO_2 Injected vs. Square Root of Time for Diffusivity Experiments No. 41, 42, 43, and 44.

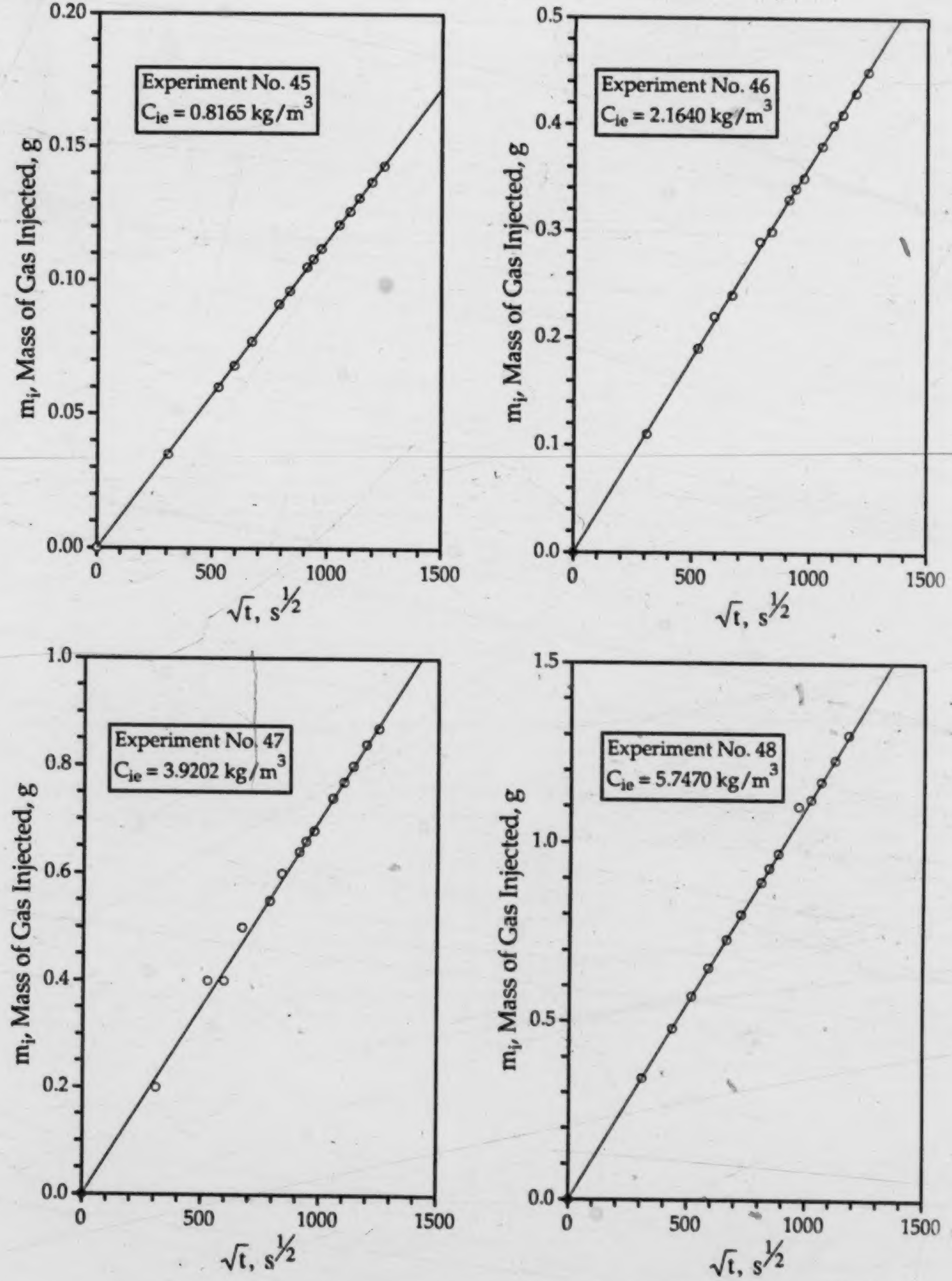

Figure D12 - Mass of CO_2 Injected vs. Square Root of Time for Diffusivity Experiments No. 45, 46, 47, and 48.

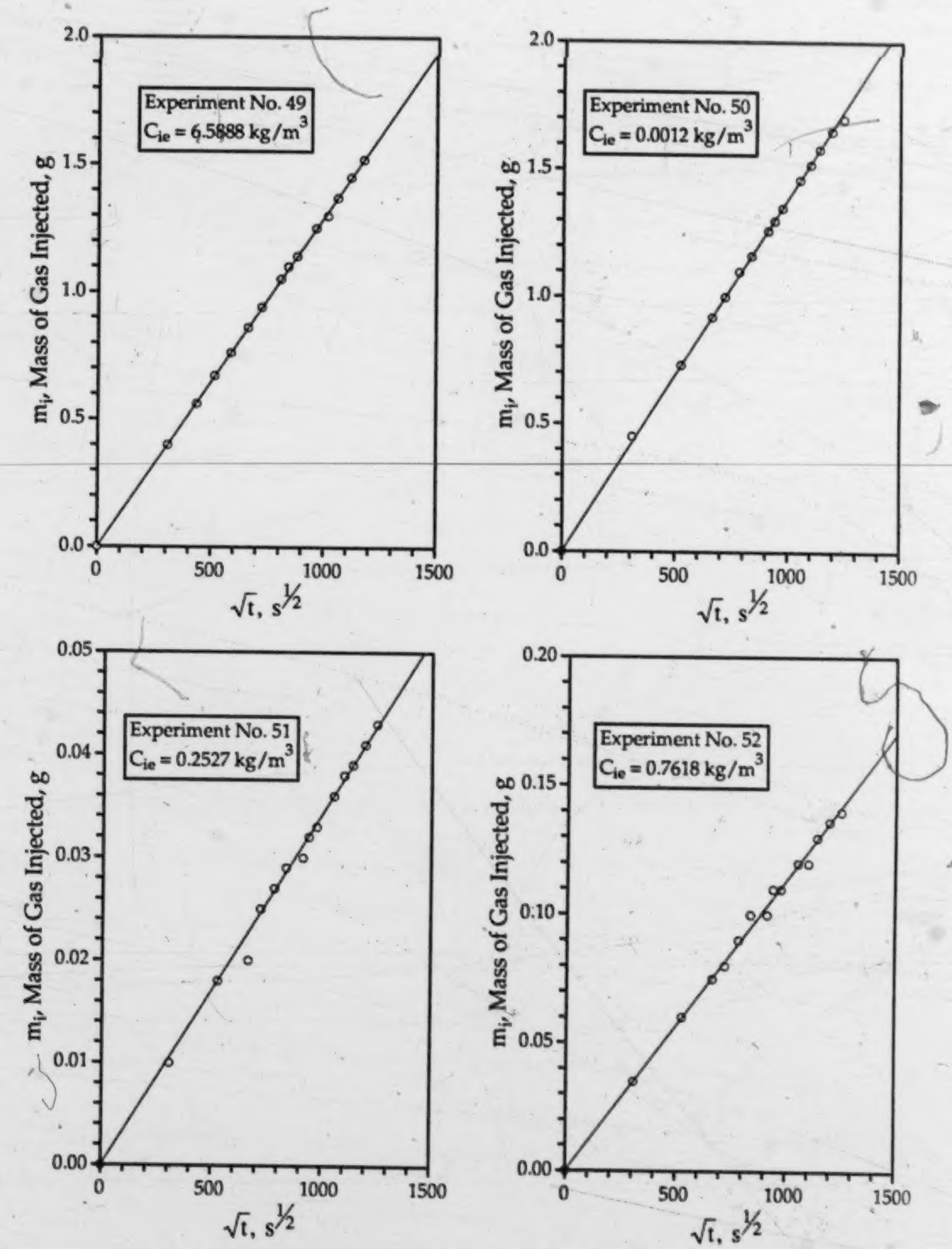

Figure D13 - Mass of CO_2 Injected vs. Square Root of Time for Diffusivity Experiments No. 49, 50, 51, and 52.

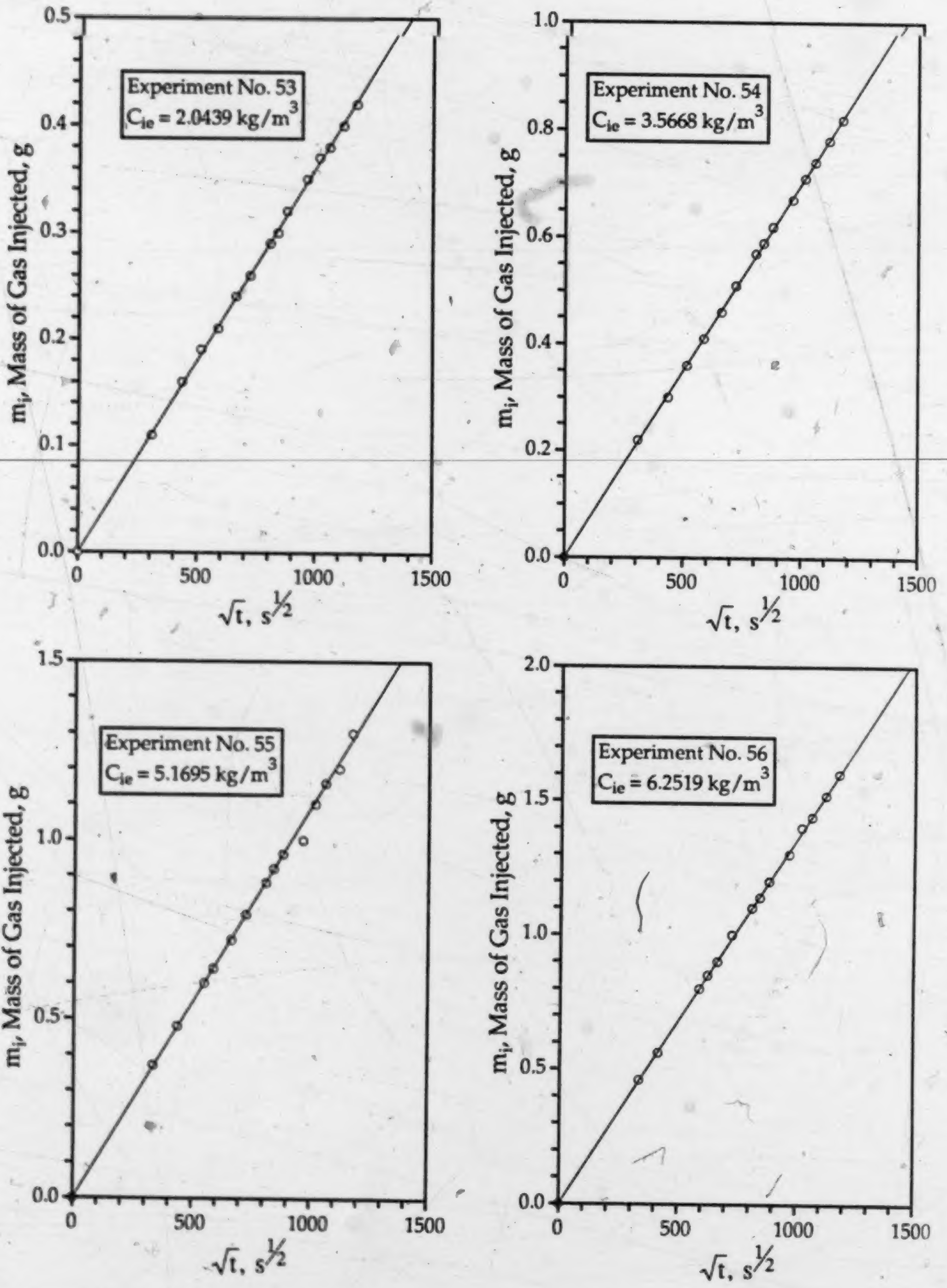

Figure D14 - Mass of CO_2 Injected vs. Square Root of Time for Diffusivity Experiments No. 53, 54, 55, and 56.

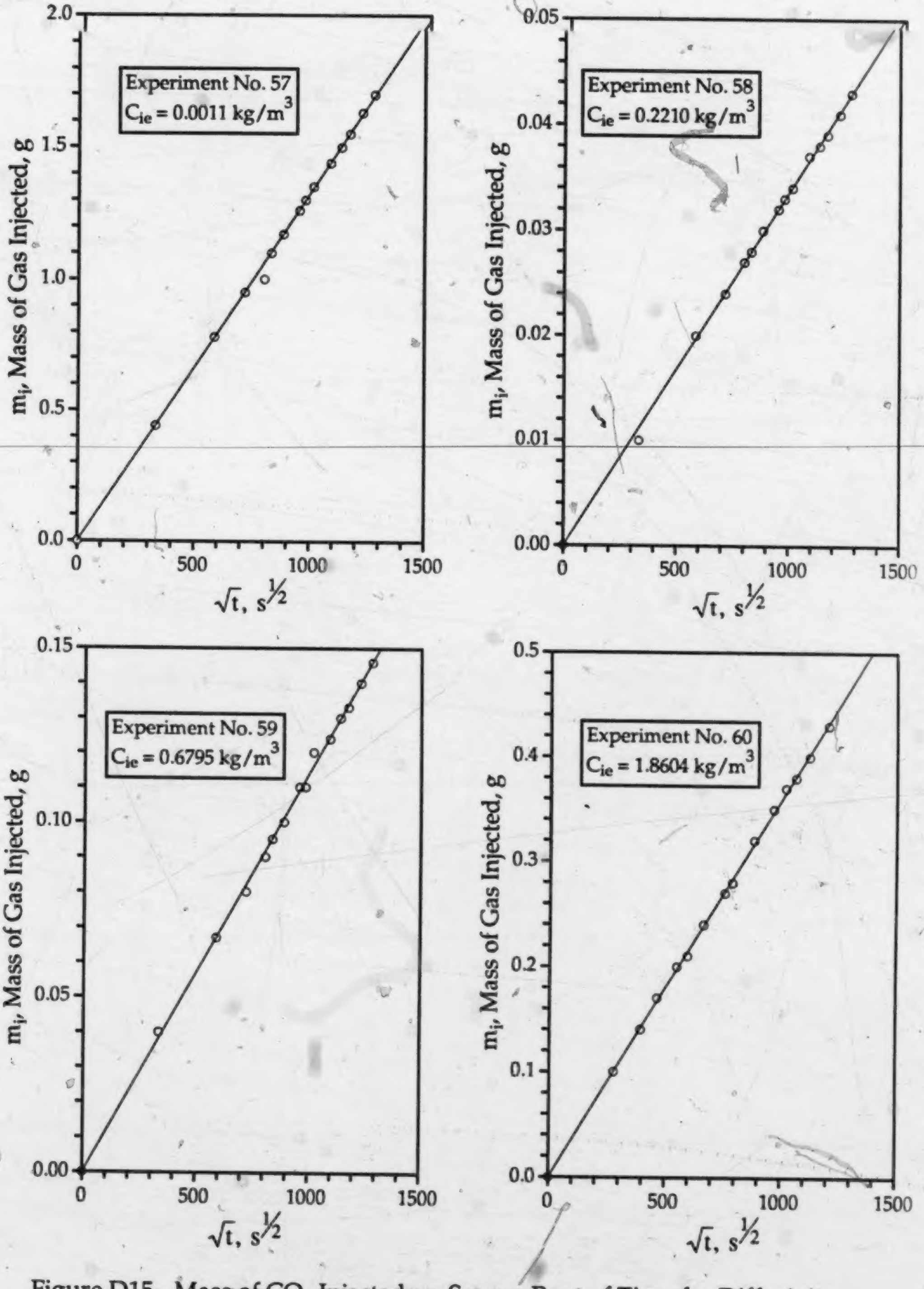

Figure D15 - Mass of CO_2 Injected vs. Square Root of Time for Diffusivity Experiments No. 57, 58, 59, and 60.

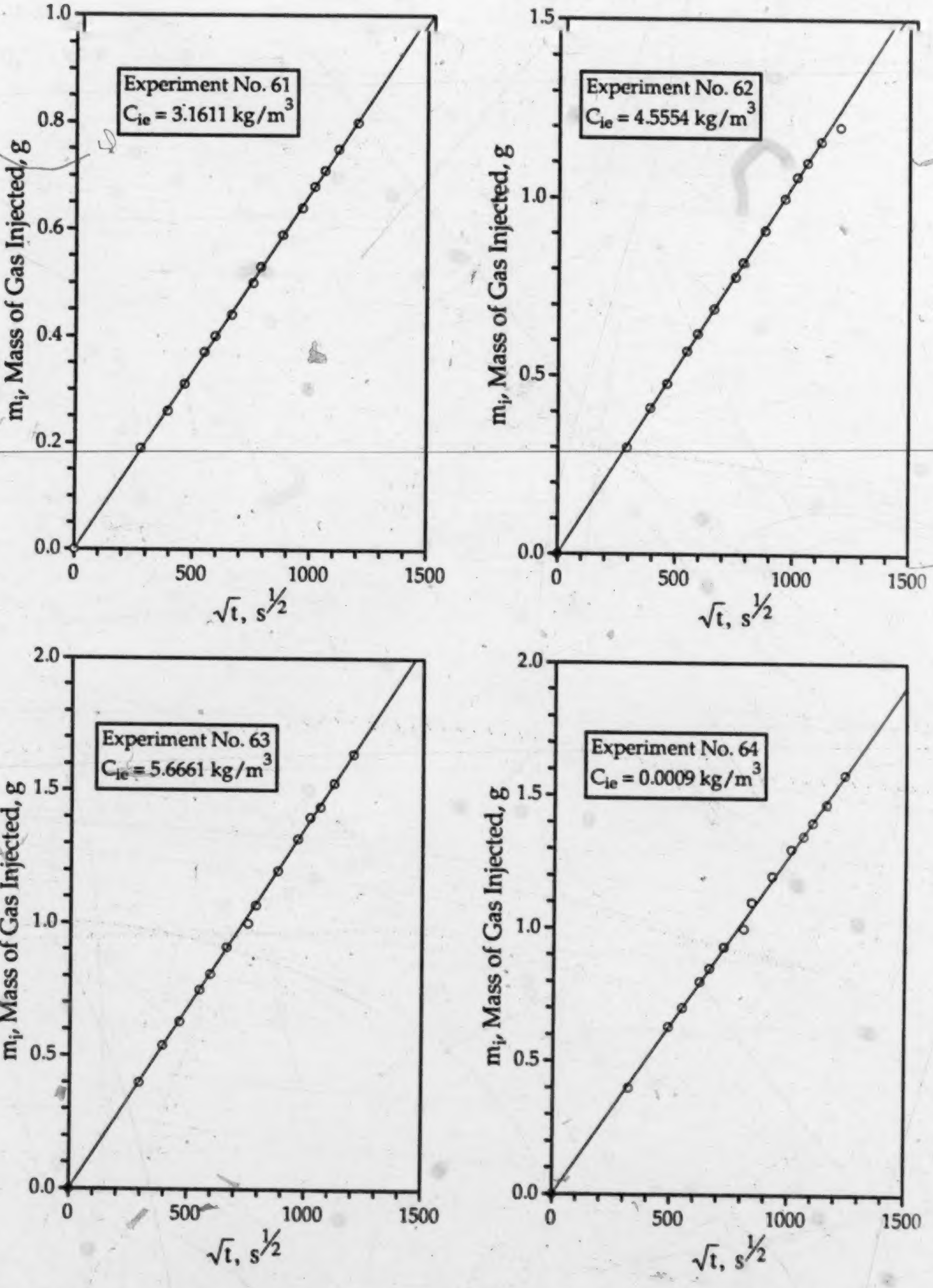

Figure D16 - Mass of CO_2 Injected vs. Square Root of Time for Diffusivity Experiments No. 61, 62, 63, and 64.

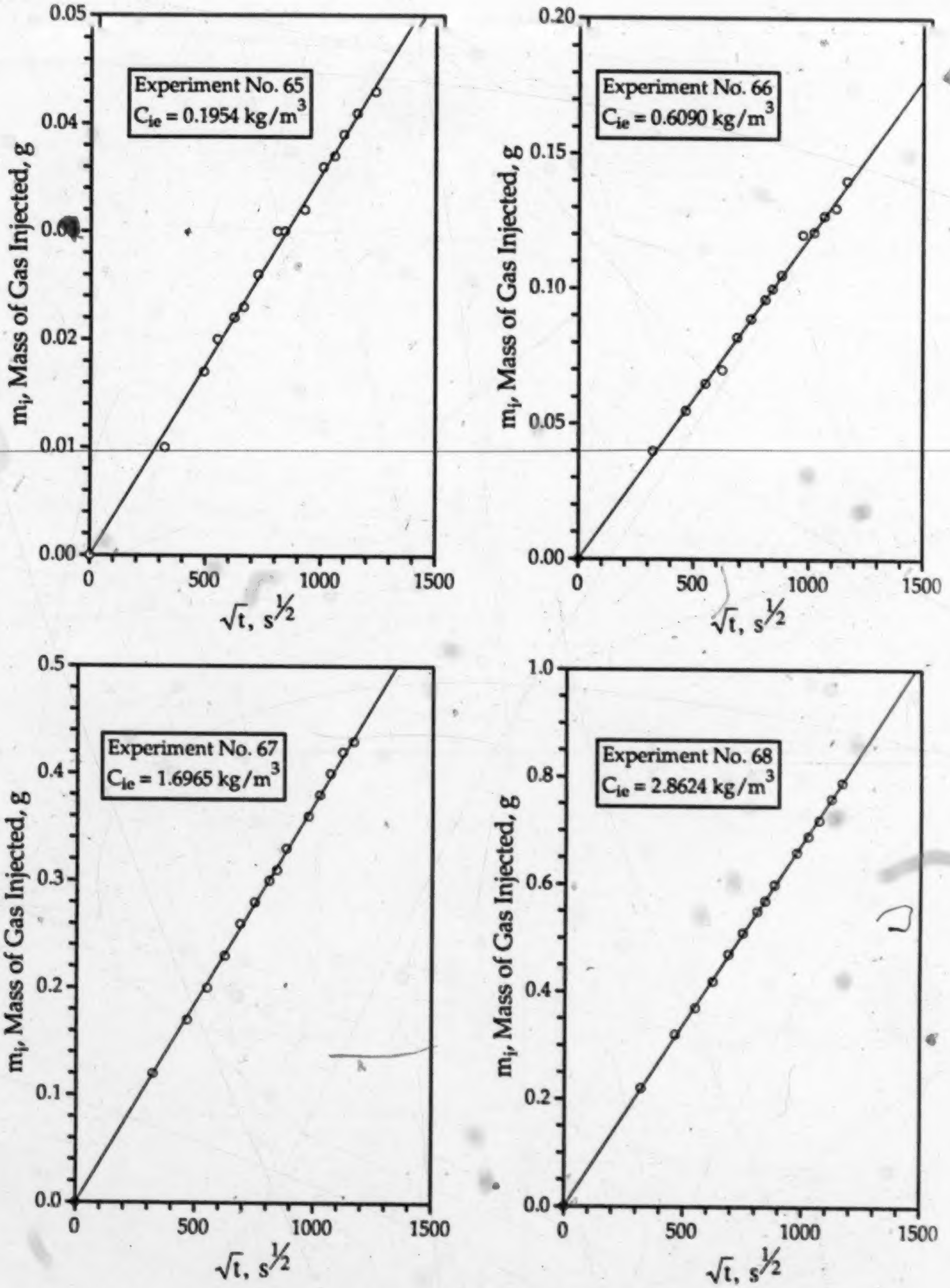

Figure D17 - Mass of CO_2 Injected vs. Square Root of Time for Diffusivity Experiments No. 65, 66, 67, and 68.

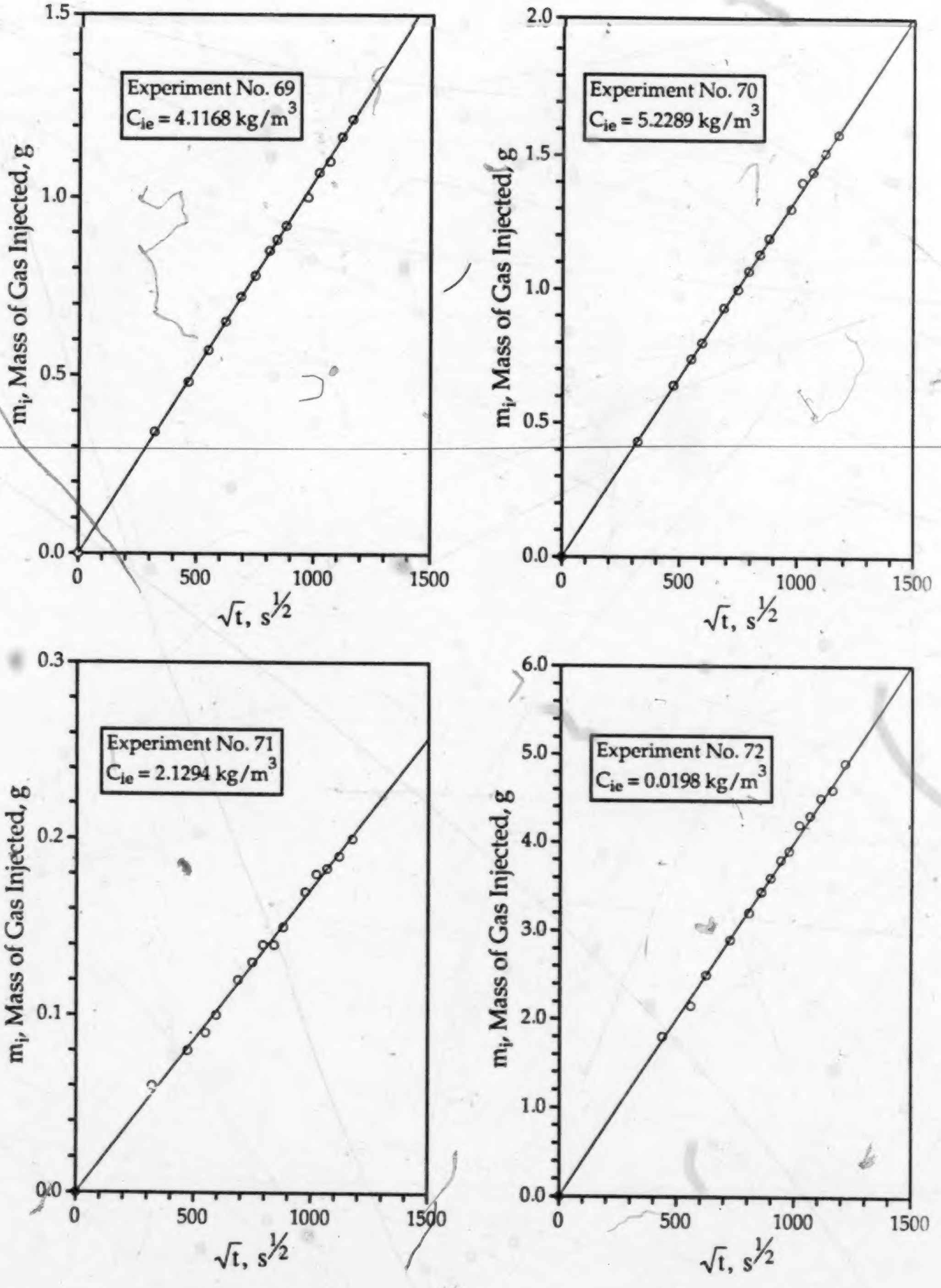

Figure D18 - Mass of CO_2 Injected vs. Square Root of Time for Diffusivity Experiments No. 69, 70, 71, and 72.

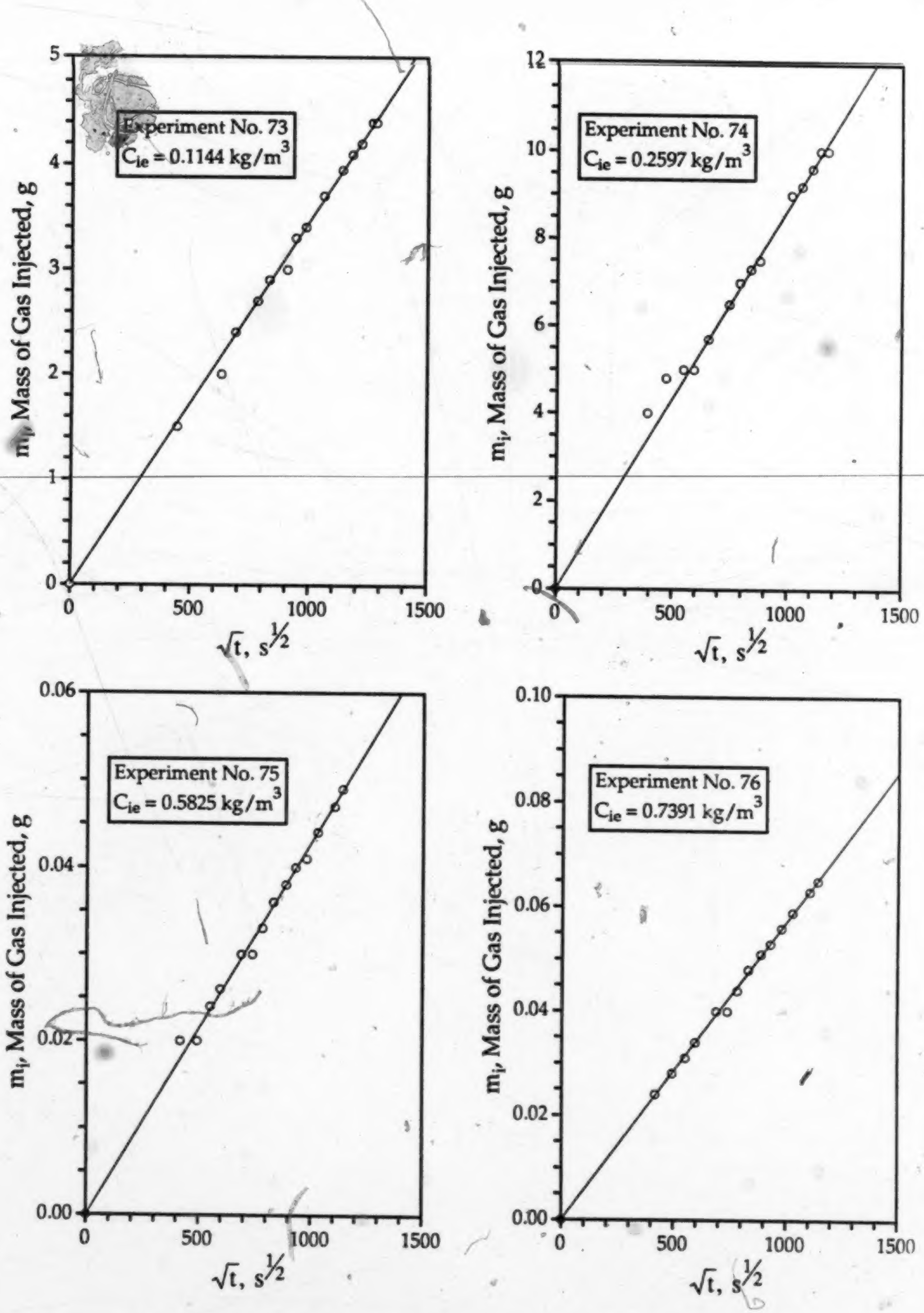

Figure D19 - Mass of CH_4 Injected vs. Square Root of Time for Diffusivity Experiments No. 73, 74, 75, and 76.

APPENDIX E

Tabulated Results of Displacement Experiments

TABLE E01

Tabulated Experimental Results of Run CWF1

(Carbonated Waterflood @ 2.5 MPa (1.532 moles), 21°C)

Porosity (%) = 35.80
Oil Viscosity (mPa.s) = 1842.3
Ave. Run Temp.(K) = 294.15
CO_2 Req. (sm^3/sm^3) = 63.40
V_p (cm^3) = 1113
S_{oi} (%) = 92.18
HCPV (cm3) = 1026
CO_2 Ret. (%inj.) = 29.76
S_{wc} (%) = 7.82
Molar Den. ($kmol/m^3$) = 0.04166
Abs. k (darcies) = 11.44
Ave. Flow Vel. (m/d) = 0.894

Press Inj. (MPa)	Press Prod. (MPa)	Gas Inj. (cm^3)	Water Inj. (cm^3)	Cum. PV Injected	Gas Prod (s.ltr)	Water Prod. (cm^3)	Oil Prod. (cm^3)	Cum. Oil Prod. (cm^3)	Percent Rec. (%)	WOR (sm^3/sm^3)	GOR (sm^3/sm^3)	OPFIR (sm^3/sm^3)
2.70	2.50	0.0	261.2	0.235	0	40.00	223.00	223.00	21.73	0.00	0	0.854
2.60	2.50	0.0	250.3	0.460	0	168.00	83.50	306.50	29.87	2.01	0	0.334
2.60	2.40	0.0	271.8	0.704	0.335	206.00	72.00	378.50	36.89	0.00	4.65	0.265
2.70	2.50	0.0	248.9	0.927	1.697	205.00	45.00	423.50	41.28	4.56	37.71	0.181
2.80	2.50	0.0	245.4	1.148	2.301	211.00	37.50	461.00	44.93	5.63	61.36	0.153
2.70	2.60	0.0	178.6	1.308	2.528	218.50	30.50	491.50	47.90	7.16	82.89	0.171
2.70	2.40	0.0	66.2	1.368	2.501	236.00	13.00	504.50	49.17	18.15	92.38	0.196
2.70	2.50	0.0	250.9	1.593	2.744	234.50	14.50	519.00	50.58	16.17	189.21	0.058
2.70	2.50	0.0	247.3	1.816	2.565	239.00	11.50	530.50	51.71	20.78	223.04	0.047
0.10	0.10	0.0	0.0	1.816	11.211	227.00	49.50	580.00	56.53	4.59	226.48	

TABLE E02

Tabulated Experimental Results of Run CWF2

[Carbonated Waterflood @ 1.0 MPa (0.143 moles), 20% HCPV of CO_2 Mixed With Water @ 4:1 Ratio, 21°C]

Porosity (%) = 37.84
Oil Viscosity (mPa.s) = 1058.0
Ave. Run Temp.(K) = 294.15
CO_2 Req. (sm^3/sm^3) = 5.30

V_p (cm^3) = 1843
S_{oi} (%) = 89.94
HCPV (cm3) = 1650
CO_2 Ret. (%inj.) = 36.62

S_{wc} (%) = 10.06
Molar Den. ($kmol/m^3$) = 0.04166
Abs. k (darcies) = 11.56
Ave. Flow Vel. (m/d) = 2.6

Press Inj. (MPa)	Press Prod. (MPa)	Gas Inj. (cm^3)	Water Inj. (cm^3)	Cum. PV Injected	Gas Prod (s.ltr)	Water Prod. (cm^3)	Oil Prod. (cm^3)	Cum. Oil Prod. (cm^3)	Percent Rec. (%)	WOR (sm^3/sm^3)	GOR (sm^3/sm^3)	OPFIR (sm^3/sm^3)
1.00	1.00	0.0	522.0	0.283	0.250	215.00	306.25	306.25	18.56	0.70	0.82	0.587
1.05	1.00	0.0	520.0	0.565	0.348	379.75	138.25	444.50	26.94	2.75	2.52	0.266
1.00	1.00	0.0	510.0	0.842	0.398	442.00	67.75	512.25	31.05	6.52	5.87	0.133
1.30	1.00	0.0	112.2	0.903	0.082	100.25	11.50	523.75	31.74	8.72	7.13	0.103
1.10	1.00	0.0	255.0	1.041	0.178	233.00	21.50	545.25	33.05	10.84	8.28	0.084
1.20	1.00	0.0	253.9	1.179	0.198	229.50	21.50	566.75	34.35	10.67	9.21	0.085
1.30	1.00	0.0	250.1	1.315	0.285	230.50	20.00	586.75	35.56	11.53	14.25	0.080
1.10	1.00	0.0	260.0	1.456	0.245	238.00	20.50	607.25	36.80	11.61	11.95	0.079
1.10	1.00	0.0	251.5	1.592	0.127	235.00	15.25	622.50	37.73	15.41	8.33	0.061
1.05	1.00	0.0	251.9	1.729	0.057	238.00	12.80	635.30	38.50	18.59	4.45	0.051
1.20	1.00	0.0	250.3	1.865	0.008	239.00	10.50	645.80	39.14	22.76	0.76	0.042
1.00	1.00	0.0	0.0	1.865	0.254	76.00	25.00	647.50	39.24	3.04	10.16	

TABLE E03

Tabulated Experimental Results of Run CWF3

(Carbonated Waterflood @ 2.5 MPa (1.608 moles), 21°C)

Porosity (%) = 36.02
Oil Viscosity (mPa.s) = 1058
Ave. Run Temp.(K) = 294.15
CO_2 Req. (sm³/sm³) = 62.74
V_p (cm³) = 1120
S_{oi} (%) = 96.16
HCPV (cm3) = 1077
CO_2 Ret. (%inj.) = 31.14
S_{wc} (%) = 3.84
Molar Den. (kmol/m³) = 0.04166
Abs. k (darcies) = 11.25
Ave. Flow Vel. (m/d) = 0.894

Press Inj. (MPa)	Press Prod. (MPa)	Gas Inj. (cm³)	Water Inj. (cm³)	Cum. PV Injected	Gas Prod (s.ltr)	Water Prod. (cm³)	Oil Prod. (cm³)	Cum. Oil Prod. (cm³)	Percent Rec. (%)	WOR (sm³/sm³)	GOR (sm³/sm³)	OPFIR (sm³/sm³)
2.70	2.50	0.0	251.3	0.224	0	40.00	211.50	211.50	19.64	0.00	0.00	0.842
2.60	2.50	0.0	262.0	0.458	0	158.00	94.50	306.00	28.41	1.67	0.00	0.361
2.60	2.40	0.0	262.2	0.692	0.276	185.00	85.00	391.00	36.30	2.18	3.25	0.324
2.70	2.50	0.0	261.8	0.926	0.710	228.00	44.50	435.50	40.44	5.12	15.96	0.170
2.80	2.50	0.0	261.4	1.160	2.536	223.00	40.00	475.50	44.15	5.58	63.40	0.153
2.70	2.60	0.0	251.9	1.385	2.551	218.50	31.50	507.00	47.08	6.94	80.98	0.125
2.70	2.40	0.0	252.3	1.610	2.482	219.00	22	529.00	49.12	9.95	112.82	0.087
2.70	2.50	0.0	250.1	1.833	2.802	229.00	14	543.00	50.42	16.36	200.14	0.056
2.70	2.50	0.0	249.4	2.056	2.830	233.00	11	554.00	51.44	21.18	257.27	0.044
2.70	2.50	0.0	252.1	2.281	2.865	239.50	11.5	565.50	52.51	20.83	249.13	0.046
0.10	0.10	0.0	0.0	2.281	9.541	171.00	49.5	615.00	57.10	3.45	192.75	

TABLE E04

Tabulated Experimental Results of Run CWF4

[Carbonated Waterflood @ 1.0 MPa (0.143 moles), 20% HCPV of CO_2 Mixed With Water @ 4:1 Ratio, 21°C]

Porosity (%) = 37.47
Oil Viscosity (mPa.s) = 1058.0
Ave. Run Temp.(K) = 294.15
CO_2 Req. (sm^3/sm^3) = 4.93
V_p (cm^3) = 1825
S_{oi} (%) = 90.14
HCPV (cm3) = 1645
CO_2 Ret. (%inj.) = 23.57
S_{wc} (%) = 9.86
Molar Den. ($kmol/m^3$) = 0.04166
Abs. k (darcies) = 10.89
Ave. Flow Vel. (m/d) = 2.6

Press Inj. (MPa)	Press Prod. (MPa)	Gas Inj. (cm^3)	Water Inj. (cm^3)	Cum. PV Injected	Gas Prod (s.ltr)	Water Prod. (cm^3)	Oil Prod. (cm^3)	Cum. Oil Prod. (cm^3)	Percent Rec. (%)	WOR (sm^3/sm^3)	GOR (sm^3/sm^3)	OPFIR (sm^3/sm^3)
1.00	1.00	0.0	500.0	0.273	0.350	212.50	302.50	302.50	18.39	0.70	1.16	0.605
1.05	1.00	0.0	506.0	0.550	0.505	362.50	145.00	447.50	27.20	2.50	3.48	0.287
1.00	1.00	0.0	500.0	0.823	0.469	420.00	78.50	526.00	31.98	5.35	5.97	0.157
1.30	1.00	0.0	140.0	0.900	0.129	123.00	10.00	536.00	32.58	12.30	7.9	0.071
1.00	1.00	0.0	252.5	1.038	0.251	228.00	24.00	560.00	34.04	9.50	10.46	0.095
1.00	1.00	0.0	250.1	1.175	0.249	224.00	20.00	580.00	35.26	11.20	12.45	0.080
1.00	1.00	0.0	250.1	1.311	0.249	227.00	15.00	595.00	36.17	15.13	14.6	0.060
1.00	1.00	0.0	274.9	1.462	0.273	238.00	20.00	615.00	37.39	11.90	13.65	0.073
1.00	1.00	0.0	250.2	1.599	0.119	230.00	15.00	630.00	38.30	15.33	7.93	0.060
1.00	1.00	0.0	250.8	1.736	0.019	241.00	8.50	638.50	38.81	28.35	2.24	0.034
0.10	0.10	0.0	0.0	1.736	0.002	230.00	19.50	649.50	39.48	11.79	0.10	

TABLE E05

Tabulated Experimental Results of Run VLC01

(20% HCPV CO_2 @ 1.0 MPa (0.089 moles), 10 Slugs, 4:1 WAG, 21°C, Bottom Injection)

Porosity (%) =	35.90	Vp (cm^3) =	1116	S_{wc} (%) =	4.57
Oil Viscosity (mPa.s) =	1058.0	S_{oi} (%) =	95.43	Molar Den. (kmol/m^3) =	0.04166
Ave. Run Temp.(K) =	294.15	HCPV (cm3) =	1025	Abs. k (darcies) =	11.33
CO_2 Req. (sm^3/sm^3) =	3.82	CO_2 Ret. (%inj.) =	37.17	Ave. Flow Vel. (m/d) =	0.984

Press Inj. (MPa)	Press Prod. (MPa)	Gas Inj. (cm^3)	Water Inj. (cm^3)	Cum. PV Injected	Gas Prod (s.ltr)	Water Prod. (cm^3)	Oil Prod. (cm^3)	Cum. Oil Prod. (cm^3)	Percent Rec. (%)	WOR (sm^3/sm^3)	GOR (sm^3/sm^3)	OPFIR (sm^3/sm^3)
1.10	1.00	21.2	0.0	0.019	0.000	0.00	0.00	0.00	0.00	0.00	0.00	0.000
1.40	1.00	0.0	85.2	0.095	0.004	0.00	85.50	85.50	8.34	0.00	0.05	1.004
1.10	1.00	21.2	0.0	0.114	0.000	0.00	6.50	92.00	8.98	0.00	0.00	0.306
1.30	1.00	0.0	85.2	0.191	0.000	6.30	76.20	168.20	16.41	0.08	0.00	0.894
1.00	1.00	21.2	0.0	0.210	0.001	3.00	6.50	174.70	17.04	0.46	0.15	0.306
1.20	1.00	0.0	85.2	0.286	0.000	34.30	44.70	219.40	21.40	0.77	0.00	0.525
1.10	1.00	21.2	0.0	0.305	0.000	8.50	5.10	224.50	21.90	1.67	0.00	0.240
1.20	1.00	0.0	85.2	0.381	0.000	41.30	33.30	257.80	25.15	1.24	0.00	0.391
1.20	1.00	21.2	0.0	0.400	0.000	9.00	3.00	260.80	25.44	3.00	0.00	0.141
1.20	1.00	0.0	85.2	0.477	0.000	43.10	33.40	294.20	28.70	1.29	0.00	0.392
1.10	1.00	21.2	0.0	0.496	0.050	18.00	4.80	299.00	29.17	3.75	10.42	0.226
1.20	1.00	0.0	85.2	0.572	0.003	40.40	24.60	323.60	31.57	1.64	0.12	0.289
1.10	1.00	21.2	0.0	0.591	0.004	25.70	4.80	328.40	32.04	5.35	0.83	0.226
1.20	1.00	0.0	85.2	0.667	0.000	44.80	23.70	352.10	34.35	1.89	0.00	0.278
1.20	1.00	21.2	0.0	0.686	0.001	32.00	5.00	357.10	34.84	6.40	0.20	0.236
1.20	1.00	0.0	85.2	0.763	0.000	42.00	26.50	383.60	37.42	1.58	0.00	0.311
1.20	1.00	21.2	0.0	0.782	0.001	33.00	4.50	388.10	37.86	7.33	0.22	0.212
1.20	1.00	0.0	85.2	0.858	0.002	41.50	14.00	402.10	39.23	2.96	0.14	0.164
1.20	1.00	21.2	0.0	0.877	0.001	33.40	5.10	407.20	39.73	6.55	0.20	0.240

TABLE E05 (Cont'd)

Tabulated Experimental Results of Run VLC01

(20% HCPV CO_2 @ 1.0 MPa (0.089 moles), 10 Slugs, 4:1 WAG, 21°C, Bottom Injection)

Porosity (%) = 35.90
Oil Viscosity (mPa.s) = 1058.0
Ave. Run Temp.(K) = 294.15
CO_2 Req. (sm^3/sm^3) = 3.82
Vp (cm^3) = 1116
S_{oi} (%) = 95.43
HCPV (cm3) = 1025
CO_2 Ret. (%inj.) = 37.17
S_{wc} (%) = 4.57
Molar Den. ($kmol/m^3$) = 0.04166
Abs. k (darcies) = 11.33
Ave. Flow Vel. (m/d) = 0.984

Press Inj. (MPa)	Press Prod. (MPa)	Gas Inj. (cm^3)	Water Inj. (cm^3)	Cum. PV Injected	Gas Prod (s.ltr)	Water Prod. (cm^3)	Oil Prod. (cm^3)	Cum. Oil Prod. (cm^3)	Percent Rec. (%)	WOR (sm^3/sm^3)	GOR (sm^3/sm^3)	OPFIR (sm^3/sm^3)
1.20	1.00	0.0	85.2	0.953	0.042	41.00	19.20	426.40	41.60	2.14	2.19	0.225
1.20	1.00	0.0	224.8	1.155	0.275	157.00	54.00	480.40	46.87	2.91	5.09	0.240
1.20	1.00	0.0	478.3	1.584	0.324	179.00	36.00	516.40	50.38	4.97	9.00	0.075
1.20	1.00	0.0	483.4	2.017	0.251	227.50	13.50	529.90	51.70	16.85	18.59	0.028
1.20	1.00	0.0	441.5	2.412	0.161	235.50	9.50	539.40	52.62	24.79	16.95	0.022
0.10	0.10	0.0	0.0	2.412	0.220	139.00	19.00	558.40	54.48	7.32	11.58	

TABLE E06

Tabulated Experimental Results of Run VLC02

(20% HCPV CO_2 @ 1.0 MPa (0.087 moles), 10 Slugs, 4:1 WAG, 21°C, Injection at Top)

Porosity (%) = 35.54
Oil Viscosity (mPa.s) = 1058.0
Ave. Run Temp.(K) = 294.15
CO_2 Req. (sm^3/sm^3) = 4.34

Vp (cm^3) = 1105
S_{oi} (%) = 90.68
HCPV (cm3) = 1002
CO_2 Ret. (%inj.) = 54.05

S_{wc} (%) = 9.32
Molar Den. ($kmol/m^3$) = 0.04166
Abs. k (darcies) = 11.12
Ave. Flow Vel. (m/d) = 0.984

Press Inj. (MPa)	Press Prod. (MPa)	Gas Inj. (cm^3)	Water Inj. (cm^3)	Cum. PV Injected	Gas Prod (s.ltr)	Water Prod. (cm^3)	Oil Prod. (cm^3)	Cum. Oil Prod. (cm^3)	Percent Rec. (%)	WOR (sm^3/sm^3)	GOR (sm^3/sm^3)	OPFIR (sm^3/sm^3)
1.10	1.00	20.0	0.0	0.018	0.000	0.00	2.00	2.00	0.20	0.00	0.00	0.100
1.20	1.00	0.0	80.2	0.091	0.000	0.00	81.00	83.00	8.28	0.00	0.00	1.010
1.10	1.00	20.0	0.0	0.109	0.000	0.00	7.80	90.80	9.06	0.00	0.00	0.389
1.20	1.00	0.0	80.2	0.181	0.000	1.00	80.00	170.80	17.05	0.01	0.00	0.998
1.20	1.00	20.0	0.0	0.199	0.000	1.50	10.00	180.80	18.04	0.15	0.00	0.499
1.30	1.00	0.0	80.2	0.272	0.000	35.00	44.50	225.30	22.49	0.79	0.00	0.555
1.25	1.00	20.0	0.0	0.290	0.000	9.00	4.90	230.20	22.97	1.84	0.00	0.245
1.20	1.00	0.0	80.2	0.363	0.000	45.00	34.50	264.70	26.42	1.30	0.00	0.430
1.10	1.00	20.0	0.0	0.381	0.000	1.50	2.50	267.20	26.67	0.60	0.00	0.125
1.10	1.00	0.0	80.2	0.453	0.000	57.50	20.00	287.20	28.66	2.88	0.00	0.250
1.20	1.00	20.0	0.0	0.472	0.000	6.40	1.80	289.00	28.84	3.56	0.00	0.090
1.20	1.00	0.0	80.2	0.544	0.000	59.50	21.50	310.50	30.99	2.77	0.00	0.268
1.10	1.00	20.0	0.0	0.562	0.000	5.00	1.50	312.00	31.14	3.33	0.00	0.075
1.20	1.00	0.0	80.2	0.635	0.000	58.00	21.50	333.50	33.28	2.70	0.00	0.268
1.20	1.00	20.0	0.0	0.653	0.000	24.00	1.80	335.30	33.46	13.33	0.00	0.090
1.20	1.00	0.0	80.2	0.725	0.000	43.50	16.50	351.80	35.11	2.64	0.00	0.206
1.20	1.00	20.0	0.0	0.744	0.000	28.50	2.00	353.80	35.31	14.25	0.00	0.100
1.20	1.00	0.0	80.2	0.816	0.000	45.50	15.20	369.00	36.83	2.99	0.00	0.190
1.20	1.00	20.0	0.0	0.834	0.000	12.50	1.00	370.00	36.93	12.50	0.00	0.050

TABLE E06 (Cont'd)

Tabulated Experimental Results of Run VLC02

(20% HCPV CO_2 @ 1.0 MPa (0.087 moles), 10 Slugs, 4:1 WAG, 21°C, Injection at Top)

Porosity (%) =	35.54	Vp (cm^3) =	1105	S_{wc} (%) =	9.32
Oil Viscosity (mPa.s) =	1058.0	S_{oi} (%) =	90.68	Molar Den. (kmol/m^3) =	0.04166
Ave. Run Temp.(K) =	294.15	HCPV (cm3) =	1002	Abs. k (darcies) =	11.12
CO_2 Req. (sm^3/sm^3) =	4.34	CO_2 Ret. (%inj.) =	54.05	Ave. Flow Vel. (m/d) =	0.984

Press Inj. (MPa)	Press Prod. (MPa)	Gas Inj. (cm^3)	Water Inj. (cm^3)	Cum. PV Injected	Gas Prod (s.ltr)	Water Prod. (cm^3)	Oil Prod. (cm^3)	Cum. Oil Prod. (cm^3)	Percent Rec. (%)	WOR (sm^3/sm^3)	GOR (sm^3/sm^3)	OPFIR (sm^3/sm^3)
1.20	1.00	0.0	80.2	0.907	0.000	60.50	12.50	382.50	38.17	4.84	0.00	0.156
1.10	1.00	0.0	229.8	1.115	0.026	212.00	18.00	400.50	39.97	11.78	1.44	0.078
1.10	1.00	0.0	478.3	1.548	0.070	196.00	23.00	423.50	42.27	8.52	3.04	0.048
1.10	1.00	0.0	475.9	1.978	0.309	195.00	17.50	441.00	44.01	11.14	17.66	0.037
1.10	1.00	0.0	444.0	2.380	0.290	232.00	14.00	455.00	45.41	16.57	20.68	0.032
0.10	1.00	0.0	0.0	2.380	0.264	137.00	25.00	480.00	47.90	5.48	10.54	

TABLE E07

Tabulated Experimental Results of Run VLC03

(20% HCPV CO_2 @ 1.0 MPa (0.088 moles), 21°C, Single Slug, Injection at Bottom)

Porosity (%) =	34.74	Vp (cm^3) =	1080	S_{wc} (%) =	5.65
Oil Viscosity (mPa.s) =	1058.0	S_{oi} (%) =	94.35	Molar Den. ($kmol/m^3$) =	0.04166
Ave. Run Temp.(K) =	294.15	HCPV (cm^3) =	1019	Abs. k (darcies) =	9.18
CO_2 Req. (sm^3/sm^3) =	5.43	CO_2 Ret. (%inj.) =	59.61	Ave. Flow Vel. (m/d) =	0.984

Press Inj. (MPa)	Press Prod. (MPa)	Gas Inj. (cm^3)	Water Inj. (cm^3)	Cum. PV Injected	Gas Prod (s.ltr)	Water Prod. (cm^3)	Oil Prod. (cm^3)	Cum. Oil Prod. (cm^3)	Percent Rec. (%)	WOR (sm^3/sm^3)	GOR (sm^3/sm^3)	OPFIR (sm^3/sm^3)
1.10	1.00	211.8	0.0	0.196	0.001	0.00	2.00	2.00	0.20	0.00	0.00	0.009
1.20	1.00	0.0	232.3	0.411	0.000	39.50	209.50	211.50	20.76	0.19	0.00	0.902
1.10	1.00	0.0	233.2	0.627	0.000	197.50	75.00	286.50	28.12	2.63	0.00	0.322
1.20	1.00	0.0	250.7	0.859	0.000	227.00	35.40	321.90	31.59	6.41	0.00	0.141
1.20	1.00	0.0	90.9	0.944	0.000	84.00	20.00	341.90	33.55	4.20	0.00	0.220
1.30	1.00	0.0	250.6	1.176	0.095	219.50	18.20	360.10	35.34	12.06	5.21	0.073
1.25	1.00	0.0	250.2	1.407	0.223	215.50	14.50	374.60	36.76	14.86	15.34	0.058
1.25	1.00	0.0	265.7	1.653	0.296	244.00	12.20	386.80	37.96	20.00	24.29	0.046
1.10	1.00	0.0	0.0	1.653	0.276	22.00	11.10	397.90	39.05	1.98	24.86	

TABLE E08

Tabulated Experimental Results of Run VLC04

(20% HCPV CO_2 @ 1.0 MPa (0.088 moles), 21°C, Single Slug, Injection at Bottom)

Porosity (%) = 35.50
Oil Viscosity (mPa.s) = 1058.0
Ave. Run Temp.(K) = 294.15
CO_2 Req. (sm^3/sm^3) = 5.64

Vp (cm^3) = 1103.8
S_{oi} (%) = 91.96
HCPV (cm^3) = 1015
CO_2 Ret. (%inj.) = 57.45

S_{wc} (%) = 8.04
Molar Den. ($kmol/m^3$) = 0.04166
Abs. k (darcies) = 10.23
Ave. Flow Vel. (m/d) = 0.984

Press Inj. (MPa)	Press Prod. (MPa)	Gas Inj. (cm^3)	Water Inj. (cm^3)	Cum. PV Injected	Gas Prod (s.ltr)	Water Prod. (cm^3)	Oil Prod. (cm^3)	Cum. Oil Prod. (cm^3)	Percent Rec. (%)	WOR (sm^3/sm^3)	GOR (sm^3/sm^3)	OPFIR (sm^3/sm^3)
1.10	1.00	211.0	0.0	0.191	0.001	0.00	7.50	7.50	0.74	0.00	0.00	0.036
1.10	1.00	0.0	237.6	0.406	-0.001	22.00	208.50	216.00	21.28	0.11	0.00	0.877
1.20	1.00	0.0	231.9	0.617	0.000	161.00	70.00	286.00	28.18	2.30	0.00	0.302
1.10	1.00	0.0	250.9	0.844	0.000	227.00	26.00	312.00	30.74	8.73	0.00	0.104
1.20	1.00	0.0	255.0	1.075	0.001	235.00	21.00	333.00	32.81	11.19	0.02	0.082
1.20	1.00	0.0	251.5	1.303	0.102	238.00	17.00	350.00	34.48	14.00	5.97	0.068
1.20	1.00	0.0	251.3	1.530	0.185	240.00	12.00	362.00	35.67	20.00	15.38	0.048
1.20	1.00	0.0	253.6	1.760	0.242	244.50	10.50	372.50	36.70	23.29	23.00	0.041
0.10	0.10	0.0	0.0	1.760	0.406	48.00	17.00	389.50	38.37	2.82	23.88	

TABLE E09

Tabulated Experimental Results of Run VLC05

(20% HCPV CO_2 @ 1.0 MPa (0.087 moles), 21°C, Single Slug Injection at Top)

Porosity (%) = 35.38 Vp (cm^3) = 1100 S_{wc} (%) = 8.18

Oil Viscosity (mPa.s) = 1058.0 S_{oi} (%) = 91.82 Molar Den. (kmol/m^3) = 0.04166

Ave. Run Temp.(K) = 294.15 HCPV (cm^3) = 1010 Abs. k (darcies) = 11.34

CO_2 Req. (sm^3/sm^3) = 7.20 CO_2 Ret. (%inj.) = 99.19 Ave. Flow Vel. (m/d) = 0.984

Press Inj. (MPa)	Press Prod. (MPa)	Gas Inj. (cm^3)	Water Inj. (cm^3)	Cum. PV Injected	Gas Prod (s.ltr)	Water Prod. (cm^3)	Oil Prod. (cm^3)	Cum. Oil Prod. (cm^3)	Percent Rec. (%)	WOR (sm^3/sm^3)	GOR (sm^3/sm^3)	OPFIR (sm^3/sm^3)
1.10	1.00	209.9	0.0	0.191	0.006	0.00	17.50	17.50	1.73	0.00	0.00	0.083
1.10	1.00	0.0	239.0	0.408	0.000	21.00	209.40	226.90	22.47	0.10	0.00	0.876
1.20	1.00	0.0	233.2	0.620	0.000	97.50	25.80	252.70	25.02	3.78	0.00	0.111
1.10	1.00	0.0	251.4	0.849	0.000	226.00	7.00	259.70	25.71	32.29	0.00	0.028
1.20	1.00	0.0	252.0	1.078	0.000	234.00	12.90	272.60	26.99	18.14	0.00	0.051
1.20	1.00	0.0	251.9	1.307	0.000	239.50	16.40	289.00	28.61	14.60	0.00	0.065
1.20	1.00	0.0	251.0	1.535	0.003	239.00	10.90	299.90	29.69	21.93	0.28	0.043
0.10	0.10	0.0	0.0	1.535	0.009	86.00	3.40	303.30	30.03	25.29	2.53	

TABLE E10

Tabulated Experimental Results of Run VLC06

(20% HCPV CO_2 @ 2.5 MPa (0.087 moles), 10 Slugs, 4:1 WAG, 21°C, Injection at Bottom)

Porosity (%) = 35.32
Oil Viscosity (mPa.s) = 1058.0
Ave. Run Temp.(K) = 294.15
CO_2 Req. (sm^3/sm^3) = 12.05

V_p (cm^3) = 1098
S_{oi} (%) = 91.99
HCPV (cm^3) = 1010
CO_2 Ret. (%inj.) = 75.31

S_{wc} (%) = 8.01
Molar Den. ($kmol/m^3$) = 1.20426
Abs. k (darcies) = 9.87
Ave. Flow Vel. (m/d) = 0.984

Press Inj. (MPa)	Press Prod. (MPa)	Gas Inj. (cm^3)	Water Inj. (cm^3)	Cum. PV Injected	Gas Prod (s.ltr)	Water Prod. (cm^3)	Oil Prod. (cm^3)	Cum. Oil Prod. (cm^3)	Percent Rec. (%)	WOR (sm^3/sm^3)	GOR (sm^3/sm^3)	OPFIR (sm^3/sm^3)
2.60	2.50	21.0	0.0	0.019	0.000	0.00	1.00	1.00	0.10	0.00	0.00	0.048
3.00	2.50	0.0	84.0	0.096	0.001	2.00	81.50	82.50	8.17	0.02	0.01	0.970
2.60	2.50	21.0	0.0	0.115	0.000	0.00	4.00	86.50	8.56	0.00	0.00	0.191
2.80	2.50	0.0	84.0	0.191	0.000	0.00	82.00	168.50	16.68	0.00	0.00	0.976
2.60	2.50	21.0	0.0	0.210	0.000	0.00	7.50	176.00	17.43	0.00	0.00	0.358
2.80	2.50	0.0	87.6	0.290	0.000	30.00	53.00	229.00	22.67	0.57	0.00	0.605
2.70	2.50	21.0	0.0	0.309	0.001	7.60	5.40	234.40	23.21	0.00	0.09	0.258
2.80	2.50	0.0	84.0	0.386	0.000	53.50	29.10	263.50	26.09	1.84	0.00	0.346
2.60	2.50	21.0	0.0	0.405	0.000	2.00	2.00	265.50	26.29	0.00	0.00	0.095
2.80	2.50	0.0	86.1	0.483	0.000	66.50	17.00	282.50	27.97	3.91	0.00	0.198
2.60	2.50	21.0	0.0	0.502	0.000	2.50	2.00	284.50	28.17	0.00	0.00	0.095
2.60	2.50	0.0	85.2	0.580	0.000	64.50	18.50	303.00	30.00	3.49	0.00	0.217
2.60	2.50	21.0	0.0	0.599	0.000	3.00	2.00	305.00	30.20	0.00	0.00	0.095
2.60	2.50	0.0	84.0	0.675	0.000	65.00	15.50	320.50	31.73	4.19	0.00	0.185
2.70	2.50	21.0	0.0	0.695	0.000	5.50	1.50	322.00	31.88	0.00	0.00	0.072
2.80	2.50	0.0	84.1	0.771	0.003	61.50	19.00	341.00	33.76	3.24	0.13	0.226
2.60	2.50	21.0	0.0	0.790	0.001	3.00	1.50	342.50	33.91	0.00	0.33	0.072
2.90	2.50	0.0	84.0	0.867	0.003	63.50	17.00	359.50	35.59	3.74	0.18	0.202
2.60	2.50	21.0	0.0	0.886	0.001	2.50	2.50	362.00	35.84	0.00	0.20	0.119

TABLE E10 (Cont'd)

Tabulated Experimental Results of Run VLC06

(20% HCPV CO_2 @ 2.5 MPa (0.087 moles), 10 Slugs, 4:1 WAG, 21°C, Injection at Bottom)

Porosity (%) = 35.32
Oil Viscosity (mPa.s) = 1058.0
Ave. Run Temp.(K) = 294.15
CO_2 Req. (sm^3/sm^3) = 12.05

V_p (cm^3) = 1098
S_{oi} (%) = 91.99
HCPV (cm^3) = 1010
CO_2 Ret. (%inj.) = 75.31

S_{wc} (%) = 8.01
Molar Den. ($kmol/m^3$) = 1.20426
Abs. k (darcies) = 9.87
Ave. Flow Vel. (m/d) = 0.984

Press Inj. (MPa)	Press Prod. (MPa)	Gas Inj. (cm^3)	Water Inj. (cm^3)	Cum. PV Injected	Gas Prod (s.ltr)	Water Prod. (cm^3)	Oil Prod. (cm^3)	Cum. Oil Prod. (cm^3)	Percent Rec. (%)	WOR (sm^3/sm^3)	GOR (sm^3/sm^3)	OPFIR (sm^3/sm^3)
2.80	2.50	0.0	84.0	0.962	0.028	66.00	16.50	378.50	37.48	4.00	1.70	0.196
2.80	2.50	0.0	235.1	1.176	0.376	200.00	20.00	398.50	39.46	10.00	18.81	0.085
2.60	2.50	0.0	240.5	1.395	0.376	225.00	18.00	416.50	41.24	12.50	20.89	0.075
2.70	2.50	0.0	245.2	1.619	0.299	232.00	12.50	429.00	42.48	18.56	23.88	0.051
2.80	2.50	0.0	248.2	1.845	0.201	236.00	12.50	441.50	43.71	18.88	16.04	0.050
2.60	2.50	0.0	248.6	2.071	0.096	238.00	11.50	453.00	44.85	20.70	8.30	0.046
2.60	2.50	0.0	251.1	2.300	0.024	245.00	13.00	466.00	46.14	18.85	1.81	0.052
2.70	2.50	0.0	269.2	2.545	0.013	262.00	11.50	477.50	47.28	22.78	1.09	0.043
0.10	2.50	0.0	0.0	2.545	0.023	30.00	7.00	484.50	47.97	4.29	3.29	

TABLE E11

Tabulated Experimental Results of Run VLC07

(Continuous Injection of CO_2 @ Top Until Gas Breakthrough @ 1.0 MPa (0.391 moles), 21°C, Water Injection at Bottom)

Porosity (%) = 35.38
Oil Viscosity (mPa.s) = 1055.3
Ave. Run Temp.(K) = 294.15
CO_2 Req. (sm^3/sm^3) = 15.55

V_p (cm^3) = 1100
S_{oi} (%) = 95.27
HCPV (cm^3) = 1048
CO_2 Ret. (%inj.) = 74.07

S_{wc} (%) = 4.73
Molar Den. ($kmol/m^3$) = 0.04166
Abs. k (darcies) = 10.02
Ave. Flow Vel. (m/d) = 0.984

Press Inj. (MPa)	Press Prod. (MPa)	Gas Inj. (cm^3)	Water Inj. (cm^3)	Cum. PV Injected	Gas Prod (s.ltr)	Water Prod. (cm^3)	Oil Prod. (cm^3)	Cum. Oil Prod. (cm^3)	Percent Rec. (%)	WOR (sm^3/sm^3)	GOR (sm^3/sm^3)	OPFIR (sm^3/sm^3)
1.10	1.00	902.6	0.0	0.821	0.465	0.00	50.00	50.00	4.77	0.00	9.30	0.055
1.10	1.00	0.0	252.2	1.050	1.197	54.00	168.50	218.50	20.85	0.32	6.87	0.668
1.10	1.00	0.0	229.2	1.258	0.577	120.00	128.00	346.50	33.06	0.94	4.20	0.559
1.10	1.00	0.0	251.4	1.487	0.032	187.00	63.00	409.50	39.07	2.97	0.50	0.251
1.10	1.00	0.0	250.4	1.714	0.029	210.00	41.00	450.50	42.99	5.12	0.71	0.164
1.10	1.00	0.0	250.5	1.942	0.012	218.00	31.00	481.50	45.94	7.03	0.37	0.124
1.10	1.00	0.0	251.8	2.171	0.021	233.00	17.50	499.00	47.61	13.31	1.17	0.070
1.10	1.00	0.0	262.1	2.409	0.017	240.00	21.50	520.50	49.67	11.16	0.77	0.082
1.10	1.00	0.0	251.8	2.638	0.021	235.00	16.80	537.30	51.27	13.99	1.26	0.067
1.10	1.00	0.0	250.9	2.866	0.017	236.00	14.90	552.20	52.69	15.84	1.15	0.059
1.10	1.00	0.0	255.0	3.098	0.018	239.75	15.25	567.45	54.15	15.72	1.18	0.060
1.10	1.00	0.0	252.6	3.328	0.032	240.00	12.60	580.05	55.35	19.05	2.57	0.050
1.10	1.00	0.0	250.9	3.556	0.034	240.00	10.90	590.95	56.39	22.02	3.13	0.043
0.10	0.10	0.0	0.0	3.556	0.044	43.00	13.00	603.95	57.63	3.31	3.38	

TABLE E12

Tabulated Experimental Results of Run VLC08

(Continuous Injection of CO_2 @ Top Until Gas Breakthrough @ 1.0 MPa (0.748 moles), 21°C, Water Injection at Bottom)

Porosity (%) =	35.45	V_p (cm^3) =	1102	S_{wc} (%) =	4.45
Oil Viscosity (mPa.s) =	1055.3	S_{oi} (%) =	95.55	Molar Den. ($kmol/m^3$) =	0.04166
Ave. Run Temp.(K) =	294.15	HCPV (cm^3) =	1053	Abs. k (darcies) =	9.44
CO_2 Req. (sm^3/sm^3) =	15.51	CO_2 Ret. (%inj.) =	72.51	Ave. Flow Vel. (m/d) =	0.984

Press Inj. (MPa)	Press Prod. (MPa)	Gas Inj. (cm^3)	Water Inj. (cm^3)	Cum. PV Injected	Gas Prod (s.ltr)	Water Prod. (cm^3)	Oil Prod. (cm^3)	Cum. Oil Prod. (cm^3)	Percent Rec. (%)	WOR (sm^3/sm^3)	GOR (sm^3/sm^3)	OPFIR (sm^3/sm^3)
1.10	1.00	925.5	0.0	0.840	0.599	0.00	59.00	59.00	5.60	0.00	10.14	0.064
1.10	1.00	0.0	300.2	1.112	1.100	64.00	206.70	265.70	25.23	0.31	5.32	0.689
1.10	1.00	0.0	223.4	1.315	0.505	120.00	89.00	354.70	33.68	1.35	5.67	0.398
1.10	1.00	0.0	264.1	1.555	0.186	160.00	70.00	424.70	40.33	2.29	2.66	0.265
1.10	1.00	0.0	249.6	1.781	0.025	207.50	40.50	465.20	44.18	5.12	0.62	0.162
1.10	1.00	0.0	270.7	2.027	0.022	236.00	33.50	498.70	47.36	7.04	0.64	0.124
1.10	1.00	0.0	252.6	2.256	0.027	230.00	20.50	519.20	49.31	11.22	1.29	0.081
1.10	1.00	0.0	252.7	2.485	0.016	233.00	20.00	539.20	51.21	11.65	0.80	0.079
1.10	1.00	0.0	251.4	2.713	0.016	235.00	17.00	556.20	52.82	13.82	0.94	0.068
1.10	1.00	0.0	250.8	2.941	0.037	228.00	22.80	579.00	54.99	10.00	1.63	0.091
1.10	1.00	0.0	253.7	3.171	0.016	237.25	15.20	594.20	56.43	15.61	1.02	0.060
1.10	1.00	0.0	248.6	3.397	0.039	236.10	12.50	606.70	57.62	18.89	3.15	0.050
1.10	1.00	0.0	249.2	3.623	0.038	243.00	10.20	616.90	58.58	23.82	3.71	0.041
0.10	0.10	0.0	0.0	3.623	0.022	15.00	4.00	620.90	58.96	3.75	5.50	

TABLE E13

Tabulated Experimental Results of Run VLC09

(Continuous Injection of CO_2 @ Top Until Gas Breakthrough @ 1.0 MPa (0.484 moles), 21°C, Water Injection at Bottom)

Porosity (%) =	35.38	V_p (cm^3) =	1100	S_{wc} (%) =	3.82
Oil Viscosity (mPa.s) =	1055.3	S_{oi} (%) =	96.18	Molar Den. (kmol/m^3) =	0.04166
Ave. Run Temp.(K) =	294.15	HCPV (cm^3) =	1058	Abs. k (darcies) =	10.58
CO_2 Req. (sm^3/sm^3) =	15.85	CO_2 Ret. (%inj.) =	79.47	Ave. Flow Vel. (m/d) =	0.492

Press Inj. (MPa)	Press Prod. (MPa)	Gas Inj. (cm^3)	Water Inj. (cm^3)	Cum. PV Injected	Gas Prod (s.ltr)	Water Prod. (cm^3)	Oil Prod. (cm^3)	Cum. Oil Prod. (cm^3)	Percent Rec. (%)	WOR (sm^3/sm^3)	GOR (sm^3/sm^3)	OPFIR (sm^3/sm^3)
1.10	1.00	1116.3	0.0	1.015	0.557	0.00	101.00	101.00	9.55	0.00	5.51	0.090
1.10	1.00	0.0	296.3	1.284	1.188	52.50	188.00	289.00	27.32	0.28	6.32	0.634
1.10	1.00	0.0	227.4	1.491	0.063	135.00	111.50	400.50	37.85	1.21	0.56	0.490
1.10	1.00	0.0	247.2	1.716	0.048	176.00	71.00	471.50	44.57	2.48	0.68	0.287
1.10	1.00	0.0	246.6	1.940	0.042	208.00	39.00	510.50	48.25	5.33	1.08	0.158
1.10	1.00	0.0	268.3	2.184	0.022	236.00	31.00	541.50	51.18	7.61	0.71	0.116
1.10	1.00	0.0	250.7	2.412	0.012	225.00	24.00	565.50	53.45	9.38	0.50	0.096
1.10	1.00	0.0	249.9	2.639	0.012	227.00	23.50	589.00	55.67	9.66	0.51	0.094
1.10	1.00	0.0	252.6	2.868	0.054	229.00	23.60	612.60	57.90	9.70	2.31	0.093
1.10	1.00	0.0	252.7	3.098	0.016	231.00	21.70	634.30	59.95	10.65	0.75	0.086
1.10	1.00	0.0	251.4	3.327	0.027	233.00	18.40	652.70	61.69	12.66	1.45	0.073
1.10	1.00	0.0	250.4	3.554	0.031	235.00	15.40	668.10	63.15	15.26	1.99	0.062
1.10	1.00	0.0	251.2	3.783	0.040	237.00	14.20	682.30	64.49	16.69	2.80	0.057
1.10	1.00	0.0	253.3	4.013	0.069	239.00	13.30	695.60	65.75	17.97	5.17	0.053
1.10	1.00	0.0	251.1	4.241	0.060	237.00	14.10	709.70	67.08	16.81	4.25	0.056
1.10	1.00	0.0	255.8	4.474	0.045	243.00	12.80	722.50	68.29	18.98	3.53	0.050
0.10	0.10	0.0	0.0	4.474	0.100	40.00	10.00	732.50	69.23	4.00	10.00	

TABLE E14

Tabulated Experimental Results of Run VLC10

(Continuous Injection of CO_2 @ Top Until Gas Breakthrough @ 1.0 MPa (0.578 moles), 21°C, Model Inverted to Inject Water at Bottom)

Porosity (%) = 35.38
Oil Viscosity (mPa.s) = 1055.3
Ave. Run Temp.(K) = 294.15
CO_2 Req. (sm^3/sm^3) = 17.52
V_p (cm^3) = 1100
S_{oi} (%) = 95.09
HCPV (cm^3) = 1046
CO_2 Ret. (%inj.) = 87.91
S_{wc} (%) = 4.91
Molar Den. (kmol/m^3) = 0.04166
Abs. k (darcies) = 11.02
Ave. Flow Vel. (m/d) = 0.492

Press Inj. (MPa)	Press Prod. (MPa)	Gas Inj. (cm^3)	Water Inj. (cm^3)	Cum. PV Injected	Gas Prod (s.ltr)	Water Prod. (cm^3)	Oil Prod. (cm^3)	Cum. Oil Prod. (cm^3)	Percent Rec. (%)	WOR (sm^3/sm^3)	GOR (sm^3/sm^3)	OPFIR (sm^3/sm^3)
1.10	1.00	1348.6	0.0	1.226	0.298	0.00	112.50	112.50	10.76	0.00	2.64	0.083
1.10	1.00	0.0	328.7	1.525	0.522	62.50	177.50	290.00	27.72	0.35	2.94	0.540
1.10	1.00	0.0	246.9	1.749	0.247	150.50	114.50	404.50	38.67	1.31	2.16	0.464
1.10	1.00	0.0	250.4	1.977	0.122	175.00	75.50	480.00	45.89	2.32	1.61	0.302
1.10	1.00	0.0	262.0	2.215	0.026	206.00	56.00	536.00	51.24	3.68	0.46	0.214
1.10	1.00	0.0	262.8	2.454	0.008	233.00	31.00	567.00	54.21	7.52	0.24	0.118
1.10	1.00	0.0	262.0	2.692	0.001	220.00	44.00	611.00	58.41	5.00	0.02	0.168
1.10	1.00	0.0	253.3	2.922	0.010	227.00	29.00	640.00	61.19	7.83	0.34	0.114
1.10	1.00	0.0	306.5	3.201	0.078	228.50	18.50	658.50	62.95	12.35	4.19	0.060
1.10	1.00	0.0	255.5	3.433	0.012	232.00	23.50	682.00	65.20	9.87	0.49	0.092
1.10	1.00	0.0	251.7	3.662	0.040	230.00	21.70	703.70	67.28	10.60	1.83	0.086
1.10	1.00	0.0	250.9	3.890	0.021	231.00	19.90	723.60	69.18	11.61	1.04	0.079
1.10	1.00	0.0	252.1	4.119	0.055	235.00	17.10	740.70	70.81	13.74	3.24	0.068
1.10	1.00	0.0	253.4	4.350	0.078	238.00	15.40	756.10	72.28	15.45	5.07	0.061
1.10	1.00	0.0	250.8	4.578	0.061	237.00	13.80	769.90	73.60	17.17	4.40	0.055
1.10	1.00	0.0	250.9	4.806	0.041	240.00	10.90	780.80	74.65	22.02	3.72	0.043
0.10	0.10	0.0	0.0	4.806	0.081	4.00	20.00	800.80	76.56	0.20	4.05	

TABLE E15

Tabulated Experimental Results of Run VLC11

(Continuous Injection of CO_2 @ Top Until Gas Breakthrough @ 1.0 MPa (0.448 moles), 21°C, Water Injection at Bottom)

Porosity (%) = 35.56
Oil Viscosity (mPa.s) = 1055.3
Ave. Run Temp.(K) = 294.15
CO_2 Req. (sm^3/sm^3) = 16.90
V_p (cm^3) = 1105.6
S_{oi} (%) = 95.88
HCPV (cm^3) = 1060
CO_2 Ret. (%inj.) = 71.38
S_{wc} (%) = 4.12
Molar Den. ($kmol/m^3$) = 0.04166
Abs. k (darcies) = 10.75
Ave. Flow Vel. (m/d) = 0.984

Press Inj. (MPa)	Press Prod. (MPa)	Gas Inj. (cm^3)	Water Inj. (cm^3)	Cum. PV Injected	Gas Prod (s.ltr)	Water Prod. (cm^3)	Oil Prod. (cm^3)	Cum. Oil Prod. (cm^3)	Percent Rec. (%)	WOR (sm^3/sm^3)	GOR (sm^3/sm^3)	OPFIR (sm^3/sm^3)
1.10	1.00	1034.2	0.0	0.935	0.877	0.00	74.00	74.00	6.98	0.00	11.84	0.072
1.10	1.00	0.0	306.5	1.213	1.321	54.00	185.00	259.00	24.43	0.29	7.14	0.604
1.10	1.00	0.0	232.1	1.423	0.370	145.00	104.50	363.50	34.29	1.39	3.54	0.450
1.10	1.00	0.0	255.9	1.654	0.180	200.00	57.00	420.50	39.67	3.51	3.16	0.223
1.10	1.00	0.0	252.5	1.882	0.136	216.00	48.00	468.50	44.20	4.50	2.83	0.190
1.10	1.00	0.0	253.9	2.112	0.061	225.00	30.00	498.50	47.03	7.50	2.03	0.118
1.10	1.00	0.0	253.1	2.341	0.011	233.00	27.00	525.50	49.58	8.63	0.41	0.107
1.10	1.00	0.0	255.3	2.572	0.003	236.00	19.00	544.50	51.37	12.42	0.16	0.074
1.10	1.00	0.0	251.8	2.800	0.011	235.00	16.80	561.30	52.95	13.99	0.67	0.067
1.10	1.00	0.0	250.9	3.027	0.017	236.00	14.90	576.20	54.36	15.84	1.15	0.059
1.10	1.00	0.0	255.0	3.257	0.028	240.00	15.00	591.20	55.77	16.00	1.87	0.059
1.10	1.00	0.0	252.6	3.486	0.012	240.00	12.60	603.80	56.96	19.05	0.98	0.050
1.10	1.00	0.0	250.9	3.713	0.044	239.00	11.90	615.70	58.08	20.08	3.71	0.047
0.10	0.10	0.0	0.0	3.713	0.009	16.00	21.00	636.70	60.07	0.76	0.40	

TABLE E16

Tabulated Experimental Results of Run H2D1

(20% HCPV CO_2 Injected at Water Rate @ 2.5 MPa (0.450 moles), 10 Slugs, 4:1 WAG, 21°C, Horizontal Injection)

Porosity (%) = 40.13
Oil Viscosity (mPa.s) = 603
Ave. Run Temp.(K) = 294.15
CO_2 Req. (sm^3/sm^3) = 5.01

Vp (cm^3) = 2005
S_{oi} (%) = 93.27
HCPV (cm^3) = 1870
CO_2 Ret. (%inj.) = 50.21

S_{wc} (%) = 6.73
Molar Den. ($kmol/m^3$) = 0.04166
Abs. k (darcies) = 11.96
Ave. Flow Vel. (m/d) = 0.78

Press Inj. (MPa)	Press Prod. (MPa)	Gas Inj. (cm^3)	Water Inj. (cm^3)	Cum. PV Injected	Gas Prod (s.ltr)	Water Prod. (cm^3)	Oil Prod. (cm^3)	Cum. Oil Prod. (cm^3)	Percent Rec. (%)	WOR (sm^3/sm^3)	GOR (sm^3/sm^3)	OPFIR (sm^3/sm^3)
2.70	2.50	37.4	0.0	0.019	0.004	0.00	8.00	8.00	0.43	0.00	0.50	0.214
3.10	2.50	0.0	149.6	0.093	0.024	0.00	119.00	127.00	6.79	0.00	0.20	0.795
2.60	2.50	37.4	0.0	0.112	0.010	0.00	16.00	143.00	7.65	0.00	0.59	0.428
2.90	2.50	0.0	148.3	0.186	0.011	25.00	95.00	238.00	12.73	0.26	0.11	0.641
2.60	2.50	37.4	0.0	0.205	0.009	7.00	8.50	246.50	13.18	0.82	1.06	0.227
2.80	2.50	0.0	149.0	0.279	0.002	68.00	59.00	305.50	16.34	1.15	0.03	0.396
2.70	2.50	37.4	0.0	0.298	0.004	8.00	5.25	310.75	16.62	1.52	0.71	0.140
2.70	2.50	0.0	150.1	0.372	0.016	94.00	51.00	361.75	19.34	1.84	0.31	0.340
2.60	2.50	37.4	0.0	0.391	0.006	6.00	4.50	366.25	19.59	1.33	1.22	0.120
2.70	2.50	0.0	151.2	0.466	0.008	88.00	34.00	400.25	21.40	2.59	0.24	0.225
2.70	2.50	37.4	0.0	0.485	0.006	12.00	7.50	407.75	21.80	1.60	0.73	0.201
2.70	2.50	0.0	150.5	0.560	0.020	94.00	29.00	436.75	23.36	3.24	0.69	0.193
2.70	2.50	37.4	0.0	0.579	0.006	17.50	4.50	441.25	23.60	3.89	1.22	0.120
2.60	2.50	0.0	148.7	0.653	0.078	96.00	23.00	464.25	24.83	4.17	3.39	0.155
2.60	2.50	37.4	0.0	0.672	0.009	19.00	4.00	468.25	25.04	4.75	2.13	0.107
2.70	2.50	0.0	147.5	0.745	0.157	95.00	21.00	489.25	26.16	4.52	7.48	0.142
2.80	2.50	37.4	0.0	0.764	0.014	15.00	3.25	492.50	26.34	4.62	4.23	0.087
2.60	2.50	0.0	152.2	0.840	0.088	104.00	18.50	511.00	27.33	5.62	4.76	0.122
2.70	2.50	37.4	0.0	0.858	0.017	16.50	3.50	514.50	27.51	4.71	4.71	0.094

TABLE E16 (Cont'd)

Tabulated Experimental Results of Run H2D1

(20% HCPV CO_2 Injected at Water Rate @ 2.5 MPa (0.450 moles), 10 Slugs, 4:1 WAG, 21°C, Horizontal Injection)

Porosity (%) = 40.13
Oil Viscosity (mPa.s) = 1058
Ave. Run Temp.(K) = 294.15
CO_2 Req. (sm^3/sm^3) = 5.01

Vp (cm^3) = 2005
S_{oi} (%) = 93.27
HCPV (cm^3) = 1870
CO_2 Ret. (%inj.) = 50.21

S_{wc} (%) = 6.73
Molar Den. ($kmol/m^3$) = 0.04166
Abs. k (darcies) = 11.96
Ave. Flow Vel. (m/d) = 0.78

Press Inj. (MPa)	Press Prod. (MPa)	Gas Inj. (cm^3)	Water Inj. (cm^3)	Cum. PV Injected	Gas Prod (s.ltr)	Water Prod. (cm^3)	Oil Prod. (cm^3)	Cum. Oil Prod. (cm^3)	Percent Rec. (%)	WOR (sm^3/sm^3)	GOR (sm^3/sm^3)	OPFIR (sm^3/sm^3)
2.60	2.50	0.0	153.1	0.935	0.186	106.00	19.50	534.00	28.56	5.44	9.51	0.127
2.60	2.50	0.0	256.0	1.062	0.271	215.00	38.00	572.00	30.59	5.66	7.13	0.148
2.60	2.50	0.0	489.4	1.307	1.035	425.00	61.00	633.00	33.85	6.97	16.97	0.125
2.60	2.50	0.0	492.2	1.552	1.493	445.00	47.00	680.00	36.36	9.47	31.76	0.095
2.60	2.50	0.0	491.9	1.797	1.044	463.00	27.00	707.00	37.81	17.15	38.67	0.055
2.60	2.50	0.0	492.4	2.043	0.399	475.00	21.00	728.00	38.93	22.62	19.00	0.043
2.60	2.50	0.0	492.9	2.289	0.170	482.50	17.50	745.50	39.87	27.57	9.71	0.036
2.60	2.50	0.0	253.9	2.415	0.037	240.00	8.50	754.00	40.32	28.24	4.35	0.033
2.60	2.50	0.0	253.4	2.542	0.028	243.00	8.00	762.00	40.75	30.38	3.44	0.032
0.10	0.10	0.0	0.0	2.542	0.236	243.00	14.50	776.50	41.52	16.76	16.24	

TABLE E17

Tabulated Experimental Results of Run H2D2

(20% HCPV CO_2 Injected at Water Rate @ 2.5 MPa (0.423 moles), 10 Slugs, 4:1 WAG, 21°C, Horizontal Injection)

Porosity (%) = 39.71
Oil Viscosity (mPa.s) = 603
Ave. Run Temp.(K) = 294.15
CO_2 Req. (sm^3/sm^3) = 4.67
Vp (cm^3) = 1934
S_{oi} (%) = 90.74
HCPV (cm^3) = 1755
CO_2 Ret. (%inj.) = 47.0
S_{we} (%) = 9.26
Molar Den. ($kmol/m^3$) = 0.04166
Abs. k (darcies) = 14.51
Ave. Flow Vel. (m/d) = 1.55

Press Inj. (MPa)	Press Prod. (MPa)	Gas Inj. (cm^3)	Water Inj. (cm^3)	Cum. PV Injected	Gas Prod (s.ltr)	Water Prod. (cm^3)	Oil Prod. (cm^3)	Cum. Oil Prod. (cm^3)	Percent Rec. (%)	WOR (sm^3/sm^3)	GOR (sm^3/sm^3)	OPFIR (sm^3/sm^3)
2.70	2.50	35.1	0.0	0.018	0.004	0.00	8.00	8.00	0.46	0.00	0.50	0.228
3.10	2.50	0.0	140.4	0.091	0.019	0.00	124.00	132.00	7.52	0.00	0.15	0.883
2.60	2.50	35.1	0.0	0.109	0.010	0.00	16.00	148.00	8.43	0.00	0.59	0.456
2.90	2.50	0.0	140.1	0.181	0.011	25.00	95.00	243.00	13.85	0.26	0.11	0.678
2.60	2.50	35.1	0.0	0.199	0.009	7.00	8.50	251.50	14.33	0.82	1.06	0.242
2.80	2.50	0.0	140.8	0.272	0.002	68.00	59.00	310.50	17.69	1.15	0.03	0.419
2.70	2.50	35.1	0.0	0.290	0.004	8.00	5.25	315.75	17.99	1.52	0.71	0.150
2.70	2.50	0.0	141.2	0.363	0.016	94.00	51.00	366.75	20.90	1.84	0.31	0.361
2.60	2.50	35.1	0.0	0.382	0.006	6.00	4.50	371.25	21.15	1.33	1.22	0.128
2.70	2.50	0.0	141.8	0.455	0.008	88.00	34.00	405.25	23.09	2.59	0.24	0.240
2.70	2.50	35.1	0.0	0.473	0.006	12.00	7.50	412.75	23.52	1.60	0.73	0.214
2.70	2.50	0.0	140.8	0.546	0.020	94.00	29.00	441.75	25.17	3.24	0.69	0.206
2.70	2.50	35.1	0.0	0.564	0.006	17.50	4.50	446.25	25.43	3.89	1.22	0.128
2.60	2.50	0.0	140.1	0.636	0.078	96.00	23.00	469.25	26.74	4.17	3.39	0.164
2.60	2.50	35.1	0.0	0.655	0.009	19.00	4.00	473.25	26.97	4.75	2.13	0.114
2.70	2.50	0.0	142.0	0.728	0.157	95.00	21.00	494.25	28.16	4.52	7.48	0.148
2.80	2.50	35.1	0.0	0.746	0.014	15.00	3.25	497.50	28.35	4.62	4.23	0.093
2.60	2.50	0.0	141.9	0.820	0.088	104.00	18.50	516.00	29.40	5.62	4.76	0.130
2.70	2.50	35.1	0.0	0.838	0.017	16.50	3.50	519.50	29.60	4.71	4.71	0.100

TABLE E17 (Cont'd)

Tabulated Experimental Results of Run H2D2.

(20% HCPV CO_2 Injected at Water Rate @ 2.5 MPa (0.423 moles), 10 Slugs, 4:1 WAG, 21°C, Horizontal Injection)

Porosity (%) =	39.71	Vp (cm^3) =	1934	S_{wc} (%) =	9.26
Oil Viscosity (mPa.s) =	603	S_{oi} (%) =	90.74	Molar Den. ($kmol/m^3$) =	0.04166
Ave. Run Temp.(K) =	294.15	HCPV (cm^3) =	1755	Abs. k (darcies) =	14.51
CO_2 Req. (sm^3/sm^3) =	4.67	CO_2 Ret. (%inj.) =	47.0	Ave. Flow Vel. (m/d) =	1.55

Press Inj. (MPa)	Press Prod. (MPa)	Gas Inj. (cm^3)	Water Inj. (cm^3)	Cum. PV Injected	Gas Prod (s.ltr)	Water Prod. (cm^3)	Oil Prod. (cm^3)	Cum. Oil Prod. (cm^3)	Percent Rec. (%)	WOR (sm^3/sm^3)	GOR (sm^3/sm^3)	OPFIR (sm^3/sm^3)
2.60	2.50	0.0	139.8	0.910	0.186	106.00	19.50	539.00	30.71	5.44	9.51	0.139
2.60	2.50	0.0	256.0	1.042	0.271	215.00	38.00	577.00	32.88	5.66	7.13	0.148
2.60	2.50	0.0	489.4	1.295	1.035	425.00	61.00	638.00	36.35	6.97	16.97	0.125
2.60	2.50	0.0	492.2	1.550	1.493	445.00	47.00	685.00	39.03	9.47	31.76	0.095
2.60	2.50	0.0	491.9	1.804	1.044	463.00	27.00	712.00	40.57	17.15	38.67	0.055
2.60	2.50	0.0	492.4	2.059	0.399	475.00	21.00	733.00	41.77	22.62	19.00	0.043
2.60	2.50	0.0	492.9	2.314	0.170	482.50	17.50	750.50	42.76	27.57	9.71	0.036
2.60	2.50	0.0	253.9	2.445	0.037	240.00	8.50	759.00	43.25	28.24	4.35	0.033
2.60	2.50	0.0	253.4	2.576	0.028	243.00	8.00	767.00	43.70	30.38	3.44	0.032
0.10	0.10	0.0	0.0	2.576	0.236	243.00	14.50	781.50	44.53	16.76	16.24	

TABLE E18

Tabulated Experimental Results of Run H2D3

(20% HCPV CO_2 Injected at Water Rate @ 2.5 MPa (0.406 moles), 10 Slugs, 4:1 WAG, 21°C, Horizontal Injection)

Porosity (%) = 39.80
Oil Viscosity (mPa.s) = 603
Ave. Run Temp.(K) = 294.15
CO_2 Req. (sm^3/sm^3) = 4.38

Vp (cm^3) = 1939
S_{oi} (%) = 86.90
HCPV (cm^3) = 1685
CO_2 Ret. (%inj.) = 42.20

S_{wc} (%) = 13.10
Molar Den. ($kmol/m^3$) = 0.04166
Abs. k (darcies) = 13.23
Ave. Flow Vel. (m/d) = 2.54

Press Inj. (MPa)	Press Prod. (MPa)	Gas Inj. (cm^3)	Water Inj. (cm^3)	Cum. PV Injected	Gas Prod (s.ltr)	Water Prod. (cm^3)	Oil Prod. (cm^3)	Cum. Oil Prod. (cm^3)	Percent Rec. (%)	WOR (sm^3/sm^3)	GOR (sm^3/sm^3)	OPFIR (sm^3/sm^3)
2.60	2.50	33.7	0.0	0.017	0.001	0.00	12.50	12.50	0.74	0.00	0.04	0.371
3.00	2.50	0.0	135.9	0.087	0.027	0.00	120.00	132.50	7.86	0.00	0.23	0.883
2.70	2.40	33.7	0.0	0.105	0.002	0.00	18.50	151.00	8.96	0.00	0.08	0.549
2.90	2.50	0.0	139.3	0.177	0.021	21.00	103.00	254.00	15.07	0.20	0.20	0.740
2.70	2.50	33.7	0.0	0.194	0.003	4.00	12.00	266.00	15.79	0.33	0.21	0.356
2.70	2.60	0.0	138.1	0.265	0.009	60.00	69.00	335.00	19.88	0.87	0.13	0.500
2.50	2.40	33.7	0.0	0.283	0.004	11.00	7.00	342.00	20.30	1.57	0.57	0.208
2.70	2.50	0.0	133.8	0.352	0.006	82.00	37.00	379.00	22.49	2.22	0.16	0.277
2.60	2.50	33.7	0.0	0.369	0.001	23.50	6.00	385.00	22.85	3.92	0.17	0.178
2.60	2.50	0.0	135.3	0.439	0.151	78.70	32.30	417.30	24.77	2.44	4.66	0.239
2.70	2.50	33.7	0.0	0.456	0.003	18.50	6.00	423.30	25.12	3.08	0.42	0.178
2.70	2.50	0.0	135.0	0.526	0.021	94.00	27.00	450.30	26.72	3.48	0.76	0.200
2.55	2.50	33.7	0.0	0.543	0.003	11.70	4.30	454.60	26.98	2.72	0.58	0.128
2.70	2.50	0.0	134.8	0.613	0.012	94.00	23.00	477.60	28.34	4.09	0.50	0.171
2.50	2.40	33.7	0.0	0.630	0.011	21.50	4.00	481.60	28.58	5.38	2.75	0.119
2.70	2.50	0.0	161.0	0.713	0.386	108.20	24.80	506.40	30.05	4.36	15.54	0.154
2.60	2.50	33.7	0.0	0.731	0.009	16.00	2.50	508.90	30.20	6.40	3.60	0.074
2.60	2.50	0.0	134.8	0.800	0.142	102.00	21.50	530.40	31.48	4.74	6.58	0.159
2.60	2.50	33.7	0.0	0.817	0.017	19.80	3.70	534.10	31.70	5.35	4.46	0.110

TABLE E18 (Cont'd)

Tabulated Experimental Results of Run H2D3

(20% HCPV CO_2 Injected at Water Rate @ 2.5 MPa (0.406 moles), 10 Slugs, 4:1 WAG, 21°C, Horizontal Injection)

Porosity (%) = 39.80
Oil Viscosity (mPa.s) = 603
Ave. Run Temp.(K) = 294.15
CO_2 Req. (sm^3/sm^3) = 4.38
Vp (cm^3) = 1939
S_{oi} (%) = 86.90
HCPV (cm^3) = 1685
CO_2 Ret. (%inj.) = 42.20
S_{wc} (%) = 13.10
Molar Den. ($kmol/m^3$) = 0.04166
Abs. k (darcies) = 13.23
Ave. Flow Vel. (m/d) = 2.54

Press Inj. (MPa)	Press Prod. (MPa)	Gas Inj. (cm^3)	Water Inj. (cm^3)	Cum. PV Injected	Gas Prod (s.ltr)	Water Prod. (cm^3)	Oil Prod. (cm^3)	Cum. Oil Prod. (cm^3)	Percent Rec. (%)	WOR (sm^3/sm^3)	GOR (sm^3/sm^3)	OPFIR (sm^3/sm^3)
2.60	2.50	0.0	136.4	0.888	0.323	102.00	20.50	554.60	32.91	4.98	15.76	0.150
2.60	2.50	0.0	491.9	1.141	0.523	427.50	62.50	617.10	36.62	6.84	8.37	0.127
2.60	2.50	0.0	791.1	1.549	0.936	432.50	55.00	672.10	39.89	7.86	17.02	0.070
2.60	2.50	0.0	490.4	1.802	0.942	452.50	37.50	709.60	42.11	12.07	25.12	0.076
2.60	2.50	0.0	492.5	2.056	0.731	465.00	23.00	732.60	43.48	20.22	31.78	0.047
2.60	2.50	0.0	494.0	2.311	0.412	463.50	23.50	756.10	44.87	19.72	17.51	0.048
2.60	2.50	0.0	251.0	2.441	0.133	241.00	9.00	765.10	45.41	26.78	14.78	0.036
2.60	2.50	0.0	278.4	2.584	0.101	272.00	11.00	776.10	46.06	24.73	9.18	0.040
0.10	0.10	0.0	0.0	2.584	0.707	204.00	23.50	799.60	47.45	8.68	30.09	

TABLE E19

Tabulated Experimental Results of Run H2D4

(20% HCPV CO_2 Injected at Water Rate @ 2.5 MPa (0.408 moles), 10 Slugs, 4:1 WAG, 21°C, Horizontal Injection)

Porosity (%) = 38.70
Oil Viscosity (mPa.s) = 603
Ave. Run Temp.(K) = 294.15
CO_2 Req. (sm^3/sm^3) = 4.51
Vp (cm^3) = 1885
S_{oi} (%) = 89.92
HCPV (cm^3) = 1695
CO_2 Ret. (%inj.) = 45.13
S_{wc} (%) = 10.08
Molar Den. ($kmol/m^3$) = 0.04166
Abs. k (darcies) = 15.73
Ave. Flow Vel. (m/d) = 3.17

Press Inj. (MPa)	Press Prod. (MPa)	Gas Inj. (cm^3)	Water Inj. (cm^3)	Cum. PV Injected	Gas Prod (s.ltr)	Water Prod. (cm^3)	Oil Prod. (cm^3)	Cum. Oil Prod. (cm^3)	Percent Rec. (%)	WOR (sm^3/sm^3)	GOR (sm^3/sm^3)	OPFIR (sm^3/sm^3)
2.70	2.50	33.9	0.0	0.018	0.004	0.00	8.00	8.00	0.47	0.00	0.50	0.236
3.10	2.50	0.0	135.6	0.090	0.019	0.00	124.00	132.00	7.79	0.00	0.15	0.914
2.60	2.50	33.9	0.0	0.108	0.010	0.00	16.00	148.00	8.73	0.00	0.59	0.472
2.90	2.50	0.0	135.7	0.180	0.011	25.00	95.00	243.00	14.34	0.26	0.11	0.700
2.60	2.50	33.9	0.0	0.198	0.009	7.00	8.50	251.50	14.84	0.82	1.06	0.251
2.80	2.50	0.0	135.7	0.270	0.002	68.00	59.00	310.50	18.32	1.15	0.03	0.435
2.70	2.50	33.9	0.0	0.288	0.004	8.00	5.25	315.75	18.63	1.52	0.71	0.155
2.70	2.50	0.0	145.0	0.365	0.016	94.00	51.00	366.75	21.64	1.84	0.31	0.352
2.60	2.50	33.9	0.0	0.383	0.006	6.00	4.50	371.25	21.90	1.33	1.22	0.133
2.70	2.50	0.0	138.3	0.456	0.008	88.00	34.00	405.25	23.91	2.59	0.24	0.246
2.70	2.50	33.9	0.0	0.474	0.006	12.00	7.50	412.75	24.35	1.60	0.73	0.221
2.70	2.50	0.0	137.3	0.547	0.020	94.00	29.00	441.75	26.06	3.24	0.69	0.211
2.70	2.50	33.9	0.0	0.565	0.006	17.50	4.50	446.25	26.33	3.89	1.22	0.133
2.60	2.50	0.0	135.7	0.637	0.078	96.00	23.00	469.25	27.68	4.17	3.39	0.170
2.60	2.50	33.9	0.0	0.655	0.009	19.00	4.00	473.25	27.92	4.75	2.13	0.118
2.70	2.50	0.0	135.6	0.727	0.157	95.00	21.00	494.25	29.16	4.52	7.48	0.155
2.80	2.50	33.9	0.0	0.745	0.014	15.00	3.25	497.50	29.35	4.62	4.23	0.096
2.60	2.50	0.0	135.6	0.817	0.088	104.00	18.50	516.00	30.44	5.62	4.76	0.136
2.70	2.50	33.9	0.0	0.835	0.017	16.50	3.50	519.50	30.65	4.71	4.71	0.103

TABLE E19 (Cont'd)

Tabulated Experimental Results of Run H2D4

(20% HCPV CO_2 Injected at Water Rate @ 2.5 MPa (0.408 moles), 10 Slugs, 4:1 WAG, 21°C, Horizontal Injection)

Porosity (%) =	38.70	Vp (cm^3) =	1885	S_{wc} (%) =	10.08
Oil Viscosity (mPa.s) =	603	S_{oi} (%) =	89.92	Molar Den. (kmol/m^3) =	0.04166
Ave. Run Temp.(K) =	294.15	HCPV (cm^3) =	1695	Abs. k (darcies) =	15.73
CO_2 Req. (sm^3/sm^3) =	4.51	CO_2 Ret. (%inj.) =	45.13	Ave. Flow Vel. (m/d) =	3.17

Press Inj. (MPa)	Press Prod. (MPa)	Gas Inj. (cm^3)	Water Inj. (cm^3)	Cum. PV Injected	Gas Prod (s.ltr)	Water Prod. (cm^3)	Oil Prod. (cm^3)	Cum. Oil Prod. (cm^3)	Percent Rec. (%)	WOR (sm^3/sm^3)	GOR (sm^3/sm^3)	OPFIR (sm^3/sm^3)
2.60	2.50	0.0	144.1	0.911	0.186	106.00	19.50	539.00	31.80	5.44	9.51	0.135
2.60	2.50	0.0	256.0	1.047	0.271	215.00	38.00	577.00	34.04	5.66	7.13	0.148
2.60	2.50	0.0	489.4	1.307	1.035	425.00	61.00	638.00	37.64	6.97	16.97	0.125
2.60	2.50	0.0	492.2	1.568	1.493	445.00	47.00	685.00	40.41	9.47	31.76	0.095
2.60	2.50	0.0	491.9	1.829	1.044	463.00	27.00	712.00	42.01	17.15	38.67	0.055
2.60	2.50	0.0	492.4	2.090	0.399	475.00	21.00	733.00	43.24	22.62	19.00	0.043
2.60	2.50	0.0	492.9	2.351	0.170	482.50	17.50	750.50	44.28	27.57	9.71	0.036
2.60	2.50	0.0	253.9	2.486	0.037	240.00	8.50	759.00	44.78	28.24	4.35	0.033
2.60	2.50	0.0	253.4	2.621	0.028	243.00	8.00	767.00	45.25	30.38	3.44	0.032
0.10	0.10	0.0	0.0	2.621	0.236	243.00	14.50	781.50	46.11	16.76	16.24	

TABLE E20

Tabulated Experimental Results of Run H2D5

(20% HCPV CO_2 Injected at Water Rate @ 2.5 MPa (0.407 moles), 10 Slugs, 4:1 WAG, 21°C, Horizontal Injection)

Porosity (%) =	42.75	Vp (cm^3) =	2082	S_{wc} (%) =	18.83
Oil Viscosity (mPa.s) =	603	S_{oi} (%) =	81.17	Molar Den. (kmol/m^3) =	0.04166
Ave. Run Temp.(K) =	294.15	HCPV (cm^3) =	1690	Abs. k (darcies) =	12.29
CO_2 Req. (sm^3/sm^3) =	4.97	CO_2 Ret. (%inj.) =	33.55	Ave. Flow Vel. (m/d) =	3.81

Press Inj. (MPa)	Press Prod. (MPa)	Gas Inj. (cm^3)	Water Inj. (cm^3)	Cum. PV Injected	Gas Prod (s.ltr)	Water Prod. (cm^3)	Oil Prod. (cm^3)	Cum. Oil Prod. (cm^3)	Percent Rec. (%)	WOR (sm^3/sm^3)	GOR (sm^3/sm^3)	OPFIR (sm^3/sm^3)
2.70	2.50	33.8	0.0	0.016	0.009	0.00	11.90	11.90	0.70	0.00	0.72	0.352
3.00	2.50	0.0	135.2	0.081	0.266	4.80	112.00	123.90	7.33	0.04	2.38	0.829
2.80	2.50	33.8	0.0	0.097	0.009	0.10	16.00	139.90	8.28	0.00	0.56	0.473
2.70	2.50	0.0	135.3	0.162	0.165	32.50	85.30	225.20	13.33	0.38	1.94	0.631
2.70	2.50	33.8	0.0	0.179	0.010	6.90	15.80	241.00	14.26	0.44	0.65	0.467
2.70	2.50	0.0	135.3	0.244	0.410	55.10	60.10	301.10	17.82	0.92	6.83	0.444
2.70	2.50	33.8	0.0	0.260	0.014	8.90	10.00	311.10	18.41	0.89	1.36	0.296
2.70	2.50	0.0	127.7	0.321	0.273	74.20	41.90	353.00	20.89	1.77	6.51	0.328
2.70	2.50	33.8	0.0	0.337	0.015	13.30	7.20	360.20	21.31	1.85	2.01	0.213
2.70	2.50	0.0	135.4	0.402	0.284	84.80	29.40	389.60	23.05	2.88	9.65	0.217
2.70	2.50	33.8	0.0	0.419	0.022	14.70	4.80	394.40	23.34	3.06	4.58	0.142
2.70	2.50	0.0	135.4	0.484	0.328	88.90	29.05	423.45	25.06	3.06	11.29	0.215
2.60	2.50	33.8	0.0	0.500	0.024	14.70	4.40	427.85	25.32	3.34	5.43	0.130
2.60	2.50	0.0	136.4	0.565	0.334	96.10	20.70	448.55	26.54	4.64	16.12	0.152
2.70	2.50	33.8	0.0	0.582	0.033	18.20	4.30	452.85	26.80	4.23	7.56	0.127
2.60	2.50	0.0	139.6	0.649	0.492	96.70	22.80	475.65	28.14	4.24	21.56	0.163
2.60	2.50	33.8	0.0	0.665	0.037	18.10	0.85	476.50	28.20	21.29	43.59	0.025
2.60	2.50	0.0	135.8	0.730	0.444	99.10	18.80	495.30	29.31	5.27	23.62	0.138
2.60	2.50	33.8	0.0	0.746	0.039	12.20	9.10	504.40	29.85	1.34	4.25	0.269

TABLE E20 (Cont'd)

Tabulated Experimental Results of Run H2D5

(20% HCPV CO_2 Injected at Water Rate @ 2.5 MPa (0.407 moles), 10 Slugs, 4:1 WAG, 21°C, Horizontal Injection)

Porosity (%) = 42.75
Oil Viscosity (mPa.s) = 603
Ave. Run Temp.(K) = 294.15
CO_2 Req. (sm^3/sm^3) = 4.97
Vp (cm^3) = 2082
S_{oi} (%) = 81.17
HCPV (cm^3) = 1690
CO_2 Ret. (%inj.) = 33.55
S_{wc} (%) = 18.83
Molar Den. (kmol/m^3) = 0.04166
Abs. k (darcies) = 12.29
Ave. Flow Vel. (m/d) = 3.81

Press Inj. (MPa)	Press Prod. (MPa)	Gas Inj. (cm^3)	Water Inj. (cm^3)	Cum. PV Injected	Gas Prod (s.ltr)	Water Prod. (cm^3)	Oil Prod. (cm^3)	Cum. Oil Prod. (cm^3)	Percent Rec. (%)	WOR (sm^3/sm^3)	GOR (sm^3/sm^3)	OPFIR (sm^3/sm^3)
2.60	2.50	0.0	135.7	0.812	0.515	93.80	19.00	523.40	30.97	4.94	27.12	0.140
2.60	2.50	0.0	246.7	0.930	0.376	213.10	33.00	556.40	32.92	6.46	11.39	0.134
2.60	2.50	0.0	258.9	1.054	0.341	225.10	28.50	584.90	34.61	7.90	11.96	0.110
2.60	2.50	0.0	258.4	1.178	0.281	230.10	22.00	606.90	35.91	10.46	12.77	0.085
2.60	2.50	0.0	262.6	1.305	0.229	236.20	18.10	625.00	36.98	13.05	12.64	0.069
2.60	2.50	0.0	254.2	1.427	0.184	236.10	19.40	644.40	38.13	12.17	9.46	0.076
2.60	2.50	0.0	254.2	1.549	0.191	233.80	16.10	660.50	39.08	14.52	11.87	0.063
2.60	2.50	0.0	247.8	1.668	0.151	237.70	12.40	672.90	39.82	19.17	12.17	0.050
2.60	2.50	0.0	257.9	1.792	0.101	242.65	9.25	682.15	40.36	26.23	10.93	0.036
2.60	2.50	0.0	251.8	1.913	0.095	240.10	9.40	691.55	40.92	25.54	10.05	0.037
2.60	2.50	0.0	251.2	2.033	0.082	240.55	9.55	701.10	41.49	25.19	8.58	0.038
0.10	0.10	0.0	0.0	2.033	0.742	150.05	25.05	707.20	41.85	5.99	29.62	

TABLE E21

Tabulated Experimental Results of Run H2D06

(20% HCPV CO_2 Injected at Water Rate @ 2.5 MPa (0.403 moles), 10 Slugs, 4:1 WAG, 21°C, Horizontal Injection)

Porosity (%) = 37.41 Vp (cm^3) = 1822 S_{wc} (%) = 11.91
Oil Viscosity (mPa.s) = 1058 S_{oi} (%) = 88.09 Molar Den. ($kmol/m^3$) = 0.04166
Ave. Run Temp.(K) = 294.15 HCPV (cm^3) = 1605 Abs. k (darcies) = 12.18
CO_2 Req. (sm^3/sm^3) = 6.32 CO_2 Ret. (%inj.) = 75.36 Ave. Flow Vel. (m/d) = 0.78

Press Inj. (MPa)	Press Prod. (MPa)	Gas Inj. (cm^3)	Water Inj. (cm^3)	Cum. PV Injected	Gas Prod (s.ltr)	Water Prod. (cm^3)	Oil Prod. (cm^3)	Cum. Oil Prod. (cm^3)	Percent Rec. (%)	WOR (sm^3/sm^3)	GOR (sm^3/sm^3)	OPFIR (sm^3/sm^3)
1.30	1.00	33.4	0.0	0.018	0.001	0.00	10.00	10.00	0.60	0.00	0.10	0.299
1.20	1.00	0.0	133.7	0.089	0.012	0.00	122.00	132.00	7.90	0.00	0.10	0.912
1.30	1.00	33.4	0.0	0.107	0.001	0.00	12.00	144.00	8.61	0.00	0.08	0.359
1.20	1.00	0.0	133.7	0.178	0.000	20.00	87.00	231.00	13.82	0.23	0.00	0.651
1.20	1.00	33.4	0.0	0.196	0.008	8.00	14.00	245.00	14.66	0.57	0.57	0.419
1.20	1.00	0.0	133.7	0.268	0.142	50.00	61.00	306.00	18.31	0.82	2.33	0.456
1.20	1.00	33.4	0.0	0.285	0.000	2.00	3.00	309.00	18.49	0.67	0.00	0.090
1.20	1.00	0.0	133.8	0.357	0.022	90.00	40.00	349.00	20.88	2.25	0.55	0.299
1.20	1.00	33.4	0.0	0.375	0.001	7.00	3.00	352.00	21.06	2.33	0.33	0.090
1.20	1.00	0.0	133.8	0.446	0.010	96.00	28.00	380.00	22.73	3.43	0.36	0.209
1.20	1.00	33.4	0.0	0.464	0.000	25.00	11.00	391.00	23.39	2.27	0.00	0.329
1.20	1.00	0.0	133.7	0.535	0.034	86.00	23.00	414.00	24.77	3.74	1.48	0.172
1.10	1.00	33.4	0.0	0.553	0.009	16.00	5.00	419.00	25.07	3.20	1.80	0.150
1.10	1.00	0.0	133.7	0.624	0.032	94.00	20.00	439.00	26.26	4.70	1.60	0.150
1.20	1.00	33.4	0.0	0.642	0.001	6.00	3.00	442.00	26.44	2.00	0.33	0.090
1.10	1.00	0.0	133.7	0.713	0.022	112.00	18.00	460.00	27.52	6.22	1.22	0.135
1.10	1.00	33.4	0.0	0.731	0.005	27.00	5.00	465.00	27.82	5.40	1.00	0.150
1.10	1.00	0.0	133.7	0.803	0.056	86.00	13.00	478.00	28.60	6.62	4.31	0.097
1.10	1.00	33.4	0.0	0.820	0.016	27.50	4.00	482.00	28.83	6.88	4.00	0.120

TABLE E21 (Cont'd)

Tabulated Experimental Results of Run H2D06

(20% HCPV CO_2 Injected at Water Rate @ 2.5 MPa (0.403 moles), 10 Slugs, 4:1 WAG, 21°C, Horizontal Injection)

Porosity (%) = 37.41
Oil Viscosity (mPa.s) = 1058
Ave. Run Temp.(K) = 294.15
CO_2 Req. (sm^3/sm^3) = 6.32
Vp (cm^3) = 1822
S_{oi} (%) = 88.09
HCPV (cm^3) = 1605
CO_2 Ret. (%inj.) = 75.36
S_{wc} (%) = 11.91
Molar Den. ($kmol/m^3$) = 0.04166
Abs. k (darcies) = 12.18
Ave. Flow Vel. (m/d) = 0.78

Press Inj. (MPa)	Press Prod. (MPa)	Gas Inj. (cm^3)	Water Inj. (cm^3)	Cum. PV Injected	Gas Prod (s.ltr)	Water Prod. (cm^3)	Oil Prod. (cm^3)	Cum. Oil Prod. (cm^3)	Percent Rec. (%)	WOR (sm^3/sm^3)	GOR (sm^3/sm^3)	OPFIR (sm^3/sm^3)
1.10	1.00	0.0	133.7	0.892	0.069	90.00	14.00	496.00	29.67	6.43	4.93	0.105
1.10	1.00	0.0	246.3	1.023	0.155	224.00	20.00	516.00	30.87	11.20	7.75	0.081
1.10	1.00	0.0	246.3	1.155	0.098	228.00	14.00	530.00	31.71	16.29	7.00	0.057
1.10	1.00	0.0	241.9	1.284	0.090	234.00	6.00	536.00	32.07	39.00	15.00	0.025
0.10	0.10	0.0	0.0	1.284	0.073	92.00	14.00	550.00	32.90	6.57	5.21	

TABLE E22

Tabulated Experimental Results of Run H2D7

(20% HCPV CO_2 Injected at Water Rate @ 2.5 MPa (0.445 moles), 10 Slugs, 4:1 WAG, 21°C, Horizontal Injection)

Porosity (%) = 41.60
Oil Viscosity (mPa.s) = 1058
Ave. Run Temp.(K) = 294.15
CO_2 Req. (sm^3/sm^3) = 5.57

Vp (cm^3) = 2015
S_{oi} (%) = 88.34
HCPV (cm^3) = 1780
CO_2 Ret. (%inj.) = 75.27

S_{wc} (%) = 11.66
Molar Den. ($kmol/m^3$) = 0.04166
Abs. k (darcies) = 13.9
Ave. Flow Vel. (m/d) = 1.55

Press Inj. (MPa)	Press Prod. (MPa)	Gas Inj. (cm^3)	Water Inj. (cm^3)	Cum. PV Injected	Gas Prod (s.ltr)	Water Prod. (cm^3)	Oil Prod. (cm^3)	Cum. Oil Prod. (cm^3)	Percent Rec. (%)	WOR (sm^3/sm^3)	GOR (sm^3/sm^3)	OPFIR (sm^3/sm^3)
2.60	2.50	36.9	0.0	0.018	0.000	0.00	0.01	0.01	0.00	0.00	0.00	0.000
2.90	2.50	0.0	148.0	0.092	0.042	0.00	129.00	129.01	7.25	0.00	0.33	0.872
2.80	2.50	36.9	0.0	0.110	0.001	0.00	20.00	149.01	8.37	0.00	0.05	0.542
2.70	2.50	0.0	148.4	0.184	0.278	7.00	127.00	276.01	15.51	0.06	2.19	0.856
2.70	2.50	36.9	0.0	0.202	0.000	18.75	14.00	290.01	16.29	1.34	0.00	0.379
2.70	2.50	0.0	148.0	0.275	0.031	46.25	80.00	370.01	20.79	0.58	0.39	0.541
2.70	2.50	36.9	0.0	0.294	0.000	18.00	11.00	381.01	21.41	1.64	0.00	0.298
2.70	2.50	0.0	148.0	0.367	0.048	94.00	34.00	415.01	23.32	2.76	1.41	0.230
2.70	2.50	37.0	0.0	0.386	0.003	17.00	5.00	420.01	23.60	3.40	0.60	0.135
2.70	2.50	0.0	148.0	0.459	0.107	113.00	23.00	443.01	24.89	4.91	4.65	0.155
2.70	2.50	37.0	0.0	0.477	0.025	21.00	5.00	448.01	25.17	4.20	5.00	0.135
2.70	2.50	0.0	148.0	0.551	0.157	96.50	17.00	465.01	26.12	5.68	9.24	0.115
2.60	2.50	37.0	0.0	0.569	0.068	23.75	10.00	475.01	26.69	2.38	6.80	0.270
2.60	2.50	0.0	148.0	0.643	0.150	106.00	19.00	494.01	27.75	5.58	7.89	0.128
2.70	2.50	37.0	0.0	0.661	0.019	16.00	2.00	496.01	27.87	8.00	9.50	0.054
2.60	2.50	0.0	147.9	0.734	0.069	106.00	25.00	521.01	29.27	4.24	2.76	0.169
2.60	2.50	37.2	0.0	0.753	0.011	15.00	2.00	523.01	29.38	7.50	5.50	0.054
2.60	2.50	0.0	149.2	0.827	0.090	119.50	8.00	531.01	29.83	14.94	11.25	0.054
2.60	2.50	37.0	0.0	0.845	0.025	8.00	2.00	533.01	29.94	4.00	12.50	0.054

TABLE E22 (Cont'd)

Tabulated Experimental Results of Run H2D7

(20% HCPV CO_2 Injected at Water Rate @ 2.5 MPa (0.445 moles), 10 Slugs, 4:1 WAG, 21°C, Horizontal Injection)

Porosity (%) =	41.60	Vp (cm^3) =	2015	S_{wc} (%) =	11.66
Oil Viscosity (mPa.s) =	1058	S_{oi} (%) =	88.34	Molar Den. (kmol/m^3) =	0.04166
Ave. Run Temp.(K) =	294.15	HCPV (cm^3) =	1780	Abs. k (darcies) =	13.9
CO_2 Req. (sm^3/sm^3) =	5.57	CO_2 Ret. (%inj.) =	75.27	Ave. Flow Vel. (m/d) =	1.55

Press Inj. (MPa)	Press Prod. (MPa)	Gas Inj. (cm^3)	Water Inj. (cm^3)	Cum. PV Injected	Gas Prod (s.ltr)	Water Prod. (cm^3)	Oil Prod. (cm^3)	Cum. Oil Prod. (cm^3)	Percent Rec. (%)	WOR (sm^3/sm^3)	GOR (sm^3/sm^3)	OPFIR (sm^3/sm^3)
2.60	2.50	0.0	148.0	0.919	0.175	129.50	11.00	544.01	30.56	11.77	15.91	0.074
2.60	2.50	0.0	166.8	1.002	0.140	152.00	10.00	554.01	31.12	15.20	14.00	0.060
2.60	2.50	0.0	281.6	1.141	0.375	266.00	27.00	581.01	32.64	9.85	13.89	0.096
2.60	2.50	0.0	440.3	1.360	0.587	414.00	45.00	626.01	35.17	9.20	13.04	0.102
2.60	2.50	0.0	261.3	1.489	0.090	238.00	22.00	648.01	36.41	10.82	4.09	0.084
2.60	2.50	0.0	251.7	1.614	0.040	238.00	12.00	660.01	37.08	19.83	3.33	0.048
0.10	0.10	0.0	0.0	1.614	0.014	26.00	5.00	665.01	37.36	5.20	2.80	

TABLE E23

Tabulated Experimental Results of Run H2D8

(20% HCPV CO_2 Injected at Water Rate @ 2.5 MPa (0.432 moles), 10 Slugs, 4:1 WAG, 21°C, Horizontal Injection)

Porosity (%) = 40.48
Oil Viscosity (mPa.s) = 1058
Ave. Run Temp.(K) = 294.15
CO_2 Req. (sm^3/sm^3) = 4.61

Vp (cm^3) = 1975
S_{oi} (%) = 90.73
HCPV (cm^3) = 1792
CO_2 Ret. (%inj.) = 65.28

S_{wc} (%) = 9.27
Molar Den. ($kmol/m^3$) = 0.04166
Abs. k (darcies) = 12.46
Ave. Flow Vel. (m/d) = 2.6

Press Inj. (MPa)	Press Prod. (MPa)	Gas Inj. (cm^3)	Water Inj. (cm^3)	Cum. PV Injected	Gas Prod (s.ltr)	Water Prod. (cm^3)	Oil Prod. (cm^3)	Cum. Oil Prod. (cm^3)	Percent Rec. (%)	WOR (sm^3/sm^3)	GOR (sm^3/sm^3)	OPFIR (sm^3/sm^3)
2.70	2.50	33.4	0.0	0.017	0.007	0.00	14.00	14.00	0.78	0.00	0.50	0.419
3.00	2.50	0.0	133.6	0.085	0.011	1.00	115.00	129,00	7.20	0.01	0.10	0.861
2.80	2.50	33.4	0.0	0.101	0.010	0.00	18.00	147.00	8.20	0.00	0.56	0.539
2.70	2.50	0.0	133.6	0.169	0.002	30.00	91.50	238.50	13.31	0.33	0.02	0.685
2.70	2.50	33.4	0.0	0.186	0.003	9.00	11.00	249.50	13.92	0.82	0.23	0.329
2.70	2.50	0.0	133.7	0.254	0.013	50.00	60.00	309.50	17.27	0.83	0.21	0.449
2.70	2.50	33.4	0.0	0.271	0.005	10.00	11.00	320.50	17.89	0.91	0.41	0.329
2.70	2.50	0.0	133.7	0.338	0.008	64.00	58.00	378.50	21.12	1.10	0.14	0.434
2.70	2.50	33.4	0.0	0.355	0.007	16.00	11.00	389.50	21.74	1.45	0.64	0.329
2.70	2.50	0.0	133.8	0.423	0.028	96.00	41.00	430.50	24.02	2.34	0.68	0.306
2.70	2.50	34.0	0.0	0.440	0.009	4.50	5.00	435.50	24.30	0.90	1.70	0.147
2.70	2.50	0.0	133.7	0.508	0.047	90.00	20.00	455.50	25.42	4.50	2.33	0.150
2.60	2.50	33.4	0.0	0.525	0.010	16.50	6.00	461.50	25.75	2.75	1.58	0.180
2.60	2.50	0.0	133.6	0.592	0.087	90.00	20.00	481.50	26.87	4.50	4.35	0.150
2.70	2.50	33.4	0.0	0.609	0.022	14.00	6.00	487.50	27.20	2.33	3.67	0.180
2.60	2.50	0.0	133.7	0.677	0.139	103.00	17.00	504.50	28.15	6.06	8.18	0.127
2.60	2.50	35.0	0.0	0.695	0.026	18.00	9.00	513.50	28.66	2.00	2.89	0.257
2.60	2.50	0.0	133.6	0.762	0.170	95.00	20.00	533.50	29.77	4.75	8.50	0.150
2.60	2.50	33.4	0.0	0.779	0.050	28.50	5.00	538.50	30.05	5.70	9.90	0.150

TABLE E23 (Cont'd)

Tabulated Experimental Results of Run H2D8

(20% HCPV CO_2 Injected at Water Rate @ 2.5 MPa (0.432 moles), 10 Slugs, 4:1 WAG, 21°C, Horizontal Injection)

Porosity (%) = 40.48
Oil Viscosity (mPa.s) = 1058
Ave. Run Temp.(K) = 294.15
CO_2 Req. (sm^3/sm^3) = 4.61
Vp (cm^3) = 1975
S_{oi} (%) = 90.73
HCPV (cm^3) = 1792
CO_2 Ret. (%inj.) = 65.28
S_{wc} (%) = 9.27
Molar Den. ($kmol/m^3$) = 0.04166
Abs. k (darcies) = 12.46
Ave. Flow Vel. (m/d) = 2.6

Press Inj. (MPa)	Press Prod. (MPa)	Gas Inj. (cm^3)	Water Inj. (cm^3)	Cum. PV Injected	Gas Prod (s.ltr)	Water Prod. (cm^3)	Oil Prod. (cm^3)	Cum. Oil Prod. (cm^3)	Percent Rec. (%)	WOR (sm^3/sm^3)	GOR (sm^3/sm^3)	OPFIR (sm^3/sm^3)
2.60	2.50	0.0	133.6	0.847	0.367	91.50	16.00	554.50	30.94	5.72	22.94	0.120
2.60	2.50	0.0	254.3	0.976	0.571	225.00	28.00	582.50	32.51	8.04	20.38	0.110
2.60	2.50	0.0	274.9	1.115	0.381	253.00	20.00	602.50	33.62	12.65	19.03	0.073
2.60	2.50	0.0	244.4	1.239	0.206	233.00	18.00	620.50	34.63	12.94	11.42	0.074
2.60	2.50	0.0	251.2	1.366	0.113	239.00	13.00	633.50	35.35	18.38	8.69	0.052
2.60	2.50	0.0	251.1	1.493	0.048	239.00	12.00	645.50	36.02	19.92	4.00	0.048
2.60	2.50	0.0	251.4	1.620	0.030	237.50	12.00	657.50	36.69	19.79	2.50	0.048
2.60	2.50	0.0	244.3	1.744	0.019	242.00	13.00	670.50	37.42	18.62	1.46	0.053
2.60	2.50	0.0	259.2	1.875	0.016	244.00	13.00	683.50	38.14	18.77	1.23	0.050
2.60	2.50	0.0	261.7	2.008	0.008	246.00	16.00	699.50	39.03	15.38	0.50	0.061
0.10	0.10	0.0	0.0	2.008	1.189	239.00	108.50	808.00	45.09	2.20	10.95	

TABLE E24

Tabulated Experimental Results of Run H2D9

(20% HCPV CO_2 Injected at Water Rate @ 2.5 MPa (0.407 moles), 10 Slugs, 4:1 WAG, 21°C, Horizontal Injection)

Porosity (%) = 38.50
Oil Viscosity (mPa.s) = 1058
Ave. Run Temp.(K) = 294.15
CO_2 Req. (sm^3/sm^3) = 4.83

Vp (cm^3) = 1880
S_{oi} (%) = 89.89
HCPV (cm^3) = 1690
CO_2 Ret. (%inj.) = 43.29

S_{wc} (%) = 10.11
Molar Den. ($kmol/m^3$) = 0.04166
Abs. k (darcies) = 14.47
Ave. Flow Vel. (m/d) = 3.2

Press Inj. (MPa)	Press Prod. (MPa)	Gas Inj. (cm^3)	Water Inj. (cm^3)	Cum. PV Injected	Gas Prod (s.ltr)	Water Prod. (cm^3)	Oil Prod. (cm^3)	Cum. Oil Prod. (cm^3)	Percent Rec. (%)	WOR (sm^3/sm^3)	GOR (sm^3/sm^3)	OPFIR (sm^3/sm^3)
2.70	2.50	33.8	0.0	0.018	0.004	0.00	17.50	17.50	1.04	0.00	0.23	0.518
3.00	2.50	0.0	138.4	0.092	0.017	0.00	123.00	140.50	8.31	0.00	0.14	0.889
2.80	2.50	33.8	0.0	0.110	0.003	3.00	26.00	166.50	9.85	0.00	0.12	0.769
2.70	2.50	0.0	180.0	0.205	0.010	51.00	109.00	275.50	16.30	0.47	0.09	0.606
2.70	2.50	33.8	0.0	0.223	0.003	5.00	11.80	287.30	17.00	0.42	0.27	0.349
2.70	2.50	0.0	139.5	0.298	0.010	78.00	46.50	333.80	19.75	1.68	0.22	0.333
2.70	2.50	33.8	0.0	0.315	0.003	15.00	9.25	343.05	20.30	1.62	0.35	0.274
2.70	2.50	0.0	135.2	0.387	0.110	82.00	34.00	377.05	22.31	2.41	3.22	0.251
2.70	2.50	33.8	0.0	0.405	0.018	16.00	7.80	384.85	22.77	2.05	2.33	0.231
2.70	2.50	0.0	135.2	0.477	0.195	89.00	27.00	411.85	24.37	3.30	7.22	0.200
2.70	2.50	33.8	0.0	0.495	0.041	18.00	6.50	418.35	24.75	2.77	6.23	0.192
2.70	2.50	0.0	135.3	0.567	0.233	90.00	26.00	444.35	26.29	3.46	8.96	0.192
2.60	2.50	33.8	0.0	0.585	0.027	10.00	4.80	449.15	26.58	2.08	5.67	0.142
2.60	2.50	0.0	136.4	0.658	0.247	100.00	24.00	473.15	28.00	4.17	10.29	0.176
2.70	2.50	33.8	0.0	0.676	0.052	17.50	6.50	479.65	28.38	2.69	8.00	0.192
2.60	2.50	0.0	135.2	0.748	0.347	94.00	20.00	499.65	29.57	4.70	17.35	0.148
2.60	2.50	33.8	0.0	0.766	0.036	10.00	4.00	503.65	29.80	2.50	8.88	0.118
2.60	2.50	0.0	136.7	0.838	0.336	114.00	8.00	511.65	30.28	14.25	42.00	0.059
2.60	2.50	33.8	0.0	0.856	0.049	12.50	4.00	515.65	30.51	3.13	12.13	0.118

TABLE E24 (Cont'd)

Tabulated Experimental Results of Run H2D9

(20% HCPV CO_2 Injected at Water Rate @ 2.5 MPa (0.407 moles), 10 Slugs, 4:1 WAG, 21°C, Horizontal Injection)

Porosity (%) = 38.50
Oil Viscosity (mPa.s) = 1058
Ave. Run Temp.(K) = 294.15
CO_2 Req. (sm^3/sm^3) = 4.83

Vp (cm^3) = 1880
S_{oi} (%) = 89.89
HCPV (cm^3) = 1690
CO_2 Ret. (%inj.) = 43.29

S_{wc} (%) = 10.11
Molar Den. ($kmol/m^3$) = 0.04166
Abs. k (darcies) = 14.47
Ave. Flow Vel. (m/d) = 3.2

Press Inj. (MPa)	Press Prod. (MPa)	Gas Inj. (cm^3)	Water Inj. (cm^3)	Cum. PV Injected	Gas Prod (s.ltr)	Water Prod. (cm^3)	Oil Prod. (cm^3)	Cum. Oil Prod. (cm^3)	Percent Rec. (%)	WOR (sm^3/sm^3)	GOR (sm^3/sm^3)	OPFIR (sm^3/sm^3)
2.60	2.50	0.0	135.3	0.928	0.362	104.00	21.00	536.65	31.75	4.95	17.24	0.155
2.60	2.50	0.0	269.8	1.072	0.968	230.00	41.00	577.65	34.18	5.61	23.60	0.152
2.60	2.50	0.0	256.8	1.208	0.902	220.00	35.00	612.65	36.25	6.29	25.76	0.136
2.60	2.50	0.0	278.2	1.356	0.733	258.00	19.00	631.65	37.38	13.58	38.55	0.068
2.60	2.50	0.0	315.3	1.524	0.520	128.00	16.00	647.65	38.32	8.00	32.50	0.051
2.60	2.50	0.0	250.1	1.657	0.107	238.50	9.50	657.15	38.88	25.11	11.21	0.038
2.60	2.50	0.0	250.3	1.790	0.047	234.00	14.50	671.65	39.74	16.14	3.24	0.058
2.60	2.50	0.0	281.7	1.940	0.031	282.00	10.00	681.65	40.33	28.20	3.05	0.036
2.60	2.50	0.0	251.0	2.074	0.016	243.00	10.00	691.65	40.93	24.30	1.60	0.040
2.60	2.50	0.0	280.8	2.223	0.009	271.00	8.00	699.65	41.40	33.88	1.13	0.028
0.10	0.10	0.0	0.0	2.223	0.108	110.00	29.00	728.65	43.12	3.79	3.72	

TABLE E25

Tabulated Experimental Results of Run H2D10

(20% HCPV CO_2 Injected at Water Rate @ 2.5 MPa (0.407 moles), 10 Slugs, 4:1 WAG, 21°C, Horizontal Injection)

Porosity (%) = 38.05
Oil Viscosity (mPa.s) = 1058
Ave. Run Temp.(K) = 294.15
CO_2 Req. (sm^3/sm^3) = 5.10

Vp (cm^3) = 1875
S_{oi} (%) = 89.07
HCPV (cm^3) = 1670
CO_2 Ret. (%inj.) = 29.67

S_{wc} (%) = 10.93
Molar Den. ($kmol/m^3$) = 0.04166
Abs. k (darcies) = 12.29
Ave. Flow Vel. (m/d) = 3.81

Press Inj. (MPa)	Press Prod. (MPa)	Gas Inj. (cm^3)	Water Inj. (cm^3)	Cum. PV Injected	Gas Prod (s.ltr)	Water Prod. (cm^3)	Oil Prod. (cm^3)	Cum. Oil Prod. (cm^3)	Percent Rec. (%)	WOR (sm^3/sm^3)	GOR (sm^3/sm^3)	OPFIR (sm^3/sm^3)
2.70	2.50	30.3	0.0	0.016	0.008	0.00	7.50	7.50	0.45	0.00	1.00	0.248
3.00	2.50	0.0	133.6	0.087	0.003	5.00	112.00	119.50	7.16	0.04	0.03	0.838
2.80	2.50	30.3	0.0	0.104	0.001	0.00	25.25	144.75	8.67	0.00	0.03	0.833
2.70	2.50	0.0	145.7	0.181	0.154	25.00	99.00	243.75	14.60	0.25	1.55	0.680
2.70	2.50	30.3	0.0	0.197	0.032	6.00	11.50	255.25	15.28	0.52	2.78	0.380
2.70	2.50	0.0	133.9	0.269	0.269	77.50	33.50	288.75	17.29	2.31	8.01	0.250
2.70	2.50	30.3	0.0	0.285	0.069	13.50	8.00	296.75	17.77	1.69	8.56	0.264
2.70	2.50	0.0	138.9	0.359	0.338	87.00	39.50	336.25	20.13	2.20	8.56	0.284
2.70	2.50	30.3	0.0	0.375	0.056	10.00	6.25	342.50	20.51	1.60	8.92	0.206
2.70	2.50	0.0	133.6	0.446	0.442	86.00	32.50	375.00	22.46	2.65	13.58	0.243
2.70	2.50	30.3	0.0	0.463	0.088	15.00	6.00	381.00	22.81	2.50	14.67	0.198
2.70	2.50	0.0	134.0	0.534	0.559	90.00	26.00	407.00	24.37	3.46	21.48	0.194
2.60	2.50	30.3	0.0	0.550	0.094	13.00	5.00	412.00	24.67	2.60	18.80	0.165
2.60	2.50	0.0	133.8	0.622	0.634	96.00	22.00	434.00	25.99	4.36	28.82	0.164
2.70	2.50	30.3	0.0	0.638	0.104	14.00	4.50	438.50	26.26	3.11	23.11	0.149
2.60	2.50	0.0	133.6	0.709	0.636	103.00	16.00	454.50	27.22	6.44	39.75	0.120
2.60	2.50	30.3	0.0	0.725	0.118	18.00	3.50	458.00	27.43	5.14	33.57	0.116
2.60	2.50	0.0	153.5	0.807	0.750	118.00	18.00	476.00	28.50	6.56	41.67	0.117
2.60	2.50	30.3	0.0	0.823	0.129	16.50	5.50	481.50	28.83	3.00	23.45	0.182

TABLE E25 (Cont'd)

Tabulated Experimental Results of Run H2D10

(20% HCPV CO_2 Injected at Water Rate @ 2.5 MPa (0.407 moles), 10 Slugs, 4:1 WAG, 21°C, Horizontal Injection)

Porosity (%) = 38.05
Oil Viscosity (mPa.s) = 1058
Ave. Run Temp.(K) = 294.15
CO_2 Req. (sm^3/sm^3) = 5.10

Vp (cm^3) = 1875
S_{oi} (%) = 89.07
HCPV (cm^3) = 1670
CO_2 Ret. (%inj.) = 29.67

S_{wc} (%) = 10.93
Molar Den. ($kmol/m^3$) = 0.04166
Abs. k (darcies) = 12.29
Ave. Flow Vel. (m/d) = 3.81

Press Inj. (MPa)	Press Prod. (MPa)	Gas Inj. (cm^3)	Water Inj. (cm^3)	Cum. PV Injected	Gas Prod (s.ltr)	Water Prod. (cm^3)	Oil Prod. (cm^3)	Cum. Oil Prod. (cm^3)	Percent Rec. (%)	WOR (sm^3/sm^3)	GOR (sm^3/sm^3)	OPFIR (sm^3/sm^3)
2.60	2.50	0.0	155.6	0.906	0.764	118.00	18.00	499.50	29.91	6.56	42.44	0.116
2.60	2.50	0.0	257.2	1.043	1.162	224.00	33.00	532.50	31.89	6.79	35.21	0.128
2.60	2.50	0.0	248.3	1.176	0.222	232.00	15.00	547.50	32.78	15.47	14.80	0.060
2.60	2.50	0.0	242.7	1.305	0.039	230.00	20.00	567.50	33.98	11.50	1.95	0.082
2.60	2.50	0.0	268.5	1.448	0.011	240.00	22.00	589.50	35.30	10.91	0.50	0.082
2.60	2.50	0.0	254.1	1.584	0.011	245.00	16.00	605.50	36.26	15.31	0.69	0.063
2.60	2.50	0.0	292.2	1.740	0.003	260.00	8.00	613.50	36.74	32.50	0.38	0.027
2.60	2.50	0.0	242.4	1.869	0.002	242.00	10.00	623.50	37.34	24.20	0.20	0.041
2.60	2.50	0.0	251.2	2.003	0.000	253.00	8.00	631.50	37.81	31.63	0.00	0.032
0.10	0.10	0.0	0.0	2.003	0.096	100.00	49.50	681.00	40.78	2.02	1.93	

TABLE E26

Tabulated Experimental Results of Run H2D11

(20% HCPV CO_2 Injected at Water Rate @ 2.5 MPa (0.460 moles), 10 Slugs, 4:1 WAG, 21°C, Horizontal Injection)

Porosity (%) = 41.25
Oil Viscosity (mPa.s) = 1842
Ave. Run Temp.(K) = 294.15
CO_2 Req. (sm³/sm³) = 7.66

Vp (cm³) = 2050
S_{oi} (%) = 93.17
HCPV (cm³) = 1910
CO_2 Ret. (%inj.) = 55.86

S_{wc} (%) = 6.83
Molar Den. (kmol/m³) = 0.04166
Abs. k (darcies) = 12.65
Ave. Flow Vel. (m/d) = 0.78

Press Inj. (MPa)	Press Prod. (MPa)	Gas Inj. (cm³)	Water Inj. (cm³)	Cum. PV Injected	Gas Prod (s.ltr)	Water Prod. (cm³)	Oil Prod. (cm³)	Cum. Oil Prod. (cm³)	Percent Rec. (%)	WOR (sm³/sm³)	GOR (sm³/sm³)	OPFIR (sm³/sm³)
2.60	2.50	38.2	0.0	0.019	0.004	0.00	8.50	8.50	0.45	0.00	0.41	0.223
4.00	2.50	0.0	152.9	0.093	0.039	0.00	95.00	103.50	5.42	0.00	0.41	0.621
2.80	2.40	38.2	0.0	0.112	0.006	0.00	18.00	121.50	6.36	0.00	0.33	0.471
2.90	2.50	0.0	152.7	0.186	0.031	38.00	55.00	176.50	9.24	0.69	0.56	0.360
2.80	2.50	38.2	0.0	0.205	-0.001	9.00	10.50	187.00	9.79	0.86	-0.05	0.275
2.70	2.60	0.0	152.6	0.279	0.019	72.00	51.50	238.50	12.49	1.40	0.37	0.337
2.64	2.40	38.2	0.0	0.298	0.001	16.50	8.50	247.00	12.93	1.94	0.12	0.223
2.70	2.50	0.0	152.1	0.372	0.439	84.00	28.50	275.50	14.42	2.95	15.40	0.187
2.80	2.50	38.2	0.0	0.391	0.004	11.25	5.75	281.25	14.73	1.96	0.70	0.151
2.80	2.50	0.0	153.0	0.466	0.032	99.50	24.00	305.25	15.98	4.15	1.31	0.157
2.80	2.70	38.2	0.0	0.484	0.004	12.50	4.00	309.25	16.19	3.13	0.88	0.105
2.60	2.50	0.0	153.4	0.559	0.056	101.00	24.00	333.25	17.45	4.21	2.33	0.156
2.70	2.50	38.2	0.0	0.578	0.058	16.00	4.00	337.25	17.66	4.00	14.50	0.105
2.70	2.50	0.0	152.8	0.652	0.222	98.00	21.00	358.25	18.76	4.67	10.57	0.137
2.60	2.40	38.2	0.0	0.671	0.014	15.00	3.00	361.25	18.91	5.00	4.50	0.079
2.60	2.50	0.0	152.1	0.745	0.173	106.00	15.00	376.25	19.70	7.07	11.53	0.099
2.70	2.50	38.2	0.0	0.764	0.027	17.50	3.00	379.25	19.86	5.83	9.00	0.079
2.60	2.50	0.0	152.6	0.838	0.337	102.00	9.00	388.25	20.33	11.33	37.44	0.059
2.60	2.50	38.2	0.0	0.857	0.038	17.00	2.00	390.25	20.43	8.50	18.75	0.052

TABLE E26 (Cont'd)

Tabulated Experimental Results of Run H2D11

(20% HCPV CO_2 Injected at Water Rate @ 2.5 MPa (0.460 moles), 10 Slugs, 4:1 WAG, 21°C, Horizontal Injection)

Porosity (%) =	41.25	Vp (cm^3) =	2050	S_{wc} (%) =	6.83
Oil Viscosity (mPa.s) =	603	S_{oi} (%) =	93.17	Molar Den. (kmol/m^3) =	0.04166
Ave. Run Temp.(K) =	294.15	HCPV (cm^3) =	1910	Abs. k (darcies) =	12.65
CO_2 Req. (sm^3/sm^3) =	7.66	CO_2 Ret. (%inj.) =	55.86	Ave. Flow Vel. (m/d) =	0.78

Press Inj. (MPa)	Press Prod. (MPa)	Gas Inj. (cm^3)	Water Inj. (cm^3)	Cum. PV Injected	Gas Prod (s.ltr)	Water Prod. (cm^3)	Oil Prod. (cm^3)	Cum. Oil Prod. (cm^3)	Percent Rec. (%)	WOR (sm^3/sm^3)	GOR (sm^3/sm^3)	OPFIR (sm^3/sm^3)
2.60	2.50	0.0	152.5	0.931	0.294	107.50	17.00	407.25	21.32	6.32	17.26	0.111
2.60	2.50	0.0	261.7	1.059	0.500	226.50	24.50	431.75	22.60	9.24	20.41	0.094
2.60	2.50	0.0	254.1	1.183	0.556	232.00	19.50	451.25	23.63	11.90	28.49	0.077
2.60	2.50	0.0	252.3	1.306	0.519	238.00	15.00	466.25	24.41	15.87	34.60	0.059
2.60	2.50	0.0	250.3	1.428	0.428	238.00	12.50	478.75	25.07	19.04	34.20	0.050
2.60	2.50	0.0	267.4	1.558	0.340	252.00	7.00	485.75	25.43	36.00	48.50	0.026
0.10	0.10	0.0	0.0	1.558	0.738	163.75	33.00	518.75	27.16	4.96	22.36	

TABLE E27

Tabulated Experimental Results of Run H2D12

(20% HCPV CO_2 Injected at Water Rate @ 2.5 MPa (0.462 moles), 10 Slugs, 4:1 WAG, 21°C, Horizontal Injection)

Porosity (%) = 43.70
Oil Viscosity (mPa.s) = 1842
Ave. Run Temp.(K) = 294.15
CO_2 Req. (sm^3/sm^3) = 6.75
Vp (cm^3) = 2100
S_{oi} (%) = 91.43
HCPV (cm^3) = 1920
CO_2 Ret. (%inj.) = 56.75
S_{wc} (%) = 8.57
Molar Den. ($kmol/m^3$) = 0.04166
Abs. k (darcies) = 14.10
Ave. Flow Vel. (m/d) = 1.55

Press Inj. (MPa)	Press Prod. (MPa)	Gas Inj. (cm^3)	Water Inj. (cm^3)	Cum. PV Injected	Gas Prod (s.ltr)	Water Prod. (cm^3)	Oil Prod. (cm^3)	Cum. Oil Prod. (cm^3)	Percent Rec. (%)	WOR (sm^3/sm^3)	GOR (sm^3/sm^3)	OPFIR (sm^3/sm^3)
2.60	2.50	38.4	0.0	0.018	0.003	0.00	9.50	9.50	0.49	0.00	0.26	0.247
4.00	2.50	0.0	154.0	0.092	0.029	0.00	105.00	114.50	5.96	0.00	0.28	0.682
2.80	2.40	38.4	0.0	0.110	0.001	0.00	23.00	137.50	7.16	0.00	0.04	0.599
2.90	2.50	0.0	153.6	0.183	0.014	38.00	72.00	209.50	10.91	0.53	0.19	0.469
2.80	2.50	38.4	0.0	0.201	-0.001	9.00	10.50	220.00	11.46	0.86	-0.05	0.273
2.70	2.60	0.0	153.8	0.275	0.016	72.00	54.50	274.50	14.30	1.32	0.29	0.354
2.64	2.40	38.4	0.0	0.293	0.001	16.50	8.50	283.00	14.74	1.94	0.12	0.221
2.70	2.50	0.0	153.2	0.366	0.439	84.00	28.50	311.50	16.22	2.95	15.40	0.186
2.80	2.50	38.4	0.0	0.384	0.004	11.25	5.75	317.25	16.52	1.96	0.70	0.150
2.80	2.50	0.0	153.5	0.457	0.031	99.50	25.00	342.25	17.83	3.98	1.22	0.163
2.80	2.70	38.4	0.0	0.475	0.002	12.50	5.10	347.35	18.09	2.45	0.47	0.133
2.60	2.50	0.0	154.0	0.549	0.056	101.00	24.00	371.35	19.34	4.21	2.33	0.156
2.70	2.50	38.4	0.0	0.567	0.058	16.00	4.25	375.60	19.56	3.76	13.59	0.111
2.70	2.50	0.0	153.9	0.640	0.222	98.00	21.00	396.60	20.66	4.67	10.57	0.136
2.60	2.40	38.4	0.0	0.659	0.014	15.00	3.00	399.60	20.81	5.00	4.50	0.078
2.60	2.50	0.0	153.7	0.732	0.169	106.00	19.00	418.60	21.80	5.58	8.89	0.124
2.70	2.50	38.4	0.0	0.750	0.027	17.50	3.50	422.10	21.98	5.00	7.57	0.091
2.60	2.50	0.0	153.6	0.823	0.327	102.00	19.00	441.10	22.97	5.37	17.21	0.124
2.60	2.50	38.4	0.0	0.842	0.037	17.00	3.00	444.10	23.13	5.67	12.17	0.078

TABLE E27 (Cont'd)

Tabulated Experimental Results of Run H2D12

(20% HCPV CO_2 Injected at Water Rate @ 2.5 MPa (0.462 moles), 10 Slugs, 4:1 WAG, 21°C, Horizontal Injection)

Porosity (%) = 43.70
Oil Viscosity (mPa.s) = 1842
Ave. Run Temp.(K) = 294.15
CO_2 Req. (sm^3/sm^3) = 6.75
Vp (cm^3) = 2100
S_{oi} (%) = 91.43
HCPV (cm^3) = 1920
CO_2 Ret. (%inj.) = 56.75
S_{wc} (%) = 8.57
Molar Den. ($kmol/m^3$) = 0.04166
Abs. k (darcies) = 14.10
Ave. Flow Vel. (m/d) = 1.55

Press Inj. (MPa)	Press Prod. (MPa)	Gas Inj. (cm^3)	Water Inj. (cm^3)	Cum. PV Injected	Gas Prod (s.ltr)	Water Prod. (cm^3)	Oil Prod. (cm^3)	Cum. Oil Prod. (cm^3)	Percent Rec. (%)	WOR (sm^3/sm^3)	GOR (sm^3/sm^3)	OPFIR (sm^3/sm^3)
2.60	2.50	0.0	153.2	0.915	0.291	107.50	19.50	463.60	24.15	5.51	14.92	0.127
2.60	2.50	0.0	261.7	1.039	0.499	226.50	26.00	489.60	25.50	8.71	19.17	0.099
2.60	2.50	0.0	254.1	1.160	0.553	232.00	22.50	512.10	26.67	10.31	24.56	0.089
2.60	2.50	0.0	252.3	1.280	0.517	238.00	17.00	529.10	27.56	14.00	30.41	0.067
2.60	2.50	0.0	250.3	1.400	0.426	238.00	14.50	543.60	28.31	16.41	29.34	0.058
2.60	2.50	0.0	267.4	1.527	0.333	252.00	14.00	557.60	29.04	18.00	23.75	0.052
0.10	0.10	0.0	0.0	1.527	0.737	163.75	34.25	591.85	30.83	4.78	21.50	

TABLE E28

Tabulated Experimental Results of Run H2D13

(20% HCPV CO_2 Injected at Water Rate @ 2.5 MPa (0.419 moles), 10 Slugs, 4:1 WAG, 21°C, Horizontal Injection)

Porosity (%) =	41.10	Vp (cm^3) =	1981	S_{wc} (%) =	12.17
Oil Viscosity (mPa.s) =	1842	S_{oi} (%) =	87.83	Molar Den. (kmol/m^3) =	0.04166
Ave. Run Temp.(K) =	294.15	HCPV (cm^3) =	1740	Abs. k (darcies) =	13.54
CO_2 Req. (sm^3/sm^3) =	16.20	CO_2 Ret. (%inj.) =	52.56	Ave. Flow Vel. (m/d) =	2.54

Press Inj. (MPa)	Press Prod. (MPa)	Gas Inj. (cm^3)	Water Inj. (cm^3)	Cum. PV Injected	Gas Prod (s.ltr)	Water Prod. (cm^3)	Oil Prod. (cm^3)	Cum. Oil Prod. (cm^3)	Percent Rec. (%)	WOR (sm^3/sm^3)	GOR (sm^3/sm^3)	OPFIR (sm^3/sm^3)
2.60	2.50	34.8	0.0	0.018	-0.002	0.00	13.50	13.50	0.78	0.00	-0.11	0.388
2.75	2.50	0.0	139.1	0.088	0.014	0.00	120.00	133.50	7.67	0.00	0.12	0.863
2.64	2.40	34.8	0.0	0.105	0.001	0.00	23.00	156.50	8.99	0.00	0.04	0.661
2.64	2.50	0.0	140.2	0.176	0.004	38.00	82.00	238.50	13.71	0.46	0.05	0.585
2.64	2.50	34.8	0.0	0.194	-0.001	9.00	10.50	249.00	14.31	0.86	-0.05	0.302
2.68	2.60	0.0	142.0	0.265	0.016	72.00	54.50	303.50	17.44	1.32	0.29	0.384
2.54	2.40	34.8	0.0	0.283	0.001	16.50	8.50	312.00	17.93	1.94	0.12	0.244
2.55	2.50	0.0	139.3	0.353	0.439	84.00	28.50	340.50	19.57	2.95	15.40	0.205
2.72	2.50	34.8	0.0	0.371	0.004	11.25	5.75	346.25	19.90	1.96	0.70	0.165
2.92	2.50	0.0	139.3	0.441	0.031	99.50	25.00	371.25	21.34	3.98	1.22	0.180
2.70	2.70	34.8	0.0	0.459	0.002	12.50	5.10	376.35	21.63	2.45	0.47	0.147
2.60	2.50	0.0	139.6	0.529	0.056	101.00	24.00	400.35	23.01	4.21	2.33	0.172
2.65	2.50	34.8	0.0	0.547	0.058	16.00	4.25	404.60	23.25	3.76	13.59	0.122
[illegible]	2.50	0.0	139.3	0.617	0.222	98.00	21.00	425.60	24.46	4.67	10.57	0.151
[illegible]	2.40	34.8	0.0	0.635	0.014	15.00	3.00	428.60	24.63	5.00	4.50	0.086
2.60	2.50	0.0	140.0	0.705	0.169	106.00	19.00	447.60	25.72	5.58	8.89	0.136
2.75	2.50	34.8	0.0	0.723	0.027	17.50	3.50	451.10	25.93	5.00	7.57	0.101
2.62	2.50	0.0	139.3	0.793	0.327	102.00	19.00	470.10	27.02	5.37	17.21	0.136
2.60	2.50	34.8	0.0	0.811	0.037	17.00	3.00	473.10	27.19	5.67	12.17	0.086

TABLE E28 (Cont'd)

Tabulated Experimental Results of Run H2D13

(20% HCPV CO_2 Injected at Water Rate @ 2.5 MPa (0.419 moles), 10 Slugs, 4:1 WAG, 21°C, Horizontal Injection)

Porosity (%) = 41.10
Oil Viscosity (mPa.s) = 1842
Ave. Run Temp.(K) = 294.15
CO_2 Req. (sm^3/sm^3) = 16.20

Vp (cm^3) = 1981
S_{oi} (%) = 87.83
HCPV (cm^3) = 1740
CO_2 Ret. (%inj.) = 52.56

S_{wc} (%) = 12.17
Molar Den. ($kmol/m^3$) = 0.04166
Abs. k (darcies) = 13.54
Ave. Flow Vel. (m/d) = 2.54

Press Inj. (MPa)	Press Prod. (MPa)	Gas Inj. (cm^3)	Water Inj. (cm^3)	Cum. PV Injected	Gas Prod (s.ltr)	Water Prod. (cm^3)	Oil Prod. (cm^3)	Cum. Oil Prod. (cm^3)	Percent Rec. (%)	WOR (sm^3/sm^3)	GOR (sm^3/sm^3)	OPFIR (sm^3/sm^3)
2.60	2.50	0.0	144.0	0.883	0.291	107.50	19.50	492.60	28.31	5.51	14.92	0.135
2.60	2.50	0.0	261.7	1.015	0.499	226.50	26.00	518.60	29.80	8.71	19.17	0.099
2.60	2.50	0.0	254.1	1.144	0.553	232.00	22.50	541.10	31.10	10.31	24.56	0.089
2.60	2.50	0.0	252.3	1.271	0.517	238.00	17.00	558.10	32.07	14.00	30.41	0.067
2.60	2.50	0.0	250.3	1.397	0.426	238.00	14.50	572.60	32.91	16.41	29.34	0.058
2.60	2.50	0.0	267.4	1.532	0.333	252.00	14.00	586.60	33.71	18.00	23.75	0.052
0.10	0.10	0.0	0.0	1.532	0.737	163.75	34.25	620.85	35.68	4.78	21.50	

TABLE E29

Tabulated Experimental Results of Run H2D14

(20% HCPV CO_2 Injected at Water Rate @ 2.5 MPa (0.418 moles), 10 Slugs, 4:1 WAG, 21°C, Horizontal Injection)

Porosity (%) = 39.50
Oil Viscosity (mPa.s) = 1842
Ave. Run Temp.(K) = 294.15
CO_2 Req. (sm^3/sm^3) = 16.50

Vp (cm^3) = 1925
S_{oi} (%) = 90.13
HCPV (cm^3) = 1735
CO_2 Ret. (%inj.) = 52.30

S_{wc} (%) = 9.87
Molar Den. ($kmol/m^3$) = 0.04166
Abs. k (darcies) = 13.39
Ave. Flow Vel. (m/d) = 3.17

Press Inj. (MPa)	Press Prod. (MPa)	Gas Inj. (cm^3)	Water Inj. (cm^3)	Cum. PV Injected	Gas Prod (s.ltr)	Water Prod. (cm^3)	Oil Prod. (cm^3)	Cum. Oil Prod. (cm^3)	Percent Rec. (%)	WOR (sm^3/sm^3)	GOR (sm^3/sm^3)	OPFIR (sm^3/sm^3)
2.60	2.50	34.7	0.0	0.018	0.002	0.00	10.50	10.50	0.61	0.00	0.14	0.303
4.00	2.50	0.0	138.8	0.090	0.024	0.00	110.00	120.50	6.95	0.00	0.22	0.793
2.80	2.40	34.7	0.0	0.108	0.001	0.00	23.00	143.50	8.27	0.00	0.04	0.663
2.90	2.50	0.0	138.6	0.180	0.004	38.00	82.00	225.50	13.00	0.46	0.05	0.592
2.80	2.50	34.7	0.0	0.198	-0.001	9.00	10.50	236.00	13.60	0.86	-0.05	0.303
2.70	2.60	0.0	138.9	0.270	0.016	72.00	54.50	290.50	16.74	1.32	0.29	0.392
2.64	2.40	34.7	0.0	0.288	0.001	16.50	8.50	299.00	17.23	1.94	0.12	0.245
2.70	2.50	0.0	138.1	0.360	0.439	84.00	28.50	327.50	18.88	2.95	15.40	0.206
2.80	2.50	34.7	0.0	0.378	0.004	11.25	5.75	333.25	19.21	1.96	0.70	0.166
2.80	2.50	0.0	138.5	0.450	0.031	99.50	25.00	358.25	20.65	3.98	1.22	0.181
2.80	2.70	34.7	0.0	0.468	0.002	12.50	5.10	363.35	20.94	2.45	0.47	0.147
2.60	2.50	0.0	138.3	0.540	0.056	101.00	24.00	387.35	22.33	4.21	2.33	0.174
2.70	2.50	34.7	0.0	0.558	0.058	16.00	4.25	391.60	22.57	3.76	13.59	0.122
2.70	2.50	0.0	138.7	0.630	0.222	98.00	21.00	412.60	23.78	4.67	10.57	0.151
2.60	2.40	34.7	0.0	0.648	0.014	15.00	3.00	415.60	23.95	5.00	4.50	0.086
2.60	2.50	0.0	139.1	0.720	0.169	106.00	19.00	434.60	25.05	5.58	8.89	0.137
2.70	2.50	34.7	0.0	0.738	0.027	17.50	3.50	438.10	25.25	5.00	7.57	0.101
2.60	2.50	0.0	139.3	0.811	0.327	102.00	19.00	457.10	26.35	5.37	17.21	0.136
2.60	2.50	34.7	0.0	0.829	0.037	17.00	3.00	460.10	26.52	5.67	12.17	0.086

TABLE E29 (Cont'd)

Tabulated Experimental Results of Run H2D14

(20% HCPV CO_2 Injected at Water Rate @ 2.5 MPa (0.418 moles), 10 Slugs, 4:1 WAG, 21°C, Horizontal Injection)

Porosity (%) = 39.50
Oil Viscosity (mPa.s) = 1842
Ave. Run Temp.(K) = 294.15
CO_2 Req. (sm^3/sm^3) = 16.50
Vp (cm^3) = 1925
S_{oi} (%) = 90.13
HCPV (cm^3) = 1735
CO_2 Ret. (%inj.) = 52.30
S_{wc} (%) = 9.87
Molar Den. ($kmol/m^3$) = 0.04166
Abs. k (darcies) = 13.39
Ave. Flow Vel. (m/d) = 3.17

Press Inj. (MPa)	Press Prod. (MPa)	Gas Inj. (cm^3)	Water Inj. (cm^3)	Cum. PV Injected	Gas Prod (s.ltr)	Water Prod. (cm^3)	Oil Prod. (cm^3)	Cum. Oil Prod. (cm^3)	Percent Rec. (%)	WOR (sm^3/sm^3)	GOR (sm^3/sm^3)	OPFIR (sm^3/sm^3)
2.60	2.50	0.0	144.0	0.904	0.291	107.50	19.50	479.60	27.64	5.51	14.92	0.135
2.60	2.50	0.0	261.7	1.039	0.499	226.50	26.00	505.60	29.14	8.71	19.17	0.099
2.60	2.50	0.0	254.1	1.171	0.553	232.00	22.50	528.10	30.44	10.31	24.56	0.089
2.60	2.50	0.0	252.3	1.303	0.517	238.00	17.00	545.10	31.42	14.00	30.41	0.067
2.60	2.50	0.0	250.3	1.433	0.426	238.00	14.50	559.60	32.25	16.41	29.34	0.058
2.60	2.50	0.0	267.4	1.571	0.333	252.00	14.00	573.60	33.06	18.00	23.75	0.052
0.10	0.10	0.0	0.0	1.571	0.737	163.75	34.25	607.85	35.03	4.78	21.50	

TABLE E30

Tabulated Experimental Results of Run H2D15

(20% HCPV CO_2 Injected at Water Rate @ 2.5 MPa (0.421 moles), 10 Slugs, 4:1 WAG, 21°C, Horizontal Injection)

Porosity (%) =	39.75	Vp (cm^3) =	1936	S_{wc} (%) =	9.71
Oil Viscosity (mPa.s) =	1842	S_{oi} (%) =	90.29	Molar Den. (kmol/m^3) =	0.04166
Ave. Run Temp.(K) =	294.15	HCPV (cm^3) =	1748	Abs. k (darcies) =	13.14
CO_2 Req. (sm^3/sm^3) =	17.83	CO_2 Ret. (%inj.) =	45.91	Ave. Flow Vel. (m/d) =	3.81

Press Inj. (MPa)	Press Prod. (MPa)	Gas Inj. (cm^3)	Water Inj. (cm^3)	Cum. PV Injected	Gas Prod (s.ltr)	Water Prod. (cm^3)	Oil Prod. (cm^3)	Cum. Oil Prod. (cm^3)	Percent Rec. (%)	WOR (sm^3/sm^3)	GOR (sm^3/sm^3)	OPFIR (sm^3/sm^3)
2.60	2.50	35.0	0.0	0.018	0.000	0.00	11.00	11.00	0.63	0.00	0.00	0.315
4.00	2.50	0.0	139.8	0.090	0.018	12.00	107.00	118.00	6.75	0.11	0.16	0.765
3.00	2.40	35.0	0.0	0.108	0.006	5.50	13.50	131.50	7.52	0.00	0.41	0.386
2.90	2.50	0.0	138.7	0.180	0.004	66.00	71.00	202.50	11.58	0.93	0.06	0.512
2.80	2.50	35.0	0.0	0.198	0.003	11.50	5.50	208.00	11.90	2.09	0.55	0.157
3.00	2.60	0.0	139.5	0.270	-0.010	77.00	44.00	252.00	14.42	1.75	-0.23	0.315
2.64	2.40	35.0	0.0	0.288	0.004	17.50	4.50	256.50	14.67	3.89	0.89	0.129
2.70	2.50	0.0	139.1	0.360	-0.005	100.00	36.00	292.50	16.73	2.78	-0.14	0.259
2.80	2.50	35.0	0.0	0.378	0.003	28.50	6.50	299.00	17.11	4.38	0.46	0.186
2.80	2.50	0.0	140.1	0.450	0.023	87.00	26.00	325.00	18.59	3.35	0.88	0.186
2.80	2.70	35.0	0.0	0.468	0.009	15.50	4.75	329.75	18.86	3.26	1.84	0.136
2.60	2.50	0.0	142.5	0.542	0.025	111.00	21.00	350.75	20.07	5.29	1.19	0.147
2.90	2.50	35.0	0.0	0.560	0.006	20.00	4.50	355.25	20.32	4.44	1.22	0.129
2.70	2.50	0.0	139.8	0.632	0.331	90.00	19.00	374.25	21.41	4.74	17.39	0.136
2.60	2.40	35.0	0.0	0.650	0.021	20.00	3.50	377.75	21.61	5.71	5.86	0.100
2.80	2.50	0.0	143.6	0.725	0.108	111.00	18.00	395.75	22.64	6.17	6.00	0.125
2.60	2.50	35.0	0.0	0.743	0.041	20.50	4.50	400.25	22.90	4.56	9.11	0.129
2.80	2.50	0.0	139.1	0.814	0.347	100.00	16.00	416.25	23.81	6.25	21.69	0.115
2.80	2.50	35.0	0.0	0.833	0.093	23.00	3.50	419.75	24.01	6.57	26.43	0.100

TABLE E30 (Cont'd)

Tabulated Experimental Results of Run H2D15

(20% HCPV CO_2 Injected at Water Rate @ 2.5 MPa (0.421 moles), 10 Slugs, 4:1 WAG, 21°C, Horizontal Injection)

Porosity (%) = 39.75
Oil Viscosity (mPa.s) = 1842
Ave. Run Temp.(K) = 294.15
CO_2 Req. (sm^3/sm^3) = 17.83

Vp (cm^3) = 1936
S_{oi} (%) = 90.29
HCPV (cm^3) = 1748
CO_2 Ret. (%inj.) = 45.91

S_{wc} (%) = 9.71
Molar Den. ($kmol/m^3$) = 0.04166
Abs. k (darcies) = 13.14
Ave. Flow Vel. (m/d) = 3.81

Press Inj. (MPa)	Press Prod. (MPa)	Gas Inj. (cm^3)	Water Inj. (cm^3)	Cum. PV Injected	Gas Prod (s.ltr)	Water Prod. (cm^3)	Oil Prod. (cm^3)	Cum. Oil Prod. (cm^3)	Percent Rec. (%)	WOR (sm^3/sm^3)	GOR (sm^3/sm^3)	OPFIR (sm^3/sm^3)
2.60	2.50	0.0	139.8	0.905	0.702	100.00	10.00	429.75	24.59	10.00	70.20	0.072
2.60	2.50	0.0	243.5	1.031	0.723	234.00	20.00	449.75	25.73	11.70	36.15	0.082
2.60	2.50	0.0	258.7	1.164	0.729	230.00	21.50	471.25	26.96	10.70	33.88	0.083
2.60	2.50	0.0	290.4	1.314	0.628	266.00	19.00	490.25	28.05	14.00	33.05	0.065
2.60	2.50	0.0	268.4	1.453	0.479	258.00	13.00	503.25	28.79	19.85	36.85	0.048
0.10	0.10	0.0	0.0	1.453	1.182	169.00	63.50	566.75	32.42	2.66	18.61	

TABLE E31

Tabulated Experimental Results of Run H2D16

(20% HCPV CO_2 Injected at Water Rate @ 2.5 MPa (0.421 moles), 10 Slugs, 4:1 WAG, 21°C, Horizontal Injection)

Porosity (%) =	39.91	Vp (cm^3) =	1944	S_{wc} (%) =	9.98
Oil Viscosity (mPa.s) =	3295.0	S_{oi} (%) =	90.02	Molar Den. (kmol/m^3) =	0.04166
Ave. Run Temp.(K) =	294.15	HCPV (cm^3) =	1750	Abs. k (darcies) =	12.70
CO_2 Req. (sm^3/sm^3) =	25.86	CO_2 Ret. (%inj.) =	60.67	Ave. Flow Vel. (m/d) =	0.78

Press Inj. (MPa)	Press Prod. (MPa)	Gas Inj. (cm^3)	Water Inj. (cm^3)	Cum. PV Injected	Gas Prod (s.ltr)	Water Prod. (cm^3)	Oil Prod. (cm^3)	Cum. Oil Prod. (cm^3)	Percent Rec. (%)	WOR (sm^3/sm^3)	GOR (sm^3/sm^3)	OPFIR (sm^3/sm^3)
3.30	2.50	35.0	0.0	0.018	0.000	0.00	0.00	0.00	0.00	0.00	0.00	0.000
4.00	2.50	0.0	140.3	0.090	0.033	0.00	82.00	82.00	4.69	0.00	0.40	0.584
3.00	2.40	35.0	0.0	0.108	0.006	4.00	16.00	98.00	5.60	0.00	0.38	0.457
2.90	2.50	0.0	141.0	0.181	0.013	58.50	59.00	157.00	8.97	0.99	0.22	0.418
2.80	2.50	35.0	0.0	0.199	0.002	20.50	9.00	166.00	9.49	2.28	0.22	0.257
3.00	2.60	0.0	144.5	0.273	0.003	55.00	34.00	200.00	11.43	1.62	0.09	0.235
2.64	2.40	35.0	0.0	0.291	0.002	21.50	10.00	210.00	12.00	2.15	0.15	0.286
2.70	2.50	0.0	141.0	0.364	0.016	104.00	29.00	239.00	13.66	3.59	0.55	0.206
2.80	2.50	35.0	0.0	0.382	0.022	23.00	9.00	248.00	14.17	2.56	2.44	0.257
2.80	2.50	0.0	140.1	0.454	0.441	74.00	31.00	279.00	15.94	2.39	14.23	0.221
2.80	2.70	35.0	0.0	0.472	0.159	29.50	6.00	285.00	16.29	4.92	26.42	0.171
2.60	2.50	0.0	140.4	0.544	0.532	85.00	23.00	308.00	17.60	3.70	23.13	0.164
2.90	2.50	35.0	0.0	0.562	0.149	20.00	4.00	312.00	17.83	5.00	37.25	0.114
2.70	2.50	0.0	140.2	0.634	0.393	99.00	15.50	327.50	18.71	6.39	25.32	0.111
2.60	2.40	35.0	0.0	0.652	0.057	20.00	3.00	330.50	18.89	6.67	19.00	0.086
2.80	2.50	0.0	140.1	0.724	0.327	100.00	13.50	344.00	19.66	7.41	24.19	0.096
2.60	2.50	35.0	0.0	0.742	0.046	25.00	3.00	347.00	19.83	8.33	15.33	0.086
2.80	2.50	0.0	142.1	0.815	0.287	108.00	10.00	357.00	20.40	10.80	28.70	0.070
2.80	2.50	35.0	0.0	0.833	0.035	14.00	1.20	358.20	20.47	11.67	29.00	0.034

TABLE E31 (Cont'd)

Tabulated Experimental Results of Run H2D16

(20% HCPV CO_2 Injected at Water Rate @ 2.5 MPa (0.421 moles), 10 Slugs, 4:1 WAG, 21°C, Horizontal Injection)

Porosity (%) =	39.91	Vp (cm^3) =	1944	S_{wc} (%) =	9.98
Oil Viscosity (mPa.s) =	3295.0	S_{oi} (%) =	90.02	Molar Den. (kmol/m^3) =	0.04166
Ave. Run Temp.(K) =	294.15	HCPV (cm^3) =	1750	Abs. k (darcies) =	12.70
CO_2 Req. (sm^3/sm^3) =	25.86	CO_2 Ret. (%inj.) =	60.67	Ave. Flow Vel. (m/d) =	0.78

Press Inj. (MPa)	Press Prod. (MPa)	Gas Inj. (cm^3)	Water Inj. (cm^3)	Cum. PV Injected	Gas Prod (s.ltr)	Water Prod. (cm^3)	Oil Prod. (cm^3)	Cum. Oil Prod. (cm^3)	Percent Rec. (%)	WOR (sm^3/sm^3)	GOR (sm^3/sm^3)	OPFIR (sm^3/sm^3)
2.60	2.50	0.0	140.3	0.905	0.045	107.00	3.50	361.70	20.67	30.57	12.71	0.025
2.60	2.50	0.0	248.0	1.033	0.185	236.00	10.00	371.70	21.24	23.60	18.50	0.040
0.10	0.10	0.0	0.0	1.033	1.229	166.00	19.50	391.20	22.35	8.51	63.03	

TABLE E32

Tabulated Experimental Results of Run H2D17

(20% HCPV CO_2 Injected at Water Rate @ 2.5 MPa (0.436 moles), 10 Slugs, 4:1 WAG, 21°C, Horizontal Injection)

Porosity (%) = 42.41
Oil Viscosity (mPa.s) = 3295.0
Ave. Run Temp.(K) = 294.15
CO_2 Req. (sm^3/sm^3) = 22.96

Vp (cm^3) = 2065
S_{oi} (%) = 87.75
HCPV (cm^3) = 1812
CO_2 Ret. (%inj.) = 64.99

S_{wc} (%) = 12.25
Molar Den. ($kmol/m^3$) = 0.04166
Abs. k (darcies) = 13.95
Ave. Flow Vel. (m/d) = 1.55

Press Inj. (MPa)	Press Prod. (MPa)	Gas Inj. (cm^3)	Water Inj. (cm^3)	Cum. PV Injected	Gas Prod (s.ltr)	Water Prod. (cm^3)	Oil Prod. (cm^3)	Cum. Oil Prod. (cm^3)	Percent Rec. (%)	WOR (sm^3/sm^3)	GOR (sm^3/sm^3)	OPFIR (sm^3/sm^3)
3.30	2.50	36.2	0.0	0.018	0.000	0.00	2.00	2.00	0.11	0.00	0.00	0.055
4.00	2.50	0.0	145.1	0.088	0.018	0.00	97.00	99.00	5.46	0.00	0.19	0.669
3.00	2.40	36.2	0.0	0.105	0.007	4.00	15.00	114.00	6.29	0.00	0.47	0.414
2.90	2.50	0.0	146.8	0.176	-0.007	58.50	78.50	192.50	10.62	0.75	-0.08	0.535
2.80	2.50	36.2	0.0	0.194	0.001	20.50	10.00	202.50	11.18	2.05	0.10	0.276
3.00	2.60	0.0	145.4	0.264	0.003	55.00	34.00	236.50	13.05	1.62	0.09	0.234
2.64	2.40	36.2	0.0	0.282	0.001	21.50	10.70	247.20	13.64	2.01	0.07	0.295
2.70	2.50	0.0	145.3	0.352	0.016	104.00	29.00	276.20	15.24	3.59	0.55	0.200
2.80	2.50	36.2	0.0	0.370	0.022	23.00	9.20	285.40	15.75	2.50	2.37	0.254
2.80	2.50	0.0	145.5	0.440	0.441	74.00	31.00	316.40	17.46	2.39	14.23	0.213
2.80	2.70	36.2	0.0	0.458	0.158	29.50	7.00	323.40	17.85	4.21	22.50	0.193
2.60	2.50	0.0	145.8	0.528	0.412	85.00	23.00	346.40	19.12	3.70	17.91	0.158
2.90	2.50	36.2	0.0	0.546	0.133	20.00	4.60	351.00	19.37	4.35	29.00	0.127
2.70	2.50	0.0	145.8	0.617	0.385	99.00	17.50	368.50	20.34	5.66	21.97	0.120
2.60	2.40	36.2	0.0	0.634	0.057	20.00	3.50	372.00	20.53	5.71	16.14	0.097
2.80	2.50	0.0	145.7	0.705	0.333	100.00	14.50	386.50	21.33	6.90	22.93	0.100
2.60	2.50	36.2	0.0	0.722	0.056	25.00	3.00	389.50	21.50	8.33	18.67	0.083
2.80	2.50	0.0	145.2	0.793	0.293	108.00	13.00	402.50	22.21	8.31	22.50	0.090
2.80	2.50	36.2	0.0	0.810	0.116	14.00	3.20	405.70	22.39	4.38	36.19	0.088

TABLE E32 (Cont'd)

Tabulated Experimental Results of Run H2D17

(20% HCPV CO_2 Injected at Water Rate @ 2.5 MPa (0.436 moles), 10 Slugs, 4:1 WAG, 21°C, Horizontal Injection)

Porosity (%) = 42.41
Oil Viscosity (mPa.s) = 3295.0
Ave. Run Temp.(K) = 294.15
CO_2 Req. (sm^3/sm^3) = 22.96
Vp (cm^3) = 2065
S_{oi} (%) = 87.75
HCPV (cm^3) = 1812
CO_2 Ret. (%inj.) = 64.99
S_{wc} (%) = 12.25
Molar Den. ($kmol/m^3$) = 0.04166
Abs. k (darcies) = 13.95
Ave. Flow Vel. (m/d) = 1.55

Press Inj. (MPa)	Press Prod. (MPa)	Gas Inj. (cm^3)	Water Inj. (cm^3)	Cum. PV Injected	Gas Prod (s.ltr)	Water Prod. (cm^3)	Oil Prod. (cm^3)	Cum. Oil Prod. (cm^3)	Percent Rec. (%)	WOR (sm^3/sm^3)	GOR (sm^3/sm^3)	OPFIR (sm^3/sm^3)
2.60	2.50	0.0	145.9	0.881	0.304	107.00	11.50	417.20	23.02	9.30	26.39	0.079
2.60	2.50	0.0	248.0	1.001	0.327	236.00	14.00	431.20	23.80	16.86	23.36	0.056
2.60	2.50	0.0	267.5	1.130	0.402	240.00	11.00	442.20	24.40	21.82	36.55	0.041
0.10	0.10	0.0	0.0	1.130	0.193	166.00	14.00	456.20	25.18	11.86	13.75	

TABLE E33

Tabulated Experimental Results of Run H2D18

(20% HCPV CO_2 Injected at Water Rate @ 2.5 MPa (0.411 moles), 10 Slugs, 4:1 WAG, 21°C, Horizontal Injection)

Porosity (%) = 39.11
Oil Viscosity (mPa.s) = 3295.0
Ave. Run Temp.(K) = 294.15
CO_2 Req. (sm^3/sm^3) = 17.27

Vp (cm^3) = 1905
S_{oi} (%) = 89.50
HCPV (cm^3) = 1705
CO_2 Ret. (%inj.) = 56.44

S_{wc} (%) = 10.50
Molar Den. ($kmol/m^3$) = 0.04166
Abs. k (darcies) = 12.94
Ave. Flow Vel. (m/d) = 2.54

Press Inj. (MPa)	Press Prod. (MPa)	Gas Inj. (cm^3)	Water Inj. (cm^3)	Cum. PV Injected	Gas Prod (s.ltr)	Water Prod. (cm^3)	Oil Prod. (cm^3)	Cum. Oil Prod. (cm^3)	Percent Rec. (%)	WOR (sm^3/sm^3)	GOR (sm^3/sm^3)	OPFIR (sm^3/sm^3)
3.30	2.50	34.1	0.0	0.018	0.000	0.00	6.25	6.25	0.37	0.00	0.00	0.183
4.00	2.50	0.0	136.5	0.090	0.000	0.00	120.00	126.25	7.40	0.00	0.00	0.879
3.00	2.40	34.1	0.0	0.107	0.000	4.00	24.00	150.25	8.81	0.00	0.00	0.704
2.90	2.50	0.0	136.6	0.179	0.000	58.50	88.10	238.35	13.98	0.66	0.00	0.645
2.80	2.50	34.1	0.0	0.197	0.001	20.50	10.00	248.35	14.57	2.05	0.10	0.293
3.00	2.60	0.0	137.0	0.269	0.000	55.00	65.00	313.35	18.38	0.85	0.00	0.474
2.64	2.40	34.1	0.0	0.287	0.001	21.50	10.70	324.05	19.01	2.01	0.07	0.314
2.70	2.50	0.0	136.4	0.358	0.016	104.00	29.00	353.05	20.71	3.59	0.55	0.213
2.80	2.50	34.1	0.0	0.376	0.022	23.00	9.20	362.25	21.25	2.50	2.37	0.270
2.80	2.50	0.0	136.1	0.448	0.441	74.00	31.00	393.25	23.06	2.39	14.23	0.228
2.80	2.70	34.1	0.0	0.466	0.158	29.50	7.00	400.25	23.48	4.21	22.50	0.205
2.60	2.50	0.0	136.1	0.537	0.401	85.00	23.00	423.25	24.82	3.70	17.43	0.169
2.90	2.50	34.1	0.0	0.555	0.148	20.00	4.60	427.85	25.09	4.35	32.26	0.135
2.70	2.50	0.0	136.1	0.627	0.378	99.00	24.50	452.35	26.53	4.04	15.41	0.180
2.60	2.40	34.1	0.0	0.644	0.029	20.00	4.00	456.35	26.77	5.00	7.25	0.117
2.80	2.50	0.0	136.8	0.716	0.335	100.00	19.50	475.85	27.91	5.13	17.15	0.143
2.60	2.50	34.1	0.0	0.734	0.144	25.00	5.00	480.85	28.20	5.00	28.80	0.147
2.80	2.50	0.0	136.9	0.806	0.292	108.00	13.00	493.85	28.96	8.31	22.42	0.095
2.80	2.50	34.1	0.0	0.824	0.096	14.00	3.20	497.05	29.15	4.38	29.94	0.094

TABLE E33 (Cont'd)

Tabulated Experimental Results of Run H2D18

(20% HCPV CO_2 Injected at Water Rate @ 2.5 MPa (0.411 moles), 10 Slugs, 4:1 WAG, 21°C, Horizontal Injection)

Porosity (%) = 39.11
Oil Viscosity (mPa.s) = 3295.0
Ave. Run Temp.(K) = 294.15
CO_2 Req. (sm^3/sm^3) = 17.27

Vp (cm^3) = 1905
S_{oi} (%) = 89.50
HCPV (cm^3) = 1705
CO_2 Ret. (%inj.) = 56.44

S_{wc} (%) = 10.50
Molar Den. ($kmol/m^3$) = 0.04166
Abs. k (darcies) = 12.94
Ave. Flow Vel. (m/d) = 2.54

Press Inj. (MPa)	Press Prod. (MPa)	Gas Inj. (cm^3)	Water Inj. (cm^3)	Cum. PV Injected	Gas Prod (s.ltr)	Water Prod. (cm^3)	Oil Prod. (cm^3)	Cum. Oil Prod. (cm^3)	Percent Rec. (%)	WOR (sm^3/sm^3)	GOR (sm^3/sm^3)	OPFIR (sm^3/sm^3)
2.60	2.50	0.0	136.0	0.895	0.316	107.00	11.50	508.55	29.83	9.30	27.43	0.085
2.60	2.50	0.0	248.0	1.025	0.181	236.00	14.00	522.55	30.65	16.86	12.93	0.056
2.60	2.50	0.0	267.5	1.166	0.177	240.00	11.00	533.55	31.29	21.82	16.09	0.041
0.10	0.10	0.0	0.0	1.166	1.211	166.00	37.15	570.70	33.47	4.47	32.61	

TABLE E34

Tabulated Experimental Results of Run H2D19

(20% HCPV CO_2 Injected at Water Rate @ 2.5 MPa (0.405 moles), 10 Slugs, 4:1 WAG, 21°C, Horizontal Injection)

Porosity (%) = 38.50
Oil Viscosity (mPa.s) = 3295.0
Ave. Run Temp.(K) = 294.15
CO_2 Req. (sm^3/sm^3) = 20.44

Vp (cm^3) = 1880
S_{oi} (%) = 93.09
HCPV (cm^3) = 1750
CO_2 Ret. (%inj.) = 25.45

S_{wc} (%) = 6.91
Molar Den. ($kmol/m^3$) = 0.04166
Abs. k (darcies) = 13.58
Ave. Flow Vel. (m/d) = 3.17

Press Inj. (MPa)	Press Prod. (MPa)	Gas Inj. (cm^3)	Water Inj. (cm^3)	Cum. PV Injected	Gas Prod (s.ltr)	Water Prod. (cm^3)	Oil Prod. (cm^3)	Cum. Oil Prod. (cm^3)	Percent Rec. (%)	WOR (sm^3/sm^3)	GOR (sm^3/sm^3)	OPFIR (sm^3/sm^3)
3.30	2.50	35.0	0.0	0.019	0.000	0.00	6.25	6.25	0.36	0.00	0.00	0.179
4.00	2.50	0.0	140.3	0.093	0.013	0.00	102.00	108.25	6.19	0.00	0.13	0.727
3.00	2.40	35.0	0.0	0.112	0.002	4.00	20.00	128.25	7.33	0.00	0.10	0.571
2.90	2.50	0.0	141.0	0.187	0.004	58.50	68.50	196.75	11.24	0.85	0.05	0.486
2.80	2.50	35.0	0.0	0.205	0.001	20.50	10.00	206.75	11.81	2.05	0.10	0.286
3.00	2.60	0.0	144.5	0.282	0.003	55.00	34.00	240.75	13.76	1.62	0.09	0.235
2.64	2.40	35.0	0.0	0.301	0.001	21.50	10.70	251.45	14.37	2.01	0.07	0.306
2.70	2.50	0.0	141.0	0.376	0.016	104.00	29.00	280.45	16.03	3.59	0.55	0.206
2.80	2.50	35.0	0.0	0.395	0.022	23.00	9.20	289.65	16.55	2.50	2.37	0.263
2.80	2.50	0.0	140.1	0.469	0.441	74.00	31.00	320.65	18.32	2.39	14.23	0.221
2.80	2.70	35.0	0.0	0.488	0.158	29.50	7.00	327.65	18.72	4.21	22.50	0.200
2.60	2.50	0.0	140.4	0.562	0.532	85.00	23.00	350.65	20.04	3.70	23.13	0.164
2.90	2.50	35.0	0.0	0.581	0.148	20.00	4.60	355.25	20.30	4.35	32.26	0.131
2.70	2.50	0.0	140.2	0.656	0.731	99.00	17.50	372.75	21.30	5.66	41.74	0.125
2.60	2.40	35.0	0.0	0.674	0.170	20.00	3.50	376.25	21.50	5.71	48.43	0.100
2.80	2.50	0.0	140.1	0.749	0.680	100.00	14.50	390.75	22.33	6.90	46.86	0.104
2.60	2.50	35.0	0.0	0.767	0.171	25.00	3.00	393.75	22.50	8.33	57.00	0.086
2.80	2.50	0.0	142.1	0.843	0.759	108.00	13.00	406.75	23.24	8.31	58.35	0.091
2.80	2.50	35.0	0.0	0.861	0.116	14.00	3.20	409.95	23.43	4.38	36.19	0.091

TABLE E34 (Cont'd)

Tabulated Experimental Results of Run H2D19

(20% HCPV CO_2 Injected at Water Rate @ 2.5 MPa (0.405 moles), 10 Slugs, 4:1 WAG, 21°C, Horizontal Injection)

Porosity (%) = 38.50
Oil Viscosity (mPa.s) = 3295.0
Ave. Run Temp.(K) = 294.15
CO_2 Req. (sm^3/sm^3) = 20.44

Vp (cm^3) = 1880
S_{oi} (%) = 93.09
HCPV (cm^3) = 1750
CO_2 Ret. (%inj.) = 25.45

S_{wc} (%) = 6.91
Molar Den. ($kmol/m^3$) = 0.04166
Abs. k (darcies) = 13.58
Ave. Flow Vel. (m/d) = 3.17

Press Inj. (MPa)	Press Prod. (MPa)	Gas Inj. (cm^3)	Water Inj. (cm^3)	Cum. PV Injected	Gas Prod (s.ltr)	Water Prod. (cm^3)	Oil Prod. (cm^3)	Cum. Oil Prod. (cm^3)	Percent Rec. (%)	WOR (sm^3/sm^3)	GOR (sm^3/sm^3)	OPFIR (sm^3/sm^3)
2.60	2.50	0.0	140.3	0.936	0.761	107.00	11.50	421.45	24.08	9.30	66.13	0.082
2.60	2.50	0.0	248.0	1.068	1.215	236.00	14.00	435.45	24.88	16.86	86.75	0.056
2.60	2.50	0.0	267.5	1.210	0.402	240.00	11.00	446.45	25.51	21.82	36.55	0.041
0.10	0.10	0.0	0.0	1.210	1.200	166.00	48.50	494.95	28.28	3.42	24.74	

TABLE E35

Tabulated Experimental Results of Run H2D20

(20% HCPV CO_2 Injected at Water Rate @ 2.5 MPa (0.420 moles), 10 Slugs, 4:1 WAG, 21°C, Horizontal Injection)

Porosity (%) = 38.10
Oil Viscosity (mPa.s) = 3295.0
Ave. Run Temp.(K) = 294.15
CO_2 Req. (sm^3/sm^3) = 24.50
Vp (cm^3) = 1856
S_{oi} (%) = 94.02
HCPV (cm^3) = 1745
CO_2 Ret. (%inj.) = 36.83
S_{wc} (%) = 5.98
Molar Den. ($kmol/m^3$) = 0.04166
Abs. k (darcies) = 13.58
Ave. Flow Vel. (m/d) = 3.81

Press Inj. (MPa)	Press Prod. (MPa)	Gas Inj. (cm^3)	Water Inj. (cm^3)	Cum. PV Injected	Gas Prod (s.ltr)	Water Prod. (cm^3)	Oil Prod. (cm^3)	Cum. Oil Prod. (cm^3)	Percent Rec. (%)	WOR (sm^3/sm^3)	GOR (sm^3/sm^3)	OPFIR (sm^3/sm^3)
3.30	2.50	34.9	0.0	0.019	0.002	0.00	7.00	7.00	0.40	0.00	0.00	0.201
4.00	2.50	0.0	139.6	0.093	0.063	0.00	96.50	103.50	5.93	0.00	0.65	0.691
3.00	2.50	34.9	0.0	0.111	0.003	1.50	19.50	123.00	7.05	0.00	0.15	0.559
2.90	2.50	0.0	139.7	0.186	0.088	68.00	41.00	164.00	9.40	1.66	2.13	0.294
2.80	2.50	34.9	0.0	0.204	0.002	20.00	5.00	169.00	9.68	4.00	0.30	0.143
2.90	2.60	0.0	161.5	0.290	0.087	98.00	24.00	193.00	11.06	4.08	3.63	0.149
2.64	2.40	34.9	0.0	0.309	0.001	23.00	6.50	199.50	11.43	3.54	0.08	0.186
2.70	2.50	0.0	144.3	0.385	0.012	83.00	21.00	220.50	12.64	3.95	0.57	0.146
3.50	2.50	34.9	0.0	0.404	0.007	19.00	6.00	226.50	12.98	3.17	1.17	0.172
2.90	2.50	0.0	142.1	0.480	0.186	98.00	22.50	249.00	14.27	4.36	8.24	0.158
2.80	2.70	34.9	0.0	0.498	0.060	19.00	4.00	253.00	14.50	4.75	15.00	0.115
2.60	2.50	0.0	149.6	0.578	0.306	101.00	16.00	269.00	15.42	6.31	19.13	0.107
2.60	2.50	34.9	0.0	0.596	0.064	12.00	4.00	273.00	15.64	3.00	16.00	0.115
2.60	2.50	0.0	139.8	0.671	0.606	113.00	15.00	288.00	16.50	7.53	40.40	0.107
2.60	2.40	34.9	0.0	0.689	0.131	25.50	3.50	291.50	16.70	7.29	37.43	0.100
2.80	2.50	0.0	140.0	0.764	0.850	94.50	14.00	305.50	17.51	6.75	60.71	0.100
2.60	2.50	34.9	0.0	0.782	0.204	27.50	4.00	309.50	17.74	6.88	50.88	0.115
2.65	2.50	0.0	140.9	0.857	0.784	107.00	8.00	317.50	18.19	13.38	98.00	0.057
2.80	2.50	34.9	0.0	0.876	0.131	15.00	2.70	320.20	18.35	5.56	48.44	0.077

TABLE E35 (Cont'd)

Tabulated Experimental Results of Run H2D20

(20% HCPV CO_2 Injected at Water Rate @ 2.5 MPa (0.420 moles), 10 Slugs, 4:1 WAG, 21°C, Horizontal Injection)

Porosity (%) = 38.10
Oil Viscosity (mPa.s) = 3295.0
Ave. Run Temp.(K) = 294.15
CO_2 Req. (sm^3/sm^3) = 24.50
Vp (cm^3) = 1856
S_{oi} (%) = 94.02
HCPV (cm^3) = 1745
CO_2 Ret. (%inj.) = 36.83
S_{wc} (%) = 5.98
Molar Den. ($kmol/m^3$) = 0.04166
Abs. k (darcies) = 13.58
Ave. Flow Vel. (m/d) = 3.81

Press Inj. (MPa)	Press Prod. (MPa)	Gas Inj. (cm^3)	Water Inj. (cm^3)	Cum. PV Injected	Gas Prod (s.ltr)	Water Prod. (cm^3)	Oil Prod. (cm^3)	Cum. Oil Prod. (cm^3)	Percent Rec. (%)	WOR (sm^3/sm^3)	GOR (sm^3/sm^3)	OPFIR (sm^3/sm^3)
2.60	2.50	0.0	141.5	0.951	0.839	109.00	10.00	330.20	18.92	10.90	83.85	0.071
2.60	2.50	0.0	253.5	1.086	1.169	237.00	14.00	344.20	19.72	16.93	83.46	0.055
2.60	2.50	0.0	246.9	1.217	0.309	239.50	13.50	357.70	20.50	17.74	22.89	0.055
2.60	2.50	0.0	249.1	1.350	0.301	238.00	10.00	367.70	21.07	23.80	30.10	0.040
0.10	0.10	0.0	0.0	1.350	0.172	75.00	44.00	411.70	23.59	1.70	3.91	

TABLE E36

Tabulated Experimental Results of Run H2D21

(20% HCPV CO_2 Injected at Water Rate @ 2.5 MPa (0.479 moles), 10 Slugs, 4:1 WAG, 21°C, Horizontal Injection)

Porosity (%) = 44.34
Oil Viscosity (mPa.s) = 3606.6
Ave. Run Temp.(K) = 294.15
CO_2 Req. (sm^3/sm^3) = 30.90

Vp (cm^3) = 2160
S_{oi} (%) = 92.13
HCPV (cm^3) = 1990
CO_2 Ret. (%inj.) = 66.92

S_{wc} (%) = 7.87
Molar Den. ($kmol/m^3$) = 0.04166
Abs. k (darcies) = 12.62
Ave. Flow Vel. (m/d) = 0.78

Press Inj. (MPa)	Press Prod. (MPa)	Gas Inj. (cm^3)	Water Inj. (cm^3)	Cum. PV Injected	Gas Prod (s.ltr)	Water Prod. (cm^3)	Oil Prod. (cm^3)	Cum. Oil Prod. (cm^3)	Percent Rec. (%)	WOR (sm^3/sm^3)	GOR (sm^3/sm^3)	OPFIR (sm^3/sm^3)
2.60	2.50	39.8	0.0	0.018	0.000	0.00	0.00	0.00	0.00	0.00	0.00	0.000
4.00	2.50	0.0	159.2	0.092	0.141	0.00	85.00	85.00	4.27	0.00	1.66	0.534
3.00	2.40	39.8	0.0	0.111	0.014	2.00	14.50	99.50	5.00	0.00	0.93	0.364
2.90	2.50	0.0	159.2	0.184	0.051	86.00	81.00	180.50	9.07	1.06	0.62	0.509
2.80	2.50	39.8	0.0	0.203	0.003	20.00	11.00	191.50	9.62	1.82	0.27	0.276
3.00	2.60	0.0	159.4	0.276	0.006	46.25	16.75	208.25	10.46	2.76	0.36	0.105
2.64	2.40	39.8	0.0	0.295	0.003	14.00	5.50	213.75	10.74	2.55	0.45	0.138
2.70	2.50	0.0	160.0	0.369	0.154	80.00	14.00	227.75	11.44	5.71	10.96	0.088
2.80	2.50	39.8	0.0	0.387	0.011	15.50	3.50	231.25	11.62	4.43	3.14	0.088
2.80	2.50	0.0	159.8	0.461	0.207	92.50	21.00	252.25	12.68	4.40	9.86	0.131
2.80	2.70	39.8	0.0	0.480	0.045	23.00	5.25	257.50	12.94	4.38	8.52	0.132
2.60	2.50	0.0	159.7	0.554	0.623	87.00	19.00	276.50	13.89	4.58	32.76	0.119
2.90	2.50	39.8	0.0	0.572	0.065	24.00	1.25	277.75	13.96	19.20	51.80	0.031
2.70	2.50	0.0	159.7	0.646	0.229	91.00	14.00	291.75	14.66	6.50	16.32	0.088
2.60	2.40	39.8	0.0	0.665	0.164	32.50	6.25	298.00	14.97	5.20	26.28	0.157
2.80	2.50	0.0	159.9	0.739	0.289	96.00	13.25	311.25	15.64	7.25	21.79	0.083
2.60	2.50	39.8	0.0	0.757	0.059	15.50	3.00	314.25	15.79	5.17	19.50	0.075
2.80	2.50	0.0	159.4	0.831	0.451	101.50	10.50	324.75	16.32	9.67	42.95	0.066
2.80	2.50	39.8	0.0	0.849	0.135	35.00	6.00	330.75	16.62	5.83	22.50	0.151

TABLE E36 (Cont'd)

Tabulated Experimental Results of Run H2D21

(20% HCPV CO_2 Injected at Water Rate @ 2.5 MPa (0.479 moles), 10 Slugs, 4:1 WAG, 21°C, Horizontal Injection)

Porosity (%) =	44.34	Vp (cm^3) =	2160	S_{wc} (%) =	7.87
Oil Viscosity (mPa.s) =	3606.6	S_{oi} (%) =	92.13	Molar Den. (kmol/m^3) =	0.04166
Ave. Run Temp.(K) =	294.15	HCPV (cm^3) =	1990	Abs. k (darcies) =	12.62
CO_2 Req. (sm^3/sm^3) =	30.90	CO_2 Ret. (%inj.) =	66.92	Ave. Flow Vel. (m/d) =	0.78

Press Inj. (MPa)	Press Prod. (MPa)	Gas Inj. (cm^3)	Water Inj. (cm^3)	Cum. PV Injected	Gas Prod (s.ltr)	Water Prod. (cm^3)	Oil Prod. (cm^3)	Cum. Oil Prod. (cm^3)	Percent Rec. (%)	WOR (sm^3/sm^3)	GOR (sm^3/sm^3)	OPFIR (sm^3/sm^3)
2.60	2.50	0.0	159.4	0.923	0.395	98.00	7.50	338.25	17.00	13.07	52.60	0.047
2.60	2.50	0.0	263.8	1.045	0.461	239.00	11.00	349.25	17.55	21.73	41.91	0.042
0.10	0.10	0.0	0.0	1.045	0.304	74.50	23.00	372.25	18.71	3.24	13.20	

TABLE E37

Tabulated Experimental Results of Run H2D22

(20% HCPV CO_2 Injected at Water Rate @ 2.5 MPa (0.424 moles), 10 Slugs, 4:1 WAG, 21°C, Horizontal Injection)

Porosity (%) = 39.48
Oil Viscosity (mPa.s) = 3606.6
Ave. Run Temp.(K) = 294.15
CO_2 Req. (sm^3/sm^3) = 9.38

Vp (cm^3) = 1923
S_{oi} (%) = 91.52
HCPV (cm^3) = 1760
CO_2 Ret. (%inj.) = 62.92

S_{wc} (%) = 8.48
Molar Den. ($kmol/m^3$) = 0.04166
Abs. k (darcies) = 12.35
Ave. Flow Vel. (m/d) = 1.55

Press Inj. (MPa)	Press Prod. (MPa)	Gas Inj. (cm^3)	Water Inj. (cm^3)	Cum. PV Injected	Gas Prod (s.ltr)	Water Prod. (cm^3)	Oil Prod. (cm^3)	Cum. Oil Prod. (cm^3)	Percent Rec. (%)	WOR (sm^3/sm^3)	GOR (sm^3/sm^3)	OPFIR (sm^3/sm^3)
2.60	2.50	35.2	0.0	0.018	0.000	0.00	0.00	0.00	0.00	0.00	0.00	0.000
4.00	2.50	0.0	140.8	0.092	0.136	0.00	90.00	90.00	5.11	0.00	1.51	0.639
3.00	2.40	35.2	0.0	0.110	0.011	2.00	17.50	107.50	6.11	0.00	0.60	0.497
2.90	2.50	0.0	141.1	0.183	0.061	86.00	71.00	178.50	10.14	1.21	0.85	0.503
2.80	2.50	35.2	0.0	0.202	0.003	20.00	11.00	189.50	10.77	1.82	0.27	0.313
3.00	2.60	0.0	141.1	0.275	0.006	46.25	16.75	206.25	11.72	2.76	0.36	0.119
2.64	2.40	35.2	0.0	0.293	0.003	14.00	5.50	211.75	12.03	2.55	0.45	0.156
2.70	2.50	0.0	140.8	0.366	0.144	80.00	24.00	235.75	13.39	3.33	5.98	0.170
2.80	2.50	35.2	0.0	0.385	0.011	15.50	3.50	239.25	13.59	4.43	3.14	0.099
2.80	2.50	0.0	140.2	0.458	0.204	92.50	24.50	263.75	14.99	3.78	8.31	0.175
2.80	2.70	35.2	0.0	0.476	0.044	23.00	6.25	270.00	15.34	3.68	7.00	0.178
2.60	2.50	0.0	140.5	0.549	0.619	87.00	23.00	293.00	16.65	3.78	26.89	0.164
2.90	2.50	35.2	0.0	0.567	0.064	24.00	2.25	295.25	16.78	10.67	28.33	0.064
2.70	2.50	0.0	140.5	0.640	0.228	91.00	15.00	310.25	17.63	6.07	15.17	0.107
2.60	2.40	35.2	0.0	0.659	0.164	32.50	6.75	317.00	18.01	4.81	24.26	0.192
2.80	2.50	0.0	140.6	0.732	0.624	96.00	14.25	331.25	18.82	6.74	43.77	0.101
2.60	2.50	35.2	0.0	0.750	0.058	15.50	3.50	334.75	19.02	4.43	16.57	0.099
2.80	2.50	0.0	140.7	0.823	0.660	101.50	12.50	347.25	19.73	8.12	52.76	0.089
2.80	2.50	35.2	0.0	0.842	0.134	35.00	7.00	354.25	20.13	5.00	19.14	0.199

TABLE E37 (Cont'd)

Tabulated Experimental Results of Run H2D22

(20% HCPV CO_2 Injected at Water Rate @ 2.5 MPa (0.424 moles), 10 Slugs, 4:1 WAG, 21°C, Horizontal Injection)

Porosity (%) = 39.48
Vp (cm^3) = 1923
S_{wc} (%) = 8.48
Oil Viscosity (mPa.s) = 3606.6
S_{oi} (%) = 91.52
Molar Den. ($kmol/m^3$) = 0.04166
Ave. Run Temp.(K) = 294.15
HCPV (cm^3) = 1760
Abs. k (darcies) = 12.35
CO_2 Req. (sm^3/sm^3) = 9.38
CO_2 Ret. (%inj.) = 62.92
Ave. Flow Vel. (m/d) = 1.55

Press Inj. (MPa)	Press Prod. (MPa)	Gas Inj. (cm^3)	Water Inj. (cm^3)	Cum. PV Injected	Gas Prod (s.ltr)	Water Prod. (cm^3)	Oil Prod. (cm^3)	Cum. Oil Prod. (cm^3)	Percent Rec. (%)	WOR (sm^3/sm^3)	GOR (sm^3/sm^3)	OPFIR (sm^3/sm^3)
2.60	2.50	0.0	140.9	0.915	0.072	98.00	5.00	359.25	20.41	19.60	14.40	0.035
2.60	2.50	0.0	263.8	1.052	0.229	239.00	7.00	366.25	20.81	34.14	32.71	0.027
0.10	0.10	0.0	0.0	1.052	0.302	74.50	24.21	390.46	22.19	3.08	12.49	

TABLE E38

Tabulated Experimental Results of Run H2D23

(20% HCPV CO_2 Injected at Water Rate @ 2.5 MPa (0.415 moles), 10 Slugs, 4:1 WAG, 21°C, Horizontal Injection)

Porosity (%) = 39.72
Oil Viscosity (mPa.s) = 3606.6
Ave. Run Temp.(K) = 294.15
CO_2 Req. (sm^3/sm^3) = 6.90

Vp (cm^3) = 1935
S_{oi} (%) = 88.99
HCPV (cm^3) = 1722
CO_2 Ret. (%inj.) = 39.89

S_{wc} (%) = 11.01
Molar Den. ($kmol/m^3$) = 0.04166
Abs. k (darcies) = 12.41
Ave. Flow Vel. (m/d) = 2.54

Press Inj. (MPa)	Press Prod. (MPa)	Gas Inj. (cm^3)	Water Inj. (cm^3)	Cum. PV Injected	Gas Prod (s.ltr)	Water Prod. (cm^3)	Oil Prod. (cm^3)	Cum. Oil Prod. (cm^3)	Percent Rec. (%)	WOR (sm^3/sm^3)	GOR (sm^3/sm^3)	OPFIR (sm^3/sm^3)
2.60	2.50	34.4	0.0	0.018	0.000	0.00	0.00	0.00	0.00	0.00	0.00	0.000
4.00	2.50	0.0	137.8	0.089	0.136	0.00	90.00	90.00	5.23	0.00	1.51	0.653
3.00	2.40	34.4	0.0	0.107	0.011	2.00	17.50	107.50	6.24	0.00	0.60	0.508
2.90	2.50	0.0	202.2	0.211	0.026	86.00	106.00	213.50	12.40	0.81	0.24	0.524
2.80	2.50	34.4	0.0	0.229	0.003	20.00	11.00	224.50	13.04	1.82	0.27	0.319
3.00	2.60	0.0	73.3	0.267	0.006	46.25	16.75	241.25	14.01	2.76	0.36	0.228
2.64	2.40	34.4	0.0	0.285	0.003	14.00	5.50	246.75	14.33	2.55	0.45	0.160
2.70	2.50	0.0	137.8	0.356	0.144	80.00	24.00	270.75	15.72	3.33	5.98	0.174
2.80	2.50	34.4	0.0	0.374	0.011	15.50	3.50	274.25	15.93	4.43	3.14	0.102
2.80	2.50	0.0	138.8	0.446	0.204	92.50	24.50	298.75	17.35	3.78	8.31	0.177
2.80	2.70	34.4	0.0	0.463	0.044	23.00	6.25	305.00	17.71	3.68	7.00	0.181
2.60	2.50	0.0	138.5	0.535	0.619	87.00	23.00	328.00	19.05	3.78	26.89	0.166
2.90	2.50	34.4	0.0	0.553	0.064	24.00	2.25	330.25	19.18	10.67	28.33	0.065
2.70	2.50	0.0	137.8	0.624	0.228	91.00	15.00	345.25	20.05	6.07	15.17	0.109
2.60	2.40	34.4	0.0	0.642	0.164	32.50	6.75	352.00	20.44	4.81	24.26	0.196
2.80	2.50	0.0	137.9	0.713	0.624	96.00	14.25	366.25	21.27	6.74	43.77	0.103
2.60	2.50	34.4	0.0	0.731	0.058	15.50	3.50	369.75	21.47	4.43	16.57	0.102
2.80	2.50	0.0	137.8	0.802	0.652	101.50	20.50	390.25	22.66	4.95	31.78	0.149
2.80	2.50	34.4	0.0	0.820	0.134	35.00	7.00	397.25	23.07	5.00	19.14	0.203

TABLE E38 (Cont'd)

Tabulated Experimental Results of Run H2D23

(20% HCPV CO_2 Injected at Water Rate @ 2.5 MPa (0.415 moles), 10 Slugs, 4:1 WAG, 21°C, Horizontal Injection)

Porosity (%) = 39.72
Oil Viscosity (mPa.s) = 3606.6
Ave. Run Temp.(K) = 294.15
CO_2 Req. (sm³/sm³) = 6.90

Vp (cm³) = 1935
S_{oi} (%) = 88.99
HCPV (cm³) = 1722
CO_2 Ret. (%inj.) = 39.89

S_{wc} (%) = 11.01
Molar Den. (kmol/m³) = 0.04166
Abs. k_g(darcies) = 12.41
Ave. Flow Vel. (m/d) = 2.54

Press Inj. (MPa)	Press Prod. (MPa)	Gas Inj. (cm³)	Water Inj. (cm³)	Cum. PV Injected	Gas Prod (s.ltr)	Water Prod. (cm³)	Oil Prod. (cm³)	Cum. Oil Prod. (cm³)	Percent Rec. (%)	WOR (sm³/sm³)	GOR (sm³/sm³)	OPFIR (sm³/sm³)
2.60	2.50	0.0	143.5	0.894	0.702	98.00	12.50	409.75	23.80	7.84	56.12	0.087
2.60	2.50	0.0	263.8	1.030	0.455	239.00	17.00	426.75	24.78	14.06	26.76	0.064
2.60	2.50	0.0	251.0	1.160	0.392	236.00	19.00	445.75	25.89	12.42	20.61	0.076
2.60	2.50	0.0	253.9	1.291	0.519	236.00	17.00	462.75	26.87	13.88	30.53	0.067
2.60	2.50	0.0	265.3	1.428	0.278	251.00	11.00	473.75	27.51	22.82	25.27	0.041
2.60	2.50	0.0	250.5	1.558	0.221	241.00	11.50	485.25	28.18	20.96	19.22	0.046
0.10	0.10	0.0	0.0	1.558	0.292	74.50	34.25	519.50	30.17	2.18	8.53	

TABLE E39

Tabulated Experimental Results of Run H2D24

(20% HCPV CO_2 Injected at Water Rate @ 2.5 MPa (0.426 moles), 10 Slugs, 4:1 WAG, 21°C, Horizontal Injection)

Porosity (%) = 40.18
Oil Viscosity (mPa.s) = 3606.6
Ave. Run Temp.(K) = 294.15
CO_2 Req. (sm^3/sm^3) = 8.32

Vp (cm^3) = 1957
S_{oi} (%) = 90.34
HCPV (cm^3) = 1768
CO_2 Ret. (%inj.) = 59.50

S_{wc} (%) = 9.66
Molar Den. ($kmol/m^3$) = 0.04166
Abs. k (darcies) = 12.78
Ave. Flow Vel. (m/d) = 3.17

Press Inj. (MPa)	Press Prod. (MPa)	Gas Inj. (cm^3)	Water Inj. (cm^3)	Cum. PV Injected	Gas Prod (s.ltr)	Water Prod. (cm^3)	Oil Prod. (cm^3)	Cum. Oil Prod. (cm^3)	Percent Rec. (%)	WOR (sm^3/sm^3)	GOR (sm^3/sm^3)	OPFIR (sm^3/sm^3)
2.60	2.50	35.4	0.0	0.018	0.000	0.00	0.00	0.00	0.00	0.00	0.00	0.000
4.00	2.50	0.0	141.5	0.090	0.020	12.00	105.00	105.00	5.94	0.11	0.19	0.742
3.00	2.40	35.4	0.0	0.108	0.006	6.00	13.00	118.00	6.67	0.00	0.42	0.368
2.90	2.50	0.0	141.7	0.181	0.009	66.00	66.00	184.00	10.41	1.00	0.14	0.466
2.80	2.50	35.4	0.0	0.199	0.003	12.00	5.00	189.00	10.69	2.40	0.60	0.141
3.00	2.60	0.0	141.6	0.271	-0.005	77.00	39.00	228.00	12.90	1.97	-0.13	0.276
2.64	2.40	35.4	0.0	0.289	0.004	17.50	4.50	232.50	13.15	3.89	0.89	0.127
2.70	2.50	0.0	141.7	0.362	0.008	100.00	23.00	255.50	14.45	4.35	0.35	0.162
2.80	2.50	35.4	0.0	0.380	0.003	28.50	6.50	262.00	14.82	4.38	0.46	0.184
2.80	2.50	0.0	141.9	0.452	0.023	87.00	26.00	288.00	16.29	3.35	0.88	0.183
2.80	2.70	35.4	0.0	0.470	0.009	15.50	4.75	292.75	16.56	3.26	1.84	0.134
2.60	2.50	0.0	141.4	0.543	0.025	111.00	21.00	313.75	17.75	5.29	1.19	0.149
2.90	2.50	35.4	0.0	0.561	0.006	20.00	4.50	318.25	18.00	4.44	1.22	0.127
2.70	2.50	0.0	141.8	0.633	0.336	90.00	14.00	332.25	18.79	6.43	23.96	0.099
2.60	2.40	35.4	0.0	0.651	0.021	20.00	3.50	335.75	18.99	5.71	5.86	0.099
2.80	2.50	0.0	141.5	0.724	0.108	111.00	18.00	353.75	20.01	6.17	6.00	0.127
2.60	2.50	35.4	0.0	0.742	0.039	20.50	7.00	360.75	20.40	2.93	5.50	0.198
2.80	2.50	0.0	141.7	0.814	0.356	100.00	7.00	367.75	20.80	14.29	50.86	0.049
2.80	2.50	35.4	0.0	0.832	0.093	23.00	3.00	370.75	20.97	7.67	31.00	0.085

TABLE E39 (Cont'd)

Tabulated Experimental Results of Run H2D24

(20% HCPV CO_2 Injected at Water Rate @ 2.5 MPa (0.426 moles), 10 Slugs, 4:1 WAG, 21°C, Horizontal Injection)

Porosity (%) = 40.18
Oil Viscosity (mPa.s) = 3606.6
Ave. Run Temp.(K) = 294.15
CO_2 Req. (sm^3/sm^3) = 8.32

Vp (cm^3) = 1957
S_{oi} (%) = 90.34
HCPV (cm^3) = 1768
CO_2 Ret. (%inj.) = 59.50

S_{wc} (%) = 9.66
Molar Den. ($kmol/m^3$) = 0.04166
Abs. k (darcies) = 12.78
Ave. Flow Vel. (m/d) = 3.17

Press Inj. (MPa)	Press Prod. (MPa)	Gas Inj. (cm^3)	Water Inj. (cm^3)	Cum. PV Injected	Gas Prod (s.ltr)	Water Prod. (cm^3)	Oil Prod. (cm^3)	Cum. Oil Prod. (cm^3)	Percent Rec. (%)	WOR (sm^3/sm^3)	GOR (sm^3/sm^3)	OPFIR (sm^3/sm^3)
2.60	2.50	0.0	141.5	0.904	0.406	100.00	6.00	376.75	21.31	16.67	67.67	0.042
2.60	2.50	0.0	243.5	1.029	0.723	234.00	20.00	396.75	22.44	11.70	36.15	0.082
2.60	2.50	0.0	258.7	1.161	0.740	230.00	10.50	407.25	23.03	21.90	70.43	0.041
0.10	0.10	0.0	0.0	1.161	1.211	169.00	35.00	442.25	25.01	4.83	34.59	

TABLE E40

Tabulated Experimental Results of Run H2D25

(20% HCPV CO_2 Injected at Water Rate @ 2.5 MPa (0.426 moles), 10 Slugs, 4:1 WAG, 21°C, Horizontal Injection)

Porosity (%) = 41.00
Oil Viscosity (mPa.s) = 3606.6
Ave. Run Temp.(K) = 294.15
CO_2 Req. (sm^3/sm^3) = 9.42

Vp (cm^3) = 1997
S_{oi} (%) = 90.64
HCPV (cm^3) = 1810
CO_2 Ret. (%inj.) = 51.31

S_{wc} (%) = 9.36
Molar Den. ($kmol/m^3$) = 0.04166
Abs. k (darcies) = 12.89
Ave. Flow Vel. (m/d) = 3.81

Press Inj. (MPa)	Press Prod. (MPa)	Gas Inj. (cm^3)	Water Inj. (cm^3)	Cum. PV Injected	Gas Prod (s.ltr)	Water Prod. (cm^3)	Oil Prod. (cm^3)	Cum. Oil Prod. (cm^3)	Percent Rec. (%)	WOR (sm^3/sm^3)	GOR (sm^3/sm^3)	OPFIR (sm^3/sm^3)
2.60	2.50	36.2	0.0	0.018	0.000	0.00	0.00	0.00	0.00	0.00	0.00	0.000
4.00	2.50	0.0	144.8	0.091	0.136	0.00	90.00	90.00	4.97	0.00	1.51	0.622
3.00	2.40	36.2	0.0	0.109	0.011	2.00	17.50	107.50	5.94	0.00	0.60	0.483
2.90	2.50	0.0	144.8	0.181	0.073	109.80	35.00	142.50	7.87	3.14	2.08	0.242
2.80	2.50	36.2	0.0	0.199	0.003	20.00	11.00	153.50	8.48	1.82	0.27	0.304
3.00	2.60	0.0	144.8	0.272	-0.076	128.05	16.75	170.25	9.41	7.64	-4.53	0.116
2.64	2.40	36.2	0.0	0.290	0.003	14.00	5.50	175.75	9.71	2.55	0.45	0.152
2.70	2.50	0.0	144.9	0.363	0.104	120.00	24.00	199.75	11.04	5.00	4.31	0.166
2.80	2.50	36.2	0.0	0.381	0.011	15.50	3.50	203.25	11.23	4.43	3.14	0.097
2.80	2.50	0.0	144.9	0.453	0.175	120.90	24.50	227.75	12.58	4.93	7.15	0.169
2.80	2.70	36.2	0.0	0.471	0.044	23.00	6.25	234.00	12.93	3.68	7.00	0.173
2.60	2.50	0.0	149.2	0.546	0.579	127.00	23.00	257.00	14.20	5.52	25.15	0.154
2.90	2.50	36.2	0.0	0.564	0.064	24.00	2.25	259.25	14.32	10.67	28.33	0.062
2.70	2.50	0.0	149.2	0.639	0.184	135.00	15.00	274.25	15.15	9.00	12.23	0.101
2.60	2.40	36.2	0.0	0.657	0.164	32.50	6.75	281.00	15.52	4.81	24.26	0.186
2.80	2.50	0.0	150.2	0.732	0.585	134.75	14.00	295.00	16.30	9.63	41.80	0.093
2.60	2.50	36.2	0.0	0.750	0.058	15.50	3.50	298.50	16.49	4.43	16.57	0.097
2.80	2.50	0.0	148.1	0.825	0.625	137.60	10.50	309.00	17.07	13.10	59.56	0.071
2.80	2.50	36.2	0.0	0.843	0.134	35.00	7.00	316.00	17.46	5.00	19.14	0.193

TABLE E40 (Cont'd)

Tabulated Experimental Results of Run H2D25

(20% HCPV CO_2 Injected at Water Rate @ 2.5 MPa (0.426 moles), 10 Slugs, 4:1 WAG, 21°C, Horizontal Injection)

Porosity (%) =	41.00	Vp (cm^3) =	1997	S_{wc} (%) =	9.36
Oil Viscosity (mPa.s) =	3606.6	S_{oi} (%) =	90.64	Molar Den. (kmol/m^3) =	0.04166
Ave. Run Temp.(K) =	294.15	HCPV (cm^3) =	1810	Abs. k (darcies) =	12.89
CO_2 Req. (sm^3/sm^3) =	9.42	CO_2 Ret. (%inj.) =	51.31	Ave. Flow Vel. (m/d) =	3.81

Press Inj. (MPa)	Press Prod. (MPa)	Gas Inj. (cm^3)	Water Inj. (cm^3)	Cum. PV Injected	Gas Prod (s.ltr)	Water Prod. (cm^3)	Oil Prod. (cm^3)	Cum. Oil Prod. (cm^3)	Percent Rec. (%)	WOR (sm^3/sm^3)	GOR (sm^3/sm^3)	OPFIR (sm^3/sm^3)
2.60	2.50	0.0	151.1	0.918	0.561	141.60	9.50	325.50	17.98	14.91	59.04	0.063
2.60	2.50	0.0	263.8	1.050	0.447	244.80	19.00	344.50	19.03	12.88	23.54	0.072
2.60	2.50	0.0	251.0	1.176	0.396	235.00	16.00	360.50	19.92	14.69	24.72	0.064
2.60	2.50	0.0	253.9	1.303	0.518	242.90	11.00	371.50	20.52	22.08	47.10	0.043
0.10	0.10	0.0	0.0	1.303	0.298	74.50	28.25	399.75	22.09	2.64	10.56	

TABLE E41

Tabulated Experimental Results of Run H2D26

(20% HCPV CO_2 Injected at 1/10 of Water Rate @ 1.0 MPa (0.087 moles), 10 Slugs, 4:1 WAG, 21°C, Horizontal Injection)

Porosity (%) = 36.05
Oil Viscosity (mPa.s) = 1058
Ave. Run Temp.(K) = 294.15
CO_2 Req. (sm^3/sm^3) = 4.70

Vp (cm^3) = 1756
S_{oi} (%) = 92.26
HCPV (cm^3) = 1620
CO_2 Ret. (%inj.) = 96.34

S_{wc} (%) = 7.74
Molar Den. ($kmol/m^3$) = 0.04166
Abs. k (darcies) = 22.03
Ave. Flow Vel. (m/d) = 2.6

Press Inj. (MPa)	Press Prod. (MPa)	Gas Inj. (cm^3)	Water Inj. (cm^3)	Cum. PV Injected	Gas Prod (s.ltr)	Water Prod. (cm^3)	Oil Prod. (cm^3)	Cum. Oil Prod. (cm^3)	Percent Rec. (%)	WOR (sm^3/sm^3)	GOR (sm^3/sm^3)	OPFIR (sm^3/sm^3)
1.10	1.00	32.4	0.0	0.018	0.002	0.00	7.50	7.50	0.46	0.00	0.00	0.232
1.10	1.00	0.0	129.9	0.092	0.000	0.00	118.10	125.60	7.75	0.00	0.00	0.909
1.10	1.00	32.4	0.0	0.111	0.002	0.00	9.60	135.20	8.35	0.00	0.00	0.296
1.10	1.00	0.0	129.7	0.185	0.016	26.00	97.00	232.20	14.33	0.27	0.00	0.748
1.10	1.00	32.4	0.0	0.203	0.000	4.00	7.00	239.20	14.77	0.57	0.00	0.216
1.10	1.00	0.0	129.7	0.277	0.006	68.00	53.00	292.20	18.04	1.28	0.00	0.409
1.10	1.00	32.4	0.0	0.295	-0.002	5.10	4.90	297.10	18.34	1.04	0.00	0.151
1.10	1.00	0.0	177.0	0.396	0.008	116.00	52.00	349.10	21.55	2.23	0.00	0.294
1.10	1.00	32.4	0.0	0.415	0.002	13.00	8.00	357.10	22.04	1.63	0.00	0.247
1.10	1.00	0.0	142.4	0.496	-0.002	95.00	30.00	387.10	23.90	3.17	0.00	0.211
1.10	1.00	32.4	0.0	0.514	0.003	2.50	3.10	390.20	24.09	0.81	0.00	0.096
1.10	1.00	0.0	130.5	0.589	0.000	99.50	26.00	416.20	25.69	3.83	0.00	0.199
1.10	1.00	32.4	0.0	0.607	0.001	8.00	5.50	421.70	26.03	1.45	0.00	0.170
1.10	1.00	0.0	129.7	0.681	0.001	102.00	17.00	438.70	27.08	6.00	0.00	0.131
1.10	1.00	32.4	0.0	0.699	0.001	8.00	4.50	443.20	27.36	1.78	0.00	0.139
1.10	1.00	0.0	133.8	0.775	0.000	109.00	16.50	459.70	28.38	6.61	0.00	0.123
1.10	1.00	32.4	0.0	0.794	0.002	10.00	6.00	465.70	28.75	1.67	0.00	0.185
1.10	1.00	0.0	129.7	0.868	0.004	102.00	14.00	479.70	29.61	7.29	0.00	0.108
1.10	1.00	32.4	0.0	0.886	0.002	9.00	4.00	483.70	29.86	2.25	0.00	0.123

TABLE E41 (Cont'd)

Tabulated Experimental Results of Run H2D26

(20% HCPV CO_2 Injected at 1/10 of Water Rate @ 1.0 MPa (0.087 moles), 10 Slugs, 4:1 WAG, 21°C, Horizontal Injection)

Porosity (%) = 36.05

Oil Viscosity (mPa.s) = 1058

Ave. Run Temp.(K) = 294.15

CO_2 Req. (sm^3/sm^3) = 4.70

Vp (cm^3) = 1756

S_{oi} (%) = 92.26

HCPV (cm^3) = 1620

CO_2 Ret. (%inj.) = 96.34

S_{wc} (%) = 7.74

Molar Den. ($kmol/m^3$) = 0.04166

Abs. k (darcies) = 22.03

Ave. Flow Vel. (m/d) = 2.6

Press Inj. (MPa)	Press Prod. (MPa)	Gas Inj. (cm^3)	Water Inj. (cm^3)	Cum. PV Injected	Gas Prod (s.ltr)	Water Prod. (cm^3)	Oil Prod. (cm^3)	Cum. Oil Prod. (cm^3)	Percent Rec. (%)	WOR (sm^3/sm^3)	GOR (sm^3/sm^3)	OPFIR (sm^3/sm^3)
1.10	1.00	0.0	129.8	0.960	0.001	107.00	13.00	496.70	30.66	8.23	0.00	0.100
1.10	1.00	0.0	249.9	1.102	0.006	222.00	27.00	523.70	32.33	8.22	0.20	0.108
1.10	1.00	0.0	250.3	1.245	0.007	223.00	27.00	550.70	33.99	8.26	0.24	0.108
1.10	1.00	0.0	250.5	1.388	0.010	225.00	25.00	575.70	35.54	9.00	0.40	0.100
1.10	1.00	0.0	250.5	1.530	0.011	226.50	24.00	599.70	37.02	9.44	0.44	0.096
1.10	1.00	0.0	259.0	1.678	0.005	236.00	24.00	623.70	38.50	9.83	0.21	0.093
1.10	1.00	0.0	249.9	1.820	0.007	230.50	19.50	643.20	39.70	11.82	0.36	0.078
1.10	1.00	0.0	250.3	1.963	0.006	230.00	20.00	663.20	40.94	11.50	0.30	0.080
1.10	1.00	0.0	251.5	2.106	0.001	240.00	12.50	675.70	41.71	19.20	0.04	0.050
1.10	1.00	0.0	280.2	2.265	0.001	261.50	21.00	696.70	43.01	12.45	0.02	0.075
0.10	0.10	0.0	0.0	2.265	0.027	114.00	20.00	716.70	44.24	5.70	1.33	

TABLE E42

Tabulated Experimental Results of Run H2D27

(20% HCPV CO_2 Injected at 1/5 of Water Rate @ 1.0 MPa (0.087 moles), 10 Slugs, 4:1 WAG, 21°C, Horizontal Injection)

Porosity (%) = 40.03
Oil Viscosity (mPa.s) = 1058
Ave. Run Temp.(K) = 294.15
CO_2 Req. (sm^3/sm^3) = 4.88

Vp (cm^3) = 1950
S_{oi} (%) = 91.11
HCPV (cm^3) = 1776.7
CO_2 Ret. (%inj.) = 96.87

S_{wc} (%) = 8.89
Molar Den. ($kmol/m^3$) = 0.04166
Abs. k (darcies) = 14.13
Ave. Flow Vel. (m/d) = 2.6

Press Inj. (MPa)	Press Prod. (MPa)	Gas Inj. (cm^3)	Water Inj. (cm^3)	Cum. PV Injected	Gas Prod (s.ltr)	Water Prod. (cm^3)	Oil Prod. (cm^3)	Cum. Oil Prod. (cm^3)	Percent Rec. (%)	WOR (sm^3/sm^3)	GOR (sm^3/sm^3)	OPFIR (sm^3/sm^3)
1.10	1.00	37.6	0.0	0.019	0.005	0.00	17.20	17.20	0.97	0.00	0.00	0.458
1.10	1.00	0.0	142.1	0.092	-0.001	0.00	121.00	138.20	7.78	0.00	0.00	0.851
1.10	1.00	35.6	0.0	0.110	0.003	0.00	15.50	153.70	8.65	0.00	0.00	0.436
1.10	1.00	0.0	142.4	0.183	0.006	34.00	95.50	249.20	14.03	0.36	0.00	0.671
1.10	1.00	36.3	0.0	0.202	-0.002	5.00	9.50	258.70	14.56	0.00	0.00	0.261
1.10	1.00	0.0	157.9	0.283	-0.002	72.00	76.00	334.70	18.84	0.95	0.00	0.481
1.10	1.00	53.4	0.0	0.310	0.003	4.00	8.00	342.70	19.29	0.00	0.00	0.150
1.10	1.00	0.0	142.2	0.383	0.000	80.00	51.20	393.90	22.17	1.56	0.00	0.360
1.10	1.00	35.6	0.0	0.402	-0.002	5.00	2.80	396.70	22.33	0.00	0.00	0.079
1.10	1.00	0.0	142.5	0.475	0.001	93.00	41.00	437.70	24.64	2.27	0.00	0.288
1.10	1.00	78.6	0.0	0.515	0.002	0.00	2.50	440.20	24.78	0.00	0.00	0.032
1.10	1.00	0.0	142.2	0.588	-0.008	107.00	40.00	480.20	27.03	2.68	0.00	0.281
1.10	1.00	36.4	0.0	0.607	-0.001	1.50	4.10	484.30	27.26	0.00	0.00	0.113
1.10	1.00	0.0	146.2	0.681	-0.002	131.00	14.00	498.30	28.05	9.36	0.00	0.096
1.10	1.00	36.4	0.0	0.700	0.001	26.00	3.00	501.30	28.22	0.00	0.00	0.082
1.10	1.00	0.0	143.8	0.774	0.003	116.00	14.00	515.30	29.00	8.29	0.00	0.097
1.10	1.00	35.8	0.0	0.792	-0.001	9.00	4.60	519.90	29.26	0.00	0.00	0.129
1.10	1.00	0.0	142.5	0.865	0.002	121.00	13.00	532.90	29.99	9.31	0.00	0.091
1.10	1.00	35.6	0.0	0.884	0.001	15.50	4.50	537.40	30.25	0.00	0.00	0.126

TABLE E42 (Cont'd)

Tabulated Experimental Results of Run H2D27

(20% HCPV CO_2 Injected at 1/5 of Water Rate @ 1.0 MPa (0.087 moles), 10 Slugs, 4:1 WAG, 21°C, Horizontal Injection)

Porosity (%) = 40.03
Oil Viscosity (mPa.s) = 1058
Ave. Run Temp.(K) = 294.15
CO_2 Req. (sm^3/sm^3) = 4.88
Vp (cm^3) = 1950
S_{oi} (%) = 91.11
HCPV (cm^3) = 1776.7
CO_2 Ret. (%inj.) = 96.87
S_{wc} (%) = 8.89
Molar Den. ($kmol/m^3$) = 0.04166
Abs. k (darcies) = 14.13
Ave. Flow Vel. (m/d) = 2.6

Press Inj. (MPa)	Press Prod. (MPa)	Gas Inj. (cm^3)	Water Inj. (cm^3)	Cum. PV Injected	Gas Prod (s.ltr)	Water Prod. (cm^3)	Oil Prod. (cm^3)	Cum. Oil Prod. (cm^3)	Percent Rec. (%)	WOR (sm^3/sm^3)	GOR (sm^3/sm^3)	OPFIR (sm^3/sm^3)
1.10	1.00	0.0	146.5	0.959	0.005	112.50	15.50	552.90	31.12	7.26	0.00	0.106
1.10	1.00	0.0	255.0	1.089	0.007	225.00	27.50	580.40	32.67	8.18	0.24	0.108
1.10	1.00	0.0	270.0	1.228	0.017	240.00	28.00	608.40	34.24	8.57	0.59	0.104
1.10	1.00	0.0	250.5	1.356	0.018	235.00	18.00	626.40	35.26	13.06	1.00	0.072
1.10	1.00	0.0	253.5	1.486	0.011	239.00	15.00	641.40	36.10	15.93	0.70	0.059
1.10	1.00	0.0	250.2	1.615	0.010	239.00	14.50	655.90	36.92	16.48	0.66	0.058
1.10	1.00	0.0	250.7	1.743	0.012	234.00	16.50	672.40	37.85	14.18	0.73	0.066
1.10	1.00	0.0	251.2	1.872	0.009	238.00	14.50	686.90	38.66	16.41	0.62	0.058
1.10	1.00	0.0	282.6	2.017	0.003	267.00	20.00	706.90	39.79	13.35	0.15	0.071
1.10	1.00	0.0	251.8	2.146	0.003	237.00	15.00	721.90	40.63	15.80	0.20	0.060
1.10	1.00	0.0	249.5	2.274	0.001	237.00	15.00	736.90	41.48	15.80	0.07	0.060
1.10	1.00	0.0	104.1	2.327	0.003	98.50	6.50	743.40	41.84	15.15	0.46	0.062
0.10	0.10	0.0	0.0	2.327	0.012	110.00	14.50	757.90	42.66	7.59	0.79	

TABLE E43

Tabulated Experimental Results of Run H2D28

(20% HCPV CO_2 Injected at Water Rate @ 1.0 MPa (0.087 moles), 10 Slugs, 4:1 WAG, 21°C, Horizontal Injection)

Porosity (%) = 42.10
Oil Viscosity (mPa.s) = 1058
Ave. Run Temp.(K) = 294.15
CO_2 Req. (sm^3/sm^3) = 4.05

Vp (cm^3) = 2050
S_{oi} (%) = 84.94
HCPV (cm^3) = 1741.3
CO_2 Ret. (%inj.) = 54.10

S_{wc} (%) = 15.06
Molar Den. ($kmol/m^3$) = 0.04166
Abs. k (darcies) = 14.52
Ave. Flow Vel. (m/d) = 2.6

Press Inj. (MPa)	Press Prod. (MPa)	Gas Inj. (cm^3)	Water Inj. (cm^3)	Cum. PV Injected	Gas Prod (s.ltr)	Water Prod. (cm^3)	Oil Prod. (cm^3)	Cum. Oil Prod. (cm^3)	Percent Rec. (%)	WOR (sm^3/sm^3)	GOR (sm^3/sm^3)	OPFIR (sm^3/sm^3)
1.10	1.00	43.7	0.0	0.021	0.000	0.00	1.00	1.00	0.06	0.00	0.00	0.023
1.10	1.00	0.0	137.8	0.089	0.000	0.00	138.00	139.00	7.98	0.00	0.00	1.001
1.10	1.00	33.6	0.0	0.105	0.000	0.00	19.00	158.00	9.07	0.00	0.00	0.565
1.10	1.00	0.0	139.3	0.173	0.000	8.00	118.50	276.50	15.88	0.07	0.00	0.851
1.10	1.00	33.6	0.0	0.189	0.001	7.00	11.90	288.40	16.56	0.59	0.08	0.354
1.10	1.00	0.0	139.4	0.257	0.002	55.00	64.50	352.90	20.27	0.85	0.03	0.463
1.10	1.00	33.6	0.0	0.274	0.002	8.00	7.10	360.00	20.67	1.13	0.28	0.211
1.10	1.00	0.0	139.3	0.342	0.000	67.50	60.50	420.50	24.15	1.12	0.00	0.434
1.10	1.00	33.6	0.0	0.358	0.001	13.00	5.50	426.00	24.46	2.36	0.18	0.164
1.10	1.00	0.0	139.4	0.426	0.001	80.00	45.00	471.00	27.05	1.78	0.02	0.323
1.10	1.00	33.6	0.0	0.442	0.001	11.50	3.00	474.00	27.22	3.83	0.33	0.089
1.10	1.00	0.0	139.3	0.510	0.001	88.00	40.00	514.00	29.52	2.20	0.03	0.287
1.10	1.00	33.6	0.0	0.527	0.002	14.00	4.50	518.50	29.78	3.11	0.44	0.134
1.10	1.00	0.0	139.3	0.595	0.003	99.00	33.50	552.00	31.70	2.96	0.09	0.240
1.10	1.00	33.6	0.0	0.611	0.000	11.00	2.00	554.00	31.82	5.50	0.00	0.060
1.10	1.00	0.0	139.4	0.679	0.008	105.00	19.00	573.00	32.91	5.53	0.42	0.136
1.10	1.00	33.6	0.0	0.695	0.003	12.00	2.50	575.50	33.05	4.80	1.20	0.074
1.10	1.00	0.0	139.3	0.763	0.027	112.00	20.00	595.50	34.20	5.60	1.35	0.144
1.10	1.00	33.6	0.0	0.780	0.009	18.00	2.00	597.50	34.31	9.00	4.50	0.060

TABLE E43 (Cont'd)

Tabulated Experimental Results of Run H2D28

(20% HCPV CO_2 Injected at Water Rate @ 1.0 MPa (0.087 moles), 10 Slugs, 4:1 WAG, 21°C, Horizontal Injection)

Porosity (%) = 42.10
Oil Viscosity (mPa.s) = 1058
Ave. Run Temp.(K) = 294.15
CO_2 Req. (sm^3/sm^3) = 4.05

Vp (cm^3) = 2050
S_{oi} (%) = 84.94
HCPV (cm^3) = 1741.3
CO_2 Ret. (%inj.) = 54.10

S_{wc} (%) = 15.06
Molar Den. ($kmol/m^3$) = 0.04166
Abs. k (darcies) = 14.52
Ave. Flow Vel. (m/d) = 2.6

Press Inj. (MPa)	Press Prod. (MPa)	Gas Inj. (cm^3)	Water Inj. (cm^3)	Cum. PV Injected	Gas Prod (s.ltr)	Water Prod. (cm^3)	Oil Prod. (cm^3)	Cum. Oil Prod. (cm^3)	Percent Rec. (%)	WOR (sm^3/sm^3)	GOR (sm^3/sm^3)	OPFIR (sm^3/sm^3)
1.10	1.00	0.0	139.6	0.848	0.064	100.00	24.00	621.50	35.69	4.17	2.67	0.172
1.10	1.00	0.0	140.5	0.916	0.091	122.00	14.50	636.00	36.52	8.41	6.28	0.103
1.10	1.00	0.0	231.0	1.029	0.173	201.00	33.00	669.00	38.42	6.09	5.24	0.143
1.10	1.00	0.0	229.2	1.141	0.179	203.00	26.00	695.00	39.91	7.81	6.88	0.113
1.10	1.00	0.0	213.9	1.245	0.173	199.00	17.00	712.00	40.89	11.71	10.18	0.079
1.10	1.00	0.0	239.2	1.362	0.158	221.00	19.00	731.00	41.98	11.63	8.32	0.079
1.10	1.00	0.0	251.6	1.485	0.144	242.00	13.00	744.00	42.73	18.62	11.08	0.052
1.10	1.00	0.0	218.1	1.591	0.101	218.00	15.50	759.50	43.62	14.06	6.52	0.071
1.10	1.00	0.0	473.3	1.822	0.121	444.00	35.00	794.50	45.63	12.69	3.46	0.074
1.10	1.00	0.0	491.9	2.062	0.118	467.00	30.00	824.50	47.35	15.57	3.93	0.061
1.10	1.00	0.0	459.7	2.286	0.104	441.00	22.00	846.50	48.61	20.05	4.73	0.048
1.10	1.00	0.0	160.4	2.364	0.016	159.00	5.00	851.50	48.90	31.80	3.20	0.031
0.10	0.10	0.0	0.0	2.364	0.160	48.00	42.00	893.50	51.31	1.14	3.81	

TABLE E44

Tabulated Experimental Results of Run H2D29

(20% HCPV CO_2 Injected at 2 of Water Rate @ 1.0 MPa (0.087 moles), 10 Slugs, 4:1 WAG, 21°C, Horizontal Injection)

Porosity (%) = 39.54
Oil Viscosity (mPa.s) = 1058
Ave. Run Temp.(K) = 294.15
CO_2 Req. (sm^3/sm^3) = 4.52

Vp (cm^3) = 1926
S_{oi} (%) = 90.34
HCPV (cm^3) = 1740
CO_2 Ret. (%inj.) = 90.67

S_{we} (%) = 9.66
Molar Den. ($kmol/m^3$) = 0.04166
Abs. k (darcies) = 16.61
Ave. Flow Vel. (m/d) = 2.6

Press Inj. (MPa)	Press Prod. (MPa)	Gas Inj. (cm^3)	Water Inj. (cm^3)	Cum. PV Injected	Gas Prod (s.ltr)	Water Prod. (cm^3)	Oil Prod. (cm^3)	Cum. Oil Prod. (cm^3)	Percent Rec. (%)	WOR (sm^3/sm^3)	GOR (sm^3/sm^3)	OPFIR (sm^3/sm^3)
1.10	1.00	34.8	0.0	0.018	0.001	0.00	8.10	8.10	0.47	0.00	0.00	0.233
1.10	1.00	0.0	139.2	0.090	0.005	0.00	126.00	134.10	7.71	0.00	0.04	0.905
1.10	1.00	34.8	0.0	0.108	-0.001	0.00	9.00	143.10	8.22	0.00	0.00	0.259
1.10	1.00	0.0	139.3	0.181	-0.003	21.00	113.00	256.10	14.72	0.19	0.00	0.811
1.10	1.00	34.8	0.0	0.199	0.001	2.00	9.50	265.60	15.26	0.00	0.00	0.273
1.10	1.00	0.0	139.3	0.271	-0.002	56.00	75.00	340.60	19.57	0.75	0.00	0.539
1.10	1.00	34.8	0.0	0.289	0.002	10.50	11.50	352.10	20.24	0.00	0.00	0.330
1.10	1.00	0.0	139.3	0.361	-0.004	64.00	50.50	402.60	23.14	1.27	0.00	0.363
1.10	1.00	34.8	0.0	0.380	0.001	4.00	6.00	408.60	23.48	0.00	0.00	0.172
1.10	1.00	0.0	139.3	0.452	-0.006	84.00	48.50	457.10	26.27	1.73	0.00	0.348
1.10	1.00	34.8	0.0	0.470	0.001	5.00	7.00	464.10	26.67	0.00	0.00	0.201
1.10	1.00	0.0	140.7	0.543	0.001	101.00	34.00	498.10	28.63	2.97	0.00	0.242
1.10	1.00	34.8	0.0	0.561	0.001	11.00	4.50	502.60	28.89	0.00	0.00	0.129
1.10	1.00	0.0	144.5	0.636	0.006	95.00	30.00	532.60	30.61	3.17	0.00	0.208
1.10	1.00	34.8	0.0	0.654	-0.002	19.00	6.00	538.60	30.95	0.00	0.00	0.172
1.10	1.00	0.0	147.1	0.731	0.002	102.00	23.00	561.60	32.28	4.43	0.00	0.156
1.10	1.00	34.8	0.0	0.749	0.001	19.00	7.00	568.60	32.68	0.00	0.00	0.201
1.10	1.00	0.0	139.2	0.821	0.004	96.00	22.00	590.60	33.94	4.36	0.00	0.158
1.10	1.00	34.8	0.0	0.839	0.002	14.00	5.50	596.10	34.26	0.00	0.00	0.158

TABLE E44 (Cont'd)

Tabulated Experimental Results of Run H2D29

(20% HCPV CO_2 Injected at 2 of Water Rate @ 1.0 MPa (0.087 moles), 10 Slugs, 4:1 WAG, 21°C, Horizontal Injection)

Porosity (%) = 39.54
Oil Viscosity (mPa.s) = 1058
Ave. Run Temp.(K) = 294.15
CO_2 Req. (sm^3/sm^3) = 4.52

Vp (cm^3) = 1926
S_{oi} (%) = 90.34
HCPV (cm^3) = 1740
CO_2 Ret. (%inj.) = 90.67

S_{wc} (%) = 9.66
Molar Den. ($kmol/m^3$) = 0.04166
Abs. k (darcies) = 16.61
Ave. Flow Vel. (m/d) = 2.6

Press Inj. (MPa)	Press Prod. (MPa)	Gas Inj. (cm^3)	Water Inj. (cm^3)	Cum. PV Injected	Gas Prod (s.ltr)	Water Prod. (cm^3)	Oil Prod. (cm^3)	Cum. Oil Prod. (cm^3)	Percent Rec. (%)	WOR (sm^3/sm^3)	GOR (sm^3/sm^3)	OPFIR (sm^3/sm^3)
1.10	1.00	0.0	139.3	0.911	0.013	99.00	21.00	617.10	35.47	4.71	0.00	0.151
1.10	1.00	0.0	250.7	1.041	0.034	224.00	30.00	647.10	37.19	7.47	1.13	0.120
1.10	1.00	0.0	266.7	1.180	0.074	243.00	22.00	669.10	38.45	11.05	3.36	0.083
1.10	1.00	0.0	250.4	1.310	0.071	233.00	22.00	691.10	39.72	10.59	3.23	0.088
1.10	1.00	0.0	259.4	1.445	0.053	241.50	20.50	711.60	40.90	11.78	2.59	0.079
1.10	1.00	0.0	254.9	1.577	0.035	237.00	16.00	727.60	41.82	14.81	2.16	0.063
1.10	1.00	0.0	264.0	1.714	0.026	235.00	15.00	742.60	42.68	15.67	1.73	0.057
1.10	1.00	0.0	492.5	1.970	0.006	475.00	22.00	764.60	43.94	21.59	0.27	0.045
1.10	1.00	0.0	497.5	2.228	0.012	485.00	25.00	789.60	45.38	19.40	0.48	0.050
0.10	0.10	0.0	0.0	2.228	0.007	33.00	12.00	801.60	46.07	2.75	0.58	

TABLE E45

Tabulated Experimental Results of Run H2D30

(20% HCPV CO_2 Injected at 5 of Water Rate @ 1.0 MPa (0.087 moles), 10 Slugs, 4:1 WAG, 21°C, Horizontal Injection)

Porosity (%) =	40.60	Vp (cm^3) =	1977	S_{wc} (%) =	9.05
Oil Viscosity (mPa.s) =	1058	S_{oi} (%) =	90.95	Molar Den. (kmol/m^3) =	0.04166
Ave. Run Temp.(K) =	294.15	HCPV (cm^3) =	1798	Abs. k (darcies) =	13.31
CO_2 Req. (sm^3/sm^3) =	4.46	CO_2 Ret. (%inj.) =	81.88	Ave. Flow Vel. (m/d) =	0.831

Press Inj. (MPa)	Press Prod. (MPa)	Gas Inj. (cm^3)	Water Inj. (cm^3)	Cum. PV Injected	Gas Prod (s.ltr)	Water Prod. (cm^3)	Oil Prod. (cm^3)	Cum. Oil Prod. (cm^3)	Percent Rec. (%)	WOR (sm^3/sm^3)	GOR (sm^3/sm^3)	OPFIR (sm^3/sm^3)
1.10	1.00	36.0	0.0	0.018	0.000	0.00	5.00	5.00	0.28	0.00	0.00	0.139
1.10	1.00	0.0	143.9	0.091	0.010	0.00	135.00	140.00	7.79	0.00	0.07	0.938
1.10	1.00	36.0	0.0	0.109	0.000	0.00	11.00	151.00	8.40	0.00	0.00	0.306
1.10	1.00	0.0	143.9	0.182	0.005	12.00	122.00	273.00	15.18	0.10	0.04	0.848
1.10	1.00	36.0	0.0	0.200	0.000	2.50	14.50	287.50	15.99	0.17	0.00	0.403
1.10	1.00	0.0	143.9	0.273	0.000	46.00	93.00	380.50	21.16	0.49	0.00	0.646
1.10	1.00	36.0	0.0	0.291	0.000	3.00	8.00	388.50	21.61	0.38	0.00	0.222
1.10	1.00	0.0	145.5	0.365	0.000	90.00	53.00	441.50	24.56	1.70	0.00	0.364
1.10	1.00	36.0	0.0	0.383	0.000	10.50	6.50	448.00	24.92	1.62	0.00	0.181
1.10	1.00	0.0	143.9	0.456	0.000	92.00	45.00	493.00	27.42	2.04	0.00	0.313
1.10	1.00	36.0	0.0	0.474	0.000	10.60	4.40	497.40	27.66	2.41	0.00	0.122
1.10	1.00	0.0	143.9	0.547	0.252	78.00	38.00	535.40	29.78	2.05	6.63	0.264
1.10	1.00	36.0	0.0	0.565	0.025	8.00	2.50	537.90	29.92	3.20	10.00	0.070
1.10	1.00	0.0	143.9	0.638	0.011	110.00	30.00	567.90	31.59	3.67	0.35	0.208
1.10	1.00	36.0	0.0	0.656	0.000	13.00	4.60	572.50	31.84	2.83	0.00	0.128
1.10	1.00	0.0	145.6	0.729	0.017	109.00	30.50	603.00	33.54	3.57	0.54	0.209
1.10	1.00	36.0	0.0	0.748	0.021	16.00	3.00	606.00	33.70	5.33	7.00	0.083
1.10	1.00	0.0	134.9	0.816	0.260	84.00	25.50	631.50	35.12	3.29	10.20	0.189
1.10	1.00	36.0	0.0	0.834	0.055	17.00	3.50	635.00	35.32	4.86	15.71	0.097

TABLE E45 (Cont'd)

Tabulated Experimental Results of Run H2D30

(20% HCPV CO_2 Injected at 5 of Water Rate @ 1.0 MPa (0.087 moles), 10 Slugs, 4:1 WAG, 21°C, Horizontal Injection)

Porosity (%) = 40.60
Oil Viscosity (mPa.s) = 1058
Ave. Run Temp.(K) = 294.15
CO_2 Req. (sm^3/sm^3) = 4.46
Vp (cm^3) = 1977
S_{oi} (%) = 90.95
HCPV (cm^3) = 1798
CO_2 Ret. (%inj.) = 81.88
S_{wc} (%) = 9.05
Molar Den. ($kmol/m^3$) = 0.04166
Abs. k (darcies) = 13.31
Ave. Flow Vel. (m/d) = 0.831

Press Inj. (MPa)	Press Prod. (MPa)	Gas Inj. (cm^3)	Water Inj. (cm^3)	Cum. PV Injected	Gas Prod (s.ltr)	Water Prod. (cm^3)	Oil Prod. (cm^3)	Cum. Oil Prod. (cm^3)	Percent Rec. (%)	WOR (sm^3/sm^3)	GOR (sm^3/sm^3)	OPFIR (sm^3/sm^3)
1.10	1.00	0.0	277.1	0.974	0.023	229.00	30.00	665.00	36.99	7.63	0.77	0.108
1.10	1.00	0.0	254.3	1.103	0.000	224.00	25.00	690.00	38.38	8.96	0.00	0.098
1.10	1.00	0.0	256.6	1.233	0.000	234.00	23.50	713.50	39.68	9.96	0.00	0.092
1.10	1.00	0.0	498.4	1.485	0.000	460.00	42.50	756.00	42.05	10.82	0.00	0.085
1.10	1.00	0.0	494.9	1.735	0.000	467.50	32.50	788.50	43.85	14.38	0.00	0.066
1.10	1.00	0.0	494.3	1.985	0.000	475.00	25.00	813.50	45.24	19.00	0.00	0.051
1.10	1.00	0.0	252.1	2.113	0.000	243.00	10.00	823.50	45.80	24.30	0.00	0.040
0.10	0.10	0.0	0.0	2.113	0.000	74.00	15.50	839.00	46.66	4.77	0.00	

TABLE E46

Tabulated Experimental Results of Run H2D31

(20% HCPV CO_2 Injected at Water Rate @ 1.0 MPa (0.087 moles), 10 Slugs, 4:1 WAG, 21°C, Horizontal Injection)

Porosity (%) =	41.37	Vp (cm^3) =	2015	S_{wc} (%) =	13.58
Oil Viscosity (mPa.s) =	1058	S_{oi} (%) =	86.42	Molar Den. (kmol/m^3) =	0.04166
Ave. Run Temp.(K) =	294.15	HCPV (cm^3) =	1741.3	Abs. k (darcies) =	13.25
CO_2 Req. (sm^3/sm^3) =	4.49	CO_2 Ret. (%inj.) =	43.97	Ave. Flow Vel. (m/d) =	1.29

Press Inj. (MPa)	Press Prod. (MPa)	Gas Inj. (cm^3)	Water Inj. (cm^3)	Cum. PV Injected	Gas Prod (s.ltr)	Water Prod. (cm^3)	Oil Prod. (cm^3)	Cum. Oil Prod. (cm^3)	Percent Rec. (%)	WOR (sm^3/sm^3)	GOR (sm^3/sm^3)	OPFIR (sm^3/sm^3)
1.10	1.00	31.9	0.0	0.017	0.000	0.00	23.95	23.95	1.35	0.00	0.00	0.751
1.10	1.00	0.0	142.0	0.094	0.000	0.00	125.00	148.95	8.40	0.00	0.00	0.880
1.10	1.00	31.9	0.0	0.111	0.000	0.00	25.50	174.45	9.84	0.00	0.00	0.799
1.10	1.00	0.0	141.8	0.188	0.000	17.00	105.00	279.45	15.77	0.16	0.00	0.740
1.10	1.00	32.7	0.0	0.206	0.000	11.20	13.90	293.35	16.55	0.81	0.00	0.425
1.10	1.00	0.0	141.8	0.282	0.000	57.25	58.95	352.30	19.88	0.97	0.00	0.416
1.10	1.00	31.9	0.0	0.299	0.000	20.75	7.35	359.65	20.29	2.82	0.00	0.230
1.10	1.00	0.0	141.8	0.376	0.000	87.50	33.00	392.65	22.15	2.65	0.00	0.233
1.10	1.00	31.9	0.0	0.393	0.000	20.40	6.10	398.75	22.50	3.34	0.00	0.191
1.10	1.00	0.0	141.8	0.470	0.000	83.50	50.50	449.25	25.35	1.65	0.00	0.356
1.10	1.00	31.9	0.0	0.487	0.000	16.00	5.00	454.25	25.63	3.20	0.00	0.157
1.10	1.00	0.0	141.8	0.564	0.000	74.50	34.50	488.75	27.58	2.16	0.00	0.243
1.10	1.00	31.9	0.0	0.581	0.001	26.00	8.00	496.75	28.03	3.25	0.13	0.251
1.10	1.00	0.0	142.3	0.658	0.014	109.75	30.45	527.20	29.75	3.60	0.46	0.214
1.10	1.00	31.9	0.0	0.675	0.003	13.90	0.85	528.05	29.79	16.35	3.53	0.027
1.10	1.00	0.0	148.5	0.756	0.021	94.50	18.00	546.05	30.81	5.25	1.17	0.121
1.10	1.00	31.9	0.0	0.773	0.016	33.00	6.90	552.95	31.20	4.78	2.32	0.216
1.10	1.00	0.0	141.7	0.849	0.069	101.00	15.00	567.95	32.05	6.73	4.60	0.106
1.10	1.00	31.9	0.0	0.867	0.019	27.00	3.50	571.45	32.24	7.71	5.43	0.110

TABLE E46 (Cont'd)

Tabulated Experimental Results of Run H2D31

(20% HCPV CO_2 Injected at Water Rate @ 1.0 MPa (0.087 moles), 10 Slugs, 4:1 WAG, 21°C, Horizontal Injection)

Porosity (%) = 42.10
Oil Viscosity (mPa.s) = 1058
Ave. Run Temp.(K) = 294.15
CO_2 Req. (sm^3/sm^3) = 4.49

Vp (cm^3) = 2050
S_{oi} (%) = 84.94
HCPV (cm^3) = 1741.3
CO_2 Ret. (%inj.) = 43.97

S_{wc} (%) = 13.55
Molar Den. ($kmol/m^3$) = 0.04166
Abs. k (darcies) = 14.52
Ave. Flow Vel. (m/d) = 1.29

Press Inj. (MPa)	Press Prod. (MPa)	Gas Inj. (cm^3)	Water Inj. (cm^3)	Cum. PV Injected	Gas Prod (s.ltr)	Water Prod. (cm^3)	Oil Prod. (cm^3)	Cum. Oil Prod. (cm^3)	Percent Rec. (%)	WOR (sm^3/sm^3)	GOR (sm^3/sm^3)	OPFIR (sm^3/sm^3)
1.10	1.00	0.0	141.8	0.943	0.095	88.00	24.20	595.65	33.61	3.64	3.93	0.171
1.10	1.00	0.0	117.7	1.007	0.150	91.00	29.00	624.65	35.25	3.14	5.17	0.246
1.10	1.00	0.0	229.7	1.131	0.368	195.00	51.20	675.85	38.13	3.81	7.19	0.223
1.10	1.00	0.0	264.1	1.274	0.414	216.00	26.00	701.85	39.60	8.31	15.92	0.098
1.10	1.00	0.0	243.6	1.406	0.253	206.50	21.60	723.45	40.82	9.56	11.71	0.089
1.10	1.00	0.0	251.0	1.541	0.151	227.00	21.00	744.45	42.00	10.81	7.19	0.084
1.10	1.00	0.0	194.7	1.646	0.067	181.50	19.50	763.95	43.11	9.31	3.44	0.100
0.10	0.10	0.0	0.0	1.646	0.425	104.00	58.00	821.95	46.38	1.79	7.33	

TABLE C47

Tabulated Experimental Results of Run H2D32

(20% HCPV CO_2 Injected at Water Rate @ 1.0 MPa (0.087 moles), 10 Slugs, 4:1 WAG, 21°C, Horizontal Injection)

Porosity (%) = 40.60
Oil Viscosity (mPa.s) = 1058
Ave. Run Temp.(K) = 294.15
CO_2 Req. (sm^3/sm^3) = 4.81

V_p (cm^3) = 1977
S_{oi} (%) = 91.33
HCPV (cm^3) = 1805.6
CO_2 Ret. (%inj.) = 65.72

S_{wc} (%) = 8.67
Molar Den. ($kmol/m^3$) = 0.04166
Abs. k (darcies) = 13.31
Ave. Flow Vel. (m/d) = 0.831

Press Inj. (MPa)	Press Prod. (MPa)	Gas Inj. (cm^3)	Water Inj. (cm^3)	Cum. PV Injected	Gas Prod (s.ltr)	Water Prod. (cm^3)	Oil Prod. (cm^3)	Cum. Oil Prod. (cm^3)	Percent Rec. (%)	WOR (sm^3/sm^3)	GOR (sm^3/sm^3)	OPFIR (sm^3/sm^3)
1.10	1.00	36.1	0.0	0.018	0.000	0.00	0.20	0.20	0.01	0.00	0.00	0.006
1.10	1.00	0.0	144.5	0.091	0.029	0.00	130.00	130.20	7.21	0.00	0.22	0.900
1.10	1.00	36.1	0.0	0.110	0.000	0.00	20.00	150.20	8.32	0.00	0.00	0.554
1.10	1.00	0.0	144.5	0.183	0.012	30.00	107.90	258.10	14.29	0.28	0.11	0.747
1.10	1.00	36.1	0.0	0.201	0.000	7.00	12.50	270.60	14.99	0.56	0.00	0.346
1.10	1.00	0.0	144.4	0.274	0.016	67.10	66.90	337.50	18.69	1.00	0.24	0.463
1.10	1.00	36.1	0.0	0.292	0.000	6.00	5.85	343.35	19.02	1.03	0.00	0.162
1.10	1.00	0.0	144.5	0.365	0.005	89.90	44.10	387.45	21.46	2.04	0.11	0.305
1.10	1.00	36.1	0.0	0.384	0.000	11.65	5.60	393.05	21.77	2.08	0.00	0.155
1.10	1.00	0.0	144.4	0.457	0.002	95.75	36.25	429.30	23.78	2.64	0.06	0.251
1.10	1.00	36.1	0.0	0.475	0.000	9.70	10.50	439.80	24.36	0.92	0.00	0.291
1.10	1.00	0.0	144.7	0.548	0.006	105.90	29.40	469.20	25.99	3.60	0.20	0.203
1.10	1.00	36.1	0.0	0.566	0.000	20.00	6.85	476.05	26.37	2.92	0.00	0.190
1.10	1.00	0.0	144.5	0.639	0.064	97.70	21.00	497.05	27.53	4.65	3.05	0.145
1.10	1.00	36.1	0.0	0.658	0.007	22.90	12.30	509.35	28.21	1.86	0.57	0.341
1.10	1.00	0.0	144.2	0.731	0.028	96.00	17.90	527.25	29.20	5.36	1.56	0.124
1.10	1.00	36.1	0.0	0.749	0.003	24.10	5.55	532.80	29.51	4.34	0.54	0.154
1.10	1.00	0.0	144.4	0.822	0.000	109.60	16.80	549.60	30.44	6.52	0.00	0.116
1.10	1.00	36.1	0.0	0.840	0.000	20.50	4.50	554.10	30.69	4.56	0.00	0.125

TABLE E47 (Cont'd)

Tabulated Experimental Results of Run H2D32

(20% HCPV CO_2 Injected at Water Rate @ 1.0 MPa (0.087 moles), 10 Slugs, 4:1 WAG, 21°C, Horizontal Injection)

Porosity (%) = 40.60
Oil Viscosity (mPa.s) = 1058
Ave. Run Temp.(K) = 294.15
CO_2 Req. (sm^3/sm^3) = 4.81

V_p (cm^3) = 1977
S_{oi} (%) = 91.33
HCPV (cm^3) = 1805.6
CO_2 Ret. (%inj.) = 65.72

S_{wc} (%) = 8.67
Molar Den. ($kmol/m^3$) = 0.04166
Abs. k (darcies) = 13.31
Ave. Flow Vel. (m/d) = 0.831

Press Inj. (MPa)	Press Prod. (MPa)	Gas Inj. (cm^3)	Water Inj. (cm^3)	Cum. PV Injected	Gas Prod (s.ltr)	Water Prod. (cm^3)	Oil Prod. (cm^3)	Cum. Oil Prod. (cm^3)	Percent Rec. (%)	WOR (sm^3/sm^3)	GOR (sm^3/sm^3)	OPFIR (sm^3/sm^3)
1.10	1.00	0.0	146.0	0.914	0.076	109.20	14.80	568.90	31.51	7.38	5.14	0.101
1.10	1.00	0.0	161.3	0.996	0.000	145.10	18.75	587.65	32.55	7.74	0.00	0.116
1.10	1.00	0.0	175.9	1.085	0.000	160.00	18.80	606.45	33.59	8.51	0.00	0.107
1.10	1.00	0.0	268.9	1.221	0.000	246.30	25.70	632.15	35.01	9.58	0.00	0.096
1.10	1.00	0.0	314.6	1.380	0.053	287.10	27.40	659.55	36.53	10.48	1.93	0.087
1.10	1.00	0.0	301.0	1.532	0.160	280.10	23.80	683.35	37.85	11.77	6.72	0.079
1.10	1.00	0.0	365.7	1.717	0.226	342.20	25.10	708.45	39.24	13.63	9.00	0.069
1.10	1.00	0.0	181.6	1.809	0.055	172.20	10.70	719.15	39.83	16.09	5.14	0.059
1.10	1.00	0.0	315.4	1.968	0.101	299.40	17.00	736.15	40.77	17.61	5.94	0.054
1.10	1.00	0.0	294.9	2.118	0.110	280.40	14.50	750.65	41.57	19.34	7.59	0.049
0.10	0.10	0.0	0.0	2.118	0.335	85.00	31.10	781.75	43.30	2.73	10.77	

TABLE E48

Tabulated Experimental Results of Run H2D33

(20% HCPV CO_2 Injected at Water Rate @ 1.0 MPa (0.144 moles), 10 Slugs, 4:1 WAG, 21°C, Horizontal Injection)

Porosity (%) = 38.50
Oil Viscosity (mPa.s) = 1058
Ave. Run Temp.(K) = 294.15
CO_2 Req. (sm^3/sm^3) = 6.32
V_p (cm^3) = 1874
S_{oi} (%) = 89.20
HCPV (cm^3) = 1671.6
CO_2 Ret. (%inj.) = 75.36
S_{wc} (%) = 10.80
Molar Den. ($kmol/m^3$) = 0.04166
Abs. k (darcies) = 12.46
Ave. Flow Vel. (m/d) = 2.076

Press Inj. (MPa)	Press Prod. (MPa)	Gas Inj. (cm^3)	Water Inj. (cm^3)	Cum. PV Injected	Gas Prod (s.ltr)	Water Prod. (cm^3)	Oil Prod. (cm^3)	Cum. Oil Prod. (cm^3)	Percent Rec. (%)	WOR (sm^3/sm^3)	GOR (sm^3/sm^3)	OPFIR (sm^3/sm^3)
1.30	1.00	33.4	0.0	0.018	0.001	0.00	10.00	10.00	0.60	0.00	0.10	0.299
1.20	1.00	0.0	133.7	0.089	0.012	0.00	122.00	132.00	7.90	0.00	0.10	0.912
1.30	1.00	33.4	0.0	0.107	0.001	0.00	12.00	144.00	8.61	0.00	0.08	0.359
1.20	1.00	0.0	133.7	0.178	0.000	20.00	87.00	231.00	13.82	0.23	0.00	0.651
1.20	1.00	33.4	0.0	0.196	0.008	8.00	14.00	245.00	14.66	0.57	0.57	0.419
1.20	1.00	0.0	133.7	0.268	0.142	50.00	61.00	306.00	18.31	0.82	2.33	0.456
1.20	1.00	33.4	0.0	0.285	0.000	2.00	3.00	309.00	18.49	0.67	0.00	0.090
1.20	1.00	0.0	133.8	0.357	0.022	90.00	40.00	349.00	20.88	2.25	0.55	0.299
1.20	1.00	33.4	0.0	0.375	0.001	7.00	3.00	352.00	21.06	2.33	0.33	0.090
1.20	1.00	0.0	133.8	0.446	0.010	96.00	28.00	380.00	22.73	3.43	0.36	0.209
1.20	1.00	33.4	0.0	0.464	0.000	25.00	11.00	391.00	23.39	2.27	0.00	0.329
1.20	1.00	0.0	133.7	0.535	0.034	86.00	23.00	414.00	24.77	3.74	1.48	0.172
1.10	1.00	33.4	0.0	0.553	0.009	16.00	5.00	419.00	25.07	3.20	1.80	0.150
1.10	1.00	0.0	133.7	0.624	0.032	94.00	20.00	439.00	26.26	4.70	1.60	0.150
1.20	1.00	33.4	0.0	0.642	0.001	6.00	3.00	442.00	26.44	2.00	0.33	0.090
1.10	1.00	0.0	133.7	0.713	0.022	112.00	18.00	460.00	27.52	6.22	1.22	0.135
1.10	1.00	33.4	0.0	0.731	0.005	27.00	5.00	465.00	27.82	5.40	1.00	0.150
1.10	1.00	0.0	133.7	0.803	0.056	86.00	13.00	478.00	28.60	6.62	4.31	0.097
1.10	1.00	33.4	0.0	0.820	0.016	27.50	4.00	482.00	28.83	6.88	4.00	0.120

TABLE C48 (Cont'd)

Tabulated Experimental Results of Run H2D33

(20% HCPV CO_2 Injected at Water Rate @ 1.0 MPa (0.144 moles), 10 Slugs, 4:1 WAG, 21°C, Horizontal Injection)

Porosity (%) = 38.50
Oil Viscosity (mPa.s) = 1058
Ave. Run Temp.(K) = 294.15
CO_2 Req. (sm^3/sm^3) = 6.32

V_p (cm^3) = 1874
S_{oi} (%) = 89.20
HCPV (cm^3) = 1671.6
CO_2 Ret. (%inj.) = 75.36

S_{wc} (%) = 10.80
Molar Den. ($kmol/m^3$) = 0.04166
Abs. k (darcies) = 12.46
Ave. Flow Vel. (m/d) = 2.076

Press Inj. (MPa)	Press Prod. (MPa)	Gas Inj. (cm^3)	Water Inj. (cm^3)	Cum. PV Injected	Gas Prod (s.ltr)	Water Prod. (cm^3)	Oil Prod. (cm^3)	Cum. Oil Prod. (cm^3)	Percent Rec. (%)	WOR (sm^3/sm^3)	GOR (sm^3/sm^3)	OPFIR (sm^3/sm^3)
1.10	1.00	0.0	133.7	0.892	0.069	90.00	14.00	496.00	29.67	6.43	4.93	0.105
1.10	1.00	0.0	246.3	1.023	0.155	224.00	20.00	516.00	30.87	11.20	7.75	0.081
1.10	1.00	0.0	246.3	1.155	0.098	228.00	14.00	530.00	31.71	16.29	7.00	0.057
1.10	1.00	0.0	241.9	1.284	0.090	234.00	6.00	536.00	32.07	39.00	15.00	0.025
0.10	0.10	0.0	0.0	1.284	0.073	92.00	14.00	550.00	32.90	6.57	5.21	

TABLE E49

Tabulated Experimental Results of Run H2D34

(5% HCPV CO_2 Injected at Water Rate @ 2.5 MPa (0.104 moles), 21°C, Single Slug, immediate Water Injection, Horizontal Injection)

Porosity (%) = 39.21
Oil Viscosity (mPa.s) = 1058.0
Ave. Run Temp.(K) = 294.15
CO_2 Req. (sm^3/sm^3) = 5.54

V_p (cm^3) = 1910
S_{oi} (%) = 90.58
HCPV (cm^3) = 1730
CO_2 Ret. (%inj.) = 98.86

S_{wc} (%) = 9.42
Molar Den. ($kmol/m^3$) = 0.04166
Abs. k (darcies) = 14.12
Ave. Flow Vel. (m/d) = 2.54

Press Inj. (MPa)	Press Prod. (MPa)	Gas Inj. (cm^3)	Water Inj. (cm^3)	Cum. PV Injected	Gas Prod (s.ltr)	Water Prod. (cm^3)	Oil Prod. (cm^3)	Cum. Oil Prod. (cm^3)	Percent Rec. (%)	WOR (sm^3/sm^3)	GOR (sm^3/sm^3)	OPFIR (sm^3/sm^3)
2.80	2.50	86.5	0.0	0.045	0.004	0.00	29.50	29.50	1.71	0.00	0.12	0.341
2.80	2.50	0.0	269.9	0.187	0.016	7.00	243.00	272.50	15.75	0.03	0.06	0.900
2.80	2.40	0.0	256.7	0.321	-0.003	129.00	128.50	401.00	23.18	0.00	-0.02	0.501
2.70	2.50	0.0	275.8	0.465	-0.006	204.00	69.50	470.50	27.20	2.94	-0.08	0.252
2.60	2.50	0.0	274.0	0.609	0.003	234.50	31.50	502.00	29.02	7.44	0.10	0.115
2.70	2.60	0.0	241.0	0.735	0.017	228.00	19.00	521.00	30.12	12.00	0.89	0.079
2.80	2.40	0.0	252.6	0.867	0.013	228.00	27.00	548.00	31.68	8.44	0.48	0.107
2.70	2.50	0.0	239.8	0.993	0.011	214.00	30.00	578.00	33.41	7.13	0.35	0.125
2.80	2.50	0.0	248.6	1.123	0.014	230.50	19.50	597.50	34.54	11.82	0.69	0.078
2.80	2.50	0.0	245.1	1.251	0.005	240.00	7.50	605.00	34.97	32.00	0.60	0.031
2.80	2.70	0.0	272.0	1.394	-0.008	259.00	23.00	628.00	36.30	11.26	-0.35	0.085
0.10	0.10	0.0	0.0	1.394	0.050	122.00	22.00	650.00	37.57	5.55	2.27	

TABLE E50

Tabulated Experimental Results of Run H2D35

(5% HCPV CO_2 Injected at Water Rate @ 2.5 MPa (0.103 moles), 21°C, Single Slug, After 3 Days Water Injected, Horizontal Injection)

Porosity (%) = 38.49
Oil Viscosity (mPa.s) = 1058.0
Ave. Run Temp.(K) = 294.15
CO_2 Req. (sm^3/sm^3) = 5.46

V_p (cm^3) = 1875
S_{oi} (%) = 91.57
HCPV (cm^3) = 1717
CO_2 Ret. (%inj.) = 99.30

S_{wc} (%) = 8.43
Molar Den. (kmol/m^3) = 0.04166
Abs. k (darcies) = 13.98
Ave. Flow Vel. (m/d) = 3.17

Press Inj. (MPa)	Press Prod. (MPa)	Gas Inj. (cm^3)	Water Inj. (cm^3)	Cum. PV Injected	Gas Prod (s.ltr)	Water Prod. (cm^3)	Oil Prod. (cm^3)	Cum. Oil Prod. (cm^3)	Percent Rec. (%)	WOR (sm^3/sm^3)	GOR (sm^3/sm^3)	OPFIR (sm^3/sm^3)
2.60	2.50	85.9	0.0	0.046	0.002	0.00	25.50	25.50	1.49	0.00	0.09	0.297
2.80	2.50	0.0	288.1	0.199	0.042	12.00	245.50	271.00	15.78	0.05	0.17	0.852
2.80	2.40	0.0	244.3	0.330	0.000	62.00	127.00	398.00	23.18	0.00	0.00	0.520
2.70	2.50	0.0	240.9	0.458	0.005	138.50	65.50	463.50	26.99	2.11	0.08	0.272
2.60	2.50	0.0	248.3	0.591	0.000	188.50	33.00	496.50	28.92	5.71	0.00	0.133
2.70	2.60	0.0	244.0	0.721	0.000	202.00	26.00	522.50	30.43	7.77	0.00	0.107
2.80	2.40	0.0	249.4	0.854	0.009	211.00	28.00	550.50	32.06	7.54	0.33	0.112
2.70	2.50	0.0	255.6	0.990	0.003	228.50	22.50	573.00	33.37	10.16	0.13	0.088
2.80	2.50	0.0	245.2	1.121	0.001	225.50	13.50	586.50	34.16	16.70	0.07	0.055
2.80	2.50	0.0	247.7	1.253	0.000	226.00	11.00	597.50	34.80	20.55	0.02	0.044
2.80	2.70	0.0	244.5	1.383	0.000	231.80	8.20	605.70	35.28	28.27	0.00	0.034
2.60	2.50	0.0	248.1	1.516	0.000	233.00	8.00	613.70	35.74	29.13	0.00	0.032
2.90	2.50	0.0	293.0	1.672	0.000	274.00	12.00	625.70	36.44	22.83	0.00	0.041
0.10	0.10	0.0	0.0	1.672	0.027	97.00	28.00	653.70	38.07	3.46	0.96	

TABLE E51

Tabulated Experimental Results of Run H2D36

(5% HCPV CO_2 Injected at Water Rate @ 2.5 MPa (0.104 moles), 21°C, Single Slug, After 4.83 Days Water Injected, Horizontal Injection)

Porosity (%) =	38.55	V_p (cm^3) =	1877.7	S_{wc} (%) =	8.29
Oil Viscosity (mPa.s) =	1058.0	S_{oi} (%) =	91.71	Molar Den. (kmol/m^3) =	0.04166
Ave. Run Temp.(K) =	294.15	HCPV (cm^3) =	1722	Abs. k (darcies) =	10.65
CO_2 Req. (sm^3/sm^3) =	5.75	CO_2 Ret. (%inj.) =	97.42	Ave. Flow Vel. (m/d) =	2.54

Press Inj. (MPa)	Press Prod. (MPa)	Gas Inj. (cm^3)	Water Inj. (cm^3)	Cum. PV Injected	Gas Prod (s.ltr)	Water Prod. (cm^3)	Oil Prod. (cm^3)	Cum. Oil Prod. (cm^3)	Percent Rec. (%)	WOR (sm^3/sm^3)	GOR (sm^3/sm^3)	OPFIR (sm^3/sm^3)
2.60	2.50	86.1	0.0	0.046	0.000	0.00	21.50	21.50	1.25	0.00	0.00	0.250
3.10	2.50	0.0	258.2	0.183	0.059	24.00	216.50	238.00	13.82	0.11	0.27	0.839
2.80	2.50	0.0	239.4	0.311	0.019	121.00	117.00	355.00	20.62	0.00	0.16	0.489
2.60	2.40	0.0	249.9	0.444	0.015	187.00	64.00	419.00	24.33	2.92	0.23	0.256
2.62	2.50	0.0	244.2	0.574	0.017	202.00	42.00	461.00	26.77	4.81	0.40	0.172
2.60	2.50	0.0	249.3	0.707	0.021	223.00	32.00	493.00	28.63	6.97	0.64	0.128
2.70	2.60	0.0	248.4	0.839	0.012	225.00	23.20	516.20	29.98	9.70	0.51	0.093
2.60	2.50	0.0	246.9	0.971	0.013	232.00	17.00	533.20	30.96	13.65	0.76	0.069
2.60	2.50	0.0	245.7	1.101	0.010	236.00	12.50	545.70	31.69	18.88	0.76	0.051
2.60	2.50	0.0	255.0	1.237	0.013	240.00	12.00	557.70	32.39	20.00	1.04	0.047
2.50	2.30	0.0	245.8	1.368	0.007	240.00	11.00	568.70	33.03	21.82	0.59	0.045
2.40	2.30	0.0	248.9	1.501	0.004	242.00	9.50	578.20	33.58	25.47	0.37	0.038
0.10	0.10	0.0	0.0	1.501	0.071	168.00	45.00	623.20	36.19	3.73	1.58	

TABLE E52

Tabulated Experimental Results of Run H2D37

(5% HCPV CO_2 Injected at Water Rate @ 2.5 MPa (0.104 moles), 21°C, Single Slug, After 10 Days Water Injected, Horizontal Injection)

Porosity (%) =	39.36	V_p (cm^3) =	1917	S_{wc} (%) =	10.90
Oil Viscosity (mPa.s) =	1058.0	S_{oi} (%) =	89.10	Molar Den. (kmol/m^3) =	0.04166
Ave. Run Temp.(K) =	294.15	HCPV (cm^3) =	1708	Abs. k (darcies) =	11.29
CO_2 Req. (sm^3/sm^3) =	5.41	CO_2 Ret. (%inj.) =	99.02	Ave. Flow Vel. (m/d) =	2.54

Press Inj. (MPa)	Press Prod. (MPa)	Gas Inj. (cm^3)	Water Inj. (cm^3)	Cum. PV Injected	Gas Prod (s.ltr)	Water Prod. (cm^3)	Oil Prod. (cm^3)	Cum. Oil Prod. (cm^3)	Percent Rec. (%)	WOR (sm^3/sm^3)	GOR (sm^3/sm^3)	OPFIR (sm^3/sm^3)
2.60	2.50	85.4	0.0	0.045	0.002	0.00	28.50	28.50	1.67	0.00	0.08	0.334
2.80	2.50	0.0	277.1	0.189	0.074	14.00	227.00	255.50	14.96	0.06	0.33	0.819
2.80	2.40	0.0	236.2	0.312	-0.006	66.00	120.00	375.50	21.98	0.00	-0.05	0.508
2.70	2.50	0.0	238.8	0.437	-0.020	132.00	67.00	442.50	25.91	1.97	-0.29	0.281
2.60	2.50	0.0	253.2	0.569	-0.009	189.00	40.00	482.50	28.25	4.73	-0.21	0.158
2.70	2.60	0.0	249.9	0.699	0.011	196.00	43.00	525.50	30.77	4.56	0.26	0.172
2.80	2.40	0.0	278.0	0.844	0.014	227.00	41.00	566.50	33.17	5.54	0.33	0.147
2.70	2.50	0.0	272.9	0.987	0.015	237.00	36.00	602.50	35.28	6.58	0.42	0.132
2.80	2.50	0.0	249.9	1.117	0.003	225.50	21.75	624.25	36.55	10.37	0.14	0.087
2.80	2.50	0.0	253.2	1.249	0.001	238.00	12.00	636.25	37.25	19.83	0.06	0.047
2.80	2.70	0.0	253.7	1.381	0.007	240.00	10.00	646.25	37.84	24.00	0.65	0.039
0.10	0.10	0.0	0.0	1.381	0.005	61.00	11.00	657.25	38.48	5.55	0.45	

TABLE E53

Tabulated Experimental Results of Run V2D1

(5% HCPV CO_2 Injected @ Bottom@ 2.5 MPa (0.102 moles), 21°C, Water Injection at Bottom

Porosity (%) = 39.40
Oil Viscosity (mPa.s) = 1058.0
Ave. Run Temp.(K) = 294.15
CO_2 Req. (sm^3/sm^3) = 2.42

V_p (cm^3) = 1917
S_{oi} (%) = 88.68
HCPV (cm^3) = 1700
CO_2 Ret. (%inj.) = 55.02

S_{wc} (%) = 11.32
Molar Den. ($kmol/m^3$) = 0.04166
Abs. k (darcies) = 11.29
Ave. Flow Vel. (m/d) = 3.17

Press Inj. (MPa)	Press Prod. (MPa)	Gas Inj. (cm^3)	Water Inj. (cm^3)	Cum. PV Injected	Gas Prod (s.ltr)	Water Prod. (cm^3)	Oil Prod. (cm^3)	Cum. Oil Prod. (cm^3)	Percent Rec. (%)	WOR (sm^3/sm^3)	GOR (sm^3/sm^3)	OPFIR (sm^3/sm^3)
2.60	2.50	85.0	0.0	0.044	0.226	0.00	24.50	24.50	1.44	0.00	9.20	0.288
2.80	2.50	0.0	276.6	0.189	0.050	140.00	101.00	125.50	7.38	1.39	0.50	0.365
2.80	2.40	0.0	252.5	0.320	0.015	186.00	66.00	191.50	11.26	0.00	0.22	0.261
2.70	2.50	0.0	252.7	0.452	0.022	129.00	140.00	331.50	19.50	0.92	0.16	0.554
2.60	2.50	0.0	244.3	0.580	0.020	160.00	78.00	409.50	24.09	2.05	0.26	0.319
2.70	2.60	0.0	266.3	0.718	0.023	209.00	44.50	454.00	26.71	4.70	0.51	0.167
2.80	2.40	0.0	224.7	0.836	0.020	205.00	39.00	493.00	29.00	5.26	0.51	0.174
2.70	2.50	0.0	245.4	0.964	0.034	218.00	30.50	523.50	30.79	7.15	1.10	0.124
2.80	2.50	0.0	232.0	1.085	0.014	219.00	29.50	553.00	32.53	7.42	0.46	0.127
2.80	2.50	0.0	231.6	1.205	0.024	209.00	41.00	594.00	34.94	5.10	0.59	0.177
2.80	2.50	0.0	236.6	1.329	0.021	230.00	28.00	622.00	36.59	8.21	0.75	0.118
2.80	2.50	0.0	490.7	1.585	0.019	225.00	23.50	645.50	37.97	9.57	0.81	0.048
2.80	2.50	0.0	218.6	1.699	0.018	224.00	24.00	669.50	39.38	9.33	0.75	0.110
2.80	2.50	0.0	261.0	1.835	0.023	235.00	27.00	696.50	40.97	8.70	0.85	0.103
2.80	2.50	0.0	226.7	1.953	0.014	230.00	20.00	716.50	42.15	11.50	0.70	0.088
2.80	2.50	0.0	239.7	2.078	0.011	230.00	20.00	736.50	43.32	11.50	0.55	0.083
2.80	2.50	0.0	244.8	2.206	0.013	232.00	15.50	752.00	44.24	14.97	0.81	0.063
0.10	0.10	0.0	0.0	2.206	0.320	62.00	59.00	811.00	47.71	1.05	5.42	

TABLE E54

Tabulated Experimental Results of Run V2D2

(5% HCPV N_2 Injected @ Bottom @ 2.5 MPa (0.075 moles), 10 Slugs, 21°C, Water Injection at Bottom)

Porosity (%) = 40.38
Oil Viscosity (mPa.s) = 1058.0
Ave. Run Temp.(K) = 294.15
CO_2 Req. (sm^3/sm^3) = 3.42
V_p (cm^3) = 1967
S_{oi} (%) = 89.93
HCPV (cm3) = 1769
CO_2 Ret. (%inj.) = 20.80
S_{wc} (%) = 10.07
Molar Den. ($kmol/m^3$) = 0.04142004
Abs. k (darcies) = 11.99
Ave. Flow Vel. (m/d) = 2.6

Press Inj. (MPa)	Press Prod. (MPa)	Gas Inj. (cm^3)	Water Inj. (cm^3)	Cum. PV Injected	Gas Prod (s.ltr)	Water Prod. (cm^3)	Oil Prod. (cm^3)	Cum. Oil Prod. (cm^3)	Percent Rec. (%)	WOR (sm^3/sm^3)	GOR (sm^3/sm^3)	OPFIR (sm^3/sm^3)
2.60	2.50	88.5	0.0	0.045	0.382	0.00	23.34	23.34	1.32	0.00	16.35	0.264
2.80	2.50	0.0	256.6	0.175	0.686	150.00	98.01	121.35	6.86	1.53	7.00	0.382
2.80	2.40	0.0	249.5	0.302	0.345	186.00	65.31	186.66	10.55	0.00	5.29	0.262
2.70	2.50	0.0	239.7	0.424	0.160	191.00	50.40	237.06	13.40	3.79	3.17	0.210
2.60	2.50	0.0	251.3	0.552	0.055	203.50	48.95	286.01	16.17	4.16	1.11	0.195
2.70	2.60	0.0	268.3	0.688	0.068	212.50	57.91	343.92	19.44	3.67	1.17	0.216
2.80	2.40	0.0	233.7	0.807	0.055	185.70	48.96	392.88	22.21	3.79	1.12	0.210
2.70	2.50	0.0	261.4	0.940	0.045	222.00	45.29	438.17	24.77	4.90	0.99	0.173
2.80	2.50	0.0	236.9	1.060	0.024	213.80	24.15	462.32	26.13	8.85	1.00	0.102
2.80	2.50	0.0	241.6	1.183	0.031	215.00	29.66	491.98	27.81	7.25	1.04	0.123
2.80	2.50	0.0	247.6	1.309	0.020	237.00	11.84	503.82	28.48	20.02	1.70	0.048
2.80	2.50	0.0	487.7	1.557	0.078	429.00	60.82	564.64	31.92	7.05	1.28	0.125
2.80	2.50	0.0	252.3	1.685	0.003	230.00	23.14	587.78	33.23	9.94	0.12	0.092
2.80	2.50	0.0	277.3	1.826	0.047	245.00	33.27	621.05	35.11	7.36	1.40	0.120
2.80	2.50	0.0	232.1	1.944	0.013	223.50	8.60	629.65	35.59	25.99	1.56	0.037
0.10	0.10	0.0	0.0	1.944	0.027	62.00	12.00	641.65	36.27	5.17	2.25	
0.10	0.10	0.0	0.0	2.128	0.047	4.00	24.00	721.00	41.80	0.17	1.96	

TABLE E55

Tabulated Experimental Results of Run H2D38

(20% HCPV CO_2 Injected at Water Rate @ 2.5 MPa (0.372moles), 10 Slugs, 4:1 WAG, 37°C, Horizontal Injection)

Porosity (%) =	38.92	V_p (cm^3) =	1896	S_{wc} (%) =	11.39
Oil Viscosity (mPa.s) =	1058.0	S_{oi} (%) =	88.61	Molar Den. (kmol/m^3) =	0.0011067
Ave. Run Temp.(K) =	294.15	HCPV (cm^3) =	1680	Abs. k (darcies) =	12.24
CO_2 Req. (sm^3/sm^3) =	9.68	CO_2 Ret. (%inj.) =	44.24	Ave. Flow Vel. (m/d) =	2.54

Press Inj. (MPa)	Press Prod. (MPa)	Gas Inj. (cm^3)	Water Inj. (cm^3)	Cum. PV Injected	Gas Prod (s.ltr)	Water Prod. (cm^3)	Oil Prod. (cm^3)	Cum. Oil Prod. (cm^3)	Percent Rec. (%)	WOR (sm^3/sm^3)	GOR (sm^3/sm^3)	OPFIR (sm^3/sm^3)
2.90	2.50	30.9	0.0	0.016	0.000	0.00	17.25	17.25	1.03	0.00	0.00	0.559
2.60	2.50	0.0	134.4	0.087	0.000	0.00	111.00	128.25	7.63	0.00	0.00	0.826
3.00	2.90	30.9	0.0	0.103	0.000	0.00	24.50	152.75	9.09	0.00	0.00	0.793
2.60	2.50	0.0	134.4	0.174	0.000	12.50	101.00	253.75	15.10	0.12	0.00	0.751
3.10	3.00	30.9	0.0	0.191	0.000	2.50	12.25	266.00	15.83	0.20	0.00	0.397
2.60	2.50	0.0	134.9	0.262	0.000	36.00	66.00	332.00	19.76	0.55	0.00	0.489
2.60	2.50	30.9	0.0	0.278	0.000	8.00	7.75	339.75	20.22	1.03	0.00	0.251
3.60	3.50	0.0	134.5	0.349	0.000	56.00	55.00	394.75	23.50	1.02	0.00	0.409
3.40	3.30	30.9	0.0	0.365	0.000	18.50	12.75	407.50	24.26	1.45	0.00	0.413
2.60	2.50	0.0	133.9	0.436	0.000	76.00	64.00	471.50	28.07	1.19	0.00	0.478
2.60	2.50	30.9	0.0	0.452	0.000	16.50	9.50	481.00	28.63	1.74	0.00	0.308
2.70	2.50	0.0	133.8	0.523	0.104	50.00	37.00	518.00	30.83	1.35	2.81	0.276
2.50	2.40	30.9	0.0	0.539	0.017	13.50	7.50	525.50	31.28	1.80	2.27	0.243
2.60	2.40	0.0	144.8	0.615	0.172	73.00	39.00	564.50	33.60	1.87	4.41	0.269
2.75	2.70	30.9	0.0	0.632	0.002	0.00	0.50	565.00	33.63	0.00	4.00	0.016
3.10	3.00	0.0	116.7	0.693	0.400	81.00	37.00	602.00	35.83	2.19	10.81	0.317
2.50	2.40	37.4	0.0	0.713	0.136	24.25	10.00	612.00	36.43	2.43	13.58	0.267
2.10	2.00	0.0	136.4	0.785	0.714	86.00	32.50	644.50	38.36	2.65	21.95	0.238
2.70	2.60	37.4	0.0	0.805	0.037	7.00	2.00	646.50	38.48	3.50	18.50	0.053

TABLE E55 (Cont'd)

Tabulated Experimental Results of Run H2D4158

(20% HCPV CO_2 Injected at Water Rate @ 2.5 MPa (0.372moles), 10 Slugs, 4:1 WAG, 37°C, Horizontal Injection)

Porosity (%) = 38.92
Oil Viscosity (mPa.s) = 1058.0
Ave. Run Temp.(K) = 294.15
CO_2 Req. (sm^3/sm^3) = 9.68

V_p (cm^3) = 1896
S_{oi} (%) = 88.61
HCPV (cm^3) = 1680
CO_2 Ret. (%inj.) = 44.24

S_{we} (%) = 11.39
Molar Den. ($kmol/m^3$) = 0.0011067
Abs. k (darcies) = 12.24
Ave. Flow Vel. (m/d) = 2.54

Press Inj. (MPa)	Press Prod. (MPa)	Gas Inj. (cm^3)	Water Inj. (cm^3)	Cum. PV Injected	Gas Prod (s.ltr)	Water Prod. (cm^3)	Oil Prod. (cm^3)	Cum. Oil Prod. (cm^3)	Percent Rec. (%)	WOR (sm^3/sm^3)	GOR (sm^3/sm^3)	OPFIR (sm^3/sm^3)
2.65	2.60	0.0	135.0	0.876	0.503	96.00	26.00	672.50	40.03	3.69	19.35	0.193
2.60	2.50	0.0	266.3	1.016	0.679	229.00	29.50	702.00	41.79	7.76	23.00	0.111
2.50	2.42	0.0	242.8	1.144	0.585	224.00	24.00	726.00	43.21	9.33	24.38	0.099
2.64	2.57	0.0	101.5	1.198	0.169	94.40	7.60	733.60	43.67	12.42	22.24	0.075
2.48	2.40	0.0	97.5	1.249	0.155	92.50	7.50	741.10	44.11	12.33	20.67	0.077
2.50	2.40	0.0	105.8	1.305	0.143	95.50	8.50	749.60	44.62	11.24	16.82	0.080
2.60	2.50	0.0	103.2	1.360	0.131	94.00	8.50	758.10	45.13	11.06	15.35	0.082
2.60	2.50	0.0	119.1	1.422	0.112	100.50	7.40	765.50	45.57	13.58	15.15	0.062
2.60	2.50	0.0	95.3	1.473	0.097	93.00	9.00	774.50	46.10	10.33	10.78	0.094
2.60	2.50	0.0	270.1	1.615	0.189	244.00	21.00	795.50	47.35	11.62	9.00	0.078
2.60	2.50	0.0	242.5	1.743	0.137	230.00	23.75	819.25	48.76	9.68	5.78	0.098
2.60	2.50	0.0	248.3	1.874	0.108	230.00	22.50	841.75	50.10	10.22	4.78	0.091
2.60	2.50	0.0	106.0	1.930	0.040	95.00	5.25	847.00	50.42	18.10	7.57	0.050
2.60	2.50	0.0	91.2	1.978	0.035	93.80	5.20	852.20	50.73	18.04	6.73	0.057
2.60	2.50	0.0	102.2	2.032	0.029	95.70	5.80	858.00	51.07	16.50	4.91	0.057
2.55	2.50	0.0	94.2	2.082	0.020	94.00	6.00	864.00	51.43	15.67	3.33	0.064
0.10	0.10	0.0	0.0	2.082	0.265	170.00	58.00	922.00	54.88	2.93	4.57	

TABLE E56

Tabulated Experimental Results of Run H2D39

(20% HCPV CO_2 Injected at Water Rate @ 2.5 MPa (0.354 moles), 10 Slugs, 4:1 WAG, 37°C, Horizontal Injection)

Porosity (%) =	37.65	V_p (cm^3) =	1834	S_{wc} (%) =	12.87
Oil Viscosity (mPa.s) =	5200.0	S_{oi} (%) =	87.13	Molar Den. (kmol/m^3) =	0.04166
Ave. Run Temp.(K) =	294.15	HCPV (cm^3) =	1598	Abs. k (darcies) =	4.35
CO_2 Req. (sm^3/sm^3) =	12.94	CO_2 Ret. (%inj.) =	54.97	Ave. Flow Vel. (m/d) =	2.54

Press Inj. (MPa)	Press Prod. (MPa)	Gas Inj. (cm^3)	Water Inj. (cm^3)	Cum. PV Injected	Gas Prod (s.ltr)	Water Prod. (cm^3)	Oil Prod. (cm^3)	Cum. Oil Prod. (cm^3)	Percent Rec. (%)	WOR (sm^3/sm^3)	GOR (sm^3/sm^3)	OPFIR (sm^3/sm^3)
2.80	2.50	27.0	0.0	0.015	0.000	0.00	3.50	3.50	0.22	0.00	0.00	0.130
3.40	2.50	0.0	127.8	0.084	0.080	0.00	109.00	112.50	7.04	0.00	0.73	0.853
3.00	2.90	27.0	0.0	0.099	0.006	0.00	9.50	122.00	7.63	0.00	0.58	0.352
3.00	2.50	0.0	127.9	0.169	0.020	44.00	71.50	193.50	12.11	0.62	0.28	0.559
3.10	2.50	27.0	0.0	0.184	0.004	7.50	6.00	199.50	12.48	1.25	0.58	0.222
3.20	2.50	0.0	127.9	0.253	0.019	66.50	48.00	247.50	15.49	1.39	0.40	0.375
2.90	2.50	27.0	0.0	0.268	0.004	10.00	6.50	254.00	15.89	1.54	0.54	0.241
3.00	2.00	0.0	128.4	0.338	0.052	74.00	40.00	294.00	18.40	1.85	1.29	0.312
3.00	2.50	27.0	0.0	0.353	0.007	6.00	2.50	296.50	18.55	2.40	2.60	0.093
2.60	2.50	0.0	128.3	0.423	0.127	74.50	13.75	310.25	19.41	5.42	9.25	0.107
2.60	2.50	27.0	0.0	0.437	0.029	15.00	6.00	316.25	19.79	2.50	4.83	0.222
2.70	2.50	0.0	127.9	0.507	0.146	88.00	29.00	345.25	21.61	3.03	5.03	0.227
2.80	2.70	27.0	0.0	0.522	0.020	9.00	5.00	350.25	21.92	1.80	4.00	0.185
2.60	2.40	0.0	127.8	0.592	0.156	86.00	27.00	377.25	23.61	3.19	5.76	0.211
3.00	2.80	27.0	0.0	0.606	0.036	11.50	4.20	381.45	23.87	2.74	8.64	0.156
3.10	3.00	0.0	127.8	0.676	0.233	88.00	22.00	403.45	25.25	4.00	10.57	0.172
2.90	2.50	27.0	0.0	0.691	0.038	13.50	3.50	406.95	25.47	3.86	10.86	0.130
2.90	2.50	0.0	127.9	0.761	0.244	95.00	17.00	423.95	26.53	5.59	14.35	0.133
2.90	2.80	35.0	0.0	0.780	0.061	20.50	4.25	428.20	26.80	4.82	14.41	0.121

TABLE E56 (Cont'd)

Tabulated Experimental Results of Run H2D39

(20% HCPV CO_2 Injected at Water Rate @ 2.5 MPa (0.354 moles), 10 Slugs, 4:1 WAG, 37°C, Horizontal Injection)

Porosity (%) =	37.65	V_p (cm^3) =	1834	S_{wc} (%) =	12.87
Oil Viscosity (mPa.s) =	5200.0	S_{oi} (%) =	87.13	Molar Den. (kmol/m^3) =	0.04166
Ave. Run Temp.(K) =	294.15	HCPV (cm^3) =	1598	Abs. k (darcies) =	4.35
CO_2 Req. (sm^3/sm^3) =	12.94	CO_2 Ret. (%inj.) =	54.97	Ave. Flow Vel. (m/d) =	2.54

Press Inj. (MPa)	Press Prod. (MPa)	Gas Inj. (cm^3)	Water Inj. (cm^3)	Cum. PV Injected	Gas Prod (s.ltr)	Water Prod. (cm^3)	Oil Prod. (cm^3)	Cum. Oil Prod. (cm^3)	Percent Rec. (%)	WOR (sm^3/sm^3)	GOR (sm^3/sm^3)	OPFIR (sm^3/sm^3)
2.70	2.50	0.0	127.9	0.849	0.341	86.00	15.75	443.95	27.78	5.46	21.63	0.123
2.60	2.40	0.0	251.9	0.987	0.690	220.00	32.00	475.95	29.78	6.88	21.56	0.127
2.50	2.42	0.0	257.7	1.127	0.293	222.00	24.00	499.95	31.29	9.25	12.21	0.093
2.64	2.57	0.0	249.6	1.263	0.246	222.00	22.00	521.95	32.66	10.09	11.16	0.088
2.80	2.70	0.0	244.2	1.396	0.184	230.50	24.00	545.95	34.16	9.60	7.65	0.098
2.50	2.40	0.0	268.3	1.543	0.152	240.00	19.50	565.45	35.38	12.31	7.79	0.073
2.42	2.38	0.0	240.3	1.674	0.120	235.00	12.00	577.45	36.14	19.58	10.00	0.050
2.50	2.40	0.0	253.3	1.812	0.082	226.00	20.00	597.45	37.39	11.30	4.10	0.079
2.50	2.40	0.0	255.9	1.951	0.061	244.00	14.00	611.45	38.26	17.43	4.36	0.055
2.50	2.40	0.0	252.5	2.089	0.045	237.50	11.50	622.95	38.98	20.65	3.87	0.046
0.10	0.10	0.0	0.0	2.089	0.331	129.00	33.00	655.95	41.05	3.91	10.03	

TABLE E57

Tabulated Experimental Results of Run H2D40

(20% HCPV CO_2 Injected at Water Rate @ 3.14 MPa (0.354 moles), 10 Slugs, 4:1 WAG, 37°C, Horizontal Injection)

Porosity (%) = 37.57
Oil Viscosity (mPa.s) = 5200.0
Ave. Run Temp.(K) = 294.15
CO_2 Req. (sm^3/sm^3) = 15.91

V_p (cm^3) = 1830
S_{oi} (%) = 86.89
HCPV (cm^3) = 1590
CO_2 Ret. (%inj.) = 52.01

S_{wc} (%) = 13.11
Molar Den. ($kmol/m^3$) = 1.45E-03
Abs. k (darcies) = 3.23
Ave. Flow Vel. (m/d) = 2.54

Press Inj. (MPa)	Press Prod. (MPa)	Gas Inj. (cm^3)	Water Inj. (cm^3)	Cum. PV Injected	Gas Prod (s.ltr)	Water Prod. (cm^3)	Oil Prod. (cm^3)	Cum. Oil Prod. (cm^3)	Percent Rec. (%)	WOR (sm^3/sm^3)	GOR (sm^3/sm^3)	OPFIR (sm^3/sm^3)
3.34	3.14	31.8	0.0	0.017	0.002	4.00	5.25	5.25	0.33	0.00	0.33	0.165
4.80	3.14	0.0	129.0	0.088	0.059	5.00	95.00	100.25	6.31	0.05	0.62	0.736
3.64	2.80	31.8	0.0	0.105	0.009	0.00	18.75	119.00	7.48	0.00	0.46	0.590
3.00	3.14	0.0	127.3	0.175	0.022	30.00	79.00	198.00	12.45	0.38	0.27	0.620
3.10	3.14	31.8	0.0	0.192	0.003	6.50	9.00	207.00	13.02	0.76	0.35	0.283
3.38	3.14	0.0	127.5	0.262	0.039	66.50	64.00	271.00	17.04	1.96	0.62	0.502
3.38	3.14	31.8	0.0	0.279	0.006	17.00	9.50	280.50	17.64	1.79	0.58	0.299
3.32	3.14	0.0	127.3	0.349	0.041	69.00	54.00	334.50	21.04	2.09	0.77	0.424
3.54	3.14	31.8	0.0	0.366	0.011	13.00	6.00	340.50	21.42	2.17	1.83	0.189
3.24	3.14	0.0	127.2	0.436	0.115	79.00	41.00	381.50	23.99	2.72	2.83	0.322
3.20	3.14	31.8	0.0	0.453	0.021	16.00	5.00	386.50	24.31	2.56	4.12	0.157
3.58	3.14	0.0	125.2	0.522	0.097	78.00	17.00	403.50	25.38	3.00	5.69	0.136
3.38	3.14	31.8	0.0	0.539	0.029	12.00	5.25	408.75	25.71	2.29	5.48	0.165
3.28	3.14	0.0	127.3	0.608	0.148	87.00	18.00	426.75	26.84	3.48	8.20	0.141
3.18	3.14	31.8	0.0	0.626	0.025	7.00	3.00	429.75	27.03	2.33	8.33	0.094
3.24	3.14	0.0	123.6	0.693	0.194	89.00	17.00	446.75	28.10	4.14	11.42	0.138
3.30	3.14	31.8	0.0	0.711	0.041	13.00	3.75	450.50	28.33	3.47	11.00	0.118
3.18	3.14	0.0	128.9	0.781	0.293	96.00	15.00	465.50	29.28	6.40	19.80	0.116
3.16	3.14	31.8	0.0	0.799	0.048	9.50	8.50	474.00	29.81	1.12	5.65	0.267

TABLE E57 (Cont'd)

Tabulated Experimental Results of Run H2D40

(20% HCPV CO_2 Injected at Water Rate @ 3.14 MPa (0.354 moles), 10 Slugs, 4:1 WAG, 37°C, Horizontal Injection)

Porosity (%) = 37.57
Oil Viscosity (mPa.s) = 5200.0
Ave. Run Temp.(K) = 294.15
CO_2 Req. (sm^3/sm^3) = 15.91

V_p (cm^3) = 1830
S_{oi} (%) = 86.89
HCPV (cm^3) = 1590
CO_2 Ret. (%inj.) = 52.01

S_{wc} (%) = 13.11
Molar Den. ($kmol/m^3$) = 1.45E-03
Abs. k (darcies) = 3.23
Ave. Flow Vel. (m/d) = 2.54

Press Inj. (MPa)	Press Prod. (MPa)	Gas Inj. (cm^3)	Water Inj. (cm^3)	Cum. PV Injected	Gas Prod (s.ltr)	Water Prod. (cm^3)	Oil Prod. (cm^3)	Cum. Oil Prod. (cm^3)	Percent Rec. (%)	WOR (sm^3/sm^3)	GOR (sm^3/sm^3)	OPFIR (sm^3/sm^3)
3.26	3.10	0.0	127.2	0.868	0.297	89.50	15.00	489.00	30.75	5.97	19.77	0.118
3.20	3.17	0.0	266.0	1.013	0.539	201.00	24.00	513.00	32.26	8.38	22.63	0.090
3.25	3.14	0.0	271.3	1.162	0.730	226.00	19.00	532.00	33.46	11.89	38.39	0.070
3.40	3.20	0.0	248.6	1.298	0.505	228.00	16.00	548.00	34.47	14.25	31.53	0.064
3.40	3.35	0.0	269.4	1.445	0.328	247.00	13.00	561.00	35.28	19.00	25.19	0.048
3.22	3.14	0.0	244.4	1.578	0.345	231.00	15.00	576.00	36.23	15.40	23.17	0.061
3.30	3.14	0.0	251.3	1.716	0.239	236.00	13.00	589.00	37.04	18.15	18.38	0.052
3.22	3.20	0.0	247.6	1.851	0.189	234.00	13.00	602.00	37.86	18.00	14.54	0.053
3.22	3.14	0.0	243.9	1.984	0.143	232.00	12.00	614.00	38.62	19.33	11.92	0.049
3.18	3.14	0.0	252.3	2.122	0.126	240.00	12.00	626.00	39.37	20.00	10.25	0.048
3.20	3.14	0.0	246.8	2.257	0.088	242.00	11.00	637.00	40.06	22.00	7.73	0.045
3.20	3.14	0.0	245.6	2.391	0.066	243.00	10.00	647.00	40.69	24.30	6.30	0.041
0.10	0.10	0.0	0.0	2.391	0.513	185.00	48.00	695.00	43.71	3.85	10.65	

TABLE E58

Tabulated Experimental Results of Run H2D41

(10% HCPV CO_2 Injected at Water Rate @ 2.5 MPa (0.177 moles), 10 Slugs, 4:1 WAG, 37°C, Horizontal Injection)

Porosity (%) = 37.55
Oil Viscosity (mPa.s) = 5200.0
Ave. Run Temp.(K) = 294.15
CO_2 Req. (sm^3/sm^3) = 8.83

V_p (cm^3) = 1829
S_{oi} (%) = 86.93
HCPV (cm^3) = 1590
CO_2 Ret. (%inj.) = 59.15

S_{wc} (%) = 13.07
Molar Den. ($kmol/m^3$) = 1.11E-03
Abs. k (darcies) = 3.9[illegible]
Ave. Flow Vel. (m/d) = 2.54

Press Inj. (MPa)	Press Prod. (MPa)	Gas Inj. (cm^3)	Water Inj. (cm^3)	Cum. PV Injected	Gas Prod (s.ltr)	Water Prod. (cm^3)	Oil Prod. (cm^3)	Cum. Oil Prod. (cm^3)	Percent Rec. (%)	WOR (sm^3/sm^3)	GOR (sm^3/sm^3)	OPFIR (sm^3/sm^3)
3.10	2.50	16.0	0.0	0.009	0.001	0.00	9.00	9.00	0.57	0.00	0.11	0.563
3.20	2.50	0.0	63.8	0.044	0.053	0.00	43.25	52.25	3.29	0.00	1.22	0.678
3.40	2.50	16.0	0.0	0.052	0.005	0.00	11.50	63.75	4.01	0.00	0.39	0.719
3.50	2.50	0.0	85.1	0.099	0.018	4.90	68.10	131.85	8.29	0.07	0.26	0.800
3.40	2.50	16.0	0.0	0.108	0.003	0.00	9.60	141.45	8.90	0.00	0.30	0.600
3.30	2.50	0.0	63.3	0.142	0.006	29.00	35.50	176.95	11.13	0.82	0.15	0.561
3.20	2.50	16.0	0.0	0.151	0.002	9.00	7.50	184.45	11.60	1.20	0.20	0.469
2.90	2.50	0.0	63.2	0.186	0.003	25.00	18.50	202.95	12.76	1.35	0.14	0.293
3.00	2.50	16.0	0.0	0.194	0.001	7.00	4.50	207.45	13.05	1.56	0.11	0.281
3.00	2.50	0.0	63.7	0.229	0.003	29.50	20.50	227.95	14.34	1.44	0.15	0.322
2.90	2.50	16.0	0.0	0.238	0.000	8.40	6.35	234.30	14.74	1.32	0.04	0.397
3.00	2.50	0.0	66.3	0.274	0.001	38.00	16.50	250.80	15.77	2.30	0.06	0.249
3.00	2.50	16.0	0.0	0.283	0.002	8.50	4.25	255.05	16.04	2.00	0.53	0.266
3.10	2.50	0.0	63.7	0.318	0.004	40.00	12.00	267.05	16.80	3.33	0.33	0.189
2.60	2.50	16.0	0.0	0.326	0.003	9.00	4.50	271.55	17.08	2.00	0.56	0.281
2.66	2.50	0.0	72.3	0.366	0.011	46.50	14.50	286.05	17.99	3.21	0.76	0.201
2.64	2.40	16.0	0.0	0.375	0.010	12.00	2.75	288.80	18.16	4.36	3.73	0.172
2.55	2.48	0.0	63.7	0.410	0.027	44.50	10.25	299.05	18.81	4.34	2.66	0.161
2.64	2.50	16.0	0.0	0.418	0.010	6.70	3.30	302.35	19.02	2.03	3.03	0.206

TABLE E58 (Cont'd)

Tabulated Experimental Results of Run H2D41

(10% HCPV CO_2 Injected at Water Rate @ 2.5 MPa (0.177 moles), 10 Slugs, 4:1 WAG, 37°C, Horizontal Injection)

Porosity (%) = 37.55
Oil Viscosity (mPa.s) = 5200.0
Ave. Run Temp.(K) = 294.15
CO_2 Req. (sm^3/sm^3) = 8.83

V_p (cm^3) = 1829
S_{oi} (%) = 86.93
HCPV (cm^3) = 1590
CO_2 Ret. (%inj.) = 59.15

S_{wc} (%) = 13.07
Molar Den. ($kmol/m^3$) = 1.11E-03
Abs. k (darcies) = 3.90
Ave. Flow Vel. (m/d) = 2.54

Press Inj. (MPa)	Press Prod. (MPa)	Gas Inj. (cm^3)	Water Inj. (cm^3)	Cum. PV Injected	Gas Prod (s.ltr)	Water Prod. (cm^3)	Oil Prod. (cm^3)	Cum. Oil Prod. (cm^3)	Percent Rec. (%)	WOR (sm^3/sm^3)	GOR (sm^3/sm^3)	OPFIR (sm^3/sm^3)
2.60	2.50	0.0	63.7	0.453	0.043	41.00	10.00	312.35	19.64	4.10	4.30	0.157
2.50	2.40	0.0	251.1	0.590	0.557	213.00	37.00	349.35	21.97	5.76	15.05	0.147
2.70	2.50	0.0	249.3	0.727	0.397	225.00	22.00	371.35	23.36	10.23	18.02	0.088
2.62	2.50	0.0	243.9	0.860	0.210	235.00	15.00	386.35	24.30	15.67	13.97	0.061
2.60	2.50	0.0	246.1	0.995	0.113	231.00	14.70	401.05	25.22	15.71	7.71	0.060
2.90	2.70	0.0	248.6	1.130	0.082	228.00	16.25	417.30	26.25	14.03	5.03	0.065
2.60	2.50	0.0	241.9	1.263	0.072	229.00	16.70	434.00	27.30	13.71	4.33	0.069
2.80	2.50	0.0	250.4	1.400	0.028	237.00	12.50	446.50	28.08	18.96	2.20	0.050
2.60	2.50	0.0	244.3	1.533	0.026	229.00	12.00	458.50	28.84	19.08	2.17	0.049
2.60	2.50	0.0	245.7	1.668	0.020	236.00	10.00	468.50	29.47	23.60	1.95	0.041
2.60	2.50	0.0	247.6	1.803	0.019	242.00	10.00	478.50	30.09	24.20	1.90	0.040
0.10	0.10	0.0	0.0	1.803	0.257	100.00	17.00	495.50	31.16	5.88	15.09	

TABLE E59

Tabulated Experimental Results of Run H2D42a

(Waterflood at 4.8 MPa and 37°C)

Porosity (%) =	37.28	V_p (cm^3) =	1816	S_{wc} (%) =	17.95
Oil Viscosity (mPa.s) =	603.0	S_{oi} (%) =	82.05	Molar Den. (kmol/m^3) =	2.52E-03
Ave. Run Temp.(K) =	294.15	HCPV (cm^3) =	1490	Abs. k (darcies) =	6.16
CO_2 Req. (sm^3/sm^3) =	0	CO_2 Ret. (%inj.) =	0	Ave. Flow Vel. (m/d) =	2.54

Press Inj. (MPa)	Press Prod. (MPa)	Gas Inj. (cm^3)	Water Inj. (cm^3)	Cum. PV Injected	Gas Prod (s.ltr)	Water Prod. (cm^3)	Oil Prod. (cm^3)	Cum. Oil Prod. (cm^3)	Percent Rec. (%)	WOR (sm^3/sm^3)	GOR (sm^3/sm^3)	OPFIR (sm^3/sm^3)
5.10	4.80	0.0	490.4	0.270	0.000	195.00	257.50	257.50	17.28	0.00	0.00	0.525
5.10	4.80	0.0	491.9	0.541	0.000	362.00	140.00	397.50	26.68	2.59	0.00	0.285
5.10	4.80	0.0	493.8	0.813	0.000	415.00	79.00	476.50	31.98	0.00	0.00	0.160
5.10	4.80	0.0	491.4	1.083	0.000	458.00	37.00	513.50	34.46	12.38	0.00	0.075
5.10	4.80	0.0	491.9	1.354	0.000	440.00	55.00	568.50	38.15	8.00	0.00	0.112
5.10	4.80	0.0	491.8	1.625	0.000	462.50	50.00	618.50	41.51	9.25	0.00	0.102
5.10	4.80	0.0	491.3	1.896	0.000	447.50	38.50	657.00	44.09	11.62	0.00	0.078
5.10	4.80	0.0	491.4	2.166	0.000	482.50	30.00	687.00	46.11	16.08	0.00	0.061
5.10	4.80	0.0	493.0	2.438	0.000	455.00	27.00	714.00	47.92	16.85	0.00	0.055
5.10	4.80	0.0	493.0	2.709	0.000	472.00	20.50	734.50	49.30	23.02	0.00	0.042
5.10	4.80	0.0	494.1	2.981	0.000	477.00	21.00	755.50	50.70	22.71	0.00	0.043

TABLE ~~C~~E60

Tabulated Experimental Results of Run H2D42b

(20% HCPV CO_2 Injected at Water Rate @ 4.8 MPa (0.370 moles), 10 Slugs, 2:1 WAG, 37°C, Horizontal Injection)

Porosity (%) = 37.28

Oil Viscosity (mPa.s) = 603.0

Ave. Run Temp.(K) = 294.15

CO_2 Req. (sm^3/sm^3) = 96.39

V_p (cm^3) = 1816

S_{oi} (%) = 40.45

HCPV (cm^3) = 734.5

CO_2 Ret. (%inj.) = 33.27

S_{wc} (%) = 59.55

Molar Den. ($kmol/m^3$) = 2.52E-03

Abs. k (darcies) = 6.16

Ave. Flow Vel. (m/d) = 2.54

Press Inj. (MPa)	Press Prod. (MPa)	Gas Inj. (cm^3)	Water Inj. (cm^3)	Cum. PV Injected	Gas Prod (s.ltr)	Water Prod. (cm^3)	Oil Prod. (cm^3)	Cum. Oil Prod. (cm^3)	Percent Rec. (%)	WOR (sm^3/sm^3)	GOR (sm^3/sm^3)	OPFIR (sm^3/sm^3)
4.92	4.82	14.7	0.0	0.008	0.000	18.50	0.50	0.50	0.07	37.00	0.00	0.034
4.92	4.82	0.0	29.7	0.024	0.000	8.00	0.50	1.00	0.14	16.00	0.00	0.017
5.10	4.80	14.7	0.0	0.033	0.000	6.00	0.50	1.50	0.20	12.00	0.00	0.034
5.10	4.80	0.0	29.7	0.049	0.000	29.50	1.75	3.25	0.44	16.86	0.00	0.059
4.84	4.50	14.7	0.0	0.057	0.000	20.00	0.50	3.75	0.51	40.00	0.00	0.034
4.84	4.50	0.0	31.1	0.074	0.000	14.00	1.00	4.75	0.65	14.00	0.00	0.032
4.84	4.56	14.7	0.0	0.082	0.000	0.00	0.00	4.75	0.65	0.00	0.00	0.000
4.84	4.56	0.0	29.8	0.099	0.015	25.00	2.00	6.75	0.92	12.50	7.25	0.067
5.00	4.82	14.7	0.0	0.107	0.000	0.00	0.00	6.75	0.92	0.00	0.00	0.000
5.00	4.80	0.0	30.5	0.123	0.070	28.00	2.00	8.75	1.19	14.00	35.00	0.066
4.87	4.56	14.7	0.0	0.132	0.010	15.00	1.00	9.75	1.33	15.00	10.00	0.068
4.92	4.62	0.0	29.7	0.148	0.012	20.00	1.00	10.75	1.46	20.00	11.50	0.034
4.92	4.80	14.7	0.0	0.156	0.000	0.00	0.00	10.75	1.46	0.00	0.00	0.000
5.04	4.82	0.0	30.1	0.173	0.096	27.50	1.50	12.25	1.67	18.33	64.00	0.050
5.04	4.82	14.7	0.0	0.181	0.000	0.00	0.00	12.25	1.67	0.00	0.00	0.000
5.04	4.82	0.0	32.8	0.199	0.099	28.50	1.00	13.25	1.80	28.50	99.00	0.031
5.04	4.82	14.7	0.0	0.207	0.000	0.00	0.00	13.25	1.80	0.00	0.00	0.000
5.04	4.82	0.0	29.8	0.223	0.057	26.00	1.75	15.00	2.04	14.86	32.57	0.059
5.04	4.82	14.7	0.0	0.231	0.006	11.00	1.25	16.25	2.21	8.80	4.60	0.085

TABLE E60 (Cont'd)

Tabulated Experimental Results of Run H2D42b

(20% HCPV CO_2 Injected at Water Rate @ 4.8 MPa (0.370 moles), 10 Slugs, 2:1 WAG, 37°C, Horizontal Injection)

Porosity (%) =	37.28	V_p (cm^3) =	1816	S_{wc} (%) =	59.55
Oil Viscosity (mPa.s) =	603.0	S_{oi} (%) =	40.45	Molar Den. ($kmol/m^3$) =	2.52E-03
Ave. Run Temp.(K) =	294.15	HCPV (cm^3) =	734.5	Abs. k (darcies) =	6.16
CO_2 Req. (sm^3/sm^3) =	96.39	CO_2 Ret. (%inj.) =	33.27	Ave. Flow Vel. (m/d) =	2.54

Press Inj. (MPa)	Press Prod. (MPa)	Gas Inj. (cm^3)	Water Inj. (cm^3)	Cum. PV Injected	Gas Prod (s.ltr)	Water Prod. (cm^3)	Oil Prod. (cm^3)	Cum. Oil Prod. (cm^3)	Percent Rec. (%)	WOR (sm^3/sm^3)	GOR (sm^3/sm^3)	OPFIR (sm^3/sm^3)
5.04	4.82	0.0	33.1	0.250	0.063	29.00	1.00	17.25	2.35	29.00	62.50	0.030
4.82	4.62	0.0	260.4	0.393	0.546	238.00	9.00	26.25	3.57	26.44	60.67	0.035
4.82	4.62	0.0	250.9	0.531	0.409	234.00	12.00	38.25	5.21	19.50	34.08	0.048
4.82	4.62	0.0	255.4	0.672	0.623	247.00	12.00	50.25	6.84	20.58	51.92	0.047
4.82	4.62	0.0	251.5	0.810	0.627	237.00	13.00	63.25	8.61	18.23	48.23	0.052
4.82	4.62	0.0	253.4	0.950	0.568	238.00	10.00	73.25	9.97	23.80	56.75	0.039
4.82	4.62	0.0	252.8	1.089	0.440	235.00	10.00	83.25	11.33	23.50	43.95	0.040
0.10	0.10	0.0	0.0	1.089	2.295	206.00	9.00	92.25	12.56	22.89	255.00	

TABLE E61

Tabulated Experimental Results of Run H2D43a

(20% HCPV CO_2 Injected at Water Rate @ 3.58 MPa (0.279 moles), 10 Slugs, 2:1 WAG, 21°C, Horizontal Injection)

Porosity (%) = 36.95
Oil Viscosity (mPa.s) = 282.0
Ave. Run Temp.(K) = 294.15
CO_2 Req. (sm^3/sm^3) = 0

V_p (cm^3) = 1800
S_{oi} (%) = 82.78
HCPV (cm^3) = 1490
CO_2 Ret. (%inj.) = 0

S_{wc} (%) = 17.22
Molar Den. ($kmol/m^3$) = 1.90E-03
Abs. k (darcies) = 11.91
Ave. Flow Vel. (m/d) = 2.54

Press Inj. (MPa)	Press Prod. (MPa)	Gas Inj. (cm^3)	Water Inj. (cm^3)	Cum. PV Injected	Gas Prod (s.ltr)	Water Prod. (cm^3)	Oil Prod. (cm^3)	Cum. Oil Prod. (cm^3)	Percent Rec. (%)	WOR (sm^3/sm^3)	GOR (sm^3/sm^3)	OPFIR (sm^3/sm^3)
3.70	3.58	0.0	490.4	0.270	0.000	195.00	257.50	257.50	17.28	0.00	0.00	0.525
3.70	3.58	0.0	491.9	0.541	0.000	362.00	140.00	397.50	26.68	2.59	0.00	0.285
3.70	3.58	0.0	493.8	0.813	0.000	415.00	79.00	476.50	31.98	0.00	0.00	0.160
3.70	3.58	0.0	491.4	1.083	0.000	458.00	37.00	513.50	34.46	12.38	0.00	0.075
3.70	3.58	0.0	491.9	1.354	0.000	440.00	55.00	568.50	38.15	8.00	0.00	0.112
3.70	3.58	0.0	491.8	1.625	0.000	462.50	50.00	618.50	41.51	9.25	0.00	0.102
3.70	3.58	0.0	491.3	1.896	0.000	447.50	38.50	657.00	44.09	11.62	0.00	0.078
3.70	3.58	0.0	491.4	2.166	0.000	482.50	30.00	687.00	46.11	16.08	0.00	0.061
3.70	3.58	0.0	493.0	2.438	0.000	455.00	27.00	714.00	47.92	16.85	0.00	0.055
3.70	3.58	0.0	493.0	2.709	0.000	472.00	20.50	734.50	49.30	23.02	0.00	0.042
3.70	3.58	0.0	494.1	2.981	0.000	477.00	21.00	755.50	50.70	22.71	0.00	0.043

TABLE E62

Tabulated Experimental Results of Run H2D43b

(20% HCPV CO_2 Injected at Water Rate @ 3.58 MPa (0.279 moles), 10 Slugs, 2:1 WAG, 21°C, Horizontal Injection)

Porosity (%) =	36.95	V_p (cm^3) =	1800	S_{wc} (%) =	59.19
Oil Viscosity (mPa.s) =	282.0	S_{oi} (%) =	40.81	Molar Den. (kmol/m^3) =	1.90E-03
Ave. Run Temp.(K) =	294.15	HCPV (cm^3) =	734.5	Abs. k (darcies) =	11.91
CO_2 Req. (sm^3/sm^3) =	61.94	CO_2 Ret. (%inj.) =	27.58	Ave. Flow Vel. (m/d) =	2.54

Press Inj. (MPa)	Press Prod. (MPa)	Gas Inj. (cm^3)	Water Inj. (cm^3)	Cum. PV Injected	Gas Prod (s.ltr)	Water Prod. (cm^3)	Oil Prod. (cm^3)	Cum. Oil Prod. (cm^3)	Percent Rec. (%)	WOR (sm^3/sm^3)	GOR (sm^3/sm^3)	OPFIR (sm^3/sm^3)
3.50	3.48	14.7	0.0	0.008	0.000	21.50	1.75	1.75	0.24	12.29	0.00	0.119
3.62	3.58	0.0	29.7	0.025	0.000	14.50	1.00	2.75	0.37	14.50	0.00	0.034
3.22	3.12	14.7	0.0	0.033	0.000	27.50	0.50	3.25	0.44	55.00	0.00	0.034
2.98	2.94	0.0	30.7	0.050	0.000	13.00	0.50	3.75	0.51	26.00	0.00	0.016
3.60	3.56	14.7	0.0	0.058	0.000	0.00	0.00	3.75	0.51	0.00	0.00	0.000
3.66	3.60	0.0	31.1	0.075	0.000	19.50	1.50	5.25	0.71	13.00	0.00	0.048
3.54	3.48	14.7	0.0	0.084	0.000	11.50	0.50	5.75	0.78	23.00	0.00	0.034
3.72	3.68	0.0	31.7	0.101	0.000	23.00	1.00	6.75	0.92	23.00	0.00	0.032
3.70	3.64	14.7	0.0	0.109	0.065	17.00	0.25	7.00	0.95	0.00	0.00	0.017
3.48	3.42	0.0	31.4	0.127	0.027	18.00	1.00	8.00	1.09	18.00	27.00	0.032
3.64	3.63	14.7	0.0	0.135	0.022	7.00	0.50	8.50	1.16	0.00	0.00	0.034
3.64	3.62	0.0	29.4	0.151	0.019	20.50	1.75	10.25	1.40	11.71	10.71	0.060
3.66	3.62	14.7	0.0	0.159	0.000	11.50	0.75	11.00	1.50	15.33	0.00	0.051
3.68	3.64	0.0	29.4	0.176	0.019	20.00	1.00	12.00	1.63	20.00	19.00	0.034
3.65	3.62	14.7	0.0	0.184	0.073	7.00	1.50	13.50	1.84	0.00	0.00	0.102
3.50	3.44	0.0	29.7	0.200	0.066	22.50	1.50	15.00	2.04	15.00	44.00	0.051
3.68	3.66	14.7	0.0	0.208	0.077	8.50	0.50	15.50	2.11	0.00	0.00	0.034
3.68	3.64	0.0	29.4	0.225	0.034	19.30	1.20	16.70	2.27	16.08	27.92	0.041
3.64	3.58	14.7	0.0	0.233	0.130	13.00	2.00	18.70	2.55	0.00	0.00	0.136

TABLE E62 (Cont'd)

Tabulated Experimental Results of Run H2D43b

(20% HCPV CO_2 Injected at Water Rate @ 3.58 MPa (0.279 moles), 10 Slugs, 2:1 WAG, 21°C, Horizontal Injection)

Porosity (%) = 36.95
Oil Viscosity (mPa.s) = 282.0
Ave. Run Temp.(K) = 294.15
CO_2 Req. (sm^3/sm^3) = 61.54

V_p (cm^3) = 1800
S_{oi} (%) = 40.81
HCPV (cm^3) = 734.5
CO_2 Ret. (%inj.) = 27.98

S_{wc} (%) = 59.19
Molar Den. ($kmol/m^3$) = 1.90E-03
Abs. k (darcies) = 11.91
Ave. Flow Vel. (m/d) = 2.54

Press Inj. (MPa)	Press Prod. (MPa)	Gas Inj. (cm^3)	Water Inj. (cm^3)	Cum. PV Injected	Gas Prod (s.ltr)	Water Prod. (cm^3)	Oil Prod. (cm^3)	Cum. Oil Prod. (cm^3)	Percent Rec. (%)	WOR (sm^3/sm^3)	GOR (sm^3/sm^3)	OPFIR (sm^3/sm^3)
3.58	3.54	0.0	31.9	0.251	0.071	23.50	2.00	20.70	2.82	11.75	35.25	0.063
3.53	3.48	0.0	265.1	0.398	0.265	240.00	8.00	28.70	3.91	30.00	33.13	0.030
3.62	3.56	0.0	248.7	0.536	0.594	236.00	12.00	40.70	5.54	19.67	49.50	0.048
3.70	3.68	0.0	250.9	0.676	0.673	238.00	12.00	52.70	7.17	19.83	56.08	0.048
3.70	3.67	0.0	260.7	0.820	0.523	248.00	13.00	65.70	8.94	19.08	40.23	0.050
3.64	3.62	0.0	248.3	0.958	0.394	246.00	11.00	76.70	10.44	22.36	35.82	0.044
3.62	3.58	0.0	250.3	1.097	0.282	243.00	12.00	88.70	12.08	20.25	23.50	0.048
0.10	0.10	0.0	0.0	1.097	1.486	130.00	20.00	108.70	14.80	6.50	74.30	

TABLE E63

Tabulated Experimental Results of Run H2D44a

Waterflood at 3.58 MPa and 21°C

Porosity (%) =	37.28	V_p (cm^3) =	1816	S_{wc} (%) =	19.05
Oil Viscosity (mPa.s) =	282.0	S_{oi} (%) =	80.95	Molar Den. (kmol/m^3) =	1.90E-03
Ave. Run Temp.(K) =	294.15	HCPV (cm^3) =	1470	Abs. k (darcies) =	8.11
CO_2 Req. (sm^3/sm^3) =	0.00	CO_2 Ret. (%inj.) =	0.00	Ave. Flow Vel. (m/d) =	2.54

Press Inj. (MPa)	Press Prod. (MPa)	Gas Inj. (cm^3)	Water Inj. (cm^3)	Cum. PV Injected	Gas Prod (s.ltr)	Water Prod. (cm^3)	Oil Prod. (cm^3)	Cum. Oil Prod. (cm^3)	Percent Rec. (%)	WOR (sm^3/sm^3)	GOR (sm^3/sm^3)	OPFIR (sm^3/sm^3)
3.70	3.58	0.0	938.5	0.517	0.000	647.00	281.00	281.00	19.12	0.00	0.00	0.299
3.70	3.58	0.0	489.8	0.786	0.000	337.50	140.50	421.50	28.67	2.40	0.00	0.287
3.70	3.58	0.0	486.6	1.054	0.000	437.00	53.00	474.50	32.28	8.25	0.00	0.109
3.70	3.58	0.0	490.7	1.325	0.000	450.00	50.00	524.50	35.68	9.00	0.00	0.102
3.70	3.58	0.0	491.4	1.595	0.000	460.00	35.00	559.50	38.06	13.14	0.00	0.071
3.70	3.58	0.0	493.0	1.867	0.000	467.00	35.00	594.50	40.44	13.34	0.00	0.071
3.70	3.58	0.0	491.4	2.137	0.000	467.00	28.00	622.50	42.35	16.68	0.00	0.057
3.70	3.58	0.0	489.7	2.407	0.000	465.00	25.00	647.50	44.05	18.60	0.00	0.051
3.70	3.58	0.0	491.4	2.677	0.000	467.00	21.00	668.50	45.48	22.24	0.00	0.043
3.70	3.58	0.0	492.2	2.949	0.000	487.00	20.00	688.50	46.84	24.35	0.00	0.041
3.70	3.58	0.0	489.7	3.218	0.000	477.50	21.50	710.00	48.30	22.21	0.00	0.044

TABLE E64

Tabulated Experimental Results of Run H2D44b

(20% HCPV CO_2 Injected at Water Rate @ 3.58 MPa (0.288 moles), 10 Slugs, 2:1 WAG, 21°C, Horizontal Injection)

Porosity (%) = 37.28
Oil Viscosity (mPa.s) = 280.0
Ave. Run Temp.(K) = 294.15
CO_2 Req. (sm^3/sm^3) = 60.58

V_p (cm^3) = 1816
S_{oi} (%) = 41.85
HCPV (cm^3) = 760
CO_2 Ret. (%inj$_d$) = 37.97

S_{wc} (%) = 58.15
Molar Den. (kmol/m^3) = 1.90E-03
Abs. k (darcies) = 8.11
Ave. Flow Vel. (m/d) = 2.54

Press Inj. (MPa)	Press Prod. (MPa)	Gas Inj. (cm^3)	Water Inj. (cm^3)	Cum. PV Injected	Gas Prod (s.ltr)	Water Prod. (cm^3)	Oil Prod. (cm^3)	Cum. Oil Prod. (cm^3)	Percent Rec. (%)	WOR (sm^3/sm^3)	GOR (sm^3/sm^3)	OPFIR (sm^3/sm^3)
3.32	3.30	15.2	0.0	0.008	0.000	20.00	0.50	0.50	0.07	40.00	0.00	0.033
3.62	3.60	0.0	30.5	0.025	0.000	23.00	1.00	1.50	0.20	23.00	0.00	0.033
3.60	3.56	15.2	0.0	0.034	0.000	9.00	0.50	2.00	0.26	18.00	0.00	0.033
3.30	3.28	0.0	30.5	0.050	0.000	36.00	2.00	4.00	0.53	18.00	0.00	0.066
3.58	3.57	15.2	0.0	0.059	0.000	18.00	0.50	4.50	0.59	0.00	0.00	0.033
3.80	3.77	0.0	30.8	0.076	0.000	22.00	1.00	5.50	0.72	22.00	0.00	0.032
3.62	3.58	15.2	0.0	0.084	0.000	15.50	1.00	6.50	0.86	15.50	0.00	0.066
3.60	3.58	0.0	30.8	0.101	0.000	26.50	1.00	7.50	0.99	26.50	0.00	0.032
3.58	3.52	15.2	0.0	0.109	0.000	14.50	1.25	8.75	1.15	0.00	0.00	0.082
3.58	3.48	0.0	30.1	0.126	0.029	31.50	1.00	9.75	1.28	31.50	29.00	0.033
3.60	3.48	15.2	0.0	0.134	0.072	8.00	0.50	10.25	1.35	0.00	0.00	0.033
3.52	3.48	0.0	30.9	0.151	0.013	27.00	1.50	11.75	1.55	18.00	8.67	0.049
3.64	3.59	15.2	0.0	0.160	0.007	14.00	1.00	12.75	1.68	14.00	7.00	0.066
3.64	3.58	0.0	30.9	0.177	0.016	26.00	1.00	13.75	1.81	26.00	16.00	0.032
3.54	3.46	15.2	0.0	0.185	0.120	14.00	1.00	14.75	1.94	0.00	0.00	0.066
3.62	3.60	0.0	30.1	0.202	0.033	39.60	1.00	15.75	2.07	39.60	33.00	0.033
3.04	3.02	15.2	0.0	0.210	0.217	16.00	1.00	16.75	2.20	0.00	0.00	0.066
3.60	3.58	0.0	29.3	0.226	0.023	8.50	1.50	18.25	2.40	5.67	15.33	0.051
3.62	3.56	15.2	0.0	0.235	0.000	0.00	1.00	19.25	2.53	0.00	0.00	0.066

TABLE E64 (Cont'd)

Tabulated Experimental Results of Run H2D44b

(20% HCPV CO_2 Injected at Water Rate @ 3.58 MPa (0.288 moles), 10 Slugs, 2:1 WAG, 21°C, Horizontal Injection)

Porosity (%) =	37.28	V_p (cm^3) =	1816	S_{wc} (%) =	58.15
Oil Viscosity (mPa.s) =	280.0	S_{oi} (%) =	41.85	Molar Den. (kmol/m^3) =	1.90E-03
Ave. Run Temp.(K) =	294.15	HCPV (cm^3) =	760	Abs. k (darcies) =	8.11
CO_2 Req. (sm^3/sm^3) =	60.58	CO_2 Ret. (%inj.) =	37.97	Ave. Flow Vel. (m/d) =	2.54

Press Inj. (MPa)	Press Prod. (MPa)	Gas Inj. (cm^3)	Water Inj. (cm^3)	Cum. PV Injected	Gas Prod (s.ltr)	Water Prod. (cm^3)	Oil Prod. (cm^3)	Cum. Oil Prod. (cm^3)	Percent Rec. (%)	WOR (sm^3/sm^3)	GOR (sm^3/sm^3)	OPFIR (sm^3/sm^3)
3.62	3.56	0.0	30.5	0.251	0.164	36.50	2.50	21.75	2.86	14.60	65.60	0.082
3.60	3.56	0.0	257.6	0.393	0.364	237.00	10.00	31.75	4.18	23.70	36.40	0.039
3.58	3.56	0.0	251.5	0.532	0.538	232.00	10.00	41.75	5.49	23.20	53.80	0.040
3.64	3.54	0.0	241.6	0.665	0.947	230.00	14.50	56.25	7.40	15.86	65.28	0.060
3.56	3.54	0.0	250.4	0.803	0.430	234.00	12.00	68.25	8.98	19.50	35.83	0.048
3.56	3.54	0.0	261.4	0.947	0.272	237.00	12.00	80.25	10.56	19.75	22.63	0.046
3.56	3.54	0.0	230.4	1.073	0.214	235.00	11.00	91.25	12.01	21.36	19.45	0.048
0.10	0.10	0.0	0.0	1.073	0.836	100.00	23.00	114.25	15.03	4.35	36.33	

APPENDIX F

Production Histories of All Experiments Conducted

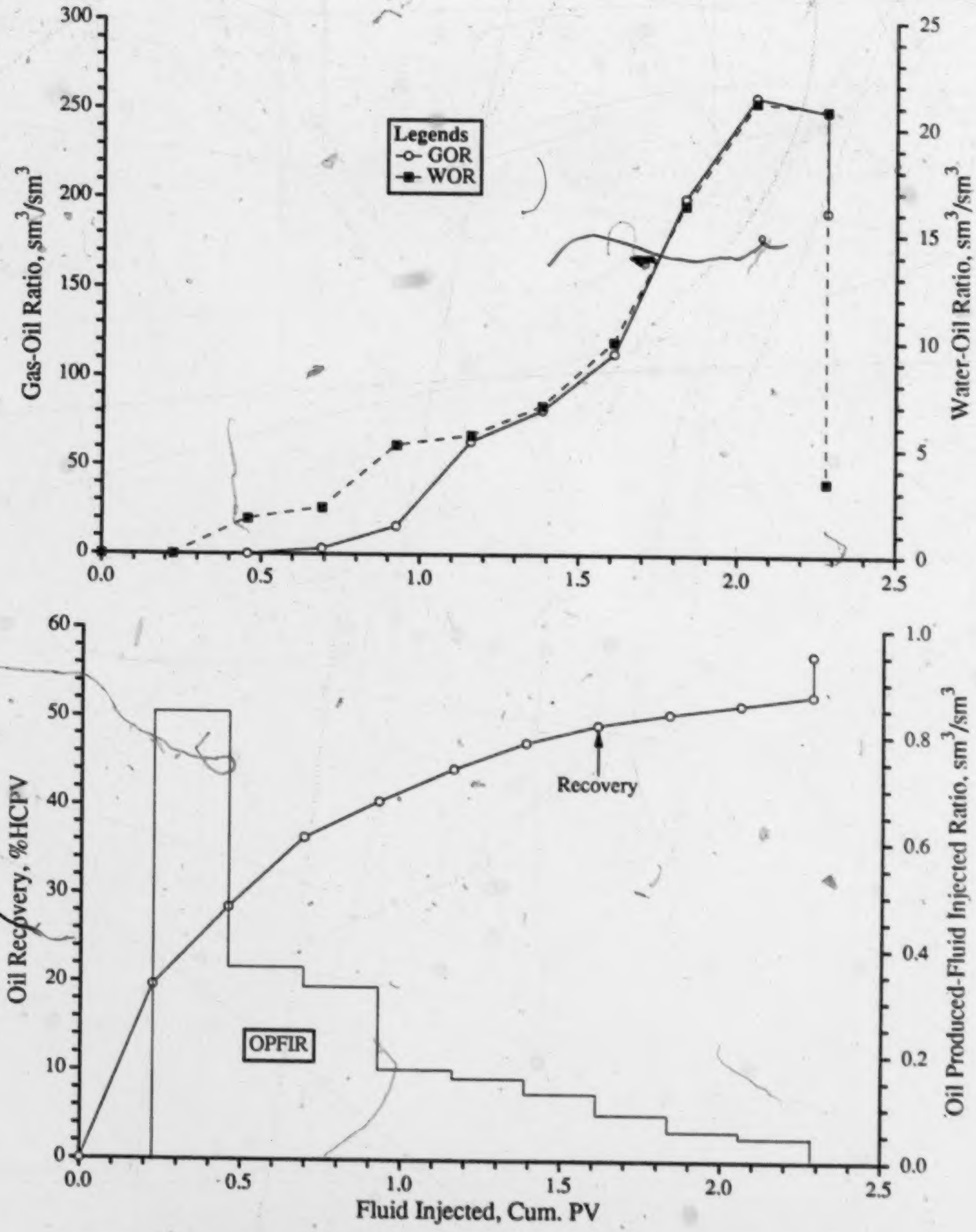

NOTE: Average Run Conditions: Carbonated Waterflood, 2.5 MPa, 21°C

Model Parameters: Average Injection Rate = 308 cc/hr, μ_o = 1053.0 mPa.s,

ø = 36.0%, k = 11.3 darcies, S_o = 96.2 %, S_{wc} = 3.8 %

Model Type: Linear

[1.608 moles of CO_2]

Figure F1 - Production History of Run CWF3.

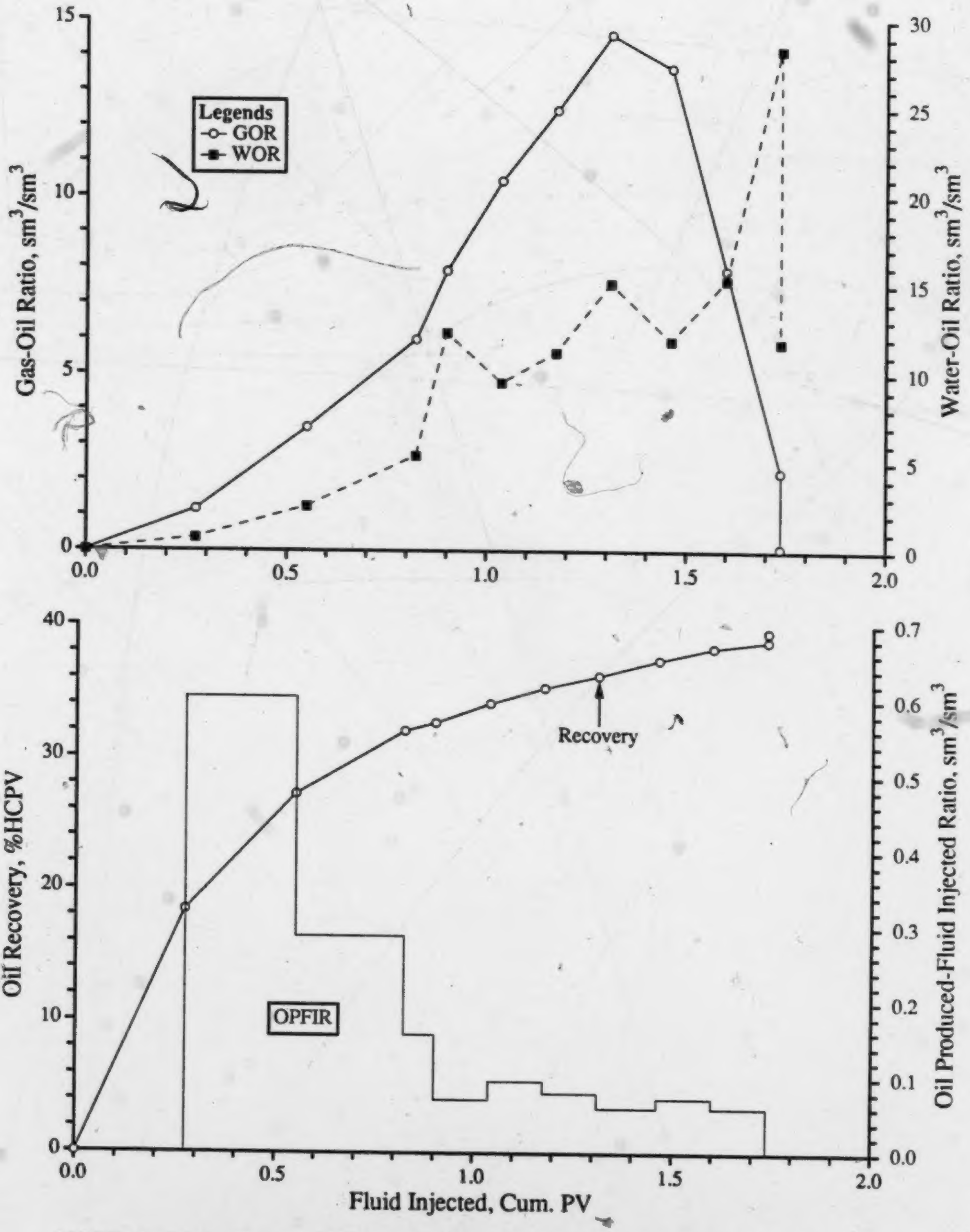

NOTE: Average Run Conditions: Carbonated Waterflood, 1.0 MPa, 21°C
Model Parameters: Average Injection Rate = 308 cc/hr, μ_o = 1058.0 mPa.s,
ϕ = 37.5 %, k = 10.9 darcies, S_o = 90.1 %, S_{wc} = 9.9 %
Model Type: Linear
[20% HCPV of CO_2 (0.143 moles) Mixed with Water at 4:1 Ratio]

Figure F2 - Production History of Run CWF4.

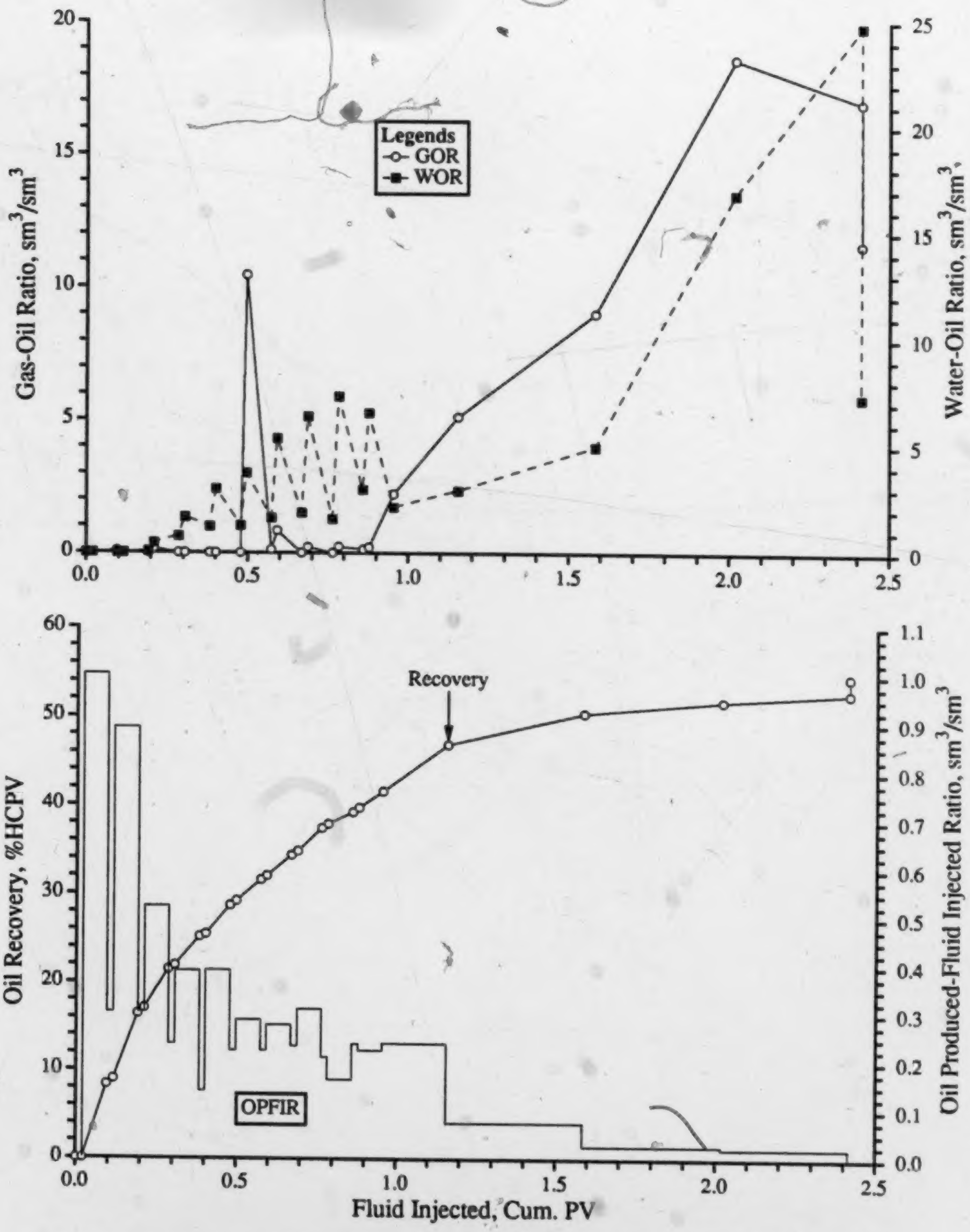

NOTE: Average Run Conditions: Vertical WAG Flood at Bottom, 1.0 MPa, 21°C
Model Parameters: Average Injection Rate = 308 cc/hr, μ_o = 1053.0 mPa.s,
ϕ = 35.9 %, k = 11.33 darcies, S_o = 95.4 %, S_{wc} = 4.6 %
Model Type: Linear
[0.20 HCPV CO_2 @ 1.0 MPa (0.089 moles) 4:1 WAG, 10 Slugs]

Figure F3 - Production History of Run VLC1.

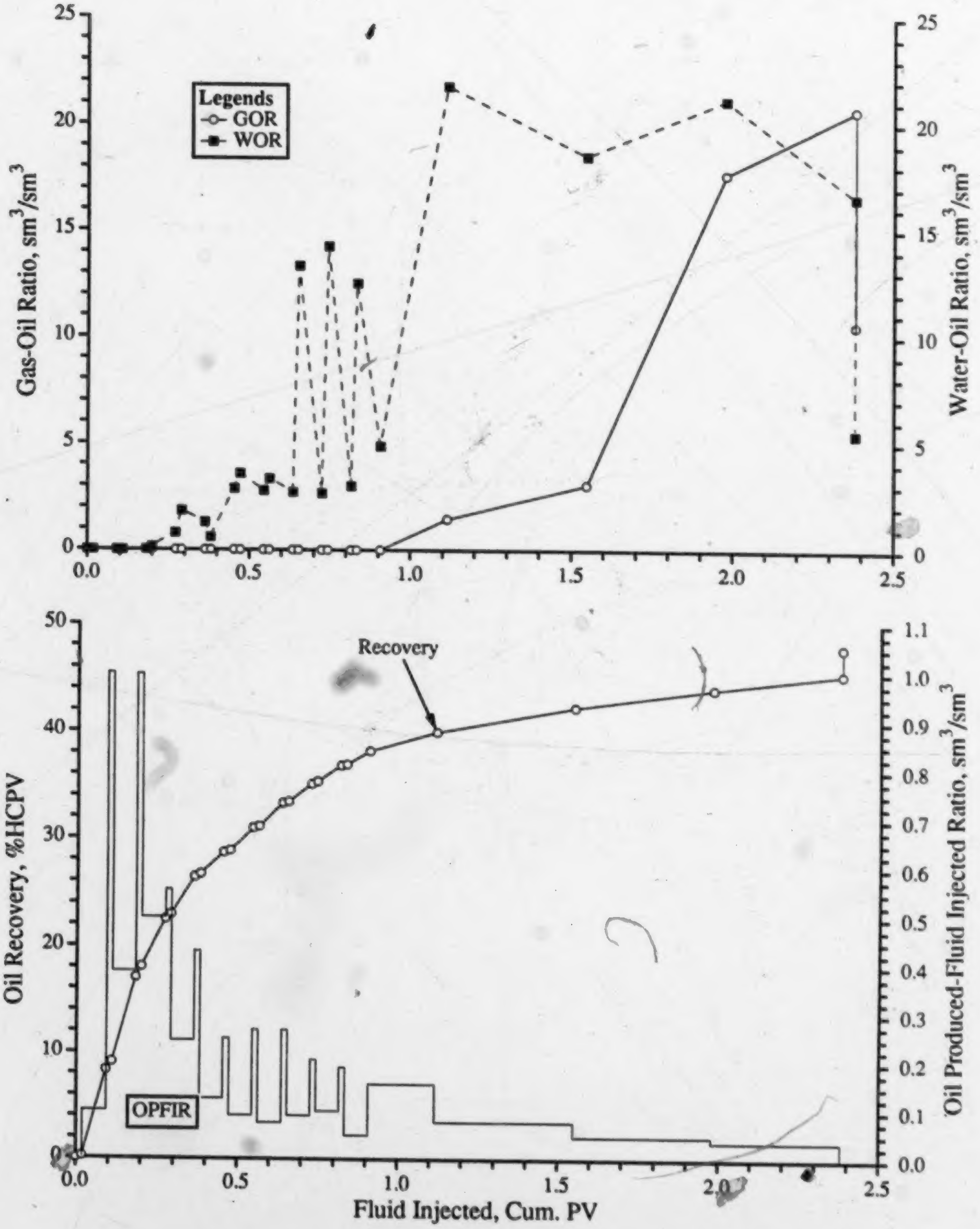

NOTE: Average Run Conditions: Vertical WAG Flood at Top, 1.0 MPa, 21°C
Model Parameters: Average Injection Rate = 308 cc/hr, μ_o = 1058.0 mPa.s,
ϕ = 35.5 %, k = 11.12 darcies, S_o = 90.7 %, S_{wc} = 9.3 %
Model Type: Linear
[0.20 HCPV CO_2 @ 1.0 MPa (0.087 moles) 4:1 WAG, 10 Slugs]

Figure F4 - Production History of Run VLC2.

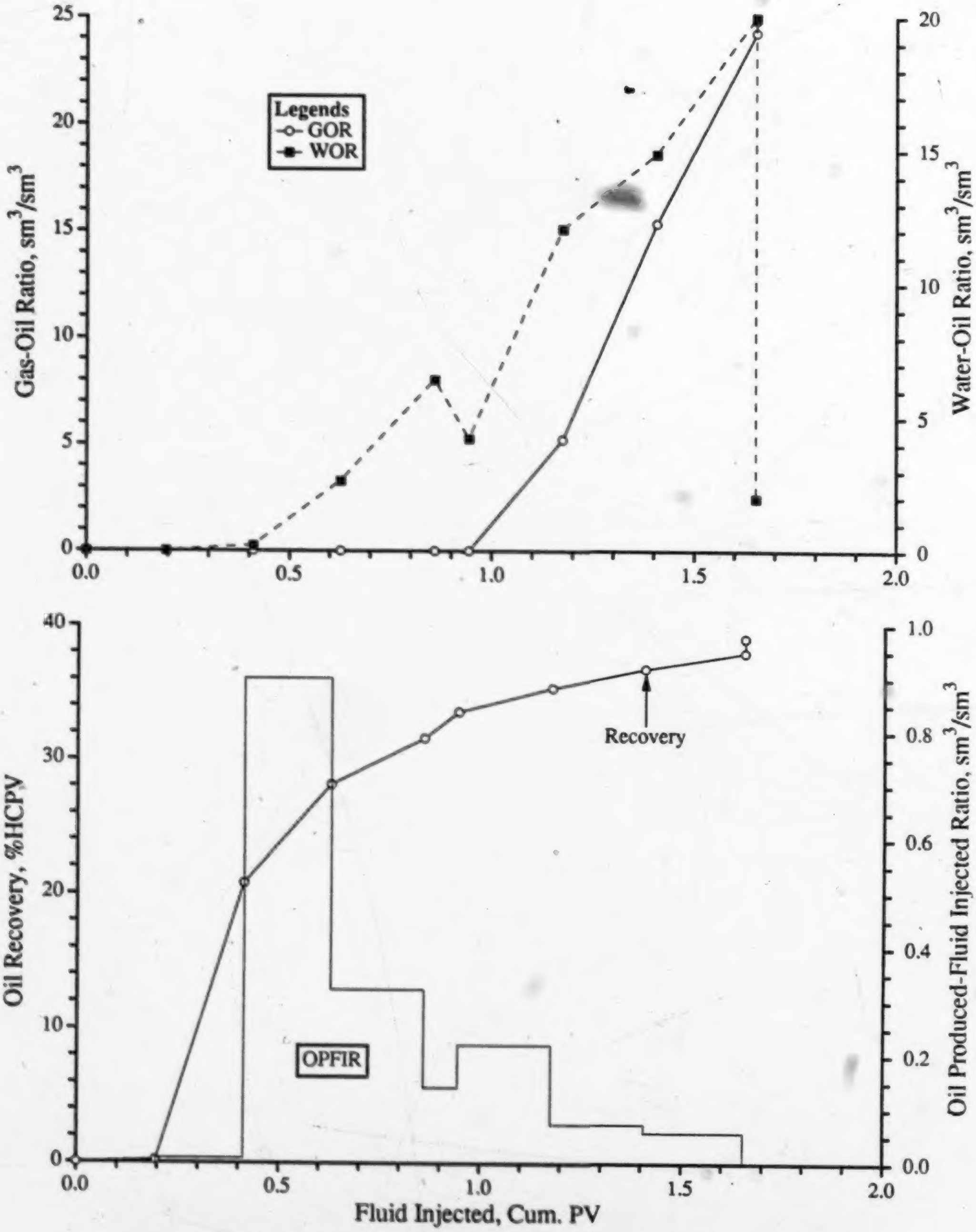

NOTE: Average Run Conditions: Continuous Injection at Bottom, 1.0 MPa, 21°C
Model Parameters: Average Injection Rate = 308 cc/hr, μ_o = 1058.0 mPa.s,
ϕ = 34.74%, k = 9.18 darcies, S_o = 94.35%, S_{wc} = 5.65%
Model Type: Linear
[0.20 HCPV CO_2 @ 1.0 MPa (0.088 moles)]

Figure F5 - Production History of Run VLC3.

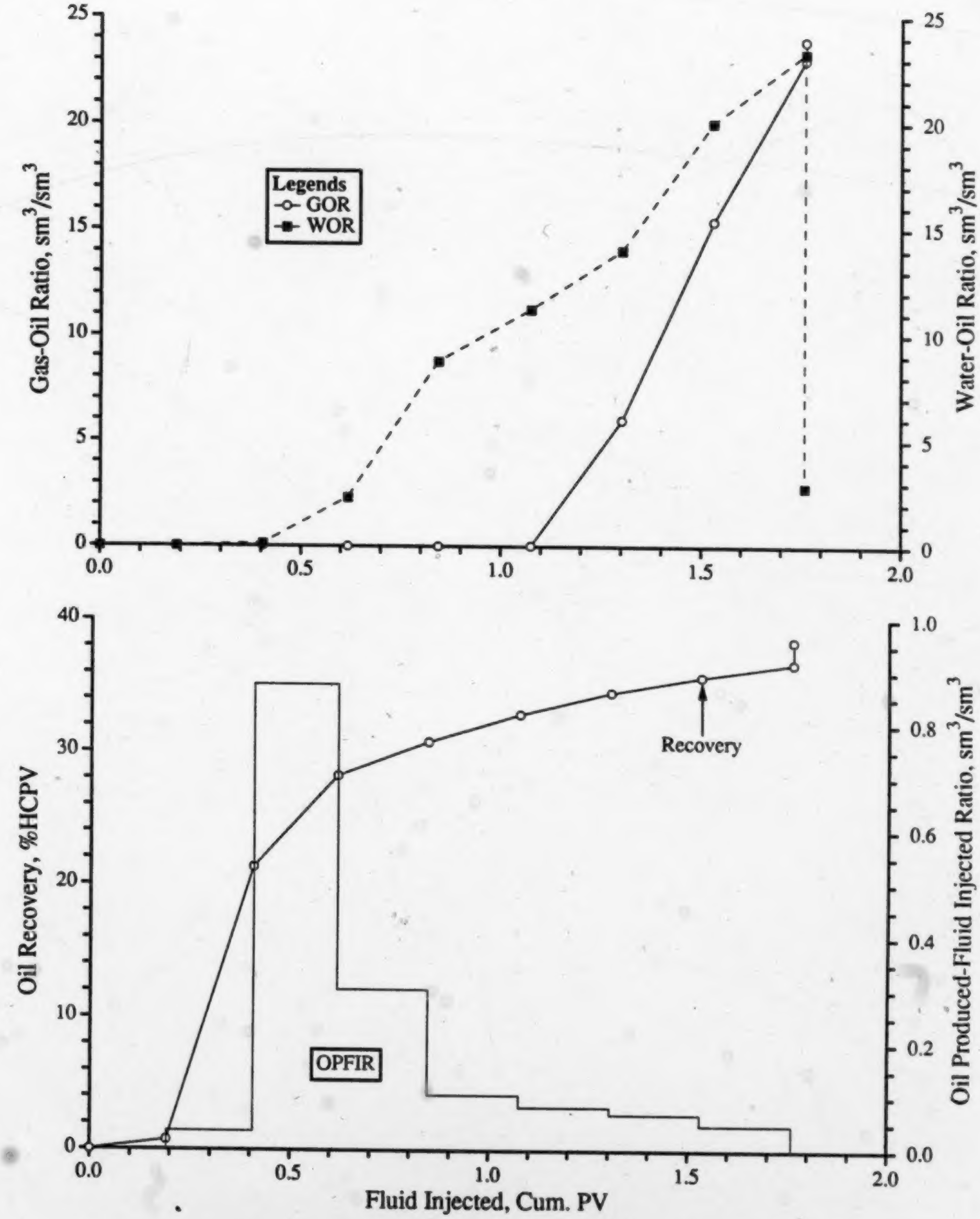

NOTE: Average Run Conditions: Continuous Injection at Bottom, 1.0 MPa, 21°C
Model Parameters: Average Injection Rate = 308 cc/hr, μ_o = 1058.0 mPa.s,
ϕ = 35.50%, k = 10.23 darcies, S_o = 91.96%, S_{wc} = 8.04%
Model Type: Linear
[0.20 HCPV CO_2 @ 1.0 MPa (0.088 moles)]

Figure F6 - Production History of Run VLC4.

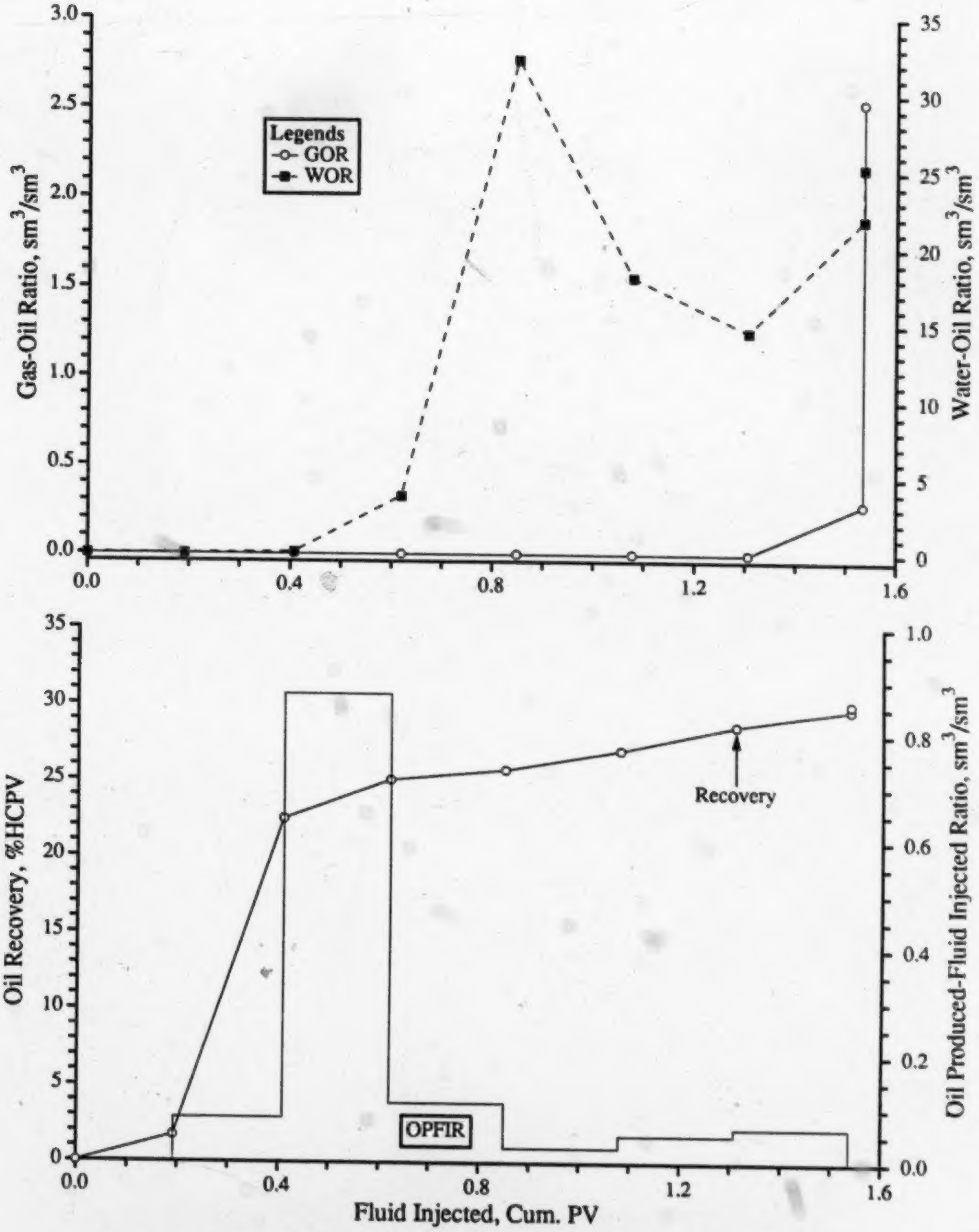

NOTE: Average Run Conditions: Continuous Injection at Top, 1.0 MPa, 21°C
Model Parameters: Average Injection Rate = 308 cc/hr, μ_o = 1058.0 mPa.s, ϕ = 35.38%, k = 11.34 darcies, S_o = 91.82%, S_{wc} = 8.18%
Model Type: Linear
[0.20 HCPV CO_2 @ 1.0 MPa (0.088 moles)]

Figure F7 - Production History of Run VLC5.

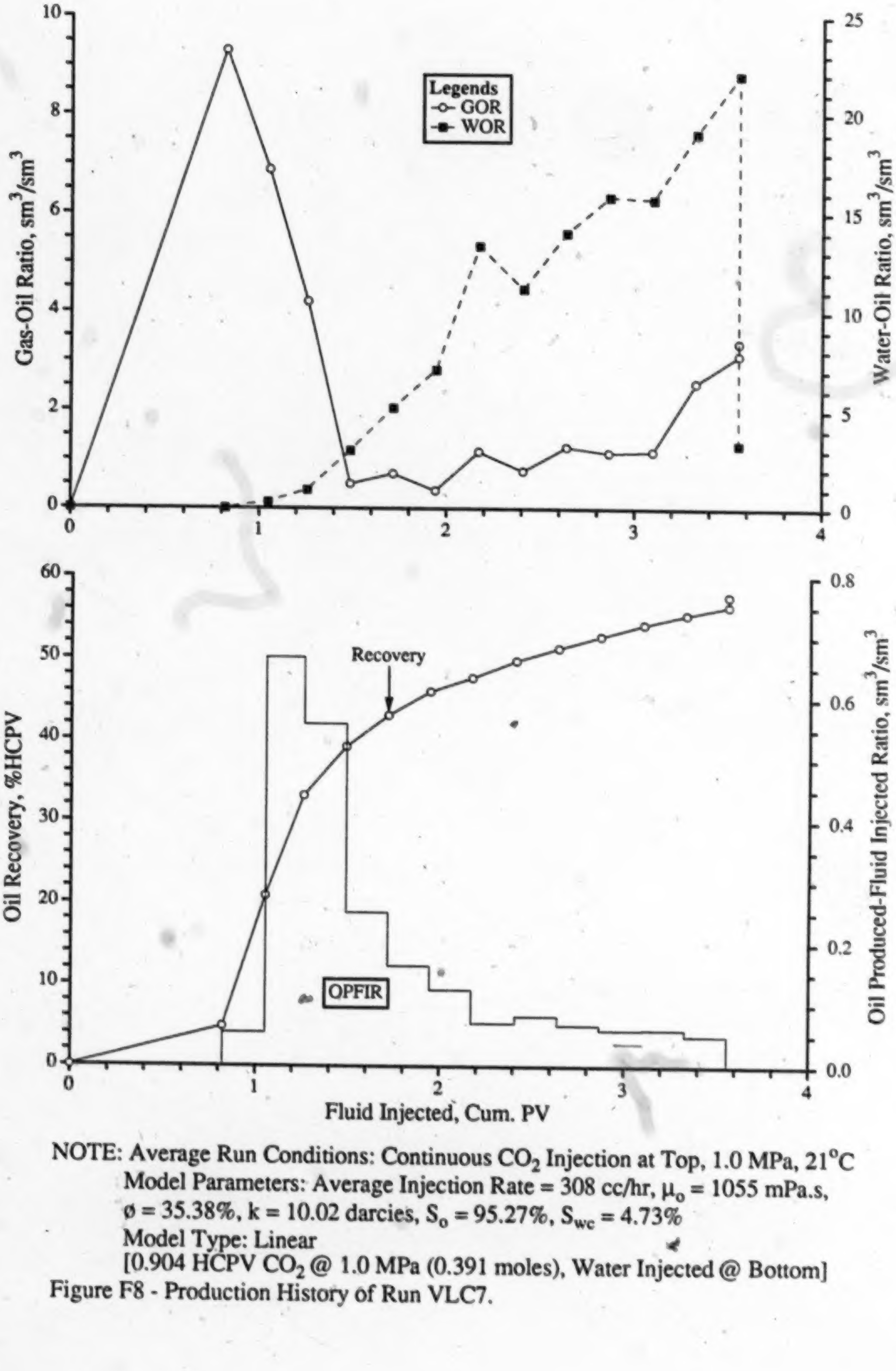

NOTE: Average Run Conditions: Continuous CO_2 Injection at Top, 1.0 MPa, 21°C
Model Parameters: Average Injection Rate = 308 cc/hr, μ_o = 1055 mPa.s,
ϕ = 35.38%, k = 10.02 darcies, S_o = 95.27%, S_{wc} = 4.73%
Model Type: Linear
[0.904 HCPV CO_2 @ 1.0 MPa (0.391 moles), Water Injected @ Bottom]

Figure F8 - Production History of Run VLC7.

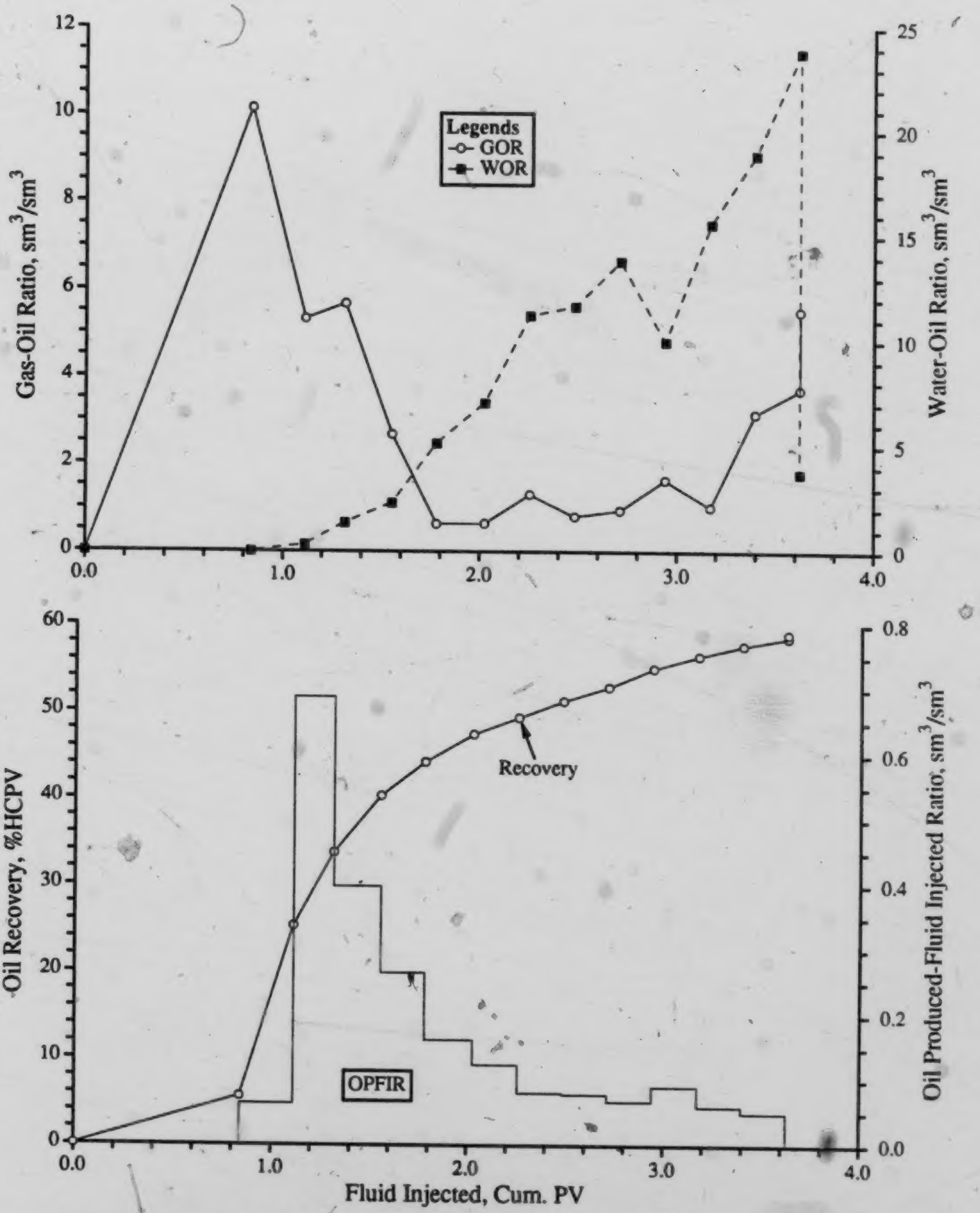

NOTE: Average Run Conditions: Continuous CO_2 Injection at Top, 1.0 MPa, 21°C
Model Parameters: Average Injection Rate = 308 cc/hr, μ_o = 1055 mPa.s,
ϕ = 35.45%, k = 9.44 darcies, S_o = 95.55%, S_{wc} = 4.45%
Model Type: Linear
[1.703 HCPV CO_2 @ 1.0 MPa (0.748 moles), Water Injected @ Bottom]

Figure F9 - Production History of Run VLC8.

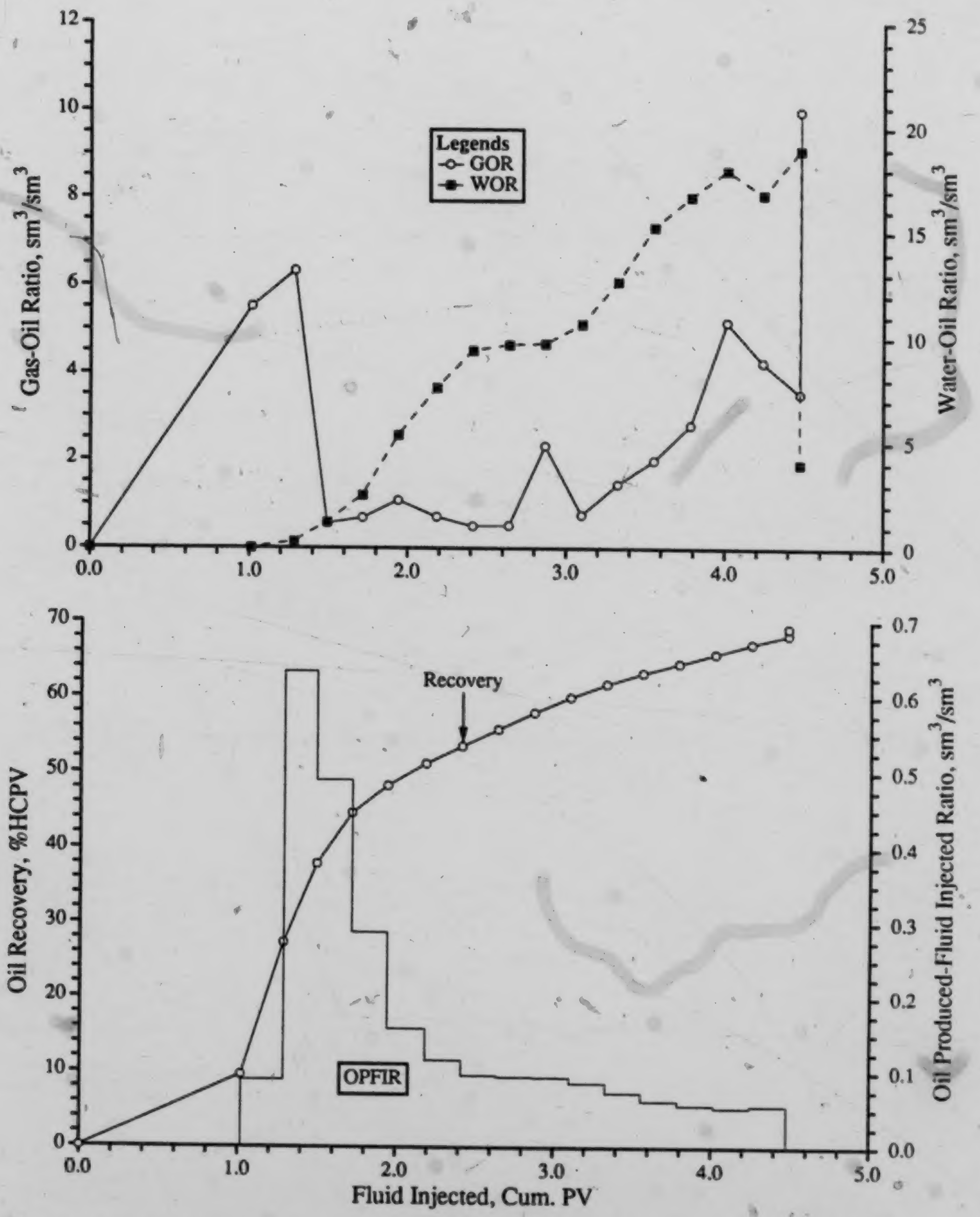

NOTE: Average Run Conditions: Continuous CO_2 Injection at Top, 1.0 MPa, 21°C
Model Parameters: Average Injection Rate = 154 cc/hr, μ_o = 1053.0 mPa.s,
ϕ = 35.38%, k = 10.58 darcies, S_o = 96.18%, S_{wc} = 3.82%
Model Type: Linear
[1.015 HCPV CO_2 @ 1.0 MPa (0.484 moles), Water Injected @ Bottom]

Figure F10 - Production History of Run VLC9.

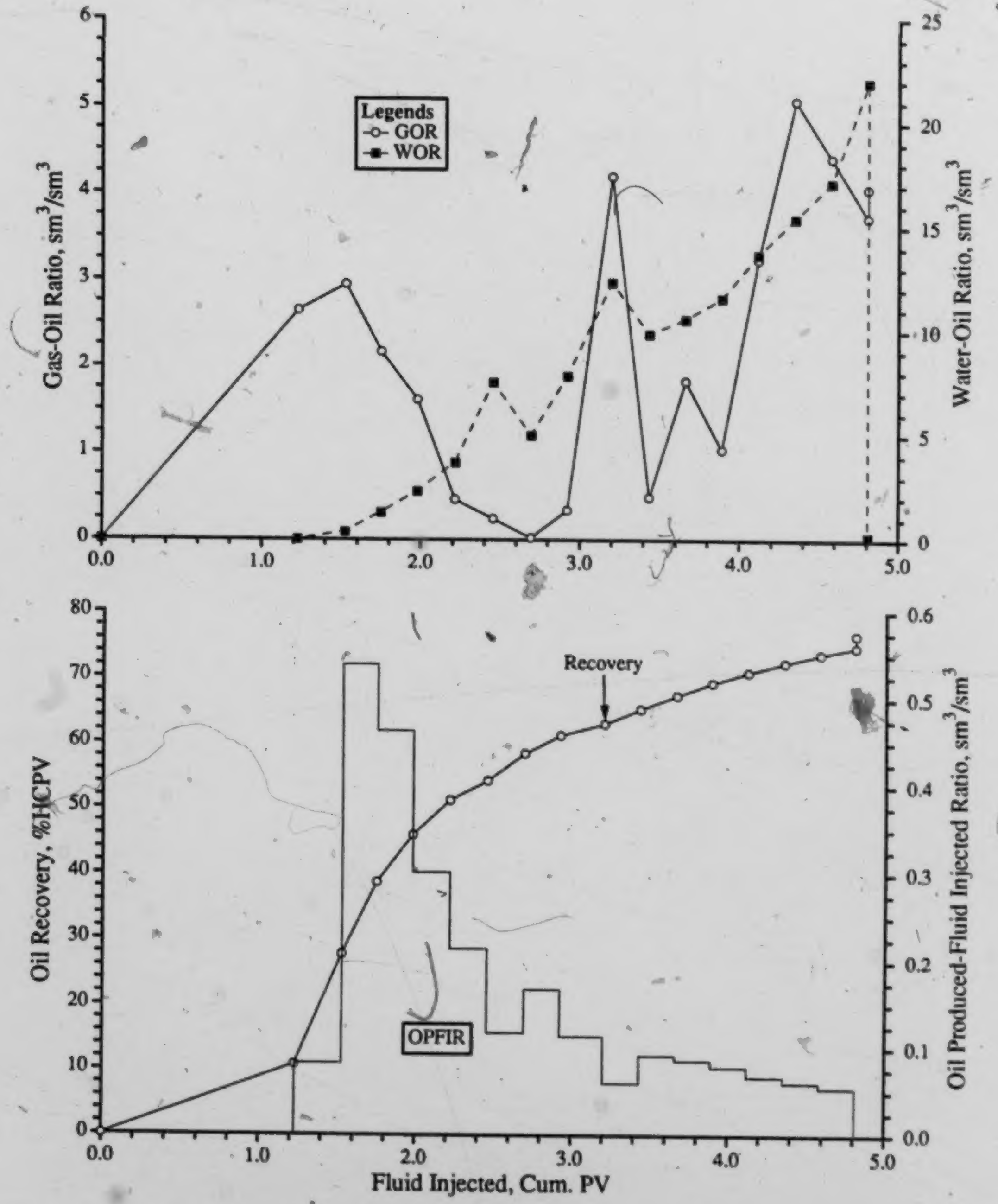

NOTE: Average Run Conditions: Continuous CO_2 Injection at Top, 1.0 MPa, 21°C
Model Parameters: Average Injection Rate = 154 cc/hr, μ_o = 10550 mPa.s,
ϕ = 35.38%, k = 11.02 darcies, S_o = 5.09%, S_{wc} = 4.91%
Model Type: Linear
[1.341 HCPV CO_2 @ 1.0 MPa (0.578 moles), Water Injected @ Bottom]

Figure F11 - Production History of Run VLC10.

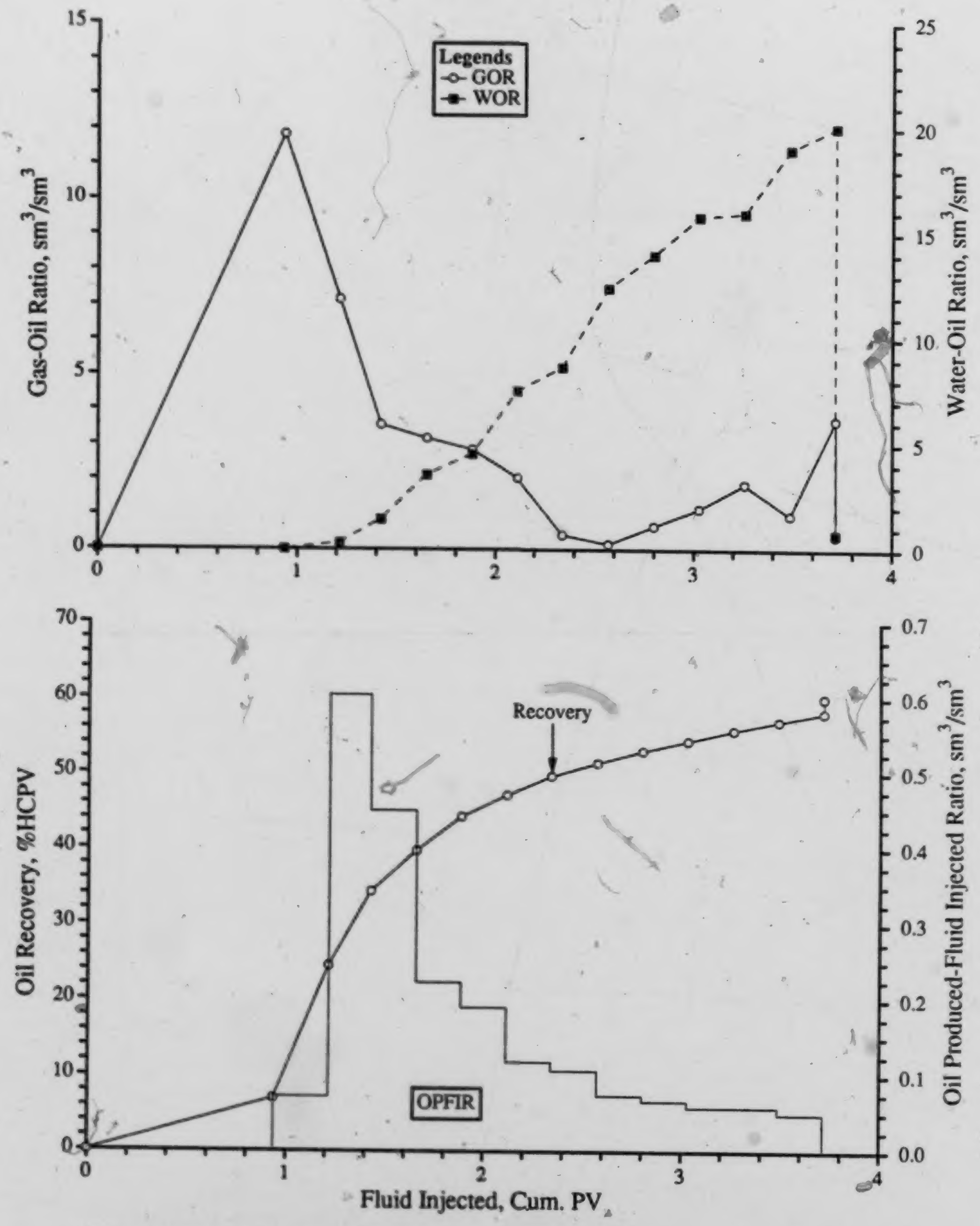

NOTE: Average Run Conditions: Continuous CO_2 Injection at Top, 1.0 MPa, 21°C
Model Parameters: Average Injection Rate = 308 cc/hr, μ_o = 1053.0 mPa.s,
ϕ = 35.56%, k = 10.75 darcies, S_o = 95.88%, S_{wc} = 4.12%
Model Type: Linear
[0.935 HCPV CO_2 @ 1.0 MPa (0.448 moles), Water Injected @ Bottom]

Figure F12 - Production History of Run VLC11.

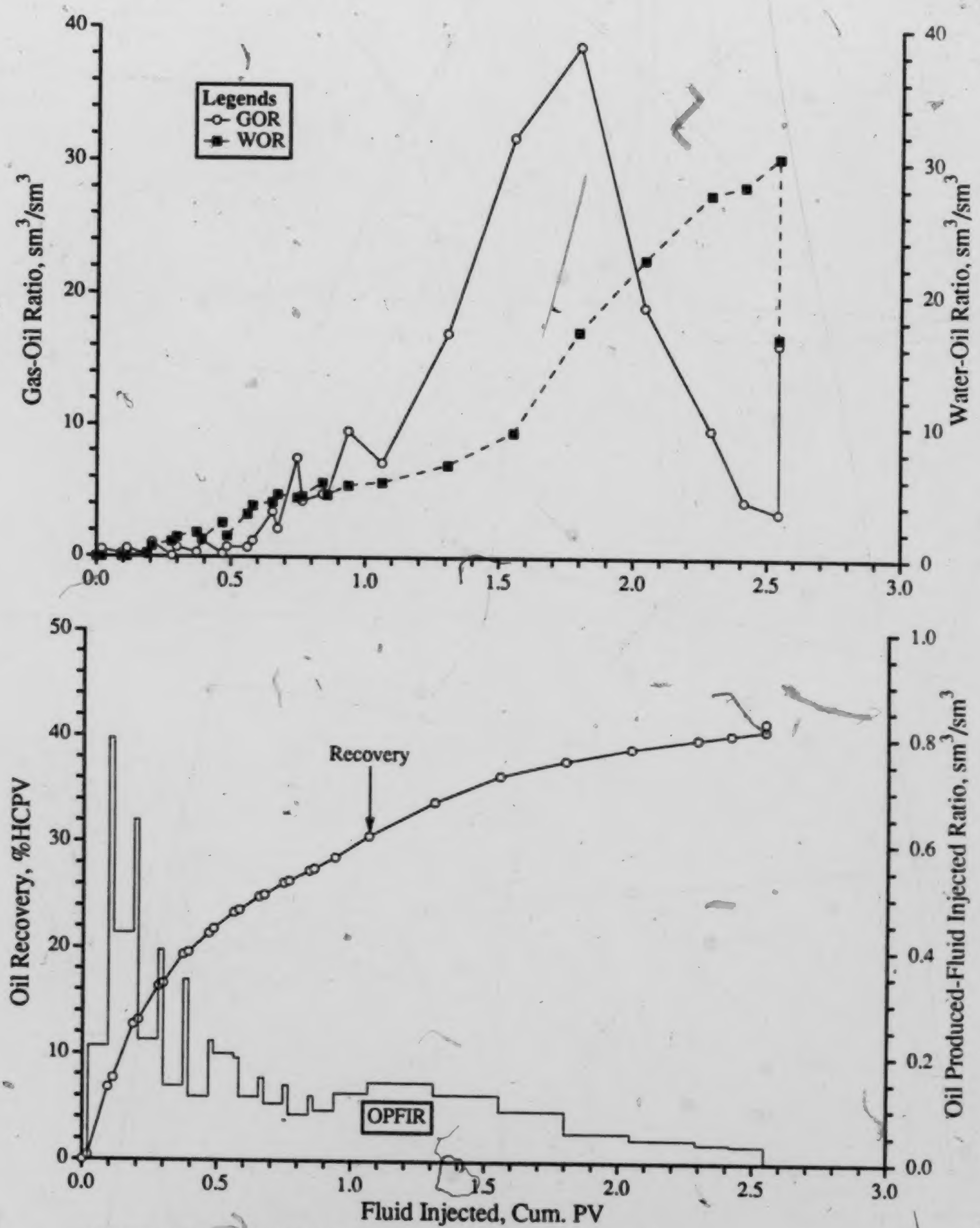

NOTE: Quarter of A 5-Spot

Model Parameters: Average Injection Rate =92.42 cc/hr, μ_o = 603 mPa.s, ϕ = 40.1 %, k = 12.0 darcies, S_{oi} = 93.3 %, S_{wc} = 6.7 %

[0.20 HCPV CO_2 @ 2.5 MPa & 21°C (0.450 mol), 4:1 WAG, 10 Slugs]

Figure F13 - Production History of Run H2D1.

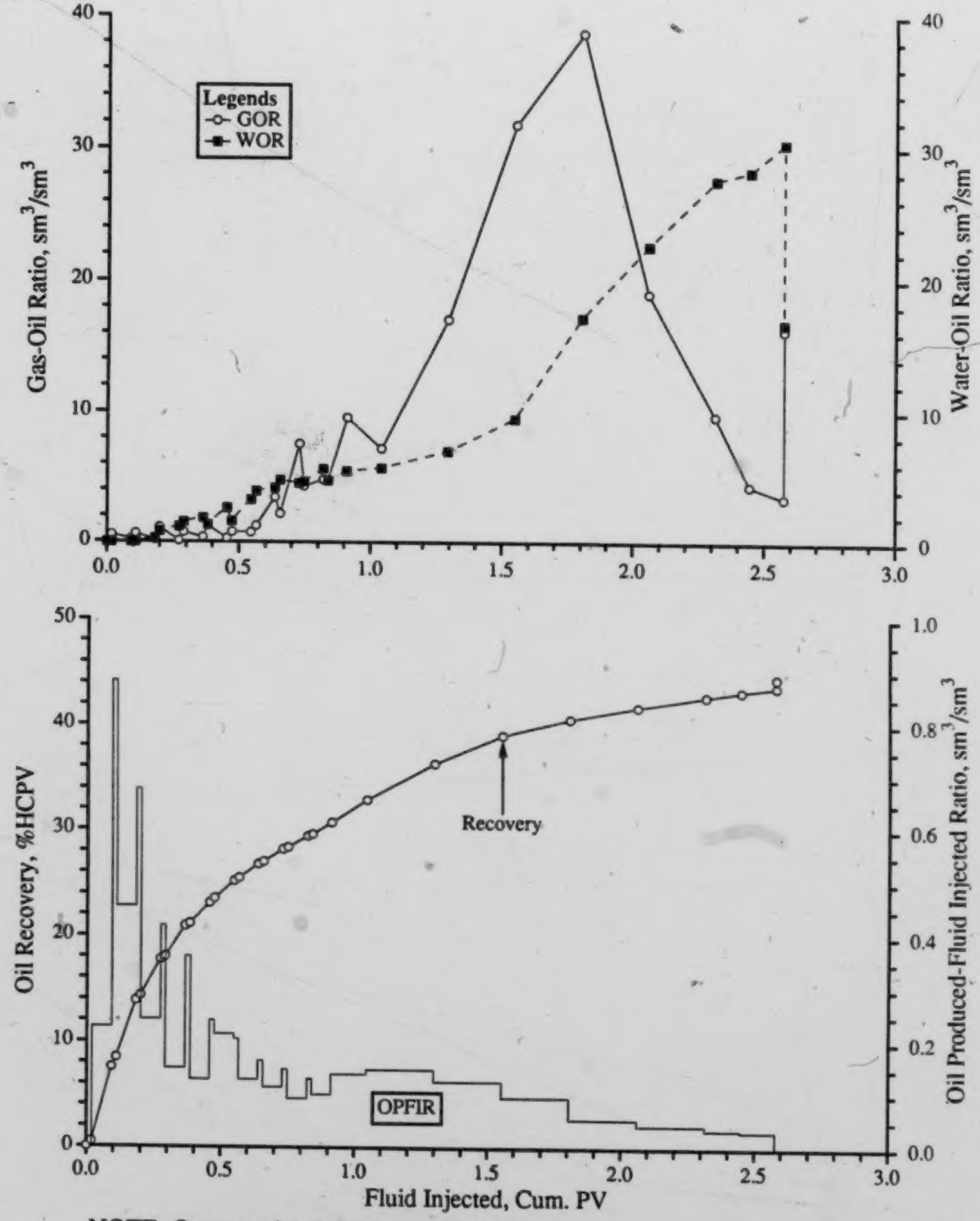

NOTE: Quarter of A 5-Spot

Model Parameters: Average Injection Rate = 1.55 m/d, μ_o = 603.0 mPa.s, ϕ = 39.7 %, k = 14.5 darcies, S_{oi} = 90.7 %, S_{wc} = 9.3 %

[0.20 HCPV CO_2 @ 2.5 MPa & 21°C (0.423 mol), 4:1 WAG, 10 Slugs]

Figure F14 - Production History of Run H2D2.

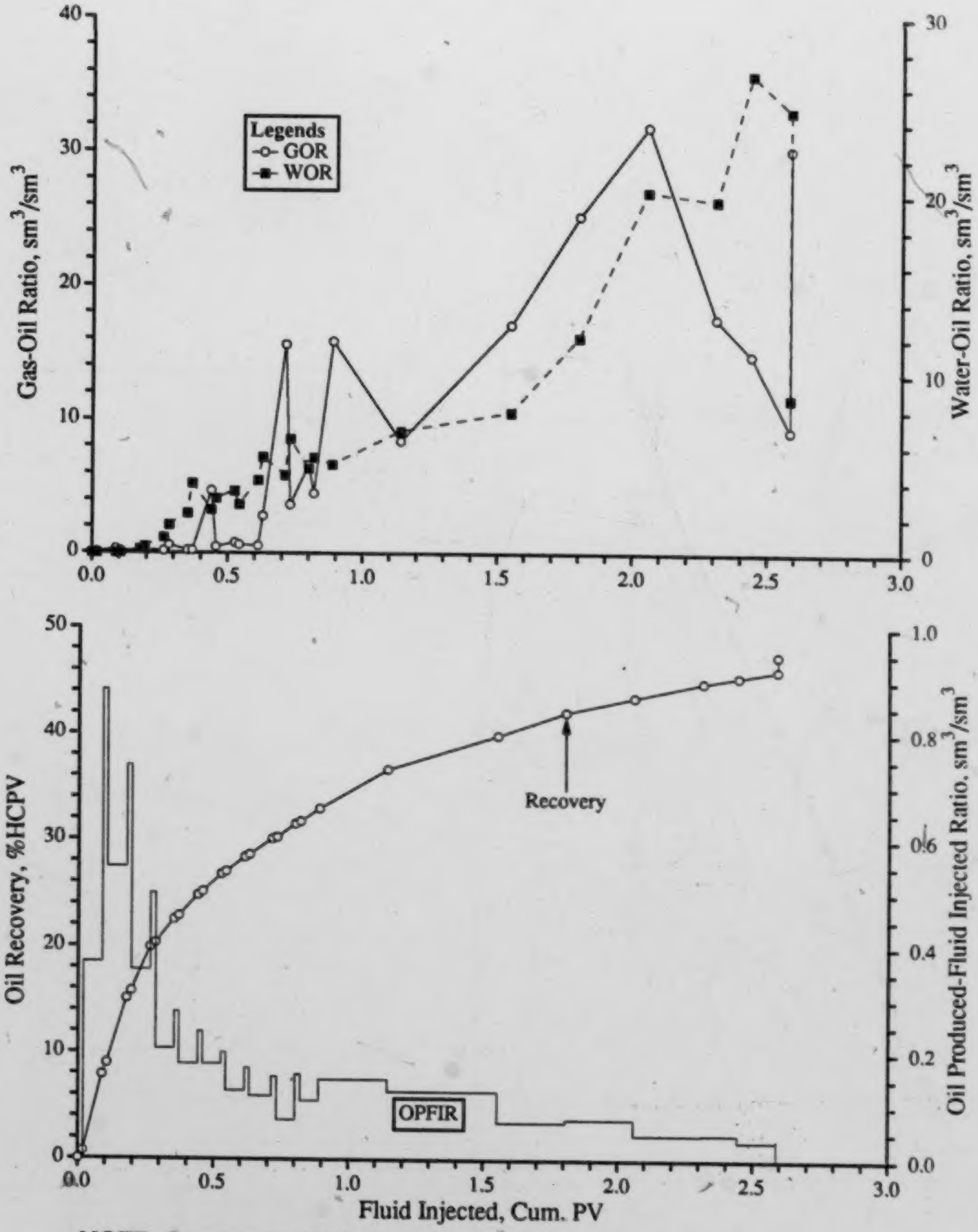

NOTE: Quarter of A 5-Spot

Model Parameters: Average Injection Rate = 2.54 m/d, μ_o = 603.0 mPa.s, ϕ = 39.8%, k = 13.2 darcies, S_{oi} = 86.9 %, S_{wc} = 13.1%

[0.20 HCPV CO_2 @ 2.5 MPa & 21°C (0.406 mol), 4:1 WAG, 10 Slugs]

Figure F15 - Production History of Run H2D3.

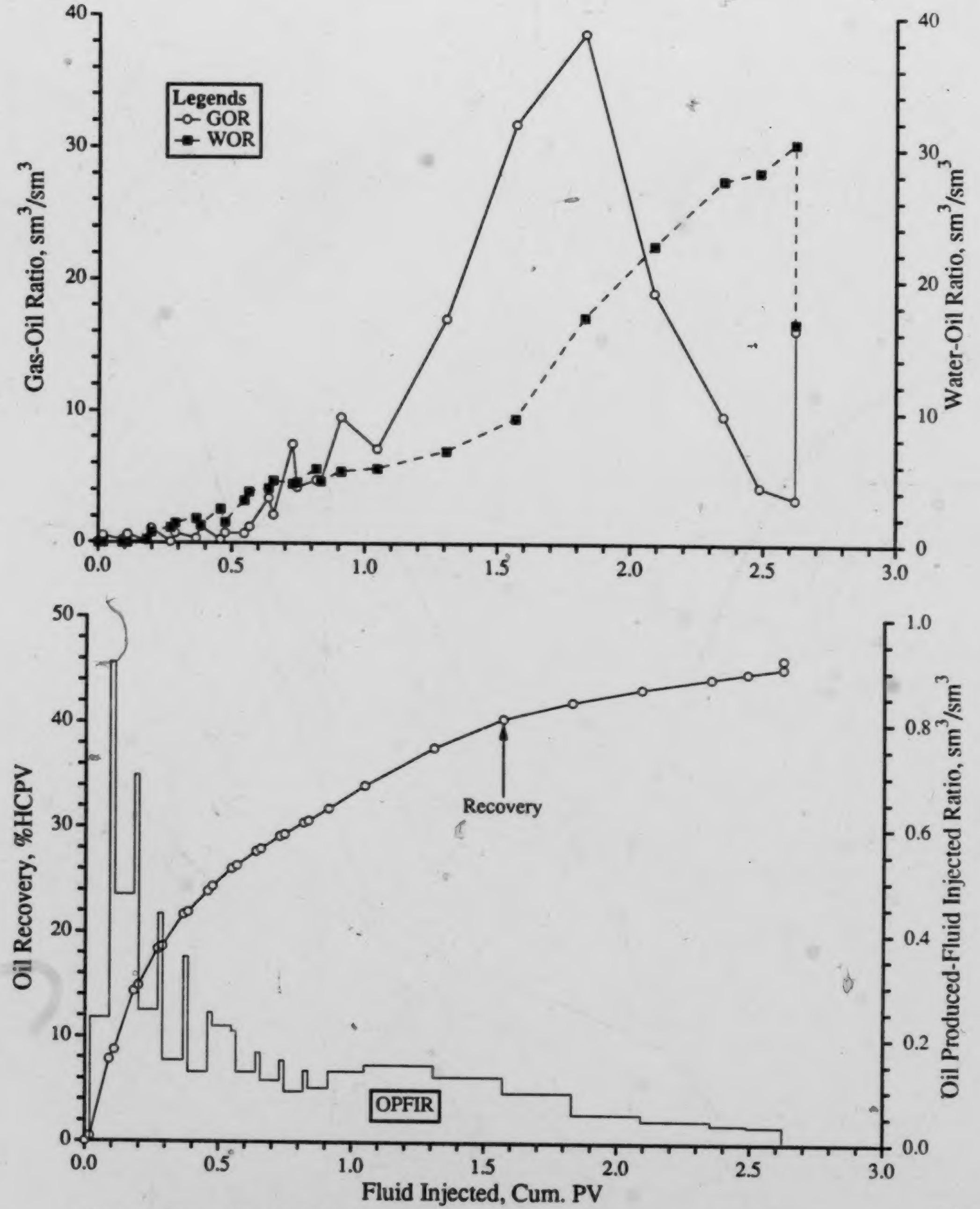

NOTE: Quarter of A 5-Spot

Model Parameters: Average Flow Velocity = 3.17 m/d, μ_o = 603.0 mPa.s,
ø = 38.7 %, k = 15.7 darcies, S_{oi} = 89.9 %, S_{wc} = 10.1 %

[0.20 HCPV CO_2 @ 2.5 MPa & 21°C (0.408 moles), 4:1 WAG, 10 Slugs]

Figure F16 - Production History of Run H2D4.

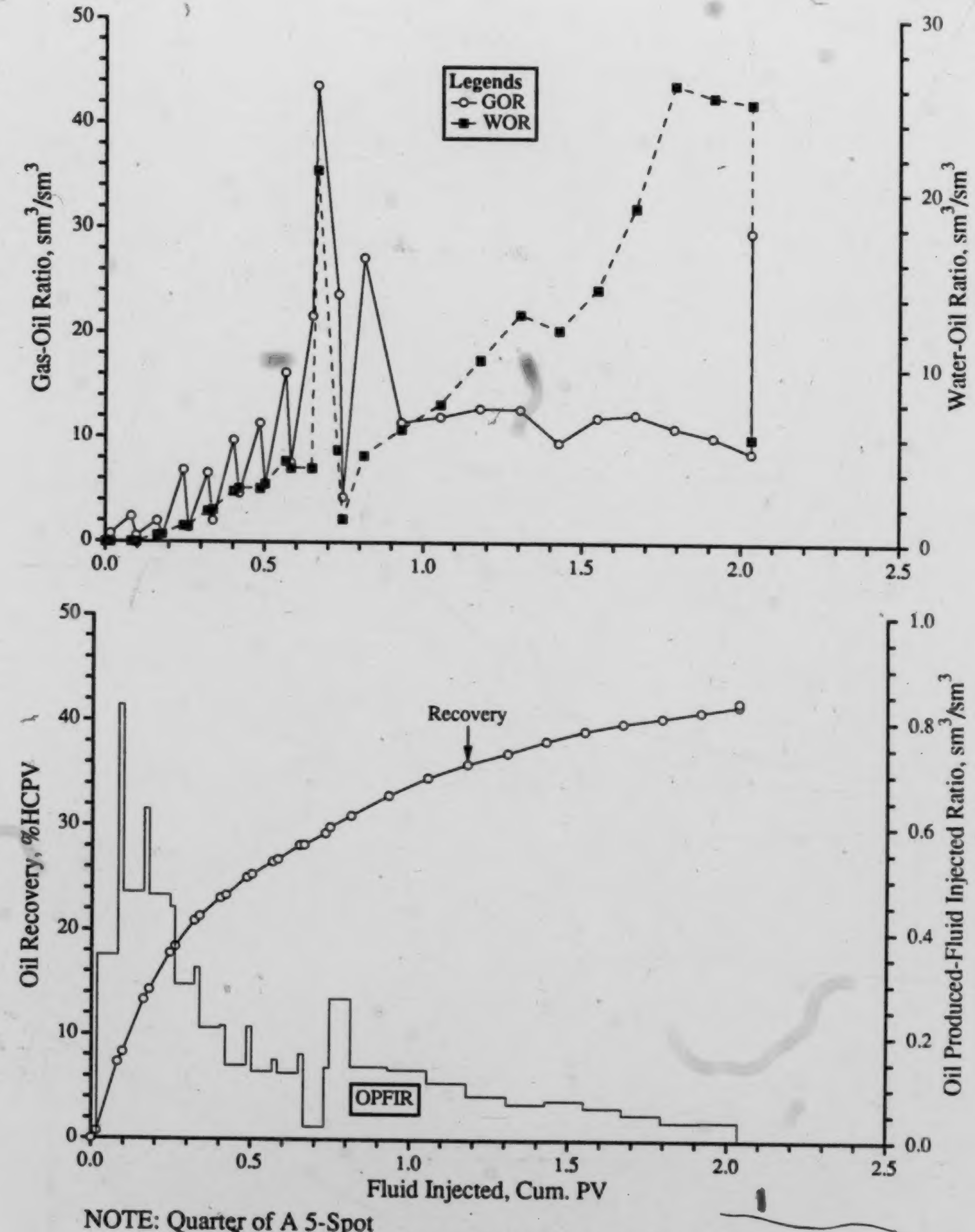

NOTE: Quarter of A 5-Spot

Model Parameters: Average Injection Rate = 451.23 cc/hr, μ_o = 603 mPa.s, ϕ = 42.8 %, k = 12.3 darcies, S_{oi} = 81.2 %, S_{wc} = 18.8 %

[0.20 HCPV CO_2 @ 2.5 MPa & 21°C (0.407 mol), 4:1 WAG, 10 Slugs]

Figure F17 - Production History of Run H2D5.

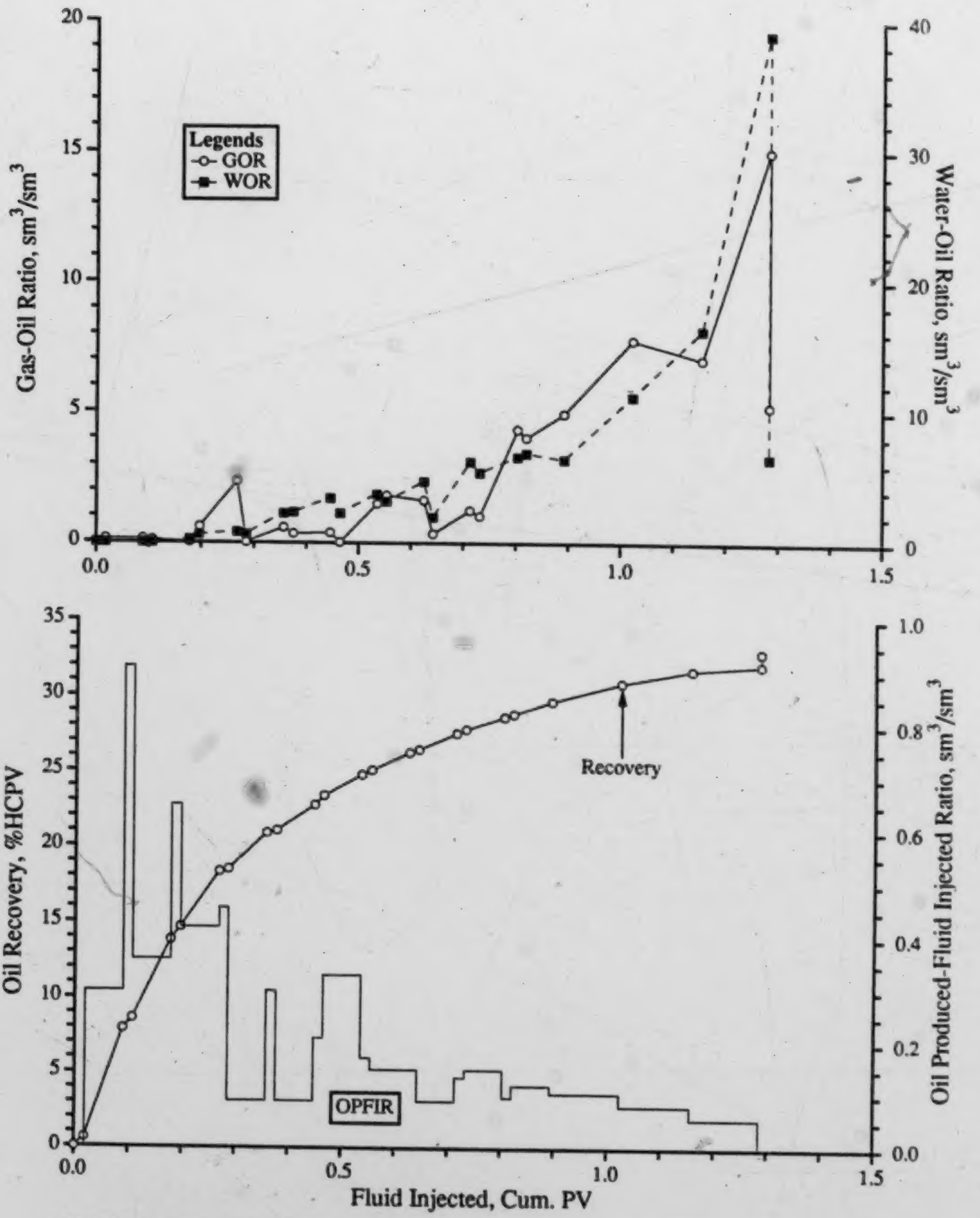

NOTE: Quarter of A 5-Spot

Model Parameters: Average Injection Velocity = 0.78 m/d, μ_o = 1058 mPa.s, ϕ = 37.4 %, k = 12.18 darcies, S_{oi} = 88.1 %, S_{wc} = 11.9 %

[0.20 HCPV CO_2 @ 2.5 MPa & 21°C (0.403 mol), 4:1 WAG, 10 Slugs]

Figure F18 - Production History of Run H2D6.

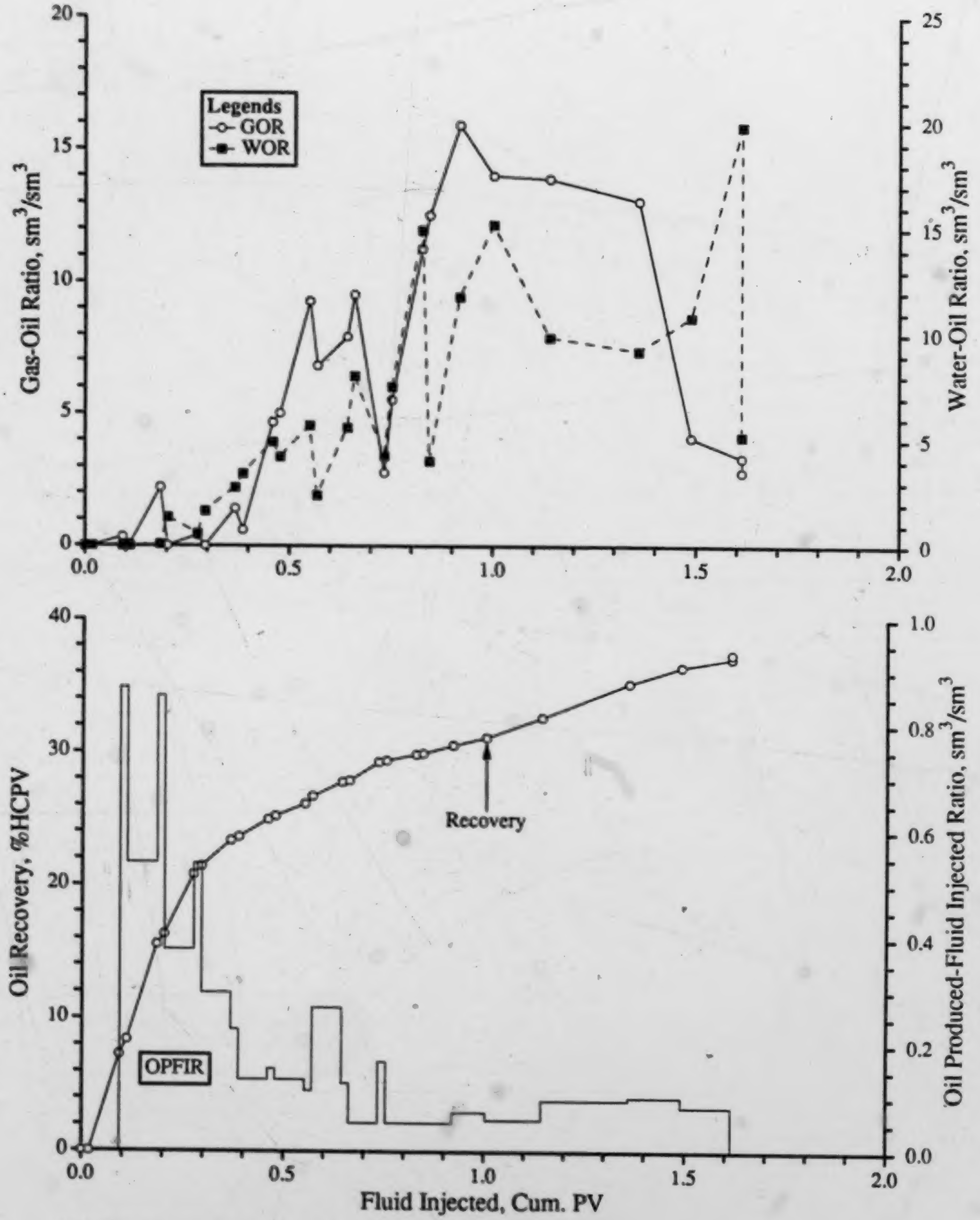

NOTE: Quarter of A 5-Spot

Model Parameters: Average Injection Velocity = 1.55 m/d, μ_o = 1058 mPa.s, ø = 41.6 %, k = 13.9 darcies, S_{oi} = 88.3 %, S_{wc} = 11.7 %

[0.20 HCPV CO_2 @ 2.5 MPa & 21°C (0.445 mol), 4:1 WAG, 10 Slugs]

Figure F19 - Production History of Run H2D7.

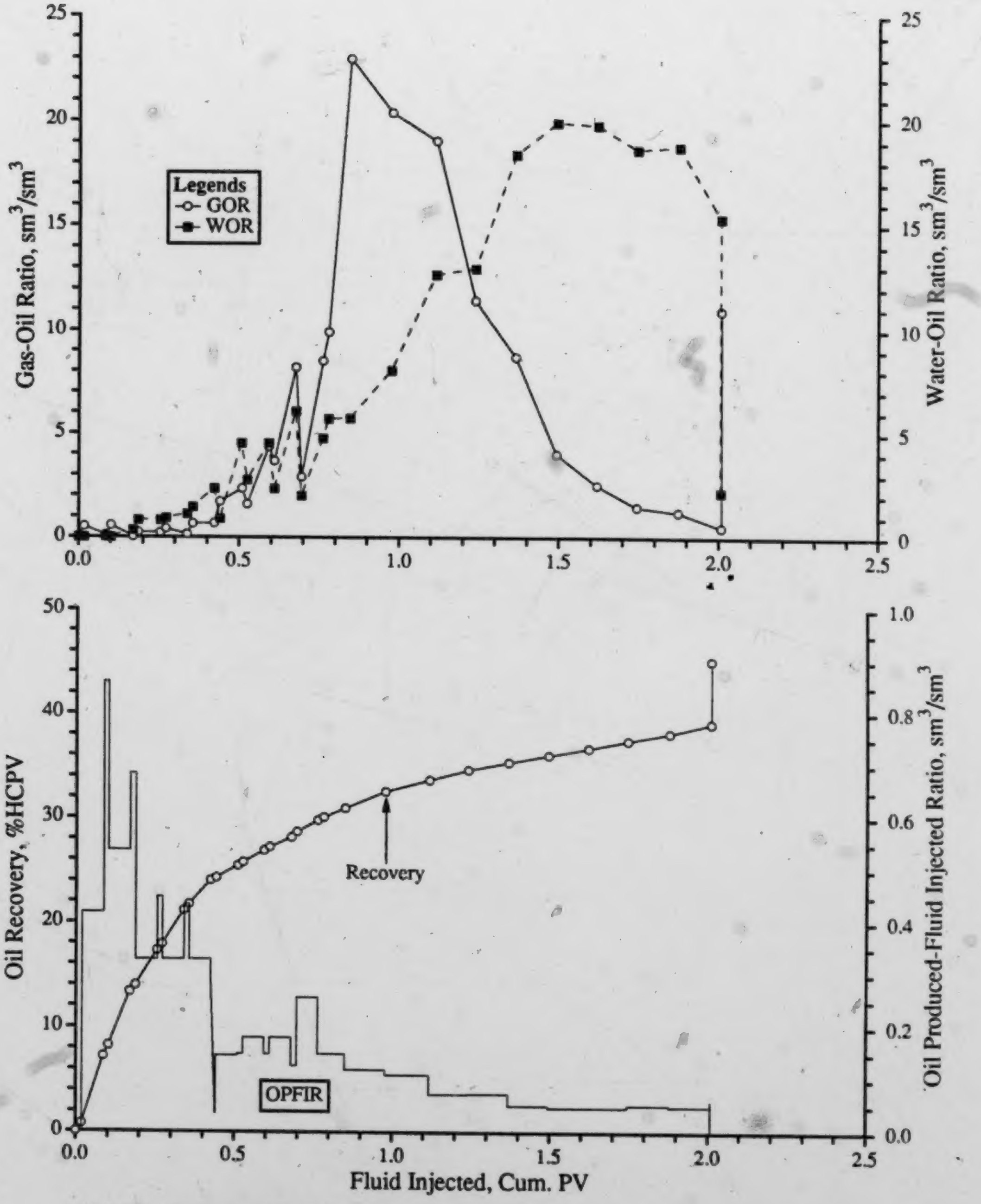

NOTE: Quarter of A 5-Spot

Model Parameters: Average Injection Rate = 2.6 m/d, μ_o = 1058 mPa.s, ø = 40.5 %, k = 12.5 darcies, S_{oi} = 90.7 %, S_{wc} = 9.3 %

[0.20 HCPV CO_2 @ 2.5 MPa & 21°C (0.432 mol), 4:1 WAG, 10 Slugs]

Figure F20 - Production History of Run H2D8.

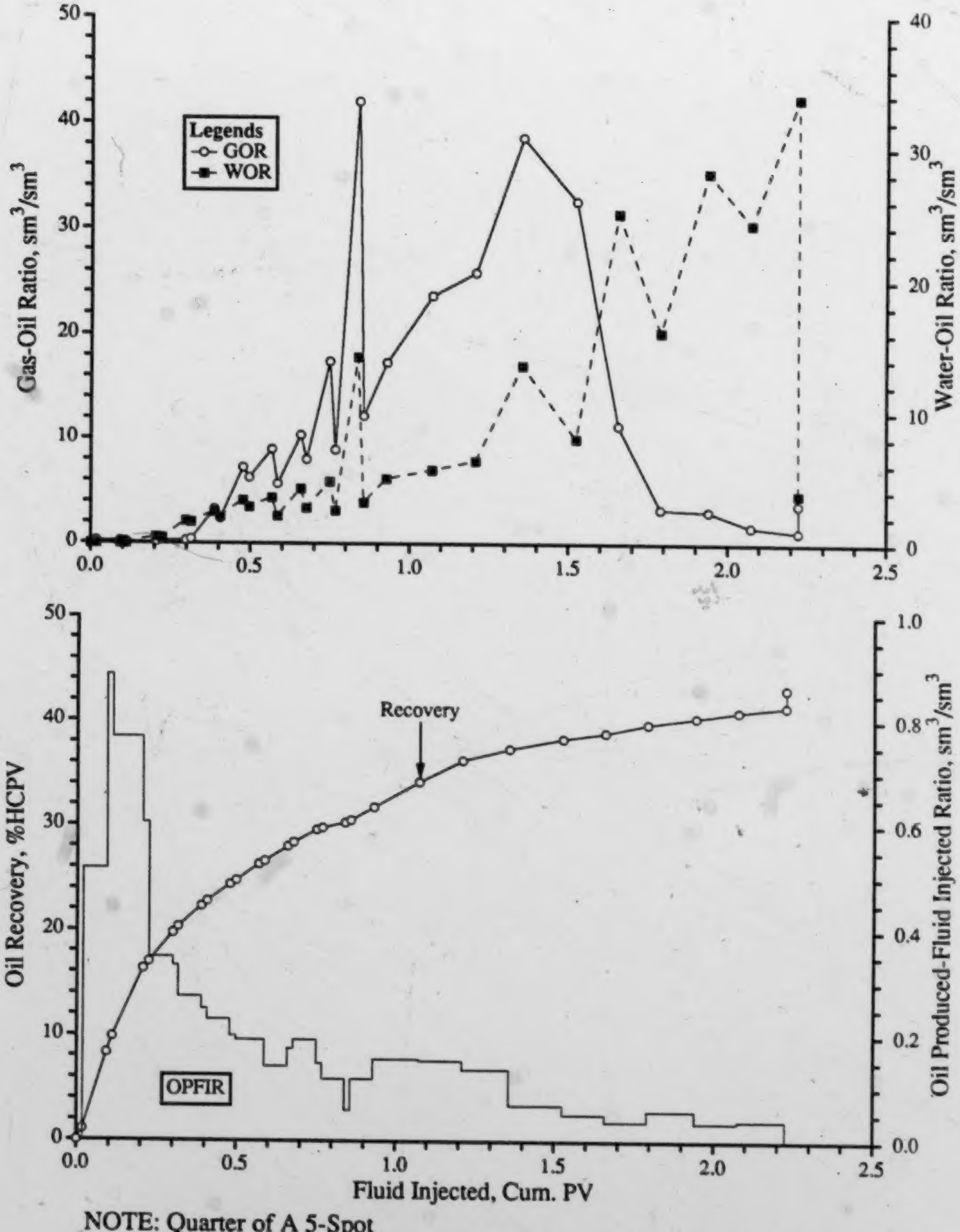

NOTE: Quarter of A 5-Spot

Model Parameters: Average Injection Rate =3.2 m/d, μ_o = 1058 mPa.s, ϕ = 38.5 %, k = 14.5 darcies, S_{oi} = 89.9 %, S_{wc} = 10.1 %

[0.20 HCPV CO_2 @ 2.5 MPa & 21°C (0.407 mol), 4:1 WAG, 10 Slugs]

Figure F21 - Production History of Run H2D9.

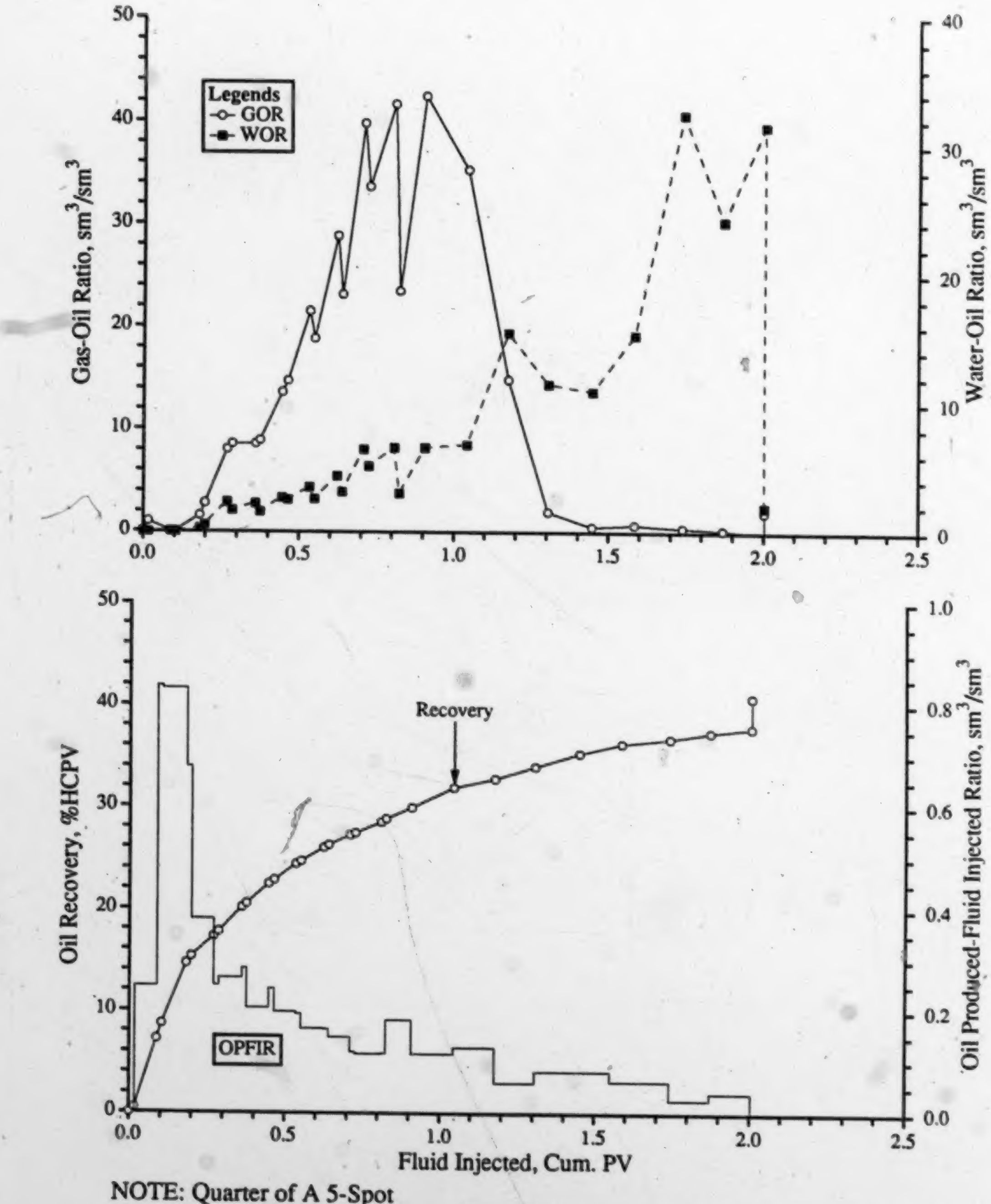

NOTE: Quarter of A 5-Spot

Model Parameters: Average Flow Velocity =3.81 m/d, μ_o = 1058.0 mPa.s, ø = 38.1 %, k = 12.3 darcies, S_{oi} = 89.1 %, S_{wc} = 10.9 %

[0.20 HCPV CO_2 @ 2.5 MPa & 21°C (0.407 mol), 4:1 WAG, 10 Slugs]

Figure F22 - Production History of Run H2D10.

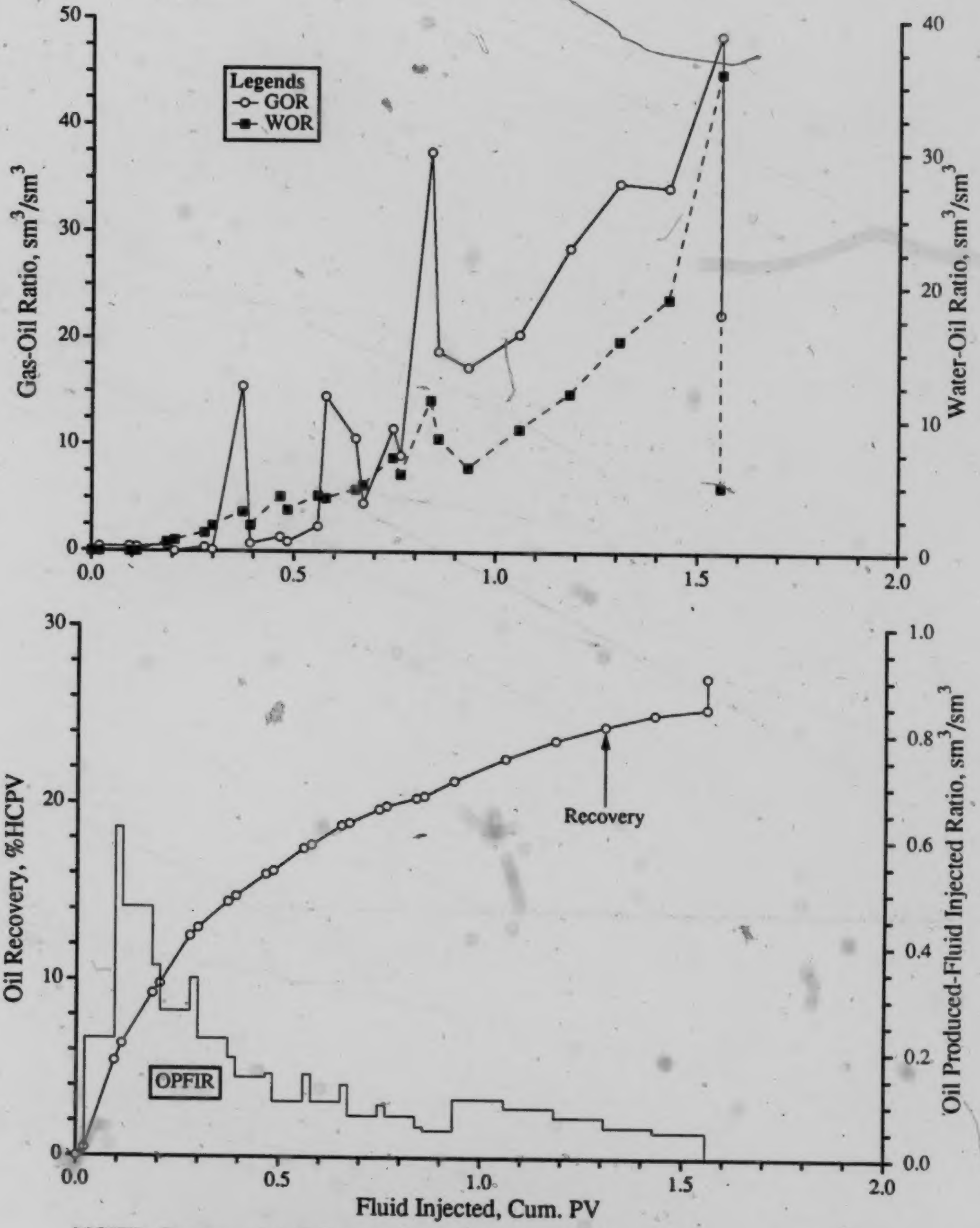

NOTE: Quarter of A 5-Spot

Model Parameters: Average Injection Rate = 0.78 m/d, μ_o = 1842 mPa.s, ϕ = 41.3 %, k = 12.7 darcies, S_{oi} = 93.2 %, S_{wc} = 6.8 %

[0.20 HCPV CO_2 @ 2.5 MPa & 21°C (0.460 moles), 4:1 WAG, 10 Slugs]

Figure F23 - Production History of Run H2D11.

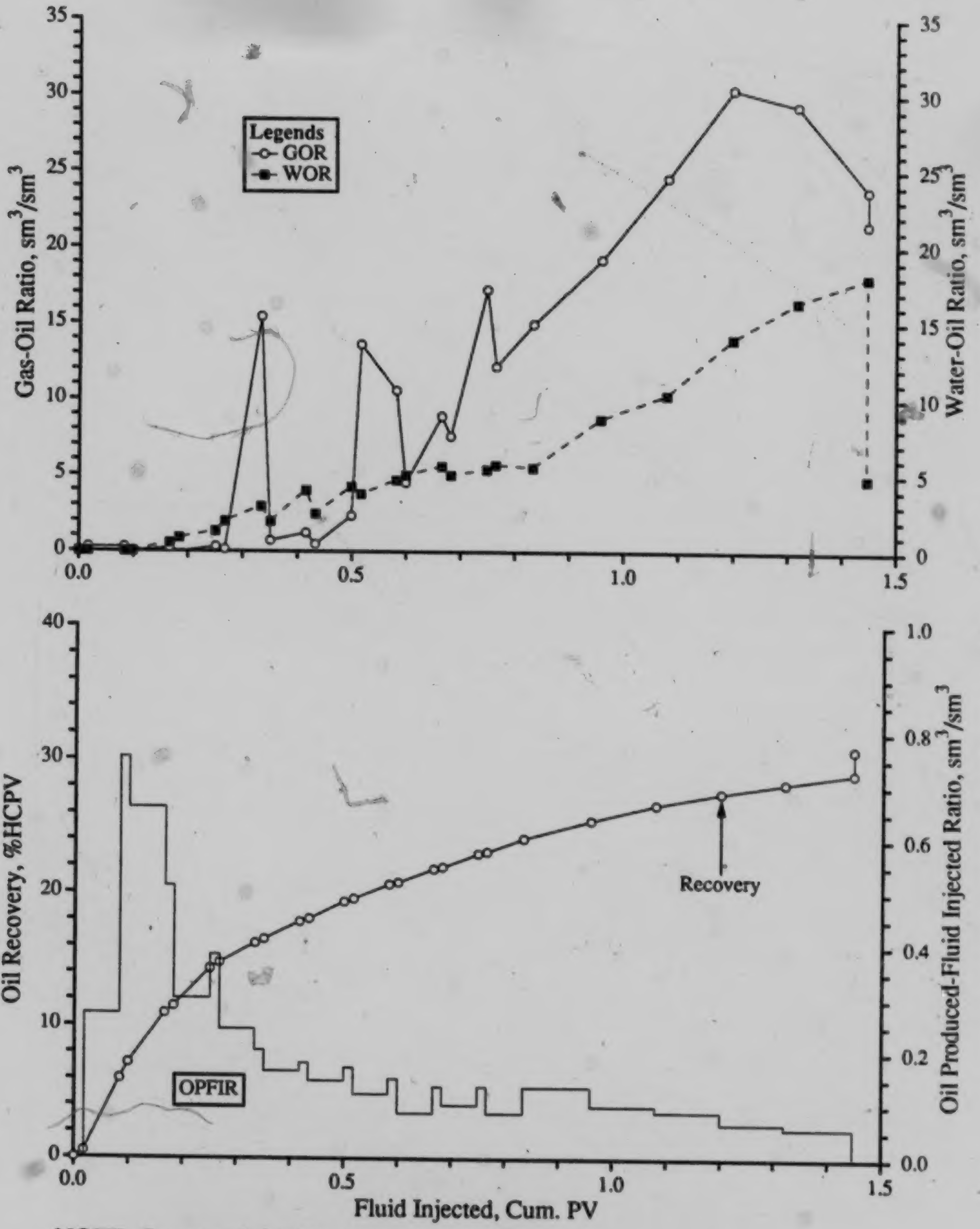

NOTE: Quarter of A 5-Spot

Model Parameters: Average Injection Rate = 1.55 m/d, μ_o = 1842 mPa.s, ø = 43.7 %, k = 14.1 darcies, S_{oi} = 91.4 %, S_{wc} = 8.6 %

[0.20 HCPV CO_2 @ 2.5 MPa & 21°C (0.462 mol), 4:1 WAG, 10 Slugs]

Figure F24 - Production History of Run H2D12.

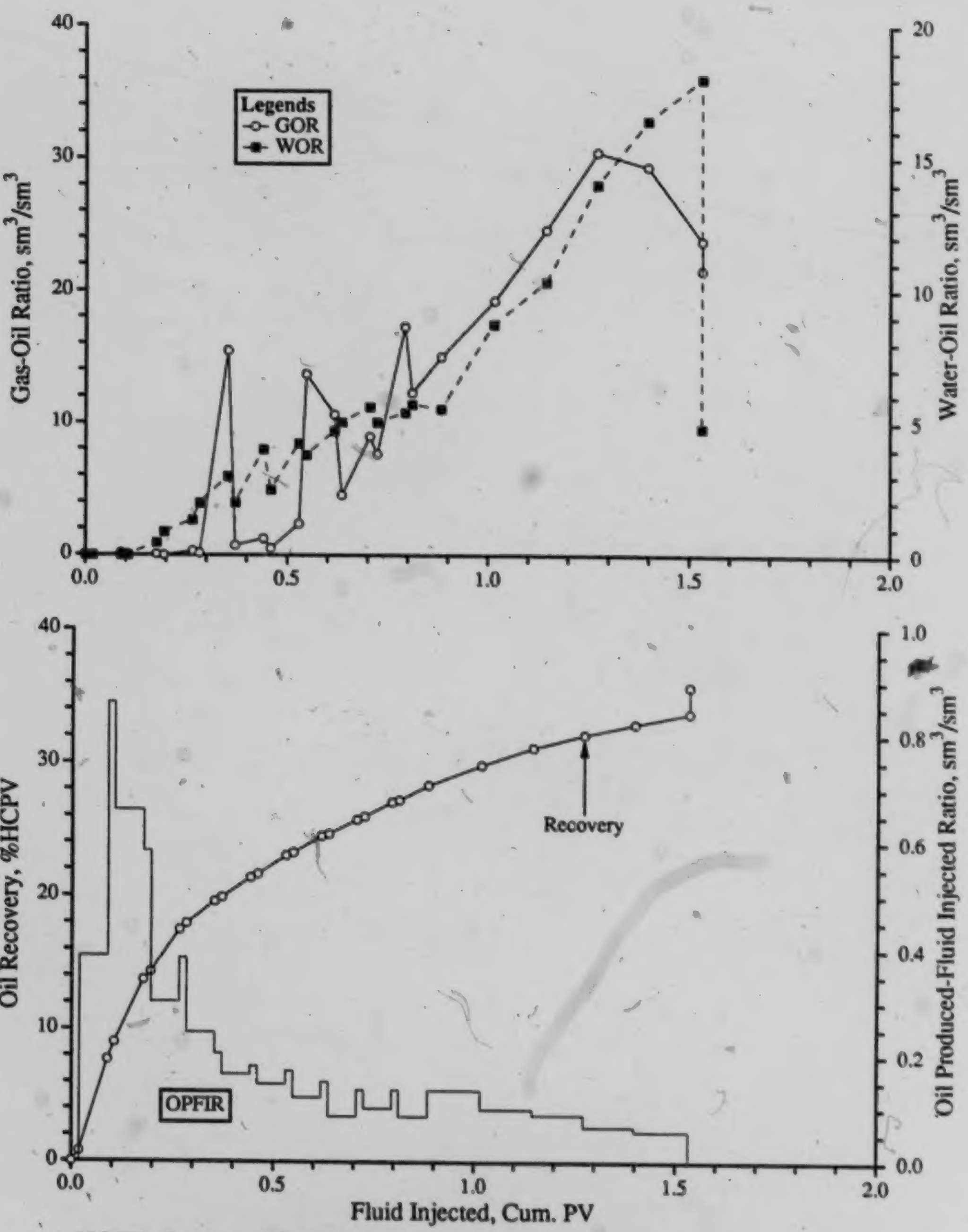

NOTE: Quarter of A 5-Spot

Model Parameters: Average Injection Rate = 2.54 m/d, μ_o = 1842 mPa.s, ϕ = 41.1 %, k = 12.5 darcies, S_{oi} = 87.8%, S_{wc} = 12.2 %

[0.20 HCPV CO_2 @ 2.5 MPa & 21°C (0.419 mol), 4:1 WAG, 10 Slugs]

Figure F25 - Production History of Run H2D13.

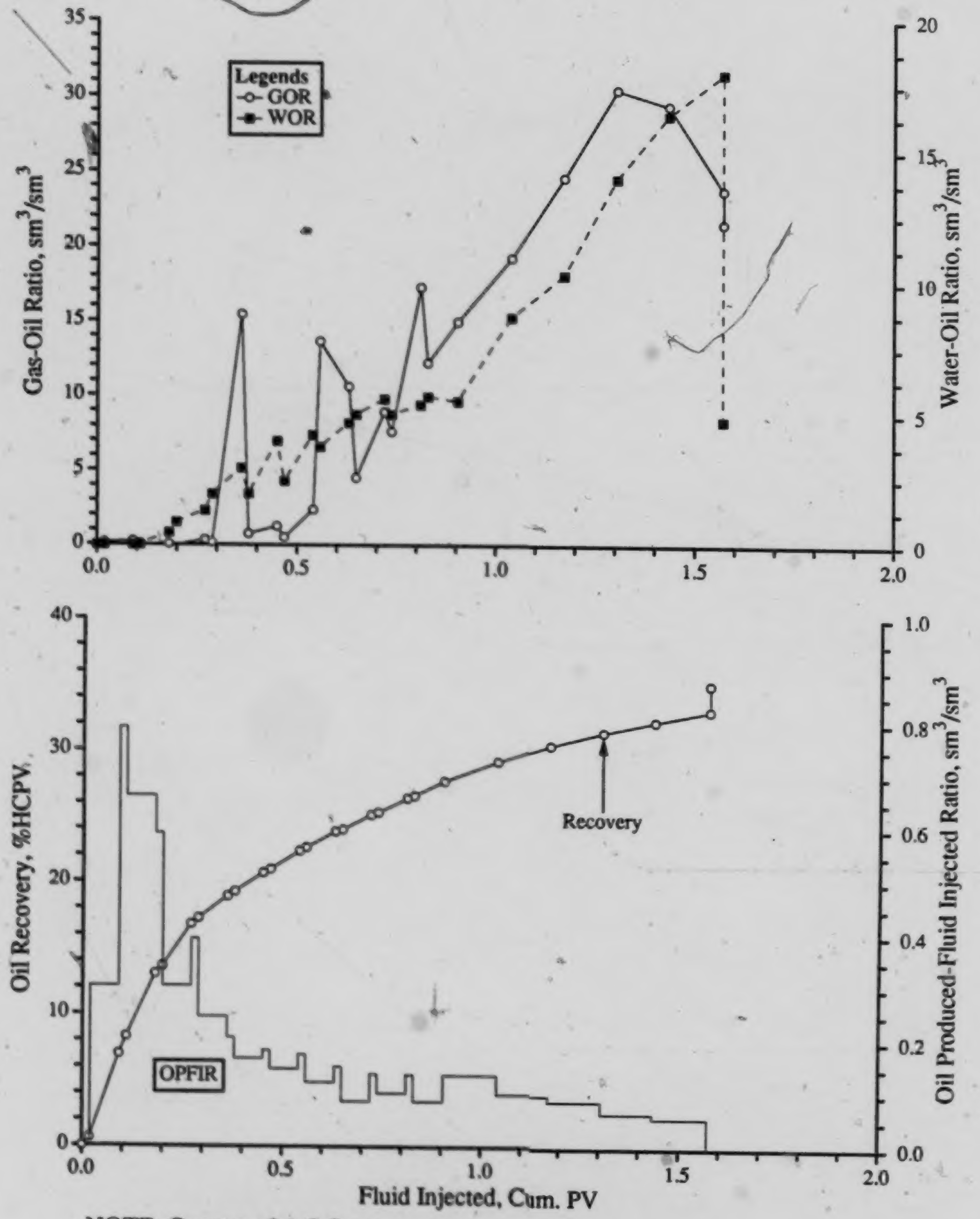

NOTE: Quarter of A 5-Spot

Model Parameters: Average Flow Velocity = 3.17 m/d, μ_o = 1842 mPa.s, $ø$ = 39.5 %, k = 13.4 darcies, S_{oi} = 90.1 %, S_{wc} = 9.9 %

[0.20 HCPV CO_2 @ 2.5 MPa & 21°C (0.418 mol), 4:1 WAG, 10 Slugs]

Figure F26 - Production History of Run H2D14.

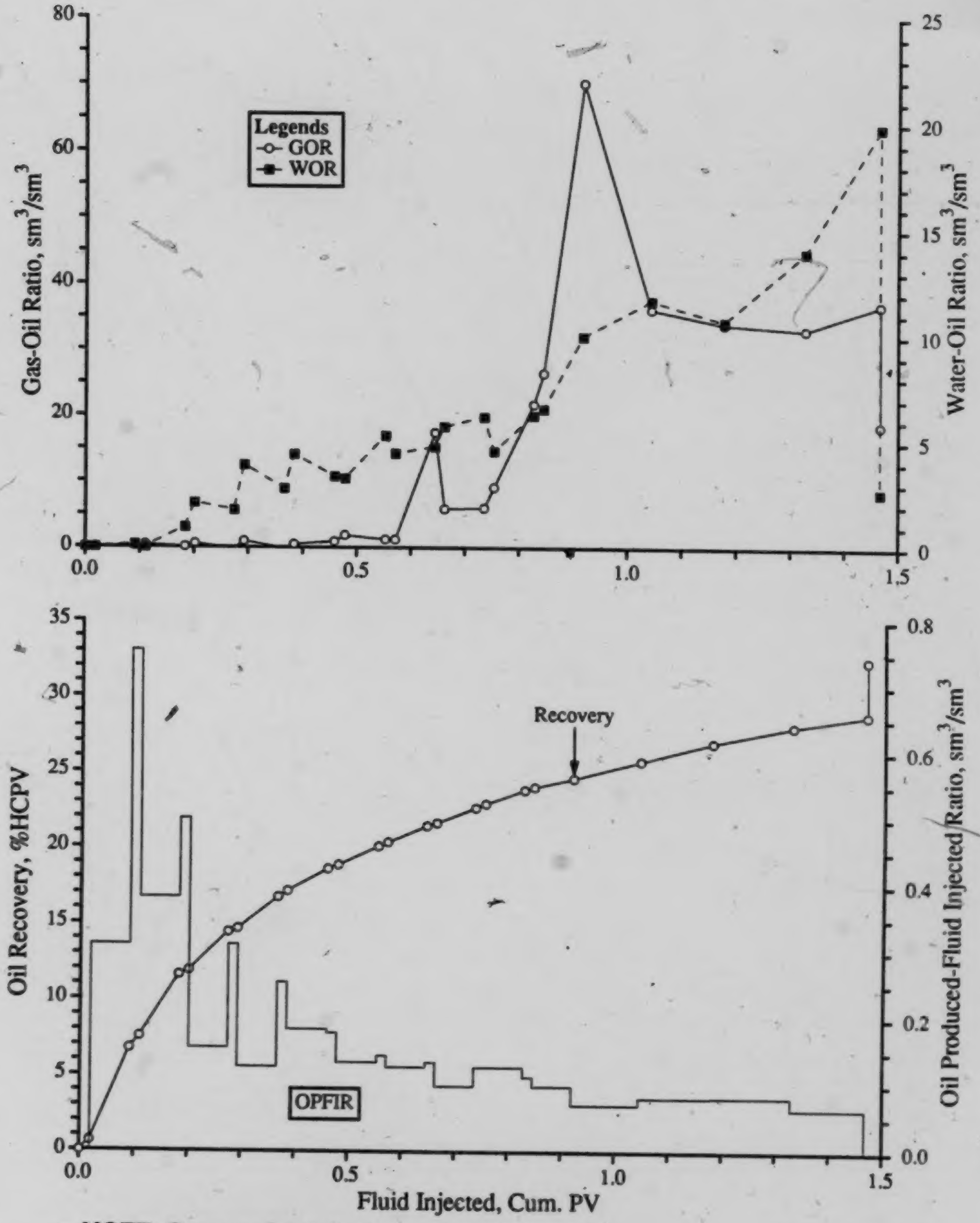

NOTE: Quarter of A 5-Spot

Model Parameters: Average Flow Velocity = 3.81 m/d, μ_o = 1842 mPa.s, ϕ = 39.8 %, k = 13.1 darcies, S_{oi} = 90.3 %, S_{wc} = 9.7 %

[0.20 HCPV CO_2 @ 2.5 MPa & 21°C (0.421 mol), 4:1 WAG, 10 Slugs]

Figure F27 - Production History of Run H2D15.

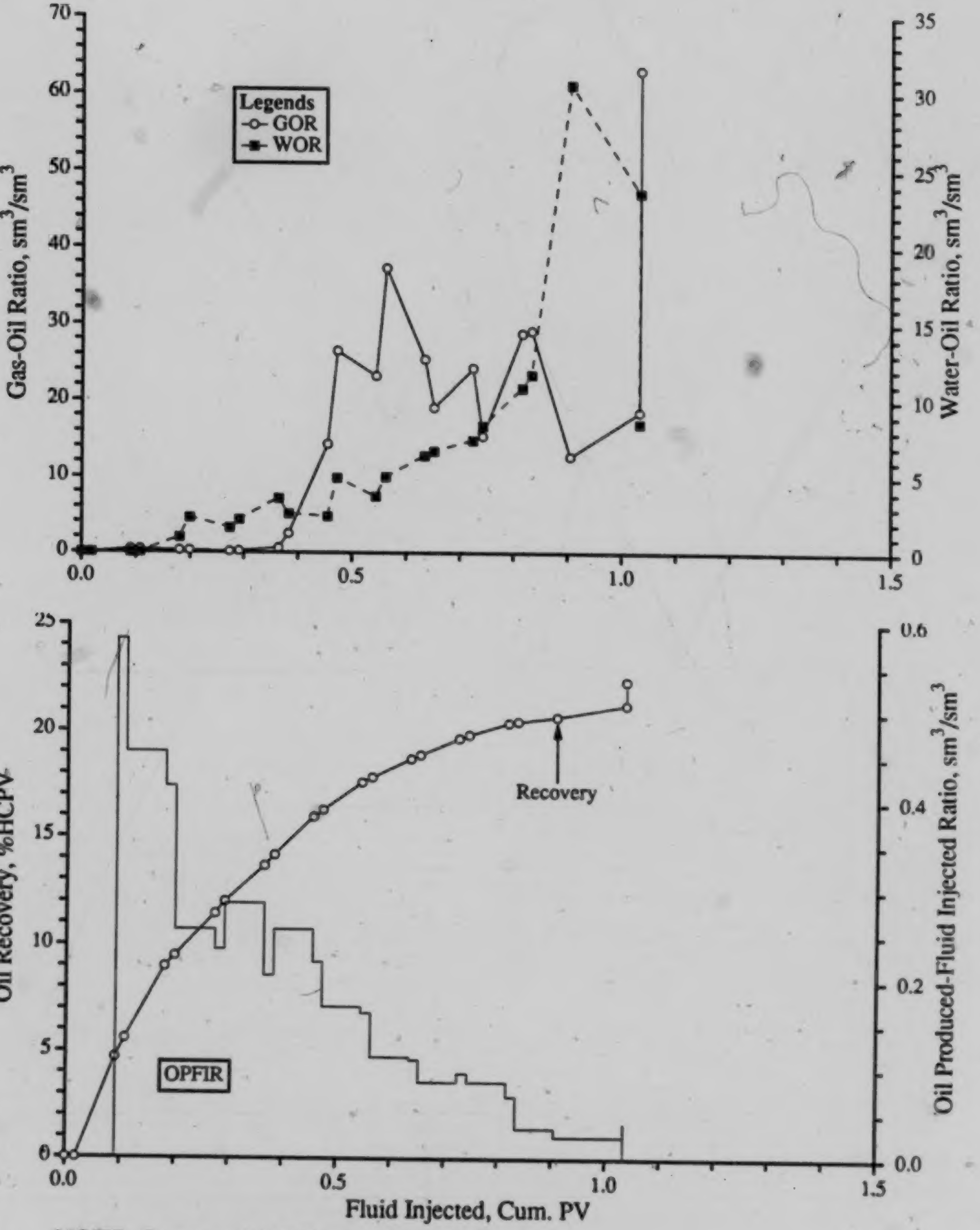

NOTE: Quarter of A 5-Spot

Model Parameters: Average Flow Velocity = 0.78 cc/hr, μ_o = 3295 mPa.s, ϕ = 39.9 %, k = 12.7 darcies, S_{oi} = 90.0 %, S_{wc} = 10.0 %

[0.20 HCPV CO_2 @ 2.5 MPa & 21°C (0.421 mol), 4:1 WAG, 10 Slugs]

Figure F28 - Production History of Run H2D16.

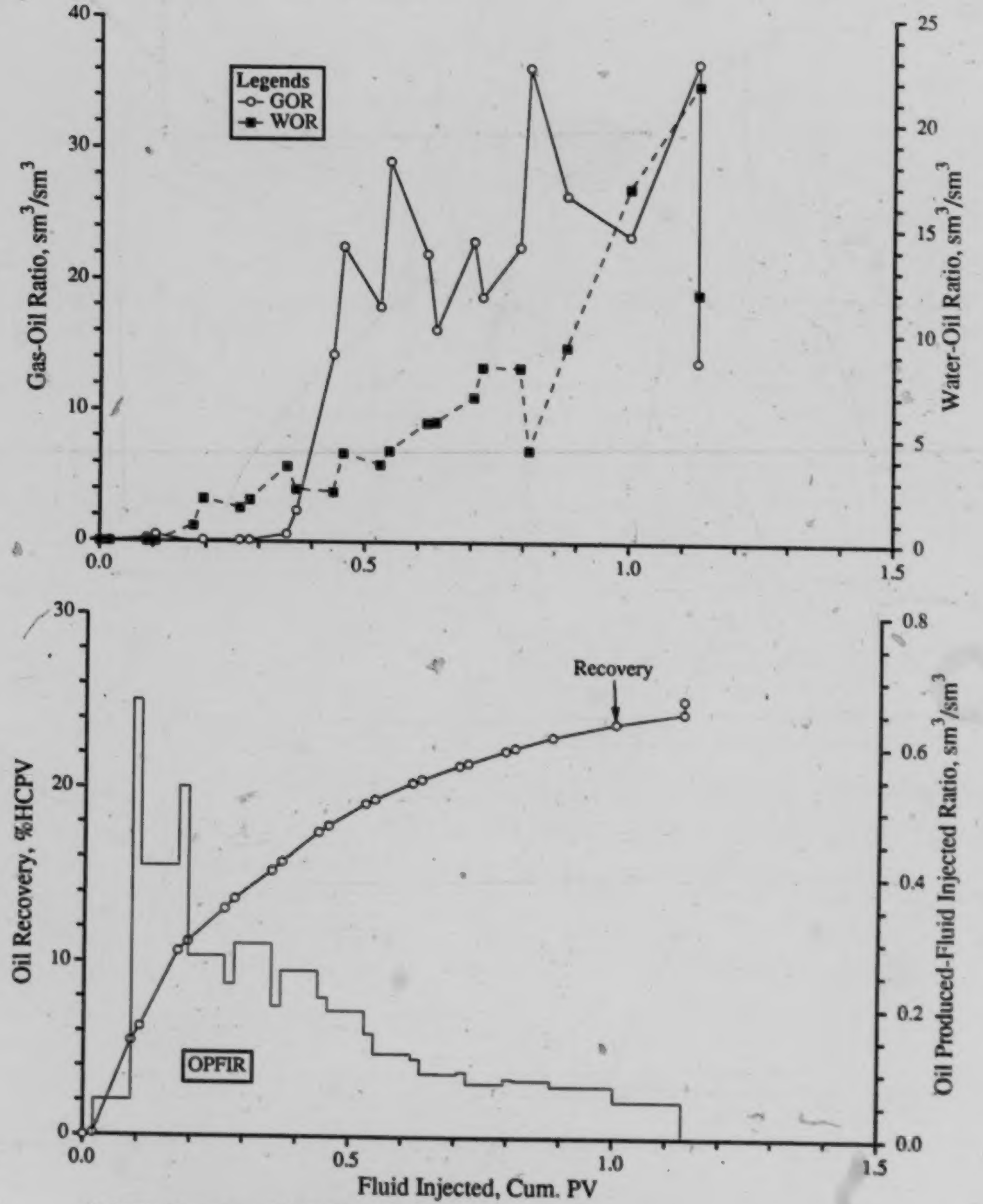

NOTE: Quarter of A 5-Spot

Model Parameters: Average Flow Velocity = 1.55 m/d, μ_o = 3295 mPa.s, ϕ = 42.4 %, k = 14.0 darcies, S_{oi} = 87.8 %, S_{wc} = 12.3 %

[0.20 HCPV CO_2 @ 2.5 MPa & 21°C (0.436 mol), 4:1 WAG, 10 Slugs]

Figure F29 - Production History of Run H2D17.

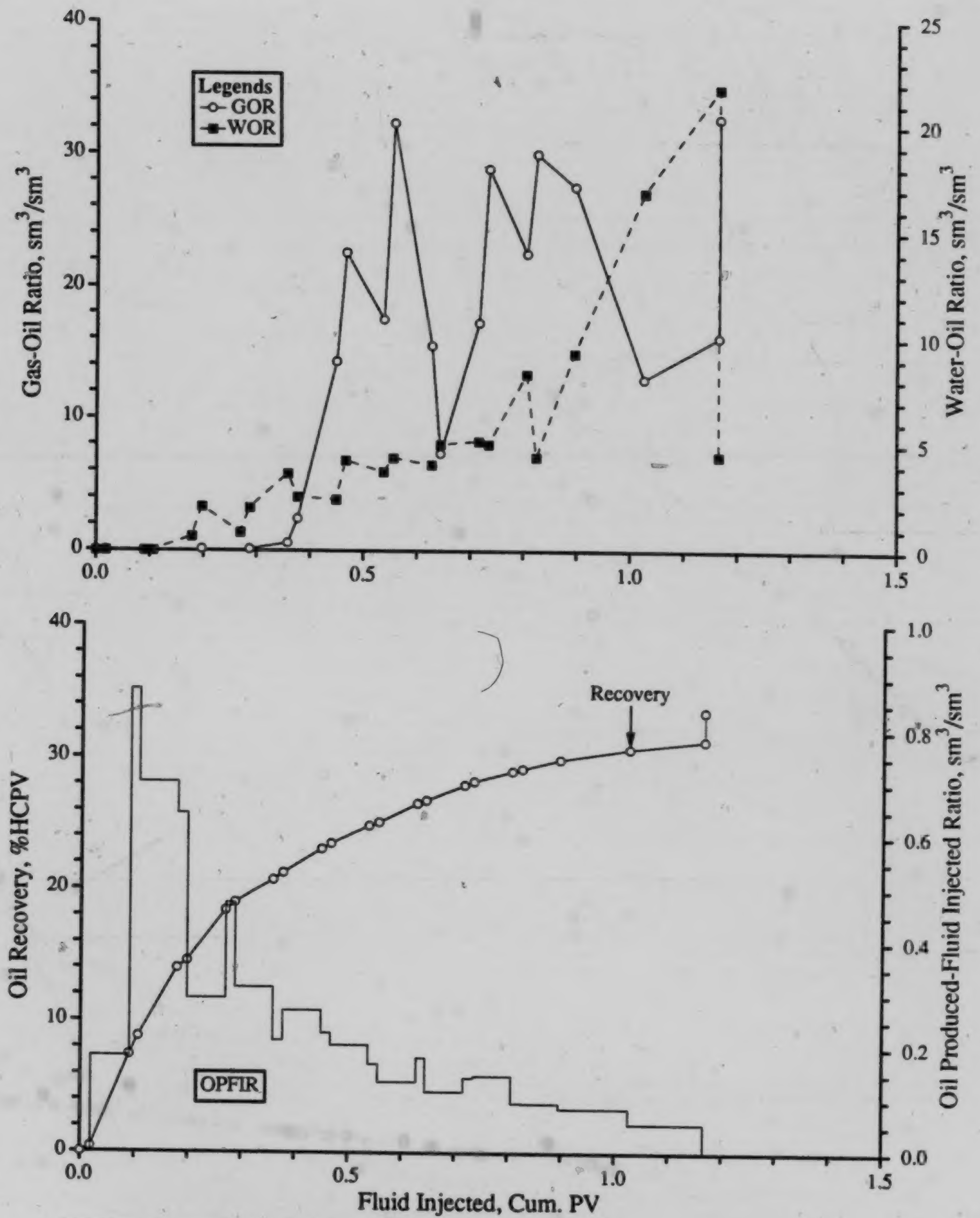

NOTE: Quarter of A 5-Spot

Model Parameters: Average Flow Velocity = 2.54 m/d, μ_o = 3295 mPa.s, ϕ = 39.1 %, k = 12.9 darcies, S_{oi} = 89.5 %, S_{wc} = 10.5 %

[0.20 HCPV CO_2 @ 2.5 MPa & 21°C (0.411 mol), 4:1 WAG, 10 Slugs]

Figure F30 - Production History of Run H2D18.

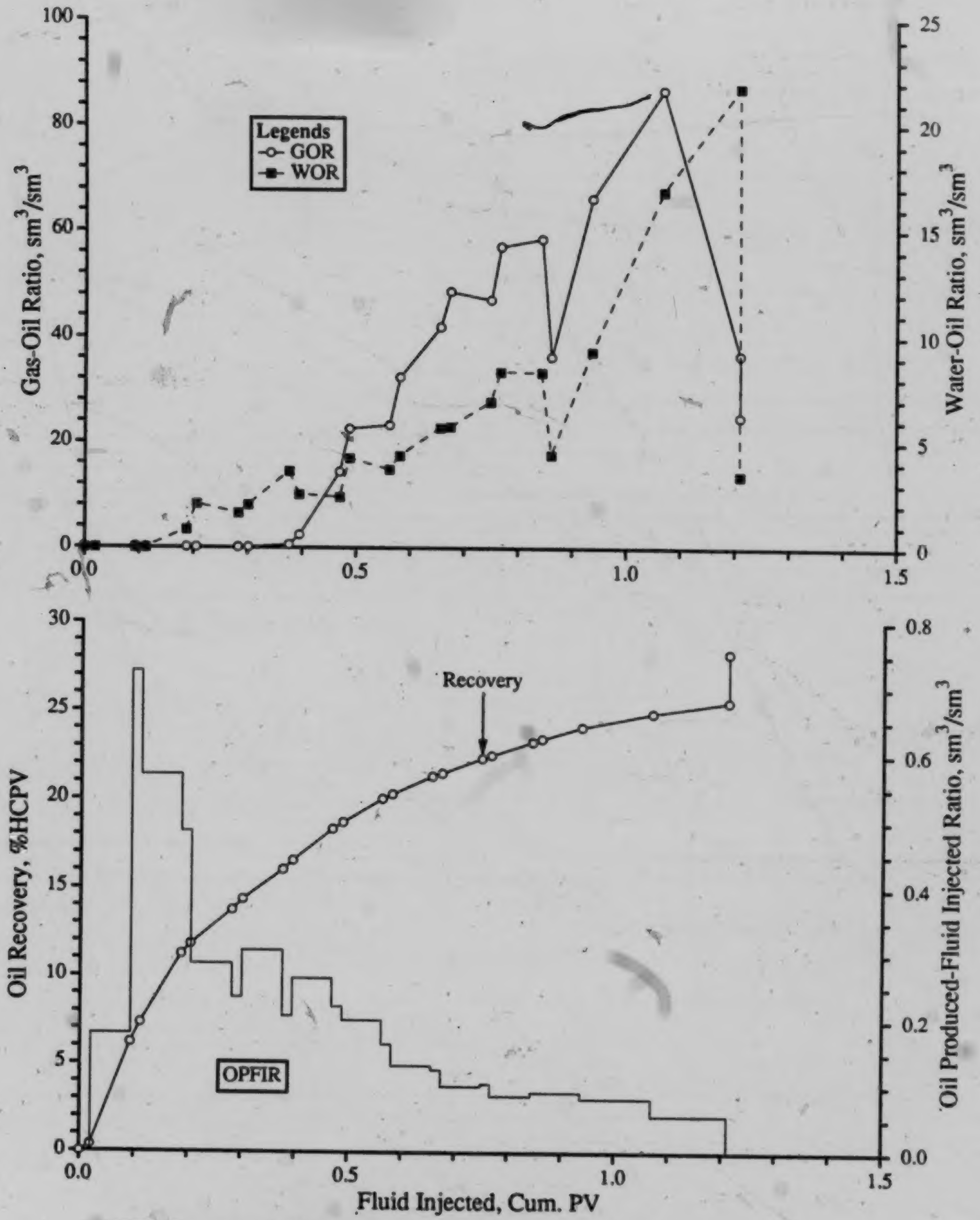

NOTE: Quarter of A 5-Spot

Model Parameters: Average Flow Velocity = 3.17 m/d, μ_o = 3295 mPa.s, ϕ = 38.5 %, k = 13.6 darcies, S_{oi} = 93.1 %, S_{wc} = 6.9 %

[0.20 HCPV CO_2 @ 2.5 MPa & 21°C (0.405 mol), 4:1 WAG, 10 Slugs]

Figure F31 - Production History of Run H2D19.

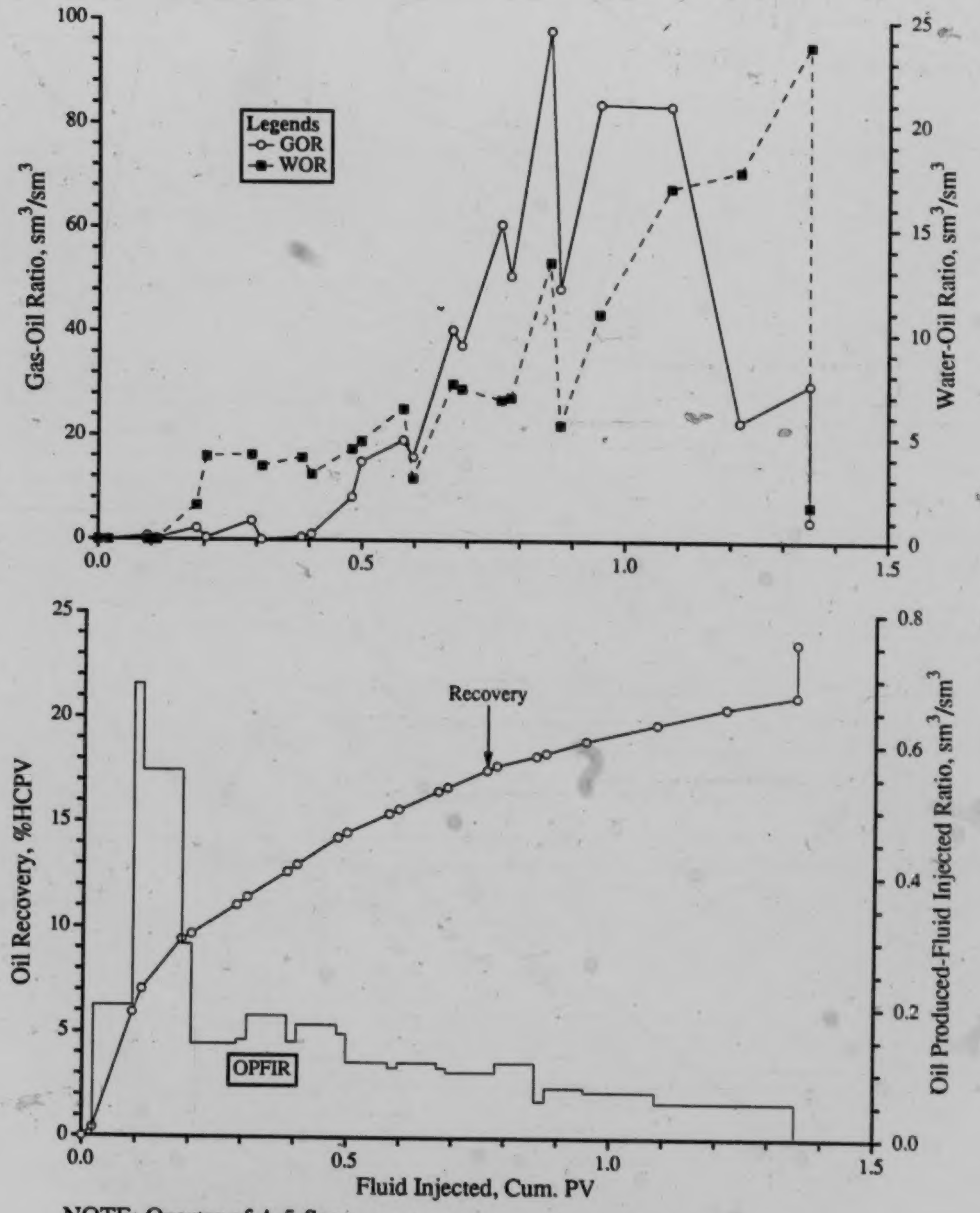

NOTE: Quarter of A 5-Spot

Model Parameters: Average Injection Rate = 3.81 m/d, μ_o = 3295 mPa.s, ø = 38.1 %, k = 13.6 darcies, S_{oi} = 94.0 %, S_{wc} = 6.0 %

[0.20 HCPV CO_2 @ 2.5 MPa & 21°C (0.420 mol), 4:1 WAG, 10 Slugs]

Figure F32 - Production History of Run H2D20.

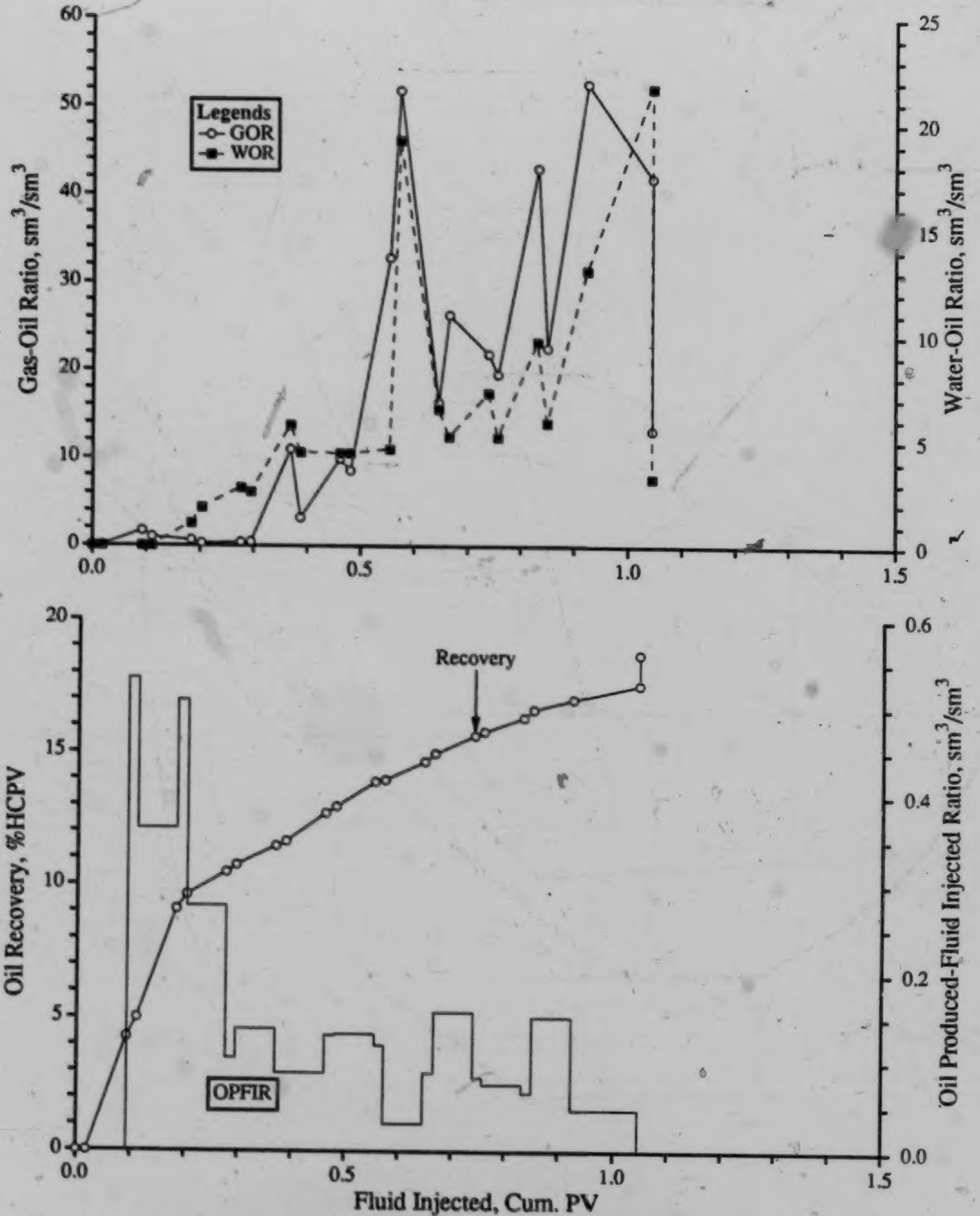

NOTE: Quarter of A 5-Spot

Model Parameters: Average Injection Rate = 0.78 m/d, μ_o = 3607 mPa.s, ϕ = 44.3 %, k = 12.6 darcies, S_{oi} = 92.1 %, S_{wc} = 7.9 %

[0.20 HCPV CO_2 @ 2.5 MPa & 21°C (0.479 mol), 4:1 WAG, 10 Slugs]

Figure F33 - Production History of Run H2D21.

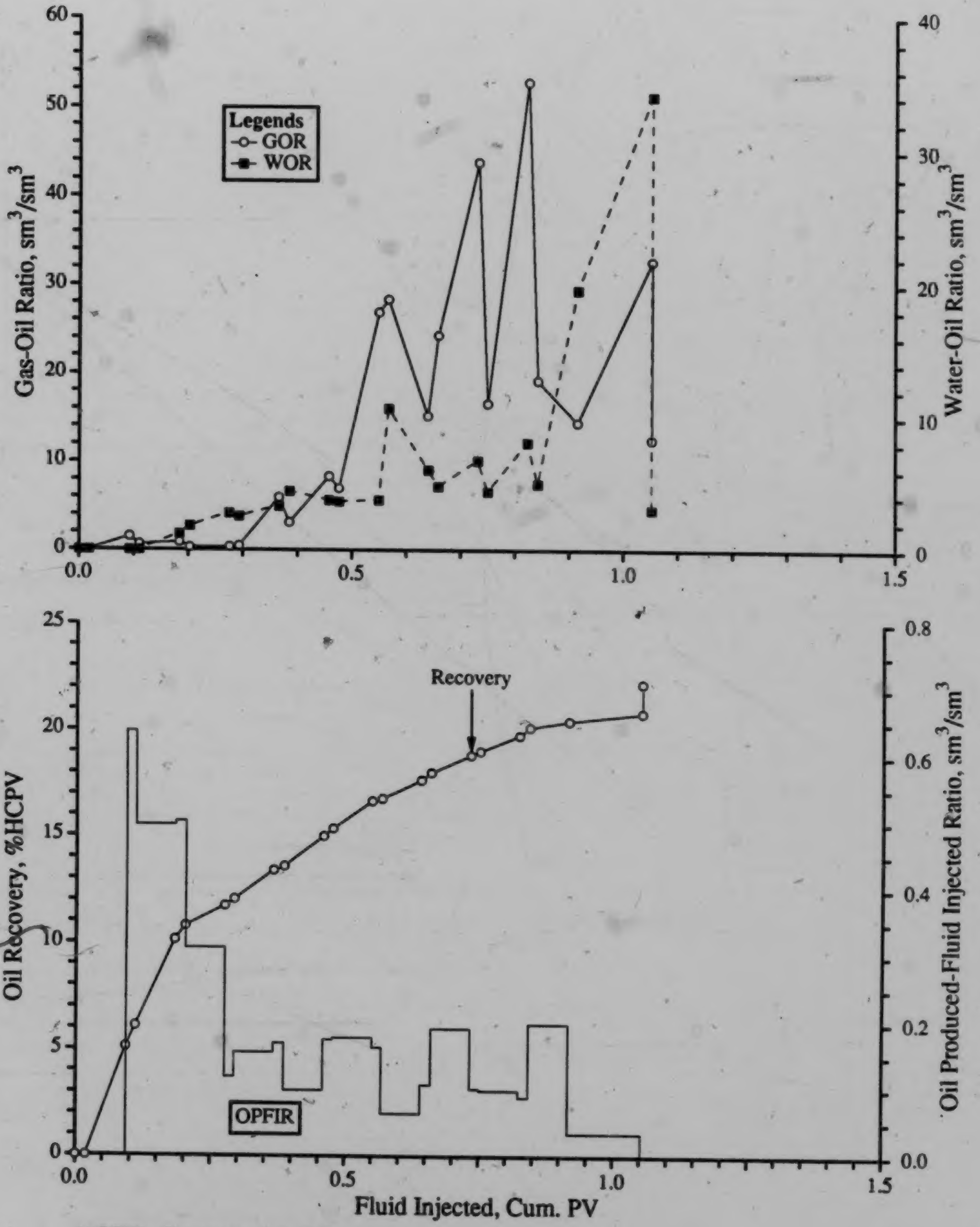

NOTE: Quarter of A 5-Spot

Model Parameters: Average Injection Rate = 1.55 cc/hr, μ_o = 3607 mPa.s, ϕ = 39.5 %, k = 12.4 darcies, S_{oi} = 91.5 %, S_{wc} = 8.5 %

[0.20 HCPV CO_2 @ 2.5 MPa & 21°C (0.424 mol), 4:1 WAG, 10 Slugs]

Figure F34 - Production History of Run H2D22.

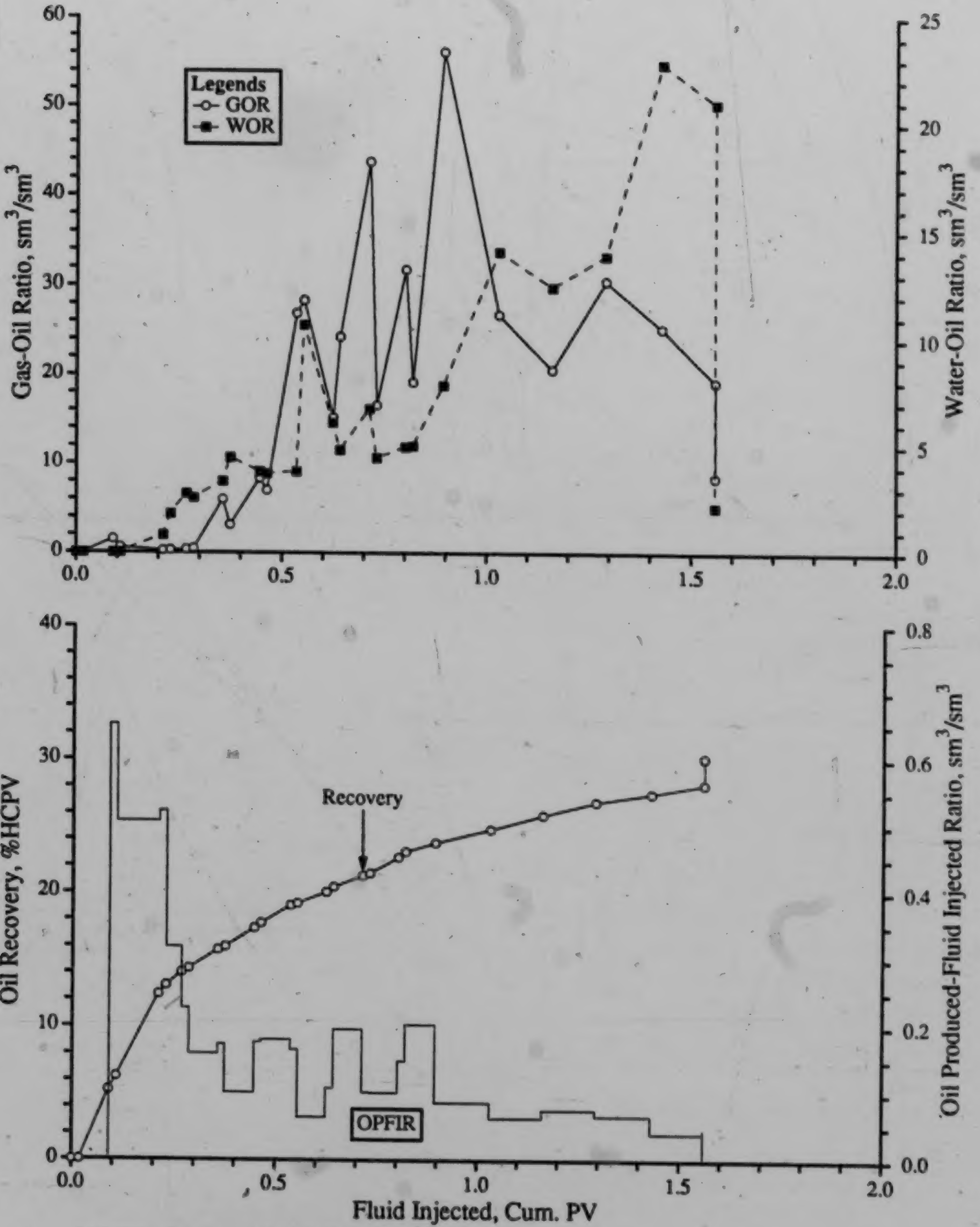

NOTE: Quarter of A 5-Spot

Model Parameters: Average Injection Rate = 2.54 m/d, μ_o = 3607 mPa.s, ϕ = 39.7 %, k = 12.4 darcies, S_{oi} = 89.0 %, S_{wc} = 11.0 %

[0.20 HCPV CO_2 @ 2.5 MPa & 21°C (0.415 mol), 4:1 WAG, 10 Slugs]

Figure F35 - Production History of Run H2D23.

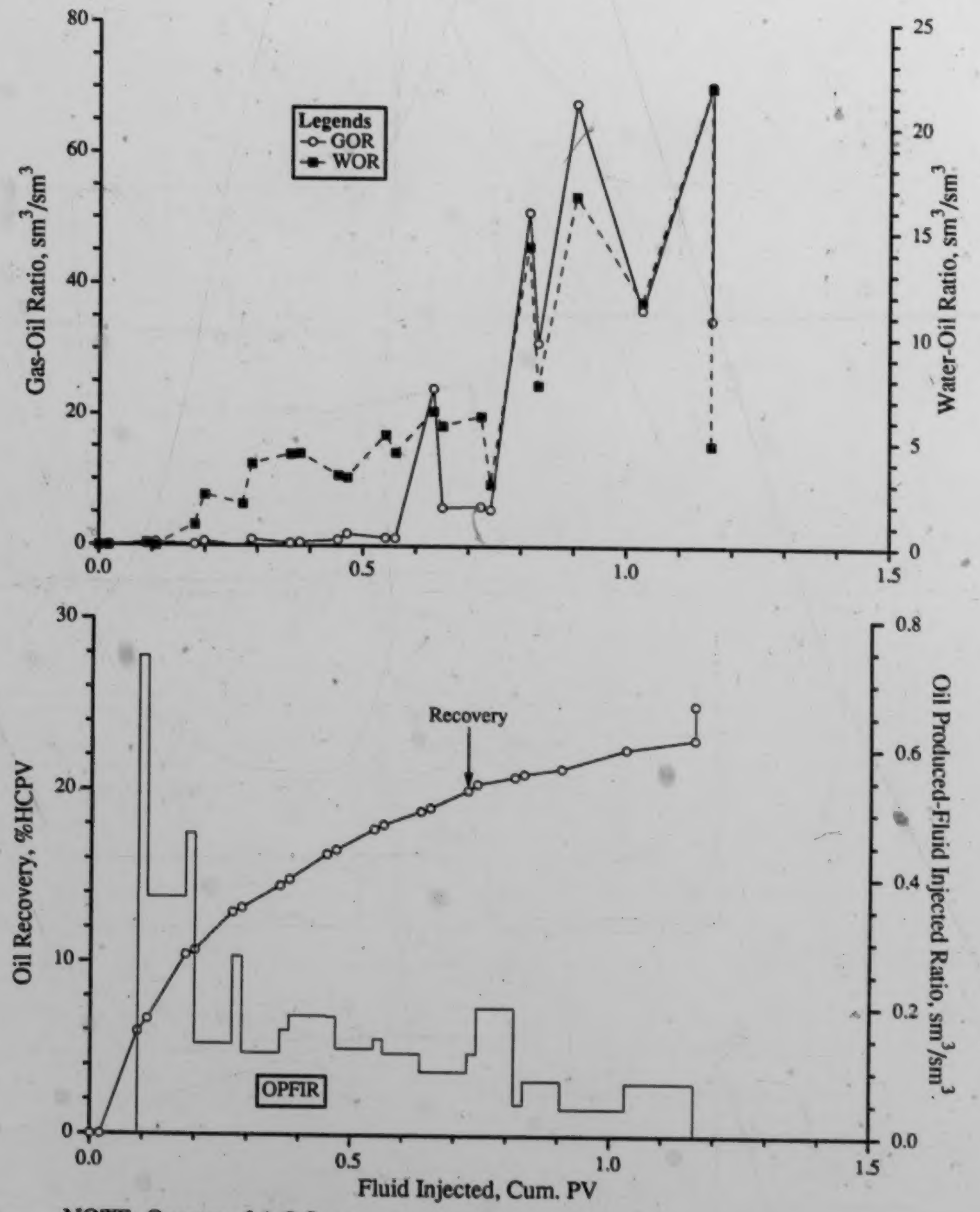

NOTE: Quarter of A 5-Spot

Model Parameters: Average Flow Velocity = 3.17 m/d, μ_o = 3607 mPa.s, ø = 40.2 %, k = 12.8 darcies, S_{oi} = 90.3 %, S_{wc} = 9.7 %

[0.20 HCPV CO_2 @ 2.5 MPa & 21°C (0.426 mol), 4:1 WAG, 10 Slugs]

Figure F36 - Production History of Run H2D24.

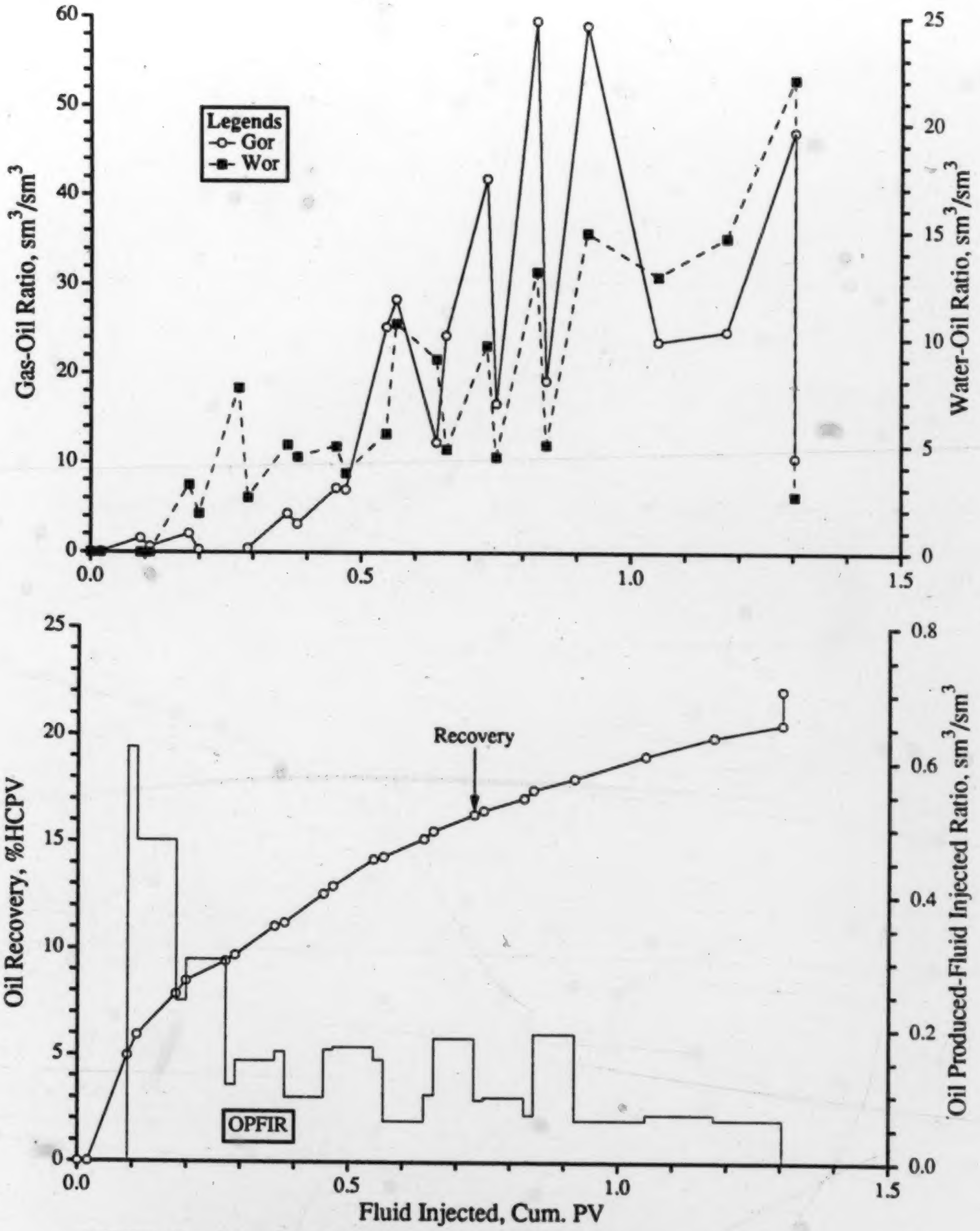

NOTE: Quarter of A 5-Spot

Model Parameters: Average Flow Velocity = 3.81m/d, μ_o = 3607 mPa.s, ϕ = 41.0 %, k = 12.9 darcies, S_{oi} = 90.6 %, S_{wc} = 9.4 %

[0.20 HCPV CO_2 @ 2.5 MPa & 21°C (0.436 mol), 4:1 WAG, 10 Slugs]

Figure F37 - Production History of Run H2D25.

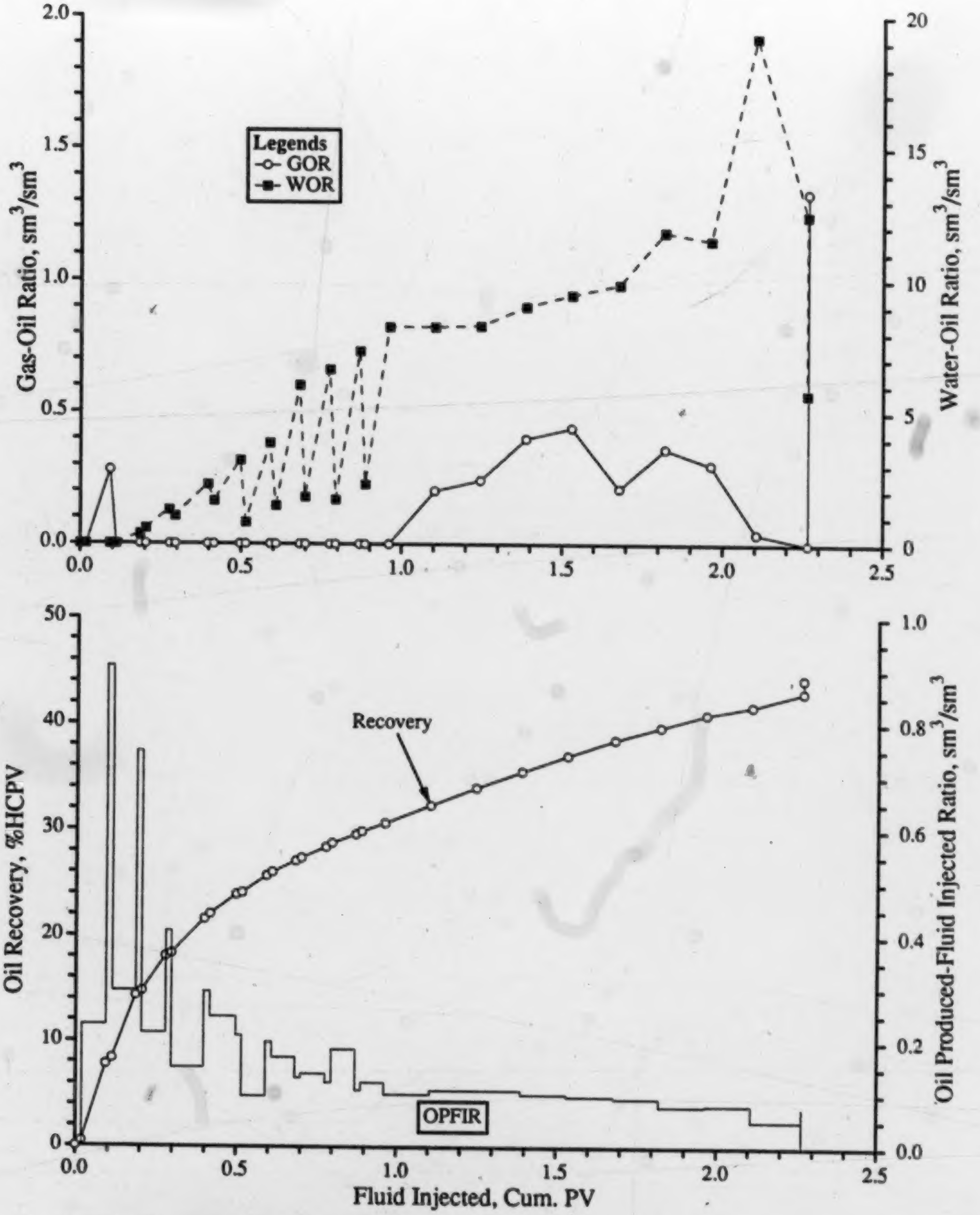

NOTE: Quarter of A 5-Spot

Model Parameters: Average Injection Rate = 308 cc/hr, μ_o = 1058 mPa.s, ϕ = 36.1 %, k = 22.0 darcies, S_{oi} = 92.3 %, S_{wc} = 7.7 %

CO_2 Injected at 1/10 of Water Rate

[0.20 HCPV CO_2 @ 1.0 MPa & 21°C (1.12 mol), 4:1 WAG, 10 Slugs]

Figure F38 - Production History of Run H2D26.

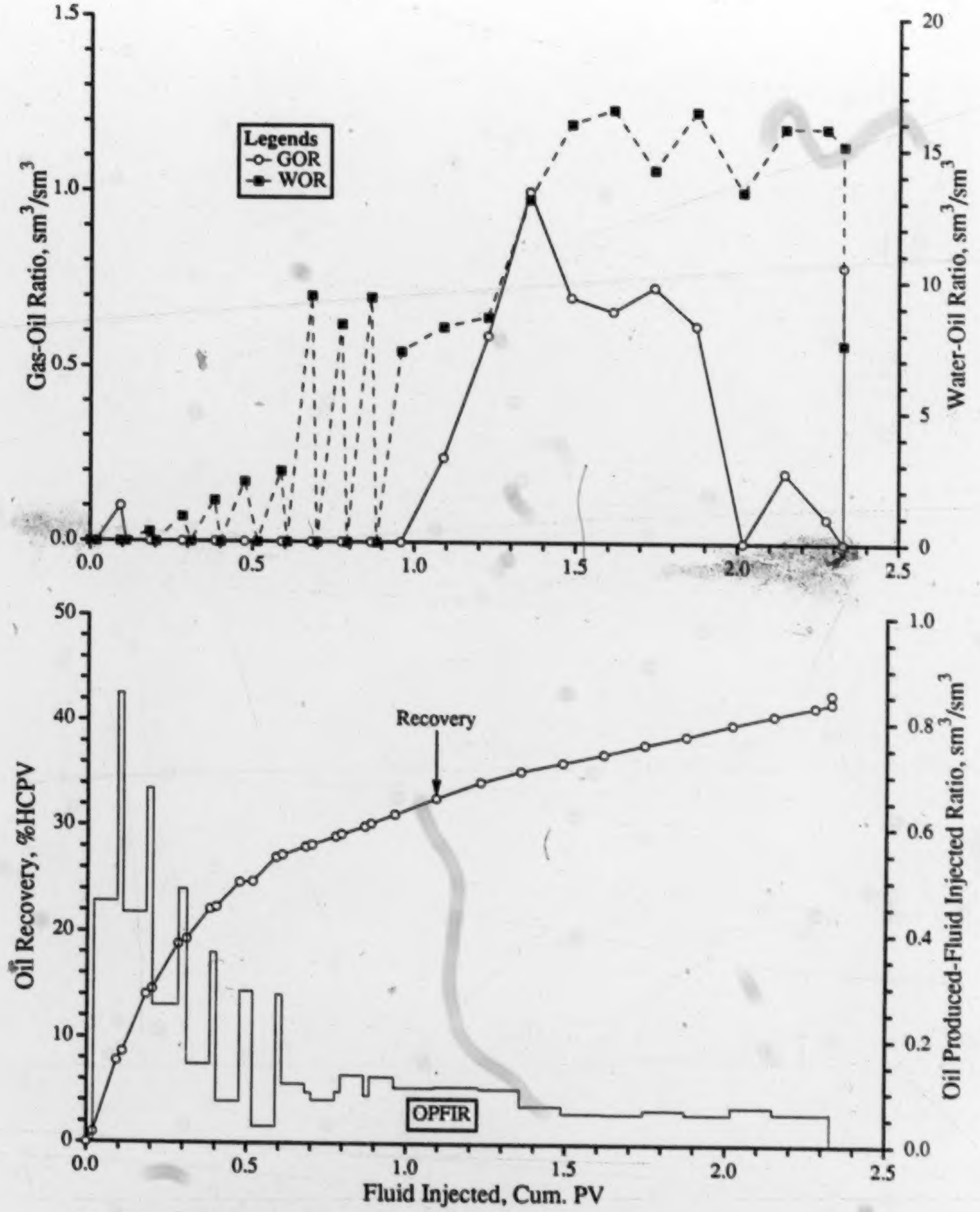

NOTE: Quarter of A 5-Spot

Model Parameters: Average Injection Rate = 308 cc/hr, μ_o = 1055 mPa.s, ø = 40.0 %, k = 14.1 darcies, S_{oi} = 91.1 %, S_{wc} = 8.9 %

CO_2 Injected at 1/5 of Water Rate

[0.20 HCPV CO_2 @ 1.0 MPa & 21°C (0.154 mol), 4:1 WAG, 10 Slugs]

Figure F39 - Production History of Run H2D27.

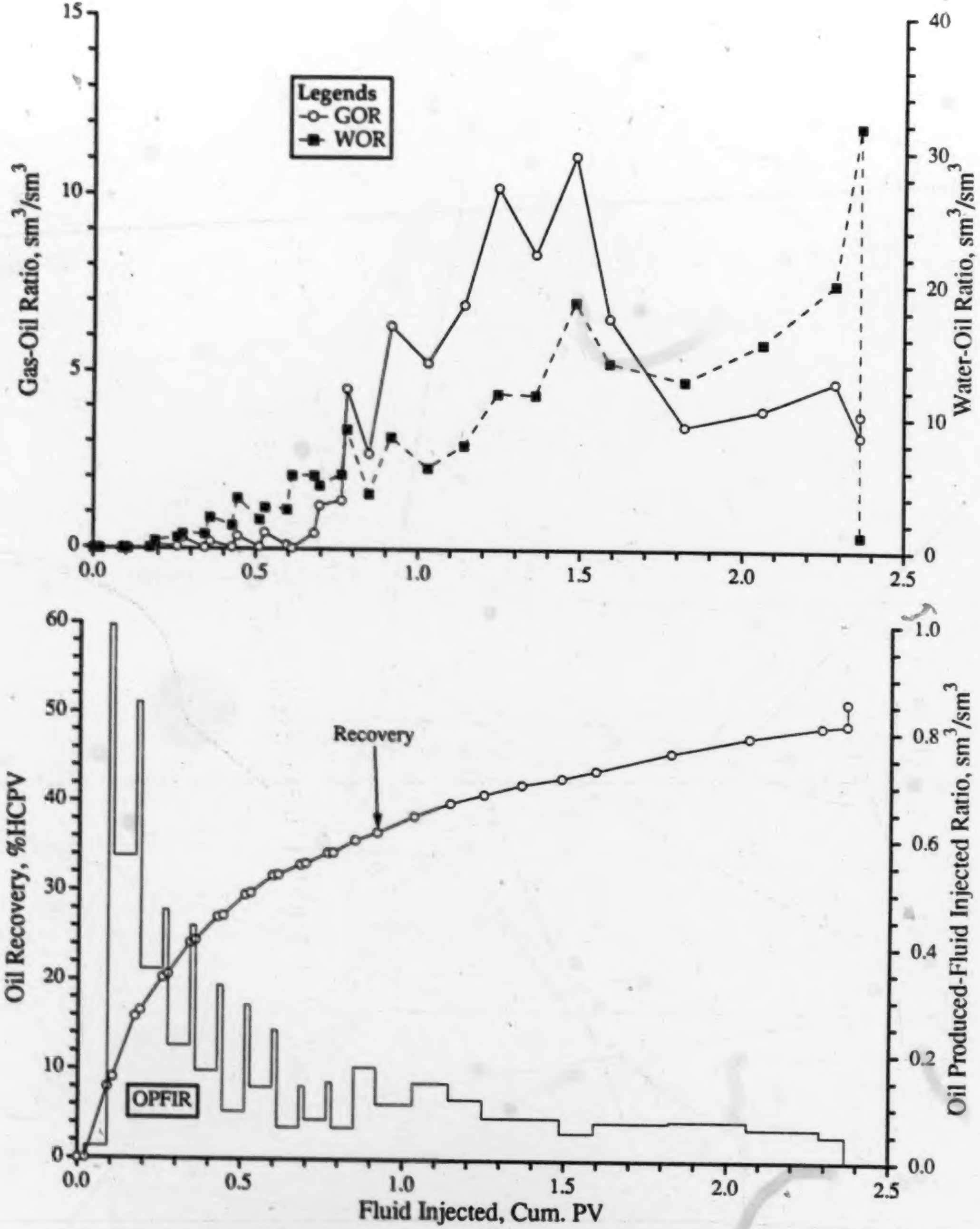

NOTE: Quarter of A 5-Spot

Model Parameters: Average Injection Rate = 308 cc/hr, μ_o = 1055 mPa.s,
ϕ = 42.1 %, k = 14.5 darcies, S_{oi} = 84.9 %, S_{wc} = 15.1 %
CO_2 Injected at Water Rate

[0.20 HCPV CO_2 @ 1.0 MPa & 21° C (0.178 mol), 4:1 WAG, 10 Slugs]

Figure F40 - Production History of Run H2D28.

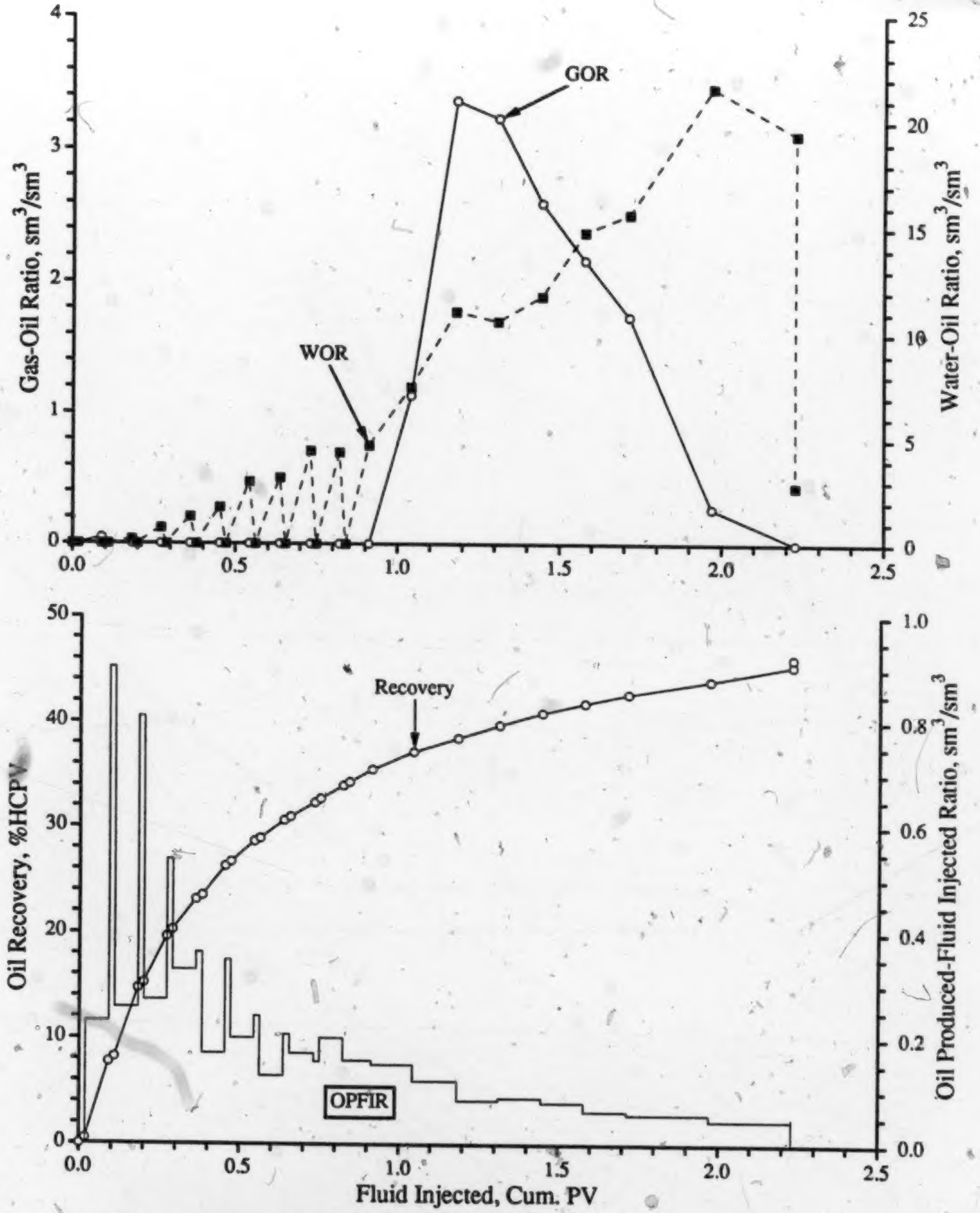

NOTE: Quarter of A 5-Spot

Model Parameters: Average Injection Rate = 308 cc/hr, μ_o = 1055 mPa.s,
ø = 39.5 %, k = 16.6 darcies, S_{oi} = 90.3 %, S_{wc} = 9.7 %
CO_2 Injected at 2 times of Water Rate

[0.20 HCPV CO_2 @ 1.0 MPa & 21°C (0.167 mol), 4:1 WAG, 10 Slugs]

Figure F41 - Production History of Run H2D29.

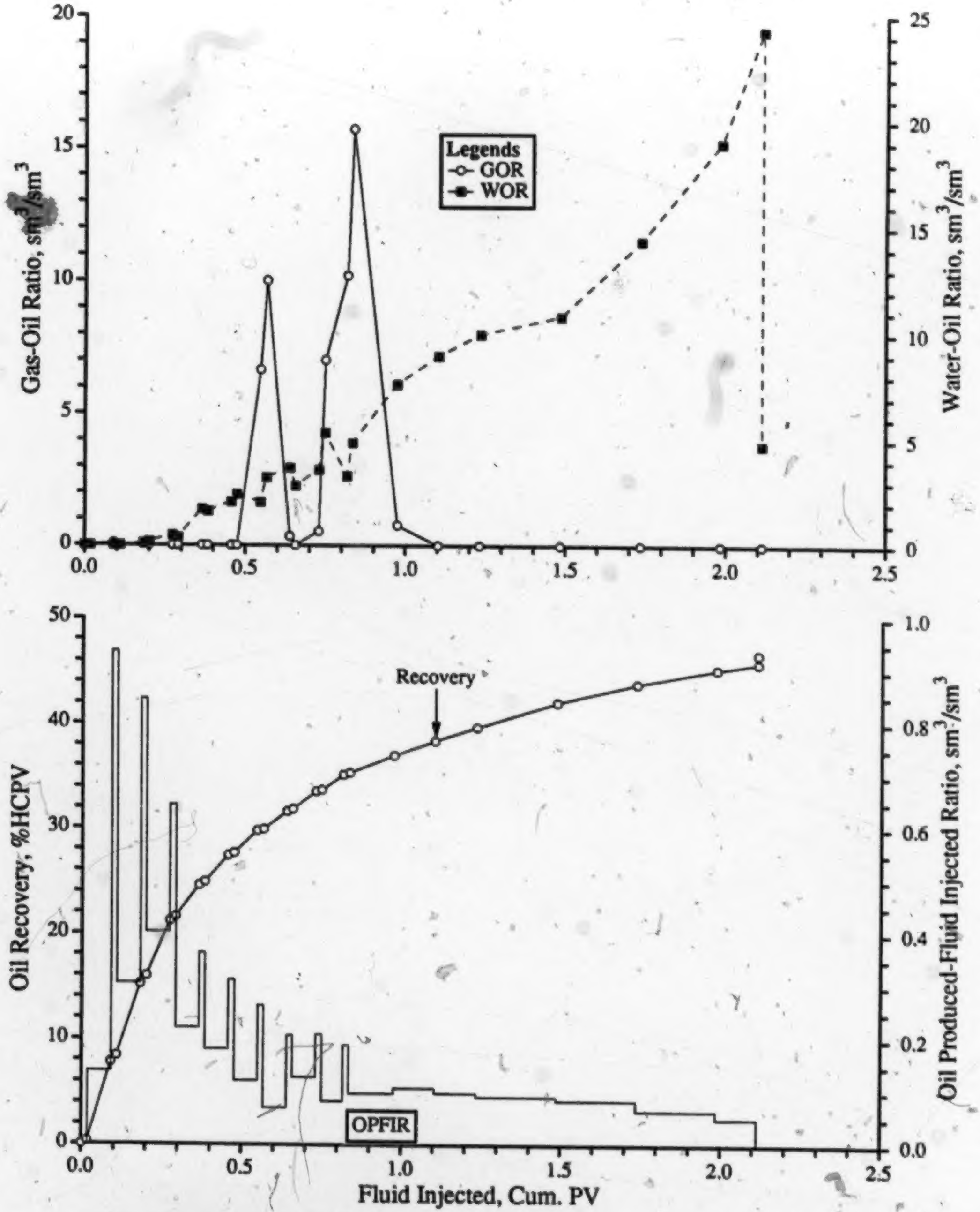

NOTE: Quarter of A 5-Spot

Model Parameters: Average Flow Velocity = 0.831 m/d, μ_o = 1058 mPa.s, ϕ = 39.5 %, k = 16.6 darcies, S_{oi} = 91.0 %, S_{wc} = 9.0 %

CO_2 Injected at 5 times of Water Rate

[0.20 HCPV CO_2 @ 1.0 MPa & 21°C (0.087 moles), 4:1 WAG, 10 Slugs]

Figure F42 - Production History of Run H2D30.

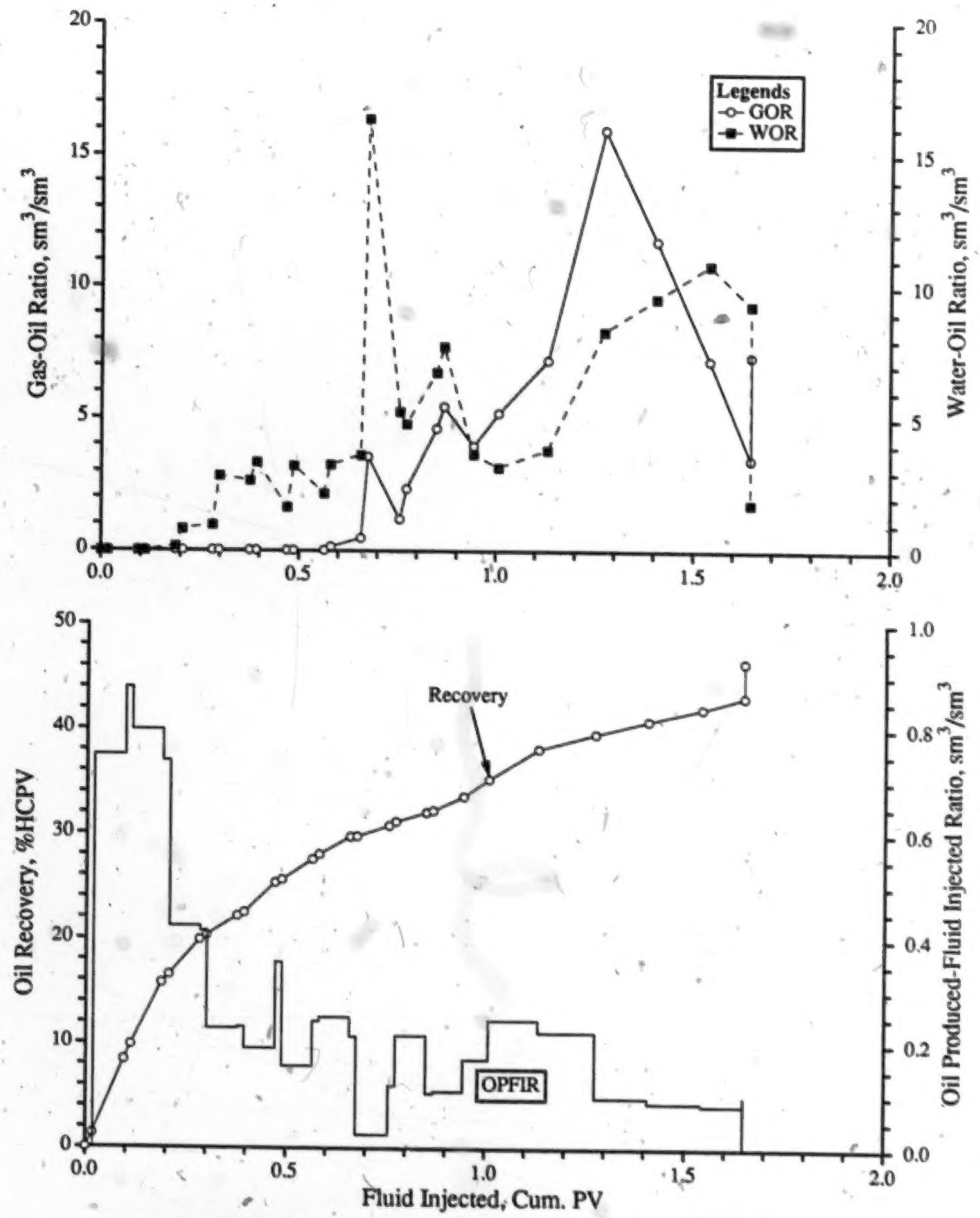

NOTE: Quarter of A 5-Spot

Model Parameters: Average Flow Velocity = 1.29 m/d, μ_o = 1055 mPa.s, ϕ = 41.4 %, k = 13.3 darcies, S_{oi} = 86.4 %, S_{wc} = 13.6 %

CO_2 Injected at Water Rate

[0.20 HCPV CO_2 @ 1.0 MPa & 21°C (0.160 mol), 4:1 WAG, 10 Slugs]

Figure F43 - Production History of Run H2D31.

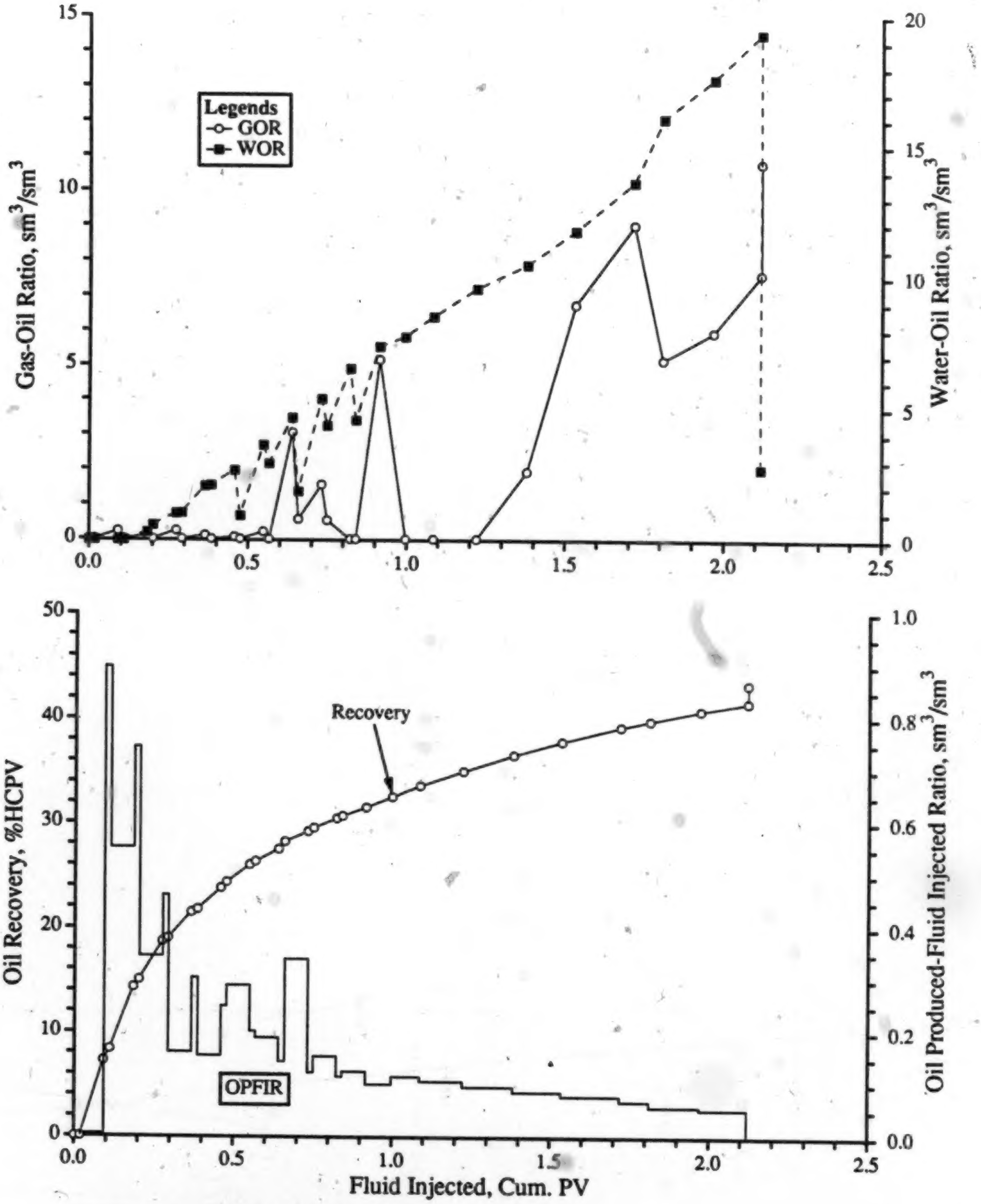

NOTE: Quarter of A 5-Spot

Model Parameters: Average Flow Velocity = 0.831 m/d, μ_o = 1055 mPa.s, ø = 40.6 %, k = 13.3 darcies, S_{oi} = 91.3 %, S_{wc} = 8.7 %

CO_2 Injected at Water Rate

[0.20 HCPV CO_2 @ 1.0 MPa & 21°C (0.171 mol), 4:1 WAG, 10 Slugs]

Figure F44 - Production History of Run H2D32.

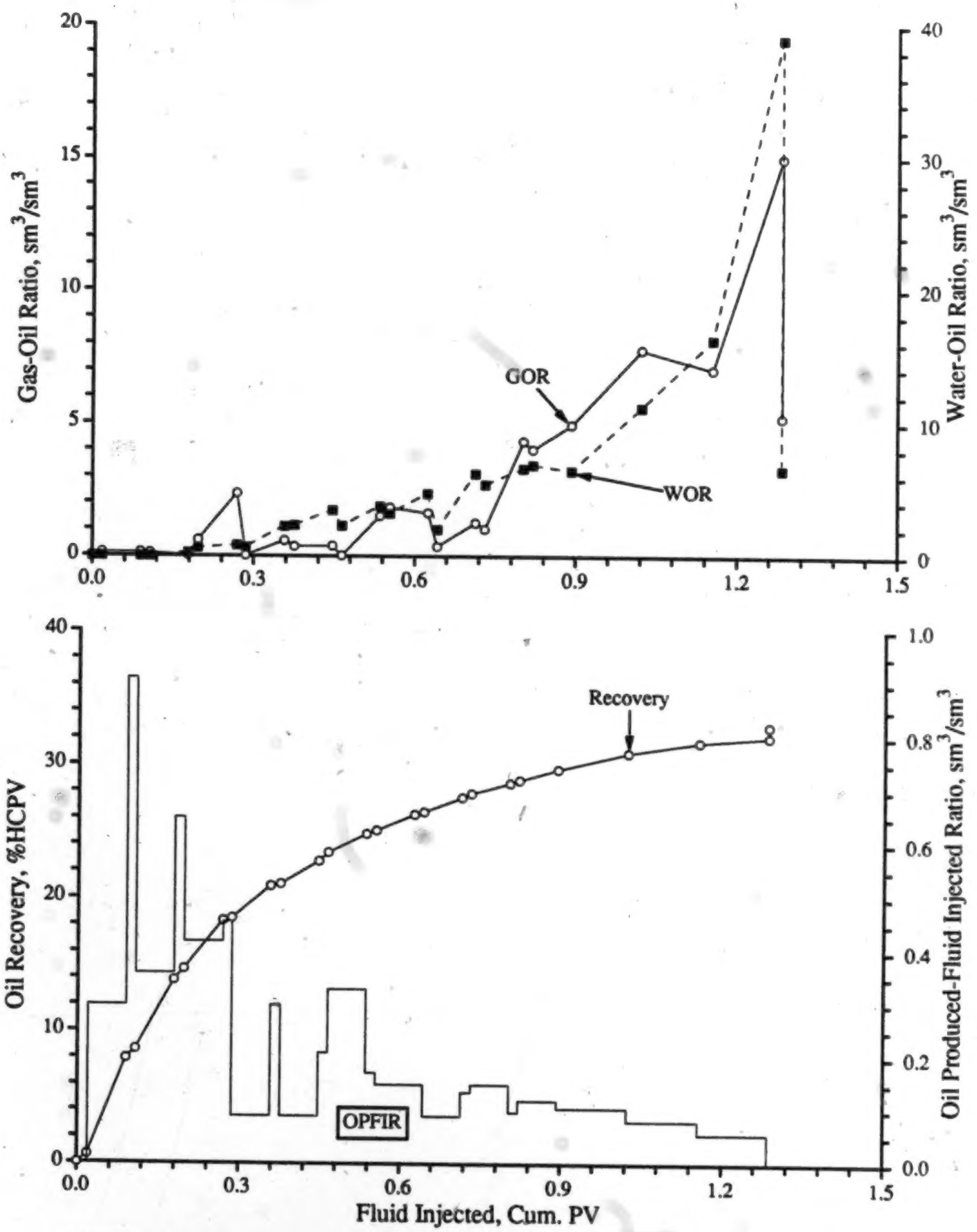

NOTE: Quarter of A 5-Spot

Model Parameters: Average Flow Velocity = 2.08 m/d, μ_o = 1055 mPa.s, ϕ = 38.5 %, k = 12.5 darcies, S_{oi} = 89.2 %, S_{wc} = 10.8 %

CO_2 Injected at Water Rate

[0.20 HCPV CO_2 @ 1.0 MPa & 21°C (0.144 mol), 4:1 WAG, 10 Slugs]

Figure F45 - Production History of Run H2D33.

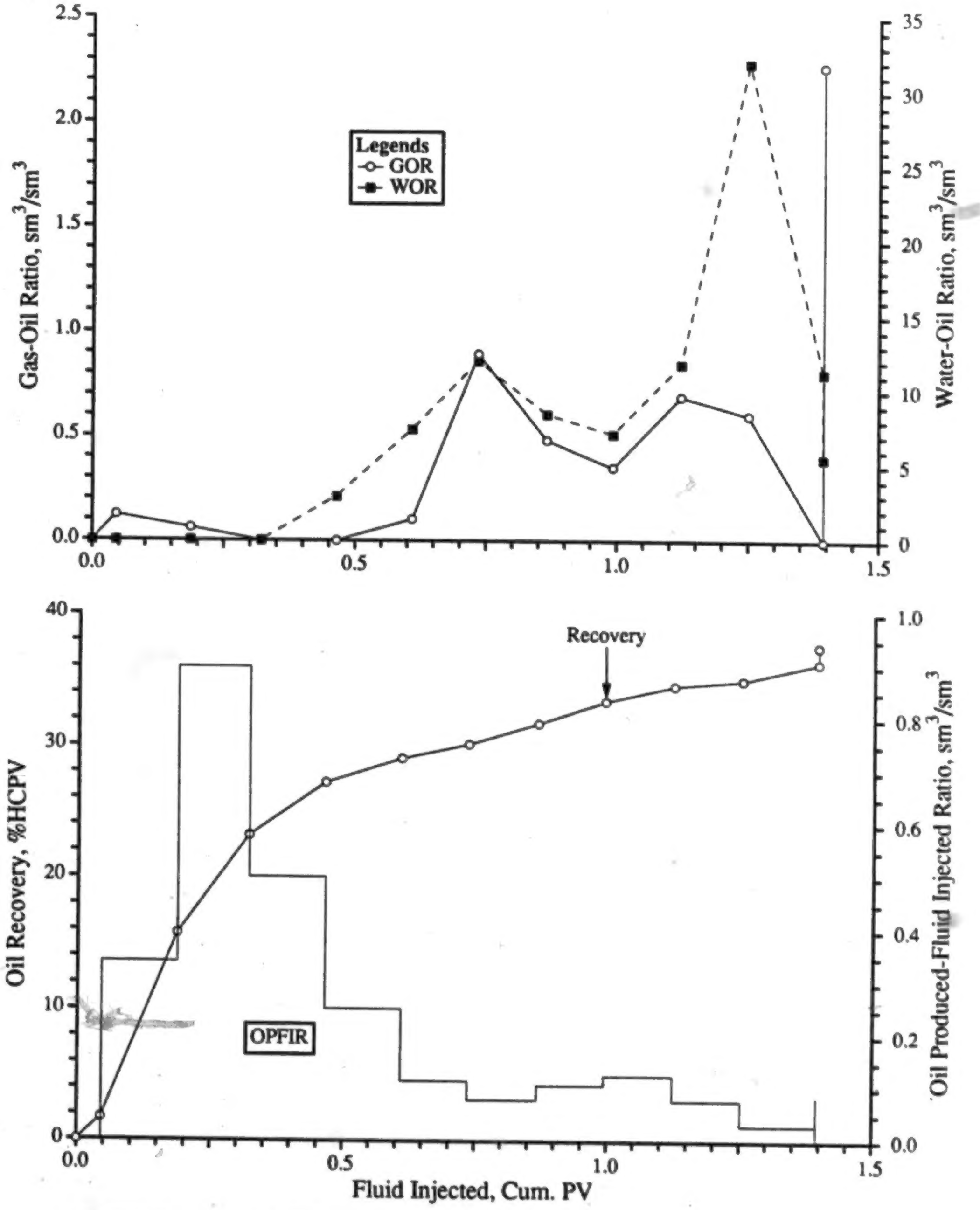

NOTE: Quarter of A 5-Spot

Model Parameters: Average Flow Velocity = 2.54 m/d, μ_o = 1058 mPa.s, ϕ = 39.2 %, k = 14.1 darcies, S_{oi} = 90.6 %, S_{wc} = 9.4 %

[0.05 HCPV CO_2 @ 2.5 MPa (0.104 moles), Soak time = 0 days]

Figure F46 - Production History of Run H2D34.

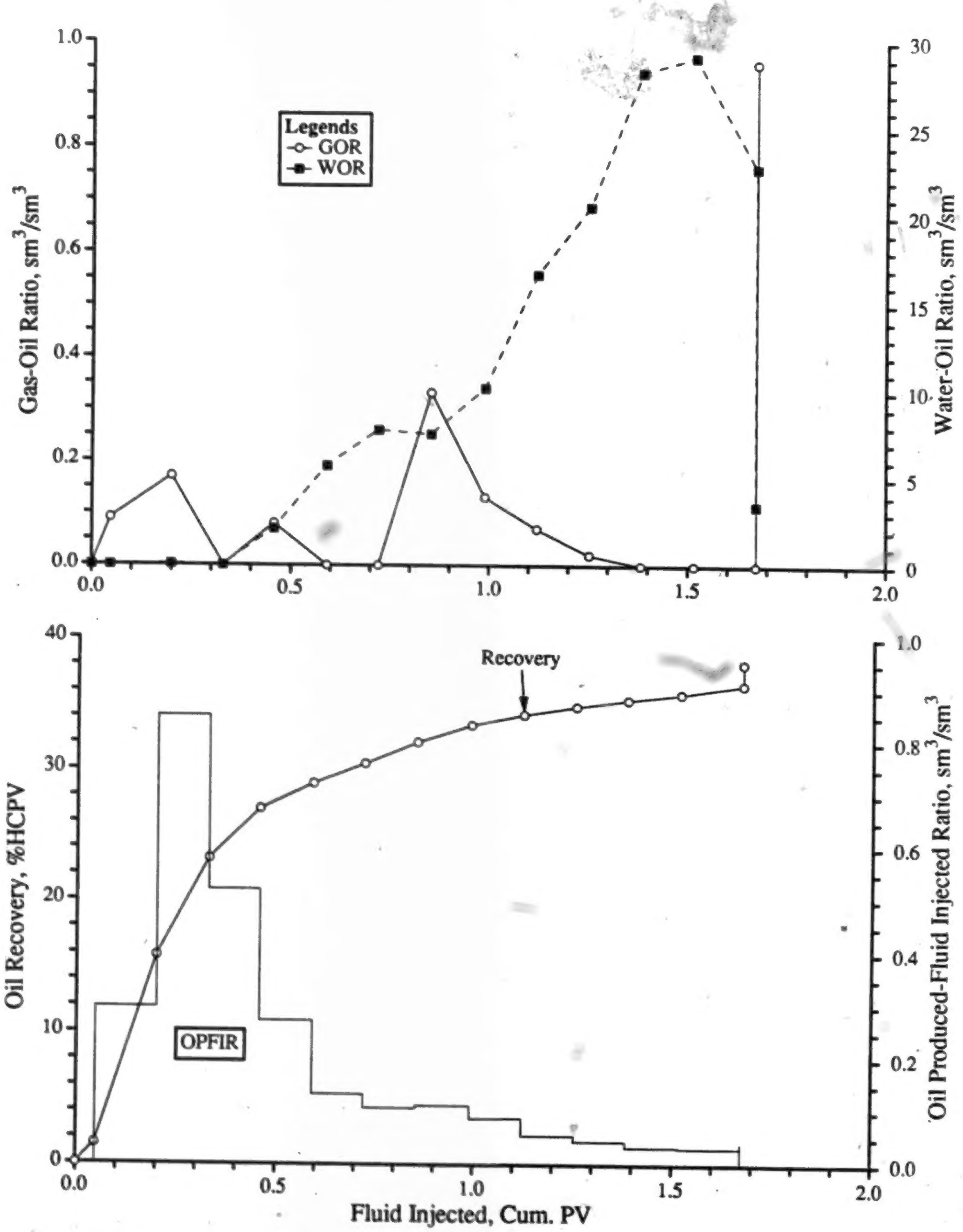

NOTE: Quarter of A 5-Spot

Model Parameters: Average Flow Velocity = 3.17 m/d, μ_o = 1058 mPa.s, ϕ = 38.5 %, k = 14.0 darcies, S_{oi} = 91.6 %, S_{wc} = 8.4 %

[0.05 HCPV CO_2 @ 2.5 MPa (0.103 moles), Soak time = 3 days]

Figure F47 - Production History of Run H2D35.

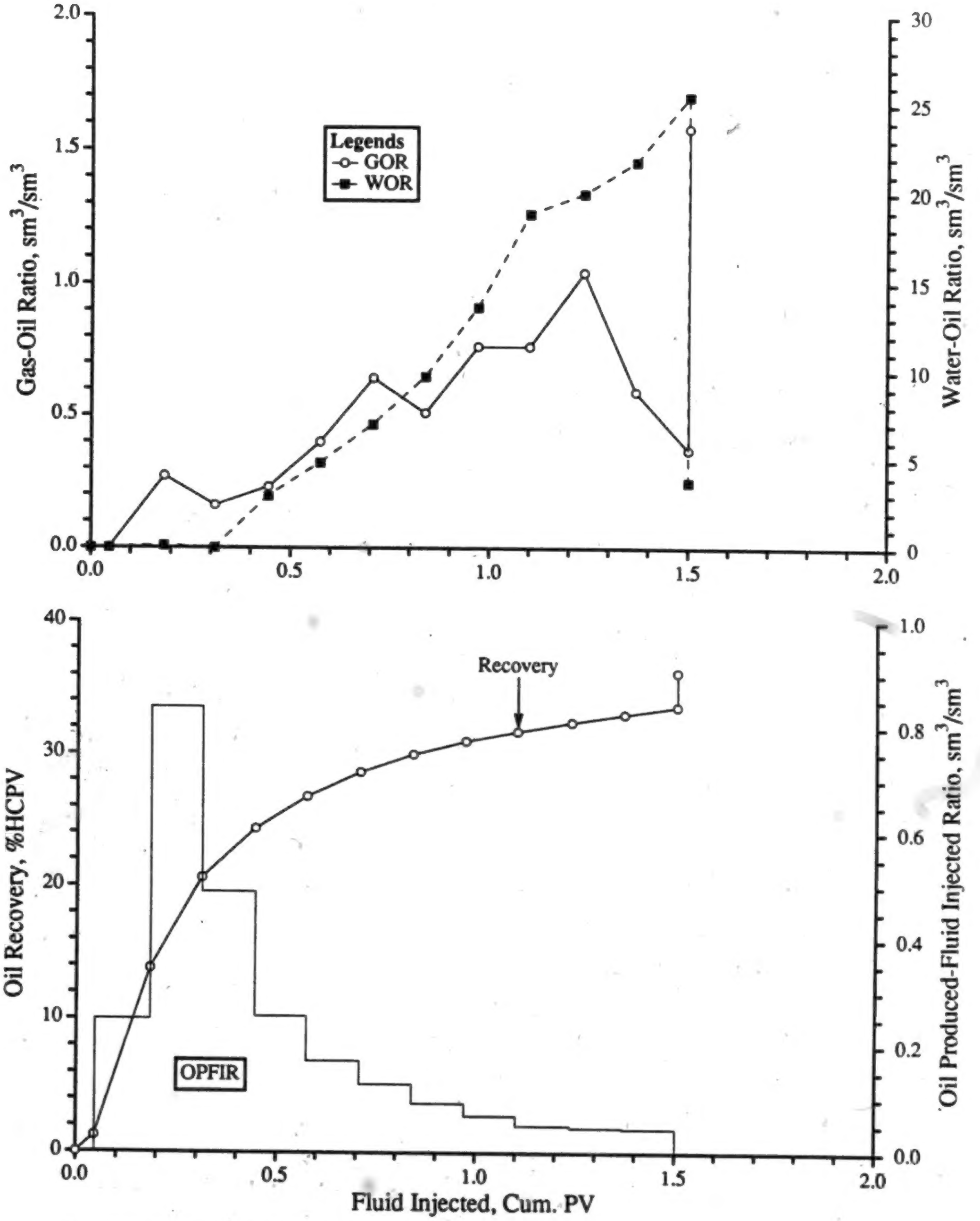

NOTE: Quarter of A 5-Spot

Model Parameters: Average Flow Velocity = 2.54 m/d, μ_o = 1058 mPa.s, ϕ = 38.6 %, k = 10.7 darcies, S_{oi} = 91.7 %, S_{wc} = 8.3 %

[0.05 HCPV CO_2 @ 2.5 MPa (0.104 moles), Soak time = 4.83 days]

Figure F48 - Production History of Run H2D36.

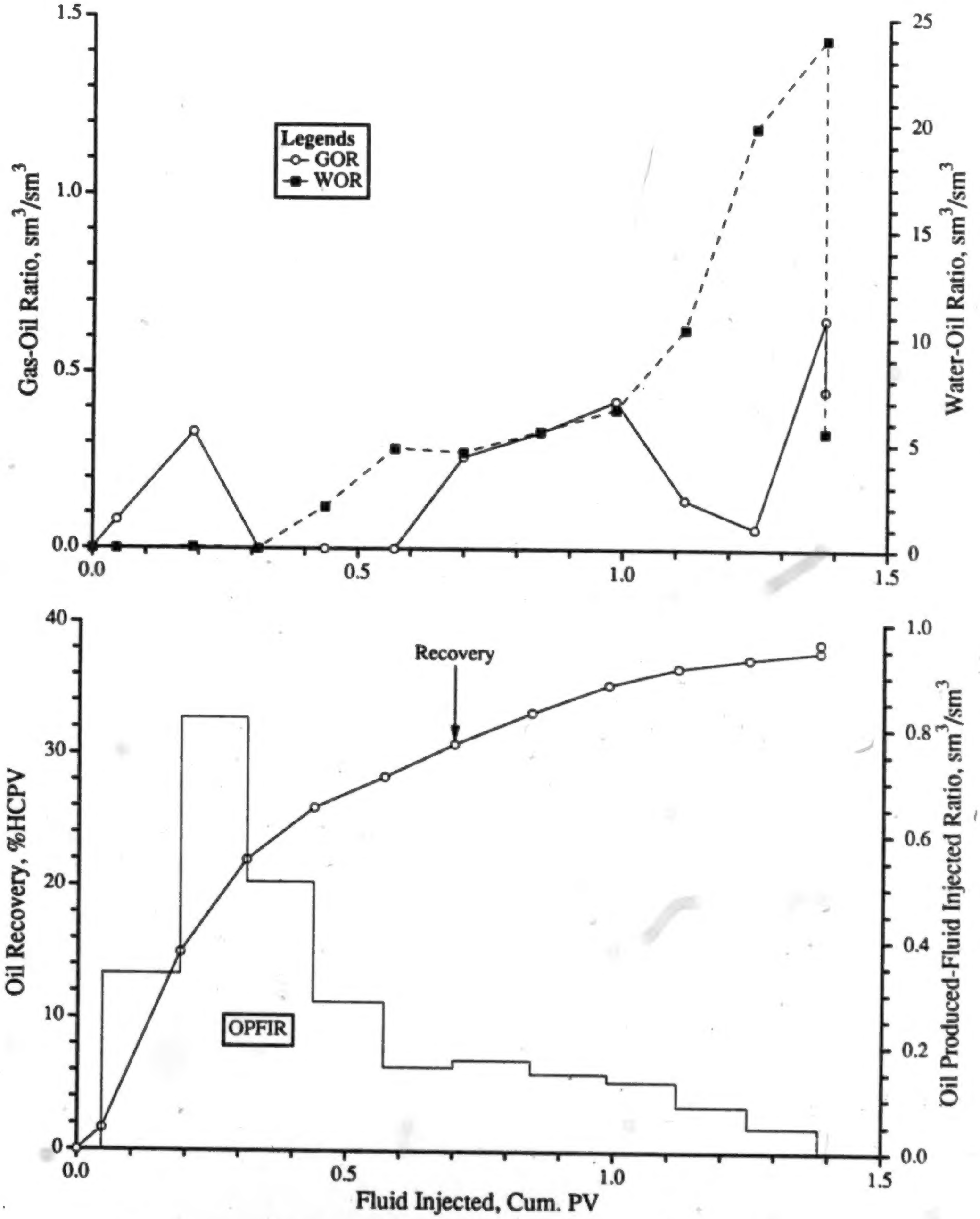

NOTE: Quarter of A 5-Spot

Model Parameters: Average Flow Velocity = 2.54 m/d, μ_o = 1058 mPa.s, ø = 39.4 %, k = 11.3 darcies, S_{oi} = 89.1 %, S_{wc} = 10.9 %

[0.05 HCPV CO_2 @ 2.5 MPa (0.104 moles), Soak time = 10 days]

Figure F49 - Production History of Run H2D37.

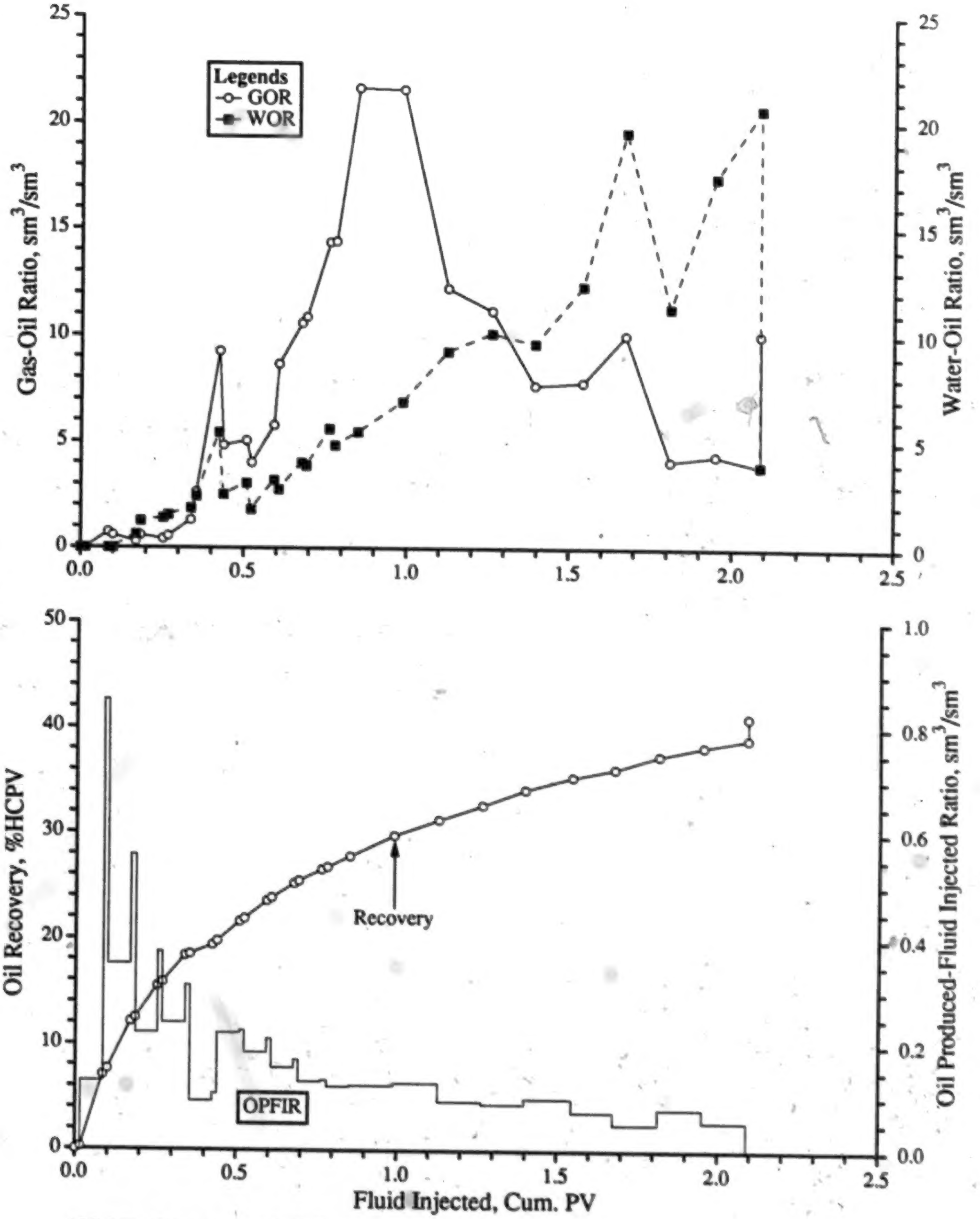

NOTE: Quarter of A 5-Spot

Model Parameters: Average Injection Rate =308.0 cc/hr, μ_o = 1058. mPa.s, ø = 37.7 %, k = 4.4 darcies, S_{oi} = 87.1 %, S_{wc} = 12.9 %

[0.20 HCPV CO_2 @ 2.5 MPa & 37°C (0.354 mol), 4:1 WAG, 10 Slugs]

Figure F50 - Production History of Run H2D39.

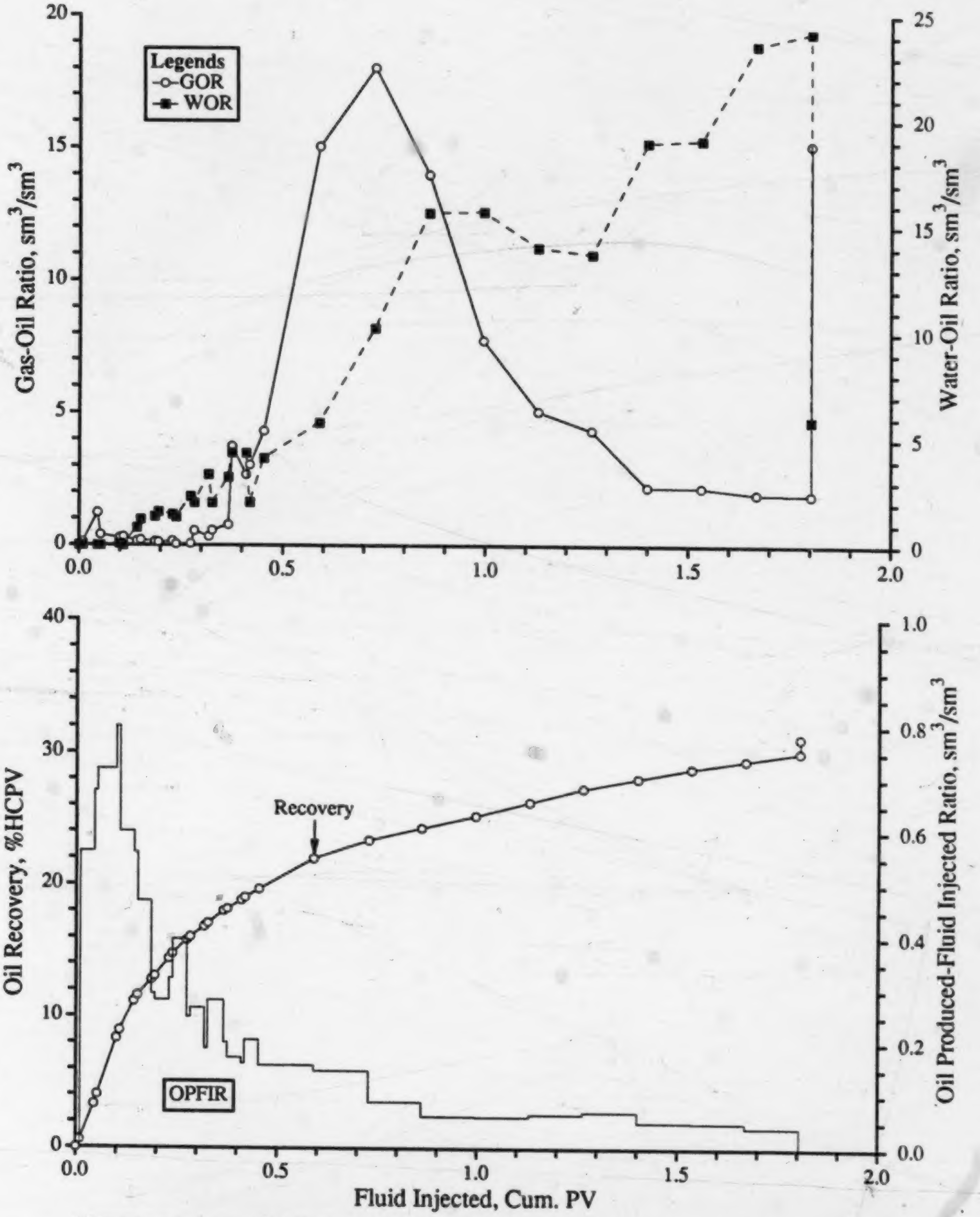

NOTE: Quarter of A 5-Spot

Model Parameters: Average Injection Rate =308.0 cc/hr, μ_o = 5200 mPa.s, ϕ = 37.6 %, k = 3.9 darcies, S_{oi} = 86.9 %, S_{wc} = 13.1%

[0.10 HCPV CO_2 @ 2.5 MPa & 37°C (0.177 mol), 4:1 WAG, 10 Slugs]

Figure F51 - Production History of Run H2D40.

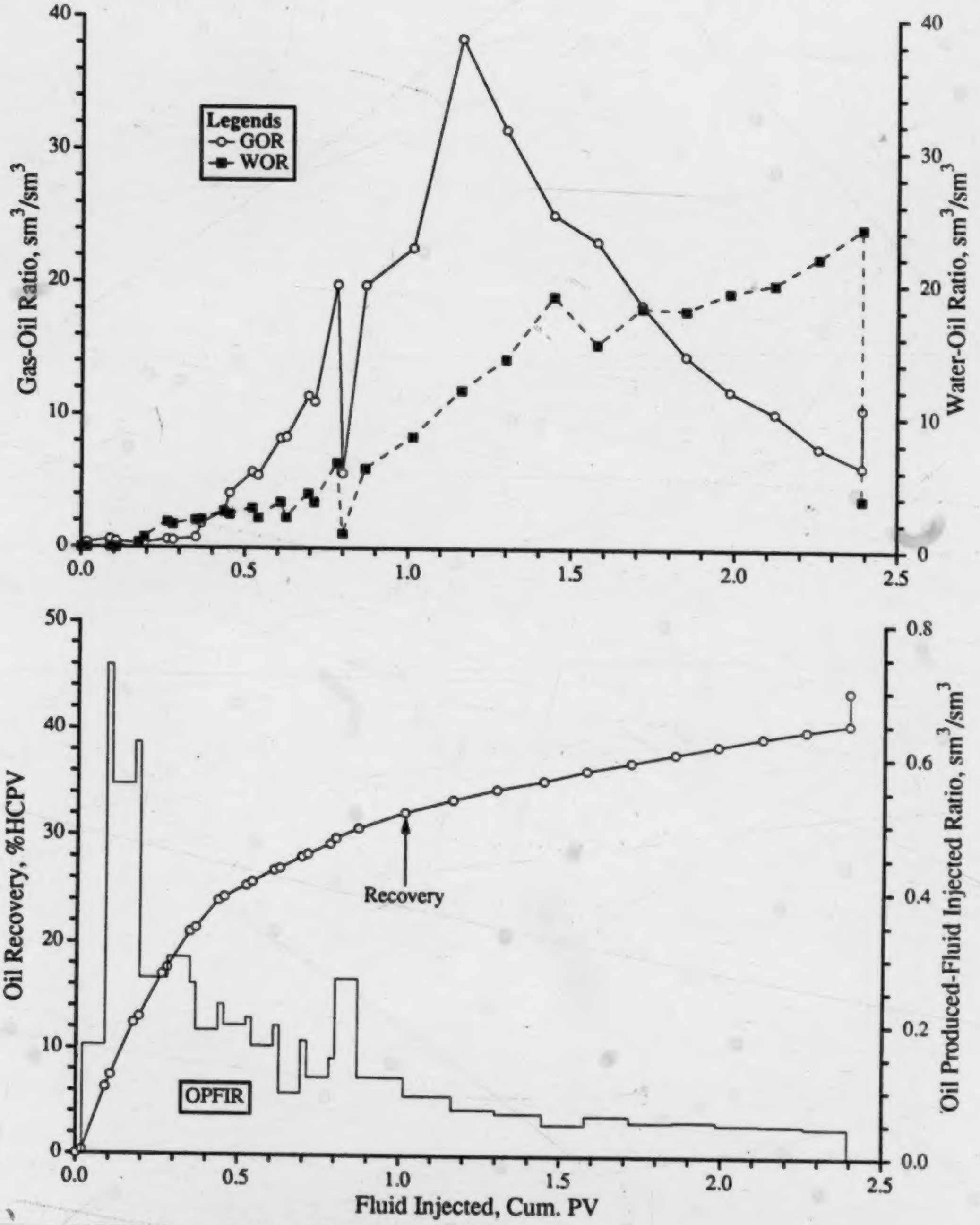

NOTE: Quarter of A 5-Spot

Model Parameters: Average Injection Rate =308.0 cc/hr, μ_o = 1058 mPa.s, ø = 37.6%, k = 3.2 darcies, S_{oi} = 86.9%, S_{wc} = 13.1%

[0.20 HCPV CO_2 @ 3.14 MPa & 37°C (0.354 mol), 4:1 WAG, 10 Slugs]

Figure F52 - Production History of Run H2D41.

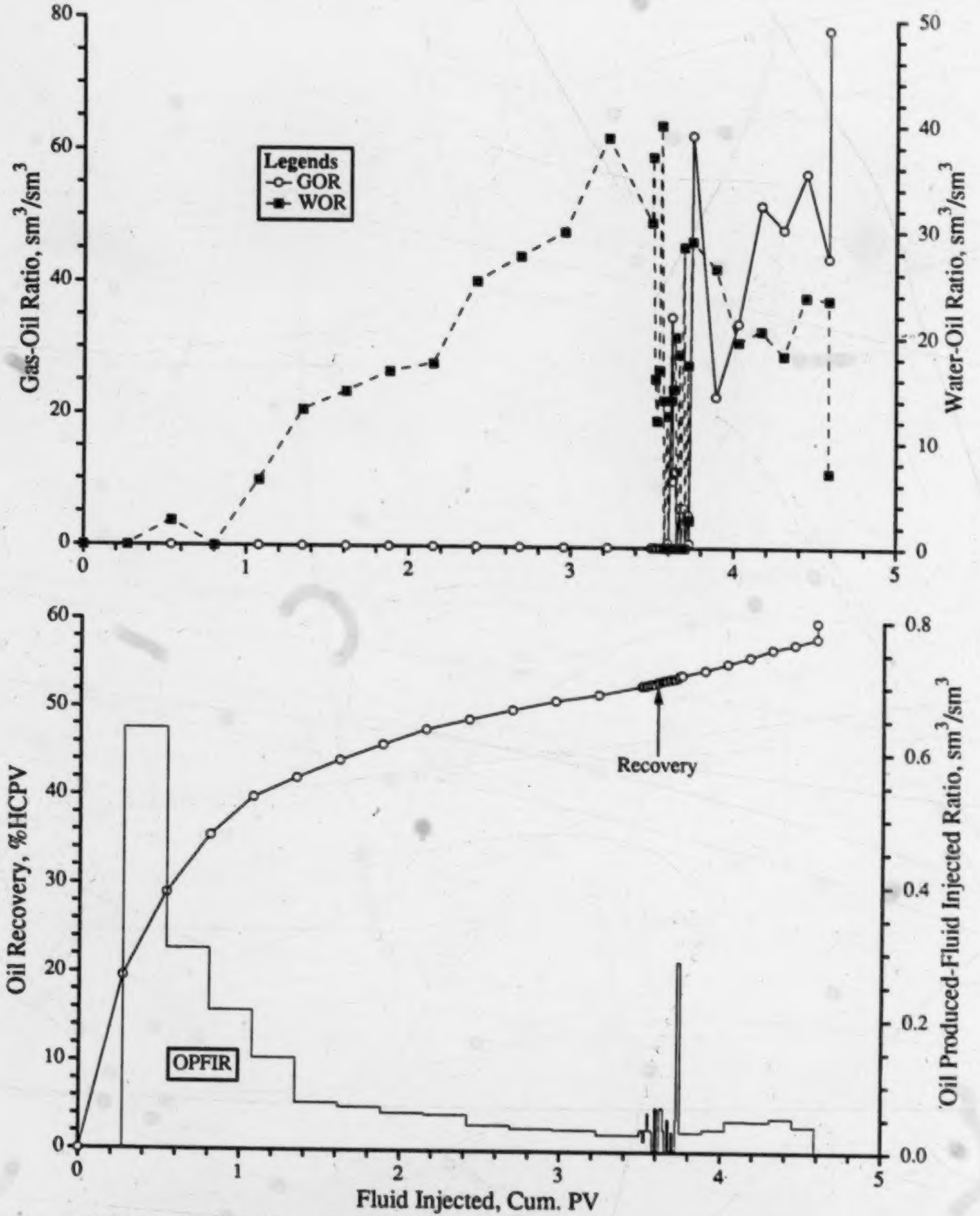

NOTE: Quarter of A 9-Spot

Model Parameters: Average Injection Rate =308.0 cc/hr, μ_o = 603 mPa.s, ϕ = 37.3%, k = 6.2 darcies, S_{oi} = 86.8%, S_{wc} = 13.2%

[0.20 HCPV CO_2 @ 4.8 MPa & 37°C (0.375 mol), 2:1 WAG, 10 Slugs]

Figure F53a - Production History of Run H2D42a.

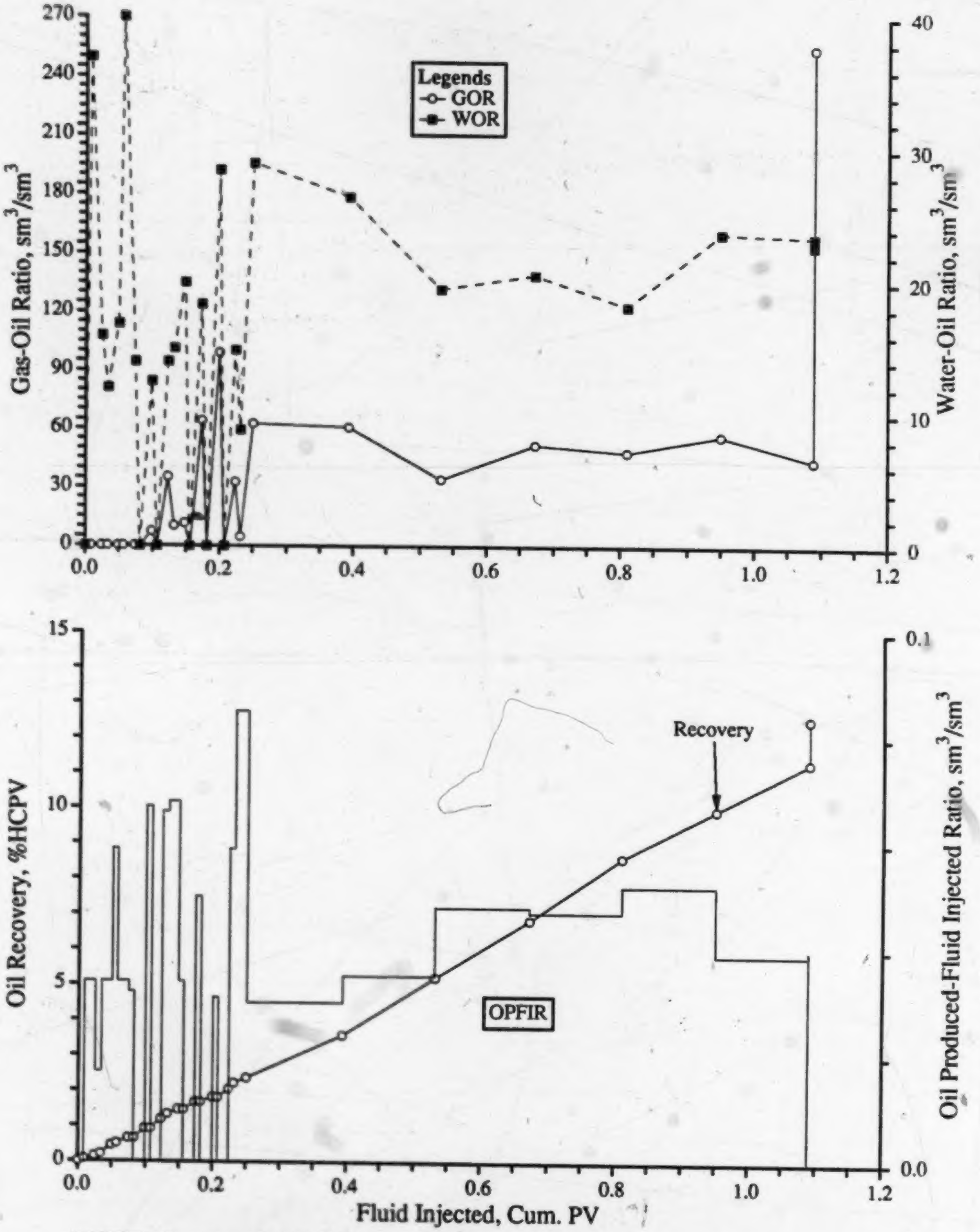

NOTE: Quarter of A 9-Spot

Model Parameters: Average Injection Rate =308.0 cc/hr, μ_o = 603 mPa.s, ø = 37.3 %, k = 6.2 darcies, S_{oi} = 40.5 %, S_{wc} = 59.5 %

[0.20 HCPV CO_2 @ 4.8 MPa & 37°C (0.370 moles), 2:1 WAG, 10 Slugs]

Figure F53b - Production History of Run H2D42b.

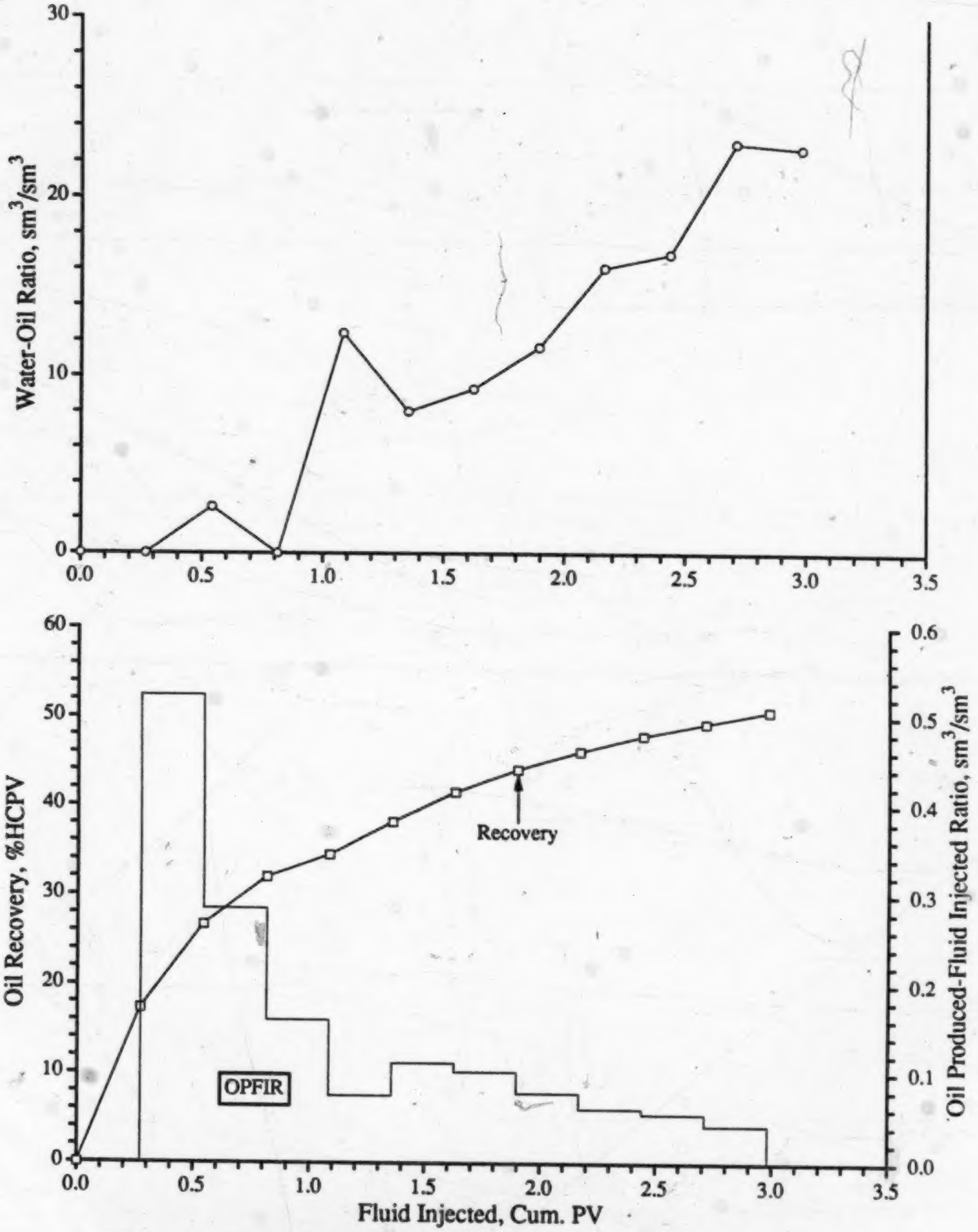

NOTE: Quarter of A 9-Spot

Model Parameters: Average Injection Rate =308.0 cc/hr, μ_o = 280 mPa.s, ø = 37.0 %, k = 11.9 darcies, S_{oi} = 87.3 %, S_{wc} = 12.7 %

[Waterflood @ 3.58 MPa & 21°C]

Figure F54a - Production History of Run H2D43a.

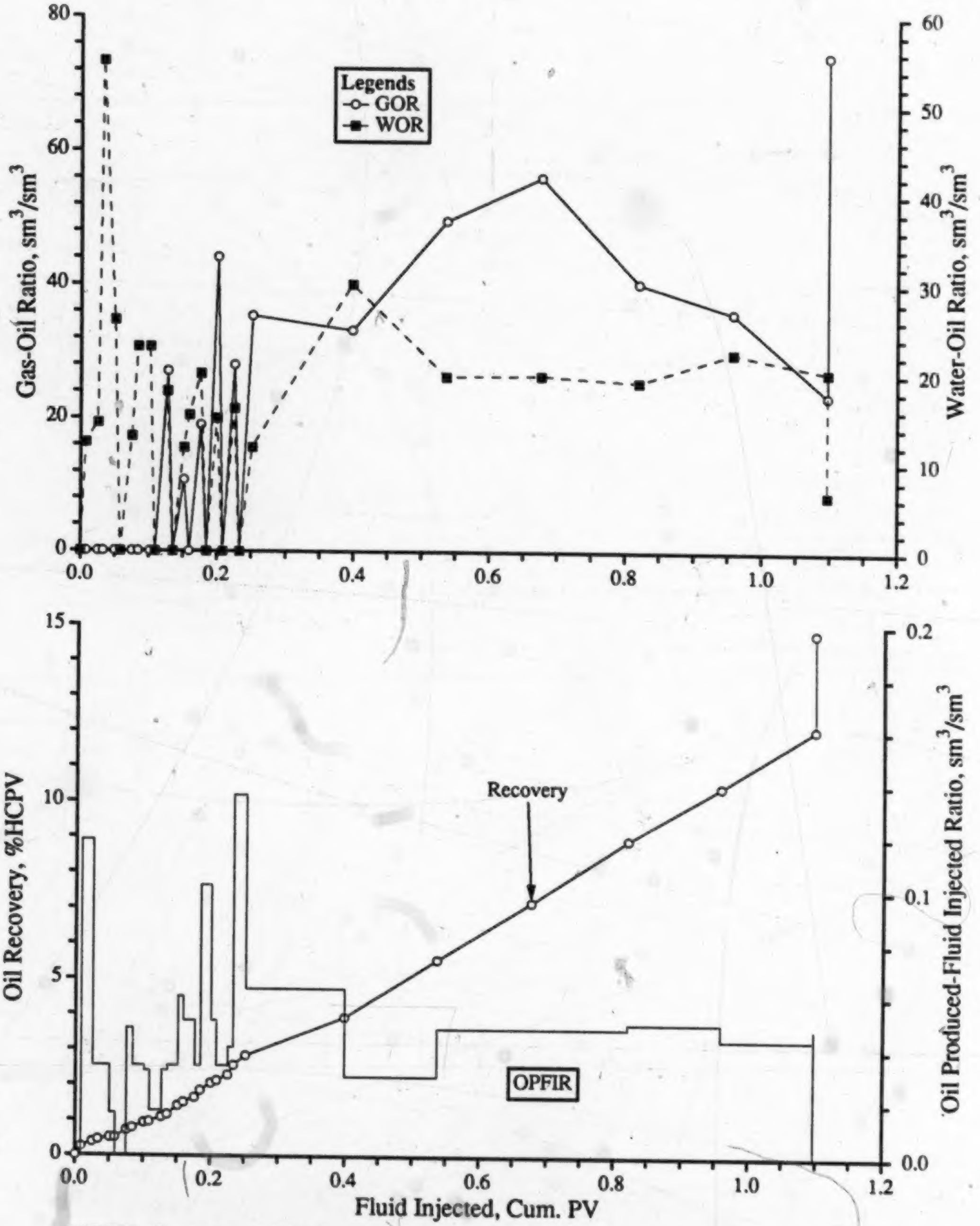

NOTE: Quarter of A 9-Spot

Model Parameters: Average Injection Rate =308.0 cc/hr, μ_o = 282.0 mPa.s, ø = 37.0%, k = 11.9 darcies, S_{oi} = 40.8%, S_{wr} = 59.2%

[0.20 HCPV CO_2 @ 3.58 MPa & 21°C (0.279 mol), 2:1 WAG, 10 Slugs]
Figure F54b - Production History of Run H2D43b.

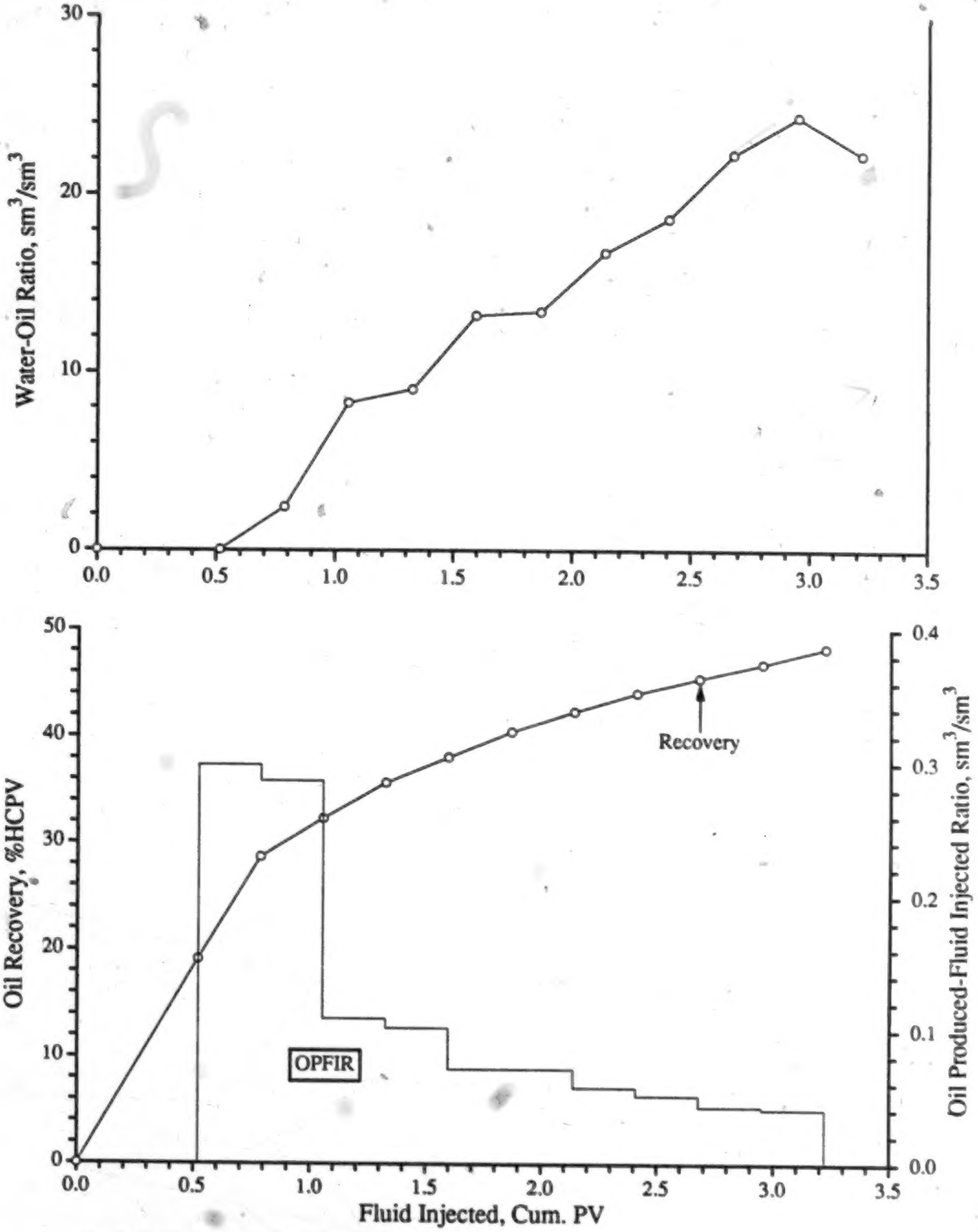

NOTE: Quarter of A 9-Spot

Model Parameters: Average Injection Rate =308.0 cc/hr, μ_o = 282 mPa.s, ϕ = 37.3 %, k = 8.1 darcies, S_{oi} = 81.0 %, S_{wc} = 19.0 %

[Waterflood @ 3.58 MPa & 21°C]

Figure F55a - Production History of Run H2D44a.

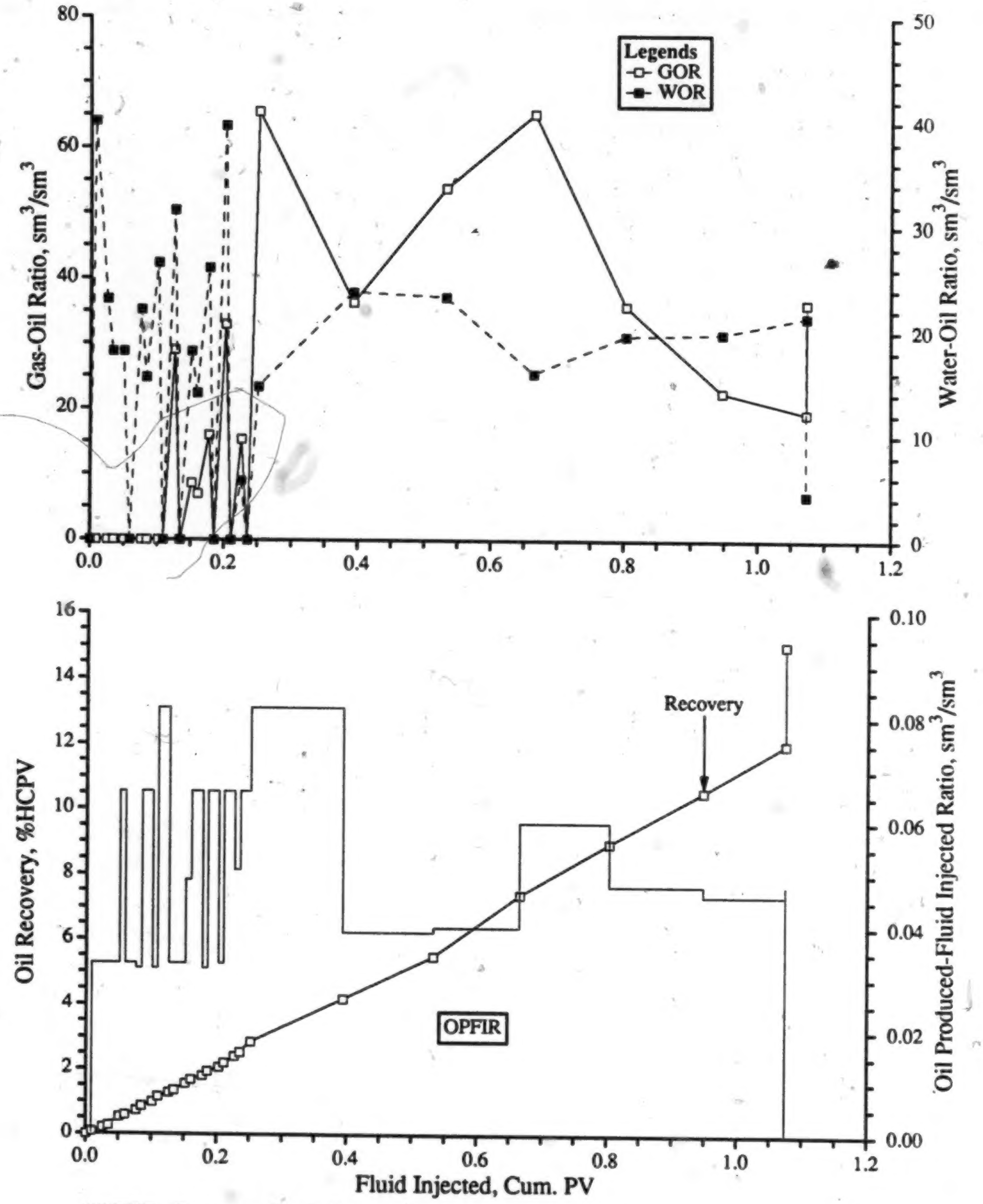

NOTE: Quarter of A 9-Spot

Model Parameters: Average Injection Rate =308.0 cc/hr, μ_o = 280 mPa.s, ø = 37.3 %, k = 8.11 darcies, S_{oi} = 41.9 %, S_{wc} = 58.1 %

[0.20 HCPV CO_2 @ 3.58 MPa & 21°C (0.288 mol), 2:1 WAG, 10 Slugs]

Figure F55b - Production History of Run H2D44b.

APPENDIX G

Viscosity-Temperature Relationship for Different Oils.

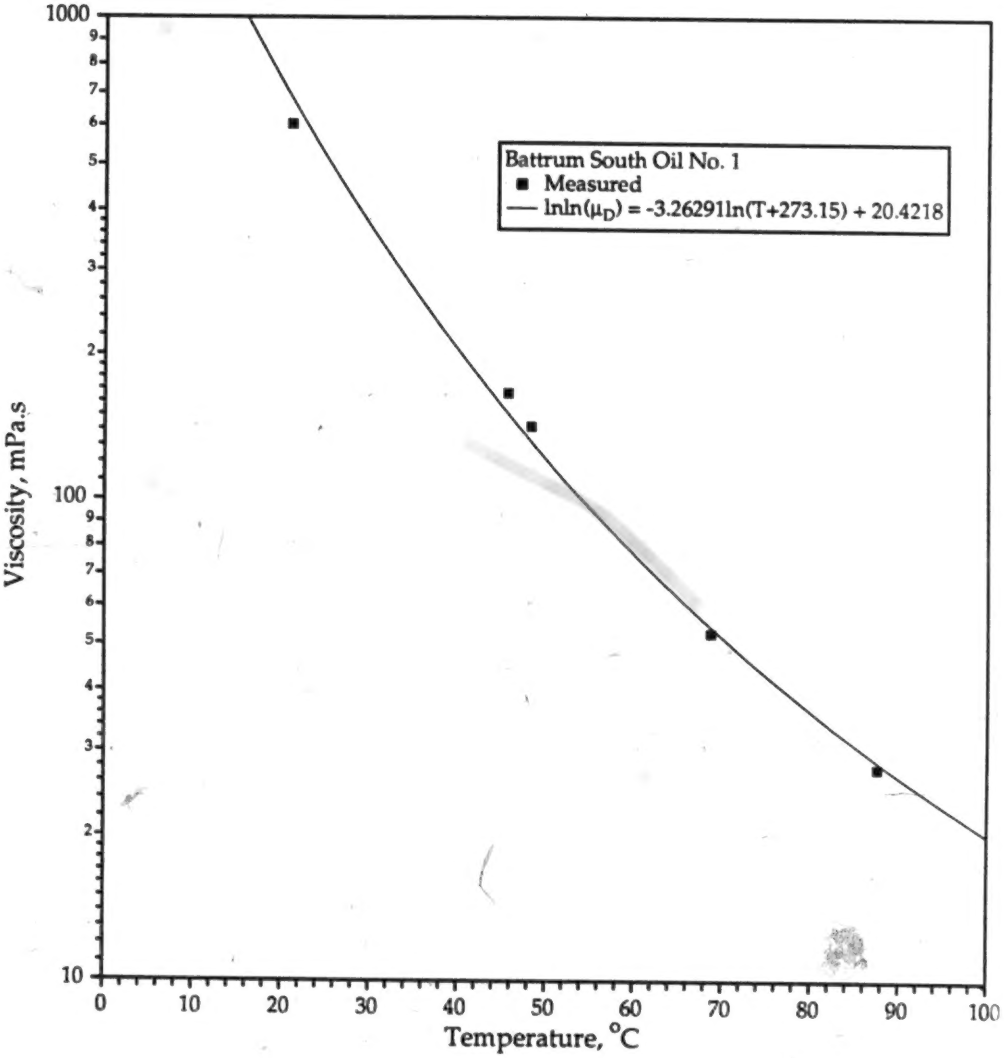

Figure G1 - Viscosity-Temperature Relationship for Battrum South Oil No.1.

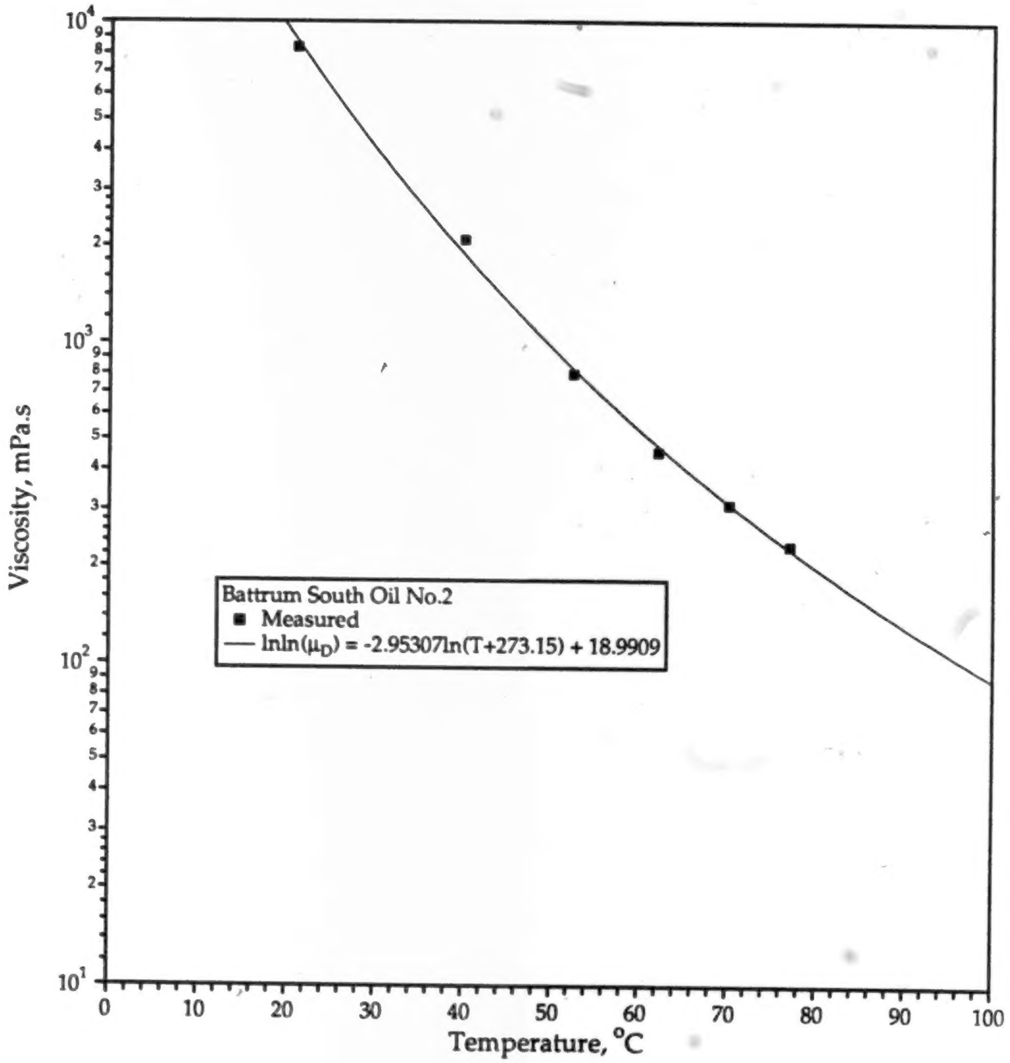

Figure G2 - Viscosity-Temperature Relationship for Battrum South Oil No.2.

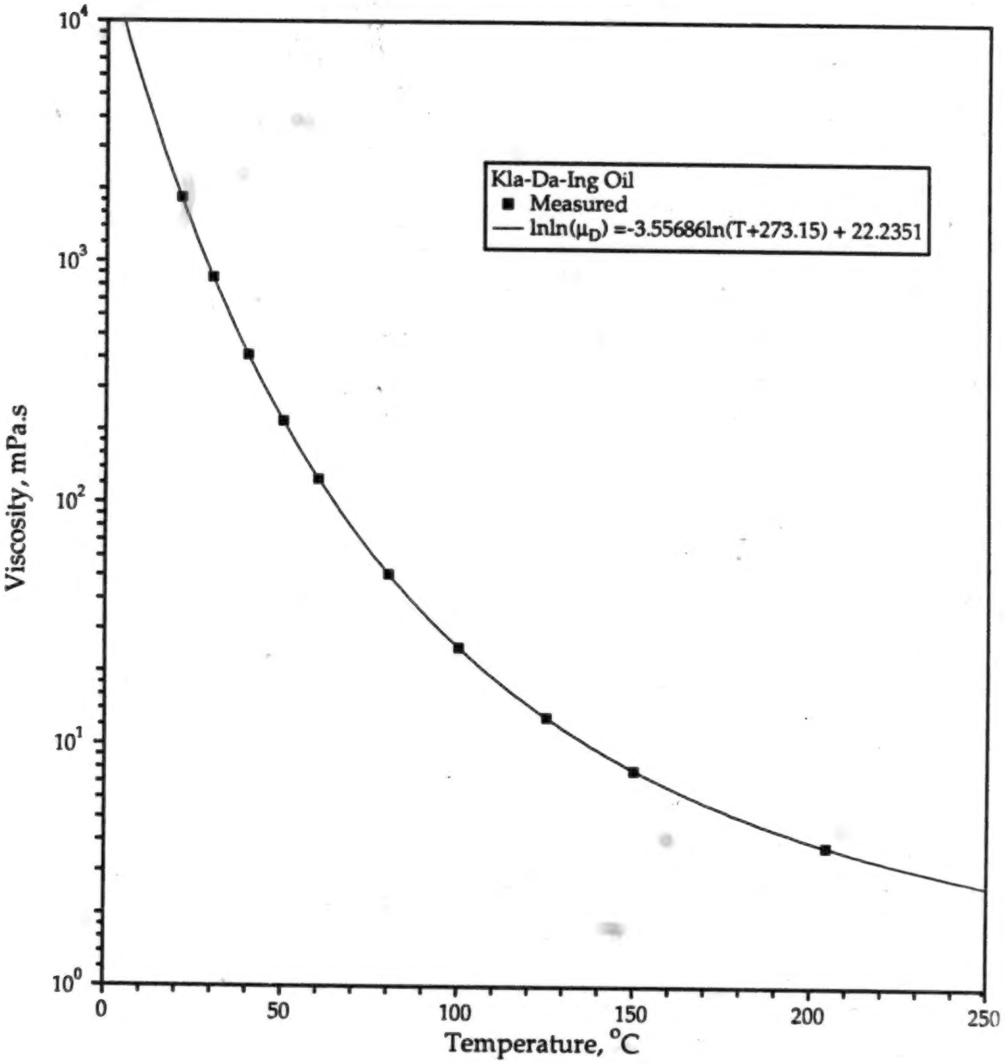

Figure G3 - Viscosity-Temperature Relationship for Kla-Da-Ing Oil.

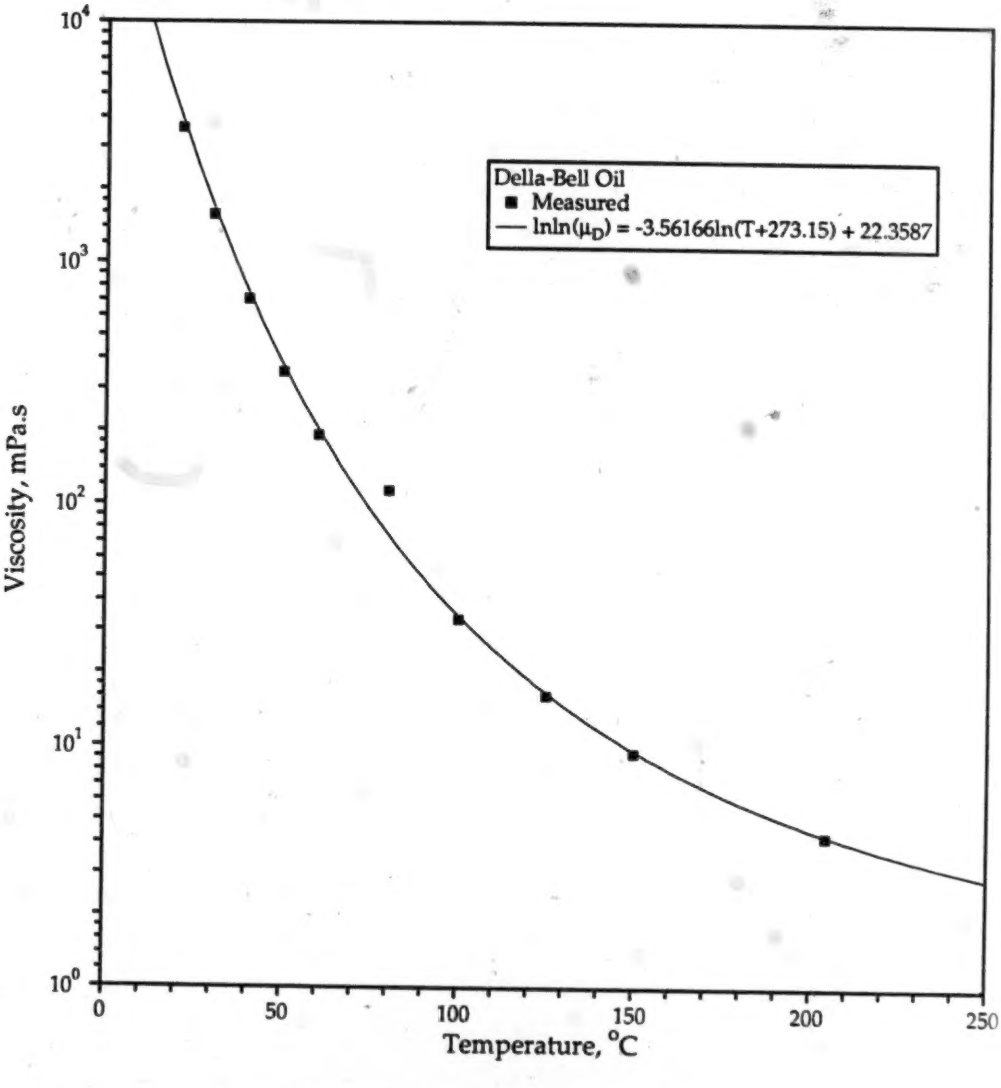

Figure G4 - Viscosity-Temperature Relationship for Della-Bell Oil.

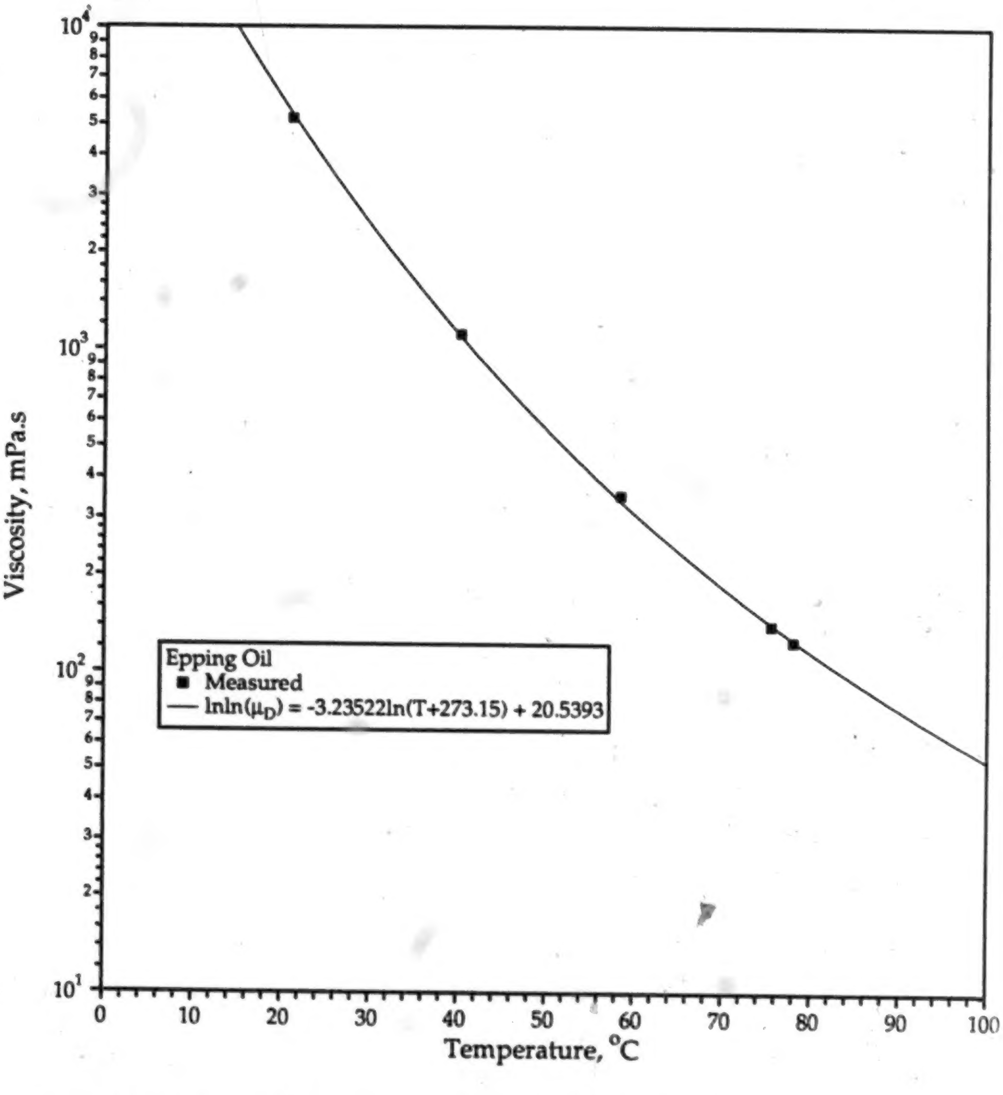

Figure G5 - Viscosity-Temperature Relationship for Epping Oil.

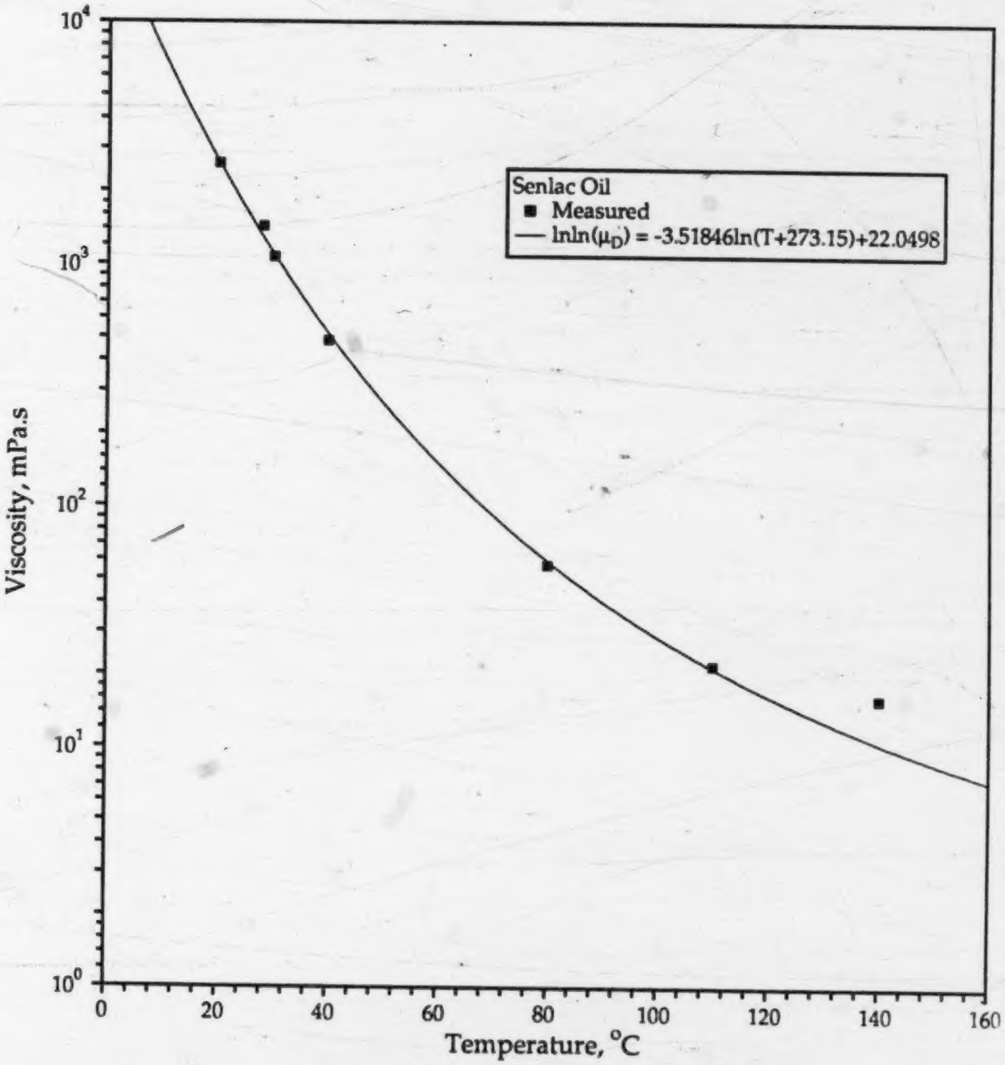

Figure G6 - Viscosity-Temperature Relationship for Senlac Oil.

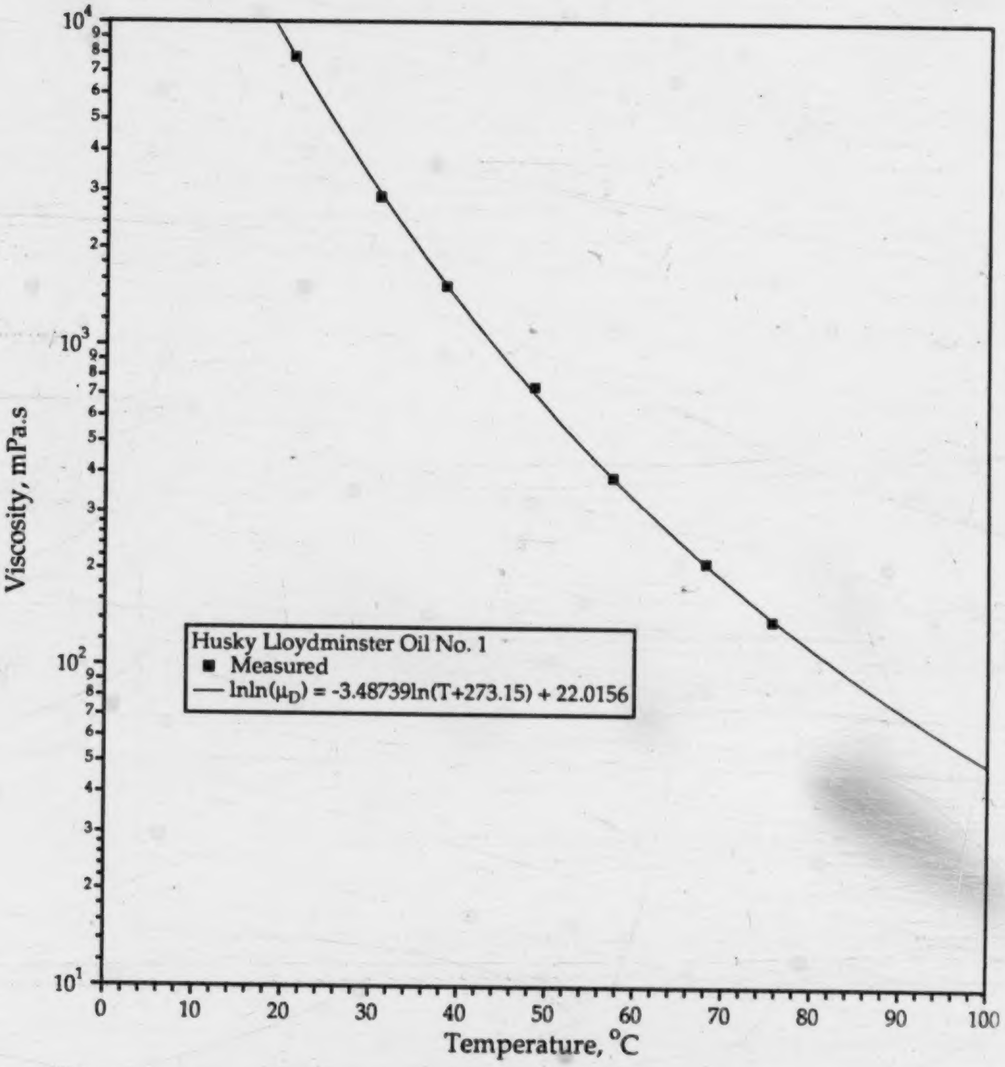

Figure G7 - Viscosity-Temperature Relationship for South Aberfeldy Oil No.1.

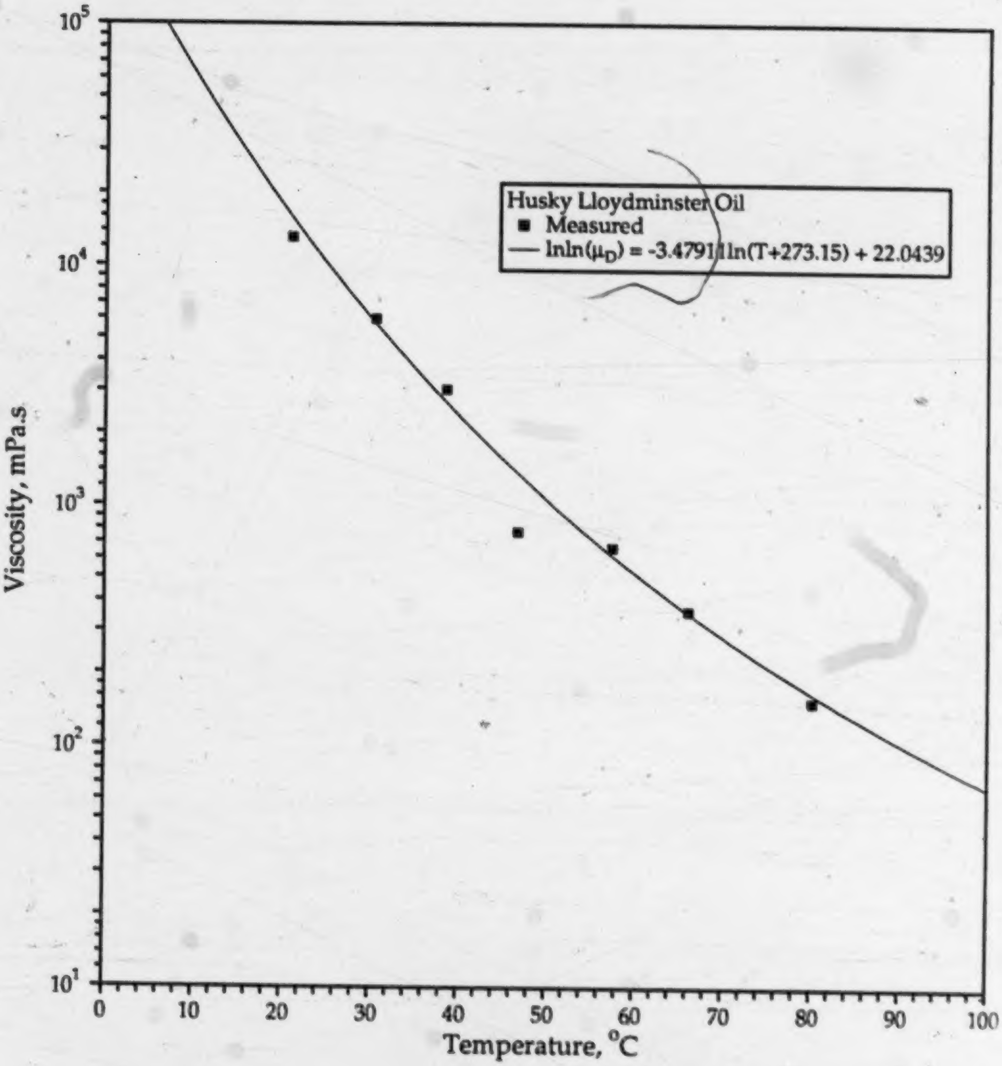

Figure G8 - Viscosity-Temperature Relationship for South Aberfeldy Oil No.2.